

Technische Universiteit Delft
Delft University of Technology



INNOVATIVE ROTOR DESIGN CONCEPTS FOR A 10 MW WIND TURBINE

Scaling Technique, Performance and Feasibility Investigation

Stefanos Kalenteridis
Student Number 4254422
Master of Science in Sustainable Energy Technology
Faculty of Applied Sciences

Supervision:
Dr. Ir. W.A.A.M. Bierbooms
Faculty of Aerospace Engineering

SUMMARY

The reduction of the Levelised Cost of Electricity (LCoE) in wind energy, and offshore in particular, is among the main objectives of research in the academia nowadays, and a demanding task as well. Offshore wind farms are capital intensive investments and lowering uncertainties and costs throughout design, planning, installation and operational phases will offer cheaper electricity production and a more competitive nature against fossil fuel powered energy.

Of course, a big part of the total cost of a wind farm is the wind turbines themselves. Innovations in the design and manufacturing processes are always welcome in order to further advance within the learning curve of the technology and achieve efficient economies of scale. Furthermore, the blades of the wind turbine rotor are its most important component because they express the most basic operation of the turbine, aerodynamics and energy capture. Yet they pose structural challenges. There are efforts to maximise energy output while keeping their mass low, which should subsequently drive down secondary costs. Additionally, another important factor is the increase of energy output in the farm level that can lead to a larger cost reduction.

This thesis aims to investigate the performance and feasibility of lightweight, low power density rotors. This investigation is made by acquiring a performance baseline with the reference rotor of the 10 MW INNWIND machine and comparing it with the proposed alternative rotor designs by means of parametrical modifications. The reference machine rotor radius is 89.166 m, with a blade mass of 41.7 tn and a rated power output of 10 MW operating at an optimal λ of 7.5. All the new designs include an increase in rotor radius to 103 m. They also include differences in operational parameters such as rated rotational speed, blade slenderness and tip speed, while rated power stays the same. These designs result in different blade masses and allocation of energy production.

The six newly proposed designs include a pure up-scale (UPS) of the reference wind turbine blade (RWT) which inherits the same aerodynamic behaviour, it is 18.6 tn heavier, shows a sound structural performance and the largest energy production increase. The second design proposed is a lower solidity rotor with higher blade twist (LSO). Due to the sub-optimal aerodynamic performance, some power is shed in the partial load region but the reduced loads result in a relatively low blade mass (ca. 45.3 tn). This poses certain structural challenges, such as blade tip-tower hits. The third design is again a slender blade (HLA) with the maximum chord location a bit further outboard. It also employs a higher λ of 8.66, closer to the Betz optimum for 3-bladed wind turbines. The blade weighs at ca. 54.2 tn and produces more energy than the RWT.

The fourth blade design is the most slender, with higher rated rotor speed (HRS) and an even higher tip speed ratio of 9.6. Its blade mass amounts to 49.9 tn with an increased energy yield as well. Because of its slender design, it produces several blade hits in extreme cases and small issues in the modal analysis. The last two designs (UPK and HRK) employ a peak shaving strategy close to the rated region for peak load reduction. Their geometries and characteristics are similar to the UPS and HRS respectively, with the exception of a slightly higher twist for the UPK. Their energy yield is also similar to the RWT. The blade mass of the UPK is 51.6 tn, and that of the HRK amounts to 42.7 tn, significantly lower than those of their aerodynamically optimal counterparts (UPS and HRS). UPK and HLA exhibit a more robust structural behaviour with less blade tip-tower hits, while the more slender designs (LSO, HRS and HRK) seem to be in need of further stiffening.

Both static and dynamic loads are a challenge for long blades as it is seen through the results of the modal analysis, the time-domain design load cases and fatigue estimation. The purpose of this thesis is not to fully certify the alternative design concepts by the International Electrotechnical

Commission (IEC) or Germanischer Lloyd (GL) standards, nor to provide a detailed finite element based structural model. The purpose of this thesis is to firstly propose an up-scaling technic that can reflect these design variations with a primary structural approach. Secondly, it is to compare the performance of all seven rotors on the individual wind turbine level through a shortlist of load cases and other structural criteria. Much interference with the rest of the wind turbine model (tower, drive-train, generator, foundation etc.) is avoided in order to maintain a consistent base of comparison. Finally, it is to investigate on how these new designs influence the original INNWIND cost model and LCoE, as a more objective criterion.

The results acquired show that, within the context of this approach, there can be a considerable energy production increase (roughly +12%) combined with a cost of energy reduction (roughly -7%), while the stresses on the blades remain at a similar level. The longer and heavier blades are indeed exposed to higher loads, especially in the extreme cases. The up-scaling method proposed though, can provide the ability for overcoming these negative effects with a well estimated material /mass increase. The most favourable designs are the aerodynamically optimal ones (UPS, HLA and HRS). The sub-optimum, lighter designs (LSO, UPK and HRK) show a marginally decent structural performance but have a disproportional energy production decrease in the effort for load reduction, resulting even in a small LCoE increase (roughly +3.5%).

FOR THE COMMITTEE

Title:

INNOVATIVE ROTOR DESIGN CONCEPTS FOR A 10 MW WIND TURBINE

Author:

Stefanos Kalenteridis

Student Number: 4254422

This Thesis is submitted in partial fulfilment of the requirements for the degree of
Master of Science in Sustainable Energy Technology (SET)

Delft University of Technology

Faculty of Applied Sciences

June 2015

Examination Committee:

Prof. Dr. Gerard J.W. van Bussel (Chair)

Dr. Ir. Michiel B. Zaaijer

Dr. Ir. Dimitrios Zarouchas

Ir. René Bos

Mrs. Özlem Ceyhan (ECN)

THANKS AND ACKNOWLEDGEMENTS

I would like to deeply thank my supervisors, Özlem Ceyhan, René Bos, Asst. Prof. Wim Bierbooms and contributors Dr. Gerard van Bussel, Francesco Grasso, Feike Savenije and all the involved ECN personnel for their help, guidance and inspiration throughout this work. Their academic and technical expertise is mostly appreciated and aided vitally in the formulation and progress of this thesis.

I would also like to express my immense gratitude to my family and friends for their continuous support during this challenging effort.

Stefanos Kalenteridis



Source of cover photograph: www.cleantechnica.com

TABLE OF CONTENTS

SUMMARY	V
FOR THE COMMITTEE	VII
THANKS AND ACKNOWLEDGEMENTS	IX
TABLE OF CONTENTS	XI
LIST OF FIGURES	XIII
LIST OF TABLES	XXI
NOMENCLATURE	XXIII
1 INTRODUCTION	1
1.1 <i>A Look on Wind Energy Today</i>	1
1.2 <i>Wind Turbine Costs</i>	5
1.3 <i>Mass and Loads Up-scaling Laws</i>	7
1.4 <i>Wind Farm Aspects of Low Power Density Rotors</i>	9
1.5 <i>Purpose, Objective, Structure</i>	11
2 THEORY	13
2.1 <i>Short Description of the Reference Model and the Proposed Designs</i>	13
2.1.1 The INNWIND 10 MW RWT	13
2.1.2 The Proposed Designs and Basic Expectations	14
2.2 <i>Performance Indicators and the Reduced List of Design Load Cases</i>	20
2.3 <i>The Cost Model</i>	22
2.3.1 Description.....	22
2.3.2 Implementation	22
2.3.3 LCoE Formulas.....	24
2.4 <i>Fatigue Loads, Damage and Power Production Estimation</i>	26
2.5 <i>Description of Software Used</i>	30
2.5.1 BOT (Blade Optimisation Tool)	30
2.5.2 FOCUS	30
3 MODELLING METHODOLOGY	37
3.1 <i>The INNWIND 10 MW Reference Wind Turbine</i>	37
3.1.1 Overall	37
3.1.2 The Blades and Aerofoils	38
3.1.3 The Tower, Nacelle, Hub and Drive-train	39
3.1.4 The BOT Results of All the Concepts.....	40
3.2 <i>The Modelling / Up-scaling Process</i>	44
3.2.1 Overview	44
3.2.2 Step 1: Definition and Assignment of the Loads	44
3.2.3 Step 2: The Bending Moments, Stiffnesses and Strains	47
3.2.4 Step 3: Towards the new blades	52

3.2.5	Step 4: Proportional Factors Analysis.....	57
3.2.6	Step 4: Up-scaling the Other Properties.....	60
3.3	A Case-Study for the Validation of the Up-scaling Method.....	64
3.3.1	From 10 to 5 MW Down-scaling	65
3.3.2	From 5 to 10 MW Up-scaling	71
4	RESULTS	79
4.1	Rotor Stationary.....	79
4.1.1	Parameters of the Simulations	79
4.1.2	Results of the Calculation.....	80
4.1.3	The Flexible Case	84
4.2	Modal Analysis	86
4.3	Cost Model and LCoE (Iteration No.1).....	99
4.4	Load Cases	101
4.4.1	Controller Modifications.....	102
4.4.2	Design Load Case Simulation Results	102
4.5	Power Production, Damage Equivalent Loads and Fatigue Results	118
4.6	LCoE (Iteration No.2) and Final Design Evaluation	127
5	CONCLUSIONS	133
5.1	Summary of Results and Concluding Remarks	133
5.2	Critical Review on the Method and Proposed Corrections.....	134
5.3	Future Work	135
REFERENCES		137
A	APPENDIX	141
A.1	Tabular Data of Tower and Blade Properties	141
A.2	Additional Time-domain Load Case Simulation Figures	155
A.3	Additional Fatigue Loads Figures (DLC 1.2)	180
A.4	Fatigue Loads Figures (DLC 4.1).....	188
A.5	Cost Model Tables.....	201
A.5.1	RWT.....	201
A.5.2	UPS	203
A.5.3	LSO	205
A.5.4	HLA	207
A.5.5	HRS	209
A.5.6	UPK	211
A.5.7	HRK	213

LIST OF FIGURES

Figure 1.1:	LCoE range of various energy sources [15].....	1
Figure 1.2:	New annual installations (upper) and cumulative capacity (lower) globally 1996 - 2013 [15]	2
Figure 1.3:	LCoE, LCoE+ and SCoE of various energy sources according to the projections of Siemens Wind while including the additional costs [15]	3
Figure 1.4:	LCoE of different energy sources [1]	4
Figure 1.5:	External costs of different energy sources [1]	5
Figure 1.6:	Break-down of basic components costs of a wind turbine (left); idem including foundation, grid connection, transportation, installation and other BoP costs. (right).....	7
Figure 1.7:	Break-down of costs for basic components and services for onshore (left) and offshore (right) installations [16].....	7
Figure 1.8:	Power density of several wind turbines (data taken from manufacturers' websites and online brochures)	9
Figure 1.9:	Rated power of several wind turbines (data taken from manufacturers' websites and online brochures)	10
Figure 2.1:	The up-scaling trend of wind energy state-of-the-art since 1985 [45]	13
Figure 2.2:	The chord distribution of the designs in comparison	18
Figure 2.3:	The aerofoil thickness distribution of the designs in comparison	19
Figure 2.4:	The blade twist distribution of the designs in comparison	19
Figure 2.5:	The turbine CAPEX and BoP for the reference and up-scaled version in [10].....	21
Figure 2.6:	A lin-log S-N curve for aluminium (source: wikipedia.org).....	27
Figure 2.7:	Two views of a Goodman Constant Life Diagram [34].	28
Figure 2.8:	Coordinate system definitions and model details in PHATAS for the overall wind turbine.....	32
Figure 2.9:	Coordinate system definitions and model details in PHATAS for the signals, loads and displacements on the Tower and Shaft.....	33
Figure 2.10:	Coordinate system definitions and model details in PHATAS for the signals, loads and displacements on the blade sections	34
Figure 3.1:	The RWT blade and coordinates (courtesy of the INNWIND database [18])	38
Figure 3.2:	A cross section of the RWT blade showing principal axes Ax.1 and Ax.2 and the different centres of interest. The "reference" point (blue square) is at 50% of the chord. x-axis runs along the chord line and y-axis along the aerofoil thickness (courtesy of the INNWIND database [18]).....	39
Figure 3.3:	The C_p values of all rotors from BOT (dashed lines are used to distinguish between similar concepts)	41
Figure 3.4:	The C_T values of all rotors from BOT (dashed lines are used to distinguish between similar concepts)	41
Figure 3.5:	Thrust on each rotor from BOT (dashed lines are used to distinguish between similar concepts)	42
Figure 3.6:	Flap-wise bending moment of each blade from BOT, with the maximum-load points denoted with the diamonds (dashed lines are used to distinguish between similar concepts)	42

Figure 3.7:	The span-wise distributions of the normal force of the maximum-load points (total rotor thrust divided by 3). The coordinate system GCS refers to the global-absolute CS, i.e. direction down-wind.....	43
Figure 3.8:	The span-wise distributions of the tangential force of the maximum-load points (total rotor torque divided by 3 and each element's distance from the rotor centre). The coordinate system GCS refers to the global-absolute CS, i.e. rotor in-plane.....	43
Figure 3.9:	Definitions of the coordinate systems GCS, LCS and PCS [#] at the blade root (left) and transformation of the forces at the blade root to the LCS (right)	45
Figure 3.10:	The normal forces per element and per unit length in the local and global coordinate system for the RWT blade, containing a small weight component in the LCS distributions	46
Figure 3.11:	The tangential forces (including the weight where indicated) per element and per unit length in the global and local coordinate system for the RWT blade	47
Figure 3.12:	Conceptual representation of the blade's most inboard and most outboard elements and edge-wise loads	48
Figure 3.13:	Flap-wise and edge-wise bending moment distributions for the RWT blade	49
Figure 3.14:	The centrifugal force distribution of the RWT	50
Figure 3.15:	The flap-wise and edge-wise bending stiffness distributions of the RWT blade for the global and local CS.....	51
Figure 3.16:	The edge-wise and flap-wise strain distributions along the span of the RWT blade	52
Figure 3.17:	The normal force per unit length distributions of the designs in comparison (including the weight component)	53
Figure 3.18:	The tangential force (including the weight) per unit length distributions of the designs in comparison	53
Figure 3.19:	The flap-wise bending moment distributions of the designs in comparison.....	54
Figure 3.20:	The edge-wise bending moment distributions of the designs in comparison.....	55
Figure 3.21:	The centrifugal force distributions of the designs in comparison	55
Figure 3.22:	The flap-wise bending stiffness distributions of the designs in comparison	56
Figure 3.23:	The edge-wise bending stiffness distributions of the designs in comparison	57
Figure 3.24:	Concept of the thin-walled rectangular cross section	58
Figure 3.25:	The torsional stiffness distribution of the designs in comparison	62
Figure 3.26:	The blade mass per unit length distribution of the designs and of the classical up-scaling law (s^3) in comparison.....	63
Figure 3.27:	The total blade mass of the designs and of the classical up-scaling law (s^3) in comparison	64
Figure 3.28:	The normal forces on the blades for the RWT, UpWind 5 MW and down-scaled RWT to 5 MW.....	65
Figure 3.29:	The tangential forces (including the weight) on the blades for the RWT, the UpWind 5 MW and the down-scaled RWT to 5 MW	65
Figure 3.30:	The flap-wise bending moments for the RWT, UpWind 5 MW and down-scaled RWT to 5 MW.....	66
Figure 3.31:	The edge-wise bending moments for the RWT, UpWind 5 MW and down-scaled RWT to 5 MW.....	66
Figure 3.32:	The centrifugal forces for the RWT, UpWind 5 MW and down-scaled RWT to 5 MW	67
Figure 3.33:	The flap-wise strains for the RWT, UpWind 5 MW and down-scaled RWT to 5 MW	67
Figure 3.34:	The edge-wise strains for the RWT, UpWind 5 MW and down-scaled RWT to 5 MW	68

Figure 3.35:	The flap-wise bending stiffness for the RWT, UpWind 5 MW and down-scaled RWT to 5 MW	68
Figure 3.36:	The edge-wise bending stiffness for the RWT, UpWind 5 MW and down-scaled RWT to 5 MW	69
Figure 3.37:	The torsional stiffness for the RWT, UpWind 5 MW and down-scaled RWT to 5 MW	69
Figure 3.38:	The mass per unit length distribution for the RWT, UpWind 5 MW and down-scaled RWT to 5 MW	70
Figure 3.39:	The axial stiffness for the RWT, UpWind 5 MW and down-scaled RWT to 5 MW	70
Figure 3.40:	The normal forces on the blades for the RWT, UpWind 5 MW and up-scaled UpWind to 10 MW	71
Figure 3.41:	The tangential forces (including the weight) on the blades for the RWT, the UpWind 5 MW and the up-scaled UpWind to 10 MW	72
Figure 3.42:	The flap-wise bending moments for the RWT, UpWind 5 MW and up-scaled UpWind to 10 MW	72
Figure 3.43:	The edge-wise bending moments for the RWT, UpWind 5 MW and up-scaled UpWind to 10 MW	73
Figure 3.44:	The centrifugal forces for the RWT, UpWind 5 MW and up-scaled UpWind to 10 MW	73
Figure 3.45:	The flap-wise strains for the RWT, UpWind 5 MW and up-scaled UpWind to 10 MW	74
Figure 3.46:	The edge-wise strains for the RWT, UpWind 5 MW and up-scaled UpWind to 10 MW	74
Figure 3.47:	The flap-wise bending stiffness for the RWT, UpWind 5 MW and up-scaled UpWind to 10 MW	75
Figure 3.48:	The edge-wise bending stiffness for the RWT, UpWind 5 MW and up-scaled UpWind to 10 MW	75
Figure 3.49:	The torsional stiffness for the RWT, UpWind 5 MW and up-scaled UpWind to 10 MW	76
Figure 3.50:	The mass per unit length distribution for the RWT, UpWind 5 MW and up-scaled UpWind to 10 MW	76
Figure 3.51:	The axial stiffness for the RWT, UpWind 5 MW and up-scaled UpWind to 10 MW	77
Figure 4.1:	C_p - λ curves for different pitch angles for the RWT	80
Figure 4.2:	C_p - λ curves for different pitch angles for the UPS	81
Figure 4.3:	C_p - λ curves for different pitch angles for the LSO	81
Figure 4.4:	C_p - λ curves for different pitch angles for the HLA	82
Figure 4.5:	C_p - λ curves for different pitch angles for the HRS	82
Figure 4.6:	C_p - λ curves for different pitch angles for the UPK	83
Figure 4.7:	C_p - λ curves for different pitch angles for the HRK	83
Figure 4.8:	C_p - λ curves at optimal pitch angle for the three designs in comparison	84
Figure 4.9:	A part of the “phatdef.mdl” model output file for the RWT flexible case showing some of the tower properties	85
Figure 4.10:	Another part of the “phatdef.mdl” model output file for the RWT flexible case showing the eigen-frequencies and eigen-modes of the rotor	85
Figure 4.11:	A part of the “towmod.out” tower model output file for the RWT flexible case showing the eigen-frequencies of the tower	85
Figure 4.12:	Coupled eigen-frequencies of the RWT rotor	87
Figure 4.13:	Aerodynamic damping versus the operating wind speed for RWT modes	87

Figure 4.14:	Coupled eigen-frequencies of the UPS rotor	88
Figure 4.15:	Aerodynamic damping versus the operating wind speed for UPS modes	88
Figure 4.16:	Coupled eigen-frequencies of the LSO rotor	89
Figure 4.17:	Aerodynamic damping versus the operating wind speed for LSO modes.....	89
Figure 4.18:	Coupled eigen-frequencies of the HLA rotor.....	90
Figure 4.19:	Aerodynamic damping versus the operating wind speed for HLA modes	90
Figure 4.20:	Coupled eigen-frequencies of the HRS rotor.....	91
Figure 4.21:	Aerodynamic damping versus the operating wind speed for HRS modes	91
Figure 4.22:	Coupled eigen-frequencies of the UPK rotor	92
Figure 4.23:	Aerodynamic damping versus the operating wind speed for UPK modes	92
Figure 4.24:	Coupled eigen-frequencies of the HRK rotor	93
Figure 4.25:	Aerodynamic damping versus the operating wind speed for HRK modes	93
Figure 4.26:	Quasi-steady state flap-wise bending moment and displacement along blade span from BLADEMODE.....	96
Figure 4.27:	Quasi-steady state edge-wise bending moment and displacement along blade span from BLADEMODE.....	97
Figure 4.28:	Quasi-steady state torsional moment and deformation along blade span from BLADEMODE	98
Figure 4.29:	Blade mass versus LCoE	100
Figure 4.30:	Wake losses versus LCoE	100
Figure 4.31:	Shaft power (excluding 6% electrical losses) from all DLCs for all designs.....	103
Figure 4.32:	Thrust on the rotor from all DLCs for all designs	104
Figure 4.33:	Rotor speed from all DLCs for all designs	105
Figure 4.34:	Torque on the low speed rotor shaft from all DLCs for all designs.....	106
Figure 4.35:	Tower bottom fore-aft bending moment from all DLCs for all designs	107
Figure 4.36:	Tower bottom side-to-side bending moment from all DLCs for all designs	108
Figure 4.37:	Tower bottom torsional moment from all DLCs for all designs	109
Figure 4.38:	Blade 1 pitch angle from all DLCs for all designs	110
Figure 4.39:	Blade 2 flap-wise blade root bending moment in the chord reference system from all DLCs for all designs. (The term “flat-wise” from PHATAS refers to the LCS instead of “flap- wise” that refers to GCS, see Figure 2.10)	111
Figure 4.40:	Blade 2 flap-wise tip deflection in the chord reference system from all DLCs for all designs	112
Figure 4.41:	Blade 1 edge-wise blade root bending moment in the chord reference system from all DLCs for all designs	113
Figure 4.42:	Blade 1 edge-wise tip displacement in the chord reference system from all DLCs for all designs	114
Figure 4.43:	Blade 1 torsional blade root moment in the chord reference system from all DLCs for all designs	115
Figure 4.44:	Blade 1 torsional tip displacement in the chord reference system from all DLCs for all designs	116

Figure 4.45:	Blade tip 1, 2 or 3 clearance from centre of tower from all DLCs for all designs. (0 value in y-axis represents the tower centre and the green line/margin, the tower radius at passing point. Treated signal, $\pm 5^\circ$ window before and after passing the tower centreline)	117
Figure 4.46:	The power curves and total energy yield (per wind turbine, NOT wind farm) of all designs from all DLC 1.2 simulations.	119
Figure 4.47:	The mean flap-wise blade root bending moment versus all operating wind speeds (not Weibull-weighted) and lifetime damage equivalent stresses of all designs from all DLC 1.2 simulations.	120
Figure 4.48:	The mean edge-wise blade root bending moment versus all operating wind speeds (not Weibull-weighted) and lifetime damage equivalent stresses of all designs from all DLC 1.2 simulations.	121
Figure 4.49:	The mean torsional blade root moment versus all operating wind speeds (not Weibull-weighted) and lifetime damage equivalent stresses of all designs from all DLC 1.2 simulations.	122
Figure 4.50:	Log-log scale S-N curve for tensile, compressive and shear loadings on GFRP material, including the damage equivalent loads at the 25 year cycles	123
Figure 4.51:	The tower bottom fore-aft moment versus all operating wind speeds (not Weibull-weighted) and lifetime damage equivalent moment of all designs from all DLC 1.2 simulations.	124
Figure 4.52:	The tower bottom extreme fore-aft (left) and side-to-side (right) bending moments on the RWT tower for load cases run by DTU [5]	125
Figure 4.53:	Wind rose direction probabilities (a - left) and wind speed Weibull probabilities (b - right) measured at Horns Rev, reported in [7]	125
Figure 4.54:	The lifetime equivalent flap- and edge-wise blade root (top) and the tower bottom fore-aft and side-to-side (bottom) bending moments versus wind speed from DTU results in [5]	127
Figure 4.55:	Graphic representation of the farm LCoE taking into account the lifetime energy yield from DLC 1.2 simulations	128
Figure 4.56:	Blade mass versus LCoE (Iter. 2)	129
Figure 4.57:	Wake losses versus LCoE (Iter. 2)	129
Figure 4.58:	Graphic representation of the rankings by group and their final sum	131
Figure A.1:	Wind speed from all DLCs for all designs	156
Figure A.2:	Wind direction from all DLCs for all designs	157
Figure A.3:	Aerodynamic power from all DLCs for all designs	158
Figure A.4:	Controller reference value for rotor speed from all DLCs for all designs	159
Figure A.5:	Controller reference value for generator torque (transformed at slow speed shaft) from all DLCs for all designs	160
Figure A.6:	Torsional deformation of rotor shaft from all DLCs for all designs	161
Figure A.7:	Blade 2 pitch angle from all DLCs for all designs	162
Figure A.8:	Blade 3 pitch angle from all DLCs for all designs	163
Figure A.9:	Blade 1 flap-wise blade root bending moment in the chord reference system from all DLCs for all designs	164
Figure A.10:	Blade 3 flap-wise blade root bending moment in the chord reference system from all DLCs for all designs	165
Figure A.11:	Blade 1 flap-wise tip displacement in the chord reference system from all DLCs for all designs	166

Figure A.12:	Blade 3 flap-wise tip displacement in the chord reference system from all DLCs for all designs	167
Figure A.13:	Blade 2 edge-wise blade root bending moment in the chord reference system from all DLCs for all designs	168
Figure A.14:	Blade 3 edge-wise blade root bending moment in the chord reference system from all DLCs for all designs	169
Figure A.15:	Blade 2 edge-wise tip displacement in the chord reference system from all DLCs for all designs	170
Figure A.16:	Blade 3 edge-wise tip displacement in the chord reference system from all DLCs for all designs	171
Figure A.17:	Blade 2 torsional blade root moment in the chord reference system from all DLCs for all designs	172
Figure A.18:	Blade 3 torsional blade root moment in the chord reference system from all DLCs for all designs	173
Figure A.19:	Blade 2 torsional tip displacement in the chord reference system from all DLCs for all designs	174
Figure A.20:	Blade 3 torsional tip displacement in the chord reference system from all DLCs for all designs	175
Figure A.21:	Tower top/nacelle fore-aft displacement from all DLCs for all designs	176
Figure A.22:	Tower top/nacelle side-to-side displacement from all DLCs for all designs	177
Figure A.23:	Tower top/nacelle torsional displacement from all DLCs for all designs	178
Figure A.24:	Blade tip 1, 2 or 3 clearance from centre of tower from all DLCs for all designs (0 value represents tower centre and green margin tower radius at passing point. Untreated signal, $\pm 60^\circ$ window)	179
Figure A.25:	The mean flap-wise blade root bending moment percent differences versus all operating wind speeds (not Weibull-weighted) for all designs from all DLC 1.2 simulations	180
Figure A.26:	Mean and maximum lifetime equivalent flap-wise blade root bending moment for all designs from all DLC 1.2 simulations	180
Figure A.27:	Mean lifetime equivalent flap-wise blade root strain of all designs from all DLC 1.2 simulations	181
Figure A.28:	The mean edge-wise blade root bending moment percent differences versus all operating wind speeds (not Weibull-weighted) for all designs from all DLC 1.2 simulations	181
Figure A.29:	Mean and maximum lifetime equivalent edge-wise blade root bending moment for all designs from all DLC 1.2 simulations	182
Figure A.30:	Mean lifetime equivalent edge-wise blade root strain of all designs from all DLC 1.2 simulations	182
Figure A.31:	The mean torsional blade root moment percent differences versus all operating wind speeds (not Weibull-weighted) for all designs from all DLC 1.2 simulations	183
Figure A.32:	Mean and maximum lifetime equivalent torsional blade root moment for all designs from all DLC 1.2 simulations	183
Figure A.33:	Mean lifetime equivalent torsional blade root strain of all designs from all DLC 1.2 simulations	184
Figure A.34:	The tower bottom side-to-side moment versus all operating wind speeds (not Weibull-weighted) and lifetime damage equivalent moment of all designs from all DLC 1.2 simulations	185
Figure A.35:	The tower bottom torsional moment versus all operating wind speeds (not Weibull-weighted) and lifetime damage equivalent moment of all designs from all DLC 1.2 simulations	186

Figure A.36:	The shaft torque versus all operating wind speeds (not Weibull-weighted) and lifetime damage equivalent torque of all designs from all DLC 1.2 simulations	187
Figure A.37:	The mean flap-wise blade root bending moment and percent differences versus shut-down wind speeds (not Weibull-weighted) for all designs from all DLC 4.1 simulations	188
Figure A.38:	Mean and maximum lifetime equivalent flap-wise blade root bending moment and stress for all designs from all DLC 4.1 simulations	189
Figure A.39:	Mean lifetime equivalent flap-wise blade root strain of all designs from all DLC 4.1 simulations.....	190
Figure A.40:	The mean edge-wise blade root bending moment and percent differences versus shut-down wind speeds (not Weibull-weighted) for all designs from all DLC 4.1 simulations	191
Figure A.41:	Mean and maximum lifetime equivalent edge-wise blade root bending moment and stress for all designs from all DLC 4.1 simulations	192
Figure A.42:	Mean lifetime equivalent edge-wise blade root strain of all designs from all DLC 4.1 simulations.....	193
Figure A.43:	The mean torsional blade root bending moment and percent differences versus shut-down wind speeds (not Weibull-weighted) for all designs from all DLC 4.1 simulations	194
Figure A.44:	Mean and maximum lifetime equivalent torsional blade root moment and stress for all designs from all DLC 4.1 simulations	195
Figure A.45:	Mean lifetime equivalent torsional blade root strain of all designs from all DLC 1.2 simulations.....	196
Figure A.46:	The tower bottom fore-aft moment versus shut-down wind speeds (not Weibull-weighted) and lifetime damage equivalent moment of all designs from all DLC 4.1 simulations.....	197
Figure A.47:	The tower bottom side-to-side moment versus shut-down wind speeds (not Weibull-weighted) and lifetime damage equivalent moment of all designs from all DLC 4.1 simulations.....	198
Figure A.48:	The tower bottom torsional moment versus shut-down wind speeds (not Weibull-weighted) and lifetime damage equivalent moment of all designs from all DLC 4.1 simulations.....	199
Figure A.49:	The rotor shaft torque versus shut-down wind speeds (not Weibull-weighted) and lifetime damage equivalent torque of all designs from all DLC 4.1 simulations.....	200

LIST OF TABLES

Table 1.1:	The sub-component masses and costs part of the INNWIND cost model#	5
Table 1.2:	Summarised results reported in [7]	11
Table 2.1:	Main parameters of the UpWind and INNWIND Wind Turbines	14
Table 2.2:	Main parameters of the proposed designs [7]	17
Table 2.3:	BOT software output at the maximum-load operating point.....	17
Table 2.4:	Corrected parameters of the proposed designs	18
Table 2.5:	The Aerofoil Distribution along the blade span, after the blade root/hub radius.....	20
Table 3.1:	Main properties of the INNWIND Reference Wind Turbine	37
Table 3.2:	Properties of the RWT Blade.....	38
Table 3.3:	Properties of the RWT Tower	39
Table 3.4:	Properties of the Nacelle and Hub	40
Table 3.5:	Properties of the Drive-train	40
Table 3.6:	The resulting Blade Masses	63
Table 3.7:	The resulting Blade Masses for the down-scaling Case Study	71
Table 3.8:	The resulting Blade Masses for the up-Scaling Case Study	77
Table 4.1:	Rotor Stationary Simulation Parameters	79
Table 4.2:	Results of the flexible case	86
Table 4.3:	Frequencies in Hz at rated rotor speed of each design and the standard deviation (StD) between concepts summarised	94
Table 4.4:	Condition combinations for maximum displacements calculations.....	94
Table 4.5:	LCoE and capacity factor estimations	99
Table 4.6:	List of load case sets and simulation details	101
Table 4.7:	LCoE and capacity factor estimations (Iteration No.2)	128
Table 4.8:	The individual parameters and values participating in the evaluation	130
Table 4.9:	The 0 to 1 rankings of the designs by individuals and groups.....	130
Table 5.1:	Summary of performance indicators	133

NOMENCLATURE

Latin Symbols

A	: Rotor swept area or Cross sectional area
B	: Blade number
c	: Chord length of aerofoil
C_D	: Drag coefficient
C_L	: Lift coefficient
C_P	: Power coefficient
$C_{P,max}$: Betz limit or wind turbine's maximum power coefficient
C_Q	: Torque coefficient
C_T	: Thrust coefficient
D, D_{Tot}	: Partial fatigue damage and total damage
$d_{x, y}$: Distance of neutral axis from stress application point
E	: Young's modulus of elasticity
E_{life}	: Lifetime energy production
EA	: Axial stiffness
$EI_{xx, yy, xy}$: Edge-wise, flap-wise or coupling bending stiffness
g	: Gravitational acceleration constant
G	: Shear modulus of elasticity
GJ_T	: Torsional stiffness
F_{ax}	: Axial aerodynamic force, thrust
F_n	: Axial force on blade
F_P	: Prandtl's tip loss correction factor
F_t	: Tangential force on blade
h, b	: Height and width of rectangular cross section
$I_{xx, yy, xy}$: Edge-wise, flap-wise or coupling area moment of inertia (second moment of area)
J_T	: Polar moment of inertia
k_w	: Weibull shape parameter
K	: Torque controller gain
L, l_{elm}	: Length, element length
m	: S-N curve material slope
m_d	: Mass distribution
M_{eq}	: Equivalent moment
M_{FA}	: Tower fore-aft bending moment
M_{SS}	: Tower side-to-side bending moment
M_y	: Flap-wise or out-of-plane bending moment on the blade
M_x	: Edge-wise or in-plane bending moment on the blade
nP	: Multiples of rotational frequencies
N, n	: Cycles to failure and occurring cycles

N_{eq}	: Equivalent 1 Hz load cycles (cycles in seconds)
N_{occur}	: Number of load case occurrences
pdf	: Probability density function
P_R	: Rated power
P_{aero}	: Aerodynamic power
Q, Q_R	: Torque and Rated torque
r, r_{elm}	: Radial position on the blade, element radial position
R, R_{Tot}	: Total rotor radius
R_f, R_e	: Flap- and edge-wise stiffness proportion factors
R_S	: Cyclic stress ratio for fatigue
R_T	: Aerofoil relative thickness
R_x, R_y, R_D	: Axes and diameter proportional factors
s_i	: Span-wise position on the blade
S	: Normal stress
s^λ	: Scaling factor raised to exponent λ
t	: Aerofoil total thickness
t_1, t_2	: Wall thicknesses of rectangular cross section
T	: Axial aerodynamic force, thrust
T_z	: Blade torsion
T_{life}	: Wind turbine lifetime
T_{sim}	: Simulation duration
V_R	: Rated wind speed
$V_{w,mean}$: Weibull annual average wind speed
z_{af}	: Aerofoil span-wise position

Greek Symbols

a	: Axial induction factor
a'	: Angular induction factor
Γ	: Gamma function
ε	: Normal strain
θ_p	: Blade pitch angle
θ_T	: Aerodynamic twist angle
θ_{st}	: Structural twist angle
λ	: Tip speed ratio (TSR) or scaling factor exponent
λ_w	: Weibull scale parameter
ρ	: Fluid density (air density)
σ	: Normal stress
τ	: Shear stress
Ω, ω	: Rotor angular velocity (rotor speed)
ω_n	: Natural frequency

Acronyms and Abbreviations

<i>AEP, AEY</i>	: Annual Energy Production, Annual Energy Yield
<i>AVATAR</i>	: AdVanced Aerodynamic Tools for Large Rotors
<i>BEM</i>	: Blade Element Momentum (Theory)
<i>bld</i>	: Blade index
<i>BoP</i>	: Balance of Plant
<i>BOT</i>	: Blade Optimisation Tool
<i>BR</i>	: Blade Root position
<i>BRBM</i>	: Blade Root Bending Moment (mostly refers to flap-wise moment)
<i>CAPEX</i>	: CAPital EXpenditure
<i>CLD</i>	: Constant Life Diagram
<i>DEqL</i>	: 1 Hz - Damage Equivalent Load
<i>DLC</i>	: Design Load Case (by context may refer to a single or a group of simulations)
<i>DT</i>	: Drive-Train assembly
<i>DTU</i>	: Denmark Technical University
<i>ECN</i>	: Energieonderzoek Centrum Nederland (Energy Research Centre of the Netherlands)
<i>elm</i>	: Element index
<i>ETM</i>	: Extreme Turbulence Model
<i>EU</i>	: European Union
<i>EWII</i>	: European Wind Industrial Initiative
<i>EWM</i>	: Extreme Wind Model (mostly refers to 1 year extreme)
<i>FA</i>	: Tower Fore-Aft motion or loads index
<i>FEM</i>	: Finite Element Method
<i>GCS</i>	: Global Coordinate System
<i>GFRP (-E)</i>	: Glass Fibre Reinforced Polymer (Epoxy)
<i>GL</i>	: Germanischer Lloyd
<i>GUI</i>	: Graphic User Interface
<i>GWEC</i>	: Global Wind Energy Council
<i>HLA</i>	: The Higher Lambda (Higher TSR) concept of the RWT
<i>HRK</i>	: The Higher Rotor Speed with Peak Shaving concept of the RWT
<i>HRS</i>	: The Higher Rotor Speed concept of the RWT
<i>HSS</i>	: High Speed Shaft
<i>IEC</i>	: International Electrotechnical Commission
<i>LCoE</i>	: Levelised Cost of Electricity / Energy
<i>LCoE+</i>	: Expanded Levelised Cost of Electricity (Term by Siemens)
<i>LCS</i>	: Local (blade) Coordinate System
<i>LSO</i>	: The Low Solidity concept of the RWT
<i>LSR</i>	: Local Speed Ratio
<i>MDO</i>	: Multi-Disciplinary Optimisation
<i>MPPT</i>	: Maximum Power Point Tracking
<i>NREL</i>	: National Renewable Energy Laboratory
<i>ONTM</i>	: Normal Turbulence Model
<i>NWP</i>	: Normal Wind Profile

<i>O&M</i>	:	Operation and Maintenance
<i>OPEX</i>	:	Operational Expenditure
<i>PHATAS</i>	:	Program for Horizontal Axis wind Turbine Analysis and Simulation
<i>PCS</i>	:	Principal axis Coordinate System
<i>PI</i>	:	Performance Indicator
<i>PPI</i>	:	Producer's Price Index
<i>PSD</i>	:	Power Spectral Density
<i>RPM, rpm</i>	:	Rounds Per Minute
<i>RSP</i>	:	Rotor Speed
<i>RWT</i>	:	Reference Wind Turbine, referring to the standard INNWIND 10 MW WT model
<i>SCoE</i>	:	Social Cost of Electricity (Term by Siemens)
<i>SETIS</i>	:	Strategic Energy Technologies Information System
<i>SF</i>	:	Scaling Factor exponent
<i>SS</i>	:	Tower Side-to-Side motion or loads index
<i>TSR</i>	:	Tip Speed Ratio
<i>UCS, UTS</i>	:	Ultimate Compressive or Tensile Strength
<i>UPK</i>	:	The Upscale with Peak Shaving concept of the RWT
<i>UPS</i>	:	The pure Upscale concept of the RWT
<i>WF</i>	:	Wind Farm
<i>WMC</i>	:	Knowledge Centre Wind turbine Materials and Constructions research institute
<i>WSP</i>	:	Wind Speed
<i>WT</i>	:	Wind Turbine

1

INTRODUCTION

1.1 A Look on Wind Energy Today

According to the GWEC annual report for 2013 [15], the global wind energy market is steadily growing despite recent setbacks in many economies worldwide. It is considered as the second most promising renewable energy source for electricity production, right after hydroelectric power, provided at an already competitive price (onshore in particular). In Figure 1.1, one can see the price range of onshore wind being reported at \$50-\$160/MWh, while offshore wind is at \$150-\$340/MWh (ca. €79/MWh and €184/MWh respectively, with a 2013 average EUR/USD exchange rate at 1.328 [11]).

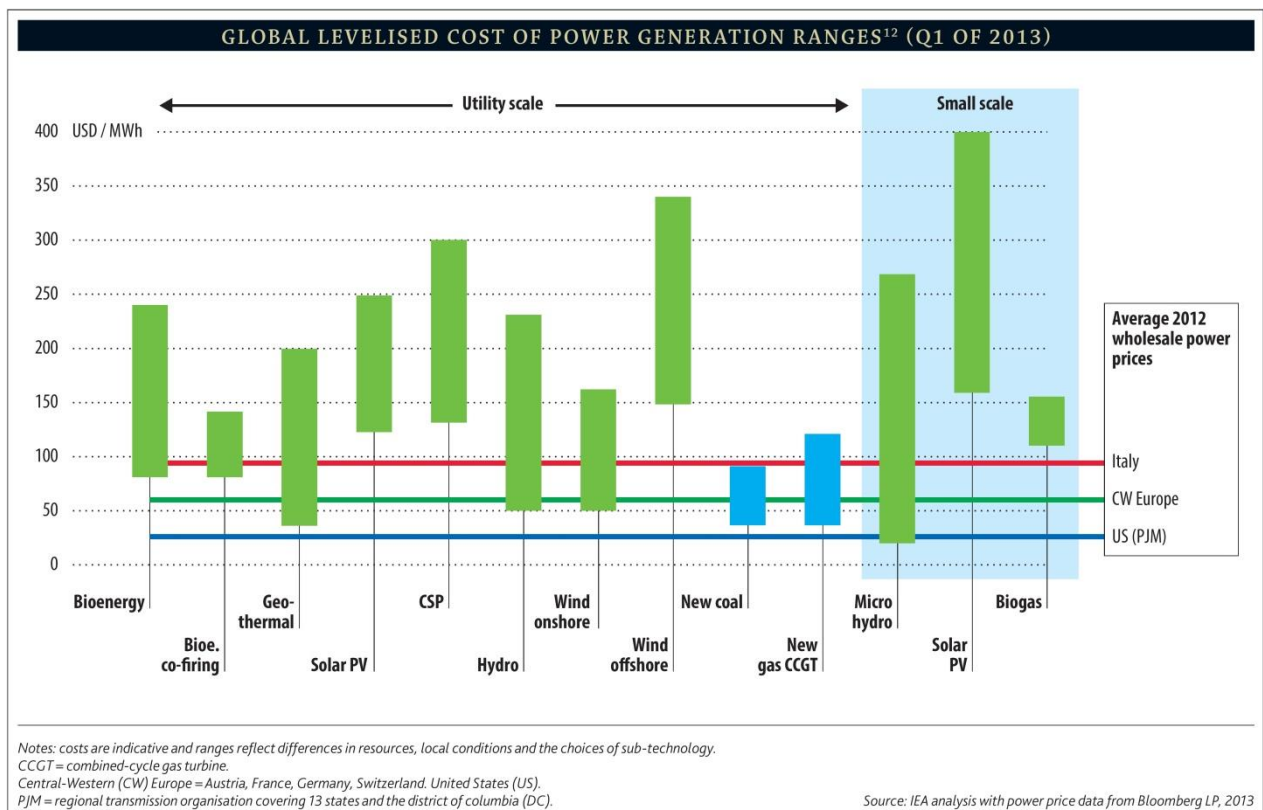


Figure 1.1: LCoE range of various energy sources [15]

New installations in wind power capacity in 2012 amounted to 45 GW followed by another 35 GW in 2013, totalling at 318 GW globally, as of today (Figure 1.2). For Europe, total capacity today is at

121.4 GW. The growth for 2012 was 13 GW and dropped slightly to 12 GW for 2013. The 14% of these 12 GW was offshore installations, a record-high yearly performance. Nonetheless, given the recent economic slowdown in Europe and uncertainty in policy-making for 2030 targets, these growth rates can be considered on-track.

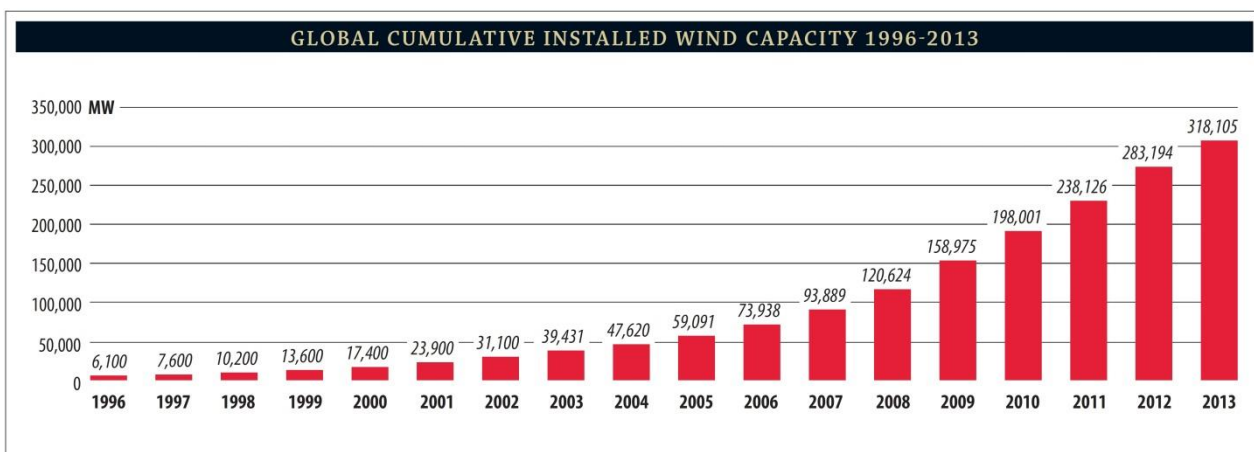
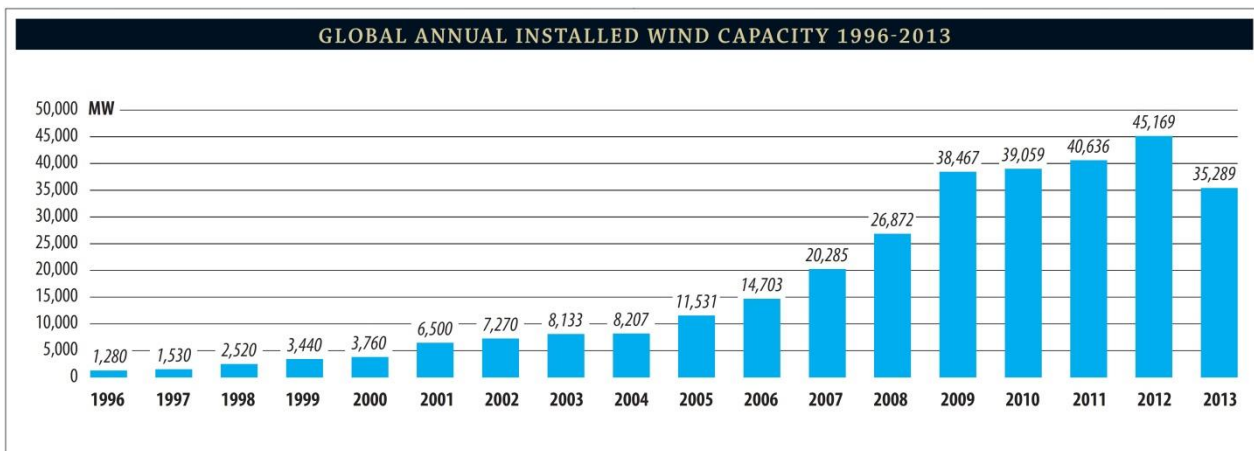
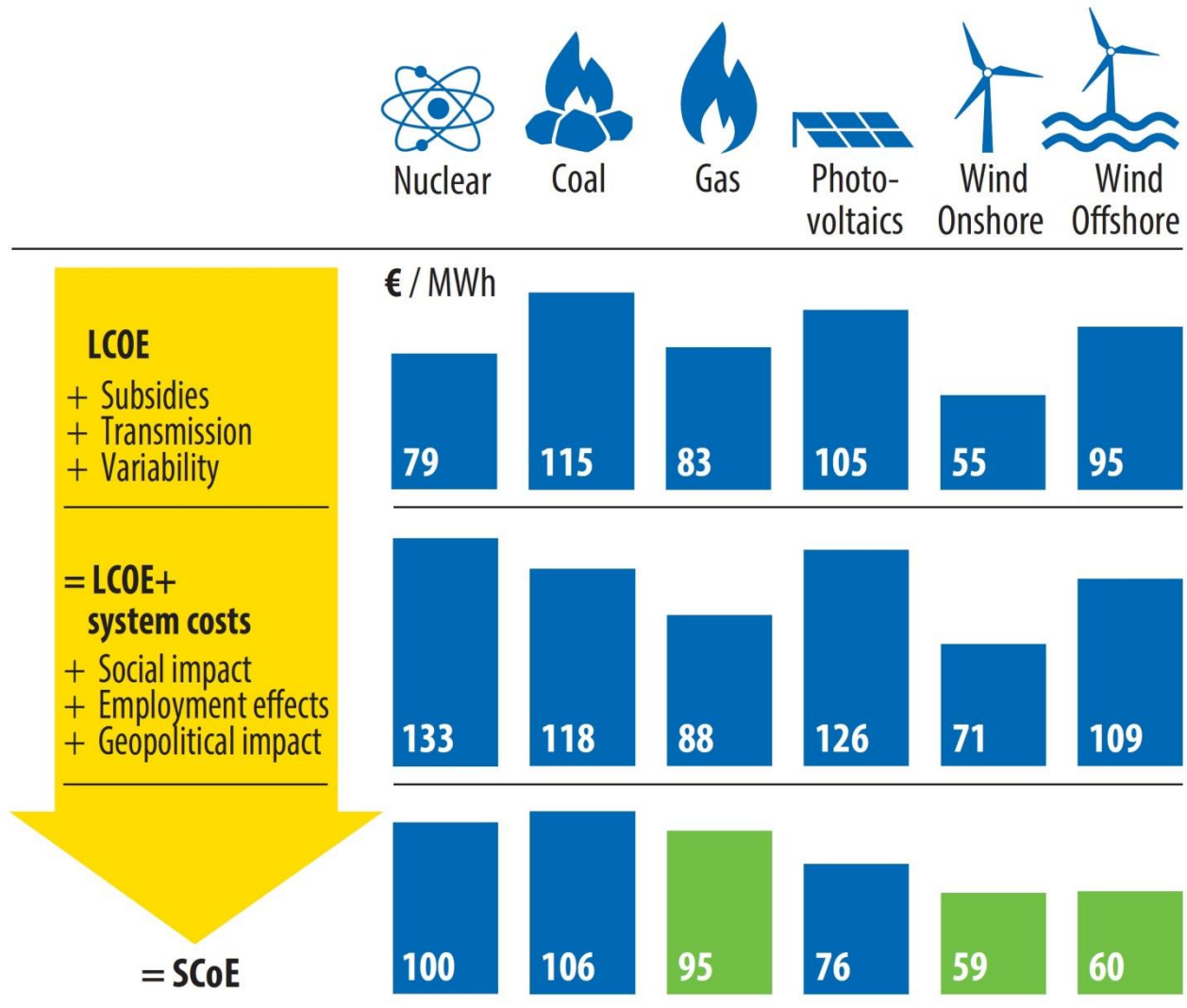


Figure 1.2: New annual installations (upper) and cumulative capacity (lower) globally 1996 - 2013 [15]

One of the main drivers for wind energy research is the reduction of LCoE (Levelised Cost of Electricity) to provide a genuinely cheap energy source, independent from subsidies. For this purpose, there is an argument by Siemens Wind about moving from the widely accepted term of LCoE to the “Expanded LCoE (LCoE+)” and furthermore to the “Society’s Cost of Electricity (SCoE)”. This serves as a more inclusive method for a realistic cost-benefit analysis of conventional (fossil fuel etc.) and renewable energy sources (Figure 1.3). This model would also consider grid access and expansion costs, production variability costs, social impacts (e.g. long-term health costs and large water consumption avoidance), economic impacts (e.g. job creation) and geopolitical impacts (e.g. fuel price volatilities, political instability and power-plays) for conventional energy sources and renewables. This method would reflect a further reduction in the cost of wind power as seen in Figure 1.3.



When judged according to the social cost of electricity (SCoE) concept, wind onshore and wind offshore will be the most competitive power sources in the UK by 2025; gas fired power plants remain the most competitive back up technology.

Figure 1.3: LCoE, LCoE+ and SCoE of various energy sources according to the projections of Siemens Wind while including the additional costs [15]

Furthermore, ECOFYS very recently conducted a study ordered by the European Commission [1] trying to evaluate government interventions (i.e. subsidies, tax cuts etc.) and negative environmental externalities for the energy market of the EU28 member-states, excluding the transportation market. In some of the graphs of the interim report (Figure 1.4 and Figure 1.5), it is shown that although certain technologies are quite cheap in terms of LCoE, their secondary impacts on the environment and health give rise to disproportional social costs.

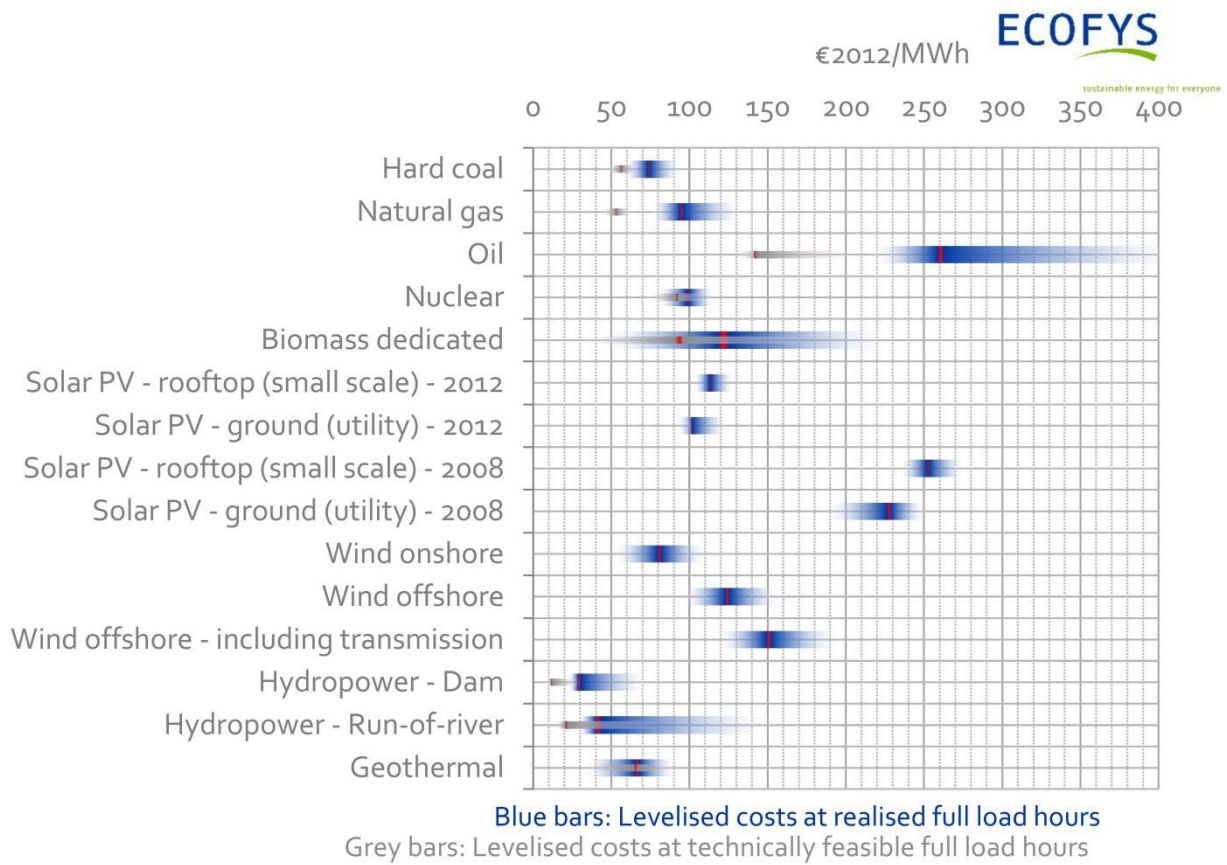


Figure 3-15: Levelised cost of electricity in the EU28 for various technologies in the EU28. The blue bars indicate the levelised cost at full load hours estimated from energy production and capacity statistics and the grey bars indicate levelised cost at technically feasible full load hours. The red vertical lines represent the median of the range.

Figure 1.4: LCoE of different energy sources [1]

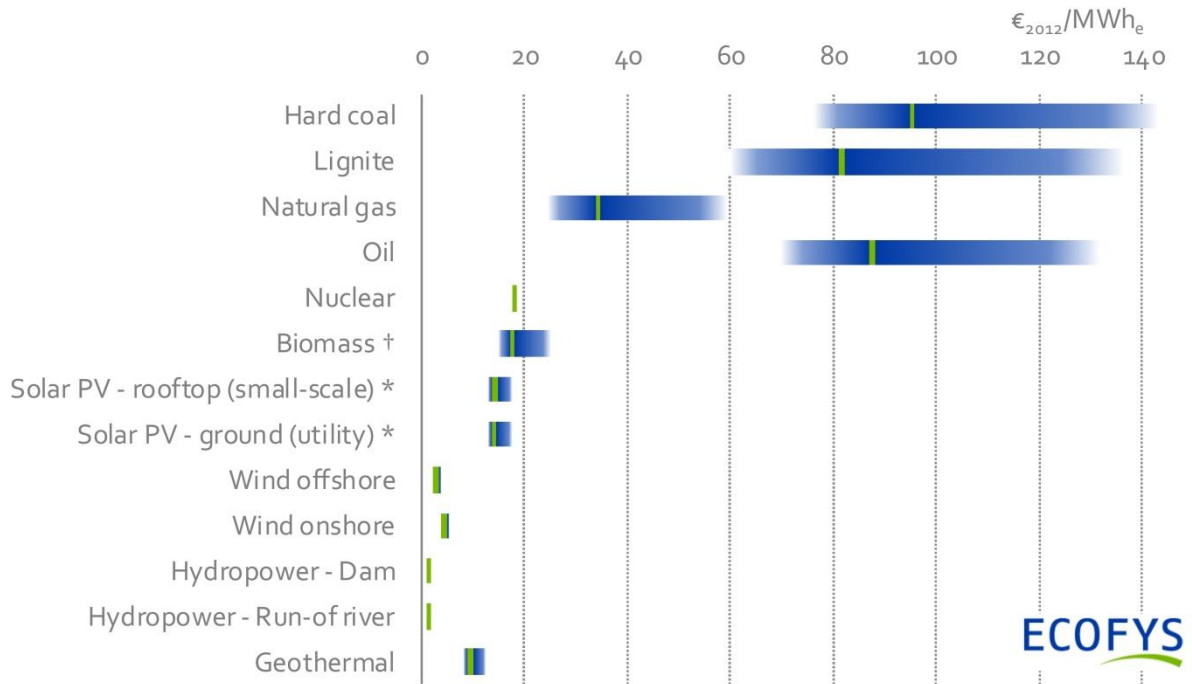


Figure 3-14: Total external costs of electricity technologies following from the sensitivity analysis of monetary values for climate change for (EU28 average) (in €₂₀₁₂/MWh_e). The blue bars indicate the range of external costs found in the sensitivity analysis; the green line indicates the results for the central assumption of 50 €₂₀₁₂/tCO_{2e}.

Figure 1.5: External costs of different energy sources [1]

Both of the claims by Siemens Wind and ECOFYS are presented merely as a reflection on the complexity of how to accurately determine the price of renewables. That is especially the case when trying to include and quantify social or environmental costs, and their direct interaction with policy-making. Although the data used were collected from realised projects, plants and markets of the EU28, there are certain assumptions and estimations employed in these reports.

1.2 Wind Turbine Costs

It is useful to obtain a more detailed view on how the costs of an individual wind turbine are broken down. The desired cost savings are put into context as the designs proposed in the next chapters concern mainly the blades. The wind turbine used as a baseline model in this report is the INNWIND 10 MW reference wind turbine (henceforth referred to as “RWT” for brevity).

Table 1.1: The sub-component masses and costs part of the INNWIND cost model[#]

%	COMPONENT	SF	Mass (kg)	Cost (\$2002)	Cost (€2012)
21.33%	ROTOR		249,973	2,316,360	2,140,821
13.39%	<i>Blades</i>		125,148	1,624,080	1,343,803
4.41%	<i>Hub</i>	2.30	88,766	377,254	442,987
3.35%	<i>Pitch mechanism</i>	2.30	33,287	299,584	335,897
0.18%	<i>Nose cone</i>		2,773	15,443	18,134
44.98%	DRIVE TRAIN & NACELLE		337,675	3,993,393	4,514,748
2.91%	<i>Low speed shaft</i>	3.00	76,962	230,885	292,104
3.48%	<i>Main bearing</i>		18,203	320,375	349,500

10.83%	Gearbox		90,604	956,782	1,087,252
0.16%	Mechanical brake & couplings	3.00	2,828	19,894	15,975
7.05%	Generator		48,787	657,593	707,411
8.17%	Power electronics			790,000	819,924
0.90%	Bed plate		32,162	76,562	89,903
1.18%	Hydraulic & cooling system		800	120,000	118,182
0.88%	Nacelle cover	2.00	26,000	104,000	88,715
5.72%	Electrical connections			400,000	574,394
3.70%	Yaw system		41,329	317,303	371,389
0.54%	CONTROL, SAFETY SYSTEM, CM			55,000	54,167
22.82%	TOWER	2.00	694,920	1,737,300	2,290,077
10.33%	MARINIZATION			1,086,352	1,036,973
100%	Cost of WT Components		1,282,568	9,188,405	10,036,785
	WT price			12,863,767	14,051,500
56.03%	Foundation system		1,920,000	8,766,277	9,496,800
9.52%	Offshore transportation			1,500,000	1,613,636
1.28%	Port and staging equipment			200,000	216,667
9.59%	Offshore turbine installation			1,500,000	1,625,000
20.07%	Offshore electrical I&C			2,600,000	3,401,667
0.00%	Offshore permits & engineering				0
0.00%	Personnel access equipment				0
3.52%	Scour protection			550,000	595,833
0.00%	Decommissioning				0
100%	Balance of Plant (BoP)		1,920,000	15,116,277	16,949,603
	CAPEX			27,980,044	31,001,103

(#NOTE: Many of the mass and cost values reported in the table above, are the original ones from the INNWIND cost model and do not reflect the precise values used for the calculations made further in this report.)

Table 1.1 is part of the INNWIND cost model (Deliverable 1.2.2 [10] and 1.2.3 [9]) for the 10 MW reference wind turbine. It estimates costs at the sub-system level by scaling other known or realised mass and cost models. It also employs a method for cost projections, taking into account the Producer Price Index (PPI) to reflect economy changes as per NREL's 2006 report [12].

The function of the cost model shall be discussed in more detail in the next chapters. It is worth noting that the model focuses mainly on the initial Capital Expenditure (CAPEX), the Balance of Plant (BoP) costs of an offshore wind farm and a large part of the Operation & Maintenance costs (OPEX). Some costs such as permits, personnel offshore access and decommissioning are not taken into account. The cost of each component derives mainly from its mass, which in turn is usually calculated either by diameter or rated power related scaling laws.

It can be seen in Table 1.1 and Figure 1.6 that the blades represent about 13.4% of the total cost of a wind turbine and a 5% when one also considers the offshore foundation, grid connection and other costs. Larger rotors can increase the energy production, but combined with an effort to keep the material costs low (i.e. blade mass), a further LCoE reduction can be expected.

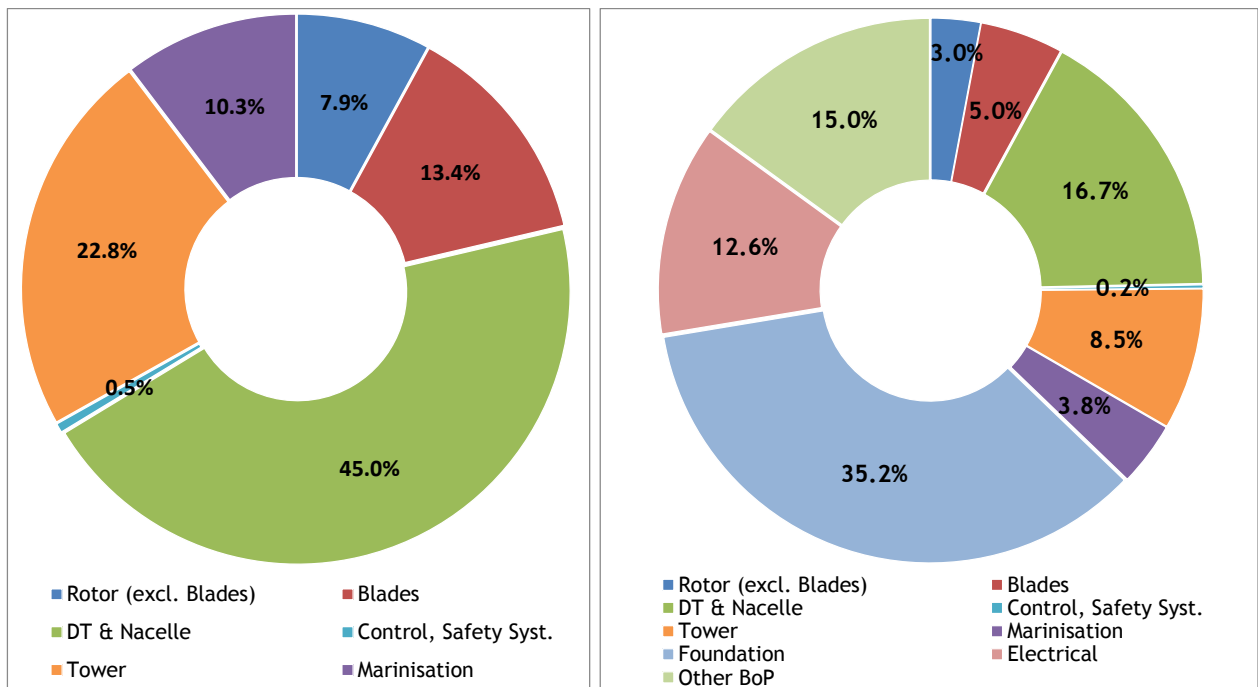


Figure 1.6: Break-down of basic components costs of a wind turbine (left); idem including foundation, grid connection, transportation, installation and other BoP costs. (right)

Similar conclusions can be drawn by NREL’s Cost of Energy Review in 2013 [16]. The rotor cost is the 15% of an onshore installation (22.06% of the turbine) and the 4.8% of an offshore installation as seen in Figure 1.7.

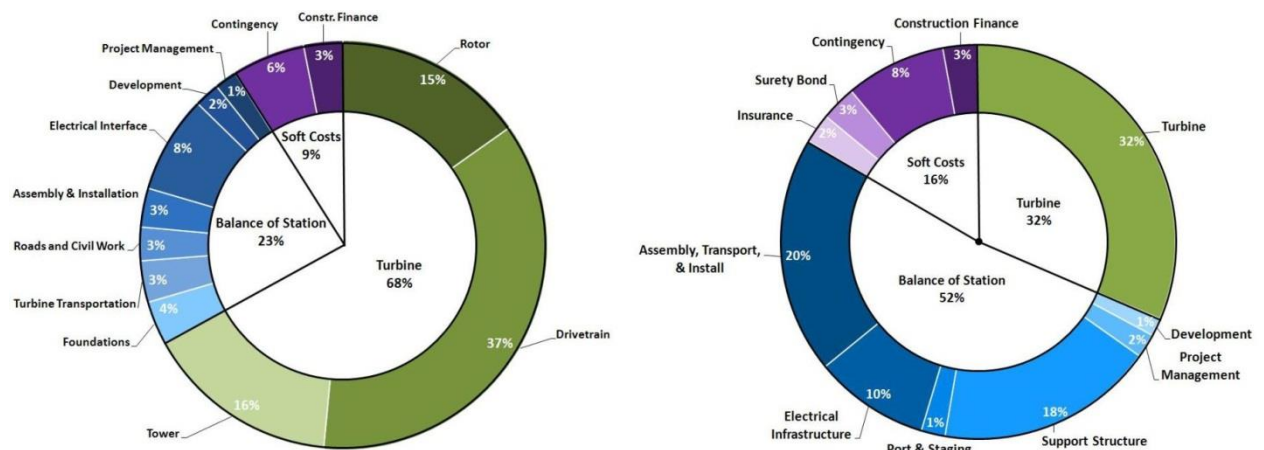


Figure 1.7: Break-down of costs for basic components and services for onshore (left) and offshore (right) installations [16]

1.3 Mass and Loads Up-scaling Laws

Following the trend in research and innovations, along with realised designs and farm projects, the turbine sizes are growing in rotor diameter, tower and hub height, and of course rated power. Especially in near future offshore wind farms, already developed machines of 5 and 6 MW are likely

to be used. The prototypes and innovations now being designed or tested may range from 7 up to 20 MW with rotor diameters of up to 250 m. It is therefore evident that loads and masses of components rise in proportion and sometimes even exponentially. The increase in size reaches for higher and more stable winds offshore and leads to larger energy yields. In an interim report of the UpWind project [40], the authors state that up-scaling will “*certainly*” lead to cost reductions.

Up-scaling laws are very useful tools in the conceptual phase of the design and can lead to converging iterations of greater detail. They mostly connect the rotor diameter, rated power and component masses of the initial and final designs.

The first classical up-scaling laws employed uniform geometrical up-scaling and assumed similar materials used and similar aerodynamic behaviour through a constant power coefficient C_p . For example, if one wants to double the rated power P_R of a wind turbine from P_1 to P_2 (assume a scaling factor s , with $s^2 = 2$), it follows, from the power equation (1.1), that the rotor diameter (or radius R) should be increased by a scaling factor of $s = \sqrt{2}$. Air density is given by ρ and V_R is the rated wind speed, at which rated power is reached.

$$P_R = C_p \frac{1}{2} \rho \pi R^2 V_R^3 \quad (1.1)$$

$$P_2 = s^2 P_1 \Rightarrow C_p \frac{1}{2} \rho \pi R_2^2 V_R^3 = s^2 C_p \frac{1}{2} \rho \pi R_1^2 V_R^3 \Rightarrow \quad (1.2)$$

$$R_2^2 = s^2 R_1^2 \Rightarrow R_2 = s R_1$$

Through material volume and constant density, the blade and other component masses would be scaled by a factor of s^3 , for all 3 dimensions. Following the same rationale and set of rules, aerodynamic forces are scaled by s^2 as they are connected to the rotor swept area. The bending moments are scaled by s^3 because an extra power from the distances is included. The bending stiffnesses (or area moments of inertia) are scaled by s^4 . Assuming aerodynamic similarity, the aerodynamic stresses are scale-independent, in contrast with those due to weight forces that increase by a factor s .

However, changes in boundary layer effects on the blades, the wind shear effect on a larger rotor area and material non-linearities imply that classical up-scaling laws fail to approach underlying technical issues with detail [40]. Furthermore as stated in the UpWind report [45], since the energy yield increases with the s^2 trend of the diameter and mass with s^3 , this disconnect could produce a limitation in ever-going up-scaling, calling for material and structural innovation.

In his PhD thesis [2], Ashuri reviewed linear scaling laws and data-based scaling trends and identified the accuracy deficiencies of linear scaling laws and their differences with realised trends. This happens mainly due to technological advancements in aerodynamics, manufacturing and design optimisations. He developed an intricate up-scaling method based on a multi-disciplinary optimisation technique using design loads and aeroelastic stability analysis criteria. With this method, he modified the design of the NREL 5 MW wind turbine [20] and up-scaled it to 10 and 20 MW. The blades were seen as one of the most material- and cost-intensive components in the up-scaling process, along with the tower, low speed shaft, yaw system and main bearing [2].

In the current thesis, an in-between up-scaling approach is proposed. Firstly, it must be noted that the up-scaling is done only with respect to rotor diameter and blade geometry modifications, while rated power and hub height remain constant. Increased energy yield is expected from this modification while the trade-off with the added blade mass is anticipated to be on the beneficial side. Secondly, the up-scaling is done in a much smaller extrapolation range so a section-by-section approach on the blade can be used efficiently. Finally, due to the modified details of the proposed

concepts, simple linear laws are not applicable. The main concept behind the up-scaling process is the following: “Having detailed distributed geometric and structural properties for a base-line (reference) wind turbine model and the detailed distributed geometrical properties for the proposed design concepts, use primary BEM and loads analyses of the reference and proposed concepts to project and calculate the distributed structural properties of the new concepts in a detailed element-by-element manner.”

1.4 Wind Farm Aspects of Low Power Density Rotors

The minimisation of LCoE and loads on wind turbines and maximisation of energy production should not only concern stand-alone performance but collective results in wind farms as well as stated in the report of Ceyhan and Grasso [7]. A recent trend, seen in Figure 1.8 and Figure 1.9, shows that power density keeps dropping in large offshore machines, meaning that rotor diameters increase more than rated power compared with past designs. The main feature of the proposed designs in this thesis, is an increase in rotor diameter from 89.166 m to 103 m, while keeping the rated power constant at 10 MW.

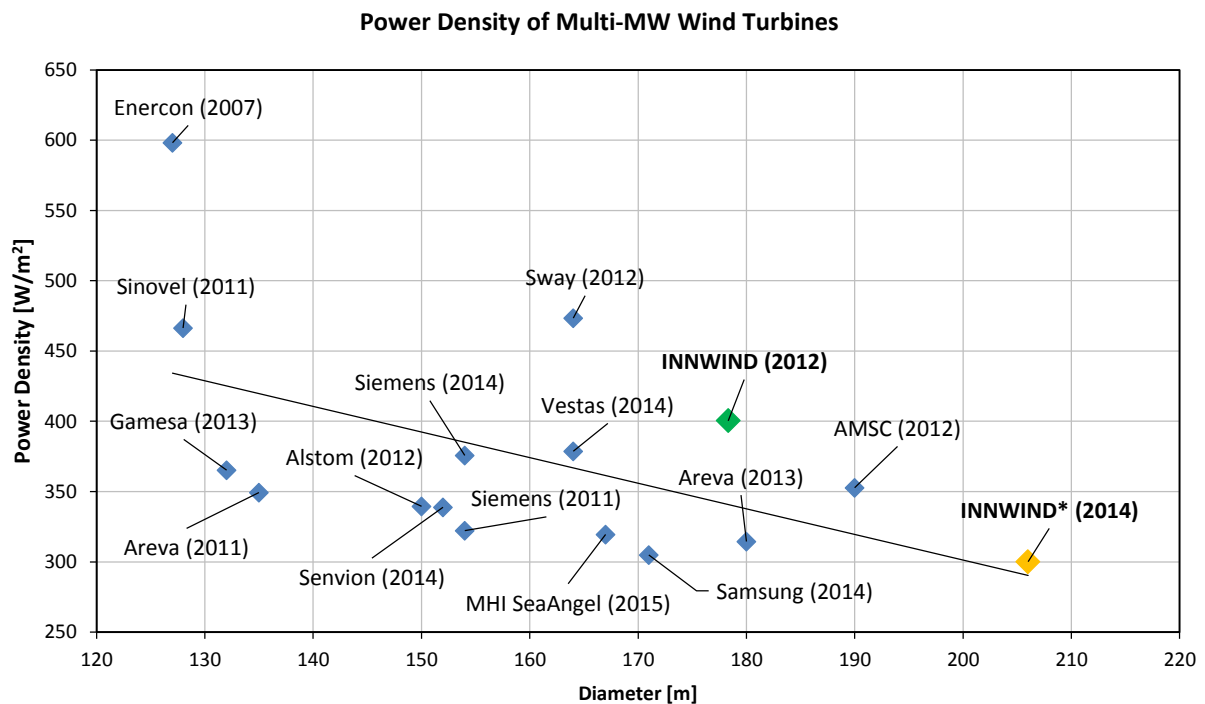


Figure 1.8: Power density of several wind turbines (data taken from manufacturers' websites and online brochures)

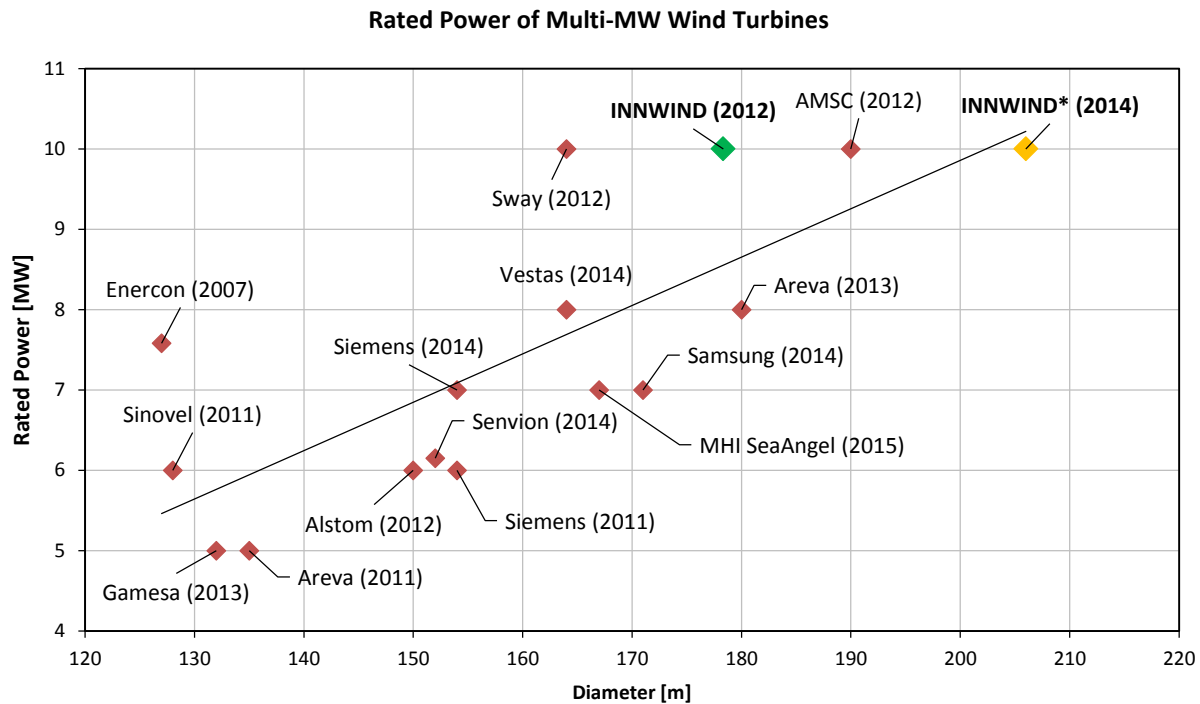


Figure 1.9: Rated power of several wind turbines (data taken from manufacturers' websites and online brochures)

The proposed concepts include modifications to geometric properties, such as the aerodynamic twist and chord distributions, the solidity of the rotor (more slender blades) and some of the operational parameters such as optimal tip speed ratio (TSR, λ), rated rotor speed and peak-shaving pitch strategy. There are six new designs, totalling to seven with the base-line model. Their main goal is to either maintain the optimal aerodynamic performance and increase energy yield while increased loads are expected or, for the sub-optimal concepts, to maintain the same loads on the blades by decreasing aerodynamic performance and expect a smaller increase in energy output.

ECN's BOT software (Blade Optimisation Tool) was previously used to analyse the individual performance of the wind turbines at a conceptual design level. BOT is a BEM-based code coupled with an optimisation tool and calculates rotor performance and energy production for a given Weibull distribution. The Farmflow software was used for the farm-level calculations. Farmflow is based on a parabolised Navier-Stokes equations solver coupled with an actuator disc method and includes turbulence and near and far wake effects. It is considered accurate enough and relatively fast for energy production estimations [7]. The results from these analyses are used as a starting-point input for the current report and some of them are given in Table 1.2.

The analysis in [7], on the turbine level, is done with a steady-state approach. Dynamic and structural behaviour is excluded altogether from the tool. On the farm level, it is done on the Horns Rev wind farm model by replacing the 80 m diameter original rotors with the INNWIND 10 MW Reference Wind Turbine (RWT) and the other concepts in order to investigate energy production results. Although the hub height of the RWT is at 119 m, wind data measurements taken between 2000 and 2004 at 62 m are not corrected. This is done so as to exclude additional energy yield due to higher average wind speeds. Analysis is done both for absolute distance between turbines kept constant (2.7D of RWT) and diameter-relative distance kept constant (7D, resulting in a larger farm area).

Hereafter, for the sake of brevity, the 10 MW Reference Wind Turbine will be referred to as "RWT", the pure Upscale concept as "UPS", the Low Solidity concept as "LSO", the Higher Tip Speed Ratio

(Lambda) as “HLA”, the Higher RPM (Rotor Speed) as “HRS”, the Upscale with Peak Shaving as “UPK” and the Higher RPM with Peak Shaving as “HRK”.

Table 1.2: Summarised results reported in [7]

Level	Parameter	RWT	UPS	LSO	HLA	HRS	UPK	HRK
WT	Theoret. Max. C_p [-]	0.480	0.480	0.440	0.498	0.494	0.480	0.494
WT	Rated Wind Speed [m/s]	11.5	10.5	11.0	10.5	10.5	11.0	11.5
WT	Max. Thrust Change [%]	-	+10.7	-17.0	+11.4	+11.1	-17.0	-11.7
WT	AEP Change [%]	-	+10.8	+5.2	+11.2	+11.4	+8.0	+9.9
WF 2.7D	AEP Change [%]	-	+10.78	+10.5	+11.2	+11.39	+11.52	+11.6
WF 2.7D	Farm Efficiency [%]	71.98	71.84	75.67	71.97	72.09	74.42	73.15
WF 7D	AEP Change [%]	-	+13.25	+9.64	+13.56	+13.64	+11.37	+12.9
WF 7D	Farm Efficiency [%]	85.83	87.57	89.54	87.64	87.71	88.62	88.24

A similar conclusion is reached by Chaviaropoulos et al. in [8], where “less-loaded” wind turbines in the stand-alone and wind-farm level show potential benefits. The first iteration seeks to maximise energy production by maximising the power coefficient. This results in a higher tip speed ratio of 8.85, and lower rotor solidity. The constraint applied is not to exceed the original aerodynamic blade root bending moment. The optimisation result is an increased rotor radius of 13.6% with an induction factor of 0.187 (far from the Betz theoretical optimum of 0.33) and a power increase of 8.7%. Considering an almost linear blade weight and cost scaling, quantifying the LCoE yields a final increase of 4.6%.

The benefits, namely a drop in LCoE, come from the second iteration in the report and in two parts. Firstly, from the increased rotor radius at the stand-alone level. The prolongation of the blade is optimised versus the minimisation of LCoE, instead of solely the power output or energy production. The axial induction factor a , is considered variable again and the constraint of not increasing the original aerodynamic bending moment is applied as well. It must be noted, that the tip speed is also variable, and actually increases without hesitation since the analysis is considered for an offshore application and noise emissions are not a constraint. The result now yields an optimal induction factor of 0.274, a rotor radius increase of 3.9%, a power increase of 5.5% and an LCoE drop of 1.6%.

A second part of LCoE reduction comes from a significant reduction in wake losses in the farm level. The authors consider a 500 MW wind farm with a 10x10 layout and 8D spacing (based on the diameter of the initial wind turbine rotor). The wind farm average capacity factor increases by 3%, with an average reduction of the wake losses by 2.5%. Another conclusion is that, with turbine spacing ranging from 5D to 8D, the accumulated 6% energy production increase is almost constant. As a final conclusion, the added weight (and subsequently cost) to the rotor design produces larger benefits in terms of energy production and LCoE than the actual cost of the design, when one considers that the rotor is the 5% of the total costs as seen in Figure 1.6 and Figure 1.7.

1.5 Purpose, Objective, Structure

The results reported in Table 1.2 above show a certain potential in the increase of energy production and load reduction in some cases. Having produced an overall image of wind energy nowadays, and a more detailed view on the innovations proposed for the INNWIND reference wind turbine, it is long

due to present the end goal of this thesis, its objectives and the structure of the way these will be pursued.

The purpose of this thesis is to investigate the performance and feasibility of the concepts proposed, in greater detail. Both through a technical and a basic economic aspect. The analysis of Ceyhan and Grasso [7] does not contain any structural modelling or dynamic behaviour at the individual wind turbine level, hence further analysis is useful.

The detailed results of the steady state analysis will be used to construct a coherent structural model in order to produce the necessary input data files for the PHATAS aeroelastic code. An ad-hoc, on-demand scaling technic is employed, that uses the structural details of the INNWIND machine and is somewhat similar to the rules mentioned in Section 1.3. The steady state loads are used to calculate the new distributed properties of the blades, based on certain assumptions.

After the new models are created, the first simulations concern the steady state aerodynamic performance. They are run for the un-deformed rotors and produce the C_p - λ and C_T - λ curves for a range of pitch angles. Along with the necessary structural properties, these curves are used to modify the original controller and also produce the new rotor speed vs. torque curves for the generator. The controller modifications are done by ECN's personnel.

The second step in calculations is the modal analysis of the blades and rotors. They are run in order to acquire the eigen-frequencies and mode shapes at rotor speeds ranging from 0 rpm to the predicted rated rotor speed of each concept. This is done as a secondary measure to evaluate the sanity of the structural models, obtain the aerodynamic damping ratios and quasi steady-state deformations. They can also provide insight on what to expect from load case time simulations. Frequency versus wind speed diagrams are produced and apparent intersections with nP frequencies are investigated. The term " nP " refers to multiples of one-per-rotor-revolution frequencies.

The third step in simulations is part of an already reduced design load case (DLC) list, also used in the AVATAR project. The simulations parameters comply with the descriptions in the IEC 61400-1 3rd Ed. standard [20]. These load cases are important for large offshore wind turbines and most probably indicate design drivers for the blades or other components. This claim comes through field experience from General Electric.

- ▲ Power production for Normal and Extreme Turbulence Models (DLC 1.2 and 1.3)
- ▲ Power production with faults and shut-down for Normal Turbulence Model (DLC 2.1)
- ▲ Normal shut-down for Normal Wind Profile (DLC 4.1)
- ▲ Parked (Idling) for Extreme 1-year Wind Model (DLC 6.3)

A reduced load case list is considered, because the certification of the rotor concepts, as per the IEC or GL standards, is outside the scope of this thesis. Additionally, the changes made only on the blades and rotor do not reflect a fully optimised design. Moreover, the computational time and the amount of data to be processed will increase disproportionately to the extra information acquired.

The results for the proposed designs will be compared and evaluated in a manner suitable for large offshore blades. The final criterion will be the LCoE calculation, through the INNWIND cost model that gives the wind farm's LCoE. The cost model inputs will be modified according to the new designs and estimations will be made on the component mass/cost that need re-evaluation. Of course, an energy production increase is expected due to the longer blades, but the increased material costs might hinder this positive effect.

2

THEORY

2.1 Short Description of the Reference Model and the Proposed Designs

2.1.1 The INNWIND 10 MW RWT

The INNWIND project is the successor of the UpWind project. As a part of UpWind, the 5 MW reference machine was up-scaled, through extrapolation, to 10 and 20 MW conceptual designs (see Table 2.1). This was done in order to explore design limitations in multi-megawatt machines that seem more likely to fulfil the European Commission's targets for 20% electricity generation from renewables by 2020 and 33% by 2030 [45]. Manufacturing, transportation and material issues are reported especially in the 20 MW case, but innovations also emerge through scientific and technological integration between the different Work Packages.

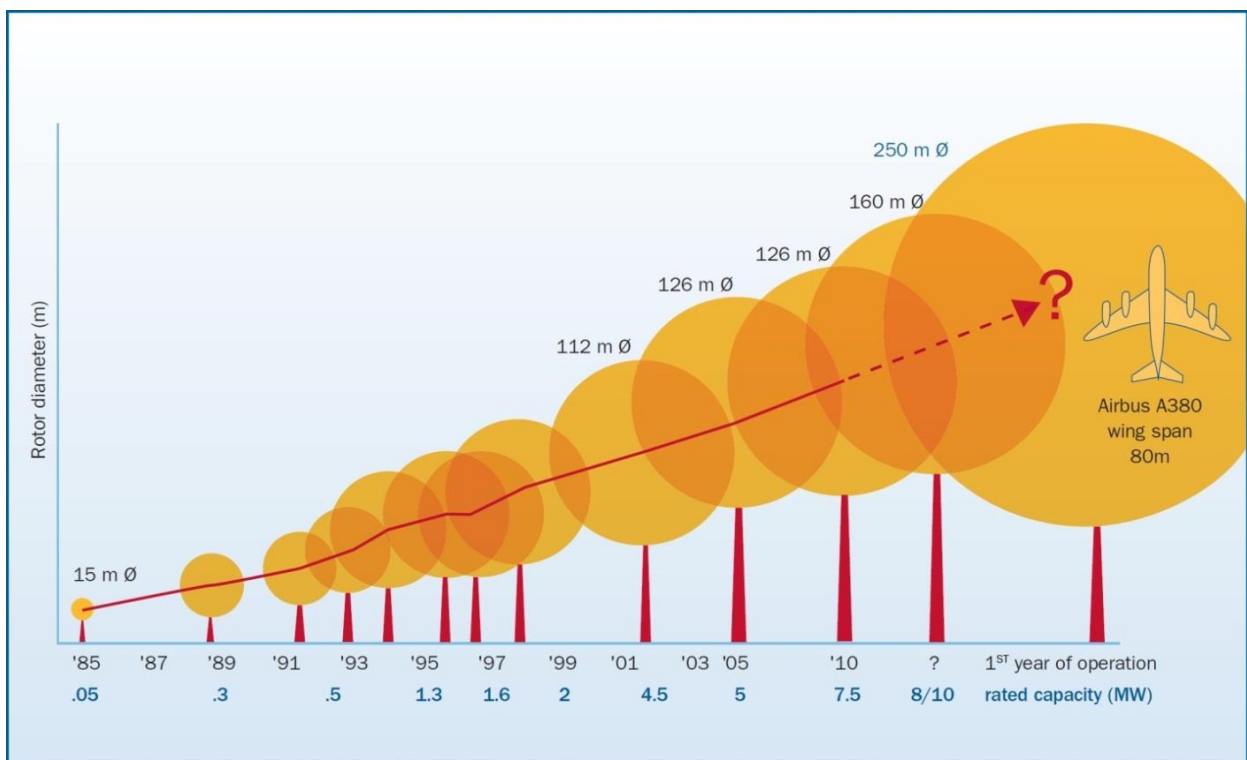


Figure 2.1: The up-scaling trend of wind energy state-of-the-art since 1985 [45]

In the effort to follow the up-scaling trend seen in Figure 2.1, the INNWIND project capitalises on the potential of these results and looks into the detailed design of a beyond-state-of-the-art 10 MW reference wind turbine. Many of the general specifications are close to the initial 10 MW concept of UpWind.

Table 2.1: Main parameters of the UpWind and INNWIND Wind Turbines

	UpWind / NREL Reference WT 5 MW	UpWind Extrapolated WT 10 MW	UpWind Extrap. Virtual WT 20 MW	INNWIND Reference WT 10 MW
Rated Power [MW]	5	10	20	10
Wind Regime (IEC Class)	1B	1B	1B	1A
No of Blades	3	3	3	3
Rotor Orientation	Upwind	Upwind	Upwind	Upwind
Control	Variable speed, control pitch	Variable speed, control pitch	Variable speed, control pitch	Variable speed, control pitch
Rotor Diameter [m]	126	178	252	178.3
Hub Height [m]	90	116	153	119
Max. Rotor Speed [rpm]	12	9	6	9.6
Rotor Mass [tn]	122	305	770	230.7
Tower Top Mass [tn]	320	760	880	676.7 [#]
Tower Mass [tn]	347	983	2,780	628.4
Power Density [W/m ²]	401	401.86	401	400.5

(#NOTE: The tower top mass of the INNWIND 10 MW RWT contains nacelle mass, mass of the blades and hub mass.)

As stated in Bak et al. 2012 [4], for the 2nd iteration of the INNWIND reference blade and rotor design, linear up-scaling does indeed produce a challenge, because the weight of the blade scales with a cubic trend (s^3) and there is a need for improvement through new materials. A multi-disciplinary system approach is chosen, so that both the aerodynamic forces and aeroelastic behaviour produce a sound structural design, keeping the blade mass low and stiffness high. For this reason, the FFA-W3-xxx aerofoil family is used, mainly because of its high relative thicknesses and its availability in the public domain.

The main driver behind this up-scaling approach is the modification of both the relative aerofoil thicknesses and the thicknesses of inner load-carrying elements to increase stiffness. The NREL 5 MW machine [20] is the reference for up-scaling in terms of power density that gives the rotor diameter. The mass is estimated based also on other novel or recently realised designs. The rest of the turbine follows classical similarity rules as described in [40]. The results described in [4] concern iteration #2 and are not the same as the final INNWIND rotor design used in this report.

2.1.2 The Proposed Designs and Basic Expectations

As stated above, the main driver for the proposed design innovations is the increase of energy output, in the wind farm level, with the ultimate objective being the reduction of the LCoE. This is done by lowering the power density of the rotor from 400 W/m² to 300 W/m² through an increase in rotor diameter to 103 m (by 15.5%) in order to achieve a relative reduction of loads on the blades (see Table 2.2). The proposed designs focus mainly on modifying the geometric blade properties. Other

blade parameters and performance characteristics - such as rated rotor speed and tip speed - change as well. This helps to obtain different conceptual design configurations and evaluate their interaction with the operation of the rest of the wind turbine and farm.

However, most of the other properties of the rest of the wind turbine structure and configuration stay the same in order to acquire an even and consistent parametrical analysis. In brief, rated power, cut-in and cut-out wind speeds, cut-in rotor speed, hub height, tower, nacelle and hub masses and gearbox ratio remain constant as in the initial reference design.

▲ *Upscale (UPS)*

The first concept under consideration is a pure up-scale in rotor diameter and absolute chord lengths, while keeping twist distribution, relative thickness and rated power constant. The shape of the chord distribution also remains constant. As expected and seen in the results, the qualitative aerodynamic performance remains unchanged, namely the C_p - λ curve.

The increase of rotor radius and swept area ($A = \pi R^2$) results in a higher energy production. Subsequently, the rated wind speed also drops as equation (1.1) implies. In turn, the rotor thrust T and flap-wise bending moments M_y increase, as shown in equations (2.1) and (2.2) [32]. C_T is the thrust coefficient and depends on the induction factor a and B is the number of blades.

$$T_{max} = C_T \frac{1}{2} \rho \pi R^2 V_R^2 \quad (2.1)$$

$$M_y = \frac{T}{B} \frac{2}{3} R \quad (2.2)$$

This implies a higher required bending stiffness EI and mass for obtaining a similar structural behaviour. The combination of keeping rated power and tip speed ratio constant, with an increase in rotor radius, results in a higher rated torque Q_R , a drop in the rated rotor speed Ω and a rise in the edge-wise bending moments M_x , without considering the added mass at this point. C_Q is the torque coefficient and is connected with tip speed ratio λ and C_p .

$$C_Q = \frac{C_p}{\lambda} \quad (2.3)$$

$$Q_R = C_Q \frac{1}{2} \rho \pi R^3 V_R^2 \quad (2.4)$$

$$M_x = \frac{Q}{B} \quad (2.5)$$

Changes in the maximum values of the aforementioned loads and their fluctuations is part of the analysis that is sought through the design load case simulations. However, since the geometry and mass of the blade change, the eigen-frequencies of the rotor and blades are bound to change. Their interaction with the rotational frequencies and harmonics (nP frequencies) is subject to investigation as well. As a crude approximation, through Euler's bending theory in equation (2.6) and the linear scaling laws, one can predict that the natural frequencies will scale by a factor of s^{-1} . For example, for the 1st natural frequency ω_n , with L being the length of an arbitrary rod and m_d its mass distribution:

$$\omega_n = \frac{3.515}{L^2} \sqrt{\frac{EI}{m_d}} \quad (2.6)^\#$$

$$\omega_n^* = \frac{3.515}{(sL)^2} \sqrt{\frac{s^4 EI}{s^2 m_d}} \Rightarrow \omega_n^* = \frac{3.515}{s^2 L^2} \sqrt{\frac{s^2 EI}{m_d}} \Rightarrow \omega_n^* = \frac{3.515s}{s^2 L^2} \sqrt{\frac{EI}{m_d}} \Rightarrow \omega_n^* = \frac{1}{s} \omega_n$$

(#NOTE: Total blade mass m scales with s^3 in the linear laws, while mass per unit length m_d scales with s^2 .)

▲ **Low Solidity (LSO)**

An in-between approach is that of the Low Solidity concept, where the rotor diameter increases also by the same amount. The flap-wise bending moment and thrust are sought to remain in the same levels of the RWT. This is done in order to take advantage of an energy output increase from the larger rotor area, while trying to keep the mass increase of the blade at a low level. This is accomplished by employing a higher twist distribution. The chord distribution is interpolated between the initial inboard values of the RWT to the outboard values of the UPS.

The higher blade twist results in a lower C_p in the partial load region, hence the design is characterised as sub-optimal. Some power is shed on the turbine level in order for the thrust and flap-wise bending moment to remain the same. However, farm efficiency is increased (as seen in Table 1.2) because of the lower induction factor and the reduced wake losses. The edge-wise moment is also expected to increase because of the larger rotor area and mass as per equations (2.3), (2.4) and (2.5), but less than in the up-scale design, as the maximum C_p drops. By keeping the tip speed and tip speed ratio the same, the rotor speed drops as in the UPS.

▲ **Higher Lambda (HLA)**

A similar design with the LSO is that of the Higher Lambda. The chord distribution is almost identical (see Figure 2.2). As the design description suggests, tip speed is slightly increased to 90.6 m/s and the tip speed ratio is chosen to be 8.66 close to the aerodynamic optimum for 3-bladed wind turbines. Rated power is reached at a rotor speed of 8.4 rpm. The reduced chord (in comparison with the UPS), helps to keep the local normal force distribution similar, as it would increase with the faster rotation and higher local wind speeds [7]. The twist, on the other hand, follows the trend of the reference machine and of the UPS. Hence, there is no power shed in the partial load region, achieving a high C_p . The bending moments are expected to increase, along with the required stiffness and mass.

▲ **Higher RPM (HRS)**

An even further increase of the tip speed ratio at 9.6, bringing the rotor speed back to the RWT levels (at 9.4 rpm), is employed in this concept. Due to the higher local wind speeds on the blade elements, the chord distribution is decreased even more, so that load distributions are kept unaffected with respect to radius increase, as mentioned above.

▲ **Upscale with Peak Shaving (UPK)**

This concept seeks to combine the geometry and operation of the LSO and the UPS. Chord distribution is identical to that of the UPS but the twist has an offset of about $+3.5^\circ$. The normal forces on the blade are sought to decrease so that the larger blade length would keep the flap-wise bending moments in the RWT levels. A peak-shaving strategy in blade pitch is used, starting at around 9 m/s wind speed, to aid in the maximum load reduction.

▲ **Higher RPM with Peak Shaving (HRK)**

Similarly, this design's operational and geometrical properties are identical to the HRS, with the peak-shaving starting from 9 m/s wind speed, so that the maximum flap-wise bending moment decreases to RWT levels. Because of that, here and also in the UPK concept, the mass of the blade

is expected to be smaller than their no-peak-shaving counterparts. However, the slender blades may pose aeroelastic challenges because of their thin shape and relatively low mass and stiffness.

It was desired in the beginning of the analysis not to have any tilt angle, cone angle and pre-bend for all the rotor designs. The latter two were indeed not present for the first calculations but the tilt angle of 5° was kept as described in the INNWIND RWT. This was done mainly because of problems with the early steady state simulations in PHATAS that gave bad numerical convergence. In terms of actual design it was also assumed necessary, as the shaft tilting has a large contribution into the tower-tip clearance; about 7.77 m for the RWT and 8.98 m for all other designs. The cone angle and pre-bend were also removed from the RWT in the first aerodynamic simulations and in the modal analysis for a consistent approach. However, the first time-domain load case simulations indicated that the forward cone angle of -2.5° had to be reinstated, because of numerous numerical convergence issues and suggested blade-tower hits.

Table 2.2: Main parameters of the proposed designs [7]

Parameter \ Concept	RWT	UPS	LSO	HLA	HRS	UPK	HRK
Rated Elec. Power [MW]	10	10	10	10	10	10	10
Tip Speed [m/s]	89.6	89.6	89.6	103.6	113.5	89.6	113.5
Optimal Lambda [-]	7.5	7.5	7.5	8.66	9.5	7.5	9.5
Rat. Rotor Sp. [rpm]	9.6	8.31	8.31	9.6	10.53	8.31	10.53
Rotor Radius [m]	89.166	103	103	103	103	103	103
Chord at BR [m]	5.38	6.21	5.38	5.25	4.56	6.21	4.56
Max. Chord [m]	6.20	7.16	6.18	6.05	5.25	7.16	5.25
Power Density [W/m^2]	400.36	300.04	300.04	300.04	300.04	300.04	300.04

BOT was used to optimise the detailed design of the proposed concepts as well as to obtain steady state performance and loads. These results are also used in the structural up-scaling process described in section 3.2. Table 2.3 contains only a strip of these results for a specific wind speed where maximum loads (flap-wise blade root bending moment and most often thrust) occur.

Table 2.3: BOT software output at the maximum-load operating point

	WSP [m/s]	P_{mech} [MW]	θ_p [$^\circ$]	λ [-]	Ω [rpm]	C_p [-]	C_T [-]	F_{ax} [kN]	M_{y-BR} [MNm]
RWT	11.0	9.77	0.12	7.50	8.84	0.480	0.809	1,498	28.5
UPS	10.0	9.80	0.10	7.50	6.95	0.480	0.810	1,653	36.3
LSO	11.0	10.64	1.83	7.50	7.65	0.392	0.509	1,257	26.6
HLA	10.0	10.16	1.00	8.66	8.03	0.498	0.820	1,674	37.1
HRS	10.0	10.09	0.80	9.60	8.90	0.494	0.822	1,678	37.5
UPK	11.0	10.93	2.50	7.16	7.30	0.402	0.537	1,326	28.3
HRK	10.5	9.74	4.45	9.60	9.35	0.412	0.571	1,284	28.5

Where: WSP = wind speed

P_{mech} = mechanical/shaft power (excluding electrical/generator losses)

θ_p = pitch angle

Ω = rotor speed

F_{ax} = rotor thrust (T)

$M_{y\text{-BR}}$ = flap-wise bending moment at blade root

During the control modification phase, it was noticed in the BOT results, that rated power in most of the concepts was reached at different conditions (lower rpm and tip speed) and further rotational acceleration was deemed unnecessary. This conclusion can also be drawn from a closer look at Table 2.3. Some of the BOT calculations were re-run with TSR values being kept the same. That would not significantly alter the structural modelling procedure and its results, as the used values came from slightly below-rated conditions shown in Table 2.3. The corrected values are given below in Table 2.4 (in **bold**). Further in the report, after the controller implementation, it shall be seen that the UPS and LSO rpm and tip speed were also corrected.

Table 2.4: Corrected parameters of the proposed designs

Parameter \ Concept	RWT	UPS	LSO	HLA	HRS	UPK	HRK
Tip Speed [m/s]	89.6	89.6	89.6	90.6	101.4	78.7	101.4
Optimal Lambda [-]	7.5	7.5	7.5	8.66	9.6	7.5	9.6
Rat. Rotor Sp. [rpm]	9.6	8.31	8.31	8.4	9.4	7.3	9.4

The distributed geometric properties of the designs are presented in the figures below.

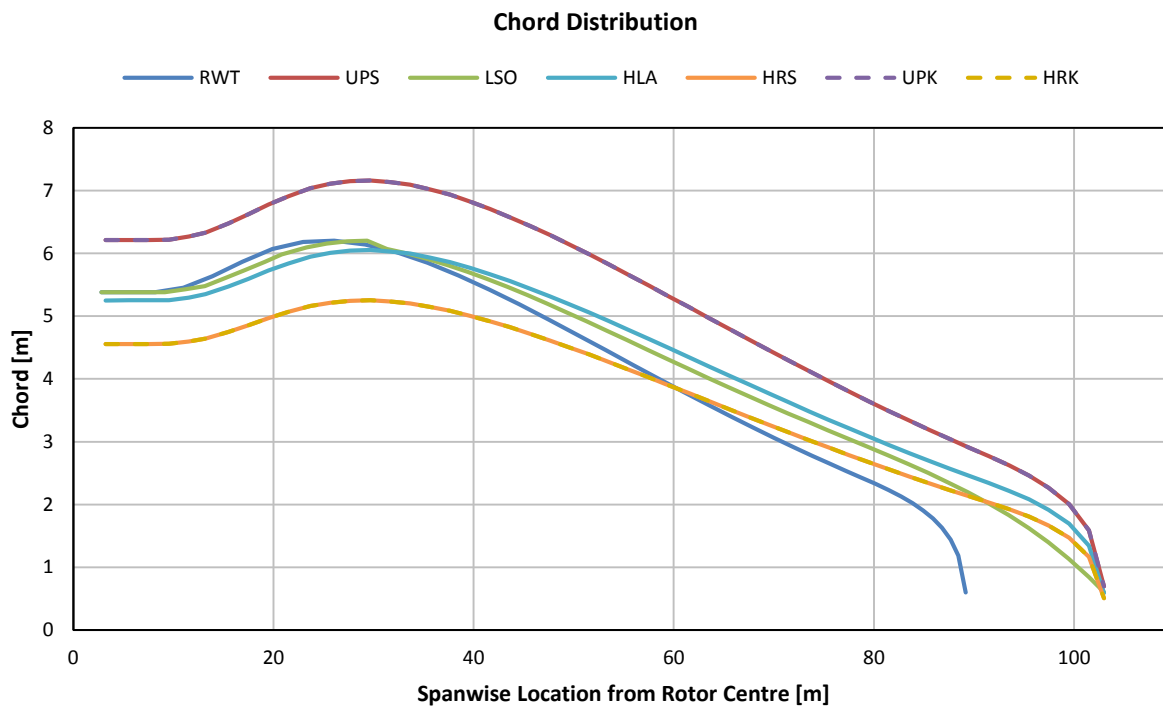


Figure 2.2: The chord distribution of the designs in comparison

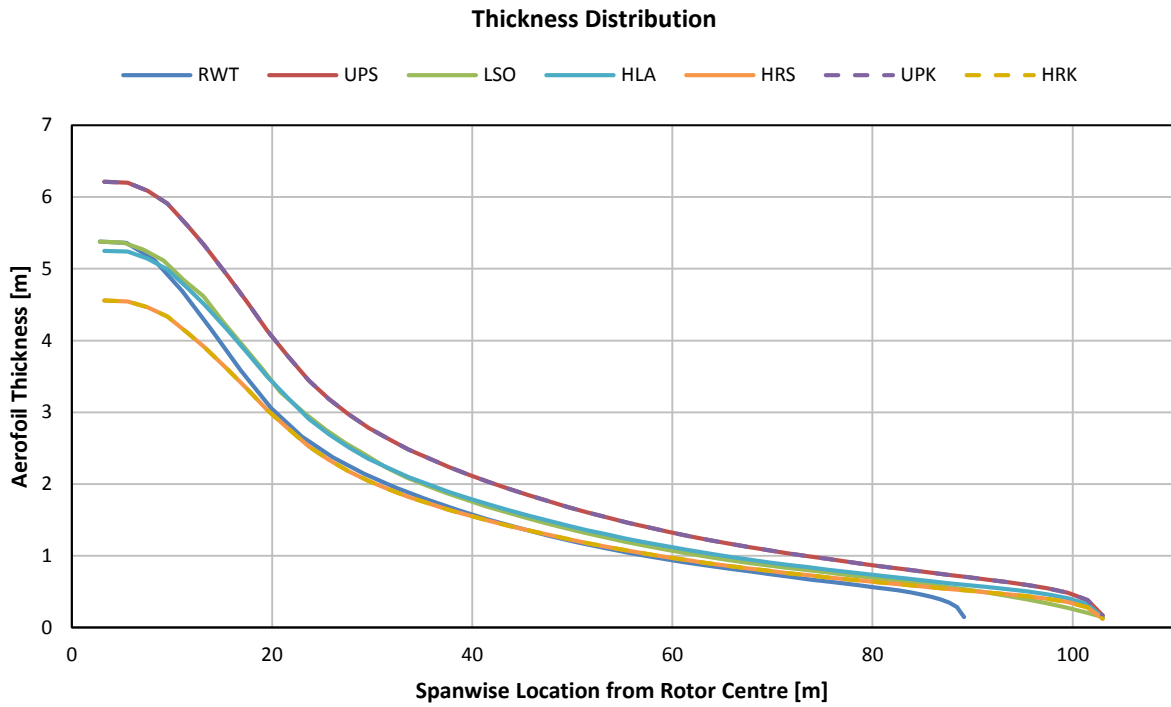


Figure 2.3: The aerofoil thickness distribution of the designs in comparison

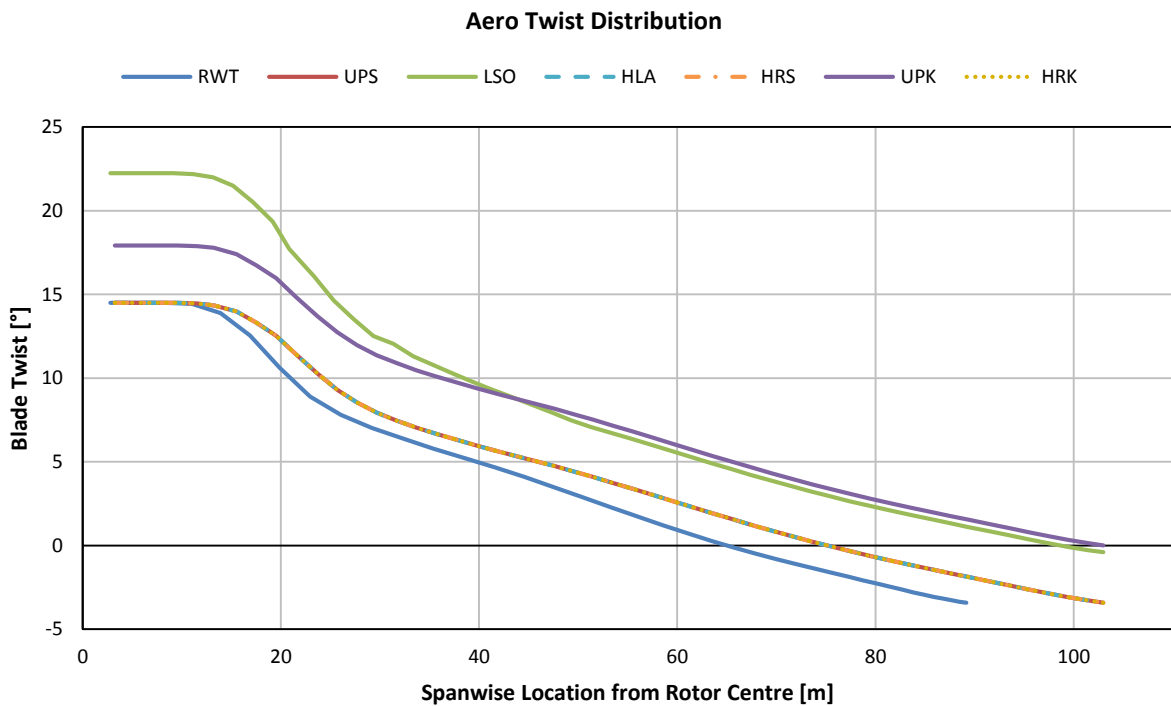


Figure 2.4: The blade twist distribution of the designs in comparison

The same FFA aerofoil family is also used, with a distribution and scheduling corresponding to the prolonged blade length (see Table 2.5).

Table 2.5: The Aerofoil Distribution along the blade span, after the blade root/hub radius

	RWT [m]	UPS, HLA, HRS, UPK, HRK [m]	LSO [m]
AF3D_CYLINDER	0.0	0.0	0.0
AF3D_FFA-W3-600	9.686	11.189	11.624
AF3D_FFA-W3-480	15.956	18.431	18.866
AF3D_FFA-W3-360	20.739	23.956	24.391
AF3D_FFA-W3-301	28.623	33.064	33.499
AF3D_FFA-W3-241	40.806	47.137	47.571
Blade Root Radius	2.8	3.234	2.8
Blade Span	86.366	99.766	100.2
Rotor Radius	89.166	103.0	103.0

The new span-wise positions were calculated with the following relation (2.7), where (*) indicates the new values, z the span-wise locations after the blade root, r_{BR} the blade root radius and R_{TOT} the rotor radius. For the case of the Low Solidity, the first z -location was manually set to 0.0 m instead of 0.4344 m that is derived.

$$z_{af}^* = \frac{z_{af,RWT} + r_{BR,RWT}}{R_{TOT,RWT}} R_{TOT}^* - r_{BR}^* \quad (2.7)$$

2.2 Performance Indicators and the Reduced List of Design Load Cases

In the INNWIND interim Deliverable 1.2.2 [10], the authors refer to the EU's SETIS-TPWind 2011 report [38] to define the Performance Indicators (PI) that are used in the INNWIND Project to assess innovative designs and a cost baseline. The Levelised Cost of Electricity, defined as the “overarching” Key Performance Indicator, connects the energy production within a given wind farm, the cost of services and the cost of components based on their masses to reach a final €/MWh indication. It is useful to concisely review this work in order to better understand the logic behind the formulation of the cost model used in this report.

The estimation excludes permitting costs, external grid connection costs, financial costs, overheads and decommissioning costs. It concludes to a value of 106.93 €/MWh and the feasibility of a 20% reduction by 2020 via up-scaling is evaluated. The reference case concerns a 300 MW farm with 5 MW wind turbines. In its first approach, the study states that, through European Wind Industrial Initiative partners (EWII) quotes and other studies, the total costs can be roughly split as follows. Turbine CAPEX 30%, BoP CAPEX 39% and OPEX 31%. The rotor amounts to 6.9% of the total costs and is accounted for in the Turbine CAPEX of course, while the tower/foundation system that is accounted for in the BoP costs, amounts to 17% of the total costs. Hence, a significant increase in energy production from an innovative rotor (although more expensive) mounted on the same tower/foundation system can be beneficial to an LCoE reduction.

The authors continue by “up-scaling” this cost model both in wind turbine size (namely rated power) and by employing innovation within an estimated learning curve in order to derive cost-over-weight proportional relations. So, the exponents of linear factors used in the classical up-scaling laws are somewhat reduced (e.g. rotor mass scales with 2.5 instead of 3). They also pursue a primary

sensitivity analysis of how these exponent reductions affect PIs such as rotor, nacelle, tower and foundation masses (Figure 2.5). The reduction of maximum design thrust appears as the most promising due to its indirect effect on most of the sub-components.

REF TURBINE (EWEA 5 MW)					UPSCALED TURBINE					
Capacity (MW)		5,00		Subcomponent costs (M€)	Turbine Upscaling Exponent 2,42	Capacity (MW)		10		
Turbine Cost (M€/MW)		1,500				Turbine Cost (M€/MW)		1,742		
Turbine Only					Turbine Only					
Rotor	Rotor lock	0,0000	0,2357	1,00	0,000	2,50	Rotor	Rotor lock	0,0000	
	Blades	0,2220			1,965	2,30	Blades	0,2121	0,2276	
	Hub	0,0137			0,103	2,80	Hub	0,0156		
	Nacelle systems					Nacelle systems				
	Gearbox	0,1291	0,2979		0,968	2,60	Gearbox	0,1368	0,3014	
	Generator	0,0703			0,527	2,00	Generator	0,0605		
	Rotor brake	0,0132			0,099	2,50	Rotor brake	0,0135		
	Nacelle cover	0,0135			0,101	2,50	Nacelle cover	0,0138		
	Nacelle structure	0,0280			0,210	2,50	Nacelle structure	0,0287		
	Couplings	0,0000			0,000	2,50	Couplings	0,0000		
	Shaft	0,0191			0,143	2,70	Shaft	0,0210		
	Yaw system	0,0125			0,094	2,70	Yaw system	0,0137		
	Bearings	0,0122			0,092	2,70	Bearings	0,0134		
Electrics & control					Electrics & control					
Pitch system	0,0266	0,0767		0,200	2,30	Pitch system	0,0254	0,0688		
Variable speed system	0,0501			0,376	2,00	Variable speed system	0,0431			
Tower					Tower					
	0,2630	0,2630		1,973	2,50		0,2693	0,2693		
Other					Other					
	0,1300	0,1300		0,975	2,50		0,1331	0,1331		
					7,528					
BoP Cost (M€/MW)					BoP Cost (M€/MW)					
2,000				Subcategory costs (M€)	BoP Upscaling Exponent 1,50	1,684				
BoP Only					BoP Only					
Foundation system		0,4400		1,00	4,400	Foundation system		0,4394		
Offshore transportation and installation		0,3000			3,000	Offshore transportation and installation		0,2519		
Offshore electrical I&C		0,2600			2,600	Offshore electrical I&C		0,3087		
					10,000					
					17,422					
					1,684					
					7,400					
					4,243					
					5,200					
					16,843					

Figure 2.5: The turbine CAPEX and BoP for the reference and up-scaled version in [10]

It is concluded that, as the water depth offshore increases, there are benefits from larger machines. That is due to the reduction of the BoP costs per MW and by assuming successful design innovations that will lower the mass exponents of the scaling laws.

On a more detailed and relevant view, the immediate subsequent of the INNWIND Deliverable 1.2.2, Deliverable 1.2.3 [9], tries to define a minimum set of DLCs needed for innovation assessment at a structural level with a 3-stage approach. The feasibility of some innovations, whether on the blades, drive-train or tower, might appear as impossible or unfavourable from early stages in the design and analysis. Hence only two or three DLCs should be run at Stage 1 to rule out the worst candidates; especially when considering a broad spectrum of concepts. The concepts can either be dropped from further analysis or re-modelled for success.

As per the nomenclature of DLCs from the IEC 61400 standards for offshore wind turbines [22], the recommended DLCs of Stage 1 are:

- ▲ DLC 1.3 and DLC 2.1 for Blade innovations
- ▲ DLC 2.3 and DLC2 .2 for Drive-train innovations
- ▲ DLC 1.1, DLC 1.2 and DLC 6.1 for Offshore Support Structures

If Stage 1 analysis is successful and before the full load set/certification of Stage 3 is run, the following DLCs are proposed. DLC 2.2 (for single blade pitch seizure), DLC 1.4, DLC 2.1 (for collective pitch runaway), DLC 6.2 (for large yaw errors), DLC 1.3, DLC 2.3, DLC 4.2 and DLC 8.2. The authors recommend that few wind seeds for primary fatigue assessments should be sufficient. That is because the extreme loads are growing more than fatigue loads in multi-MW machines and are likely to be the design drivers. Also, tower-tip clearance due to the length of the blades, rotor-lock cases during maintenance due to offshore conditions and yaw moments due to the larger tower-top mass are subject to investigation.

However, in this report DLC 1.3 and 2.1 are chosen in order to comply with INNWIND's proposals and a few others for a broader investigation. DLC 1.2 and 4.1 are fatigue related and are expected to give an estimation of lifetime 1Hz damage-equivalent loads (1HzDEqL) and accumulated damage according to Miner's rule. They refer to normal production and normal stops respectively for the 25 year lifetime of the wind turbine. More importantly, DLC 1.2 will produce a more accurate estimate on the energy production through extrapolation, which will be used in the final LCoE calculation. DLC 1.3 is also very important as it is expected to produce the extreme loads on the blades and even blade-tower hits if the blade is insufficiently stiff. DLC 2.1 is run so that faults and emergency shut-downs are simulated as extreme cases. Finally, DLC 6.3 is expected to indicate the extreme loads especially for the tower since the turbine is out of operation.

2.3 The Cost Model

2.3.1 Description

Since in [38] and [10], the overarching key performance indicator defined is the LCoE, a binary quest arises. Firstly, the LCoE of the reference and innovative designs must be formulated in sufficient detail and at a sub-component level in order to reflect the contribution of individual parts. Ergo, cost-modelling is made through cost-over-weight laws, different for each part, which are also influenced by the indirect interactions (e.g. through loads). Secondly, since the mass of each component seems to be the main cost-penalty factor, the modelling of the rotor concepts that is described in Section 3.2, must reflect in a realistic manner the changes made in the design through the blade mass parameter.

So in order to build these cost/mass relations, the performance indicators (rated power, rotor diameter, hub height, rated torque etc.) should be taken into account making the model flexible to alterations, depending also on operating conditions. The relations are built mainly from NREL's 2006 report [12], the UpWind report [45] and Ashuri's relations [2], combined with the work done in the relevant INNWIND deliverable [10] assuming some progress within a technological learning curve.

Furthermore, an interesting financial and macro-economic feature of this cost model is that its relations are based on \$2002 currency, following the findings in [12]. These prices are transformed to \$2012 by taking into account Producer Price Indices (PPIs) and then to €2012 via an average \$/€ 2012 exchange rate. In brief, PPIs reflect changes in the economy, such as GDP and raw material prices within groups of industries. In this report, there will be no analysis or alteration on these factors, because such financial details or the precise value of LCoE are not the objective; it is used only as a comparative criterion. Additionally, the plausibility of LCoE is of no great concern because the changes we inflict from the blade design alterations are not to a very large extent, such as doubling the rated power.

Finally, lack of data led the authors to include some of the offshore-related costs, such as transportation, installation etc., by assuming proportionality with the rated power.

2.3.2 Implementation

The three basic equations giving the current (i.e. for year 2012) cost of a component are the following:

$$Mass_{sub}(s) = Mass_{sub}(1) \cdot s^{\lambda_{mass}} \quad (2.8)$$

$$Cost_{sub}^{\$2002}(s) = Mass_{sub}(s) \cdot Cost_{pum}^{\$2002} \quad (2.9)$$

$$Cost_{sub}^{\$2012}(s) = Cost_{sub}^{\$2002} \cdot (1 + PPI_{sub}^{2012} - PPI_{sub}^{2002}) \cdot (\text{€} / \$)^{2012} \quad (2.10)$$

As stated above, there will be no analysis or alterations on equation (2.10) and its values. However, the first two relations should be presented in more detail. In right-hand side of equation (2.8), the sub-component $Mass_{sub}(1)$ refers to an UpWind RWT 5 MW sub-component mass. The scaling factor s refers to the diameter or power scaling factor, and λ_{mass} refers to the scaling exponent. In the right-hand side of equation (2.9), $Mass_{sub}(s)$ refers to the up-scaled sub-component mass either through an up-scaling law produced from UpWind [45] or NREL [12] or taken straight from the INNWIND wind turbine data. Lastly, $Cost_{pum}(s)$ refers to the \$2002 cost per-unit-mass or cost per-unit-power.

The costs below are referring to \$2002, except where otherwise noted. Factor s_p is equal to the square root of 2; 10 MW divided by 5 MW. The first terms in the parentheses usually represent the component mass and the second term the cost per-unit-mass (\$2002/kg) or per-unit-power (\$2002/kW). Some assumptions on cost per-unit-mass were made in the cost model but were not further investigated as they did not represent a significant part of the total turbine costs.

▲ Rotor

$$[12], [2] : \quad Cost_{bld} = 13.084 \cdot Mass_{bld} - 4452.2 \quad (2.11)$$

$$[45], [19], [12] : \quad Cost_{hub} = (40,000 \cdot s_p^{1.79}) \cdot (4.25) \quad (2.12)$$

$$[45], [19], (\text{assum.}) : \quad Cost_{pitch.mech} = (15,000 \cdot s_p^{1.79}) \cdot (9) \quad (2.13)$$

$$[12] : \quad Cost_{nose.cone} = (18.5 \cdot D - 520.5) \cdot (5.57) \quad (2.14)$$

In equation (2.11), the blade mass is either the one of the RWT or one of the proposed designs calculated from the up-scaling process. In equations (2.12) and (2.13), the original value of the s_p exponent was 2.30, but it was changed to 1.79 so that the 3 masses (hub, pitch mechanism and nose cone) summed up to the given RWT hub mass of 105,520 kg. It's also interesting to report that in the WindPACT study [41], the hub mass is given by $m=0.24 \cdot D^{2.5765}$, which would yield 151,527 kg.

▲ Drive-train and Nacelle

$$[45], (\text{assum.}) : \quad Cost_{LSS} = (27,210 \cdot s_p^{3.15}) \cdot (3) \quad (2.15)$$

$$[12] : \quad Cost_{main.bear} = (2 \cdot 0.0092 \cdot (0.0133 \cdot D - 0.033) \cdot D^{2.65}) \cdot (17.6) \quad (2.16)$$

$$[37] : \quad Cost_{GB} = (65\% \cdot 13.25 \cdot Q) \cdot (12) \quad (2.17)^{\#}$$

$$[45], [12] : \quad Mass_{mech.br.coupl} = (1,000 \cdot s_p^{3.15}) \quad \& \quad Cost_{mech.br.coupl} = (1.9894 \cdot P - 0.1141) \quad (2.18)$$

$$[37] : \quad Cost_{gen} = (35\% \cdot 13.25 \cdot Q) \cdot (14.5) \quad (2.19)^{\#}$$

$$[12] : \quad Cost_{pow.elec} = (P) \cdot (79) \quad (2.20)$$

$$[12] : \quad Mass_{bed.pl} = (1.295 \cdot D^{2.1}) \quad \& \quad Cost_{bed.pl} = (303.96 \cdot D^{1.2}) \quad (2.21)$$

$$[12] : \quad Mass_{hydr.cool} = (P) \cdot (0.08) \quad \& \quad Cost_{hydr.cool} = (P) \cdot (12) \quad (2.22)$$

$$[45], (\text{assum.}) : \quad \text{Cost}_{nac.cvr} = (13,000 \cdot s_p^{2.15}) \cdot (4) \quad (2.23)$$

$$[2] : \quad \text{Cost}_{elec.com} = (P) \cdot (40) \quad (2.24)$$

$$[12] : \quad \text{Mass}_{yaw} = (1.6 \cdot 0.0009 \cdot D^{3.45}) \quad \& \quad \text{Cost}_{yaw} = (2 \cdot 0.0339 \cdot D^{3.1}) \quad (2.25)$$

(#NOTE: These costs refer to €2012 and the PPI differences are applied inversely.)

All the exponents in the Drive-train and Nacelle section above, whether referring to the power or diameter, were increased by 0.15 so that the masses summed up to the nacelle mass given by the 10 MW RWT data.

^ Controls, Tower, Marinisation, BoP (Foundation etc.)

$$[2] : \quad \text{Cost}_{contr} = 55,000 \quad (2.26)$$

$$[45], [19], [12] (\text{adj.}) : \quad \text{Cost}_{tow} = (347,460 \cdot s_p^{1.71}) \cdot (2.5) \quad (2.27)$$

$$[12] : \quad \text{Cost}_{marin} = (\text{Cost}_{ROT+TOW+DT/NAC}) \cdot (13.5\%) \quad (2.28)$$

$$[19] : \quad \text{Cost}_{fnd.tr.pc} = (330,000) \cdot (5) \quad (2.29)^{\#}$$

$$[19] : \quad \text{Cost}_{fnd.jack} = (1,210,000) \cdot (4.8) \quad (2.30)^{\#}$$

$$[19] : \quad \text{Cost}_{fnd.piles} = (380,000) \cdot (1.2) \quad (2.31)^{\#}$$

$$[12] (\text{adj.}) : \quad \text{Cost}_{offs.trans} = (P) \cdot (150) \quad (2.32)$$

$$[12] : \quad \text{Cost}_{port.equip} = (P) \cdot (20) \quad (2.33)$$

$$[12] : \quad \text{Cost}_{offs.inst} = (P) \cdot (150) \quad (2.34)$$

$$[12] : \quad \text{Cost}_{offs.elec} = (P) \cdot (260) \quad (2.35)$$

$$[12] : \quad \text{Cost}_{scour} = (P) \cdot (55) \quad (2.36)$$

Where: $\text{Cost}_{ROT+TOW+DT/NAC}$ = Sum of component costs (Rotor + Tower + Drive-train & Nacelle)

(#NOTE: These costs refer to €2012 and the PPI differences are applied inversely. Additionally, the total costs of the foundation are multiplied with a factor of 1.2 to calculate the final price.)

In equation (2.27), the \$/kg value in [12] is reported at 1.5 but the value of 2.5 was chosen by the authors of the cost model, presumably as a conservative estimation or due to lack of data of this magnitude. The same can also be said for equation (2.32). No matter how crude these approximations, they are considered as neutral because of their connection with rated power.

2.3.3 LCoE Formulas

The relations leading to the calculation of LCoE are presented below, based on the work from [38] and [9]. The calculation of the capacity factor of a single wind turbine also comes from a drive-train efficiency model based on measurements as stated in [37] and it is drawn from the cost model Excel file.

$$\text{Levelised Cost of Electricity [€/MWh]} : \quad LCoE = \frac{LI + OM_D}{AEP} \quad (2.37)$$

$$\text{Levelised Investment [€/y]} : \quad LI = C \cdot P_{WF} \cdot CRF \quad (2.38)$$

$$\text{Annual Discounted O\&M [€/y]} : \quad OM_D = OM_{PV} \cdot CRF \quad (2.39)$$

$$\text{Annual Energy Production [MWh/y]} : \quad AEP = P_{WF} \cdot cf_{WF} \cdot 8,760 \quad (2.40)$$

$$\text{Capital Investment Cost [€/kW]} : \quad C = Cost_{wt} + BoP \quad (2.41)$$

$$\text{Total Wind Farm Capacity [MW]} : \quad P_{WF} = N_{wt} \cdot P_{wt} \quad (2.42)$$

$$\text{Capital Recovery Factor [\%]} : \quad CRF = d_R \cdot [1 - (1 + d_R)^{LT}] \quad (2.43)$$

$$\text{Present Value of Total O\&M [€]} : \quad OM_{PV} = (OM + BC) \cdot SFE \cdot AEP \quad (2.44)$$

$$\text{Wind Farm Capacity Factor [-]} : \quad cf_{WF} = cf_{wt} \cdot (1 - WkL) \cdot (1 - EIL) \cdot (1 - AvL) \quad (2.45)$$

$$\text{Turbine (Specific) Cost [€/kW]} : \quad Cost_{wt} = \frac{AbsCost_{TOT}}{P_{wt}} \quad (2.46)$$

$$\text{BoP (Specific) Cost [€/kW]} : \quad BoP = \frac{AbsCost_{BoP}}{P_{wt}} \quad (2.47)$$

$$\text{Real Discount Rate [\%]} : \quad d_R = \frac{d_N - i_R}{1 - i_R} \quad (2.48)$$

$$\text{O\&M Costs (incl. fixed an. Costs) [€/MWh]} : \quad OM = \frac{1,000 \cdot OM_F}{8,760 \cdot cf_{WF}} \quad (2.49)$$

$$\text{Summation of Discounted Future Expend [-]} : \quad SFE = \frac{(1 + d_R)^{LT} - 1}{(1 + d_R)^{LT} \cdot d_R} \quad (2.50)$$

$$\text{Wind Turbine Capacity Factor [-]} : \quad cf_{wt} = \frac{P_{out}}{P_{wt}} \quad (2.51)$$

$$\text{Expected Power Output [kW]} : \quad P_{out} = \sum_{V_{bin}=4}^{25} [P_{elec}(V_{bin}) \cdot pdf(V_{bin})] \quad (2.52)$$

$$\text{Weibull Probability Density Function} : \quad pdf(V) = \frac{k_w}{\lambda_w} \cdot \left(\frac{V}{\lambda_w}\right)^{k_w-1} \cdot e^{-(V/\lambda_w)^{k_w}} \quad (2.53)$$

$$V_{w,mean} = \lambda_w \cdot \Gamma(1 + 1/k_w)$$

$$\text{Drive-train Efficiency model [-]} : \quad n_{DT}(V) = a \cdot \exp\left(\frac{1 - P_{aero}(V)}{P_{R.aero}}\right)^n + b \quad (2.54)$$

$$\text{DT model factor a [-]} : \quad a = \frac{1}{1 - e} \cdot n_{max} \quad (2.55)$$

$$\text{DT model factor b [-]} : \quad b = \frac{e}{1 - e} \cdot n_{max} \quad (2.56)$$

$$\text{DT model factor } n [-] : \quad n = \frac{1}{\ln(1-0.1)} \cdot \ln \left[\ln \left(\frac{e \cdot n_{max} - (e-1) \cdot n_{min}}{n_{max}} \right) \right] \quad (2.57)$$

Where: N_{wt} = Number of wind turbines in the farm (50)
 P_{wt} = Rated electrical power of a single wind turbine (10 MW)
 LT = Project lifetime (25 y)
 BC = Balancing costs (3 €/MWh)
 WKL = wake losses (fixed percentage per design concept according to results in [7])
 EIL = electrical losses (2%)
 AvL = availability losses (5%)
 d_N = Nominal discount rate (5.39%)
 i_R = inflation rate (2.112%)
 OM_F = Fixed annual O&M costs (106 €/kW/y)
 P_{elec} = Electrical power output
 $pdf(V)$ = Weibull probability distribution of wind speed at mid-point with,
 $V_{w,mean}$ = Weibull mean annual speed (9.41 m/s)
 k_w = Weibull shape factor (2.33)
 λ_w = Weibull scale parameter (10.62 m/s)
 Γ = the Gamma function
 V_{bin} = Wind speed probability mid-point block (1)
 $P_{aero}(V)$ = Aerodynamic power
 $P_{R,aero}(V)$ = Rated aerodynamic power (10.6383 MW)
 n_{max} = Drive-train efficiency at 100% load (0.94)
 n_{min} = Drive-train efficiency at 10% load (0.83)

2.4 Fatigue Loads, Damage and Power Production Estimation

Aside from the extreme cases, load time-series from DLC 1.2 and 4.1 can be used to extrapolate lifetime fatigue loads and compare accumulated damage (D_{Tot}) between the designs. A common technique in damage estimation in wind turbine design is done with the use of Miner's rule, a technique also employed in the SANDIA 100m Blade [14]. In brief, Miner's rule states that material fatigue accumulates and the sum of damages from different loadings gives a good estimation of the total fatigue or remaining lifetime. For a component not to fail, the sum of the ratios of cycles with a certain loading (namely stress level and range) over the maximum allowable cycles for the same loading should be less than unity.

$$D_{Tot} = \frac{n_1(S_1)}{N_1(S_1)} + \frac{n_2(S_2)}{N_2(S_2)} + \dots + \frac{n_k(S_k)}{N_k(S_k)} \Rightarrow D_{Tot} = \sum_{i=1}^k \frac{n_i(S_i)}{N_i(S_i)} < 1 \quad (2.58)$$

Where: D = Fatigue damage
 S_i = Loading/stress level on component
 n_i = Occurring cycles for stress level S_i
 N_i = Cycles to failure for stress level S_i
 k = number of different loadings

The number of occurring cycles n_i usually comes from condition monitoring records, experimental or simulation data while the number of allowable cycles N_i comes from experimental data depicted in S-N curves (also known as Wöhler curves). A typical linear-logarithmic S-N curve for aluminium is depicted below in Figure 2.6.

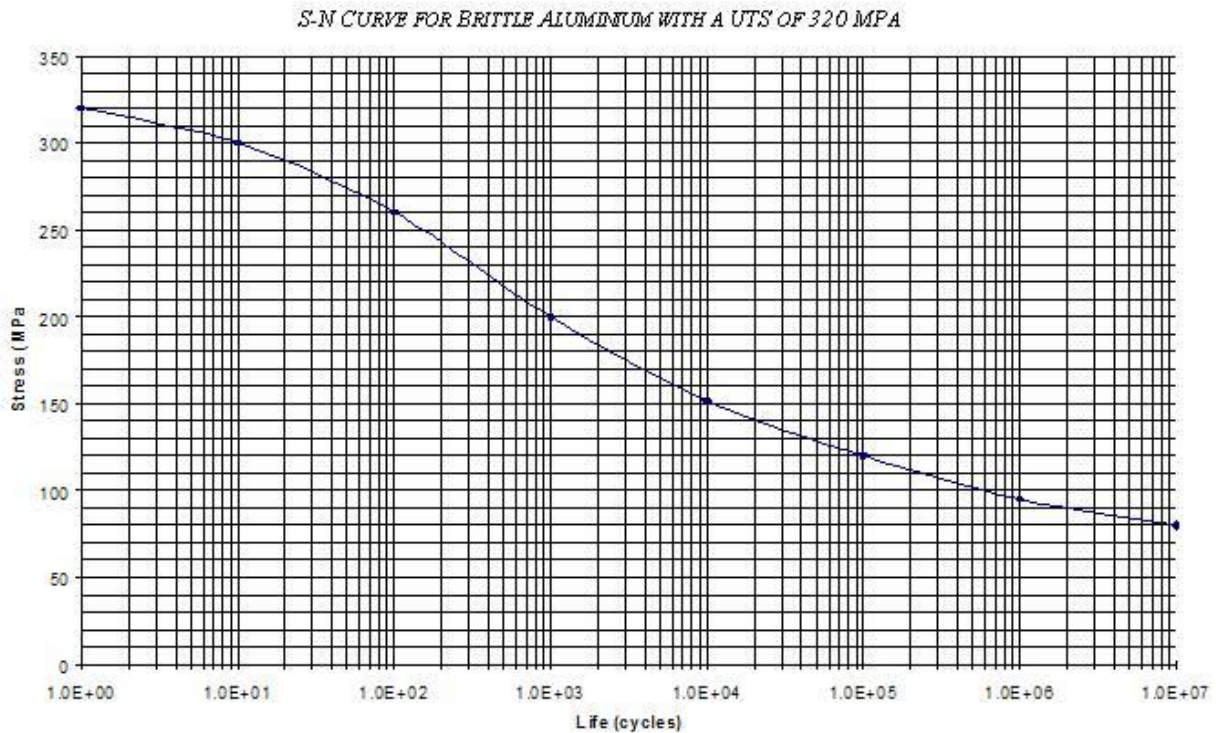


Figure 2.6: A lin-log S-N curve for aluminium (source: wikipedia.org)

The area under the curve implies that a certain combination of stress S and cycles to failure N_{FS} ensures fatigue endurance. The curve is characterised firstly by the intercepting point in the vertical axis of stress. A single-cycle failure load corresponds to the ultimate tensile (UTS - S_{UT}) or compressive strength (UCS - S_{UC}), sometimes denoted in the literature as C [42] or K [35]. Secondly, the curve is characterised by the decreasing slope exponent $-m$ that depends on the material under investigation. The mathematical expression for stresses and cycles to failure is formulated as follows.

$$\begin{aligned}
 S^m N_{FS} &= S_{UT}^m N_{FS_{UT}} \Rightarrow S^m N_{FS} = S_{UT}^m \cdot 1 \Rightarrow S^m N_{FS} = S_{UT}^m \Rightarrow \\
 N_{FS} &= \left(\frac{S_{UT}}{S} \right)^m \Rightarrow N_{FS} = \left(\frac{S}{S_{UT}} \right)^{-m} \Rightarrow S = S_{UT} N_{FS}^{-\frac{1}{m}}
 \end{aligned}
 \tag{2.59}$$

Lastly, an S-N curve is unique for different cyclic stress ratio R_S applied, with $R_S = S_{min}/S_{max}$. For example, an R_S value of -1 corresponds to equal absolute compressive S_{min} and tensile stress S_{max} with a mean value S_m of 0. An R_S value of 0 corresponds to 0 compressive stress and the full load amplitude is exhausted in the tensile direction with $S_m = S_{max}/2$. A group of S-N curves for different R_S values formulates a Goodman Constant life diagram (CLD) [34], covering multiple cases of loading ranges.

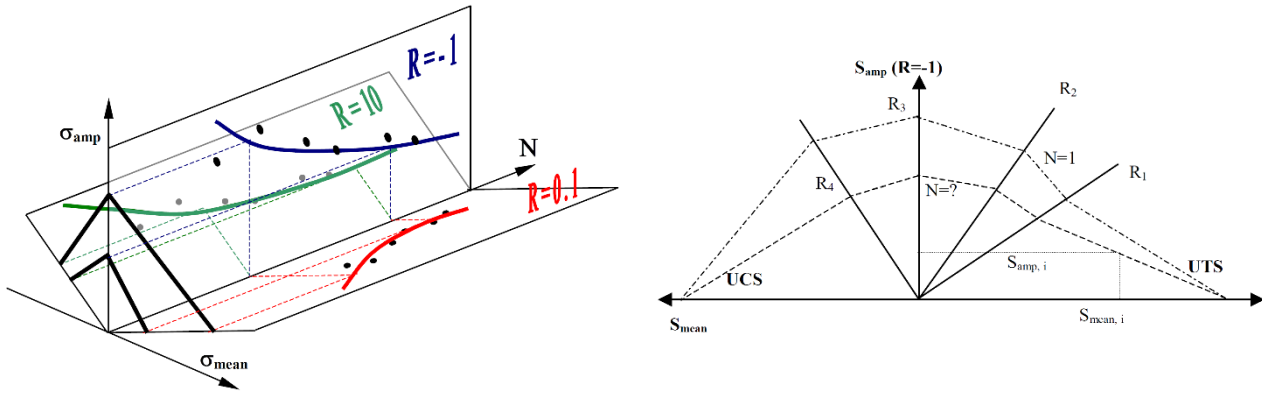


Figure 2.7: Two views of a Goodman Constant Life Diagram [34].

The outermost dotted curves in the CLD above and to the right represent a single-cycle loading with different amplitude and mean combinations. Moving inwards to the axis intersection, the cycles to failure increase to several orders of magnitude.

It is evident that detailed information for the stresses (mean, amplitude, R_5 etc.) are needed in order to accurately predict lifetime damage accumulation in the material and produce a CLD. This information is sometimes difficult to obtain or accurately extrapolate. So another method is employed in wind turbine design, involving the derivation of Damage Equivalent Load ranges (DEQL). Through a rain-flow counting algorithm, the time-series of a load case is broken down into bins of load ranges and duration in cycles. The sum of products of the cycles of each bin times each load raised to the power of m , divided by the duration in seconds of each load case seed gives the load case 1Hz equivalent load. In essence, the 1Hz Damage Equivalent Load range represents a harmonic constant amplitude load with 1 second period that for the load case seed timespan would cause the same damage to the material as the random loading of the simulation [17].

$$N_{eq} M_{eq}^m = \sum_{i=1}^{n_b} n_i M_i^m \Rightarrow M_{eq} = \left(\frac{\sum_{i=1}^{n_b} n_i M_i^m}{N_{eq}} \right)^{\frac{1}{m}} \quad (2.60)$$

The notation of loads M above concerns the blade root bending and torsional moments that were recorded from the simulations. For the tower, the bending and torsional moments in the tower bottom were recorded. The equivalent moments of all load cases within load sets 1.2 or 4.1 are then weighted and averaged with the Weibull probability density function (see Equation (2.53)) chosen with respect to the occurrences of each load range.

$$N_{occur}(V) = pdf(V) \cdot \frac{T_{life}}{T_{sim}} \quad (2.61)$$

Where: $N_{occur}(V)$ = number of occurrences of a load case at wind speed V

T_{life} = total wind turbine lifetime in seconds (25 years)

T_{sim} = duration of a load case in seconds

The lifetime 1Hz equivalent loads, similarly to equation (2.60), are extrapolated using the following formula. The derived constant amplitude load occurring harmonically for 25 years with 1Hz frequency would cause the same material damage as the equivalent loads of every simulation weighted with the occurrences.

$$M_{LT} = \left(\frac{N_{occur}(x) \sum_{i=1}^{n_{LC}} T_{sim} M_{eq.LC}^m}{T_{life}} \right)^{\frac{1}{m}} \quad (2.62)$$

Where: M_{LT} = Lifetime equivalent load

$M_{eq.LC}$ = seed/load case equivalent load

n_{LC} = number of seeds per load set

In order to compare the fatigue estimation of the blades, the equivalent loads are transformed into normal and shear stresses, to account for the stiffnesses and geometry of each design. The corresponding strains at the blade root are also derived. As for the tower and shaft, since both structures remain identical between the designs, the latter transformation was not performed.

$$\begin{aligned} S_{eq.FL} &= \frac{M_{LT,y} d_x}{I_{yy}} \Rightarrow \varepsilon_{eq.FL} = \frac{M_{LT,y} d_x}{EI_{yy}} \\ S_{eq.ED} &= \frac{M_{LT,x} d_y}{I_{xx}} \Rightarrow \varepsilon_{eq.ED} = \frac{M_{LT,x} d_y}{EI_{xx}} \\ \tau_{eq.TO} &= \frac{T_{LT,z} \max(d_x, d_y)}{J_T} \Rightarrow \gamma_{eq.TO} = \frac{T_{LT,z} \max(d_x, d_y)}{GJ_T} \end{aligned} \quad (2.63)$$

Where: $S_{eq.FL}$, $M_{LT,y}$ = lifetime equivalent normal flap-wise stress and bending moment on blade root

d_x = distance of neutral axis from point of stress application

I_{yy} , EI_{yy} = flap-wise second moment of inertia and stiffness

$\varepsilon_{eq.FL}$ = lifetime equivalent flap-wise strain

$S_{eq.ED}$, $M_{LT,x}$ = lifetime equivalent normal edge-wise stress and bending moment on blade root

d_y = distance of neutral axis from point of stress application

I_{xx} , EI_{xx} = edge-wise second moment of inertia and stiffness

$\varepsilon_{eq.ED}$ = lifetime equivalent edge-wise strain

$\tau_{eq.TO}$, $T_{LT,z}$ = lifetime equivalent maximum shear stress and torsional moment on blade root

J_T , GJ_T = polar moment of inertia and torsional stiffness

$\gamma_{eq.TO}$ = lifetime equivalent torsional strain

Therefore, in order not to speculate and proceed into assumptions on the specifics of the materials used for the RWT blade (combinations of materials, laminar weaving, ultimate strengths etc.), the comparison of lifetime equivalent stresses is considered adequate to provide an estimation of fatigue of each design. It is assumed that the RWT blade and tower exhibit a sound fatigue endurance.

In a similar manner, more realistic Power Curves are extrapolated from the power signal of the simulations. The Lifetime Energy Yield is derived by weighting these power curves with the Weibull PDF and by multiplying them with the lifetime seconds of the turbine.

$$E_{life} = T_{life} \cdot \sum_{V=4}^{25} [pdf(V) \cdot P(V)] \quad (2.64)$$

Where: E_{life} = Lifetime Energy Yield

$P(V)$ = electrical power produced

2.5 Description of Software Used

2.5.1 BOT (Blade Optimisation Tool)

The Blade Optimization Tool is an Excel workbook for wind turbine rotor design calculations. It enables optimization of the rotor geometry for maximum annual energy yield at a given wind speed distribution. The calculations are based on a model for stationary aerodynamic performance and loads of wind turbines, using the blade element momentum (BEM) theory. The user supplies an initial wind turbine blade design and coefficients C_L and C_D for the chosen aerofoils [5].

In BOT, optional corrections are available for tip and root losses according to Prandtl's tip-loss factor F_p [29], as well as for rotational effects on the aerofoils [39]. BOT can deal with single speed, dual speed and variable speed wind turbines, both with pitch or stall power regulation. The program is created in an Excel 2003 workbook using Visual Basic source code.

For the purposes of this report, BOT output results were readily available for all concepts; both the geometries of the proposed innovations and the span-wise distributions of Torque Q and Axial Force F_{ax} (Thrust) on the annuli of the rotor. Combining the known geometries, derived loads and reference blade properties, the new properties were calculated as described in Section 3.2.

2.5.2 FOCUS

FOCUS6 (ver. 6.2) is a modular modelling software developed by ECN and WMC that integrates all aspects of wind turbine design [43]. This is possible through its ability to include several independent modules and codes that exchange data through input and output files in a common database. It is based on a simplified GUI where a user can define a wide variety of parameters and geometry of the blades, support structures, generator properties, controller algorithms and all other components. It also provides aeroelastic codes/solvers, stochastic wind and wave simulators, FEM solvers, sound emissions calculator, load case generators and post-processors for data and graphs. All these tools combined can produce a complete aerodynamic and structural analysis of a wind turbine through time domain simulations.

▲ PHATAS (*Program for Horizontal Axis wind Turbine Analysis and Simulation*)

PHATAS (release JAN-2012a) is the programme/code used for the aeroelastic response calculations with time-domain simulations under the design package FOCUS [29]. It also calculates the non-linear dynamic behaviour of the wind turbine, the occurring loads and its performance characteristics while incorporating the necessary control algorithms. It abides by the BEM theory and numerical convergence is pursued through the iterative method of equating thrust and torque relations from Momentum theory and Blade Element theory and by solving for induction factors a and a' [32].

A great flexibility in setting up the appropriate simulation is provided by the ability of PHATAS to define every aspect of the turbine model and the simulation. It also provides additional modelling features such as the Snel dynamic stall model, tower shadow effect and 3D aerofoil correction. The strength of PHATAS is that it describes the integrated aerodynamic and structural dynamic response of the turbine and tower, the response of the controller, and the options to simulate normal operation, start-ups, stops, and failure conditions.

It is useful to denote some of the correction features that PHATAS uses in order to approach BEM theory more accurately, realistic flows and mechanical or structural conditions. As it is assumed for BEM theory, in PHATAS as well, there must be no aerodynamic interaction between the elements, meaning no radial, "span-wise" flow. Blade tip losses and root losses are modelled using the Prandtl approximation factor [26].

The blade bending is described by in-plane and out-of-plane degrees of freedom. Complex rotor shapes, blade twist and pitching actions, combine these two motions and should be solved together. Also, a number of 15-20 elements is recommended for proper description of the bending. Every blade element experiences relative inflow velocities in a dynamic manner due to its rotation when considering deformations and motions from the blade itself and from the rotor shaft, the tower and foundation.

For a tubular tower, the influence of the tower on the airflow (“stagnation” or “tower shadow”) can be described with the three-dimensional potential flow around a semi-infinite dipole. This approach, however, is found to give an over-estimation of the tower shadow, so a simpler double vortex model is employed in the code to describe the tower drag and the load variation on the blade. The blade-tower interaction though, is not taken into account.

A 3D correction model for the effects of rotation (span-wise gradient of the dynamic pressure, centrifugal effects of the boundary layer) is also available. It gives an empirical increase in the lift proportional to $(c/r)^2 \cdot (\Omega r)^2 / V_{\text{eff}}^2$ that also accounts for the local speed ratio [26]. However, it is not used in the current report, since the aerofoil coefficients provided are already 3D-corrected by DTU.

The dynamic stall behaviour can be described in terms of a first-order and a second-order correction on the quasi-steady lift coefficient, following the heuristic model of H. Snel based on formulations by Truong and by Leishmann and Beddoes. The first-order linear correction is similar to other dynamic stall models and it is the one used in the simulations, as the second-order non-linear part has not been validated properly [18] [27] [29].

Blade tips have a strongly decreasing mass and stiffness distribution. If stiffness decreases disproportionately to the mass, numerical problems appear, giving large local deformations. It is recommended that for the last outboard element, the stiffness is kept constant with the previous one.

The coordinate systems for the overall wind turbine structure, tower, nacelle and blades used by PHATAS should also be depicted. Note the numbering/indexing of the loads and displacements in the following graphs for a clearer view of the results in Chapter 4 of this report.

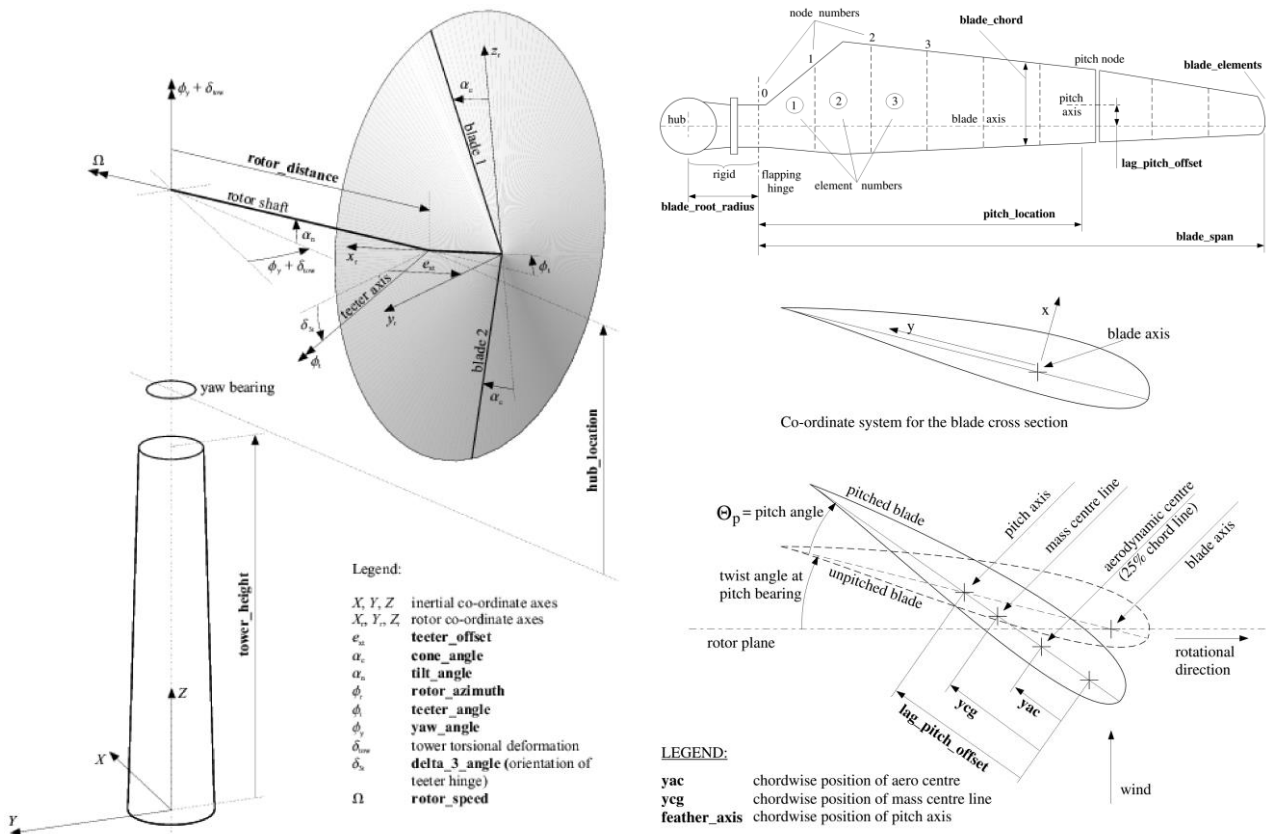


Figure 2.8: Coordinate system definitions and model details in PHATAS for the overall wind turbine

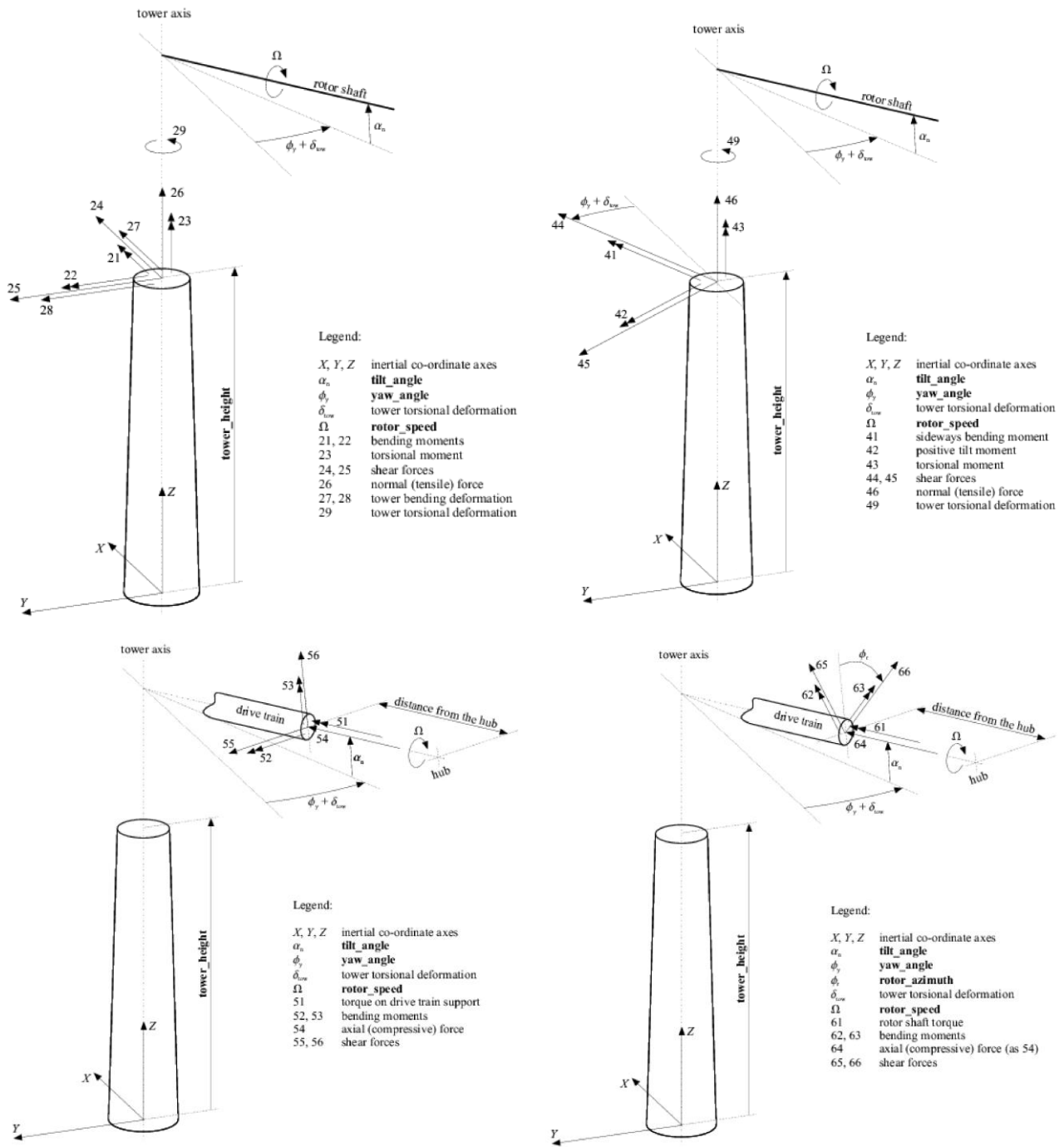


Figure 2.9: Coordinate system definitions and model details in PHATAS for the signals, loads and displacements on the Tower and Shaft

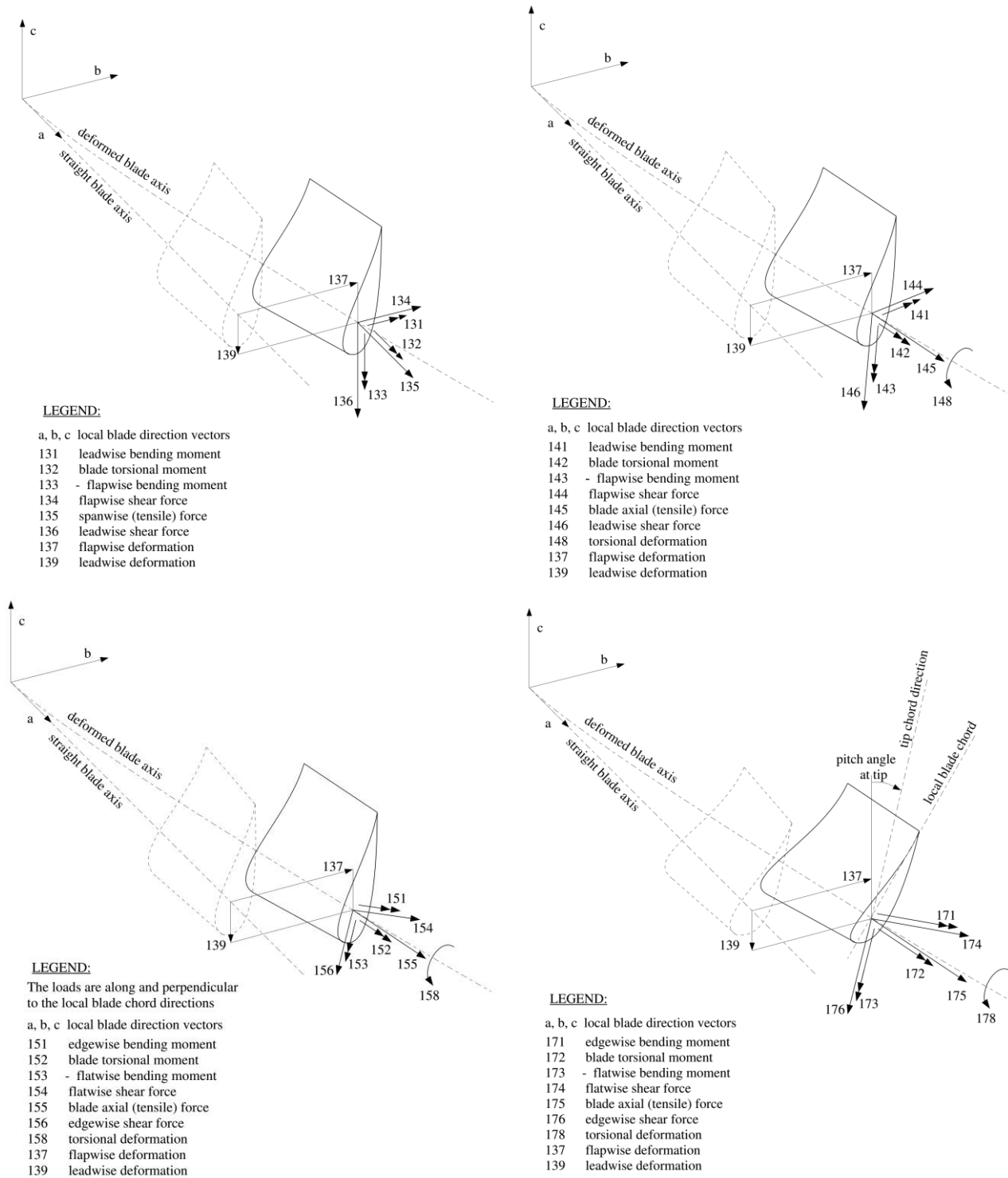


Figure 2.10: Coordinate system definitions and model details in PHATAS for the signals, loads and displacements on the blade sections

▲ **BLADEMODE**

PHATAS calculates mode shapes and frequencies of the blades and of the turbine for a number of rotational speeds, which are eigen-value solutions without aerodynamic contribution. So additionally, the BLADEMODE programme is used for the rotor modes, although it does not provide some of the modes presented by the INNWIND project partners.

The BLADEMODOE programme is used for the evaluation of the eigen-modes and frequencies of wind turbine rotor blades [27]. It contains an aerodynamic model, and gives prediction of aerodynamic damping ratios of blade vibrations.

In BLADEMODOE, the eigen-modes with coupled flap-bending, edge-bending, and torsional deformation of a rotating wind turbine blade can be calculated for a deformed equilibrium state. By expressing the tower fore-aft flexibility and drive-train dynamics (shaft torsion and drive-train inertias) in terms of edge constraints at the blade root, also the collective rotor modes can be calculated. The term “collective” indicates that the out-of-plane bending of the blades is in-phase with each other; that is the case for the in-plane bending as well. This excludes the modes that cause tower torsion, such as the asymmetric flap-wise modes. However, the reaction-less edge-wise modes can be solved too, by modelling the tower flexibility and the drive-train as rigid. The 1st collective edge-wise (Drive-train mode) is calculated by not allowing speed variations between the rotor and drive-train.

3

MODELLING METHODOLOGY

3.1 The INNWIND 10 MW Reference Wind Turbine

3.1.1 Overall

INNWIND.eu is a project for the design and simulation of innovative beyond-state-of-the-art 10 and 20 MW wind turbines for offshore applications. It is an ambitious successor for the UpWind project, where the vision of a 20MW wind turbine was put forth with specific technology advances that are required to make it happen. DTU is the coordinator of this large project with a total of 27 leading industrial partners and research establishments all across Europe [18], TU Delft and ECN among them. In the following sections and tables, the details of the model are presented.

Table 3.1: Main properties of the INNWIND Reference Wind Turbine

Parameter	Value	Units	Comment
Wind Regime	IEC Class 1A	-	-
Rotor Orientation	Clockwise Rotation - Upwind	-	-
Control	Variable Speed - Collective Pitch	-	-
Cut-in wind speed	4	[m/s]	-
Cut out wind speed	25	[m/s]	-
Rated wind speed	11.4	[m/s]	-
Rated power	10	[MW]	-
Number of blades	3	-	-
Rotor Diameter	178.3	[m]	-
Hub Diameter	5.6	[m]	-
Hub Height	119	[m]	-
Minimum Rotor Speed	6.0	[rpm]	-
Maximum Rotor Speed	9.6	[rpm]	-
Maximum Generator Speed	480	[rpm]	In the HSS
Gearbox Ratio	50 : 1	-	-
Maximum Tip Speed	90	[m/s]	-
Hub Overhang	7.1	[m]	-

Shaft Tilt Angle	5.0	[°]	-
Rotor Cone Angle	-2.5	[°]	Forward coned
Blade mass	41,716	[kg]	-
Hub mass	105,520	[kg]	-
Rotor mass (Blades + Hub)	230,667	[kg]	-
Nacelle mass	446,036	[kg]	-
Tower mass	628,442	[kg]	-
Overall mass	1,305,145	[kg]	-
Optimal Mechanical Aerodynamic Rotor Efficiency, C_P	0.4776	-	-
Thrust coefficient at rated wind speed, C_T	0.814	-	-
Design Extreme Thrust Value	4,800	[kN]	-

3.1.2 The Blades and Aerofoils

The rotor radius is 89.166 m in the rotational plane and with a hub diameter of 5.6 m, it leads to a blade span of 86.366 m, while the pre-bent span of the blade is 86.466 m. The pre-bend of the blade adds an extra 3.332 m of tower-tip clearance.

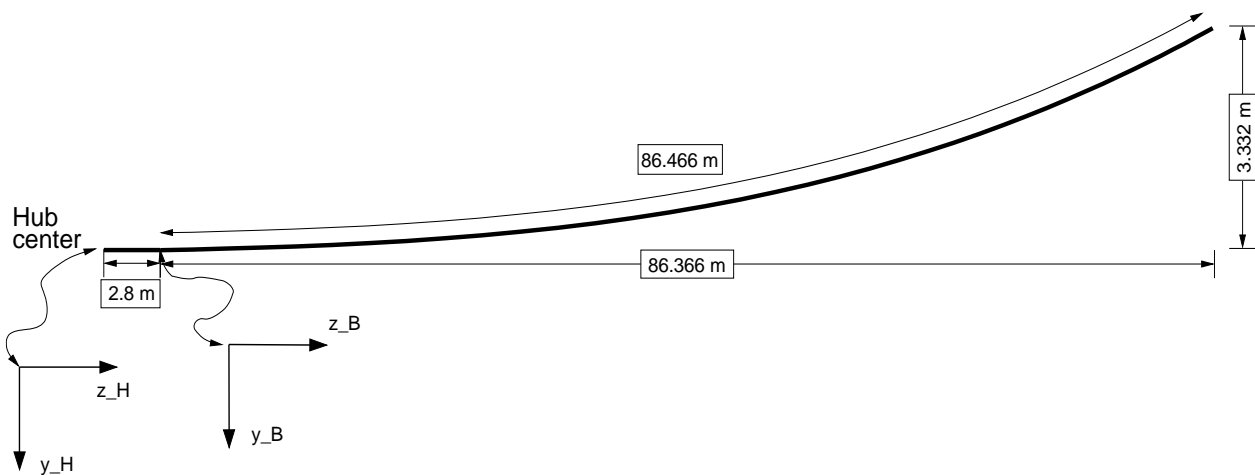


Figure 3.1: The RWT blade and coordinates (courtesy of the INNWIND database [18])

Table 3.2: Properties of the RWT Blade

Parameter	Value	Unit	Comment
Rotor radius	89.166	[m]	(In hub-coordinate system)
Blade length	86.366	[m]	(Projected onto hub-coordinate system z-axis)
Blade length	86.466	[m]	(Accumulated length along bent blade axis)
Overall (Integrated) Blade Mass	41,716	[kg]	-
Structural Damping	3	Log. Decr. [%]	Ratio (All Modes)
Body Centre of gravity	-0.118	[m]	(x _B coordinate, Figure 3.2)
Body Centre of gravity	-0.36	[m]	(y _B coordinate, Figure 3.2)

Body Centre of gravity	26.179	[m]	(z_B coordinate, Figure 3.1)
Minimum pitch angle	0.0	[°]	for maximum C_p operation
Aerofoil Distribution	0.0	[m]	CYLINDER
(after the blade root radius)	9.686	[m]	FFA-W3-600
	15.956	[m]	FFA-W3-480
	20.739	[m]	FFA-W3-360
	28.623	[m]	FFA-W3-301
	40.806	[m]	FFA-W3-241

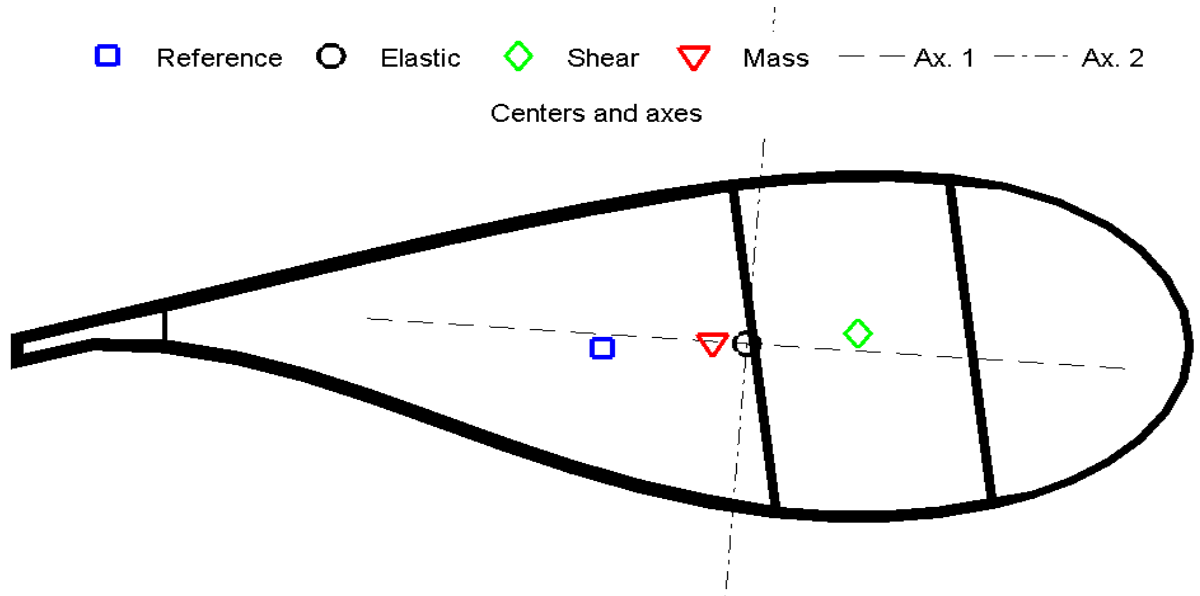


Figure 3.2: A cross section of the RWT blade showing principal axes Ax.1 and Ax.2 and the different centres of interest. The “reference” point (blue square) is at 50% of the chord. x-axis runs along the chord line and y-axis along the aerofoil thickness (courtesy of the INNWIND database [18])

3.1.3 The Tower, Nacelle, Hub and Drive-train

In the following tables, the properties of the tower, nacelle-hub assembly and drive-train are given.

Table 3.3: Properties of the RWT Tower

Parameter	Value	Unit	Comment
Hub Height	119	[m]	-
Tower Height	115.63	[m]	(up to yaw bearing)
Overall Mass	628,442	[kg]	-
Centre of Gravity	47.6	[m]	-
Structural Damping Ratio (All Modes)	6.28	Log. Decr. [%]	-
Young’s Elasticity Modulus	210	[GPa]	-
Poisson’s Ratio	0.3	-	-
Effective Density	8500	[kg/m ³]	(taking into account secondary structures)

Bottom outer Diameter	8.3	[m]	-
Bottom Wall Thickness	38	[mm]	-
Bottom Cross Section Area	0.9863	[m ²]	-
Top outer Diameter	5.5	[m]	-
Top Wall Thickness	20	[mm]	-
Top Cross Section Area	0.3443	[m ²]	-

Table 3.4: Properties of the Nacelle and Hub

Parameter	Value	Unit	Comment
Elevation of Yaw Bearing Above Ground	115.63	[m]	-
Vertical Distance Along Yaw Axis from Yaw Bearing to Shaft	2.75	[m]	-
Distance Along Shaft from Hub Centre to Yaw Axis	7.1	[m]	-
Distance Along Shaft from Hub Centre to Main Bearing	2.7	[m]	-
Nacelle c.g. Location Downwind of Yaw Axis	2.687	[m]	-
Nacelle c.g. Location Above of Yaw Bearing	2.399	[m]	-
Nacelle length (x-dir)	10	[m]	-
Nacelle width (y-dir)	10	[m]	-
Nacelle height (z-dir)	15	[m]	-
Hub Mass	105,520	[kg]	-
Hub Inertia About Shaft Axis	325,671	[kg.m ²]	-
Nacelle Mass	446,036	[kg]	-
Nacelle Inertia About Yaw Axis	7,326,346	[kg.m ²]	-

Table 3.5: Properties of the Drive-train

Parameter	Value	Unit	Comment
Rated Rotor Speed	9.6	[rpm]	-
Rated Generator Speed	480	[rpm]	-
Gearbox Ratio	50:1	-	-
Electrical Generator Efficiency	94	[%]	-
Generator Inertia About Medium-Speed Shaft	1,501	[kg.m ²]	-
Fully-Deployed Medium-Speed Shaft Brake Torque	52,254	[N.m]	-
Medium-Speed Shaft Brake Time Constant	0.74	[s]	-
Structural damping (free-free system)	5	[%] critical	-

3.1.4 The BOT Results of All the Concepts

The steady state BOT results for all seven rotors are given below. Firstly, the aerodynamic performances of the rotors, namely the C_p and C_T values against the wind speeds (Figure 3.3 and Figure 3.4). Secondly, the thrust and the flap-wise blade root bending moment (Figure 3.5 and Figure 3.6). For the point of the maximum bending moment of each rotor, the span-wise distributions of the normal and tangential (torque) forces is also given.

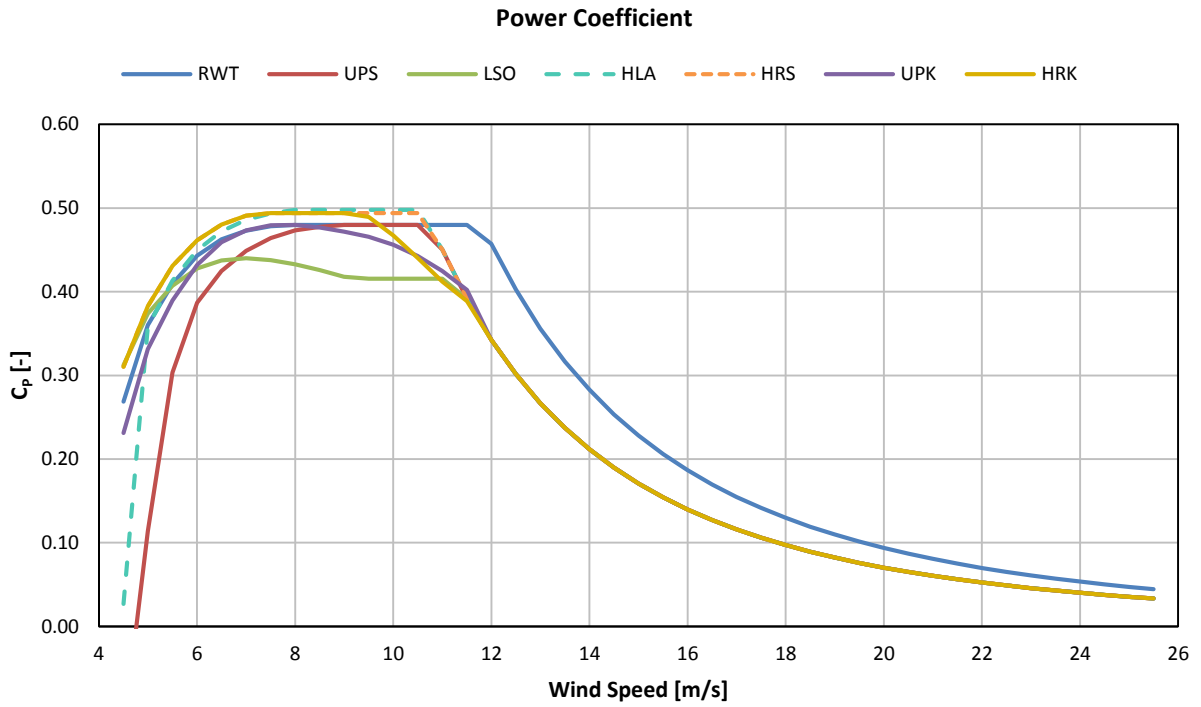


Figure 3.3: The C_p values of all rotors from BOT (dashed lines are used to distinguish between similar concepts)

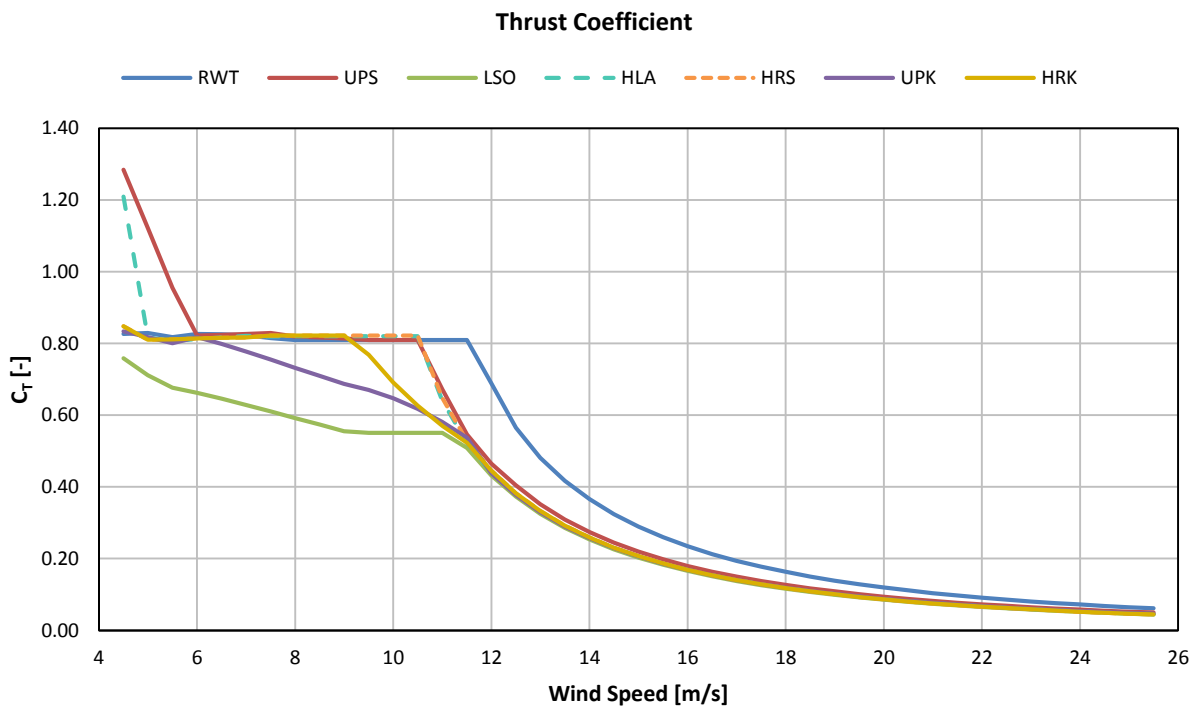


Figure 3.4: The C_t values of all rotors from BOT (dashed lines are used to distinguish between similar concepts)

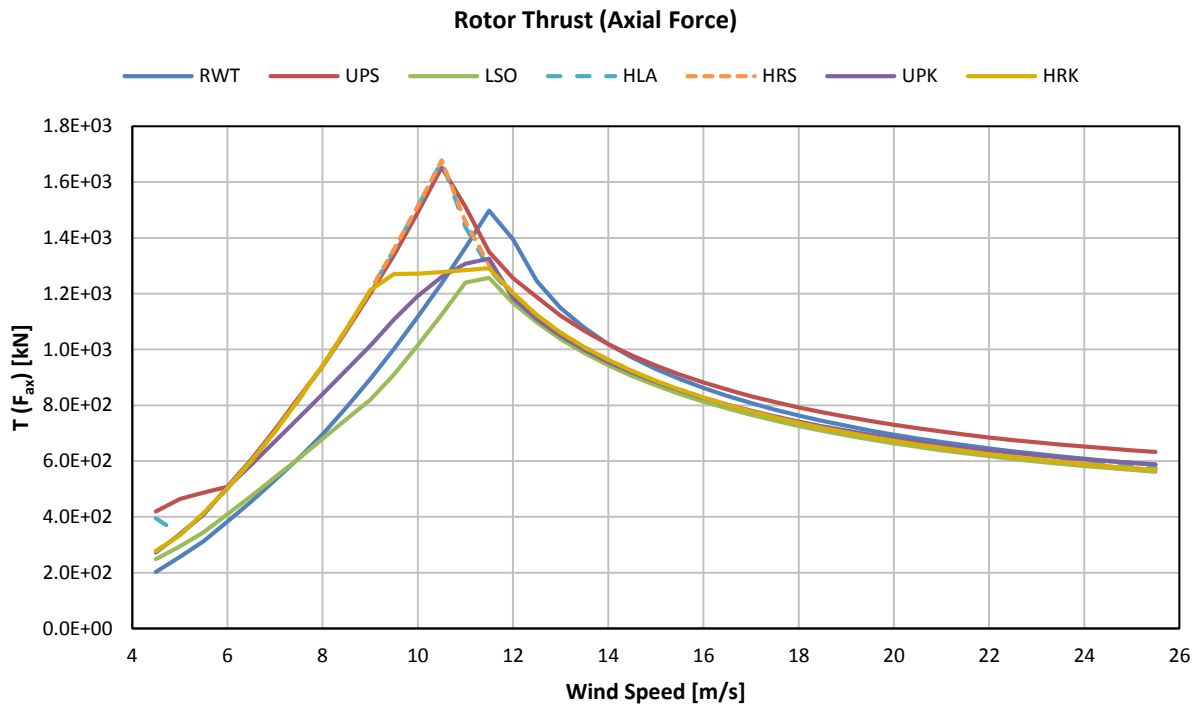


Figure 3.5: Thrust on each rotor from BOT (dashed lines are used to distinguish between similar concepts)

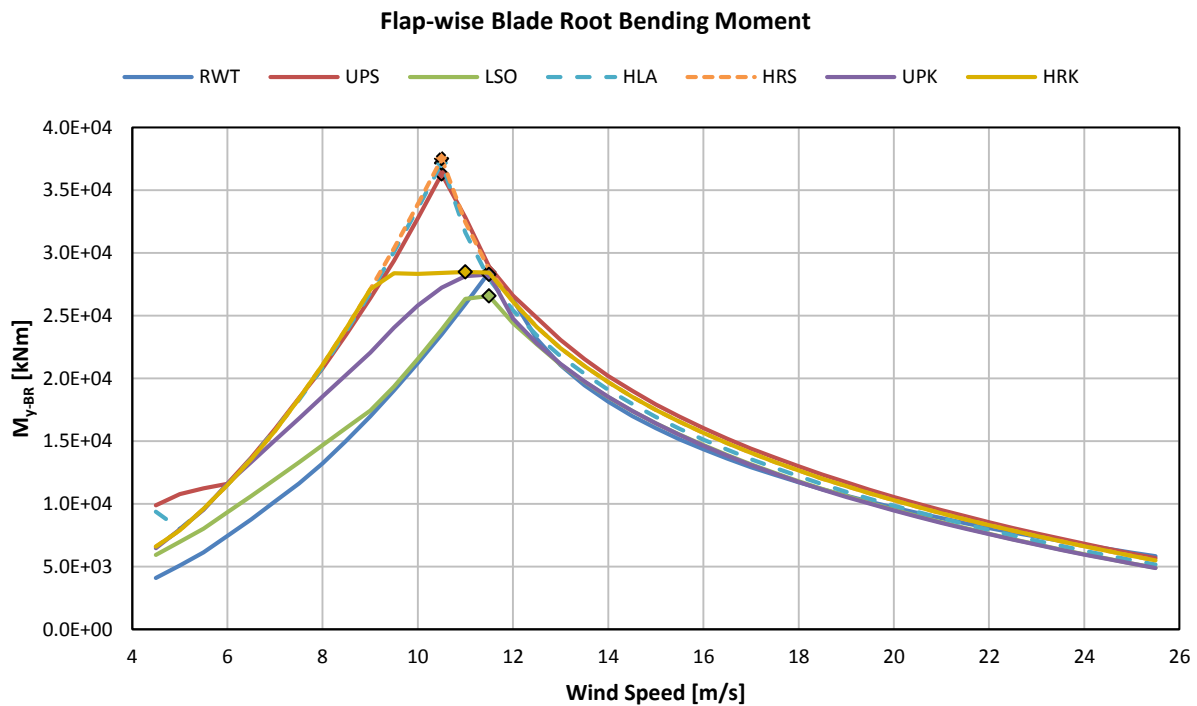


Figure 3.6: Flap-wise bending moment of each blade from BOT, with the maximum-load points denoted with the diamonds (dashed lines are used to distinguish between similar concepts)

It is interesting to note that the flap-wise moments of the sub-optimal concepts are at the RWT levels as intended, either through peak-shaving in the UPK and HRK or through power shedding in the LSO concept. Similarly in Figure 3.7 and Figure 3.8, these two groups also appear in the normal force span-wise distributions.

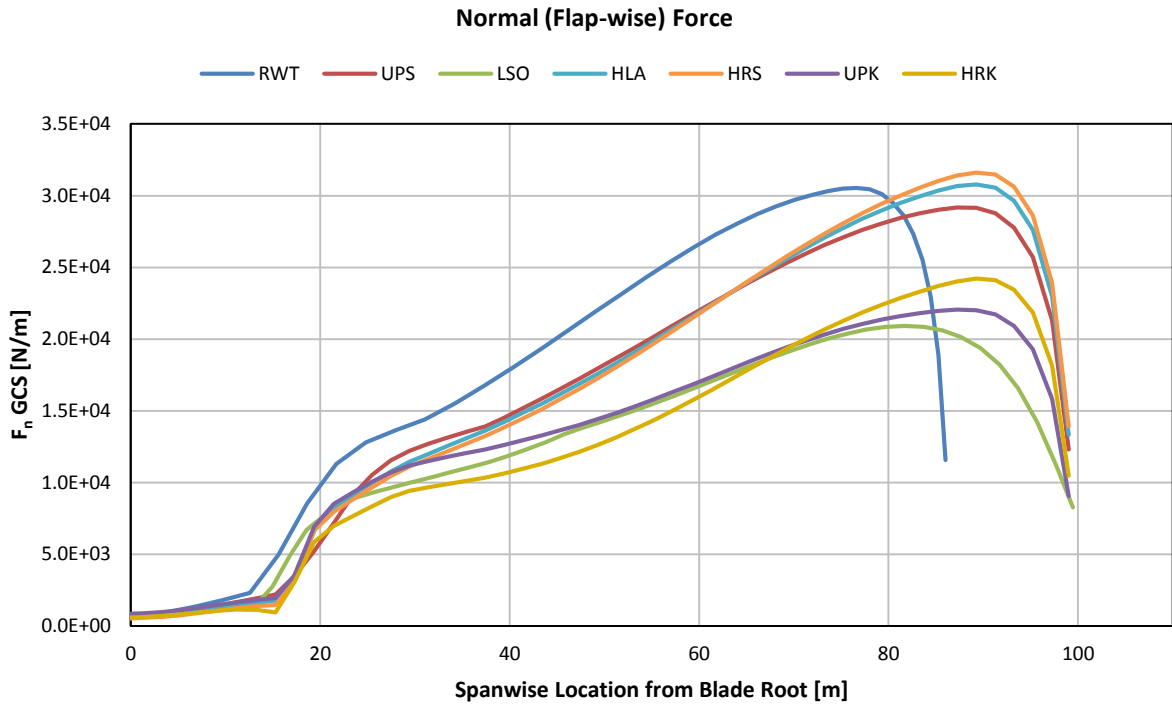


Figure 3.7: The span-wise distributions of the normal force of the maximum-load points (total rotor thrust divided by 3). The coordinate system GCS refers to the global-absolute CS, i.e. direction down-wind

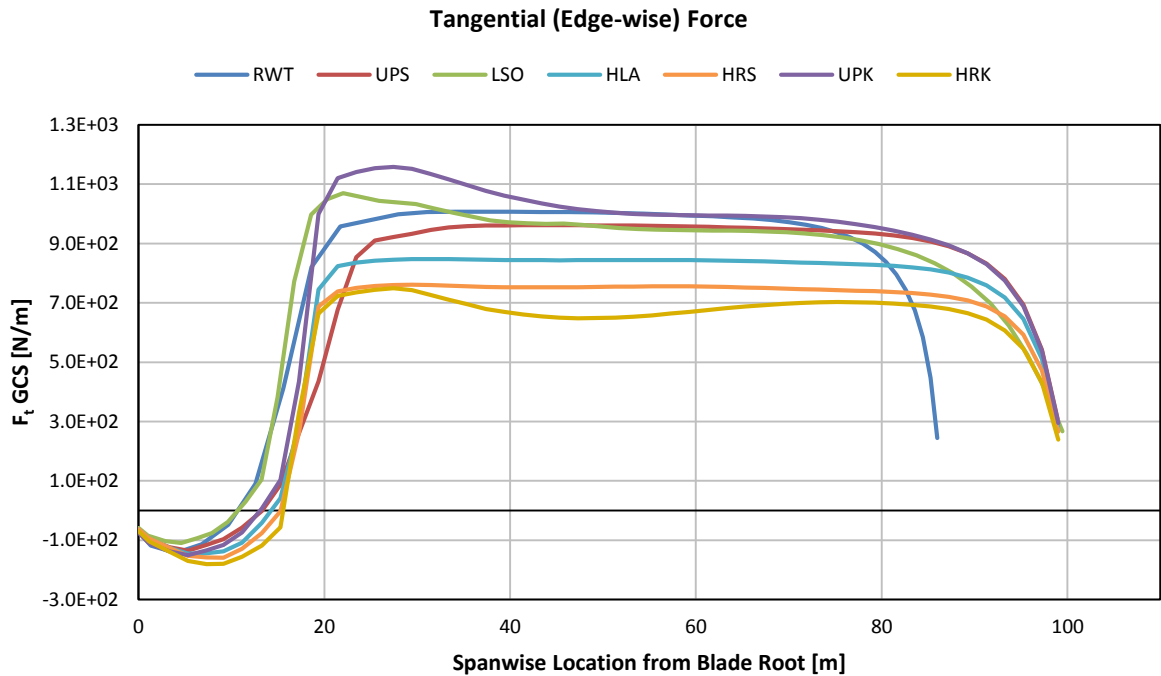


Figure 3.8: The span-wise distributions of the tangential force of the maximum-load points (total rotor torque divided by 3 and each element's distance from the rotor centre). The coordinate system GCS refers to the global-absolute CS, i.e. rotor in-plane

3.2 The Modelling / Up-scaling Process

3.2.1 Overview

The process described below is not an up-scaling method for a detailed structural description. It is merely an approach, based on a few assumptions, on how the new model input files and data should be formulated to be used in PHATAS or other aeroelastic codes. Its purpose is not to describe the properties of the new blades in full structural detail, such as spar cap and shear web exact positions and thicknesses, and aerofoil skin reinforcements. The effects of these details and reinforcements are considered to be included within the blade bending stiffness data and will be up-scaled accordingly.

The method is driven by knowing the steady-state loads (and the weight) on every blade element of the RWT operating close to its rated wind speed, where the maximum flap-wise bending moment (and usually thrust) on the rotor appears. These loads acting on the known stiffnesses provided by the INNWIND database, produce a certain strain for each element along the blade span. This strain is considered as a “pivot point” and is kept constant through the up-scaling. The approach is based on the logic that the new blades should withstand the new steady-state maximum loads, including their own weight, in a similar manner with the RWT.

It has a small innovative merit as it results in a slightly smaller total blade mass compared to other classical up-scaling methods, as described by Sieros in [26] and produces comparable results with the MDO method proposed by Ashuri in [2]. The models will be tested in PHATAS and corrected, if deemed necessary, in order to attain a final more sound design, depending on the results of the simulations. This concerns mainly dynamic loads that do not appear in the primary BEM analysis provided by the BOT software calculations. The most basic assumption, of course, is that the reference/baseline rotor operates in a proper structural manner and this performance can be projected onto other designs.

There are three basic pre-requisites for the method to function properly:

- ▲ The reference model should be given in sufficient detail both in number of parameters (necessary for many aeroelastic codes) and in an acceptable number of elements along the blade span for the distributed properties.
- ▲ The geometry of the new conceptual designs should be described at least with their chord, twist, relative (or absolute) thickness and blade elements (namely centres and lengths).
- ▲ Normal forces F_n and tangential forces F_t (or torque Q) on the blade elements should be given from a steady state analysis.

3.2.2 Step 1: Definition and Assignment of the Loads

For the RWT, the geometry and loads from BOT are given in the form of normal force F_n (F_{ax}) and torque Q distributions (N/m and Nm/m respectively) for each of the 40 elements in the global coordinate system (GCS). The GCS is defined with x-axis along the wind flow, y-axis perpendicular to the blade span and z-axis along the blade span (see Figure 3.9). The normal forces and torque vector are positive downwind, perpendicular to the rotor plane (y-z).

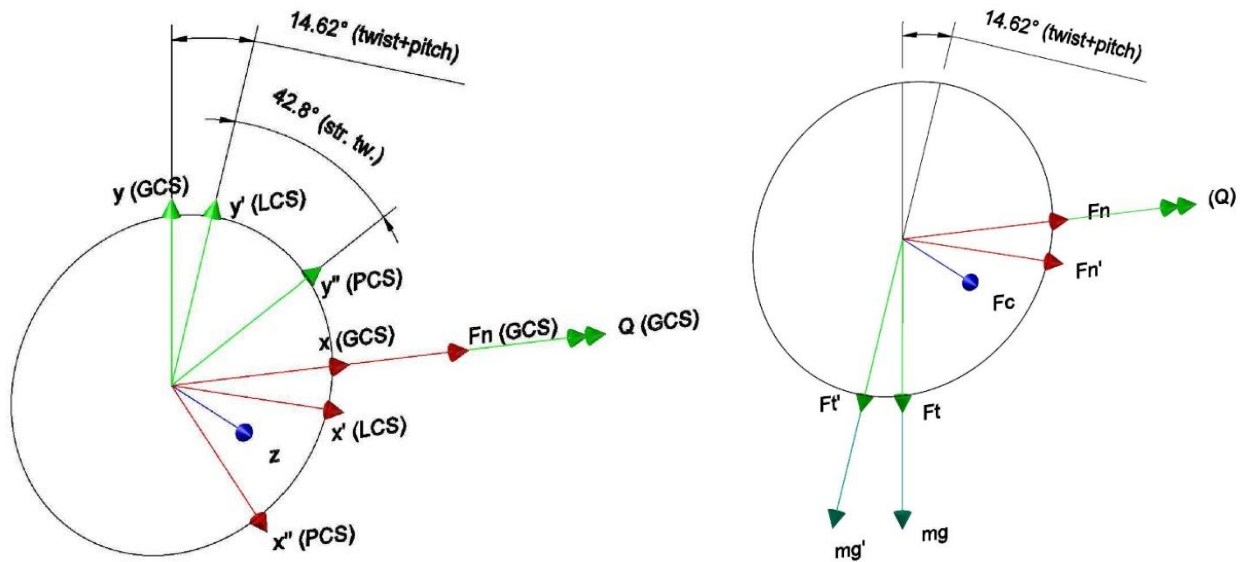


Figure 3.9: Definitions of the coordinate systems GCS, LCS and PCS# at the blade root (left) and transformation of the forces at the blade root to the LCS (right)

(#NOTE: The structural twist at the blade root is 0° because the edge-wise and flap-wise stiffnesses at the blade root are almost identical. But in the figure, the value of 42.8° from a farther span-wise location is used only to demonstrate the differences between the axes.)

Stiffnesses in FOCUS and PHATAS are defined along the chord-line (local coordinate system - LCS) taking into account the twist angle. Stiffnesses from INNWIND are given along the principal axes (principal coordinate system - PCS) with respect to the structural twist angle. The necessary transformations are made as shown in equation (3.9). The principal axis, by definition, is the axis of a beam's cross section that has the largest bending stiffness and the axis perpendicular to it. The structural twist angles with respect to the chord are given by INNWIND.

Furthermore, for the new concepts the same analysis was done for 51 elements. Linear interpolations were applied in the RWT geometry and loads to provide a proper element-by-element analysis.

The forces are taken from the operating conditions (wind speed, rotor speed, and pitch angle) that exhibit the maximum flap-wise blade root bending moment (and most often thrust). The axial/normal force distribution ($F_{n,GCS}$) on the rotor is given in the centre of each of the 40 stations along the RWT rotor. Firstly, it is divided by 3 to account for each blade and then multiplied by the length of the element (l_{elm}). Index d denotes per unit length distribution ($F_{n,d,GCS}$ in N/m), while the elm index denotes per-element distribution ($F_{n,elm,GCS}$ in N/elm).

$$F_{n,elm,GCS} = \frac{F_{n,d,GCS}}{3} l_{elm} \quad (3.1)$$

Then, the aerodynamic twist (θ_T) of each section and the blade pitch angle (θ_p) shown in Table 2.3 are used to transform the normal force from the GCS to the LCS (perpendicular to the chord line). A component of the tangential force ($F_{t,elm,GCS}$) is also added and the two angles are considered positive downwind. The tangential force here is in the GCS and also contains the weight force of each blade section. The details are given shortly after. The accent (') in the forces is used to distinguish between LCS and GCS components (see Figure 3.10).

$$F'_{n,elm,LCS} = F_{n,elm,GCS} \cos(\theta_T + \theta_P) + F_{t,elm,GCS} \sin(\theta_T + \theta_P) \quad (3.2)$$

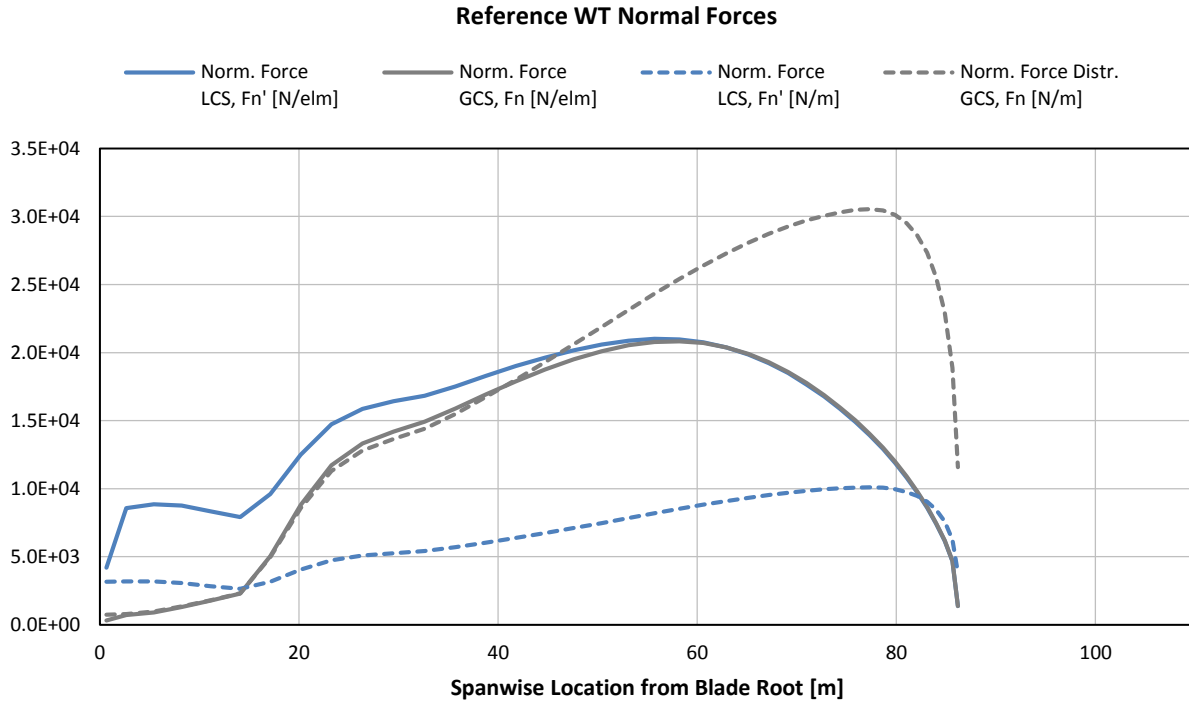


Figure 3.10: The normal forces per element and per unit length in the local and global coordinate system for the RWT blade, containing a small weight component in the LCS distributions

Similarly, since torque Q is given by BOT as a per unit length distribution (Q_d in Nm/m), it is firstly divided by 3, the number of blades. Then it is divided by the distance of each element from the rotor centre (r_{elm}). Hence, the tangential force at the GCS per unit length (N/m) is obtained.

$$F_{t,d,GCS} = \frac{Q_{d,GCS}}{3r_{elm}} \quad (3.3)$$

In the same coordinate system, the weight force of each blade element (mass per unit length m_d , times gravity constant g , times element length l_{elm}) is added to the tangential force. For the RWT blade, the mass distribution is known. For the other design concepts, an iteration of about 5 times is required, using the RWT mass distribution values as a starting point. Again, the components are multiplied with the element length (l_{elm}) to get the distribution per element. The worst loading scenario is defined while the leading edge of the blade is facing and moving downwards (at 90° azimuth) so that the weight is added to the tangential force.

$$F_{t,elm,GCS} = F_{t,d,GCS} l_{elm} + m_d g l_{elm} \quad (3.4)$$

Lastly, the GCS components are transformed to the LCS by accounting for the aerodynamic twist and pitch angle at the given operating point.

$$F'_{t,elm,LCS} = F_{t,elm,GCS} \cos(\theta_T + \theta_P) - F_{n,elm,GCS} \sin(\theta_T + \theta_P) \quad (3.5)$$

Figure 3.11 illustrates the different states of the tangential force when different distributions, coordinate systems and the weight are considered.

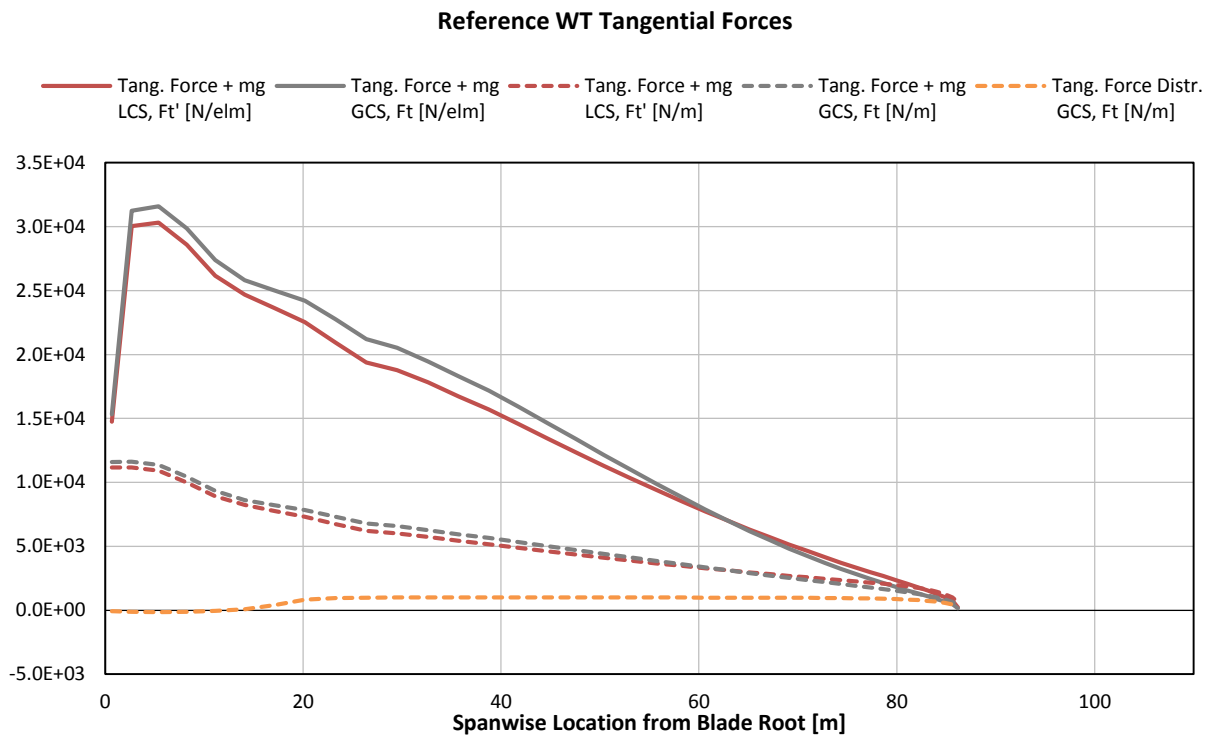


Figure 3.11: The tangential forces (including the weight where indicated) per element and per unit length in the global and local coordinate system for the RWT blade

3.2.3 Step 2: The Bending Moments, Stiffnesses and Strains

From the bending theory and mechanics it is known that the forces exert a moment on the blade segments cumulatively while moving from the tip to the blade root. A numerical method is employed to add up all the increments of the moments. The force on the most outboard element exerted on the centre of the element gives a moment on the first section. For the second section, there are two moments. One comes from the first force with a distance from the first element centre to the second section. The second moment comes from the second force with a distance from the second element centre to the second section.

A short example for the edge-wise moment M_x and the first 3 outboard elements is given below. Again, the x-axis is defined perpendicular to the chord line (parallel to and along the wind flow), y-axis is parallel to the chord line and z-axis is defined along the blade span. Distance r is the distance of an element centre from the blade root. Distance s is the distance of a section in between elements from the blade root. Figure 3.12 helps to visualise this process.

$$\begin{aligned}
 M_x(s_1) &= F'_{t,1,LCS} \cdot (r_1 - s_1) \\
 M_x(s_2) &= F'_{t,1,LCS} \cdot (r_1 - s_2) + F'_{t,2,LCS} \cdot (r_2 - s_2) \\
 M_x(s_3) &= F'_{t,1,LCS} \cdot (r_1 - s_3) + F'_{t,2,LCS} \cdot (r_2 - s_3) + F'_{t,3,LCS} \cdot (r_3 - s_3)
 \end{aligned}
 \tag{3.6}$$

(#NOTE: The numbering order of indices in these equations does not correspond to the definitions of PHATAS given in Figure 2.8. This dissonance is employed here only to serve the functionality of the mathematical sum formula.)

For $j = 1 \dots 40$ elements, the results are shown in Figure 3.13 and the more generalised form for the flap-wise (M_y) and edge-wise (M_x) bending moments at any span-wise location s_j is:

$$\begin{aligned}
 M_y(s_j) &= \sum_{i=1}^j [F'_{n,i,LCS} \cdot (r_i - s_j)] \\
 M_x(s_j) &= \sum_{i=1}^j [F'_{t,i,LCS} \cdot (r_i - s_j)]
 \end{aligned}
 \tag{3.7}$$

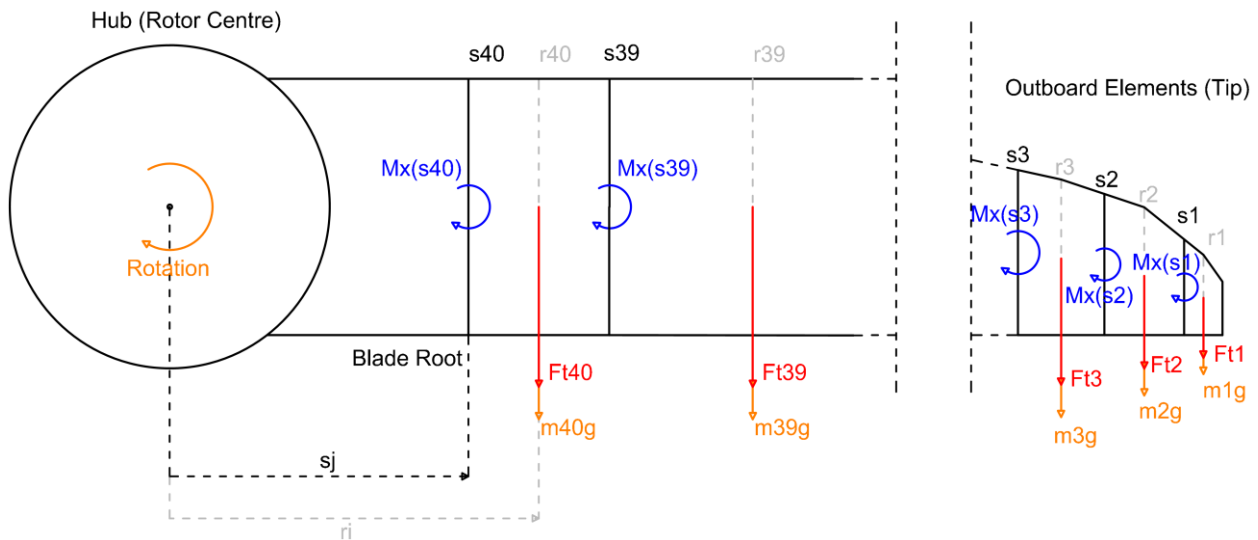


Figure 3.12: Conceptual representation of the blade's most inboard and most outboard elements and edge-wise loads

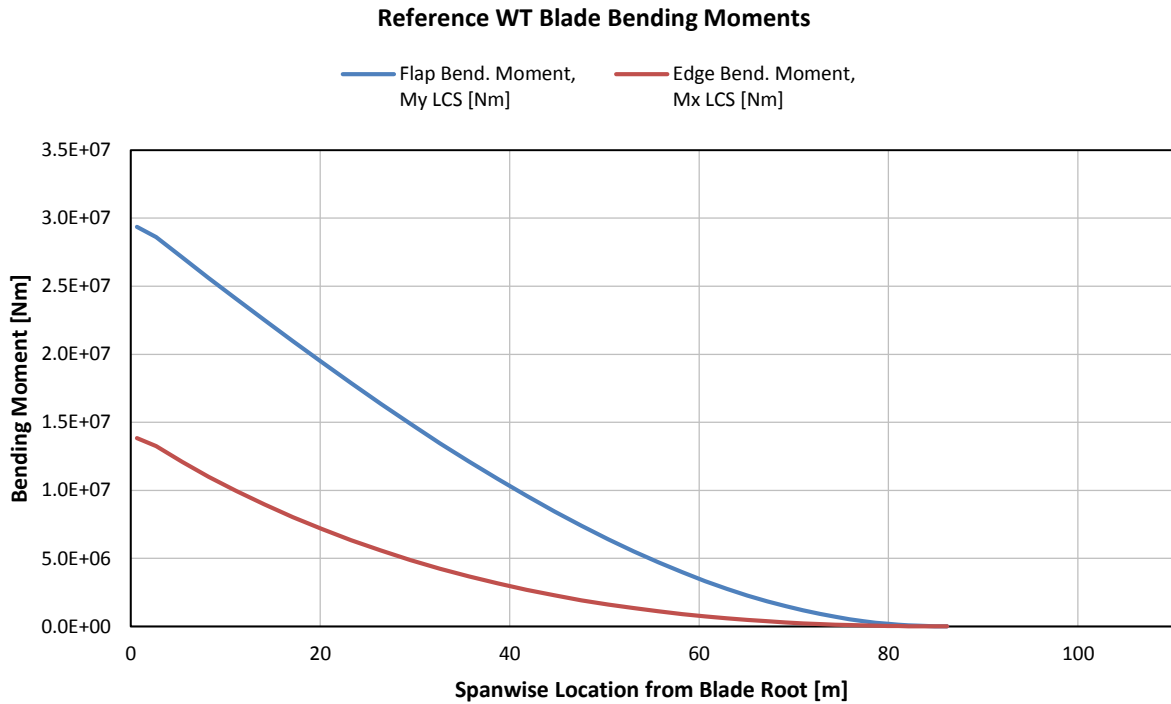


Figure 3.13: Flap-wise and edge-wise bending moment distributions for the RWT blade

The bending moment distributions, calculated above, are used in combination with the bending stiffnesses (EI_{yy} , EI_{xx} and coupled EI_{xy}) to calculate the strains on the cross sections of the blade elements. Also, the centrifugal force (F_c) is taken into account. The centrifugal forces are superimposed to the tensile strain/stress applied on the cross sections. Tensile strain in the flap-wise direction (ε_{zx}) appears on the pressure side of the aerofoil. With the blade moving downwards, tensile strain in the edge-wise direction (ε_{zy}) appears on the trailing edge. It is considered to be higher because of the greater distance from the aerodynamic centre where the forces are modelled to be exerted, hence a greater moment. The centrifugal forces in Figure 3.14 derive from the multiplication of the mass with the square of the rotational speed (rad/s) and the distance of the centre of gravity of the element from the rotor centre, similarly to the bending moments. The reaction forces add up on the blade root. The proper formula is again an integral, but instead, the sum is used due to the numerical sectional approach. Only the normal, span-wise component is taken into account. The perpendicular component of the centrifugal force due to the coupling effect of bending is not considered.

$$F_c(s_j) = \omega^2 \sum_{i=1}^j [m_i(r_i - s_j)] \quad (3.8)$$

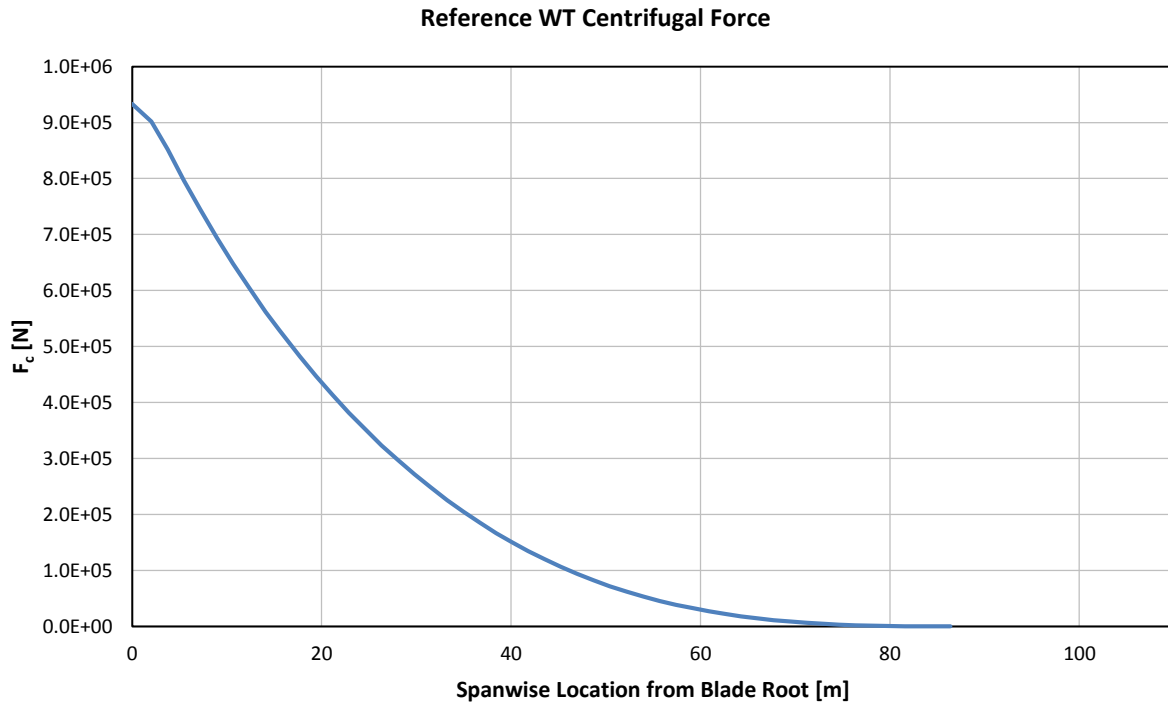


Figure 3.14: The centrifugal force distribution of the RWT

Now with the most important static and steady-state forces defined, it is useful to see how the bending stiffnesses are shaped because they play a fairly important role in the modelling process. The stiffnesses from DTU data are given in the principal axis, along with the structural twist angle (not to be confused with the aerodynamic twist angle). As mentioned earlier, the principal axis is defined at an angle where the cross section displays its largest stiffness. The structural twist (θ_{st}) given by DTU is the angle between the principal axis and the chord-line and the aerodynamic twist angle is defined from the chord line to the plane of rotation as shown in Figure 3.9. PHATAS accepts “flat-wise” and “edge-wise” stiffnesses as inputs; around the chord and perpendicular to it respectively, referring to the LCS. In contrast, the “flap-wise” and “lead-wise” terms refer to the GCS. A Mohr circle transformation for the area moment of inertia is employed to calculate the flat-wise and edge-wise stiffnesses and a crossing (coupling) stiffness is introduced to account for the changes due to the transformation. Young’s modulus E is assumed uniform around the cross section.

$$\begin{aligned}
 EI_{yy,LCS} &= \frac{EI_{xx,PCS} + EI_{yy,PCS}}{2} - \frac{EI_{xx,PCS} - EI_{yy,PCS}}{2} \cos 2\theta_{st} \\
 EI_{xx,LCS} &= \frac{EI_{xx,PCS} + EI_{yy,PCS}}{2} + \frac{EI_{xx,PCS} - EI_{yy,PCS}}{2} \cos 2\theta_{st} \\
 EI_{xy,LCS} &= \frac{EI_{yy,PCS} - EI_{xx,PCS}}{2} \sin 2\theta_{st}
 \end{aligned} \tag{3.9}$$

Below, in Figure 3.15, the bending stiffnesses in the global and local CS are given.

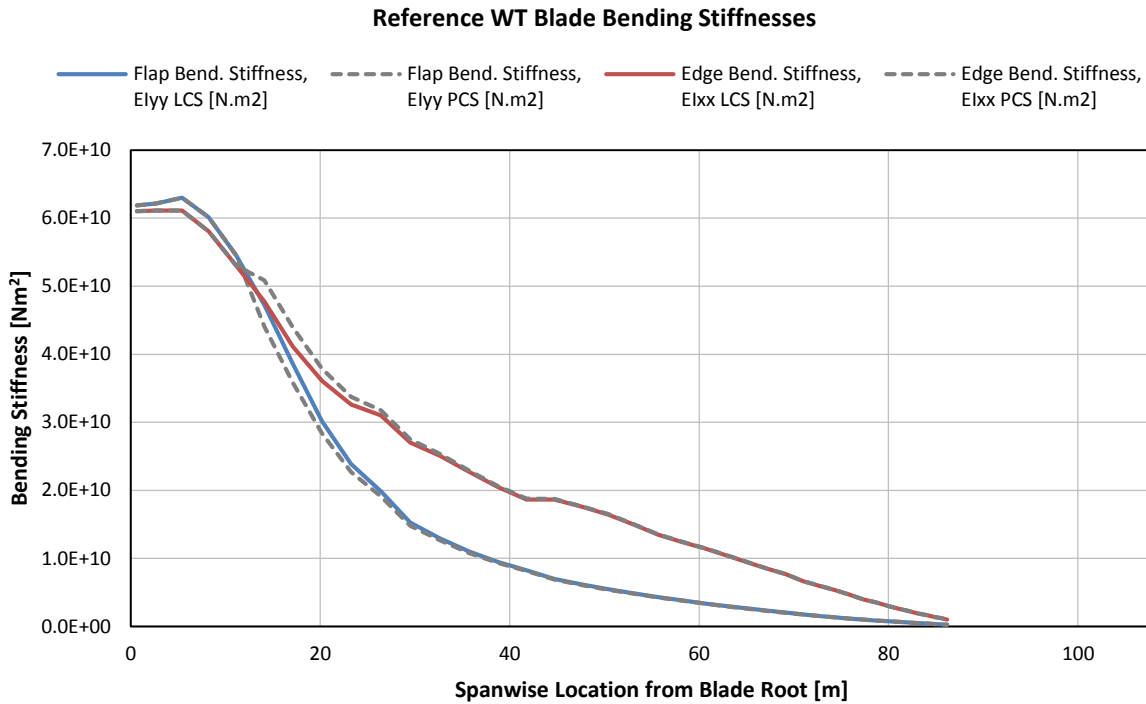


Figure 3.15: The flap-wise and edge-wise bending stiffness distributions of the RWT blade for the global and local CS

In order to up-scale the blade to the new designs, the resulting strain from the aerodynamic, gravitational and centrifugal forces is chosen to remain constant as a design driver to maintain a similar structural response. The strain is the elongation of a part of the material divided by the original length of this part ($\varepsilon = \Delta l / l$) and is directly proportional to the normal stress σ on the blade cross section divided by Young's modulus of elasticity E . In this case, it also means that, because the number of elements stays the same, while their length increases, a higher absolute elongation is implied from any higher new loads. Equation (3.10) holds for the elastic region of Hooke's law (applicable for GFRP composites) and connects the normal stress on a cross section area with Young's modulus, strain and also the axial/span-wise force and axial stiffness EA . Equation (3.11) connects stress, moment, distance from neutral axis (d_x or d_y) and area moment of inertia (I_{yy} or I_{xx}). By rearranging it, one can connect the strain and the bending stiffness (EI_{yy} or EI_{xx}).

$$\sigma = E\varepsilon \Rightarrow \frac{F}{A} = E\varepsilon \Rightarrow \varepsilon = \frac{F}{EA} \quad (3.10)$$

$$\sigma_{zx} = \frac{M_y d_x}{I_{yy}} \Rightarrow \varepsilon_{zx} = \frac{M_y d_x}{EI_{yy}} \quad (3.11)$$

The strain distribution coming from the flap-wise moment M_y and centrifugal force F_c , where t is the thickness of the aerofoil, is:

$$\varepsilon_{zx} = \frac{M_y 0.5t}{EI_{yy}} + \frac{F_c}{EA} \quad (3.12)$$

For the strain distribution coming from the edge-wise moment M_x and centrifugal force F_c in the cylindrical part of the blade root, where c is the chord length of the aerofoil:

$$\varepsilon_{zy} = \frac{M_x 0.5c}{EI_{xx}} + \frac{F_c}{EA} \quad (3.13)$$

For the strain distribution coming from the edge-wise moment M_x and centrifugal force F_c in the part of the blade from maximum chord until the tip:

$$\varepsilon_{zy} = \frac{M_x 0.75c}{EI_{xx}} + \frac{F_c}{EA} \quad (3.14)$$

For the part of the blade from the end of the cylindrical cross section until the maximum chord, the cross section is considered to be lofting as an elliptical shape (from cylinder to aerofoil shape). The distance of the aerofoil skin from neutral axis d_y is linearly interpolated from 50% of the chord up to 75% as done for the NREL 5 MW machine, reported in [36]. The strain distributions that derive are shown in Figure 3.16.

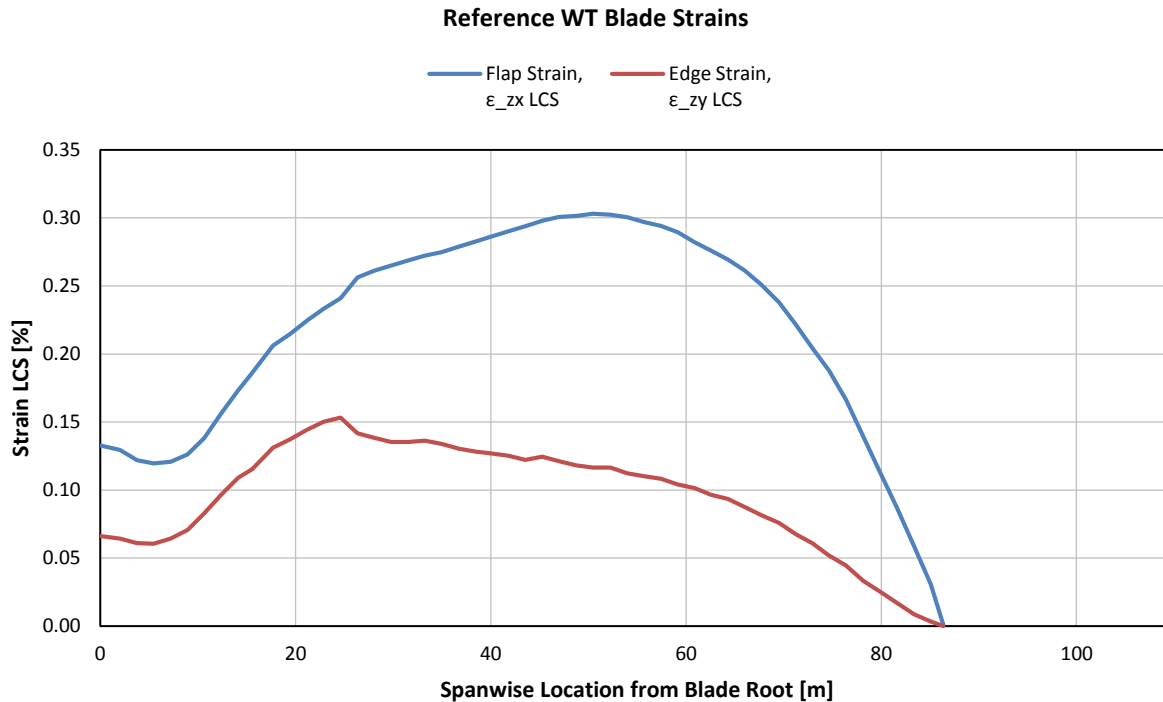


Figure 3.16: The edge-wise and flap-wise strain distributions along the span of the RWT blade

3.2.4 Step 3: Towards the new blades

Concerning the loads, the same procedure is repeated for the proposed designs. The aerodynamic steady state loads are processed with the data of the new geometries and operating conditions that correspond to the maximum flap-wise moment. The original mass distribution of the RWT as weight force is also included in the tangential force but is iteratively calculated to converge to the new masses. All the new loads are also projected in the LCS. The centrifugal force is calculated with the new rotor speeds, masses and distances.

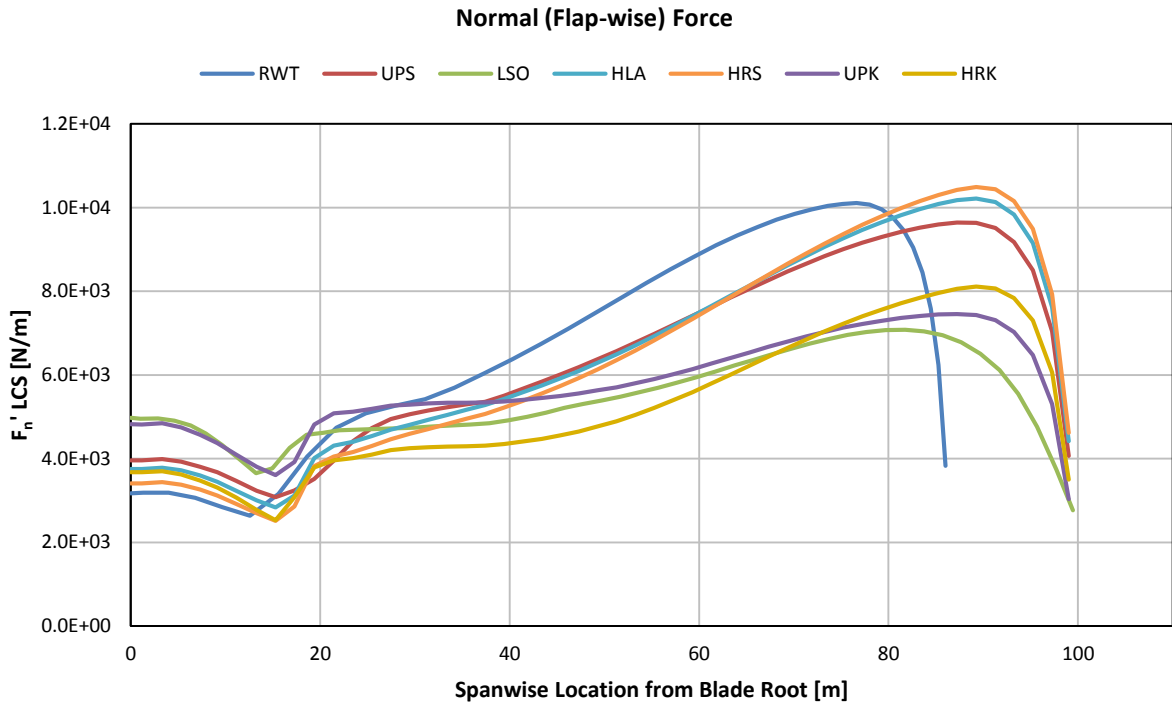


Figure 3.17: The normal force per unit length distributions of the designs in comparison (including the weight component)

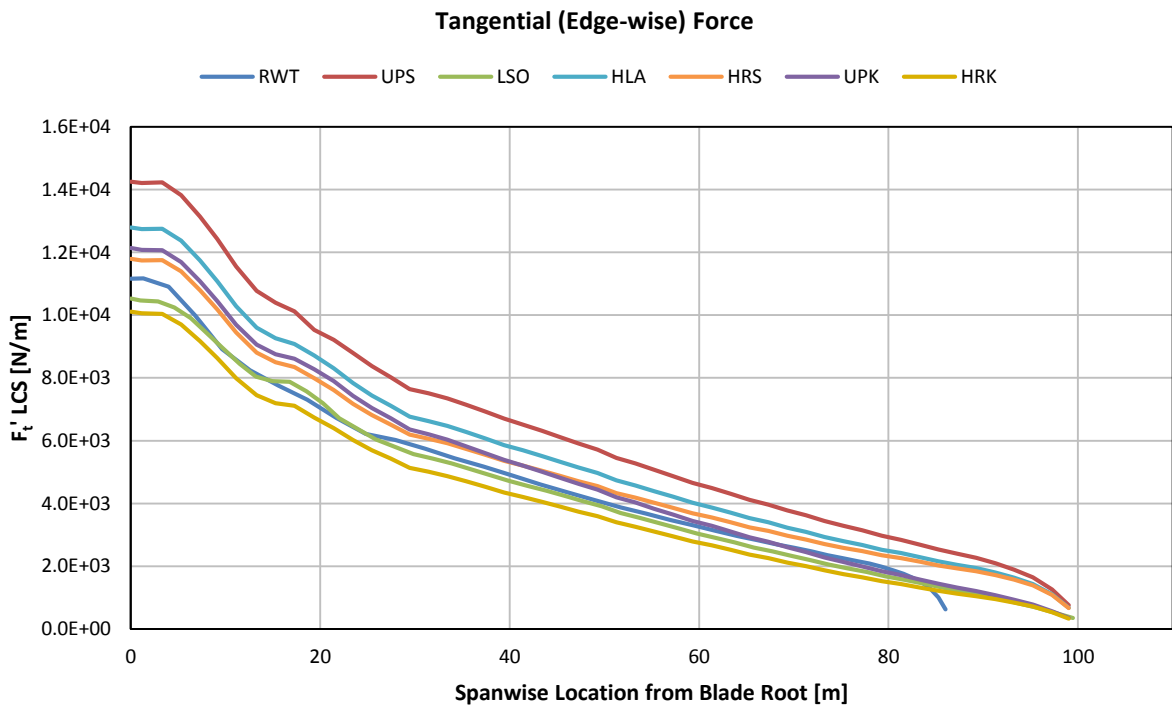


Figure 3.18: The tangential force (including the weight) per unit length distributions of the designs in comparison

It's worth noticing that the normal force distribution of the LSO and peak-shaved concepts (UPK, HRK) is considerably lower than the one of the RWT (see Figure 3.17). This is mainly due to LSO's

higher twist angle and the peak-shaving strategy for the other two that is in operation at this point. Also, the tangential force distribution (Figure 3.18) of the same concepts along with the bending moment distributions (see Figure 3.19 and Figure 3.20 below) show a similar grouping, corresponding to the main driver of the LSO, UPK and HRK designs. That is to keep the loads at a level close to the reference rotor with relatively low mass. In Figure 3.21, one can see the minimal difference of the centrifugal forces for the same TSR. As stated in [26], when the tip speed ratio is kept constant, the centrifugal forces should increase by a factor of R^2 because mass increases by R^3 , radius increases by R^1 and rotor speed decreases by R^2 . But this is not exactly the case here because the mass does not follow the R^3 law and the centrifugal force is calculated at somewhat different rotor speeds. But for the faster rotating concepts (HLA, HRS and HRK), one can see a distinguishable increase in the centrifugal force. Furthermore, its contribution to the strain is small (0.005 - 0.01%), and this implies that it could be left out of the analysis altogether when up-scaling within reasonable ranges. However, here it is included for a more precise view.

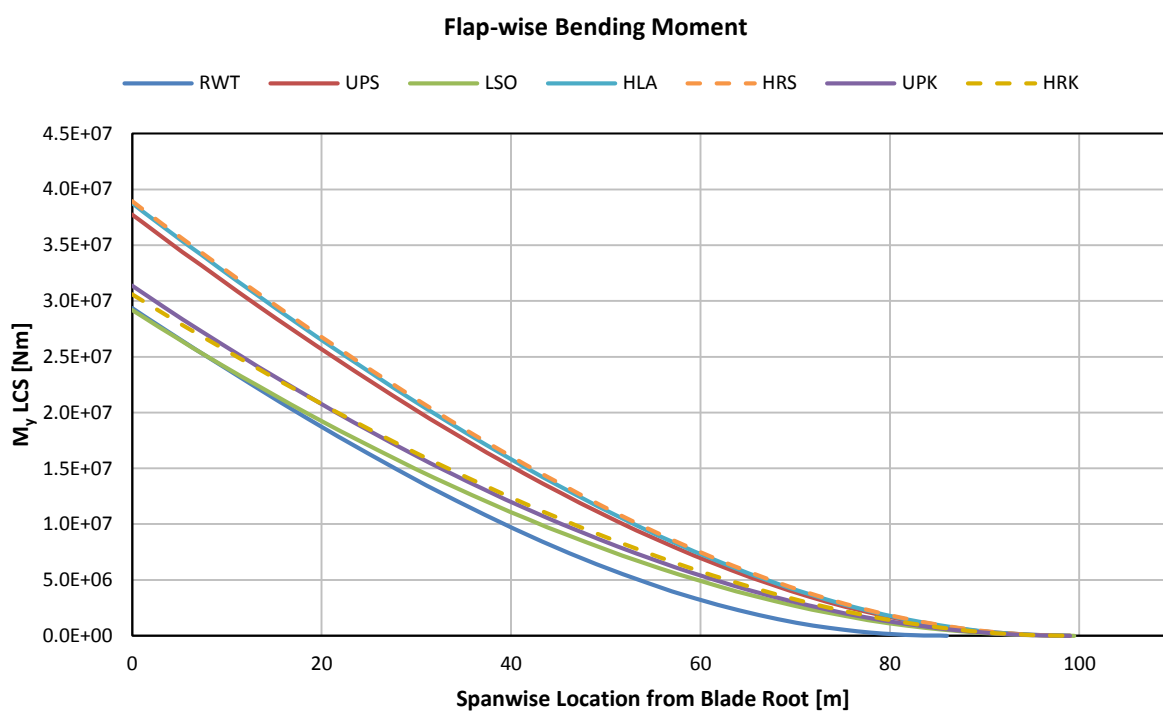


Figure 3.19: The flap-wise bending moment distributions of the designs in comparison

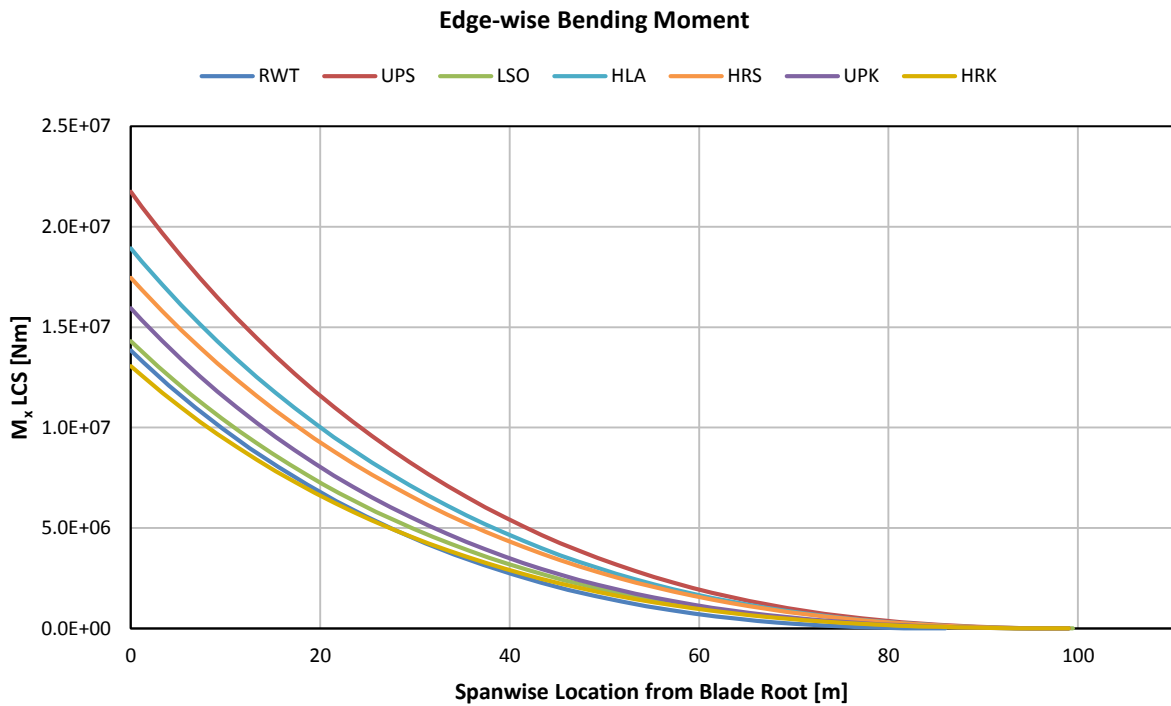


Figure 3.20: The edge-wise bending moment distributions of the designs in comparison

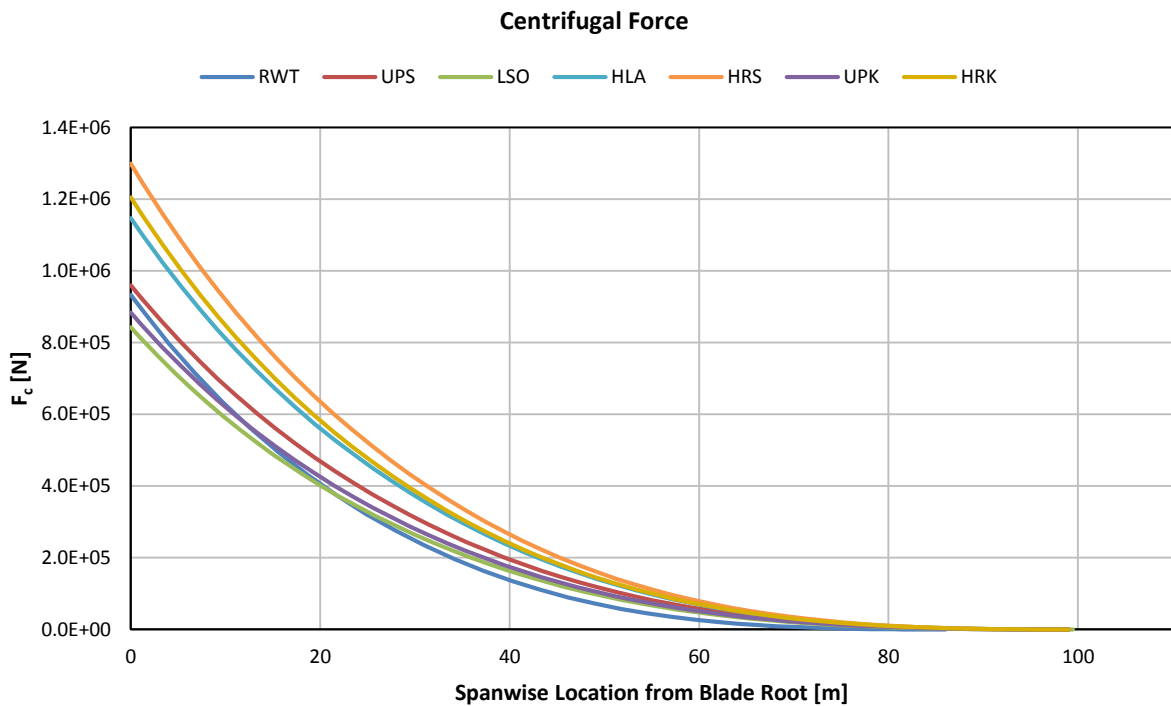


Figure 3.21: The centrifugal force distributions of the designs in comparison

The main difference with the previous analysis is that the strains on the blades are now considered as given and they contribute to calculate the new stiffnesses required (Figure 3.22 and Figure 3.23). The asterisk (*) indicates the new property values, those of the proposed designs.

$$EI_{yy}^* = \frac{M_y^* 0.5t^*}{\varepsilon_{zx} - \frac{F_c^*}{EA^*}} \quad (3.15)$$

Close to the blade root:

$$EI_{xx}^* = \frac{M_x^* 0.5c^*}{\varepsilon_{zy} - \frac{F_c^*}{EA^*}} \quad (3.16)$$

From the maximum chord location until the tip:

$$EI_{xx}^* = \frac{M_x^* 0.75c^*}{\varepsilon_{zy} - \frac{F_c^*}{EA^*}} \quad (3.17)$$

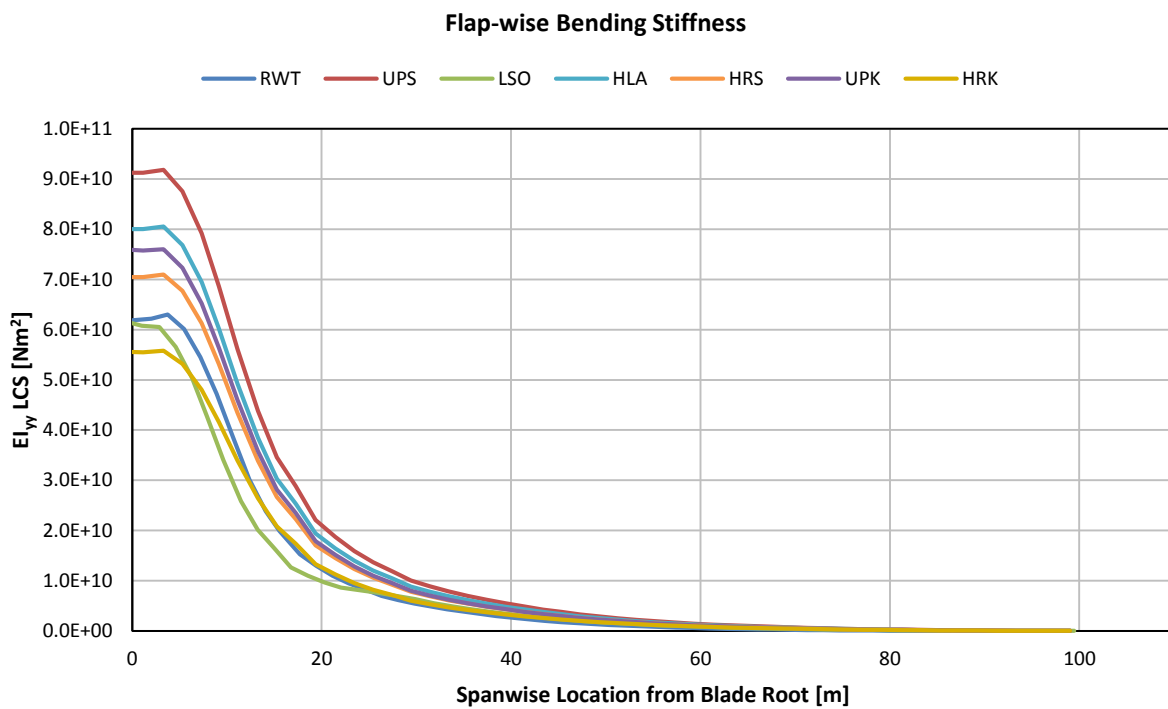


Figure 3.22: The flap-wise bending stiffness distributions of the designs in comparison

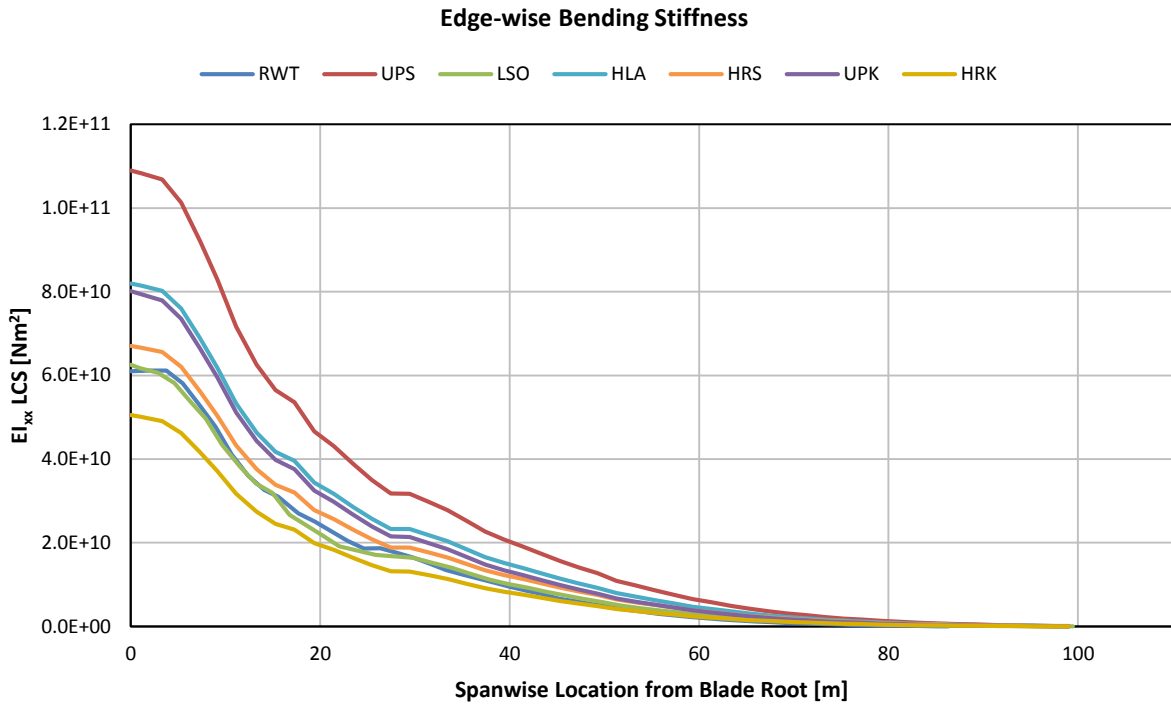


Figure 3.23: The edge-wise bending stiffness distributions of the designs in comparison

3.2.5 Step 4: Proportional Factors Analysis

From the previous analysis, two factors R_f and R_e can be defined (indices “f” and “e” refer to flap and edge) that represent the ratio between the up-scaled and the reference stiffness. By dividing the new calculated up-scaled stiffnesses with the initial ones of the reference blade, one gets up-scaling factors R_f and R_e (different for each element along the blade span). Young’s modulus can be dropped from the following relations, assuming that the proportionality and allocation of materials used within each element, stays the same. So the strain-dependent calculated stiffnesses will give the numerical values for R_f and R_e .

For the flap-wise stiffness:

$$EI_{yy}^* = R_f EI_{yy} \Rightarrow R_f = \frac{EI_{yy}^*}{EI_{yy}} \Rightarrow R_f = \frac{I_{yy}^*}{I_{yy}} \quad (3.18)$$

And for the edge-wise stiffness:

$$EI_{xx}^* = R_e EI_{xx} \Rightarrow R_e = \frac{EI_{xx}^*}{EI_{xx}} \Rightarrow R_e = \frac{I_{xx}^*}{I_{xx}} \quad (3.19)$$

The blade’s inner structure (spar cap and skin thickness) can be approximated as an arbitrary thin-walled rectangular cross-section. Height h corresponds to the chord (NOT necessarily equal), width b corresponds to the total aerofoil thickness and cross section wall thickness t corresponds to aerofoil skin, spar cap and shear web “effective thicknesses”, with t small compared to h and b . The term “effective thickness” refers to a structural response of the blade approximated as a rectangular

hollow beam, similar to the structural response emanating from its real structure. The rectangular cross-section was chosen for simplicity in order to be used in combination with flap- and edge-wise loads and stiffnesses. Still, the x-axis refers to the thickness/wind flow direction and the y-axis refers to the chord line. One can imagine squeezing all the mass of the real aerofoil cross section and inner structure into the one in Figure 3.24, in such a way that the h , b and t dimensions correspond to and behave structurally like the calculated stiffnesses. The method can be made more precise by assuming different initial wall thicknesses t_1 and t_2 for x-axis and y-axis respectively.

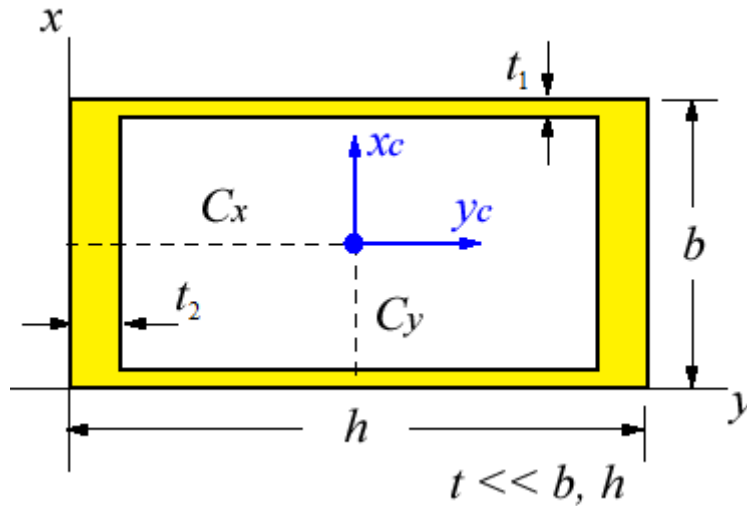


Figure 3.24: Concept of the thin-walled rectangular cross section

The edge-wise area moment of inertia is:

$$I_{xx} = 2 \left[\frac{bt_2^3}{12} + bt_2 \left(\frac{h}{2} \right)^2 \right] + 2 \frac{t_1 h^3}{12} \Rightarrow I_{xx} = \frac{bt_2^3}{6} + \frac{bt_2 h^2}{2} + \frac{t_1 h^3}{6} \Rightarrow I_{xx} = \frac{bt_2^3 + 3bt_2 h^2 + t_1 h^3}{6} \quad (3.20)$$

And similarly, the flap-wise one:

$$I_{yy} = \frac{ht_1^3 + 3ht_1 b^2 + t_2 b^3}{6} \quad (3.21)$$

Factors R_f and R_e can themselves be comprised of partial factors R_x and R_y that contribute to their respective axis, following the R^4 linear rule that is generally held for the stiffness or area moment of inertia up-scaling. This idea serves a double purpose. Firstly, the general stiffness factors R_f and R_e are broken down and will be used to up-scale every geometrical property individually and independently for x- and y-axes (e.g. centres of gravity, elastic centres etc.). This will also be done more precisely because they involve the structural behaviour of the blade and not just the geometry. Secondly, they are also detached from the constant factor R_D that comes from up-scaling the rotor diameter. This factor should only operate along the blade span, in the z-direction. This rationale can reflect different proportions in geometries and designs such as the LSO one, with its higher twist. So, one can imagine that the b dimension will increase by R_x , h dimension by R_y and uniform t (or individual t_1 and t_2) will increase by R_x in the x-axis and R_y in the y-axis. Again, the asterisk (*) indicates the new up-scaled properties.

$$b^* = R_x b$$

$$h^* = R_y h$$

(3.22)

$$t_1^* = R_x t \quad \text{or} \quad t_1^* = R_x t_1$$

$$t_2^* = R_y t \quad \text{or} \quad t_2^* = R_y t_2$$

Combining equations (3.20), (3.21) and (3.22) yields the new area moments of inertia (hence stiffnesses):

$$I_{xx}^* = \frac{b^* t_2^{*3} + 3b^* t_2^* h^{*2} + t_1^* h^{*3}}{6} \Rightarrow I_{xx}^* = \frac{R_x b R_y^3 t_2^3 + 3R_x b R_y t_2 R_y^2 h^2 + R_x t_1 R_y^3 h^3}{6} \Rightarrow$$

$$I_{xx}^* = R_x R_y^3 \frac{b t_2^3 + 3b t_2 h^2 + t_1 h^3}{6} \Rightarrow I_{xx}^* = R_x R_y^3 I_{xx}$$

(3.23)

And for the flap-wise direction:

$$I_{yy}^* = R_y R_x^3 \frac{h t_1^3 + 3h t_1 b^2 + t_2 b^3}{6} \Rightarrow I_{yy}^* = R_y R_x^3 I_{yy}$$

(3.24)

The claim above can also be confirmed by the definition of the area moments of inertia, where the R_x and R_y factors come out of the integral as constants.

$$I_{yy} = \int_A x^2 dA \Rightarrow I_{yy} = \iint x^2 dx dy \Rightarrow$$

$$I_{yy}^* = \iint (R_x x)^2 (R_x dx)(R_y dy) \Rightarrow I_{yy}^* = R_x^3 R_y \iint x^2 dx dy \Rightarrow I_{yy}^* = R_x^3 R_y I_{yy}$$

$$\text{and } I_{xx} = \int_A y^2 dA \Rightarrow I_{xx} = \iint y^2 dx dy \Rightarrow \dots \Rightarrow I_{xx}^* = R_y^3 R_x I_{xx}$$

(3.25)

The R^4 rule can be combined here to acquire the numerical values of R_x and R_y through the R_f and R_e factors/proportions coming from equations (3.23) and (3.24).

For flap-wise I_{yy} :

$$R_x^3 R_y = R_f \Rightarrow R_y = \frac{R_f}{R_x^3}$$

(3.26)

And for edge-wise I_{xx} , while plugging in equation (3.26):

$$R_x R_y^3 = R_e \Rightarrow R_x = R_e \frac{1}{R_y^3} \Rightarrow R_x = R_e \left(\frac{R_x^3}{R_f} \right)^3 \Rightarrow R_x = R_e \frac{R_x^9}{R_f^3} \Rightarrow \frac{R_f^3}{R_e} = R_x^8 \Rightarrow R_x = \left(\frac{R_f^3}{R_e} \right)^{\frac{1}{8}}$$

(3.27)

And, by combining the above:

$$R_y = R_f \frac{1}{R_x^3} \Rightarrow R_y = R_f \left(\frac{R_e^3}{R_f^9} \right)^{\frac{1}{8}} \Rightarrow R_y = \left(R_f^8 \frac{R_e^3}{R_f^9} \right)^{\frac{1}{8}} \Rightarrow R_y = \left(\frac{R_e^3}{R_f} \right)^{\frac{1}{8}} \quad (3.28)$$

This is the point where the iterative nature of the method is applied. The new values of I_{yy} and I_{xx} (or EI_{yy} and EI_{xx}) are already calculated from the analysis of loads and strains in equations (3.15), (3.16) and (3.17) and their factors R_f and R_e from equations (3.18) and (3.19). The values of R_y and R_x that come from equations (3.27) and (3.28) are used to up-scale the mass distribution and the axial stiffness EA by the following relations. Where A is the cross section area that grows by both R_x and R_y in the respective directions and R_D is the factor of up-scaling each element in the span-wise direction.

$$m_d^* = m_d \cdot R_x R_y \quad \text{or} \quad m_{elm}^* = m_{elm} \cdot R_x R_y R_D \quad (3.29)$$

$$EA^* = EA \cdot R_x R_y \quad (3.30)$$

Of course, by plugging in R_x and R_y , the weight and centrifugal force are changing and new values are calculated and plugged in again. Convergence is achieved after approximately 5 iterations. This way, two of the most basic structural properties of the new blades are calculated, i.e. stiffnesses and mass distributions.

3.2.6 Step 4: Up-scaling the Other Properties

Since a pair of values of R_x and R_y for every element is obtained, along with the z-axis growth factor R_D , all the properties are modified accordingly.

The coupling stiffness I_{xy} :

$$I_{xy} = \int_A xy dA \Rightarrow I_{xy} = \iint xy dx dy \Rightarrow I_{xy}^* = R_x^2 R_y^2 I_{xy} \quad (3.31)$$

The shear stiffness S is quoted by DTU in the INNWIND database as:

$$S = kGA \quad (3.32)$$

Where k is the flap or edge shear factor, G is the average shear modulus and A is the cross section area. In PHATAS it is quoted as the flap or edge “shear flexibility” and it is the reciprocal of S . Shear factors k_f and k_e and shear modulus G are assumed constant throughout the new concepts.

$$\frac{1}{S} = \frac{1}{kGA} \Rightarrow \frac{1}{S^*} = \frac{1}{kGA^*} \Rightarrow \frac{1}{S^*} = \frac{1}{kG(R_y R_x A)} \quad (3.33)$$

Co-ordinates of the elastic centre, centre of gravity, aerodynamic centre (lag-wise distance of the 25% chord location from the blade axis), shear centre, and radii of gyration squared (about y- and x-axis respectively) within the aerofoil:

$$\begin{aligned}
x_{ec}^* &= R_x x_{ec} & \text{and} & & y_{ec}^* &= R_y y_{ec} \\
x_{cg}^* &= R_x x_{cg} & \text{and} & & y_{cg}^* &= R_y y_{cg} \\
x_{ac}^* &= R_x x_{ac} & \text{and} & & y_{ac}^* &= R_y y_{ac} \\
x_{sc}^* &= R_x x_{sc} & \text{and} & & y_{sc}^* &= R_y y_{sc} \\
r_{delXX}^{*2} &= R_x^2 r_{delXX}^2 & \text{and} & & r_{delYY}^{*2} &= R_y^2 r_{delYY}^2
\end{aligned} \tag{3.34}$$

The latter, concerning the radii of gyration, also holds true because of their definitions:

$$\begin{aligned}
r_{delXX}^2 &= \frac{I_{yy}}{A} \Rightarrow r_{delXX}^{*2} = \frac{R_x^3 R_y I_{yy}}{R_y R_x A} \Rightarrow r_{delXX}^{*2} = R_x^2 \frac{I_{yy}}{A} \Rightarrow r_{delXX}^{*2} = R_x^2 r_{delXX}^2 \\
r_{delYY}^2 &= \frac{I_{xx}}{A} \Rightarrow r_{delYY}^{*2} = \frac{R_y^3 R_x I_{xx}}{R_y R_x A} \Rightarrow r_{delYY}^{*2} = R_y^2 \frac{I_{xx}}{A} \Rightarrow r_{delYY}^{*2} = R_y^2 r_{delYY}^2
\end{aligned} \tag{3.35}$$

Lastly, the torsion constant J_T (or torsional stiffness GJ_T) has to be scaled. For a rectangular thin-walled cross section, it is given by:

$$J_T = \frac{2b^2 h^2 t_1 t_2}{bt_1 + ht_2} \tag{3.36}$$

An extra assumption is employed here to make the calculations somewhat easier. Because h and b correspond to the chord and thickness, the idea can be extended to the point that they are connected between them with the local relative thickness R_T . The same assumption is also made for thicknesses t_1 and t_2 , on the basis that the sum of shear web, trailing and leading edge thicknesses on the chord direction are larger than the added thicknesses of the pressure side and suction side skins. One must keep in mind that this procedure should be used to derive these properties numerically and to scale them in proportion of already known distributions. There may be a considerable error from what a FEM-tool would calculate.

$$\begin{aligned}
b &= R_T h \\
t_1 &= R_T t_2
\end{aligned} \tag{3.37}$$

By making use of equation (3.37), the denominator of equation (3.36) can be rearranged.

$$J_T = \frac{2b^2 h^2 t_1 t_2}{R_T^2 h t_2 + h t_2} \Rightarrow J_T = \frac{2b^2 h^2 t_1 t_2}{(R_T^2 + 1) h t_2} \Rightarrow J_T = \frac{1}{(R_T^2 + 1)} \cdot \frac{2b^2 h^2 t_1 t_2}{h t_2} \tag{3.38}$$

As for the new torsion constant:

$$\begin{aligned}
J_T^* &= \frac{2b^* h^* t_1^* t_2^*}{b^* t_1^* + h^* t_2^*} \Rightarrow J_T^* = \frac{2 \cdot (R_x^2 b^2) \cdot (R_y^2 h^2) \cdot (R_x t_1) \cdot (R_y t_2)}{R_x^2 b t_1 + R_y^2 h t_2} \Rightarrow J_T^* = \frac{R_x^3 R_y^3 2b^2 h^2 t_1 t_2}{R_x^2 R_T^2 h t_2 + R_y^2 h t_2} \Rightarrow \\
J_T^* &= \frac{R_x^3 R_y^3}{(R_x^2 R_T^2 + R_y^2)} \cdot \frac{2b^2 h^2 t_1 t_2}{h t_2}
\end{aligned} \tag{3.39}$$

By dividing equation (3.39) with equation (3.38):

$$\frac{J_T^*}{J_T} = \left(\frac{R_x^3 R_y^3}{R_x^2 R_T^2 + R_y^2} \cdot \frac{2b^2 h^2 t_1 t_2}{ht_2} \right) \cdot \left((R_T^2 + 1) \frac{ht_2}{2b^2 h^2 t_1 t_2} \right) \Rightarrow J_T^* = J_T \frac{R_x^3 R_y^3 \cdot (R_T^2 + 1)}{(R_x^2 R_T^2 + R_y^2)} \quad (3.40)^\#$$

(#NOTE: The R_T above is the relative thickness of the reference blade.)

Use of equation (3.40) results in the following distributions shown in Figure 3.25.

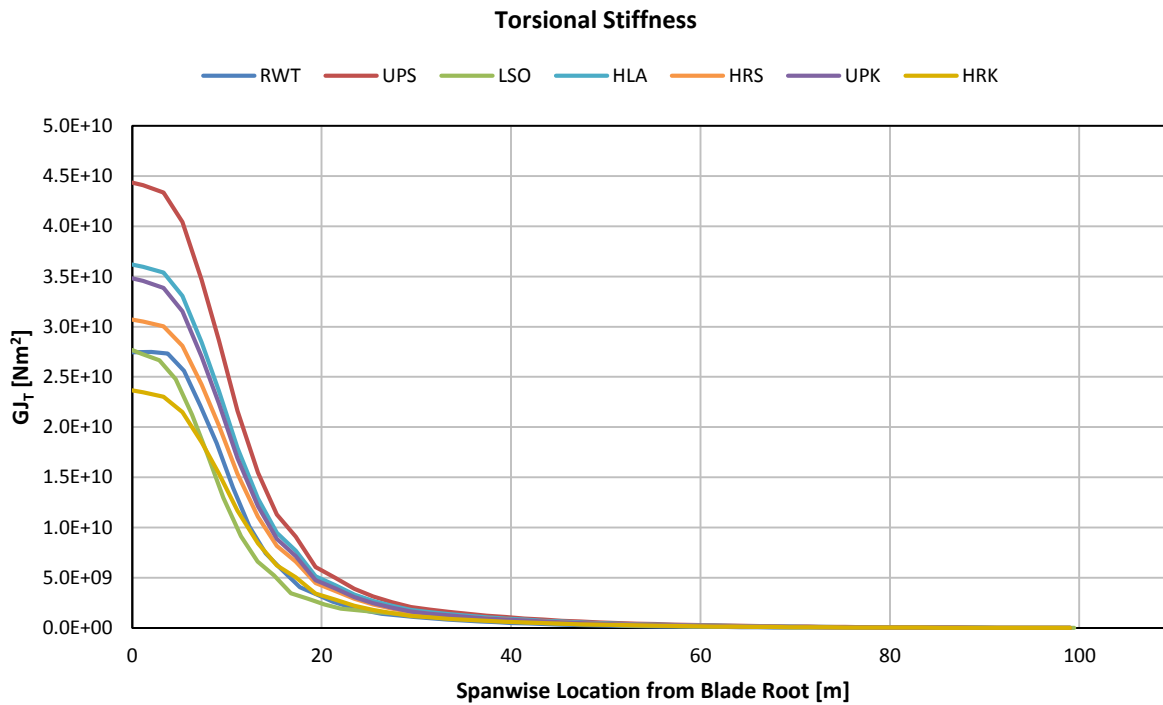


Figure 3.25: The torsional stiffness distribution of the designs in comparison

This analysis of course is made to project the new distributed properties needed for analysis in PHATAS, but most importantly to obtain the new blade masses that are the main penalty in the cost model of INNWIND. The calculated masses and distributions follow in Figure 3.26, Table 3.6 and Figure 3.27. The result of the linear up-scaling law s^3 is also included.

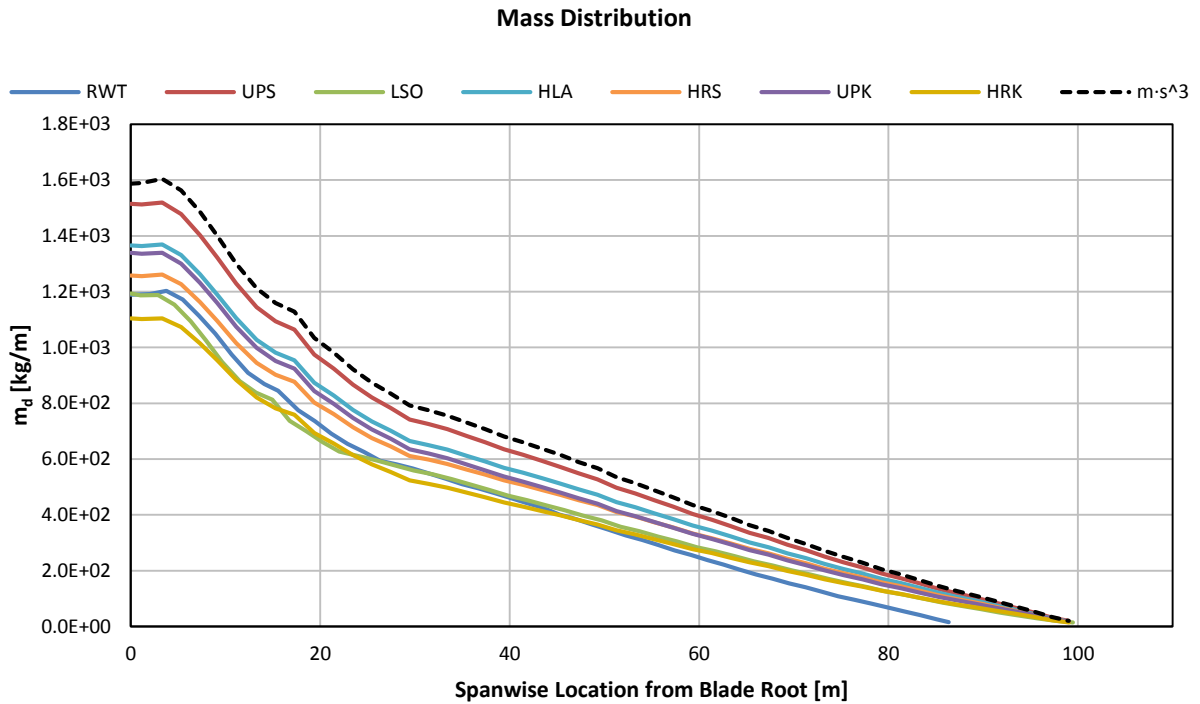


Figure 3.26: The blade mass per unit length distribution of the designs and of the classical up-scaling law (s^3) in comparison

Table 3.6: The resulting Blade Masses

Concept / Parameter	Blade Mass [kg]	Net Change [%]	Average per Unit Length Change [%]	Scaling Factor ($s=1.15515$) Exponent λ
RWT	41,722	-	-	-
UPS	60,348	+44.64	+25.21	2.559
LSO	45,309	+8.60	-5.99	0.572
HLA	54,167	+29.83	+12.39	1.810
HRS	49,871	+19.53	+3.48	1.237
UPK	51,612	+23.70	+7.09	1.475
HRK	42,695	+2.33	-11.41	0.160
$m \cdot s^3$	64,311	+54.14	+33.44	3.000

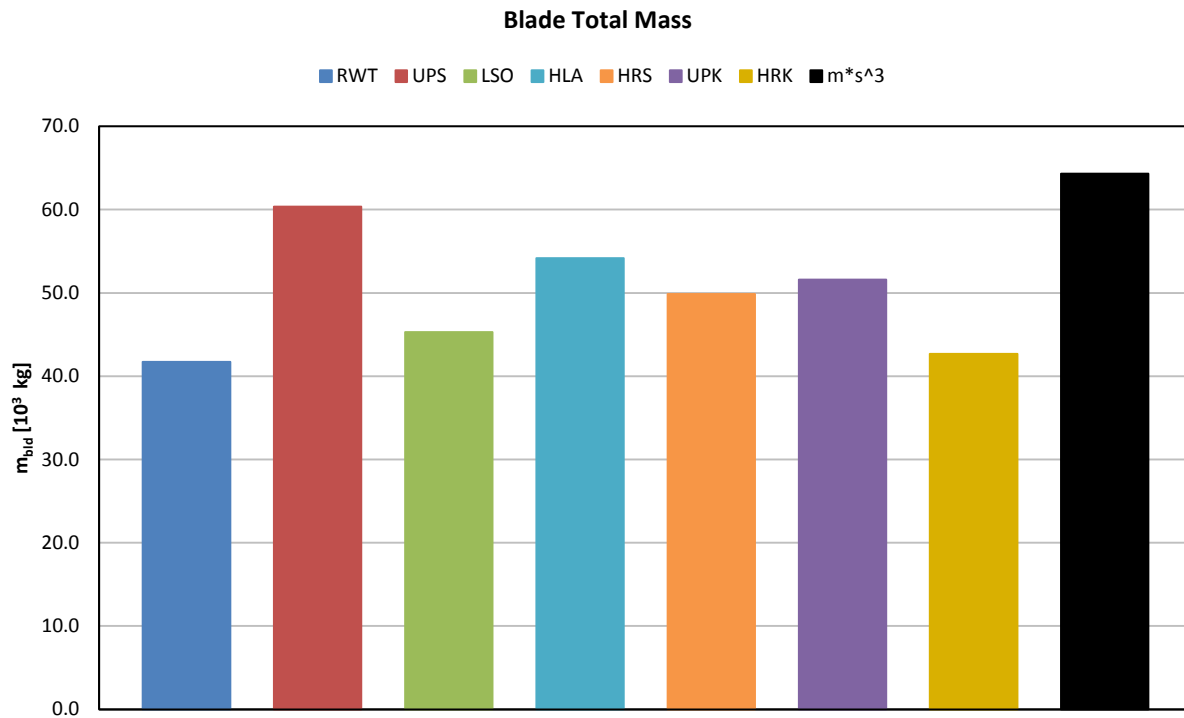


Figure 3.27: The total blade mass of the designs and of the classical up-scaling law (s^3) in comparison

It is interesting to notice that the blade mass of UPS concept, which is a pure geometric up-scale in all 3 dimensions, is relatively close to but less than what the linear up-scaling law would give. Another aspect is the furtherly reduced necessary mass of the UPK, since the loads are kept lower with peak-shaving. Whether the results of the whole process produce structurally sound properties will be evaluated further in the report. All the detailed tabular data of the properties can be found in Appendix A.1.

3.3 A Case-Study for the Validation of the Up-scaling Method

In order to investigate the method's effect on a larger scaling extent, a short validation exercise was performed. It involved down-scaling the 10 MW INNWIND RWT to a 5 MW design with the UpWind machine characteristics and the up-scaling of the 5 MW UpWind turbine to a 10 MW machine with the INNWIND characteristics. The results are presented below in brief. There was no further modal analysis, time-domain simulations or LCoE estimation for this case-study.

3.3.1 From 10 to 5 MW Down-scaling

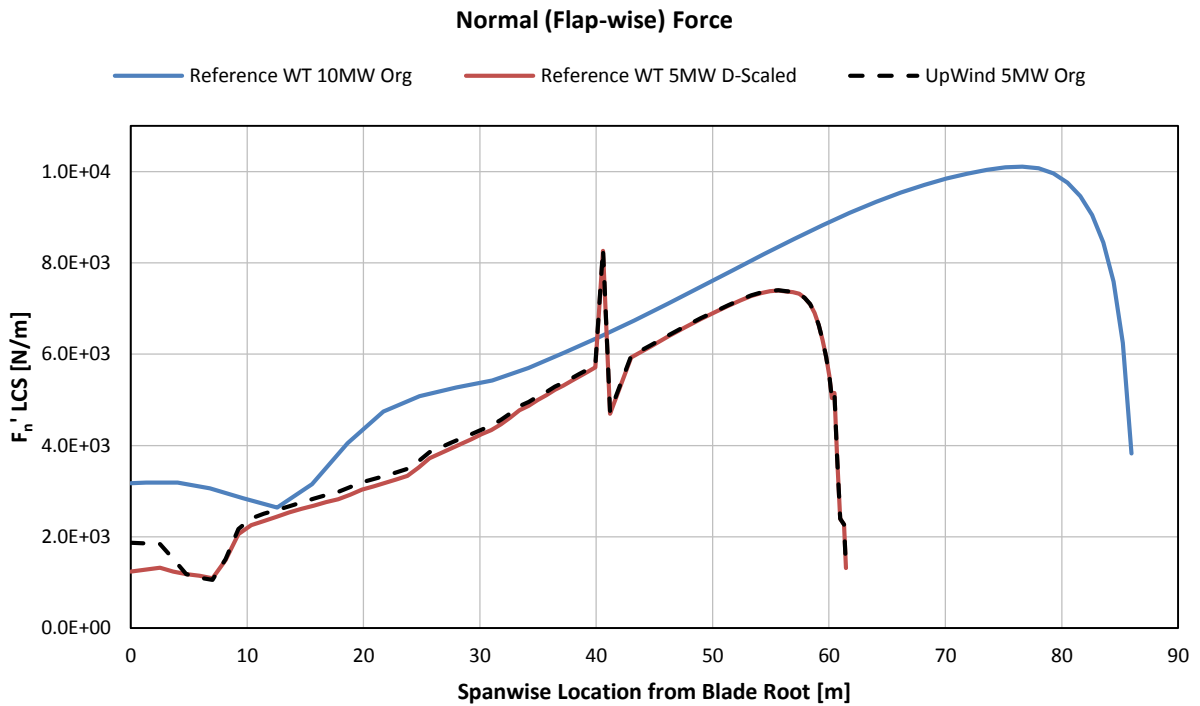


Figure 3.28: The normal forces on the blades for the RWT, UpWind 5 MW and down-scaled RWT to 5 MW

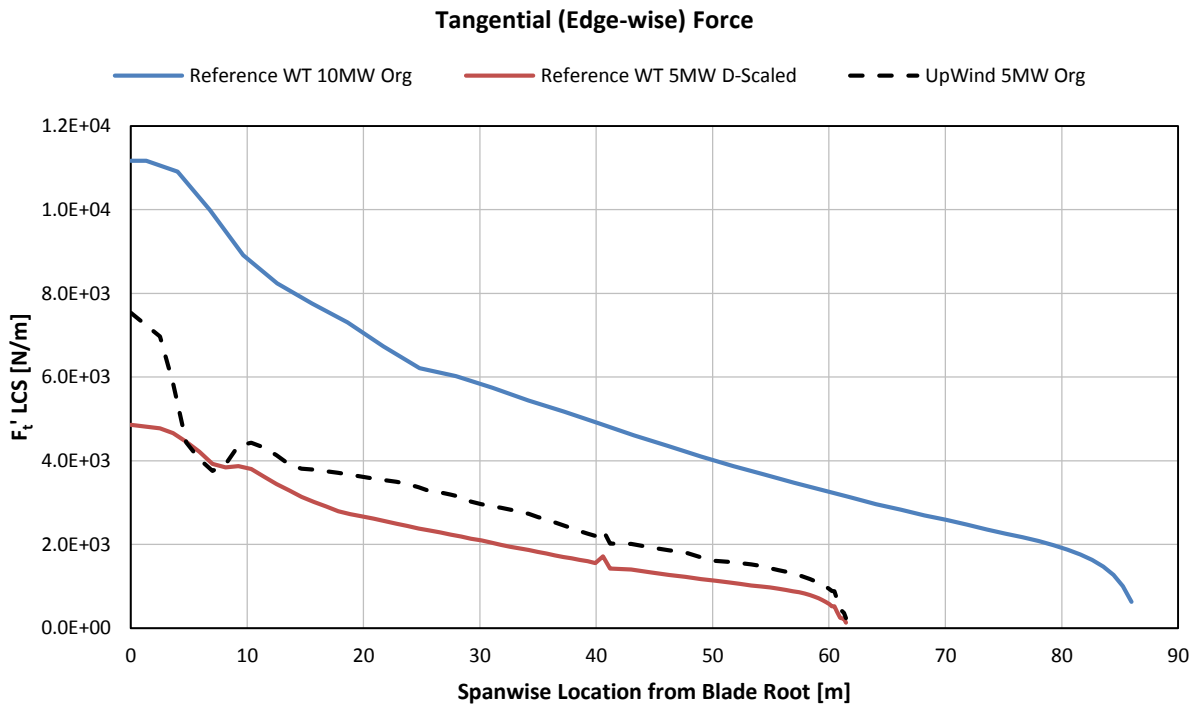


Figure 3.29: The tangential forces (including the weight) on the blades for the RWT, the UpWind 5 MW and the down-scaled RWT to 5 MW

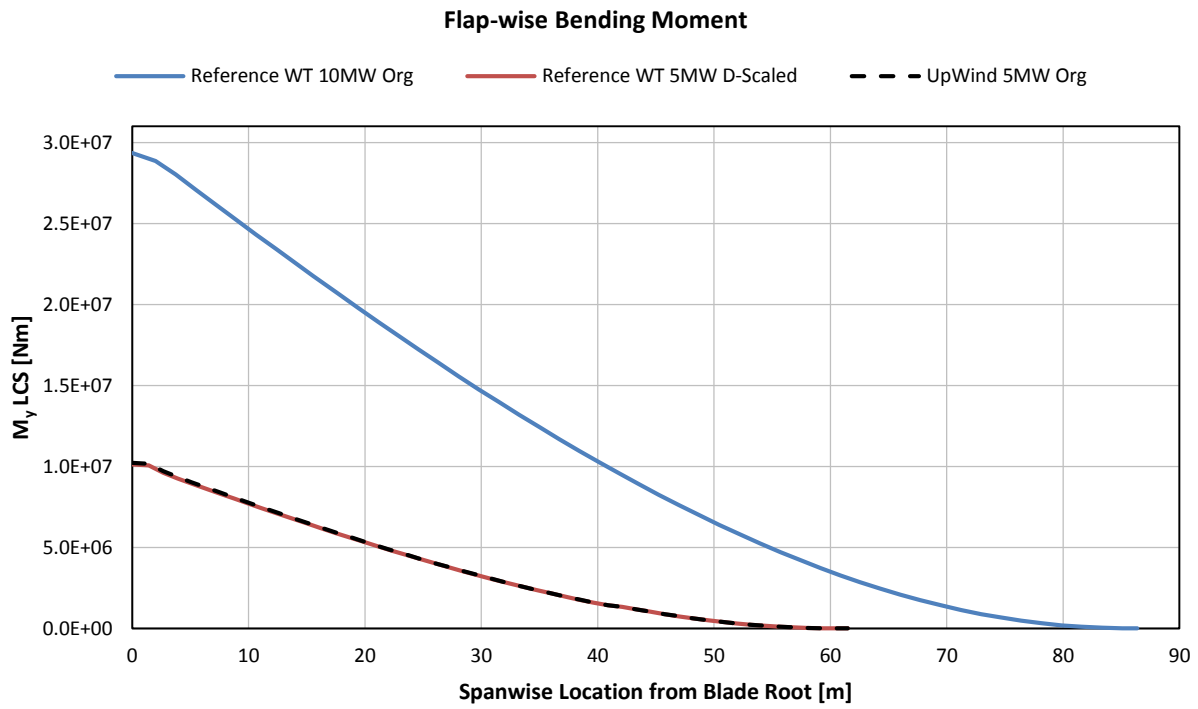


Figure 3.30: The flap-wise bending moments for the RWT, UpWind 5 MW and down-scaled RWT to 5 MW

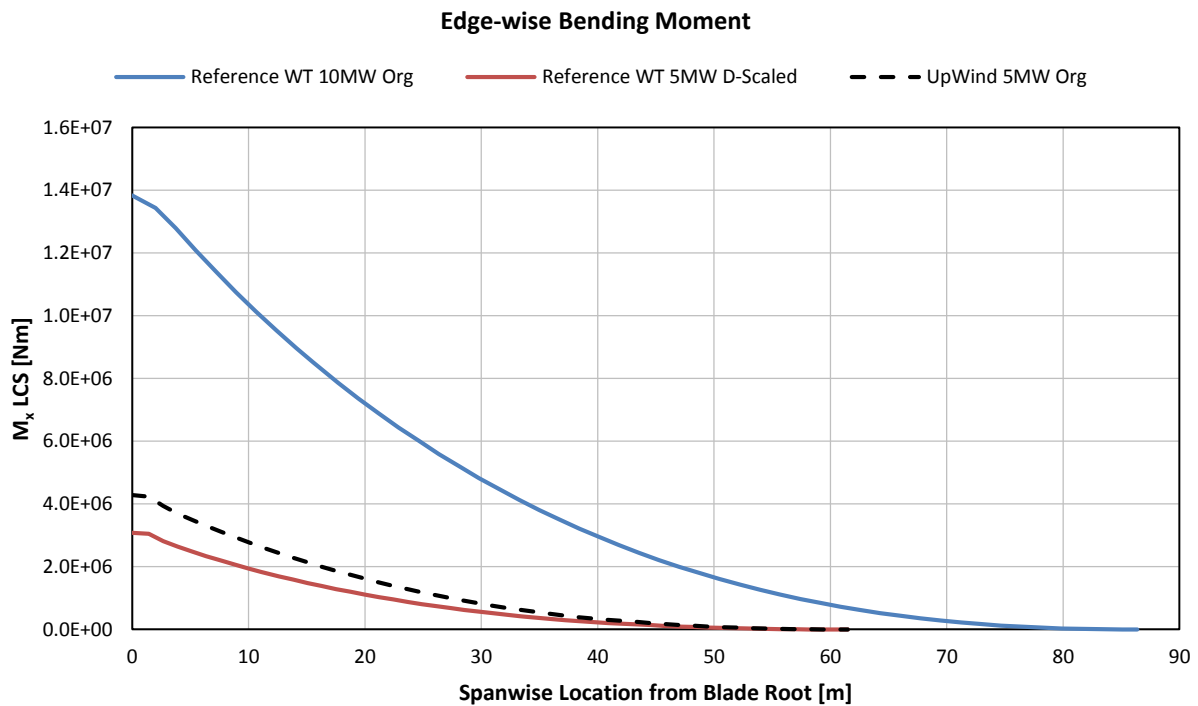


Figure 3.31: The edge-wise bending moments for the RWT, UpWind 5 MW and down-scaled RWT to 5 MW

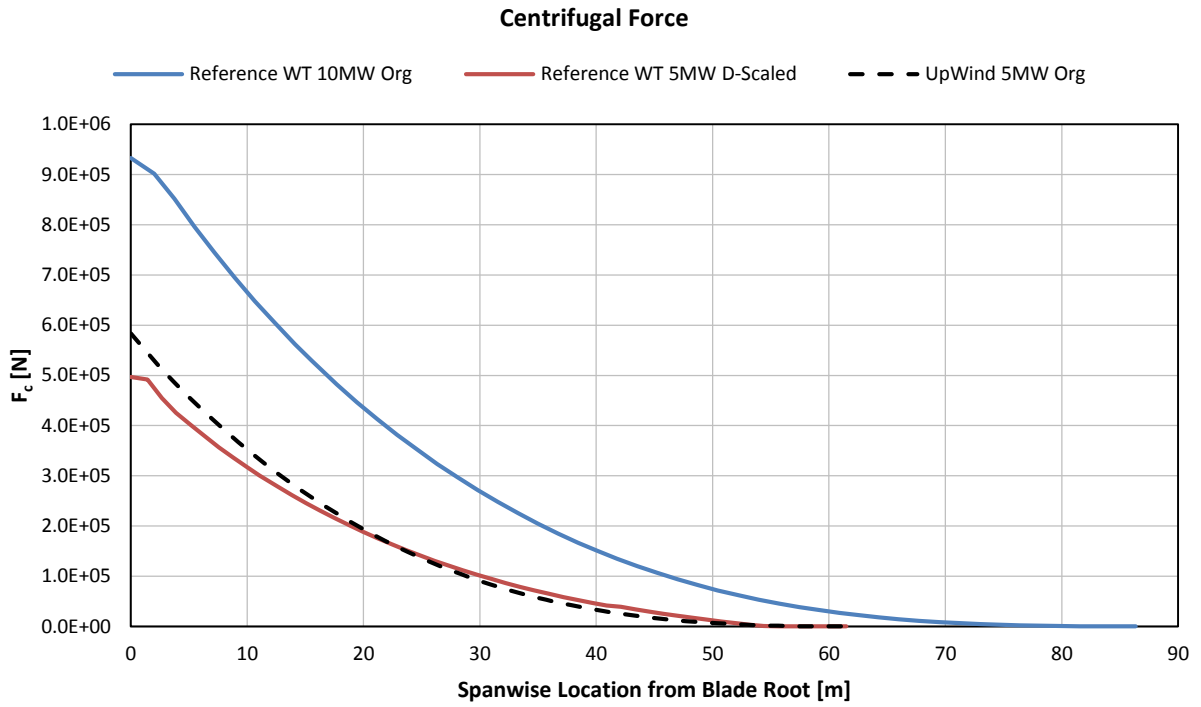


Figure 3.32: The centrifugal forces for the RWT, UpWind 5 MW and down-scaled RWT to 5 MW

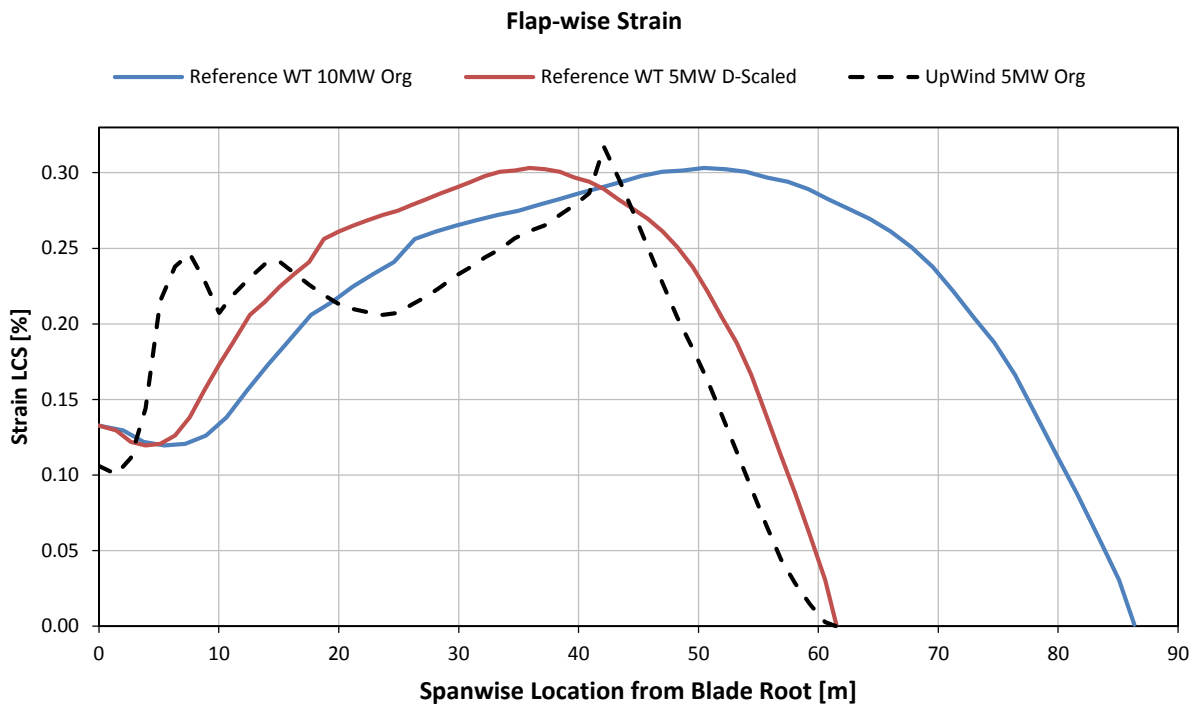


Figure 3.33: The flap-wise strains for the RWT, UpWind 5 MW and down-scaled RWT to 5 MW

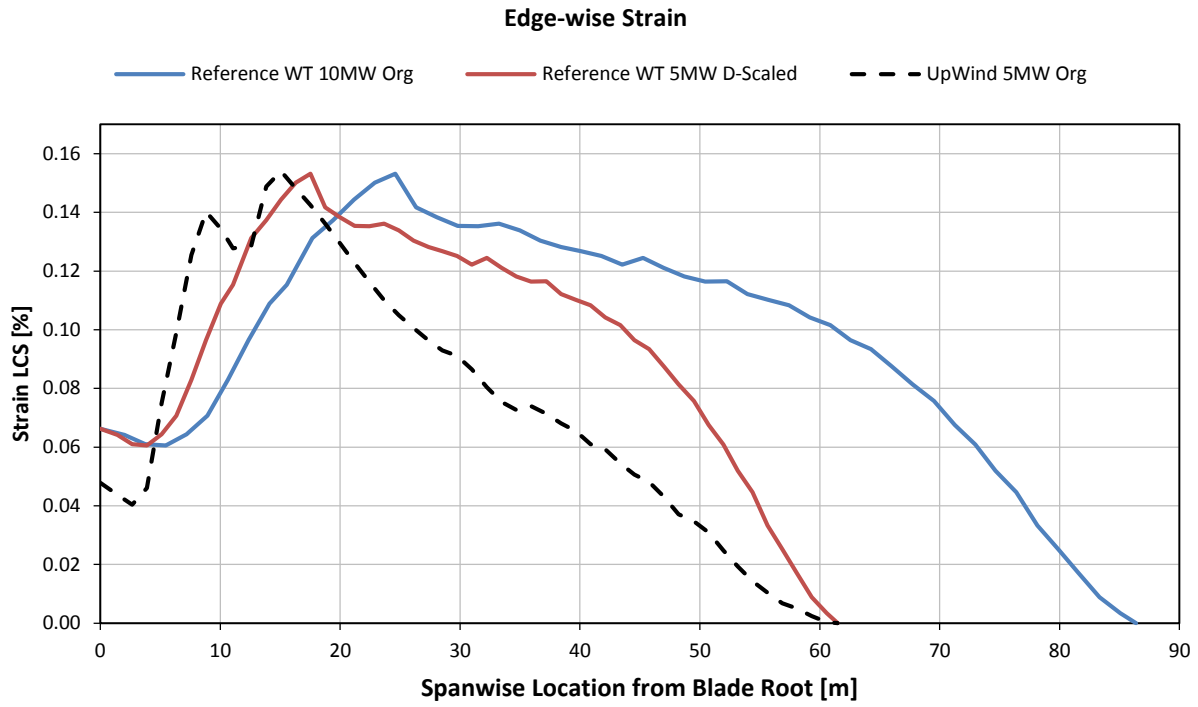


Figure 3.34: The edge-wise strains for the RWT, UpWind 5 MW and down-scaled RWT to 5 MW

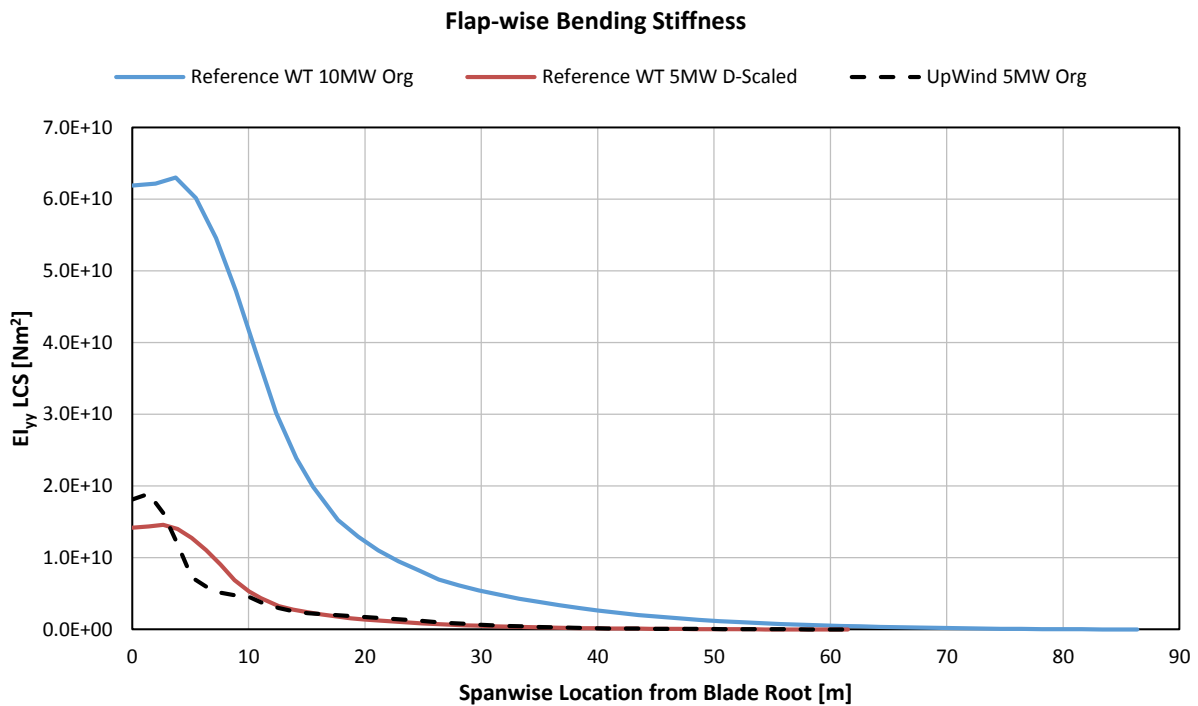


Figure 3.35: The flap-wise bending stiffness for the RWT, UpWind 5 MW and down-scaled RWT to 5 MW

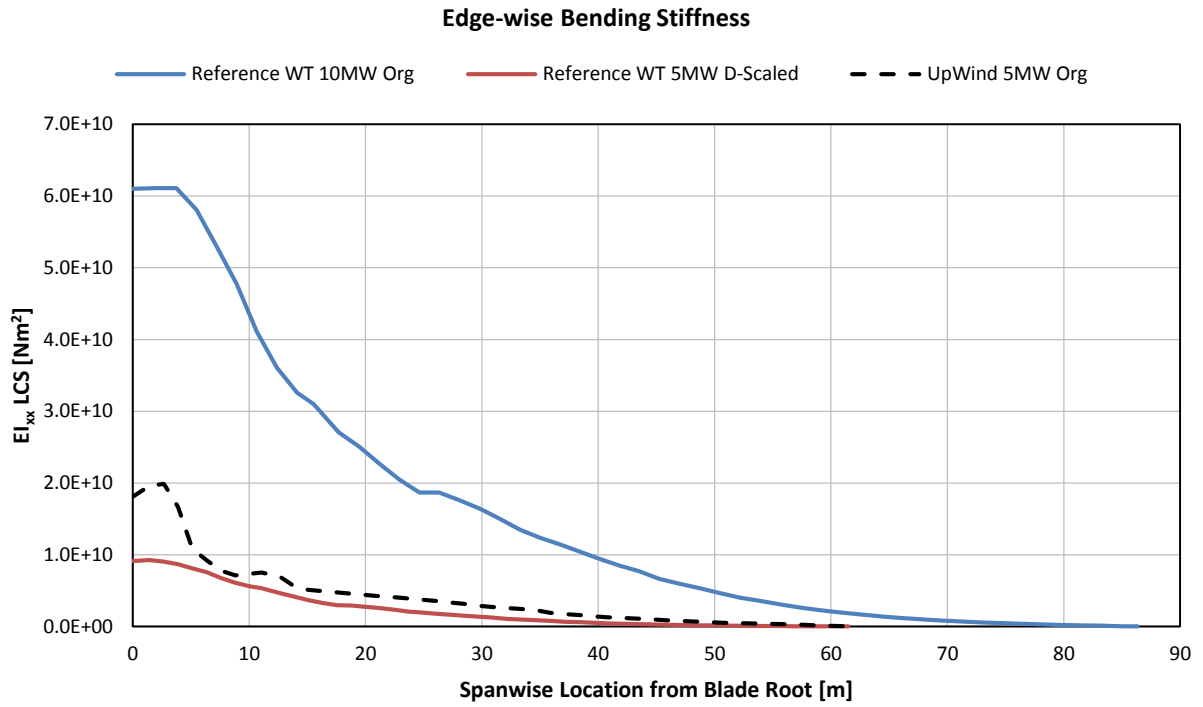


Figure 3.36: The edge-wise bending stiffness for the RWT, UpWind 5 MW and down-scaled RWT to 5 MW

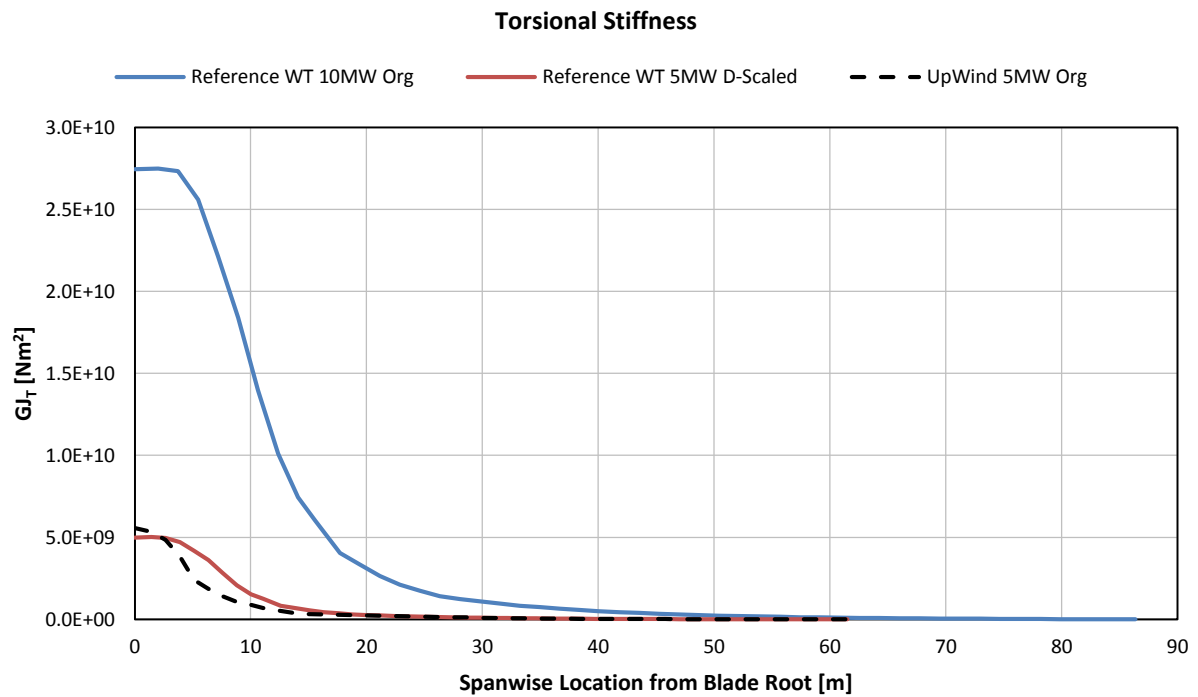


Figure 3.37: The torsional stiffness for the RWT, UpWind 5 MW and down-scaled RWT to 5 MW

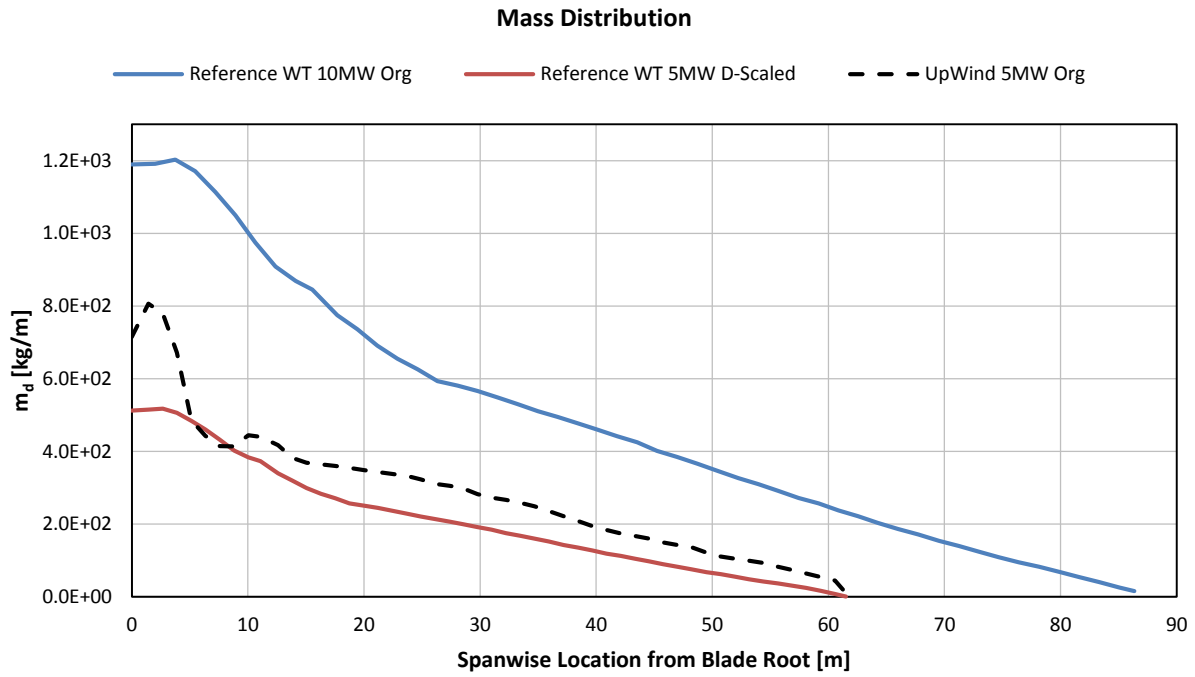


Figure 3.38: The mass per unit length distribution for the RWT, UpWind 5 MW and down-scaled RWT to 5 MW

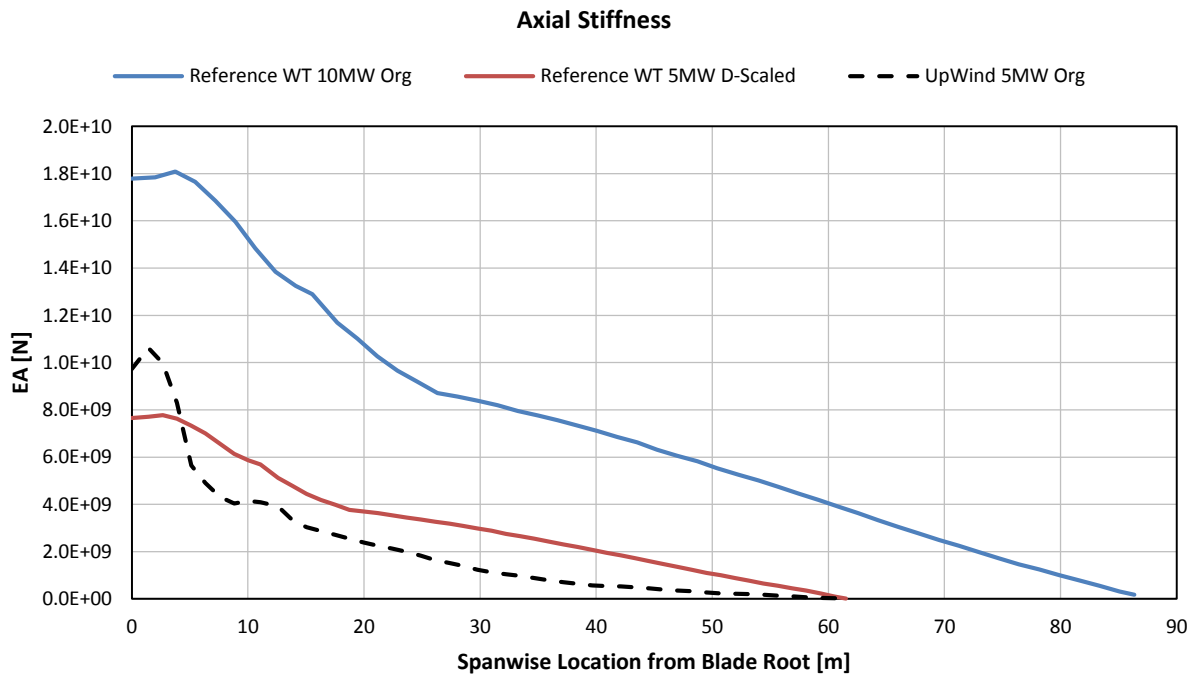


Figure 3.39: The axial stiffness for the RWT, UpWind 5 MW and down-scaled RWT to 5 MW

Table 3.7: The resulting Blade Masses for the down-scaling Case Study

Concept / Parameter	Blade Mass [kg]	Net Change [%]	Average per Unit Length Change [%]	Scaling Factor (s=0.70655) Exponent λ
INNWIND RWT 10 MW	41,722	-	-	-
RWT 5 MW	12,949	-68.96	-73.13	3.368
UpWind 5 MW	17,726	-57.51	-63.22	2.464

A certain “under-shoot” in the prediction of the mass can be seen from the table above. It is possible to explain it from the “flexible” nature of the original RWT blades. Also from the fact that the UpWind machine is using a thinner aerofoil (NACA-64618, 18% relative thickness) that needs more mass to have a high stiffness.

3.3.2 From 5 to 10 MW Up-scaling

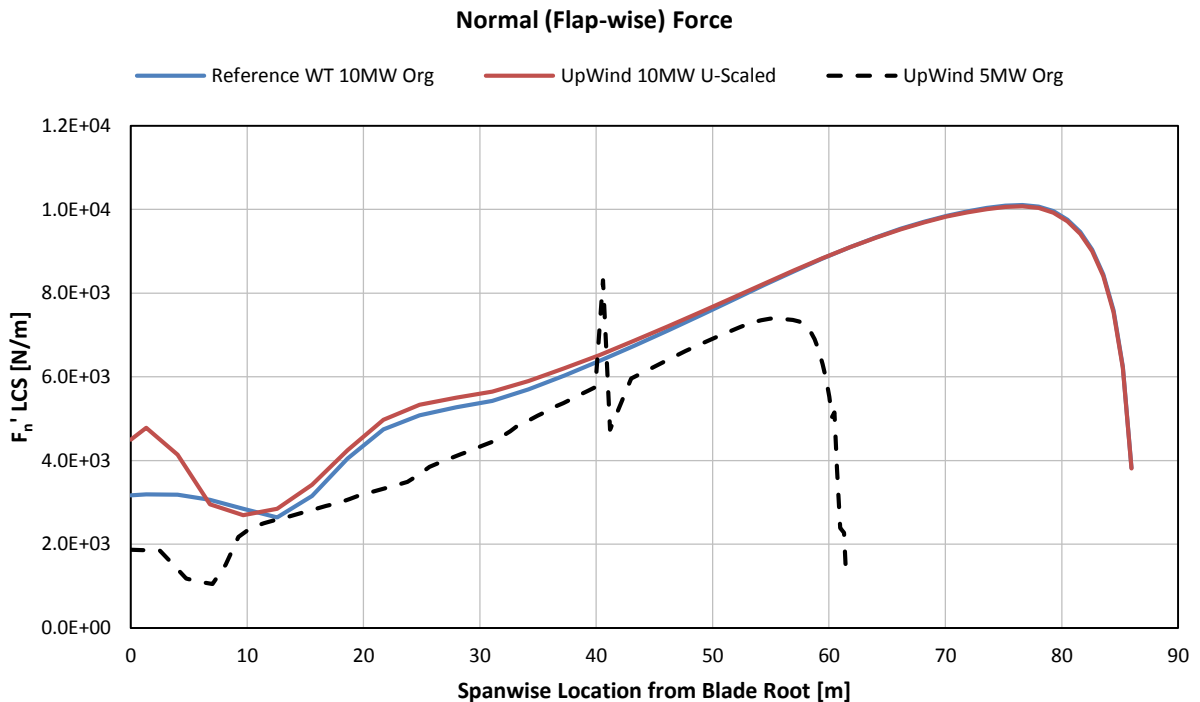


Figure 3.40: The normal forces on the blades for the RWT, UpWind 5 MW and up-scaled UpWind to 10 MW

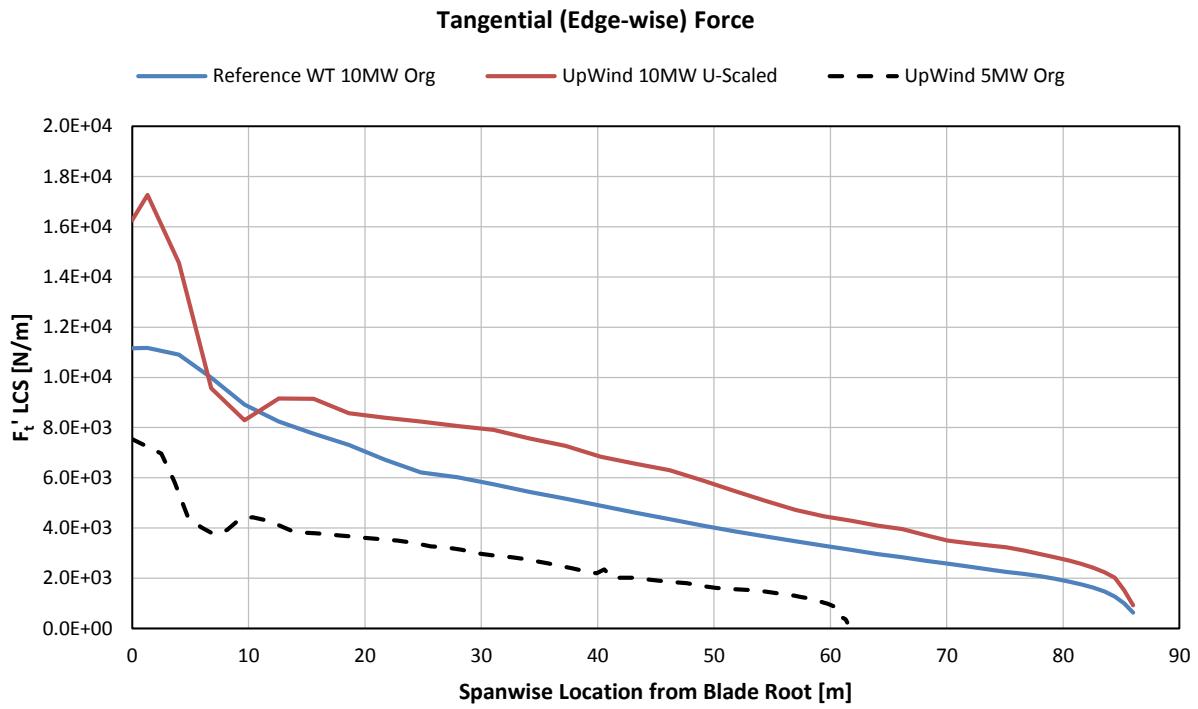


Figure 3.41: The tangential forces (including the weight) on the blades for the RWT, the UpWind 5 MW and the up-scaled UpWind to 10 MW

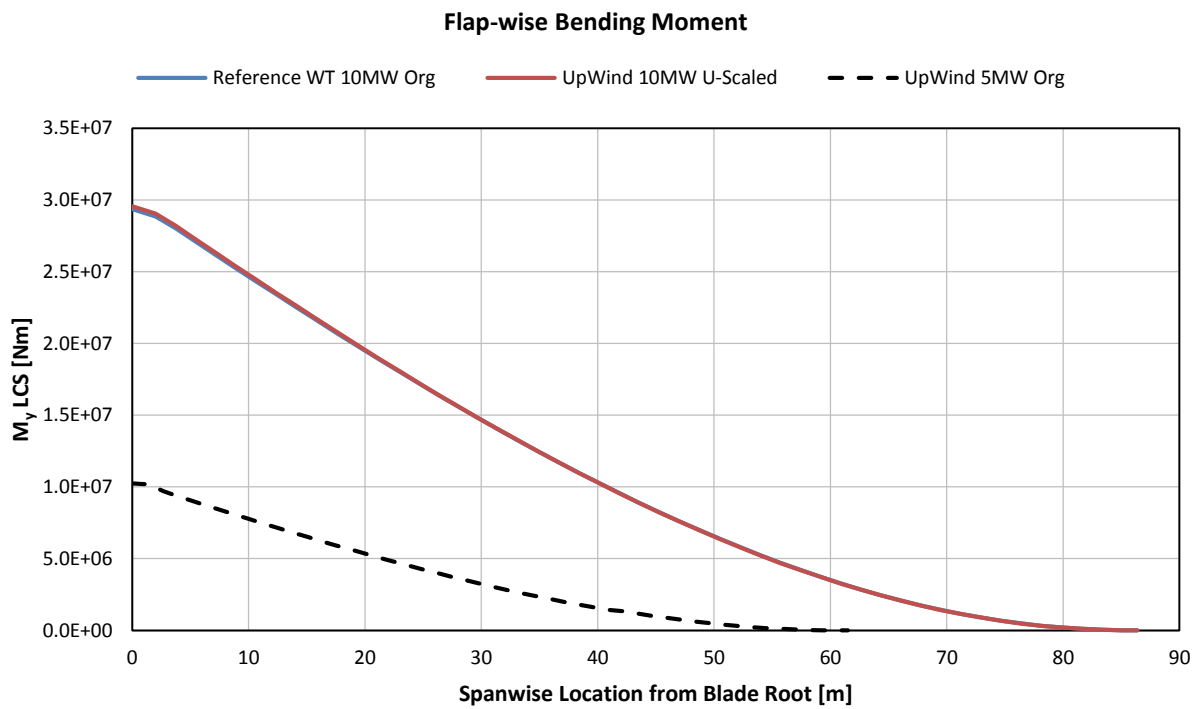


Figure 3.42: The flap-wise bending moments for the RWT, UpWind 5 MW and up-scaled UpWind to 10 MW

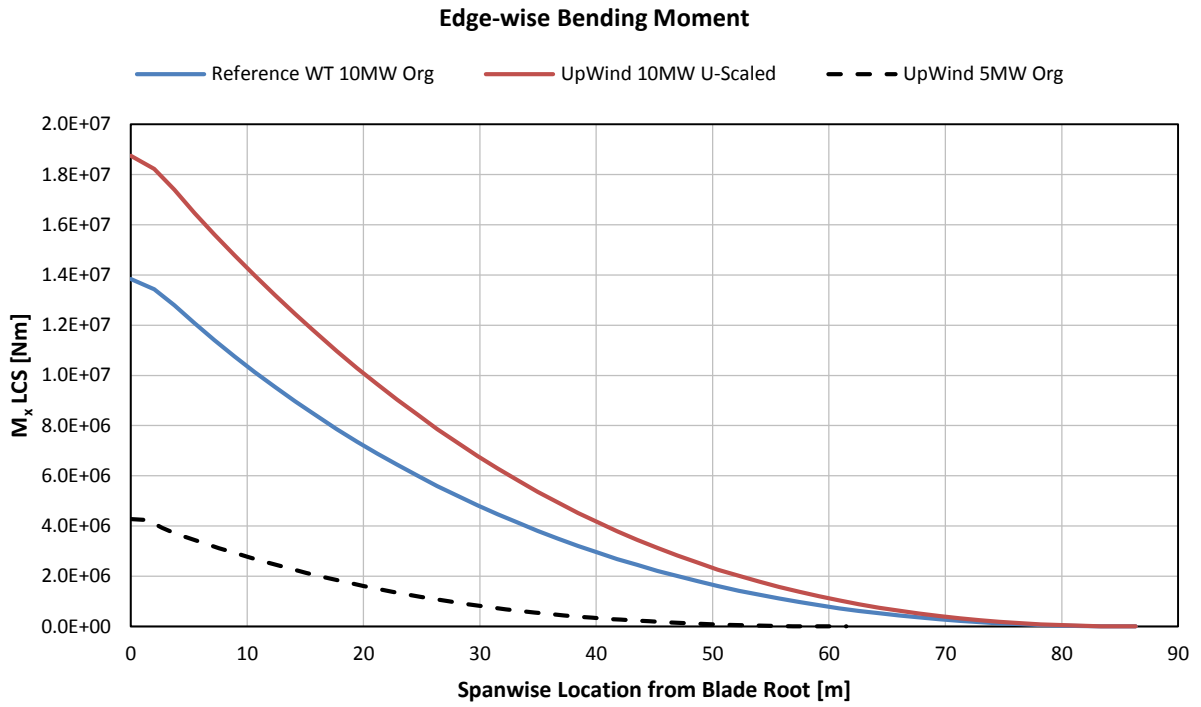


Figure 3.43: The edge-wise bending moments for the RWT, UpWind 5 MW and up-scaled UpWind to 10 MW

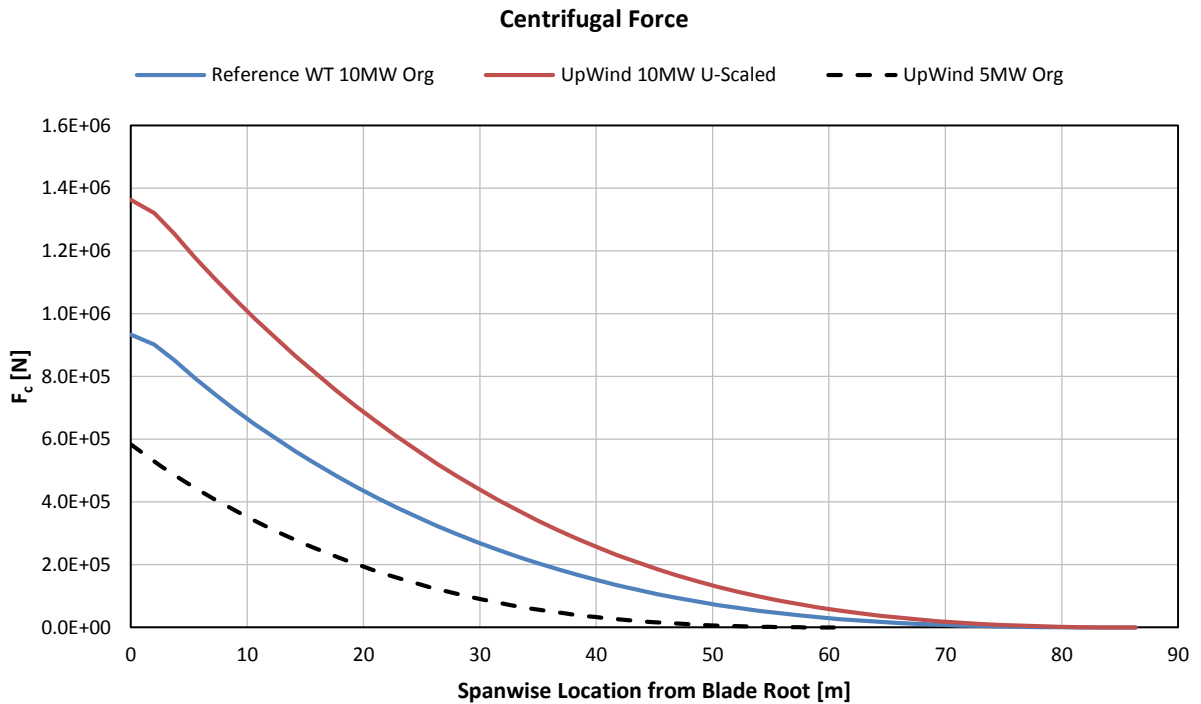


Figure 3.44: The centrifugal forces for the RWT, UpWind 5 MW and up-scaled UpWind to 10 MW

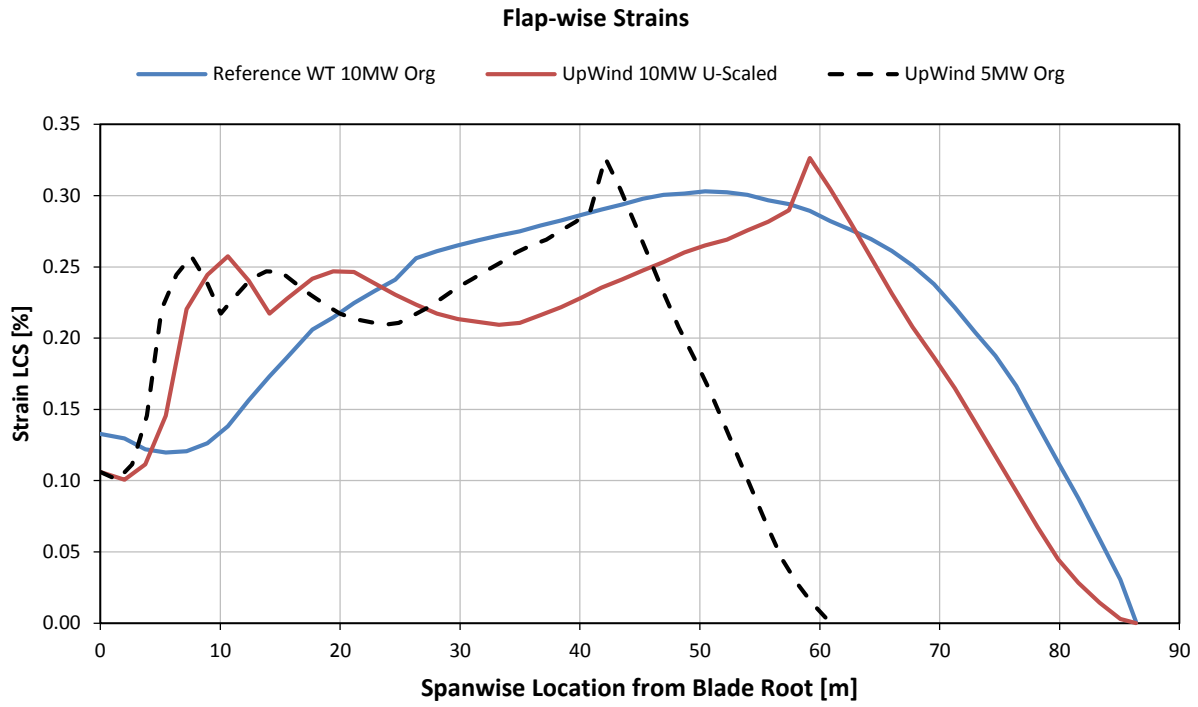


Figure 3.45: The flap-wise strains for the RWT, UpWind 5 MW and up-scaled UpWind to 10 MW

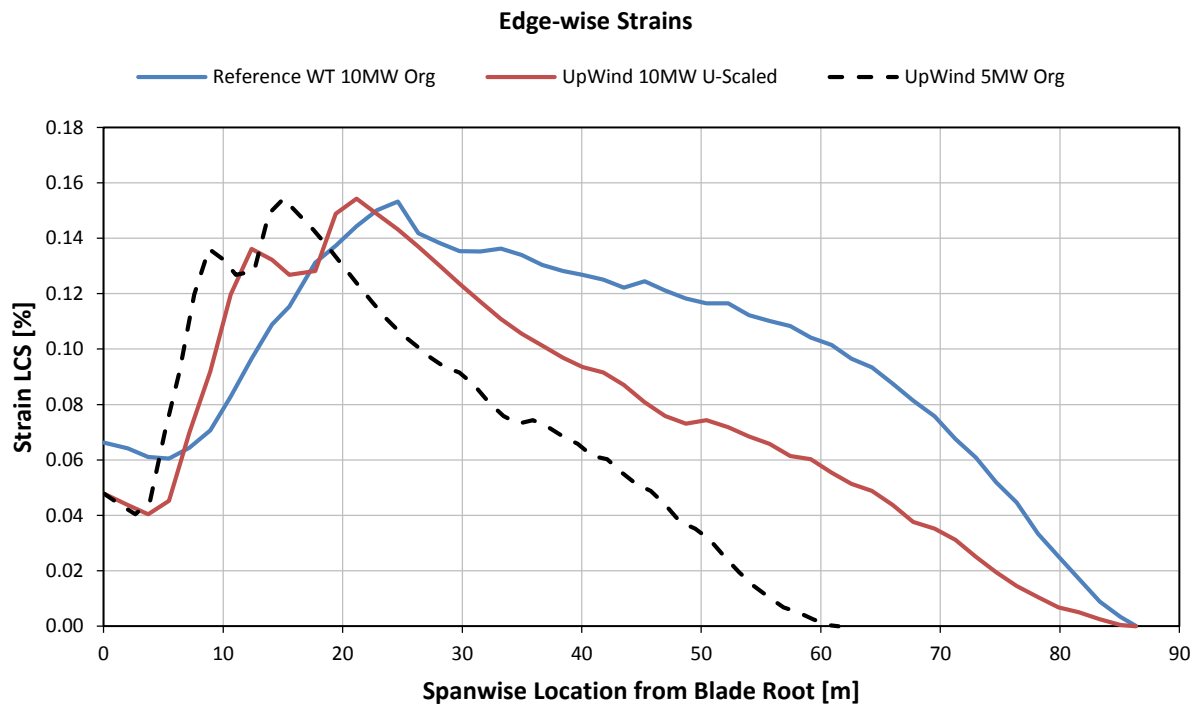


Figure 3.46: The edge-wise strains for the RWT, UpWind 5 MW and up-scaled UpWind to 10 MW

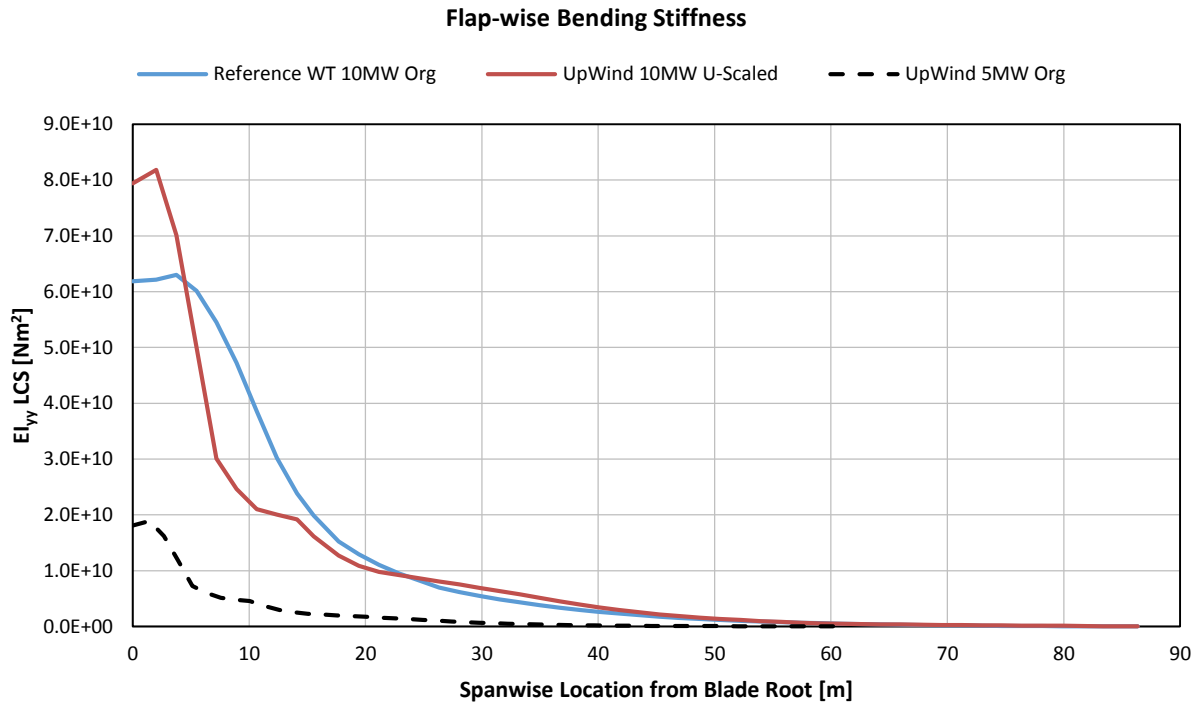


Figure 3.47: The flap-wise bending stiffness for the RWT, UpWind 5 MW and up-scaled UpWind to 10 MW

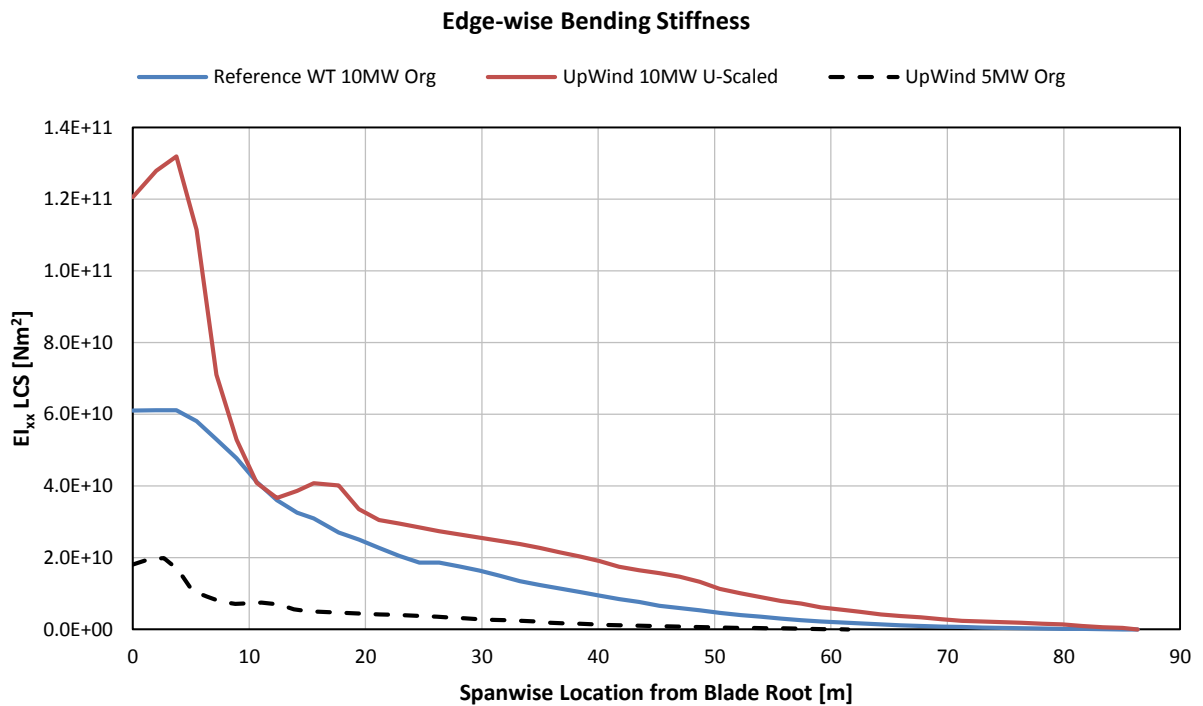


Figure 3.48: The edge-wise bending stiffness for the RWT, UpWind 5 MW and up-scaled UpWind to 10 MW

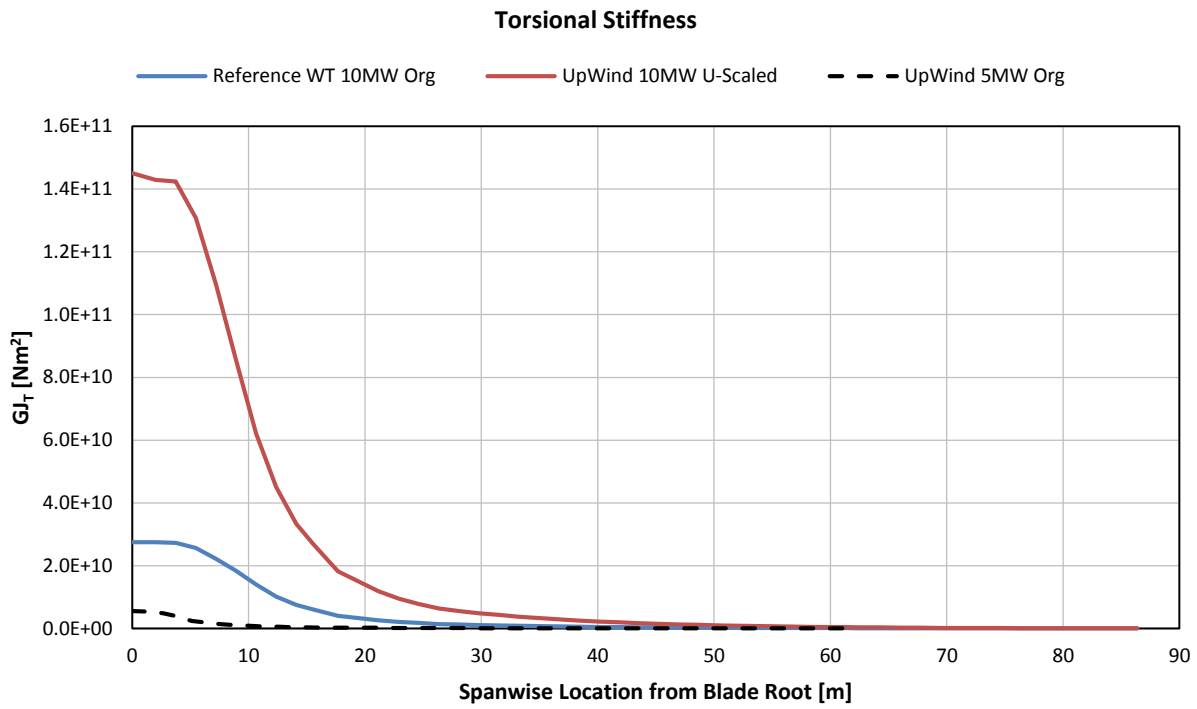


Figure 3.49: The torsional stiffness for the RWT, UpWind 5 MW and up-scaled UpWind to 10 MW

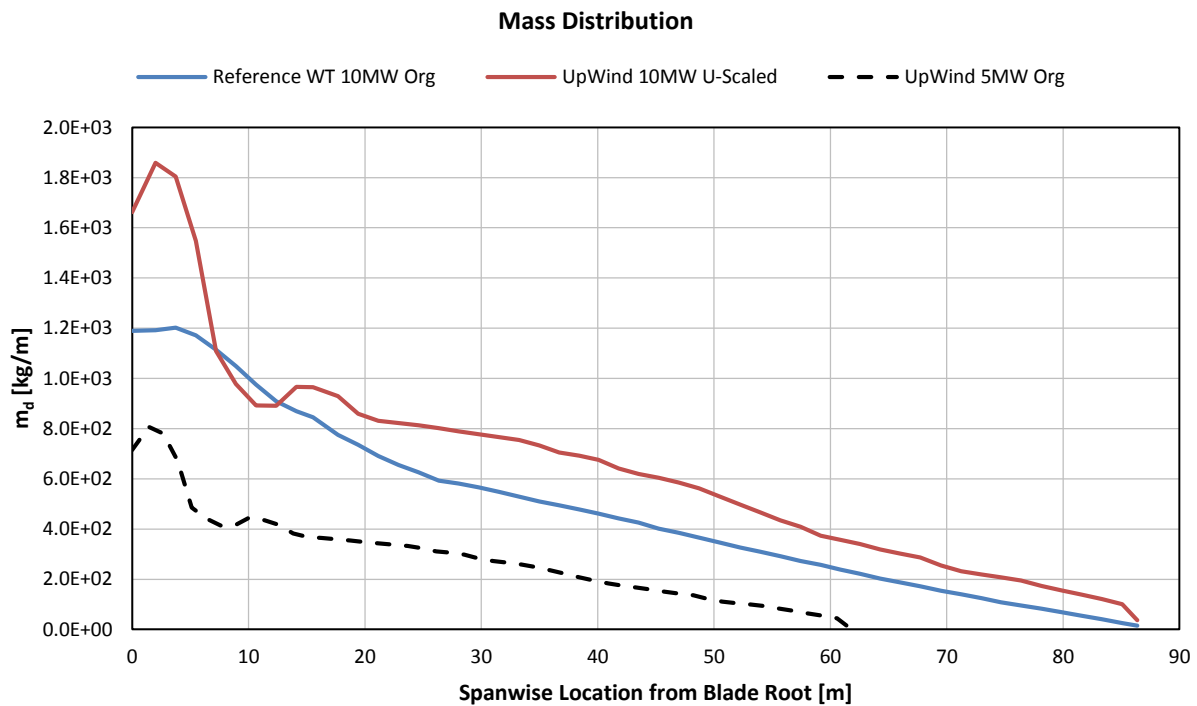


Figure 3.50: The mass per unit length distribution for the RWT, UpWind 5 MW and up-scaled UpWind to 10 MW

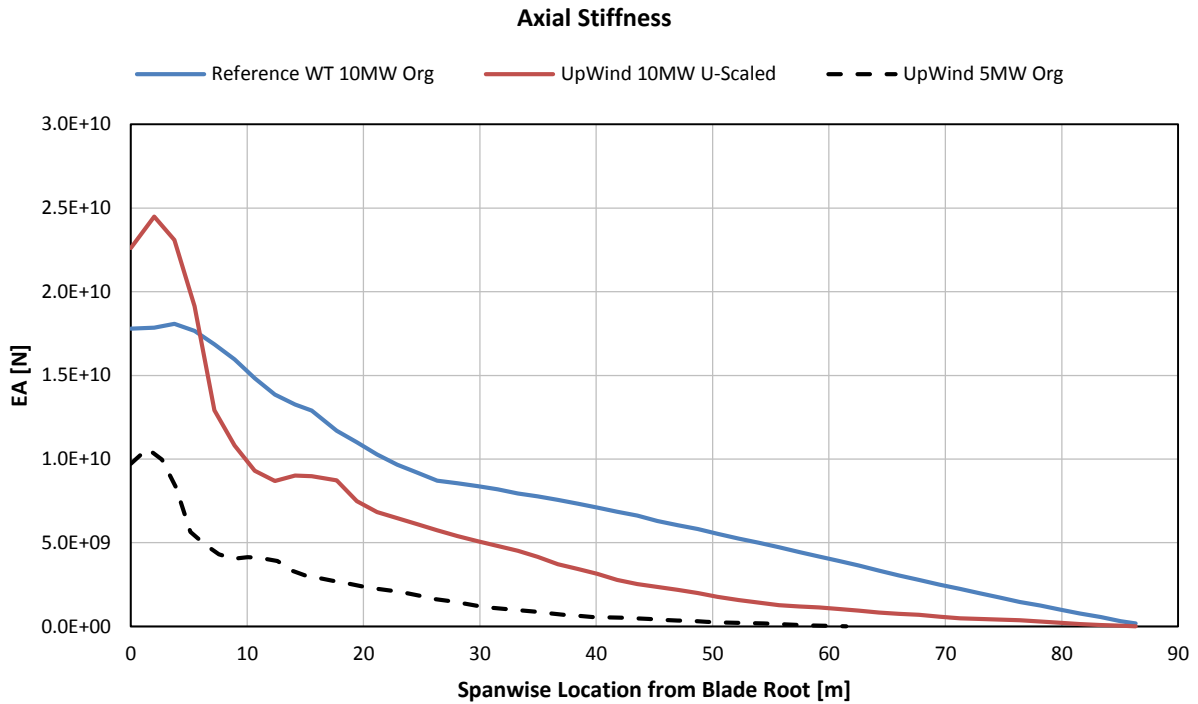


Figure 3.51: The axial stiffness for the RWT, UpWind 5 MW and up-scaled UpWind to 10 MW

Table 3.8: The resulting Blade Masses for the up-Scaling Case Study

Concept / Parameter	Blade Mass [kg]	Net Change [%]	Average per Unit Length Change [%]	Scaling Factor ($s=1.41533$) Exponent λ
UpWind 5 MW	17,726	-	-	-
UpWind 10 MW	55,748	+214.50	+122.21	3.299
INNWIND RWT 10 MW	41,722	+135.37	+66.30	2.464

The inverse phenomenon occurs in this case. When the “stiff” nature of the original UpWind 5 MW blade is up-scaled, more mass is needed to maintain the same structural response as with the loads of the INNWIND RWT blade. Mathematically, this is explained because the distance of the neutral axis, for example in the flap-wise loads, is smaller because of the smaller aerofoil absolute thickness. Hence, while trying to keep the strain constant, more stiffness is required. The method indeed is displaying a heavy dependence and sensitivity on the chosen aerofoil geometry and certain bottleneck points in the analysis such as the position of force exertion. Nevertheless, it seems to be producing reasonable results and most importantly within a recognisable range of error.

4

RESULTS

4.1 Rotor Stationary

After the modelling of the blades, as described in section 3.2, the new blade parameters and distributed properties are put in FOCUS. The first calculation carried out is the rotor stationary analysis with PHATAS Supervisor Stationary. This calculation has a binary purpose. Firstly, to obtain the steady-state aerodynamic performance of the rotors in a wide range of operational configurations with different combinations of tip speed ratios and pitch angles. This data can be used for the first LCoE estimation. Secondly, the C_p - λ and C_T - λ curves acquired are used to tune the external controller algorithm for its Maximum Power Point Tracking (MPPT) process and dynamic response. While the core function of the controller is the same for all designs, parameter modifications for a stable performance of each rotor concept are made. These controllers are used in the load case simulations.

4.1.1 Parameters of the Simulations

In Table 4.1, a summary of the simulation setup is presented. The rotor and structure (tower and shaft) are modelled as stiff/rigid in order to calculate the best possible aerodynamic performance without interactions of dynamic behaviour. Wide ranges of TSR's and pitch angles are used to cover the whole spectrum of operating points with a constant wind speed. Small steps of 0.2° and 0.5° pitch are used in the area close to the optimal pitch angle

Table 4.1: Rotor Stationary Simulation Parameters

Parameter	Value	Comment
Blade Flap-wise Flexibility	OFF	-
Blade Edge-wise Flexibility	OFF	-
Blade Torsional Flexibility	OFF	-
Rotor Shaft Flexibility	OFF	-
Tower Flexibility	OFF	-
Tip Speed Ratio range	ca. 0 : 20	Step of 0.25
Pitch Angle Range	-10° : 90°	Steps of 0.2° , 0.5° , 1° , 2.5° , 5° , 10° . The small steps are used close to the optimal pitch angle
Wind Speed	9 [m/s]	Chosen to be close to rated wind speed
Vertical Wind Shear	None	-
Air Density	1.225 [kg/m ³]	-

Dynamic Stall Model Behaviour	Linear	-
Blade Pre-bend	None	-
Cone Angle	0°	-
Tilt Angle	5°	-

4.1.2 Results of the Calculation

The results of all calculations follow. The thick green line represents the chosen partial load region optimal pitch angle curve. The highlighted point on this curve corresponds to the partial load optimal TSR.

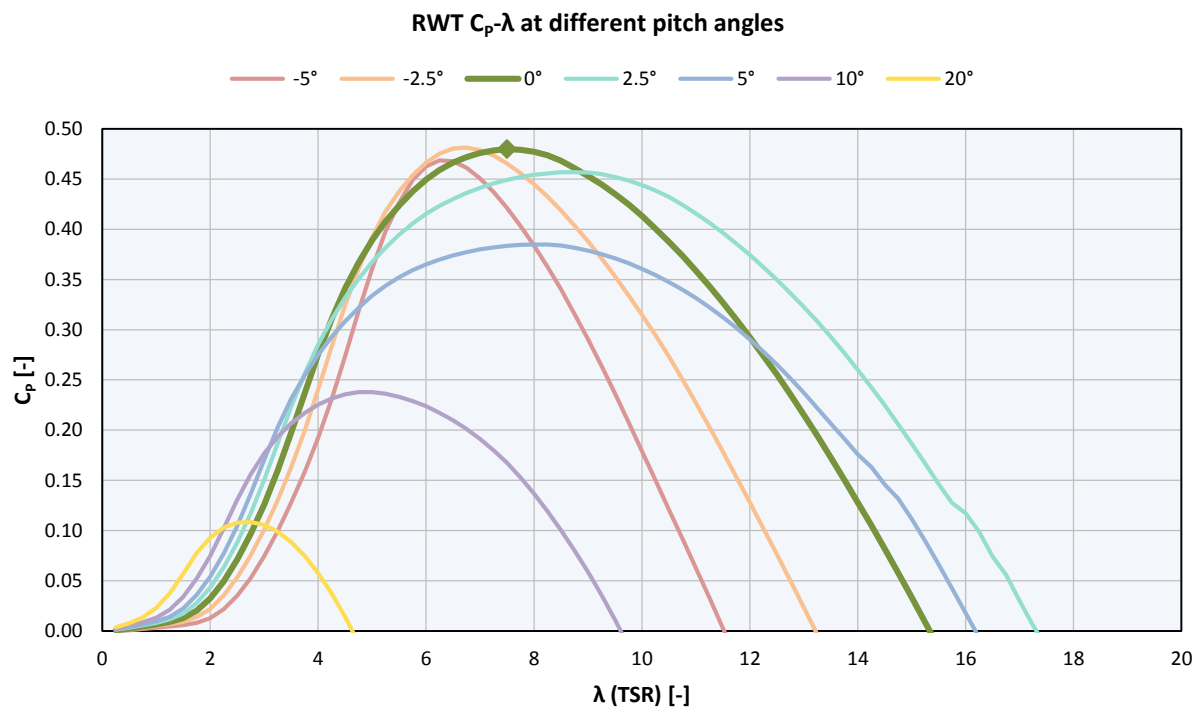


Figure 4.1: C_p - λ curves for different pitch angles for the RWT

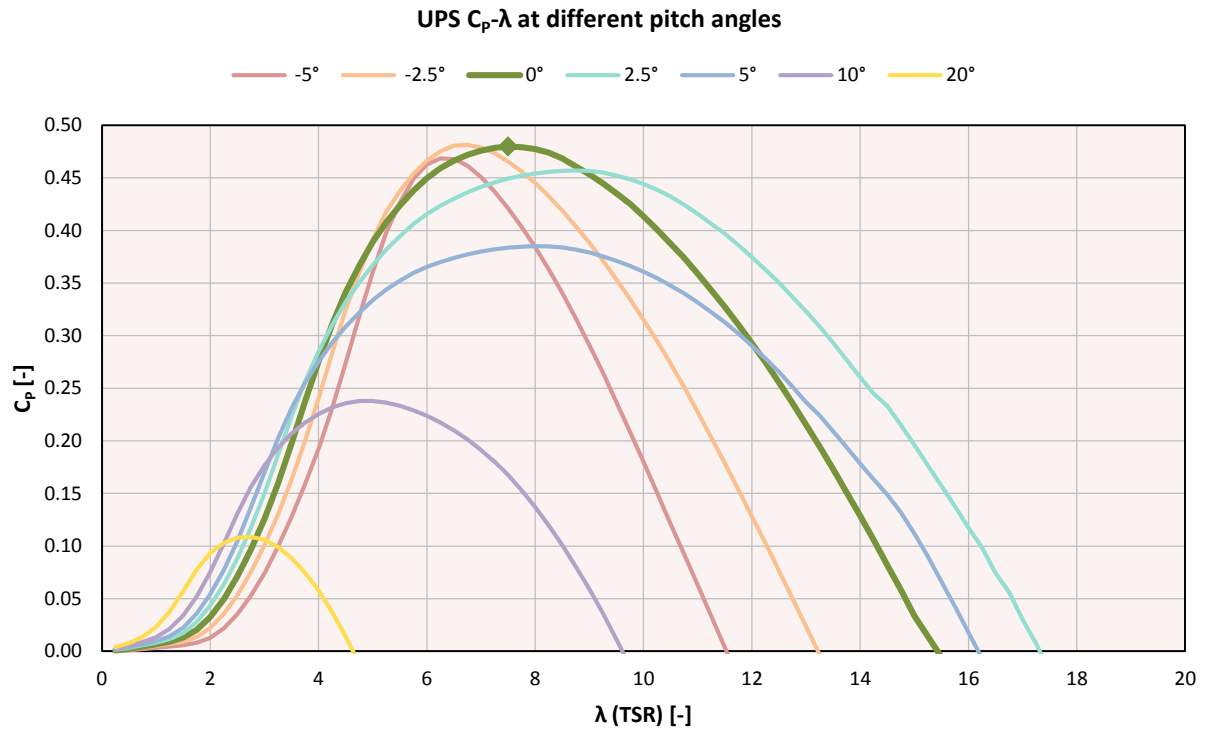


Figure 4.2: C_p - λ curves for different pitch angles for the UPS

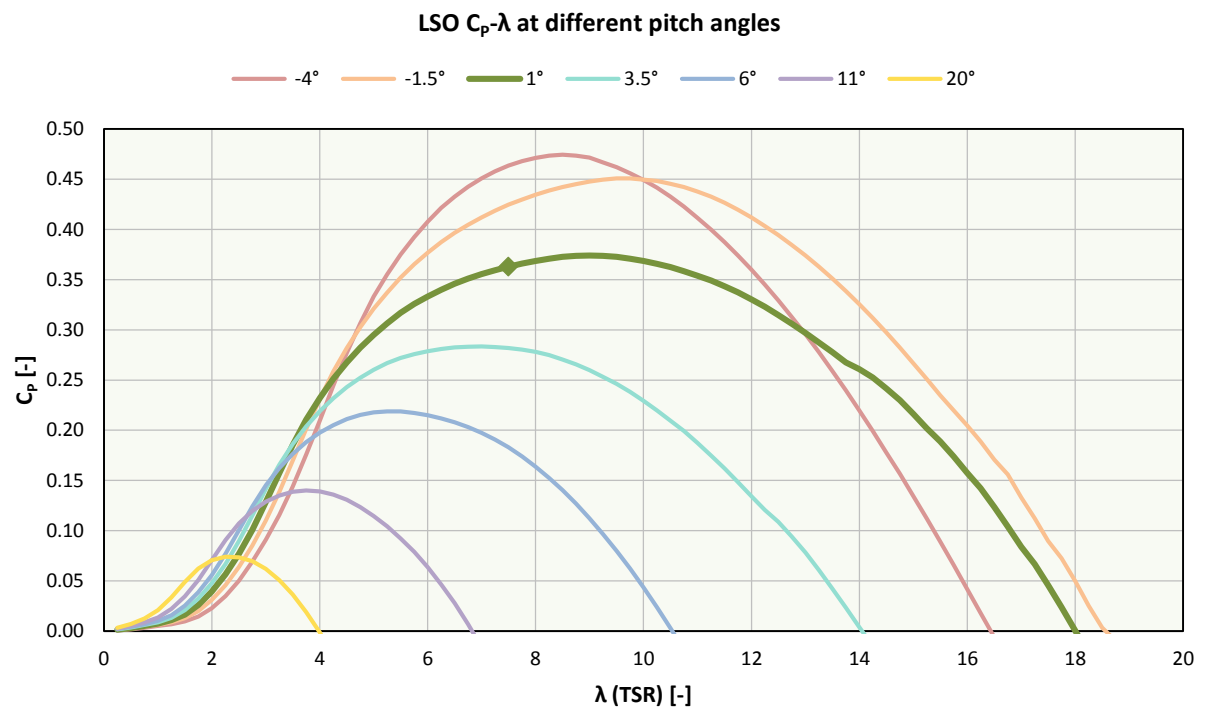


Figure 4.3: C_p - λ curves for different pitch angles for the LSO

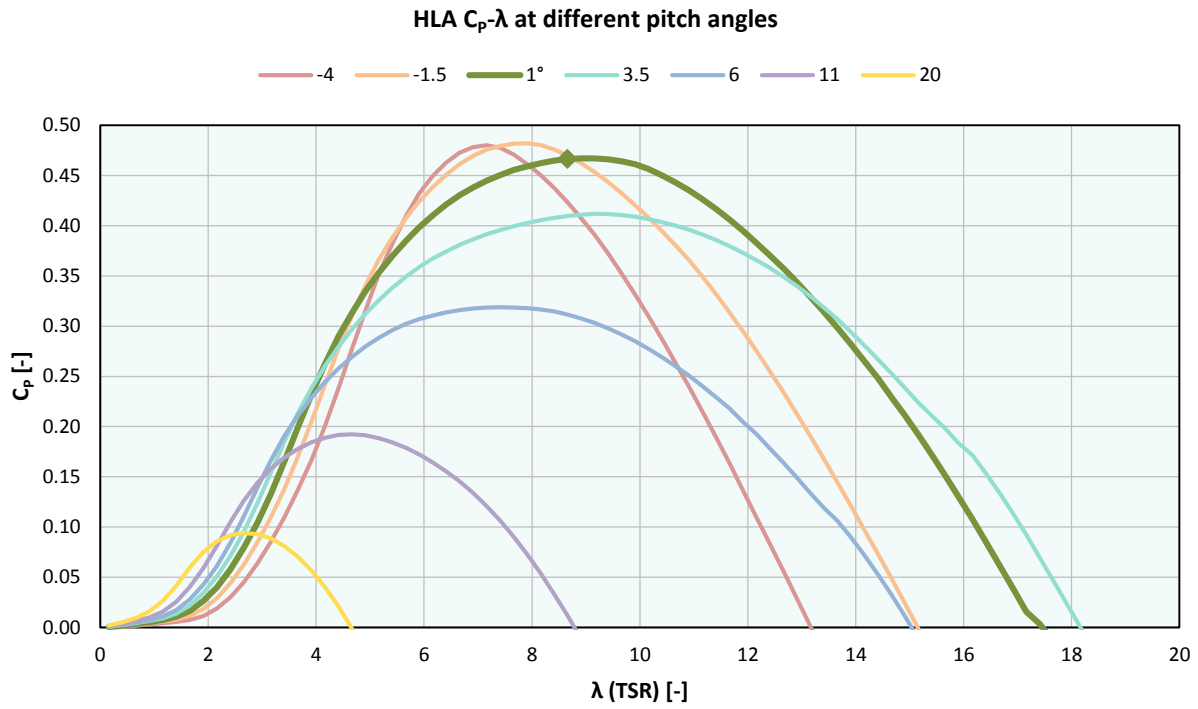


Figure 4.4: C_p - λ curves for different pitch angles for the HLA

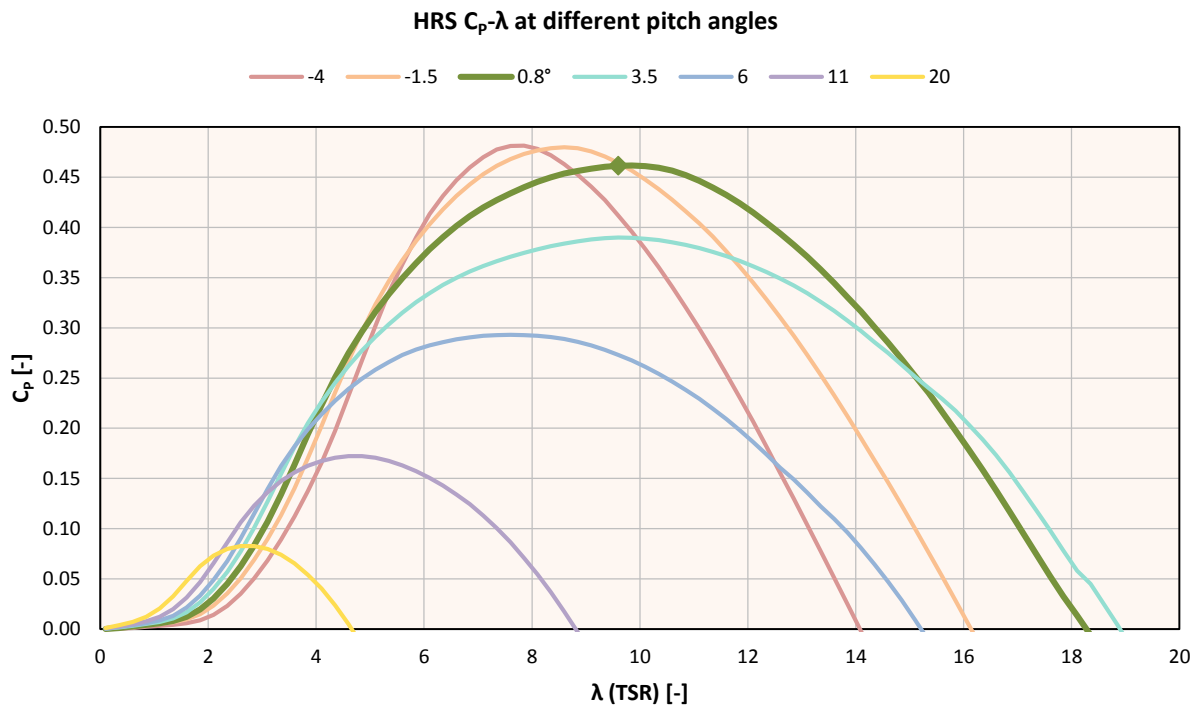


Figure 4.5: C_p - λ curves for different pitch angles for the HRS

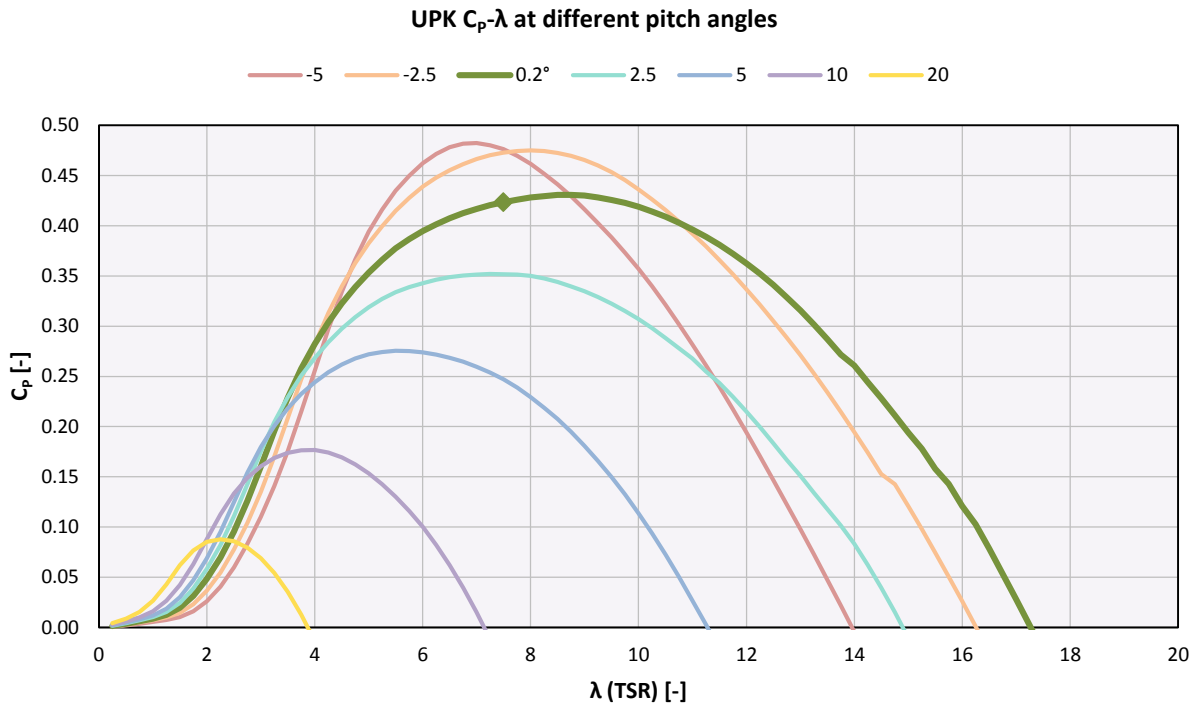


Figure 4.6: C_p - λ curves for different pitch angles for the UPK

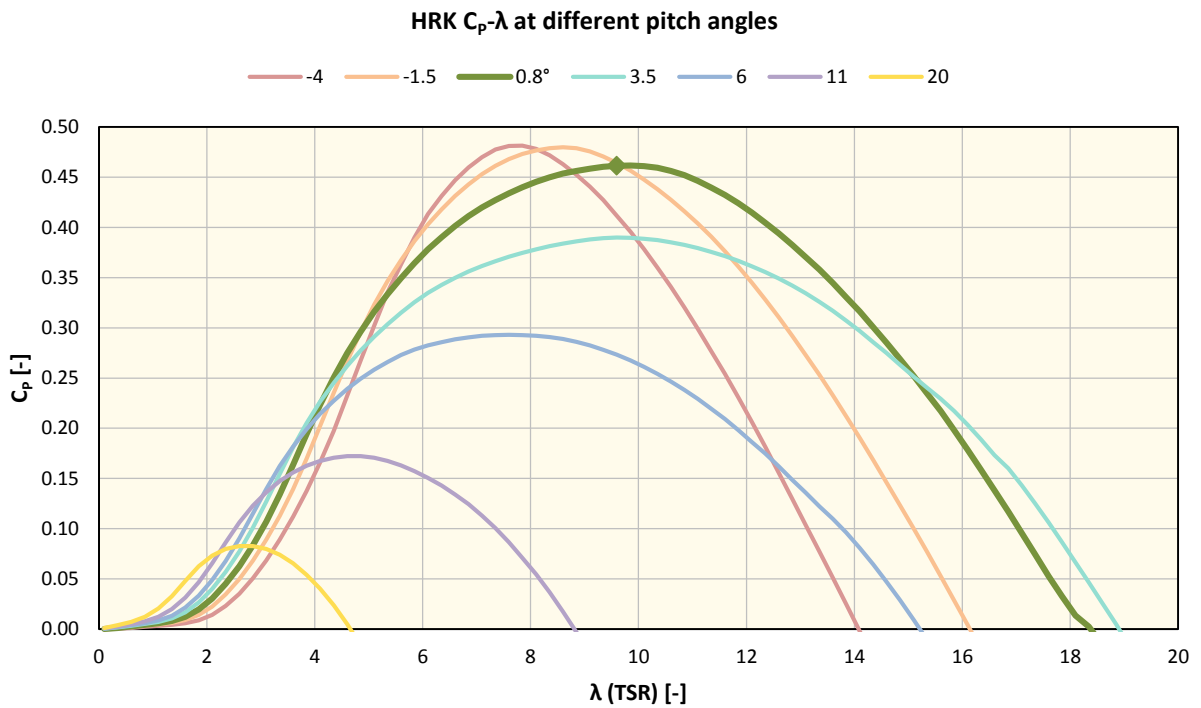


Figure 4.7: C_p - λ curves for different pitch angles for the HRK

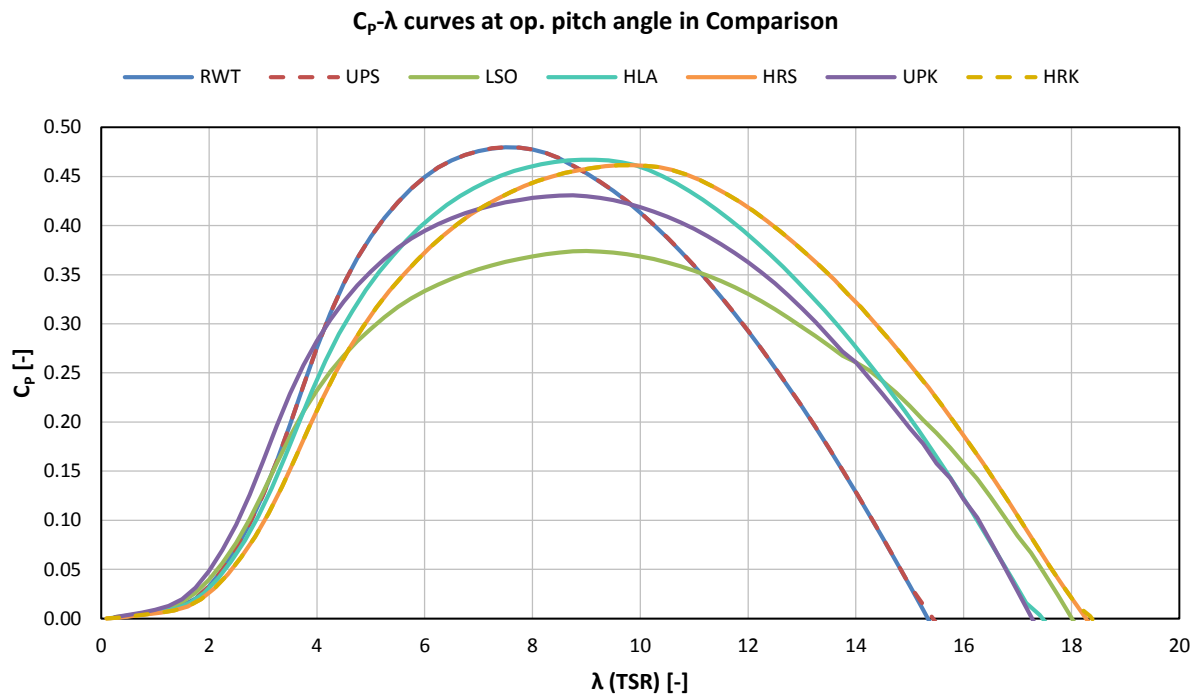


Figure 4.8: C_p - λ curves at optimal pitch angle for all the designs in comparison

In Figure 4.3, it is seen that the higher twist of the LSO rotor is producing a relatively low C_p of 0.363 at TSR 7.5 and 1° pitch angle. With negative pitch angles, the C_p value can be higher, closer to the ones of the RWT and UPS rotors, but that is not desirable with the scope of reducing the loads in the LSO concept. It is worth noting that the maximum C_p of the LSO for a TSR of 7.5 is 0.476 and occurs at ca. -6° pitch which relates to the offset of the twist distribution (see Figure 2.4) and the $+1^\circ$ of minimum/operating pitch angle. In Figure 4.8, it can be seen that the similarity in the geometry of the RWT and UPS rotor gives an (almost) identical aerodynamic performance for 0° pitch angle with a C_p of 0.47966 and 0.47972 respectively. This concerns the design TSR 7.5 and both are close to the absolute maximum of the TSR spectrum. This can also be considered as a first validation of the correct up-scaling of the geometry and input in the code. The UPK concept exhibits a somewhat lower C_p compared to the UPS because of its higher twist (Figure 2.4). The trend in the higher rotation and lower solidity concepts (LSO, HLA, HRS, HRK) show a move towards a wider, less sharp C_p - λ curve close to the optimal TSR, pointing to a 2-bladed wind turbine concept.

4.1.3 The Flexible Case

In addition, a flexible rotor and structure case is also run, but only for the optimal TSR and pitch angles (Table 4.2). This is done to obtain the tower-top mass and stiffness from the “*phatdef.mdl*” output file (Figure 4.9). These two parameters are used in the BLADEMODE module for the modal analysis. The flexible case simulation is also useful as it calculates some of the eigen-frequencies and eigen-modes of the rotor (Figure 4.10) and tower (Figure 4.11). This is used as a sanity cross-check with the modal analysis done with BLADEMODE.

PROPERTIES OF THE TOWER :		
HEIGHT OF THE TOWER TOP	115.630	[m]
TOWER RADIUS USED FOR TIP CLEARANCE	3.7888	[m]
UNDEFORMED TIP-TOWER CLEARANCE	11.0555	[m]
LUMPED TOWER TOP MASS	84243.961	[kg]
IDEM, INCL NACELLE INERTIA	615236.312	[kg]
BENDING FLEXIBILITY AT TOP	4.8546E-07	[m/N]

Figure 4.9: A part of the “phatdef.mdl” model output file for the RWT flexible case showing some of the tower properties

```

PHATAS-4
Release: JAN-2012a
Model_identif: Innwind_10MW_r1.04
FREQUENCIES OF BLADE 1 CALCULATED WITH THE PRINCIPAL STIFFNESSES
ROTOR   TOWER   SYMM   SYMM   SYMM   SYMM   SYMM   BLADE
SPEED   BEND.   FLAT 1 FLAT 2 FLAT 3 EDGE 1 EDGE 2 TORS 1
0.000   0.2484  0.6124 1.7455 3.588  0.957  2.889  5.996
0.960   0.2484  0.6128 1.7459 3.589  0.957  2.889  5.996
1.920   0.2484  0.6140 1.7471 3.590  0.957  2.890  5.996
2.880   0.2484  0.6159 1.7490 3.592  0.958  2.890  5.996
3.840   0.2484  0.6186 1.7518 3.594  0.958  2.892  5.997
4.800   0.2484  0.6220 1.7553 3.598  0.959  2.893  5.997
5.760   0.2484  0.6262 1.7596 3.602  0.960  2.895  5.997
6.720   0.2484  0.6311 1.7646 3.607  0.961  2.897  5.997
7.680   0.2484  0.6367 1.7705 3.612  0.962  2.900  5.998
8.640   0.2484  0.6429 1.7770 3.619  0.963  2.903  5.998
9.600   0.2484  0.6498 1.7843 3.626  0.964  2.906  5.998
10.560  0.2484  0.6574 1.7924 3.634  0.966  2.909  5.999
11.520  0.2484  0.6655 1.8011 3.642  0.967  2.913  5.999
12.480  0.2484  0.6742 1.8106 3.651  0.969  2.917  6.000
13.440  0.2484  0.6834 1.8208 3.661  0.971  2.922  6.000
14.400  0.2484  0.6932 1.8316 3.672  0.972  2.927  6.001

```

Figure 4.10: Another part of the “phatdef.mdl” model output file for the RWT flexible case showing the eigen-frequencies and eigen-modes of the rotor

```

# Side-bending frequencies with torsion interaction
# calculated for free rotor speed variations.
#           Freq      Transl. Rolling  Torsion
#           [Hz]      fraction fraction fraction
#   1     0.25171     0.9999  0.01506 -0.00030
#   2     1.04480     0.5541 -0.00465  0.83241
#   3     2.92512     0.2093  0.97736  0.03087
#
# Side-bending frequencies with torsion interaction
# calculated without speed variations.
#           Freq      Transl. Rolling  Torsion
#           [Hz]      fraction fraction fraction
#   1     0.24599     0.9999  0.01548 -0.00028
#   2     1.04479     0.5727 -0.00946  0.81968
#   3     1.40001     0.9976  0.06785  0.01394
#
# Mode with largest fore-aft interaction: 7
# Fore-aft bending frequencies.
#           Freq      Transl. Tilting
#           [Hz]      fraction fraction
#   1     0.24836     0.9999  0.01595
#   2     1.61618     0.9073 -0.42045

```

Figure 4.11: A part of the “towmod.out” tower model output file for the RWT flexible case showing the eigen-frequencies of the tower

Table 4.2: Results of the flexible case

	Pitch [°]	TSR [-]	[rpm]	C_p [-]	C_T [-]	Power [MW]	Thrust [kN]
RWT	0.00	7.5	7.23	0.466	0.777	5.23	962
UPS	0.00	7.5	6.26	0.463	0.771	6.95	1,280
LSO	1.00	7.5	6.26	0.346	0.466	5.21	771
HLA	1.00	8.66	7.23	0.447	0.718	6.74	1,190
HRS	0.80	9.6	8.01	0.440	0.716	6.65	1,180
UPK	0.20	7.5	6.26	0.402	0.582	6.05	962
HRK	0.80	9.6	8.01	0.437	0.707	6.64	1,170

It is worth noting the low C_p and C_T values of the LSO and UPK. The LSO gives almost the same power with the RWT with roughly 20% lower thrust while the UPK gives a higher power with the same thrust as the RWT. It seems that the higher blade twist can play an important role in loads, power production and, subsequently, farm production through the reduction of wake losses. The above results are also used for the first LCoE estimation.

4.2 Modal Analysis

The modal analysis is carried out with the BLADEM mode module. This analysis is done in order to identify clashes of the eigen-frequencies with the P frequencies that could lead to un-damped resonances. It is also done to provide extra knowledge on problems that may arise in the dynamic response in the time-domain simulations of the load cases.

The calculation is done for winds ranging from 0.5 to 25 m/s with steps of 0.5 m/s. Here, a vertical wind shear is included. It is described by the power function with a 0.1429 exponent (0.14 according to IEC 61400-3 [22]). The corresponding rotor speeds and pitch angles are applied, taken from BOT results.

It is broken down into 3 parts. The first one is run with the tower and shaft modelled as rigid and not allowing rotor speed variations in order to obtain the 1st edge-wise mode of the rotor (reaction-less R-L mode). This mode may not produce extra loads on the shaft because it is in-phase, but may produce problems with the tower 2nd side to side mode if the latter resides close to +1P or -1P of the 6P frequency. The second part is done again without allowing speed variations on the rotor but with the shaft and tower modelled as flexible. This gives the in-phase 1st edge-wise mode of the rotor, namely the torsional mode of the drive-train shaft (DT edge). The third part is run allowing rotor speed variations and with the tower and shaft modelled as flexible to get the rest of the flap- and edge-wise modes.

All of the above are run for rotor speeds ranging from 0 to rated rpm of Table 2.4 and with the corresponding pitch angles in above-rated wind speeds. The nomenclature used in the legends of the graphs below corresponds to the rated rotor speed of each concept with 0° pitch. It is characterised by the most apparent component of the coupled mode, so some differences with other definitions in the literature may arise. Modes higher than 3.8 Hz, although calculated, are not depicted for a clearer view on the lower ones, but are reported in Table 4.3. The green lines in the bottom of the graphs correspond to the tower 1st fore-aft mode. In the aerodynamic damping ratios, one should also add the dimensionless structural damping of 0.00478 and 0.01 for the blades and tower respectively.

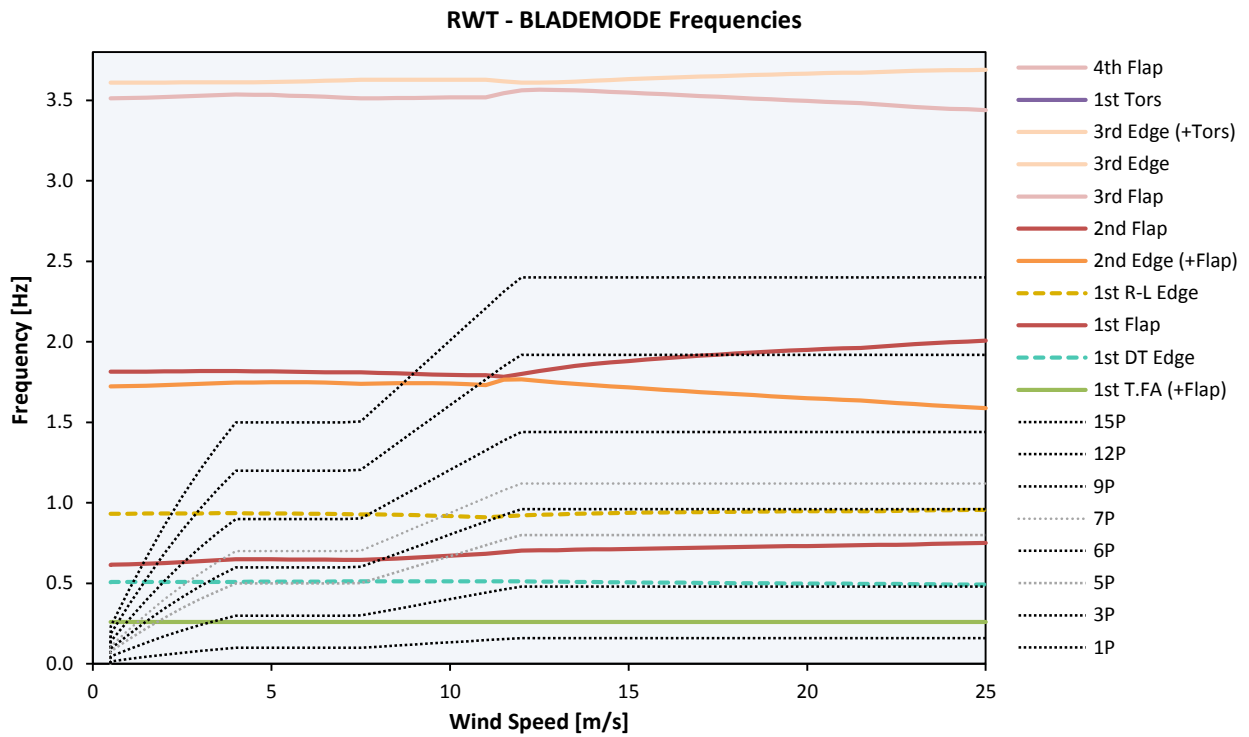


Figure 4.12: Coupled eigen-frequencies of the RWT rotor

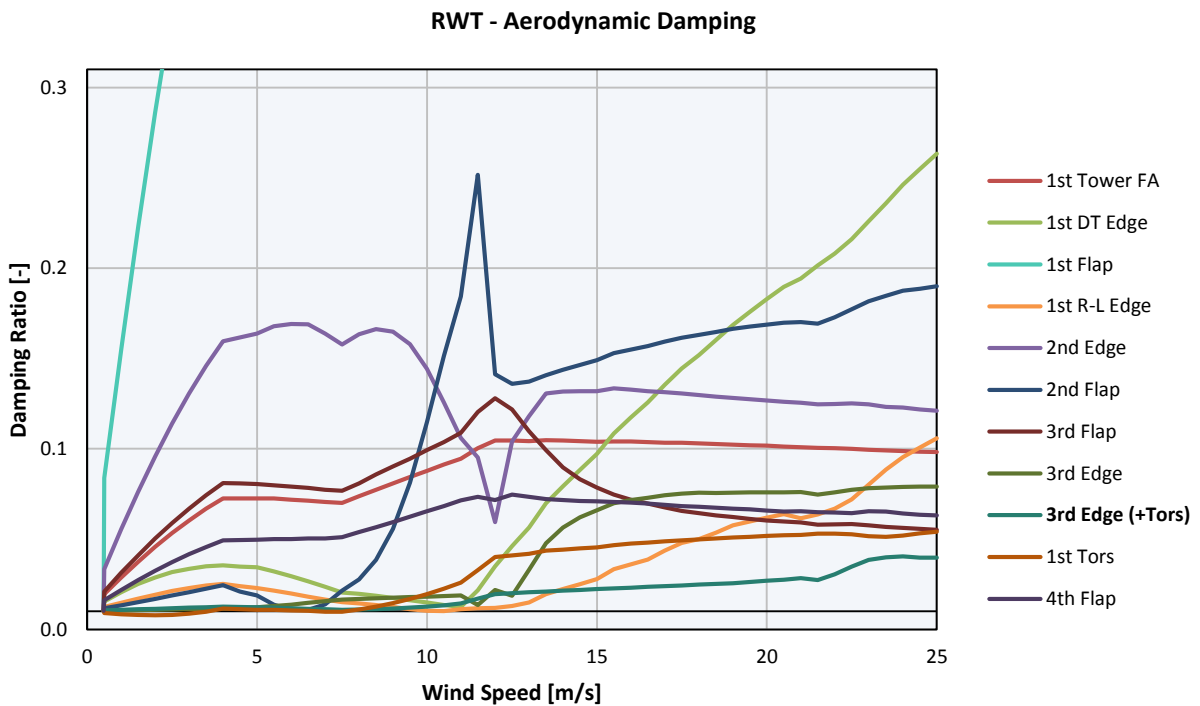


Figure 4.13: Aerodynamic damping versus the operating wind speed for RWT modes

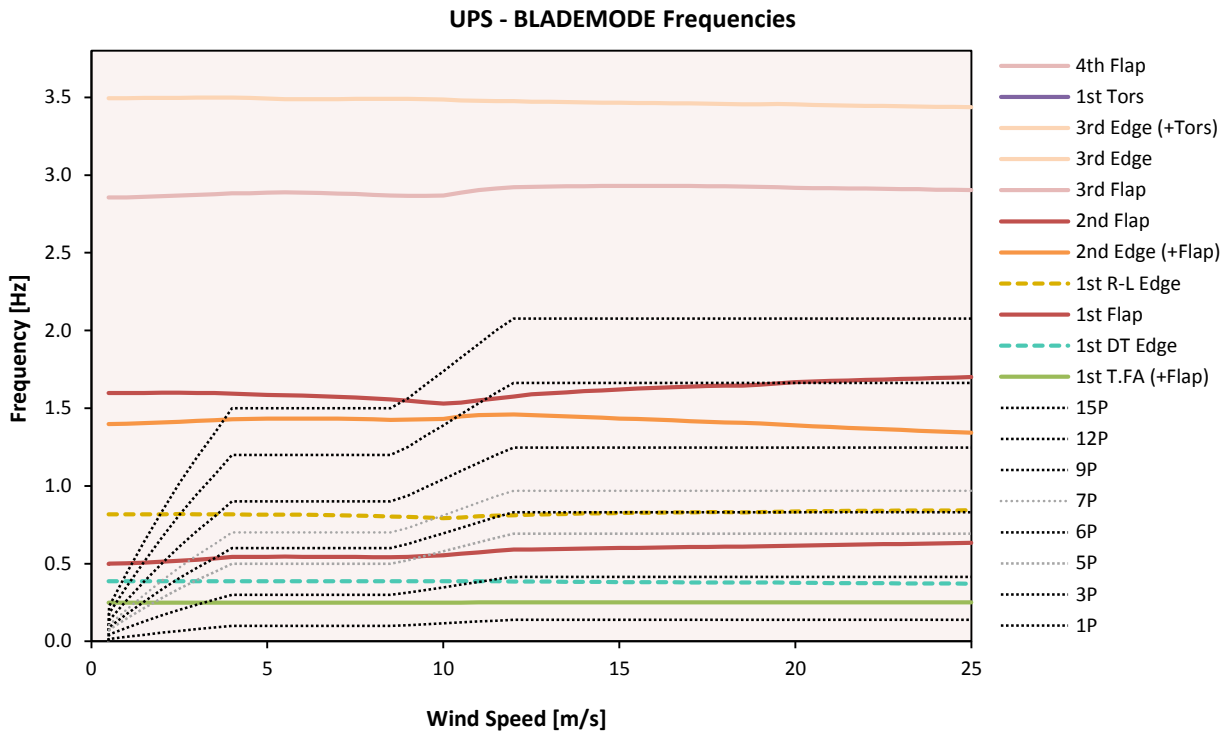


Figure 4.14: Coupled eigen-frequencies of the UPS rotor

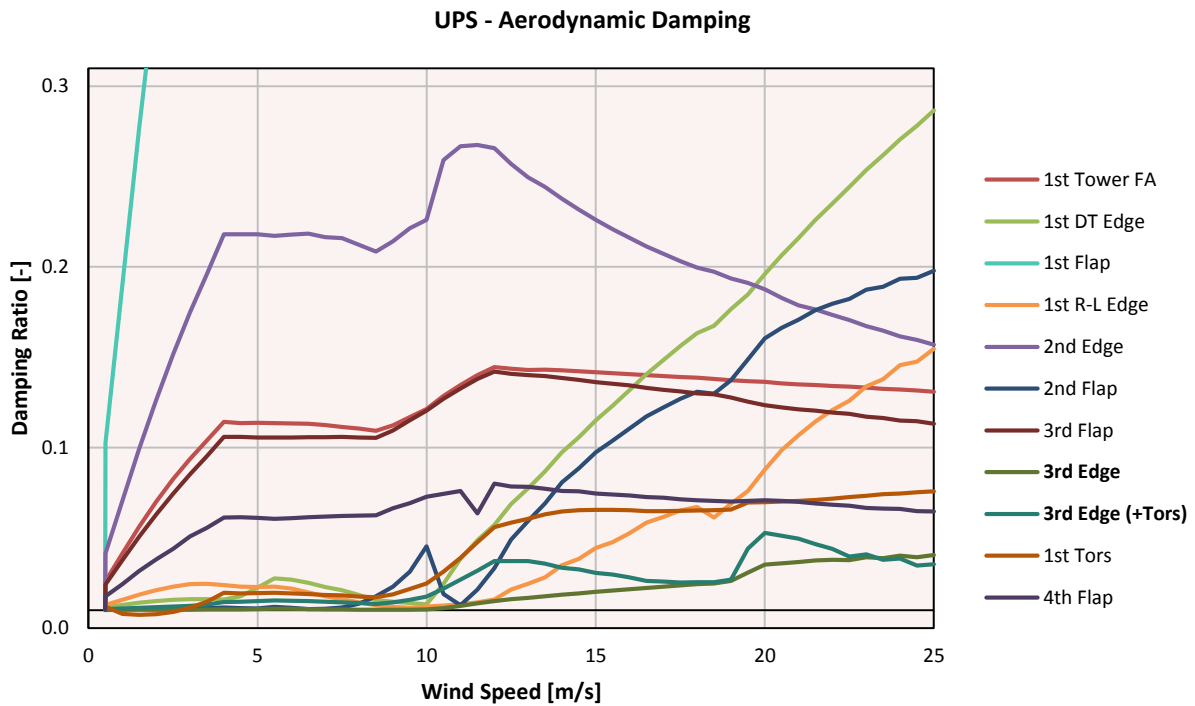


Figure 4.15: Aerodynamic damping versus the operating wind speed for UPS modes

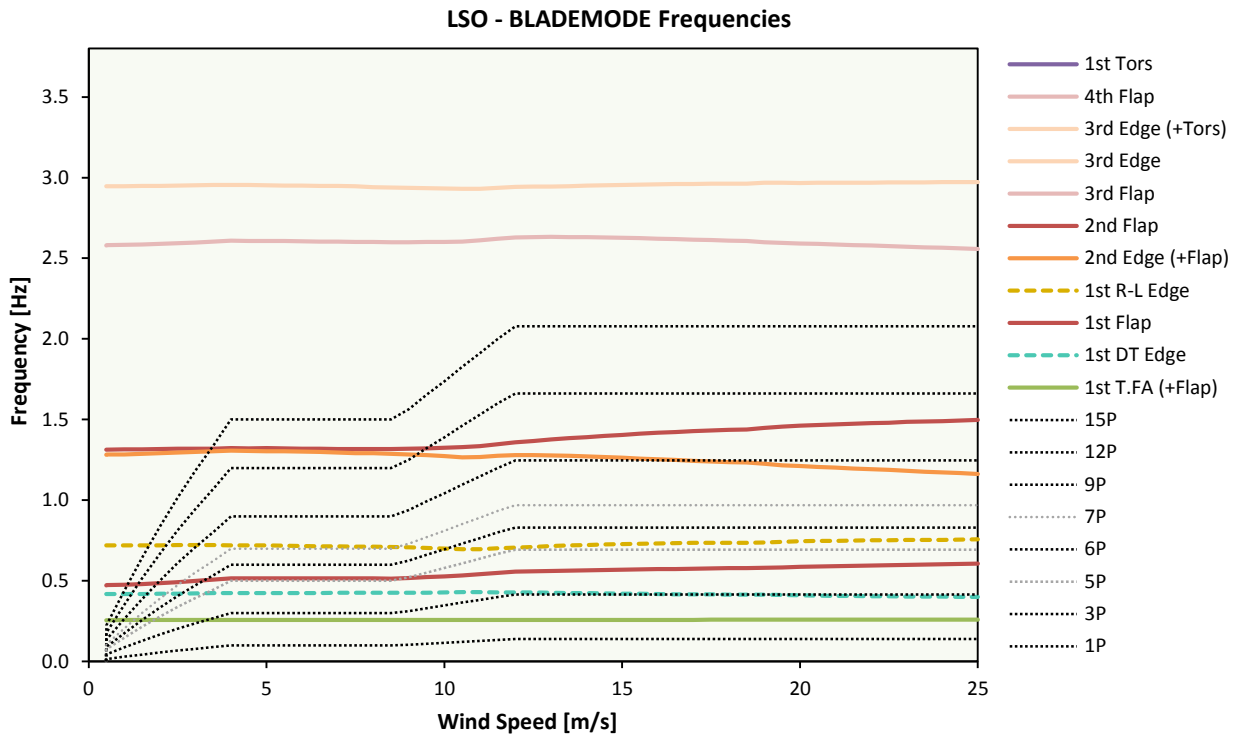


Figure 4.16: Coupled eigen-frequencies of the LSO rotor

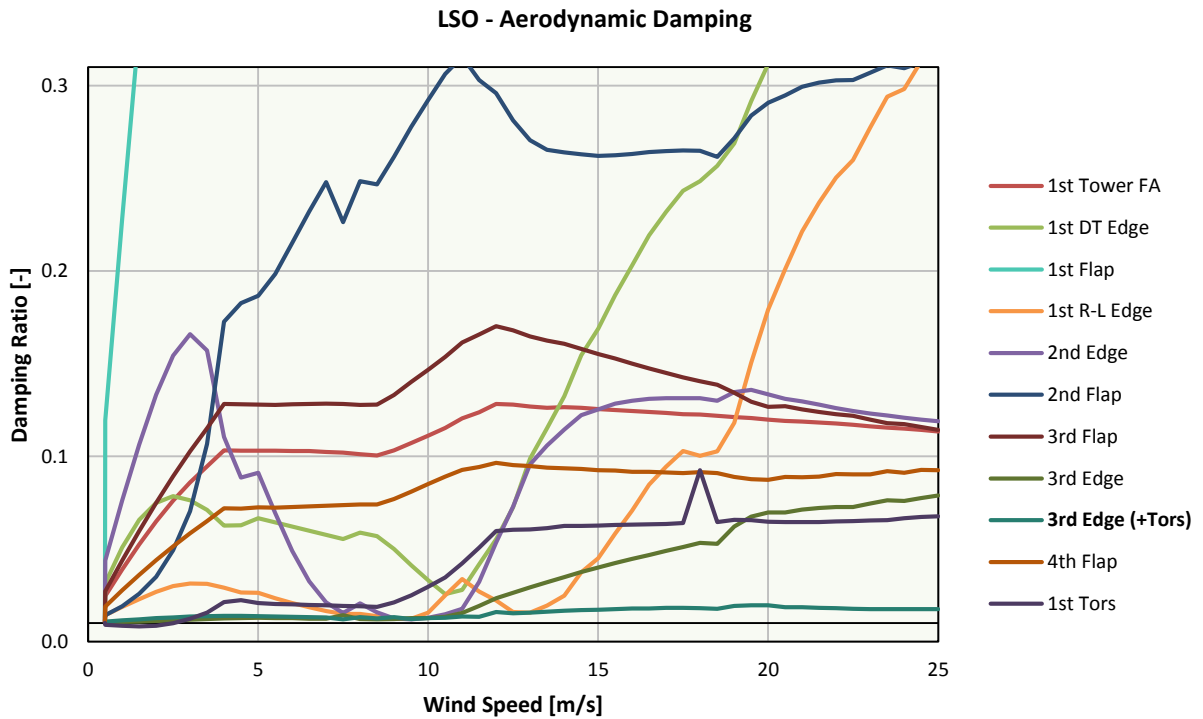


Figure 4.17: Aerodynamic damping versus the operating wind speed for LSO modes

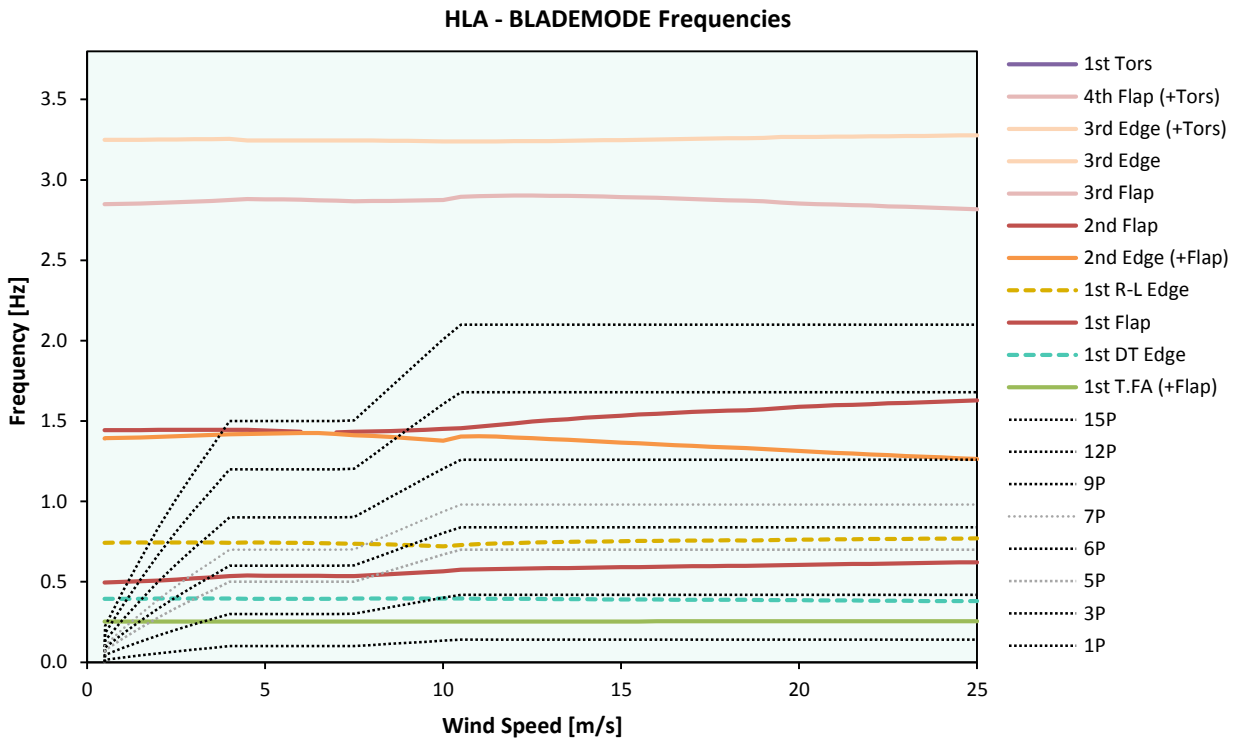


Figure 4.18: Coupled eigen-frequencies of the HLA rotor

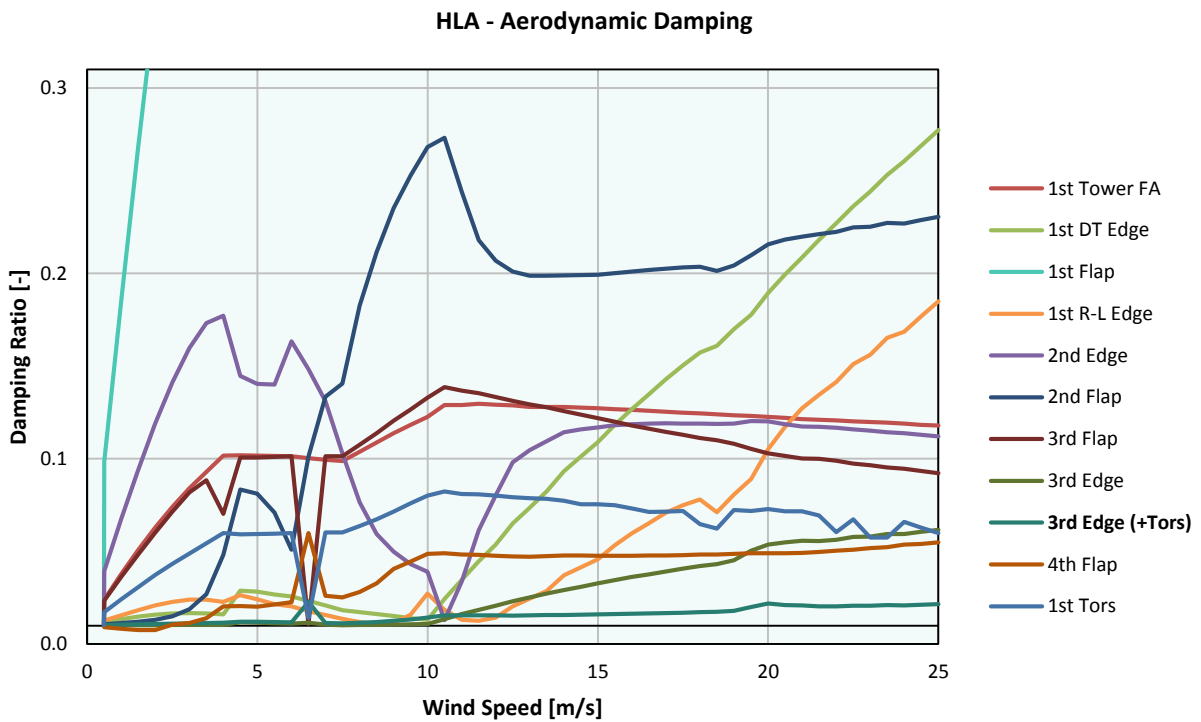


Figure 4.19: Aerodynamic damping versus the operating wind speed for HLA modes

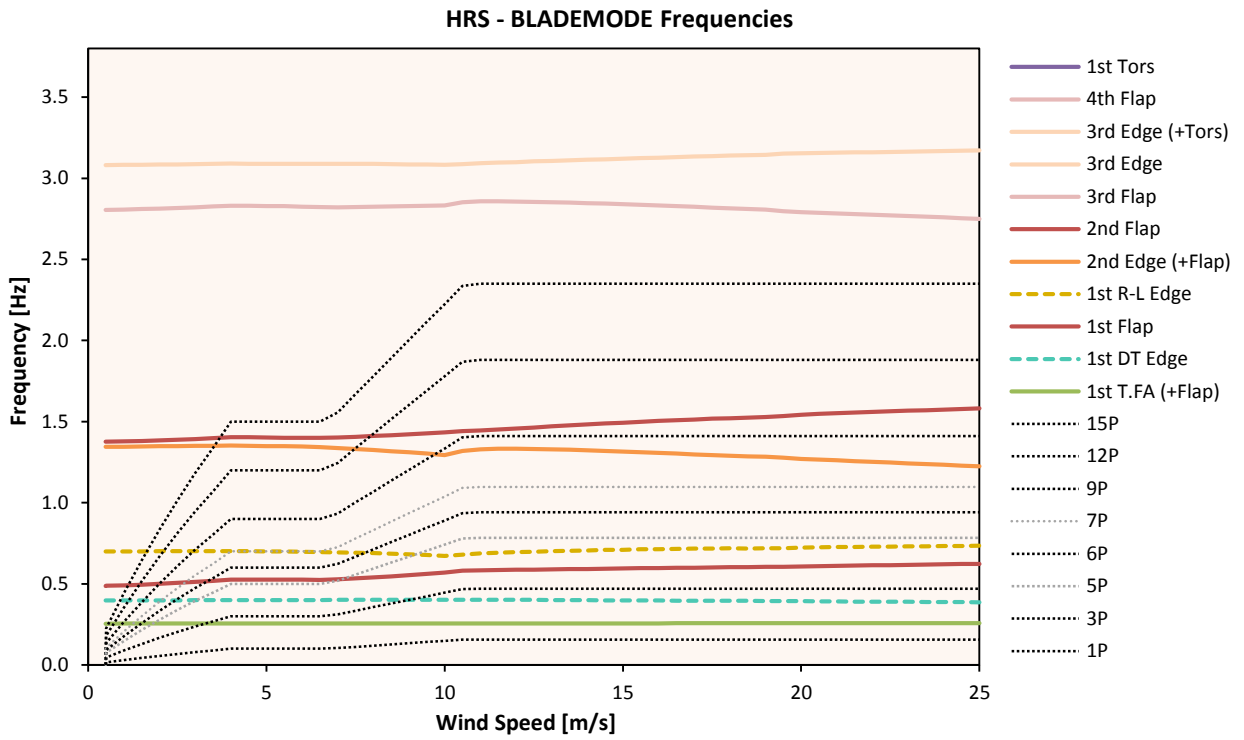


Figure 4.20: Coupled eigen-frequencies of the HRS rotor

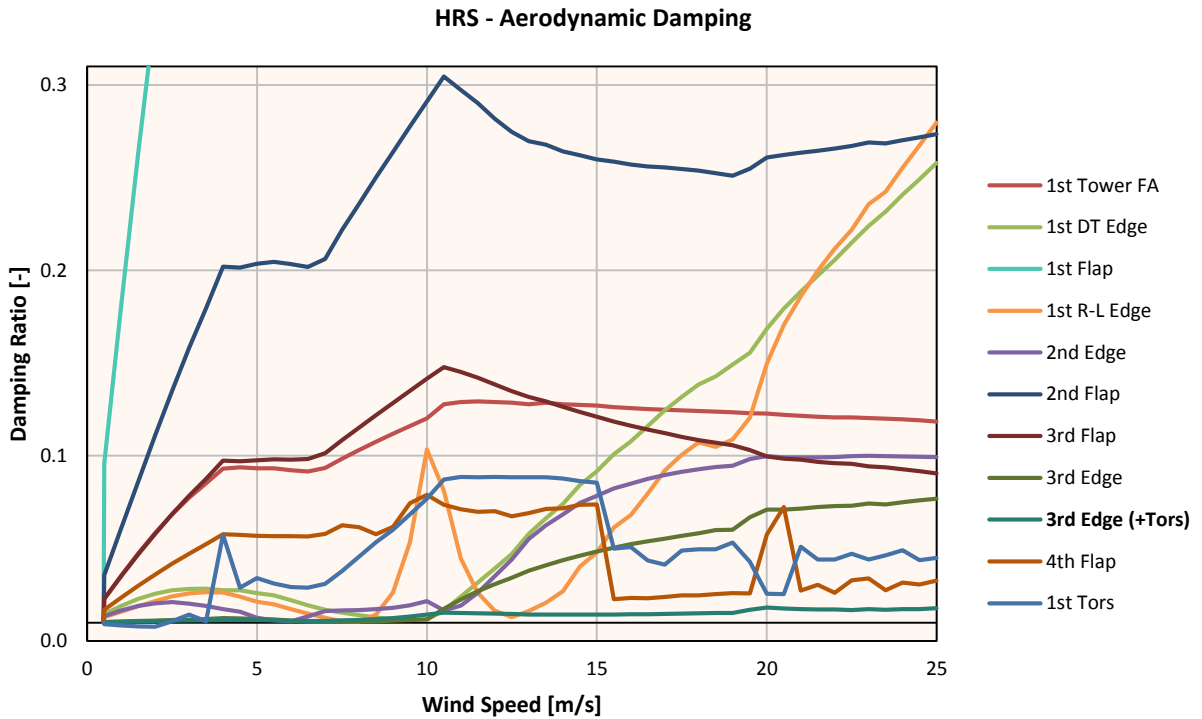


Figure 4.21: Aerodynamic damping versus the operating wind speed for HRS modes

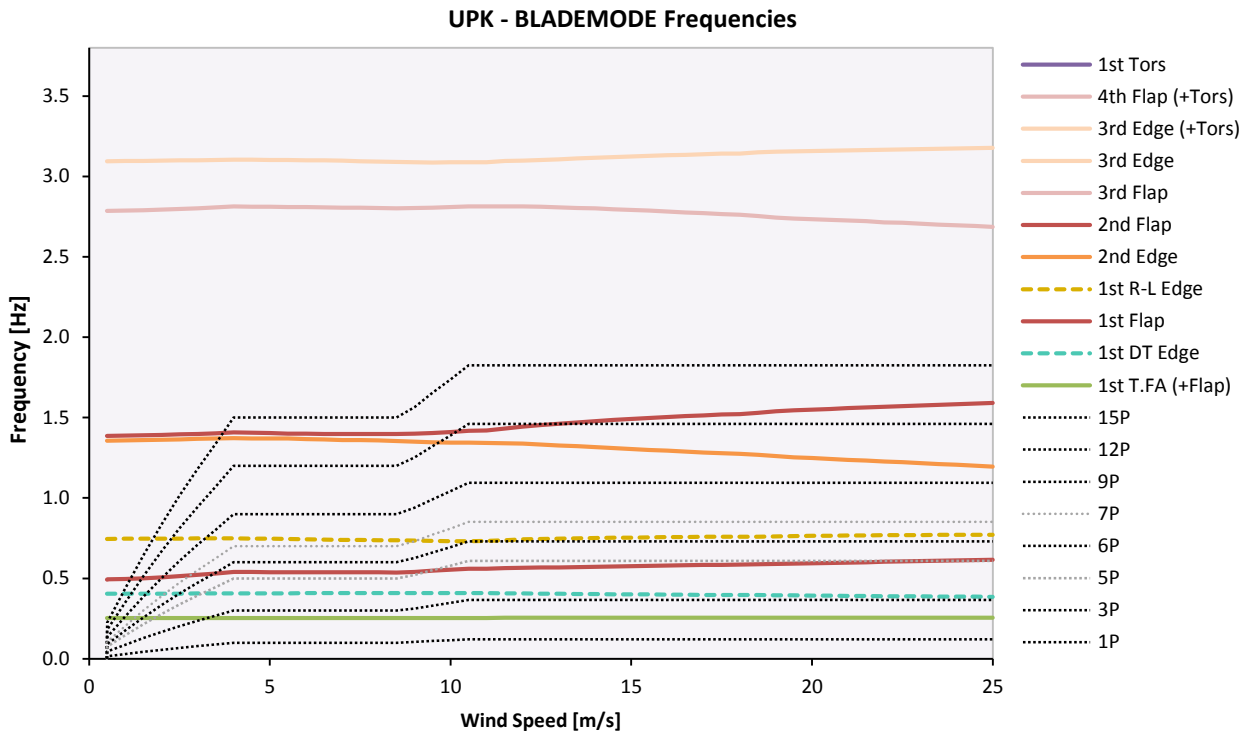


Figure 4.22: Coupled eigen-frequencies of the UPK rotor

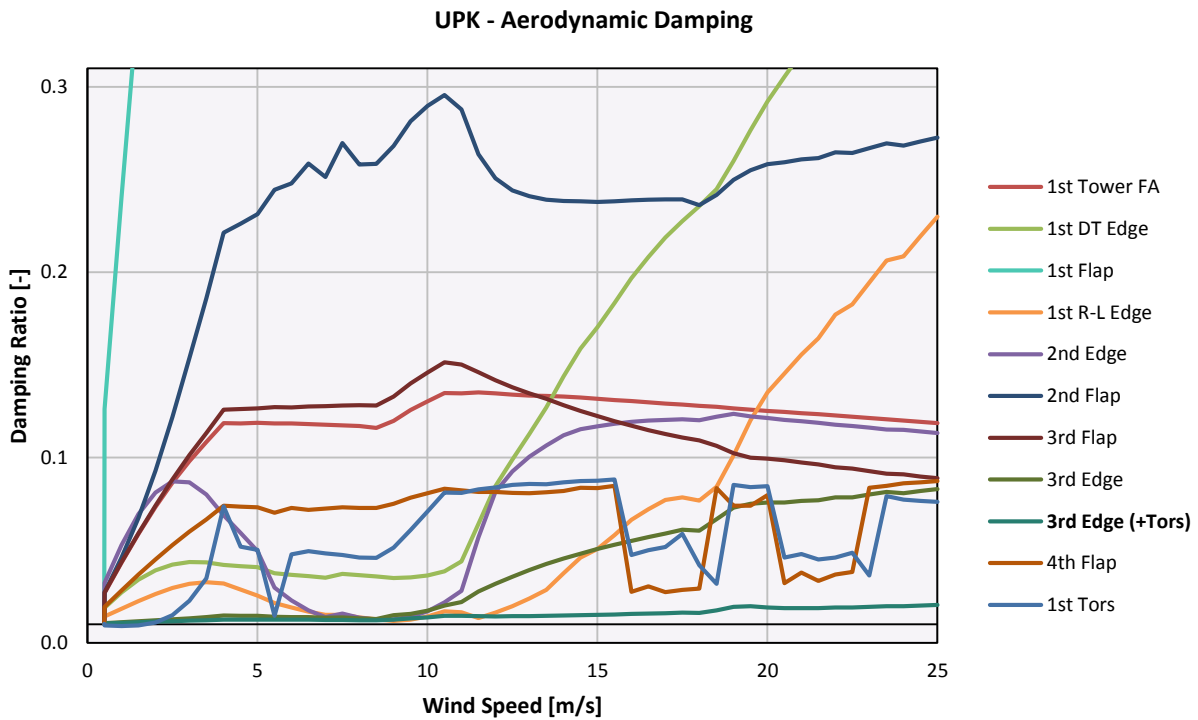


Figure 4.23: Aerodynamic damping versus the operating wind speed for UPK modes

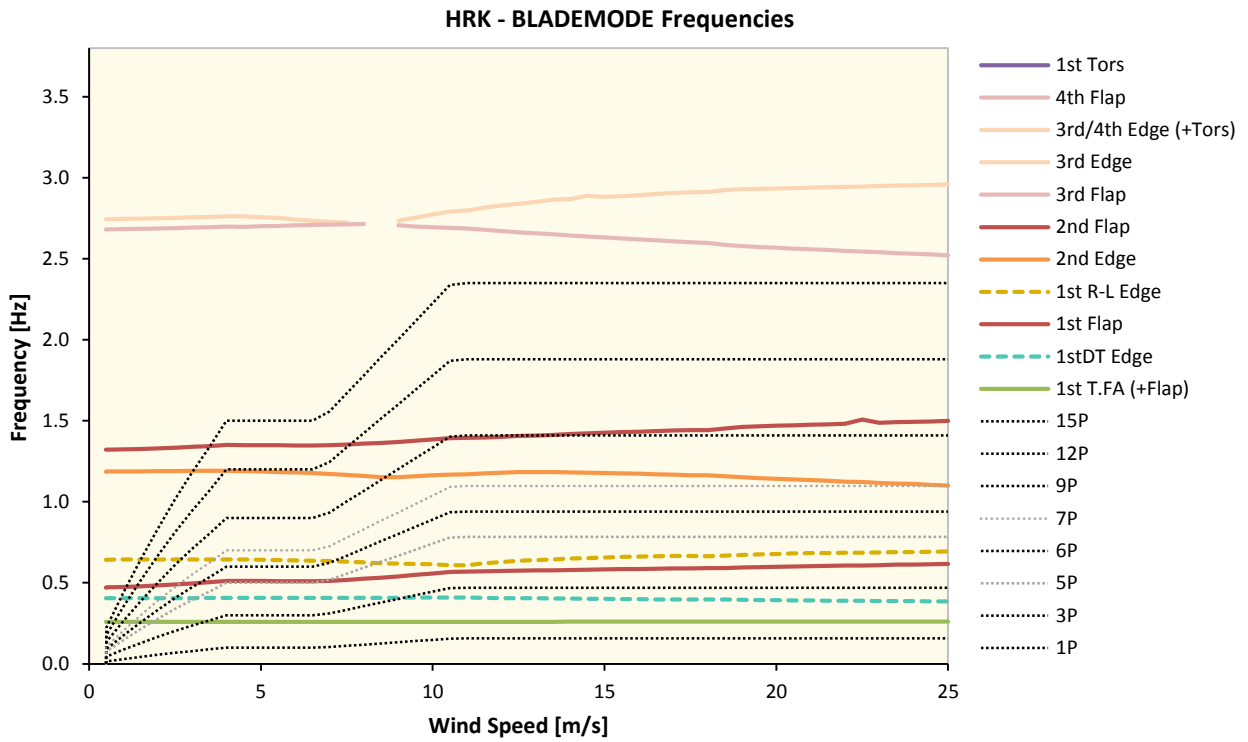


Figure 4.24: Coupled eigen-frequencies of the HRK rotor

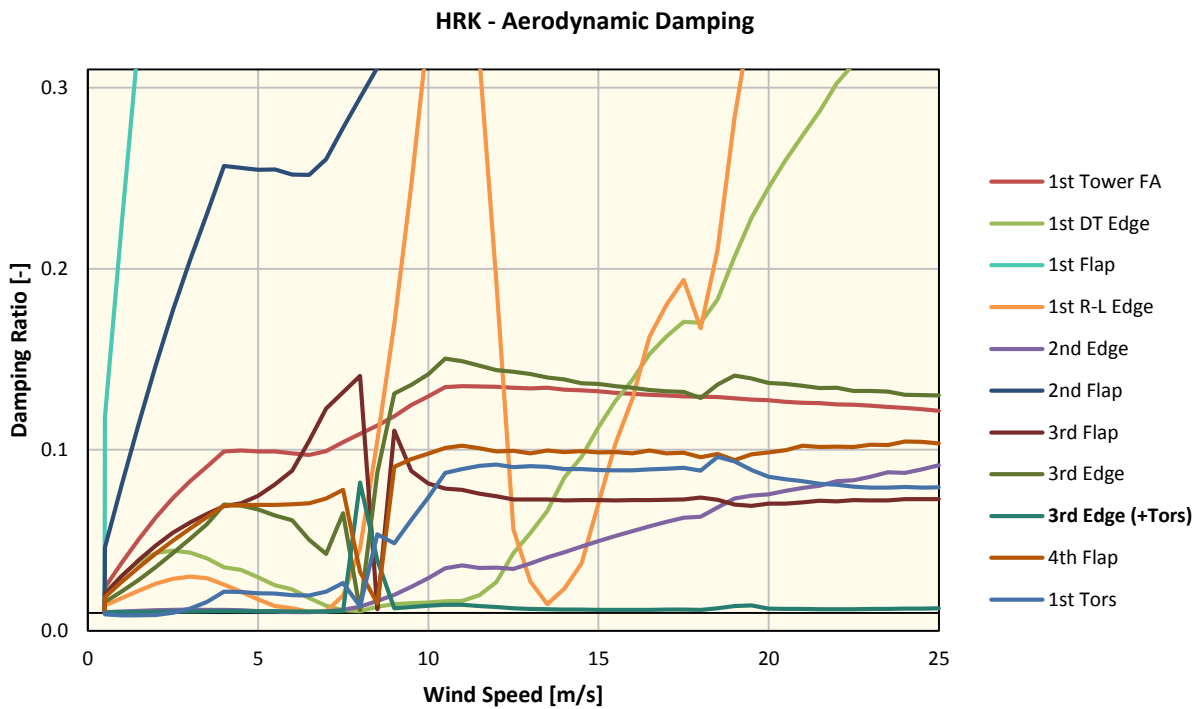


Figure 4.25: Aerodynamic damping versus the operating wind speed for HRK modes

Table 4.3: Frequencies in Hz at rated rotor speed of each design and the standard deviation (StD) between concepts summarised

	RWT	UPS	LSO	HLA	HRS	UPK	HRK	StD
1st Tower FA	0.260	0.250	0.258	0.253	0.256	0.254	0.260	0.003
1st DT Edge	0.512	0.386	0.429	0.396	0.402	0.409	0.409	0.040
1st Flap	0.703	0.590	0.558	0.576	0.583	0.560	0.569	0.047
1st R-L Edge	0.922	0.812	0.707	0.729	0.687	0.732	0.610	0.092
2nd Edge	1.767	1.459	1.280	1.403	1.329	1.344	1.169	0.175
2nd Flap	1.801	1.575	1.359	1.455	1.446	1.417	1.394	0.141
3rd Flap	3.562	2.921	2.629	2.894	2.858	2.814	2.686	0.284
3rd Edge	3.610	3.475	2.942	3.238	3.093	3.089	2.798	0.266
3rd Edge (+Tors)	4.736	4.207	3.972	4.089	4.045	4.025	3.890	0.261
1st Tors	5.312	4.380	5.031	4.887	4.881	4.879	5.190	0.276
4th Flap	5.963	4.905	4.367	4.688	4.725	4.692	4.606	0.478

From the graphs above, it can be seen that the lighter or more slender of the designs (LSO, HRS, UPK and HRK) seem to be posing certain aeroelastic challenges. The 2nd flap-wise and/or 2nd edge-wise modes lie close to the 9P frequency. In the cases of LSO and UPK, there also seems to be a dip in the aerodynamic damping ratios close to the rated wind speed for the 2nd edge-wise mode. For the HRS and HRK the damping is low throughout the partial load region for the same mode. This means that the structural behaviour of the blades at these situations depend mainly on material damping. However, the oscillations produced from these poorly damped resonances were not deemed detrimental to the operation of the turbine. Their effect was sought to be reflected either in the extreme loads and responses or in the fatigue estimations.

Out of the above results, the combination of wind speed, rotor speed and pitch angle giving the maximum flap-, edge-wise and torsional tip displacement (a different combination for each design) was re-run to acquire the span-wise distributions of moments and displacements. This would serve as a sanity check for the BOT loads used in the modelling process and as hints on the structural behaviour of the blades. The flap- and edge-wise simulations were done close to rated wind speeds while torsional simulations were run at varying wind speeds.

Table 4.4: Condition combinations for maximum displacements calculations

	Max. Flap Displacement			Max. Edge Displacement			Max. Torsional Displacement		
	WSP [m/s]	RSP [rpm]	Pitch angle [°]	WSP [m/s]	RSP [rpm]	Pitch angle [°]	WSP [m/s]	RSP [rpm]	Pitch angle [°]
RWT	11.0	8.84	0.12	12.0	9.60	4.86	22.0	9.60	19.69
UPS	10.0	6.95	0.10	10.5	7.30	2.91	19.5	8.31	17.84
LSO	10.5	7.30	1.00	11.0	7.65	1.83	18.5	8.31	13.83
HLA	10.0	8.03	1.00	10.5	8.40	3.90	20.0	8.40	18.42
HRS	10.0	8.90	0.80	10.5	9.35	3.40	21.0	9.40	17.70
UPK	10.0	6.95	1.30	11.0	7.30	2.50	11.0	7.30	2.50
HRK	9.5	8.46	2.80	11.0	9.40	4.99	18.5	9.40	15.22

From the graphs presented below, it seems that the flap-wise moment from BOT loads is slightly higher, a rough 20%, with the separation of the sub-optimal designs (LSO, UPK, and HRK) still visible, as intended. For the edge-wise moment though, the differences are much larger, approaching a factor of 4, which could be explained by leaving out the contribution of the blade weight in the BLAEMODE. A crude estimation of the torque and edge-wise moment in equations (2.4) and (2.5) confirms that claim. For the torsional moment, the much lower values of the UPK occur probably due to the different operating conditions.

The flap-wise tip displacement for the less stiff (LSO, HRS and HRK) or more loaded (UPS and HLA) designs are higher. This is partly due to the added blade length. The values of around 10 and 11 m though are small. They give hints that the undeformed blade tip-tower clearances of 11.06 m (see Figure 4.9) for the RWT and 12.09 m for the other designs, coming only from the tilt angle of 5° might be insufficient. This was also confirmed by a great number of non-converging calculations and blade-tower hits in the firstly attempted time-domain load cases for the RWT, UPS and LSO. These two facts led to the reinstatement of the 2.5° forward cone angle for all rotors that increased the tower-tip clearances to 14.92 m and 16.56 m respectively. The edge-wise and torsional displacements seem to be in-line with what would be expected from the stiffnesses and loads.

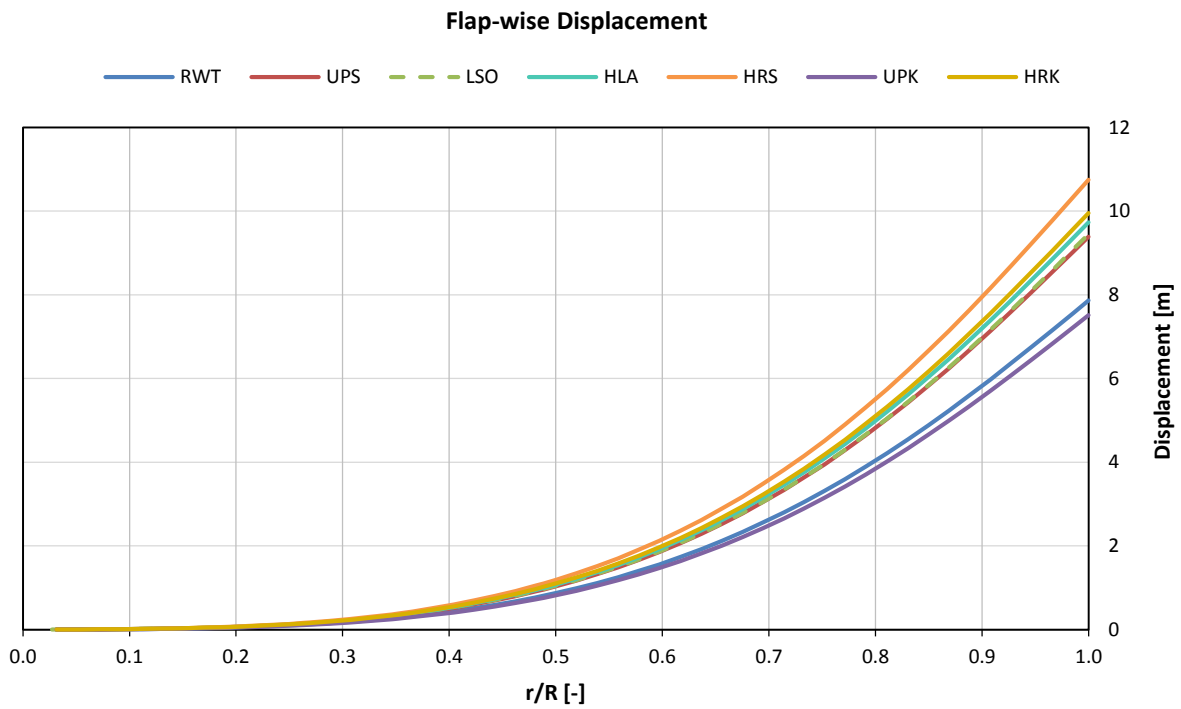
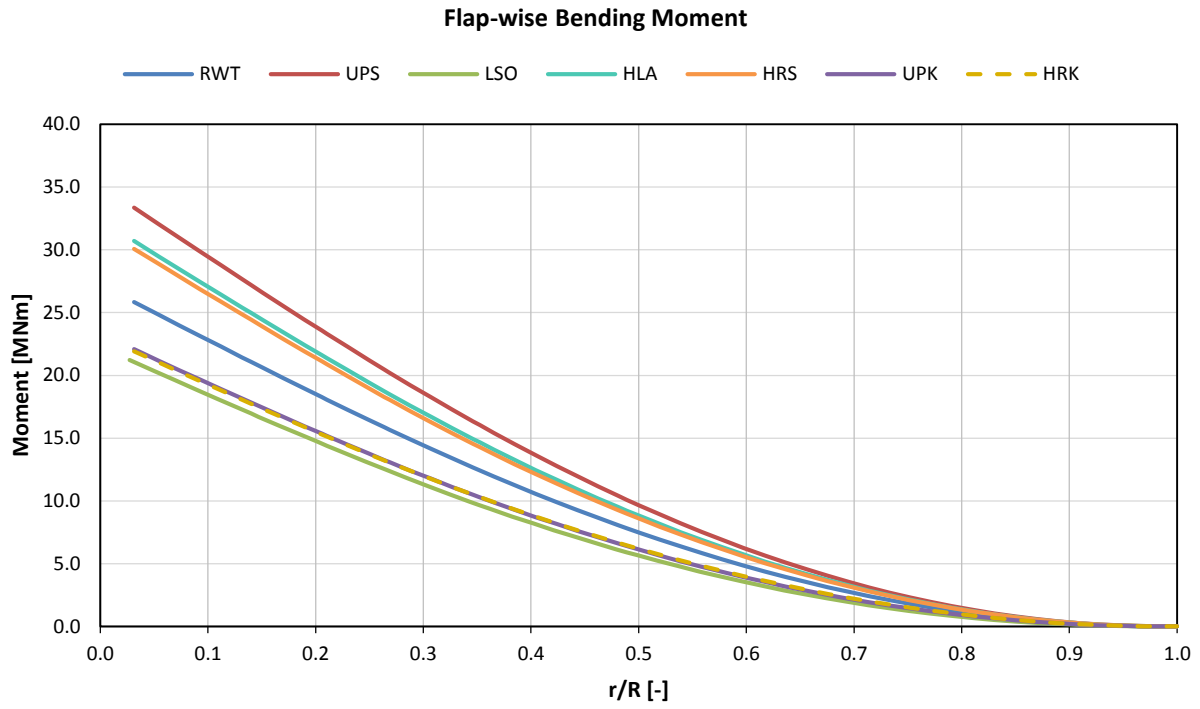


Figure 4.26: Quasi-steady state flap-wise bending moment and displacement along blade span from BLADEMODE

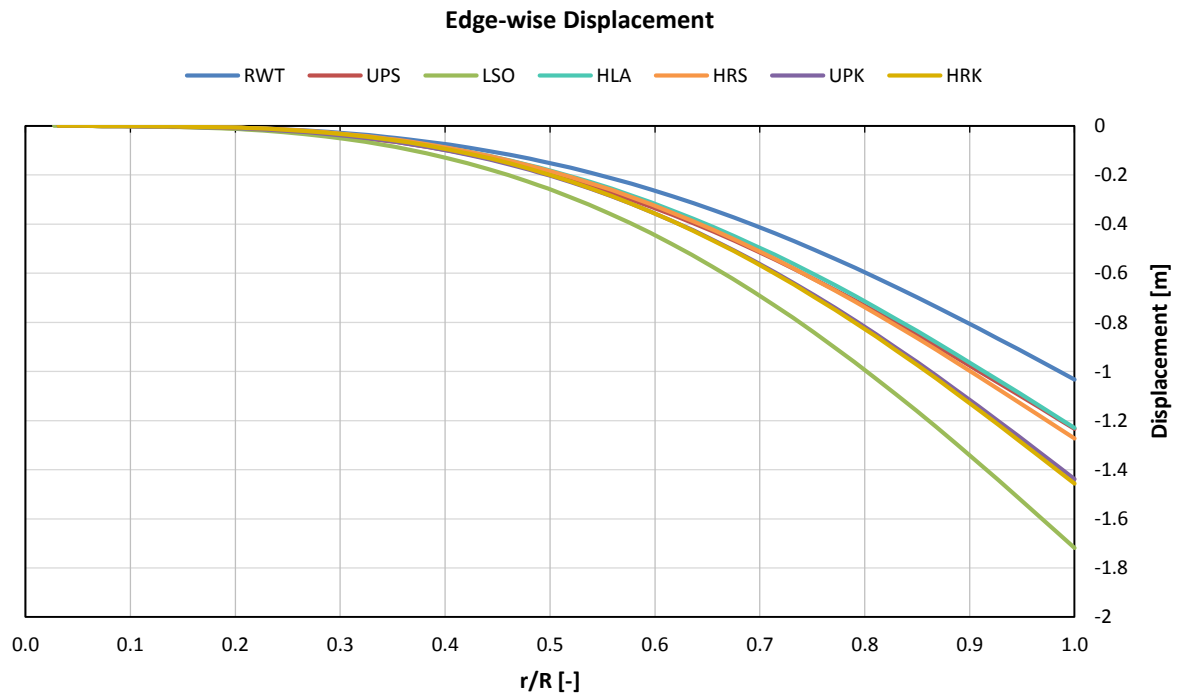
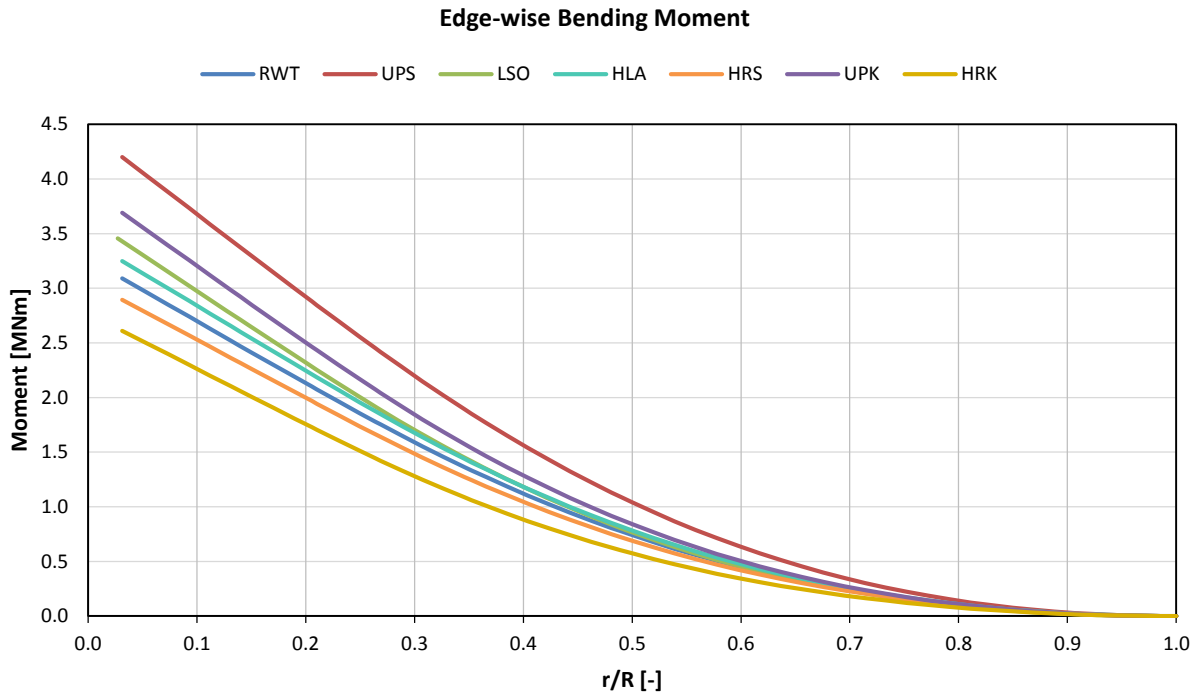


Figure 4.27: Quasi-steady state edge-wise bending moment and displacement along blade span from BLADEMODE

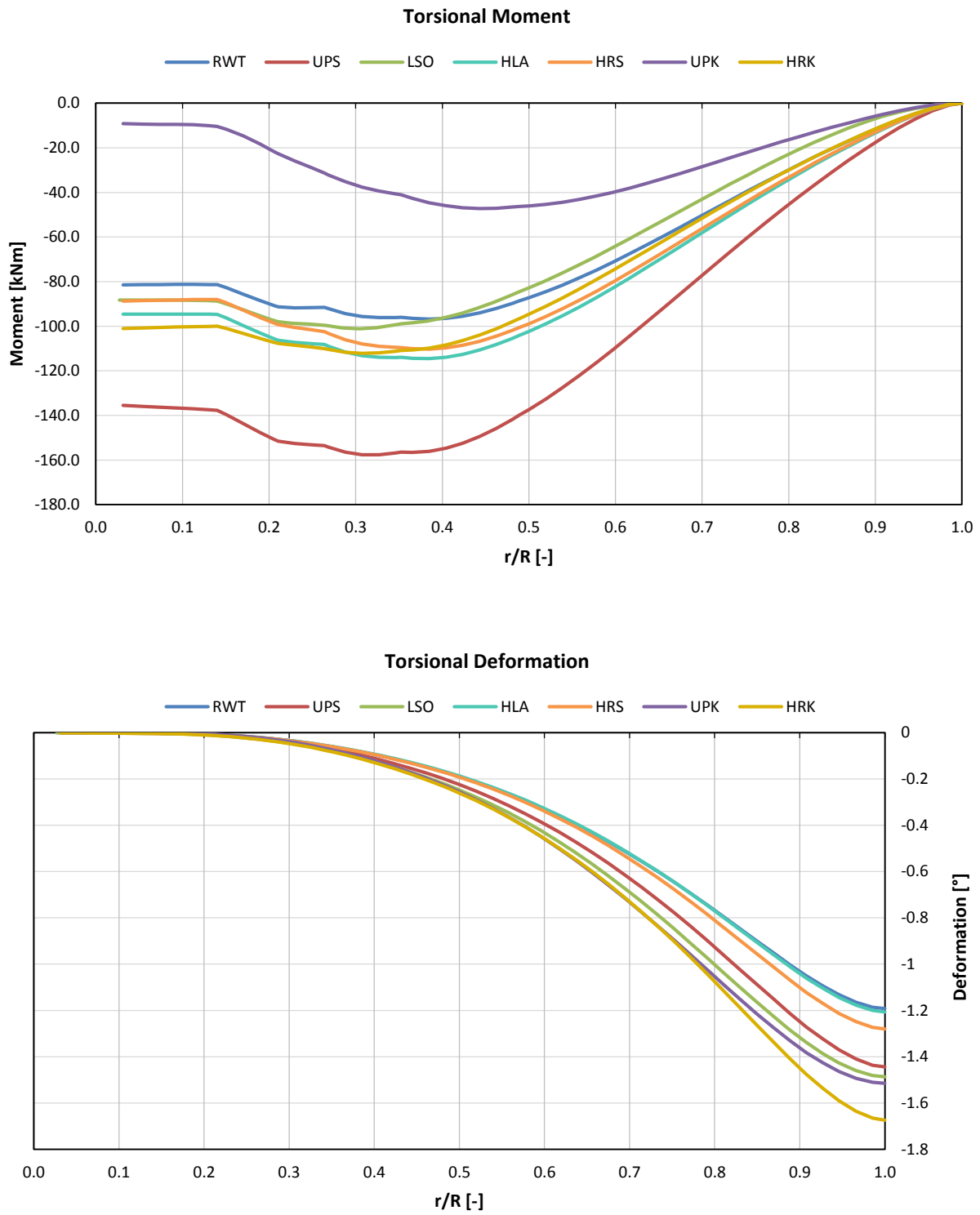


Figure 4.28: Quasi-steady state torsional moment and deformation along blade span from BLADEMODE

4.3 Cost Model and LCoE (Iteration No.1)

The calculated blade masses, C_p from the stationary flexible case and wake losses taken from [7] are plugged in into the LCoE calculator and wind turbine capacity factor, farm capacity factor and LCoE are derived, shown in Table 4.5. The Weibull wind distribution is matched with the one in [7], at 9.41 m/s mean annual wind speed and a shape factor 2.33 (scale parameter 10.62 m/s), so that the wake losses correspond better to conditions chosen in Farmflow. For the same reason the total farm capacity is set to 800 MW (80 wind turbines in Horns Rev model).

Table 4.5: LCoE and capacity factor estimations

	Blade Mass [kg]	C_p [-]	Wake Losses [%]	WT capacity factor [-]	WF capacity factor [-]	Farm AEY [GWh/y]	Farm LCoE [€/MWh]
RWT	41,722	0.466	14.17	0.537	0.429	3,006	93.85
UPS	60,348	0.463	12.43	0.601	0.490	3,432	87.68
LSO	45,309	0.346	10.46	0.534	0.445	3,120	94.66
HLA	54,167	0.447	12.36	0.593	0.484	3,391	88.09
HRS	49,871	0.440	12.29	0.589	0.481	3,373	87.54
UPK	51,612	0.402	11.38	0.571	0.471	3,300	91.04
HRK	42,695	0.437	11.76	0.588	0.483	3,385	86.57

A crude trend of the LCoE is plotted as an indication of the feasibility and performance of the designs versus the main penalty parameter, blade mass. The trend line is an automatically generated 2nd-order polynomial. It is interesting to see that there cannot be a direct link of the blade mass with the LCoE. Lighter designs can be both relatively expensive (RWT, LSO) and cheap (HRS, HRK). Even more interesting is the fact that the optimal designs (UPS, HLA) that have quite a large mass increase, give an LCoE lower than the RWT. It must also be noted that indirect costs such as port and staging equipment, offshore transportation and installation are only affected by rated power and not by the blade mass in this cost model. A more precise and inclusive estimation would probably tilt the results slightly more in favour of the lighter designs. The number of mass data-points and the automatically generated trend-line, however, do not qualify for a solid conclusion since both heavy and lightweight designs can have low LCoE.

Another interesting finding emerged from the connection of LCoE with the Farmflow results for the wake losses (*100% minus the Wind Farm capacity factor*). From the few data-points of the 7 designs it can be seen that one should take them into account in a farm LCoE estimation. The dip seen for the optimal designs (UPS, HLA, HRS) at ca. 12.5% cannot be safely concluded as an optimum, but lowering the power density on the rotor seems to play an important role. On the other hand, when minimising wake losses like in the LSO, energy yield seems to be decreasing disproportionately to the benefits gained.

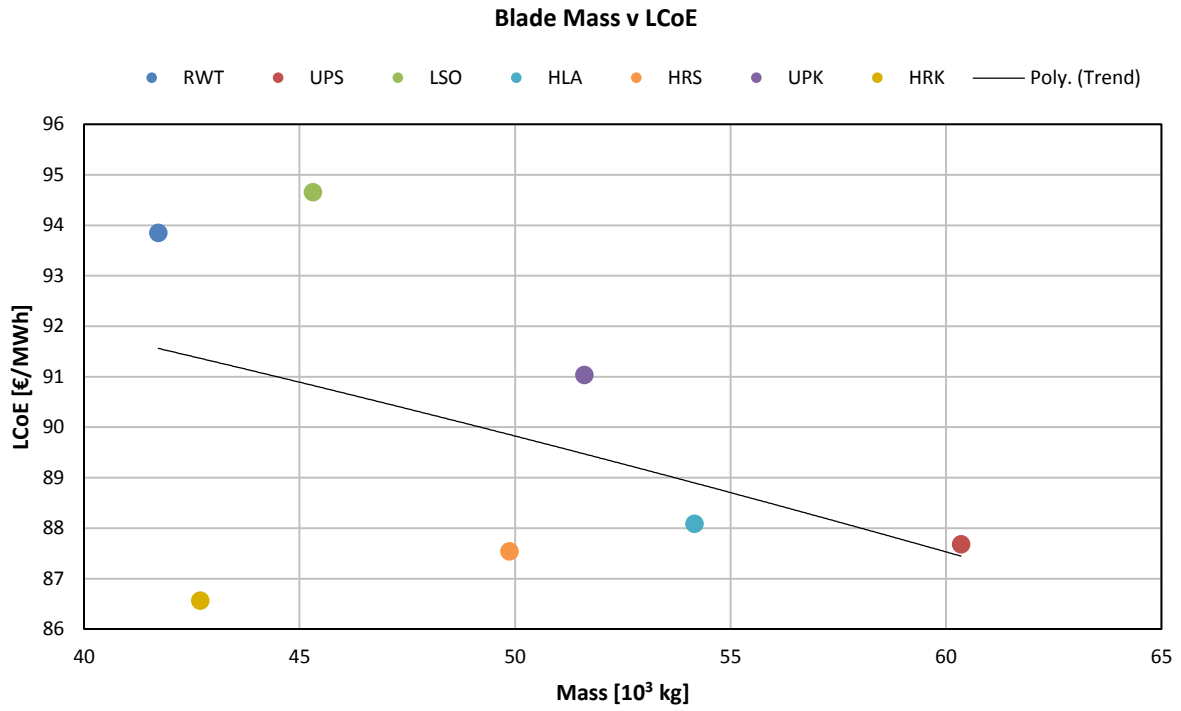


Figure 4.29: Blade mass versus LCoE

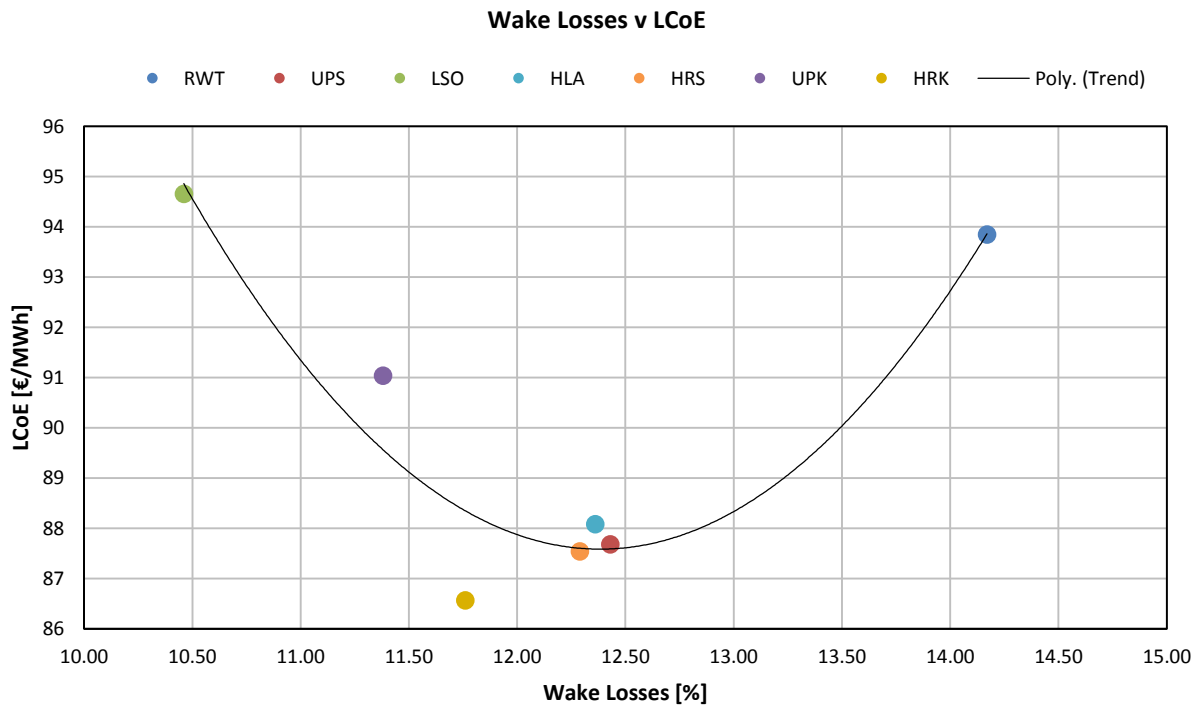


Figure 4.30: Wake losses versus LCoE

4.4 Load Cases

As stated before, time-domain simulations are run in order to investigate some of the extreme loads on the blades and tower, estimate lifetime structural fatigue loads and extrapolate energy production. This analysis would give more realistic energy production value than the one coming from the cost model based on steady-state results.

Five load case sets are run with their respective number of wind speeds and seeds. The input files are generated by the FOCUS LCPrep (Load Case Pre-processor) module as per IEC standards, set by the user. Only a few of their parameters such as simulation duration and grid loss time, where applicable, are modified to comply with AVATAR suggestions.

Table 4.6: List of load case sets and simulation details

DLC	1.2	1.3	2.1	4.1	6.3
Wind Model	NTM	ETM	NTM	NWP	EWM
Type	Fatigue	Extreme	Extreme	Fatigue	Extreme
Description	Power Production	Power Production	Power Production with Fault	Normal Shut Down	Idling with 1-year extreme
Fault	-	-	Grid loss at 80 s	Shut Down at 80 s	Extreme Yaw Misalignment
Wind Speeds	4 - 25 m/s (Steps of 1 m/s)	8 [#] - 25 m/s (Steps of 1 m/s)	Rated-2, Rated, Rated+2, Cut-out	Cut-in, Rated-2, Rated, Rated+2, Cut-out	40 m/s
Yaw Misalignments	-8°, +8°, 0°	-8°, +8°, 0°	-8°, +8°	0°	-20°, +20°
Seeds per Yaw Misalignment	2	2	6	1	6
Seeds per Wind Speed	6	6	12	1	12
Total	132	108	48	5	12
Simulation Time	670 s	670 s	370 s	170 s	670 s
Transients Skip Time			70 s		
Turbulence Intensity			0.16 ^{##}		
Turbulence Auto PSD Model			Von Karman based [44] ^{##}		
Vertical Wind Shear			Power Law		
Wind Shear Exponent			0.1429		

([#]NOTE: For DLC1.3, the load case pre-processor (LCPrep) yielded different starting speeds for every other concept (6, 7 and 8 m/s). In order to maintain a consistent approach, the maximum of these starting wind speeds (8 m/s) until cut-out are used for analysis and post-processing.)

(^{##}NOTE: Except for DLC 4.1 where a NWP is used, Focus' SWIFT module is used to generate stochastic turbulent winds of class 1A with turbulence intensity 16% and with the turbulence model described by a semi-empirical formulation proposed by ESDU (Engineering Sciences Data Unit), based on Von Karman's PSD model.)

The first 70 seconds of every simulation are dedicated to letting transient phenomena pass and are not included in the post-processing. For example, the grid loss in DLC 2.1 effectively happens at 10 seconds into the used/processed time signal.

4.4.1 Controller Modifications

The control for the wind turbine's simulated operation is performed with the use of an external Dynamic Link Library file ("*DISCON.dll*"), accompanied by a settings file ("*discon.in*"). Modifications on the original INNWIND RWT controller settings for a better operation and maximum energy production, were deemed necessary, since the physical and operational parameters of the rotor change significantly (rotor mass, inertia, rated rotor speed etc.).

The work was focused on tweaking the gains of the settings file. These changes lead to different torque vs. rotor speed operational curves (Q-n curves) for the partial load region and different responses for the pitch controller at the rated power region. In the partial load region the rotor speed is controlled with the applied-demanded generator torque following a gain-times-rotor speed squared trend ($K \cdot \omega^2$). This seeks to maximise aerodynamic torque capture while maintaining optimal TSR. In the full load region, the rotor speed is kept constant at the rated value by controlling blade pitch angle and/or pitching speed. Part of the available aerodynamic power is shed and produced electrical power is kept constant [24].

Since the structural designs themselves and their operating conditions are not optimal, the goal is not a fully optimised control design, but merely an improvement on the expected operation of each rotor. Certain issues were detected, such as unnecessary rotor acceleration pointed out in Section 2.1.2, and this feedback from the control design was taken into account for the load case simulations. The control tweaking work was done by ECN personnel. It was tested with step-wise wind simulations and a small number of normal production load cases close to controller transition regions in a trail-and-error manner. The original RWT controller already had a slightly more oscillating pitch response in the step-wise cases than other standard controllers. This behaviour was pursued to be kept throughout all designs.

4.4.2 Design Load Case Simulation Results

In the following graphs, several signals related to operational parameters and loads on the rotors and other wind turbine components are plotted. The number and size of time-series datasets were too large to be presented in an understandable manner and needed to be post-processed. The vertical lines in the following graphs depict the maximum (blue dots), minimum (red dots), mean value (coloured dots by concept) and +/- standard deviation (grey dots) of each time-series signal of every load case seed. Each graph contains seven (7) subplots corresponding to a different rotor concept. Within each of the seven subplots there are five data-groups corresponding to every load set run. From left to right, the first wide group of vertical lines corresponds to the 132 simulations of DLC 1.2, the second wide group to the 108 seeds of DLC 1.3, the third to DLC 2.1, the thin fourth group to DLC 4.1 and the rightmost group to DLC 6.3. The vertical dotted grid-lines also help to distinguish the DLC groups. Use of labels in the x-axes was avoided because useful plotting space would be lost.

For example, in Figure 4.31, for every subplot (i.e. every rotor concept), the averages of the leftmost data group of DLC 1.2 seeds practically formulate the power curve of each wind turbine. And even the groups of 6 seeds per wind speed can be distinguished in the partial load region. The maximum and minimum values in each vertical line (i.e. each seed) correspond to a single momentary value. Hence the use of the standard deviations was employed, including, by definition, the 66.6% of the values of the time-series. Most of the outliers, especially in DLC 1.3, correspond to emergency-shut downs ordered from the controller, because of exceeding maximum allowable generator speed.

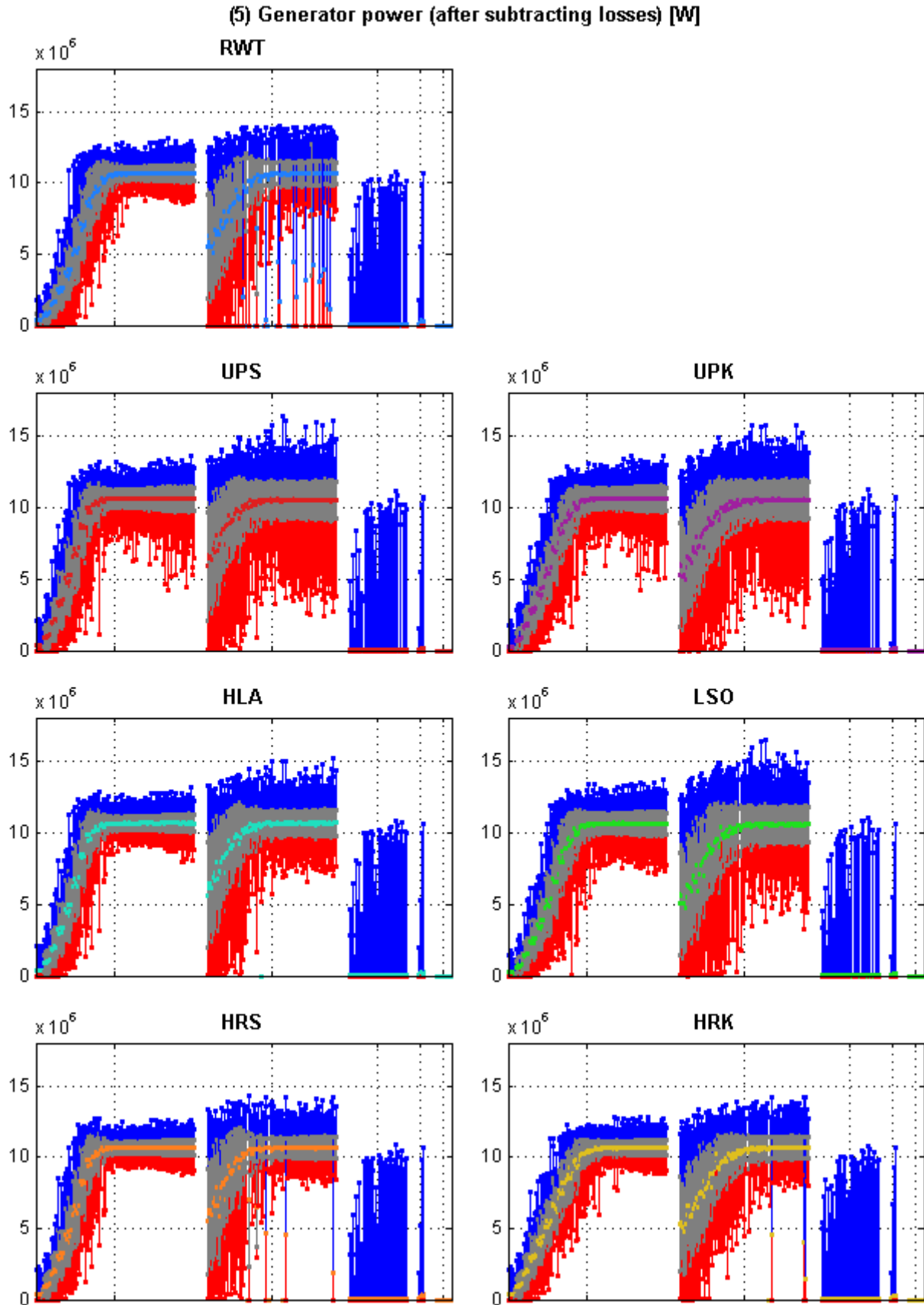


Figure 4.31: Shaft power (excluding 6% electrical losses) from all DLCs for all designs

(4) Axial aero force on rotor [N]

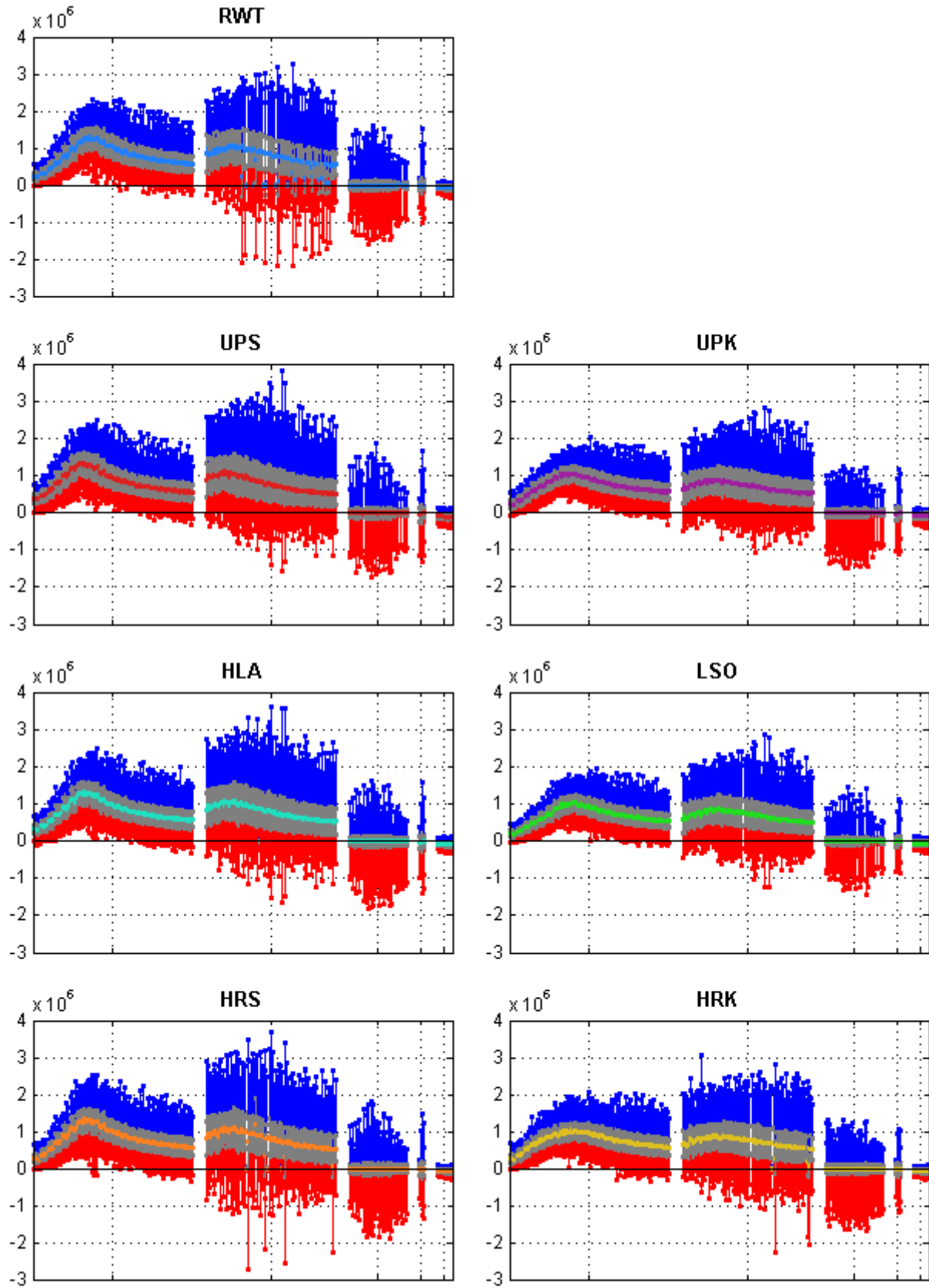


Figure 4.32: Thrust on the rotor from all DLCs for all designs

(12) Rotor speed [rpm]

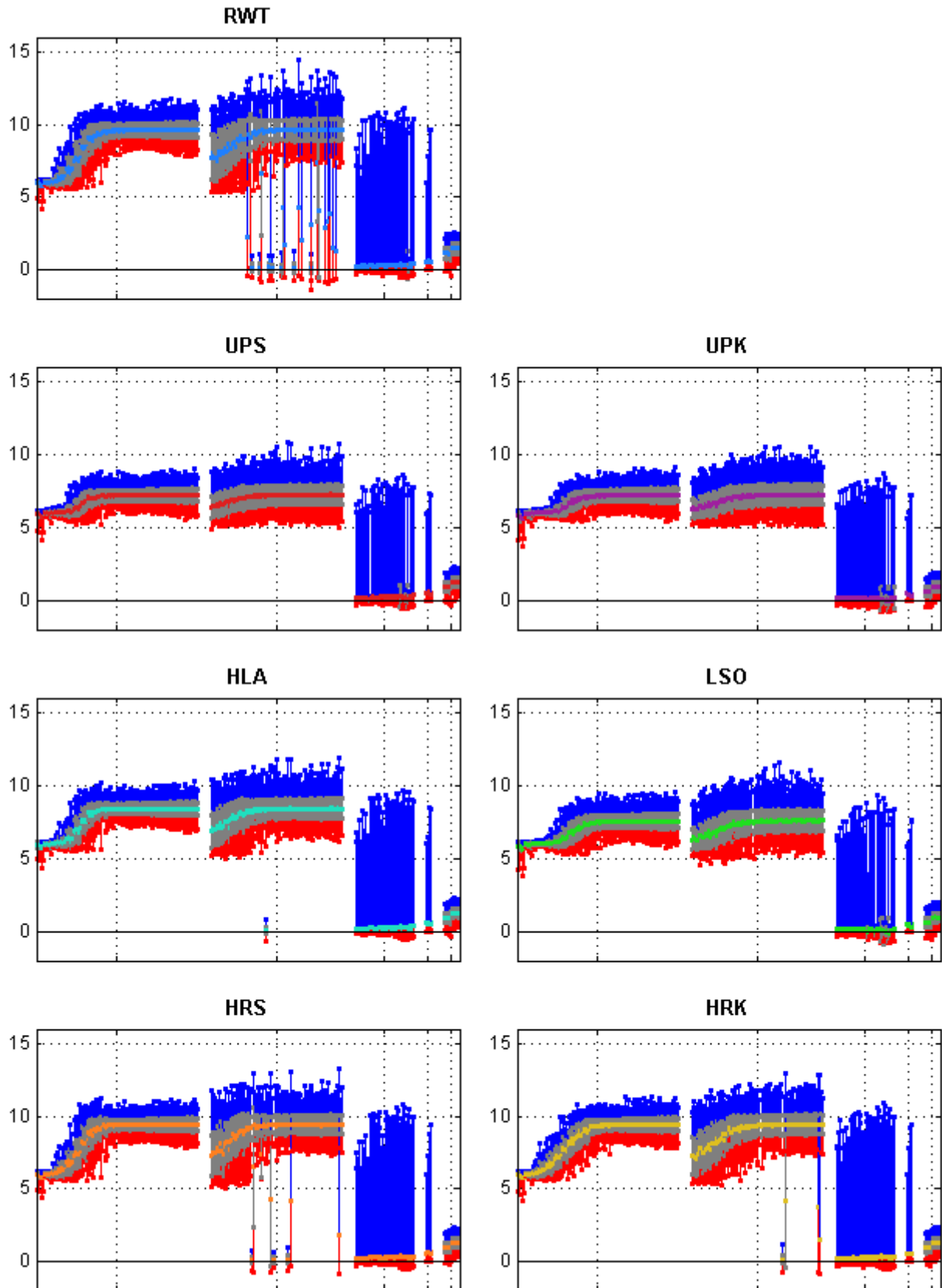


Figure 4.33: Rotor speed from all DLCs for all designs

(61) Torque on the rotor shaft [Nm]

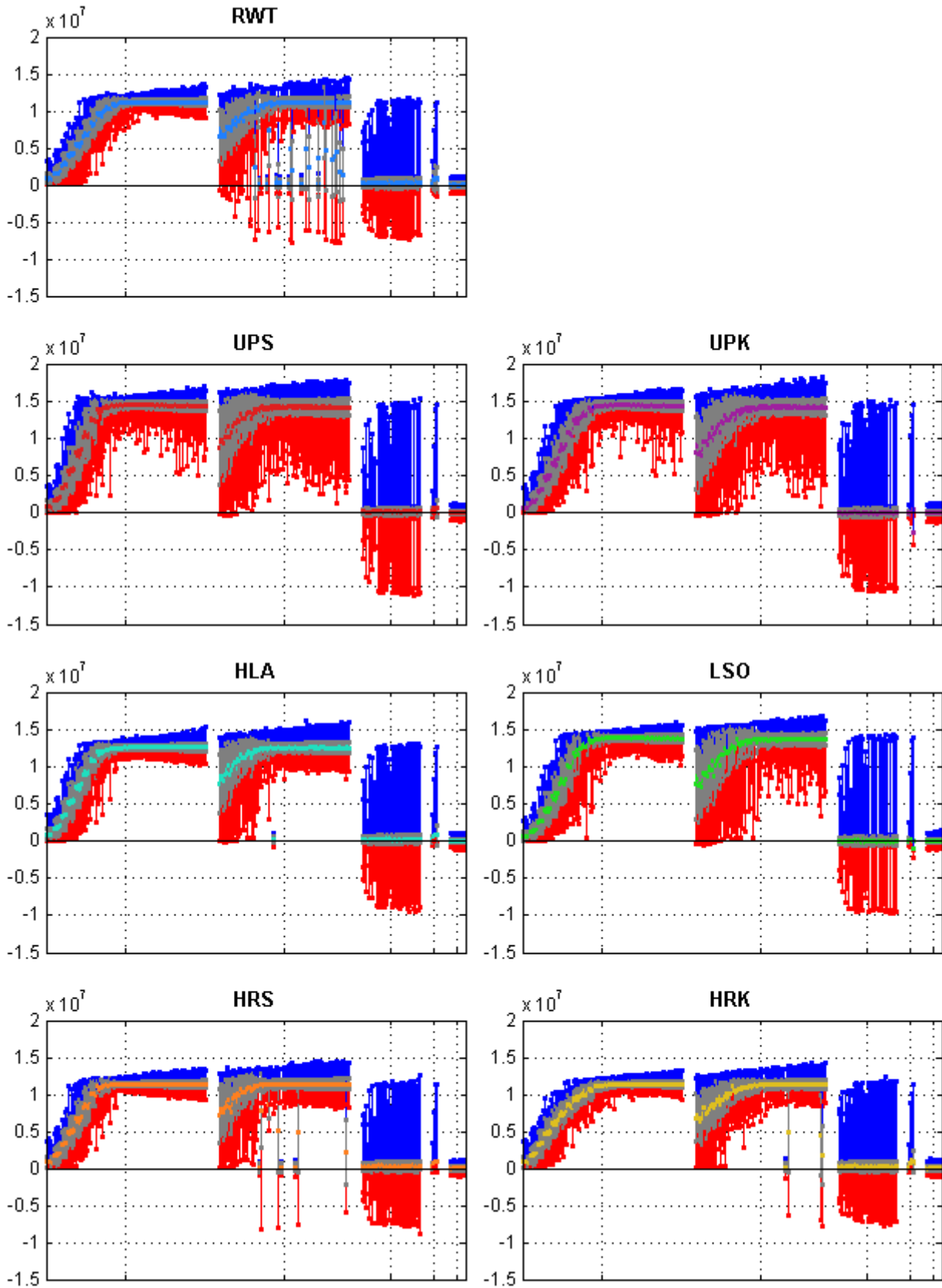


Figure 4.34: Torque on the low speed rotor shaft from all DLCs for all designs

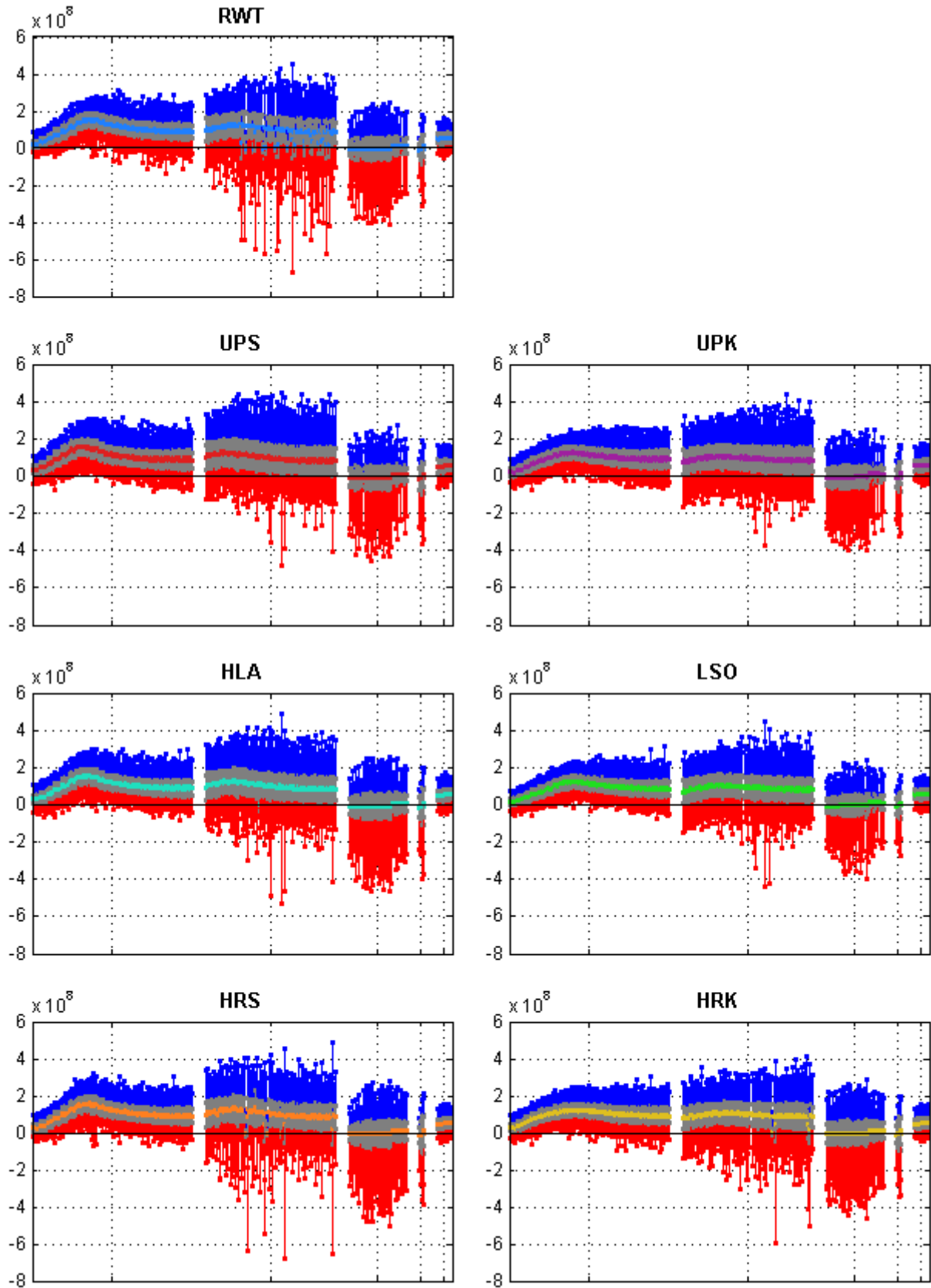
(22) Tower bending moment about Y_{GL} axis (FA) [Nm] @ TB

Figure 4.35: Tower bottom fore-aft bending moment from all DLCs for all designs

(21) Tower bending moment about X_{GL} axis (SS) [Nm] @ TB

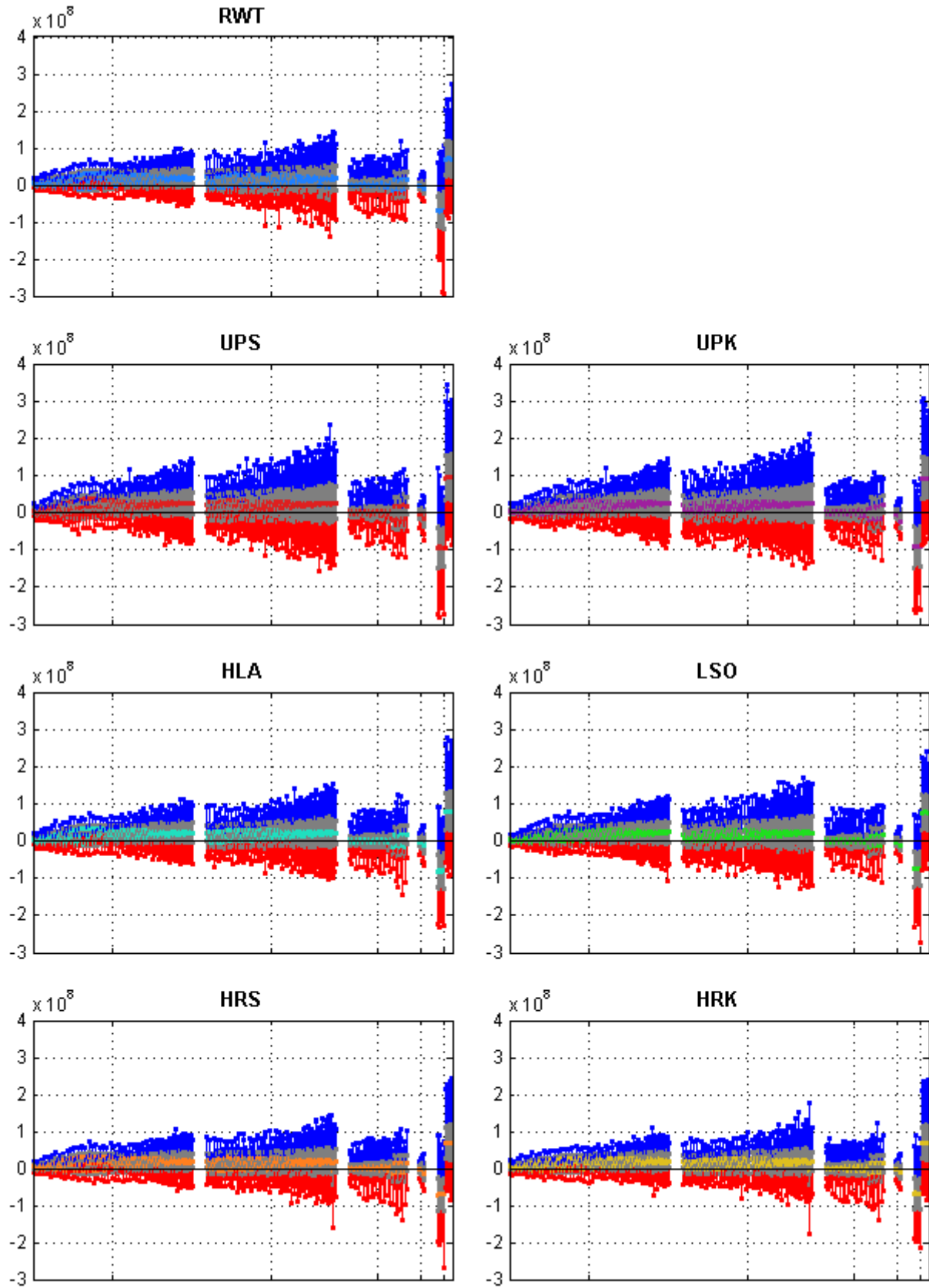


Figure 4.36: Tower bottom side-to-side bending moment from all DLCs for all designs

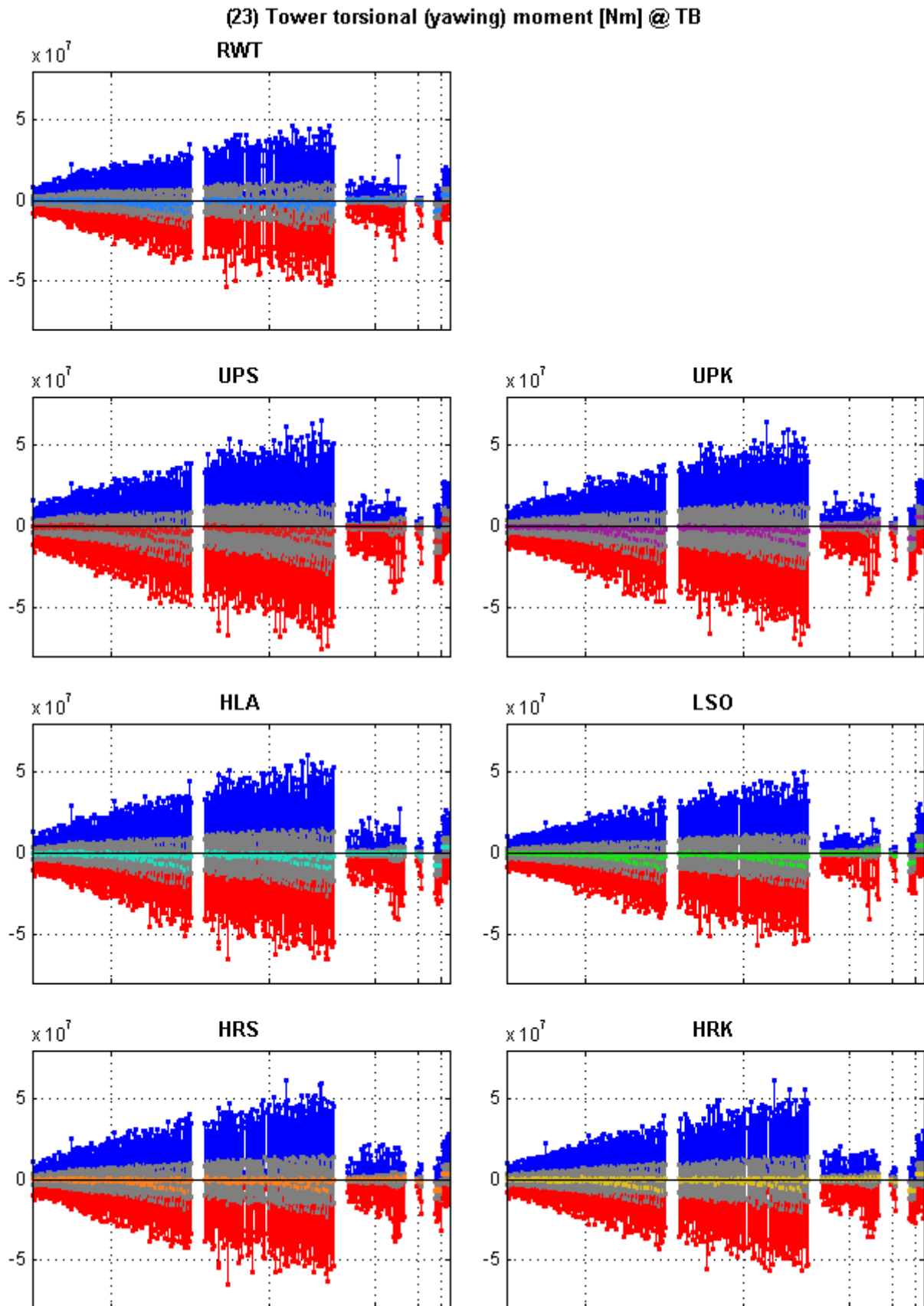


Figure 4.37: Tower bottom torsional moment from all DLCs for all designs

(104) B1: Pitch angle [deg]

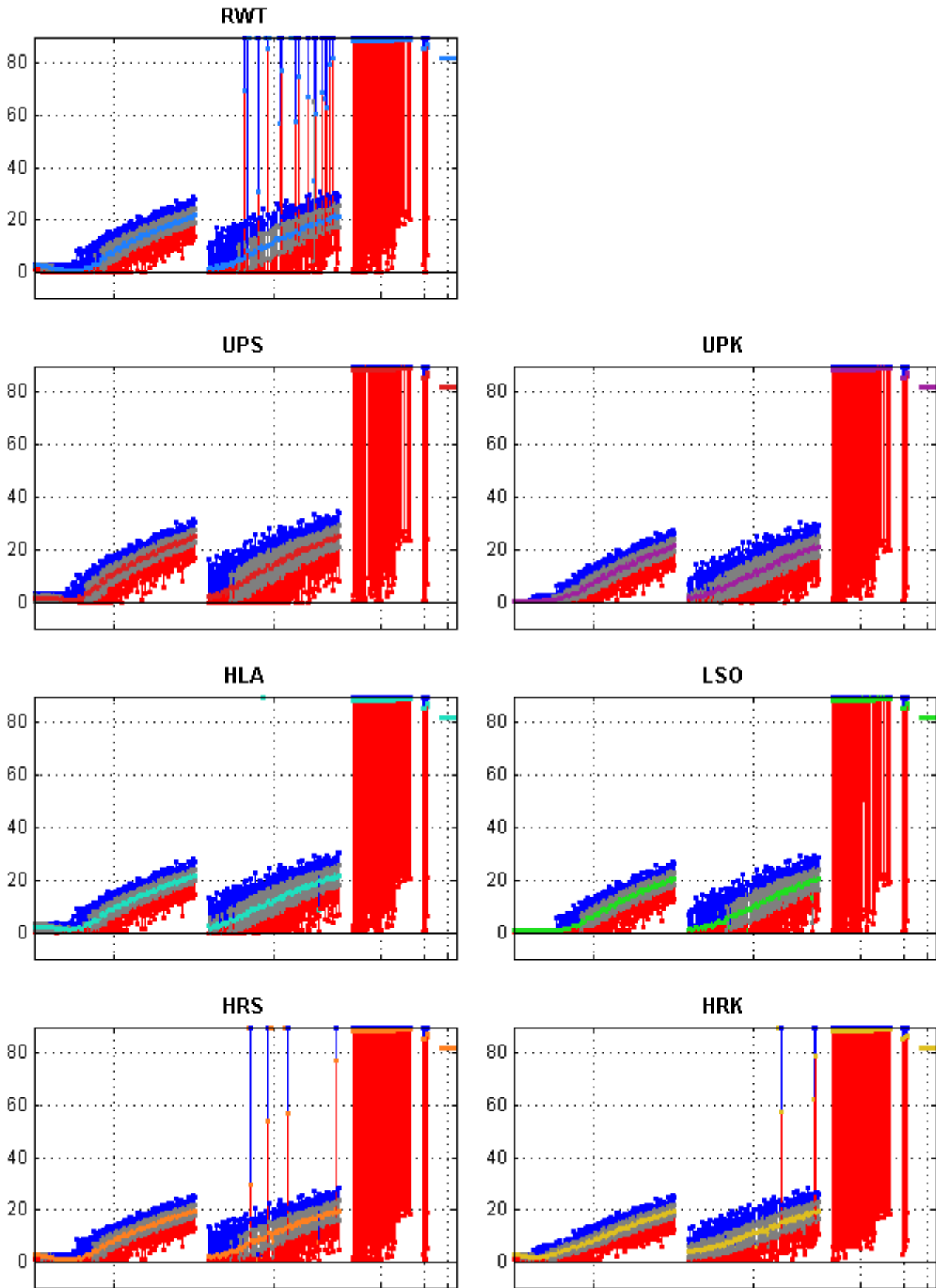


Figure 4.38: Blade 1 pitch angle from all DLCs for all designs

(-253) B2: Flatwise bending moment (chord rs) [Nm] @ BR

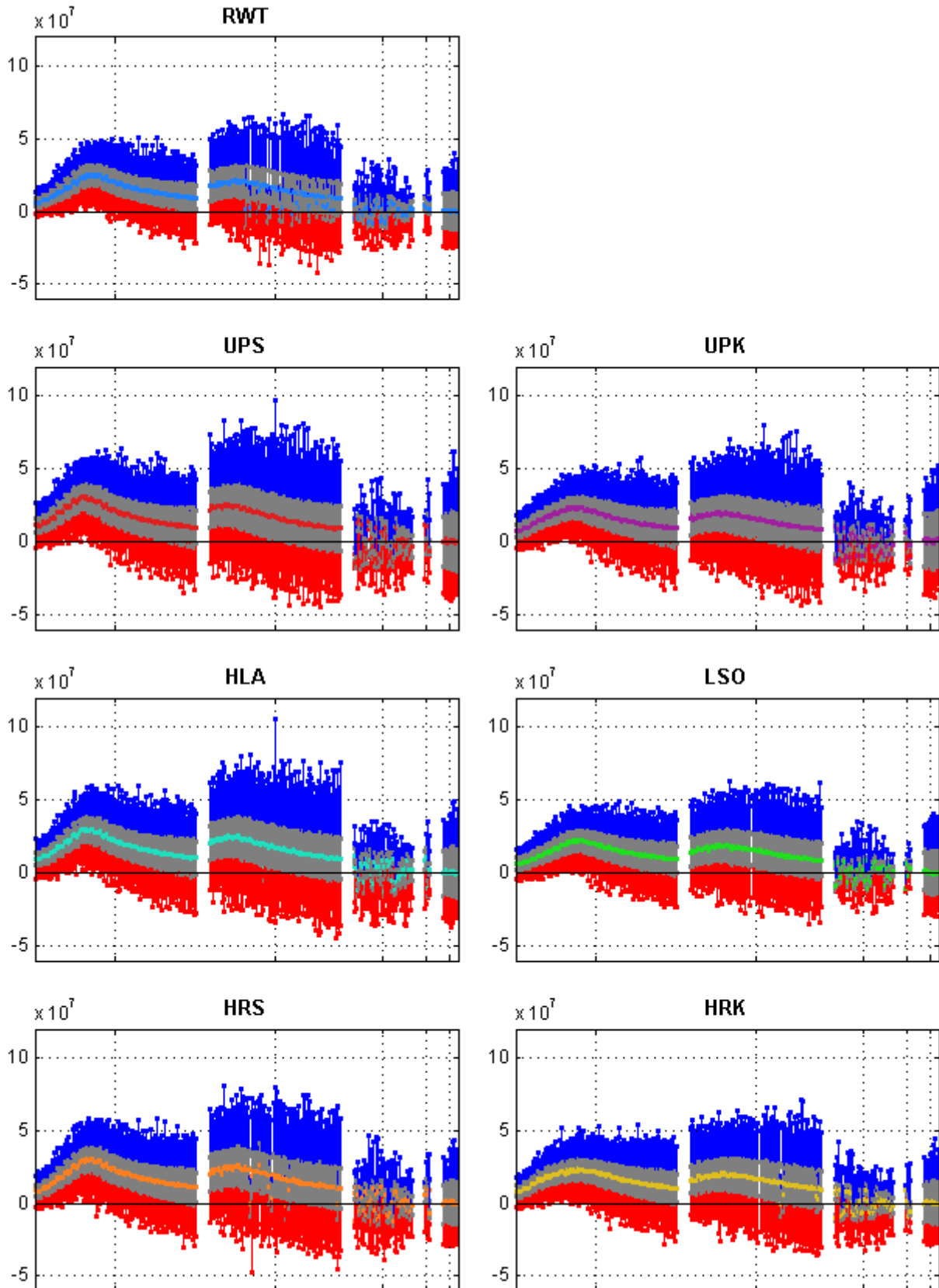


Figure 4.39: Blade 2 flap-wise blade root bending moment in the chord reference system from all DLCs for all designs. (The term “flat-wise” from PHATAS refers to the LCS instead of “flap-wise” that refers to GCS, see Figure 2.10)

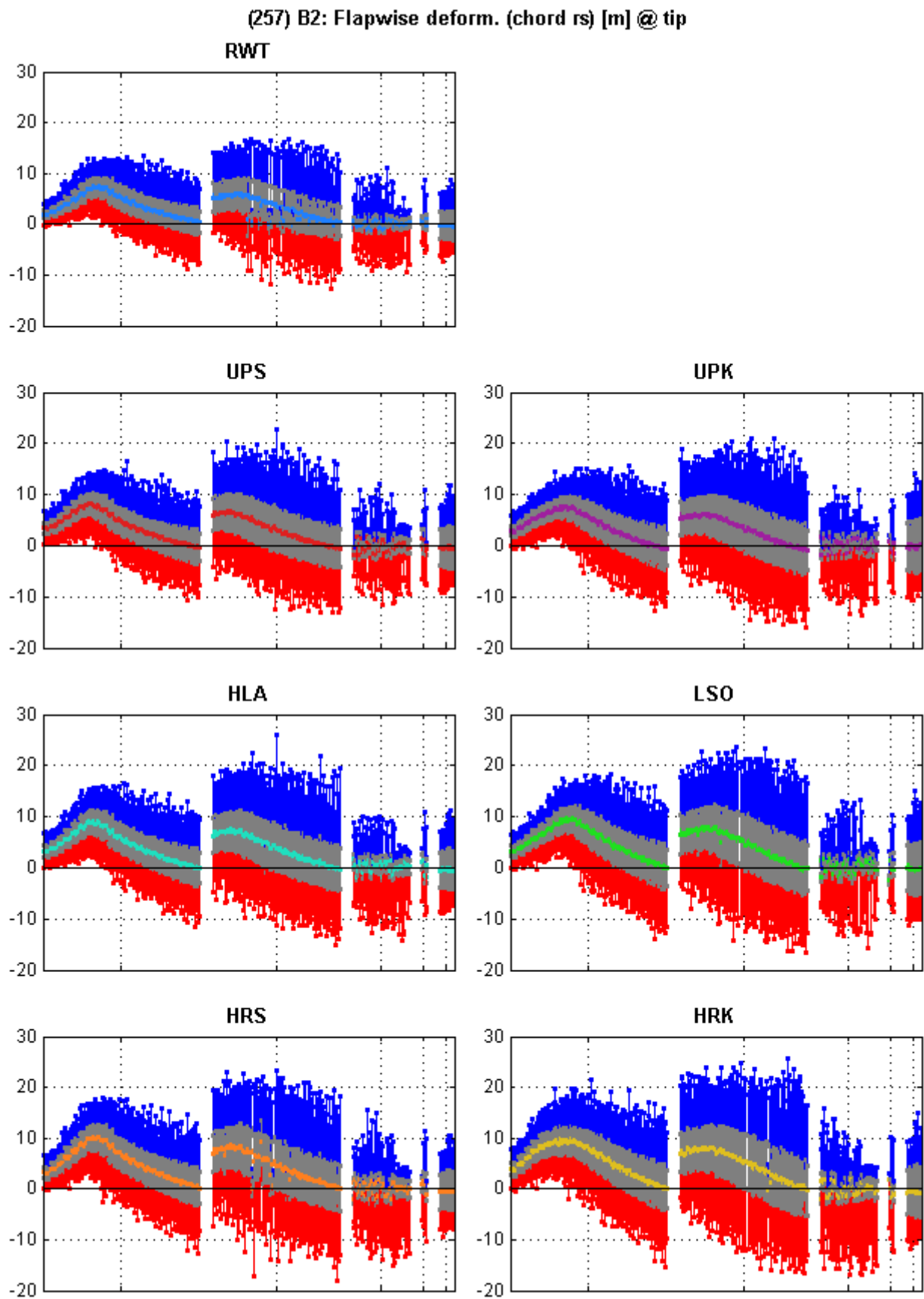


Figure 4.40: Blade 2 flap-wise tip deflection in the chord reference system from all DLCs for all designs

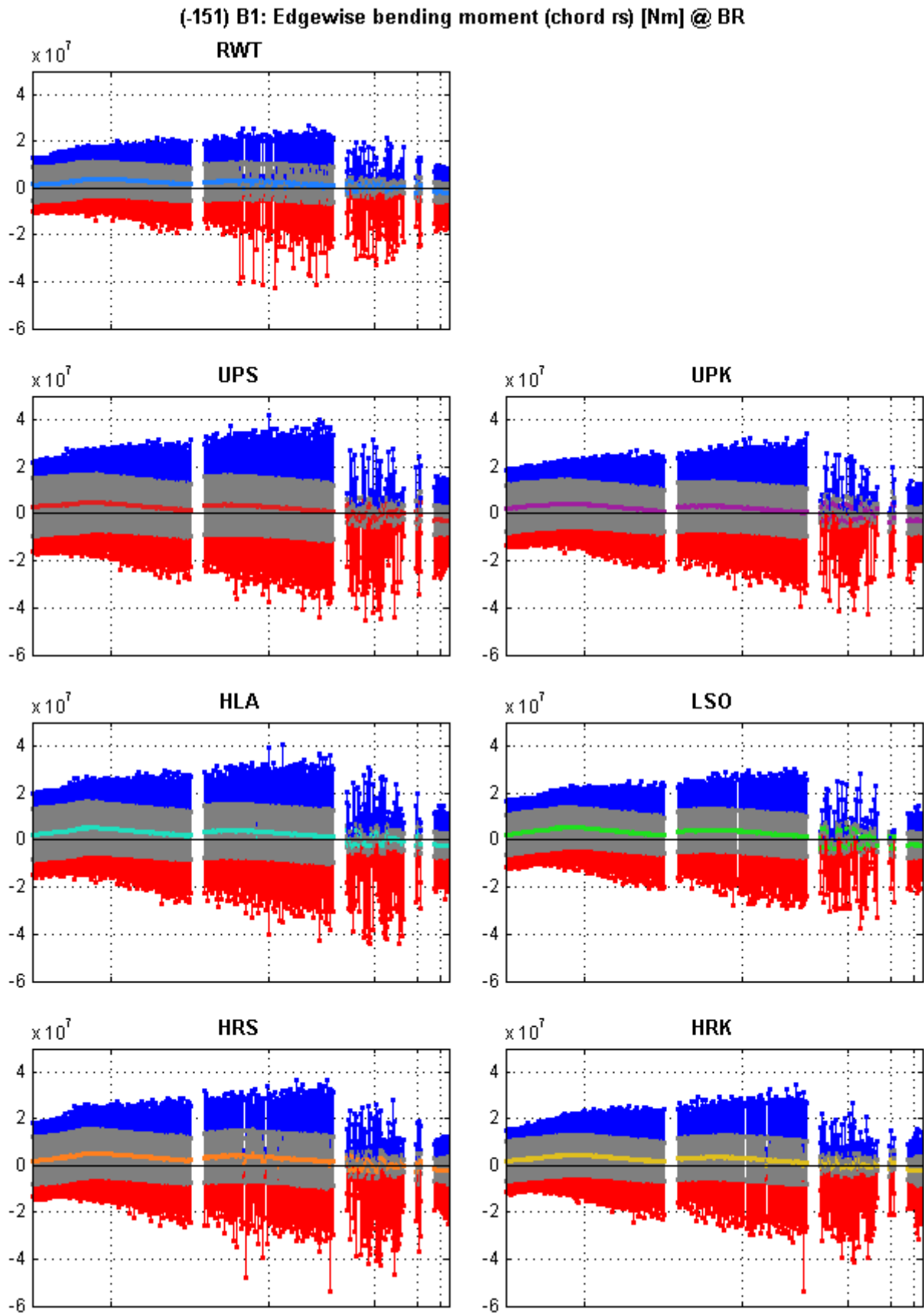


Figure 4.41: Blade 1 edge-wise blade root bending moment in the chord reference system from all DLCs for all designs

(159) B1: Leadwise deform. (chord rs) [m] @ tip

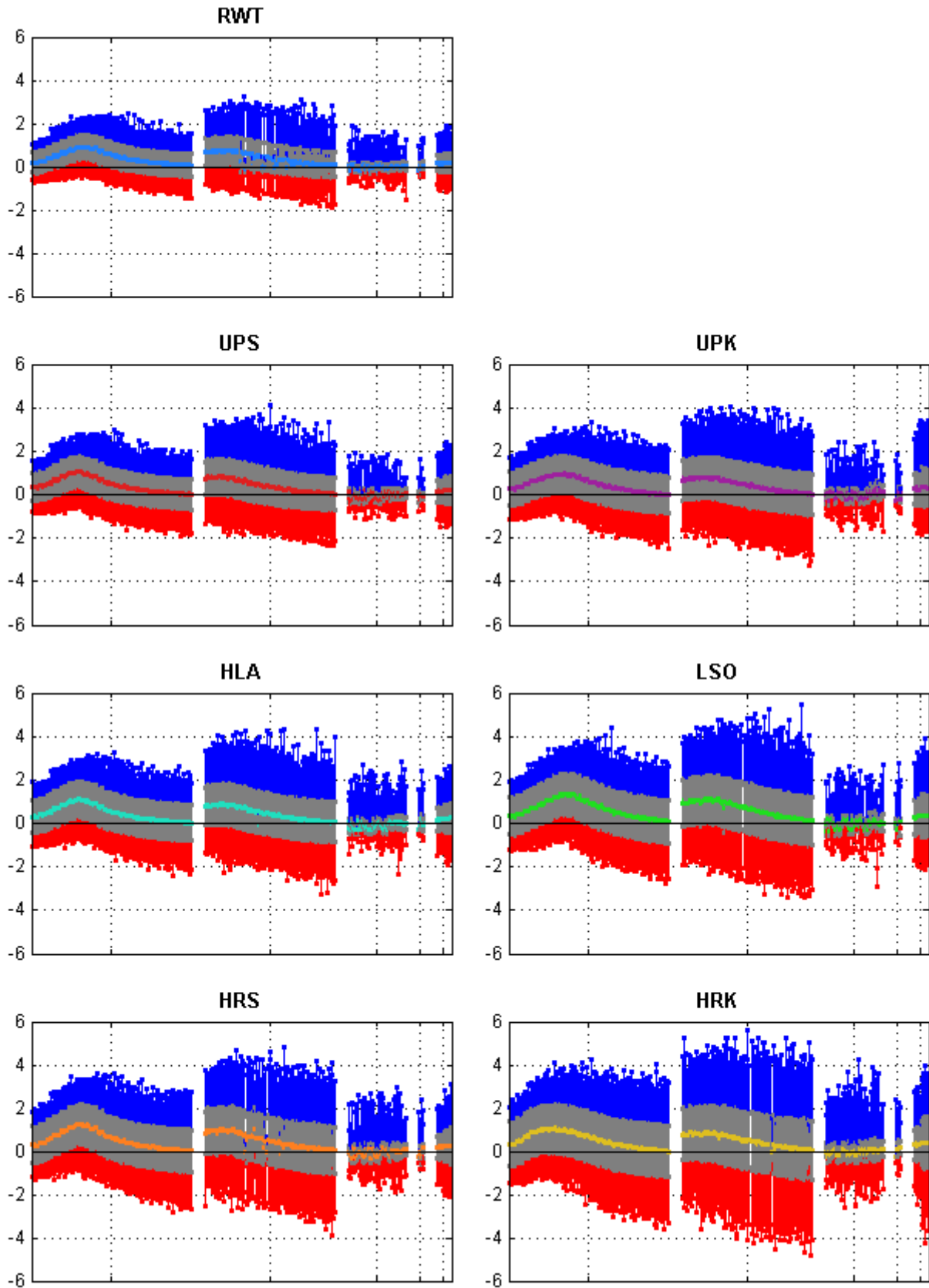


Figure 4.42: Blade 1 edge-wise tip displacement in the chord reference system from all DLCs for all designs

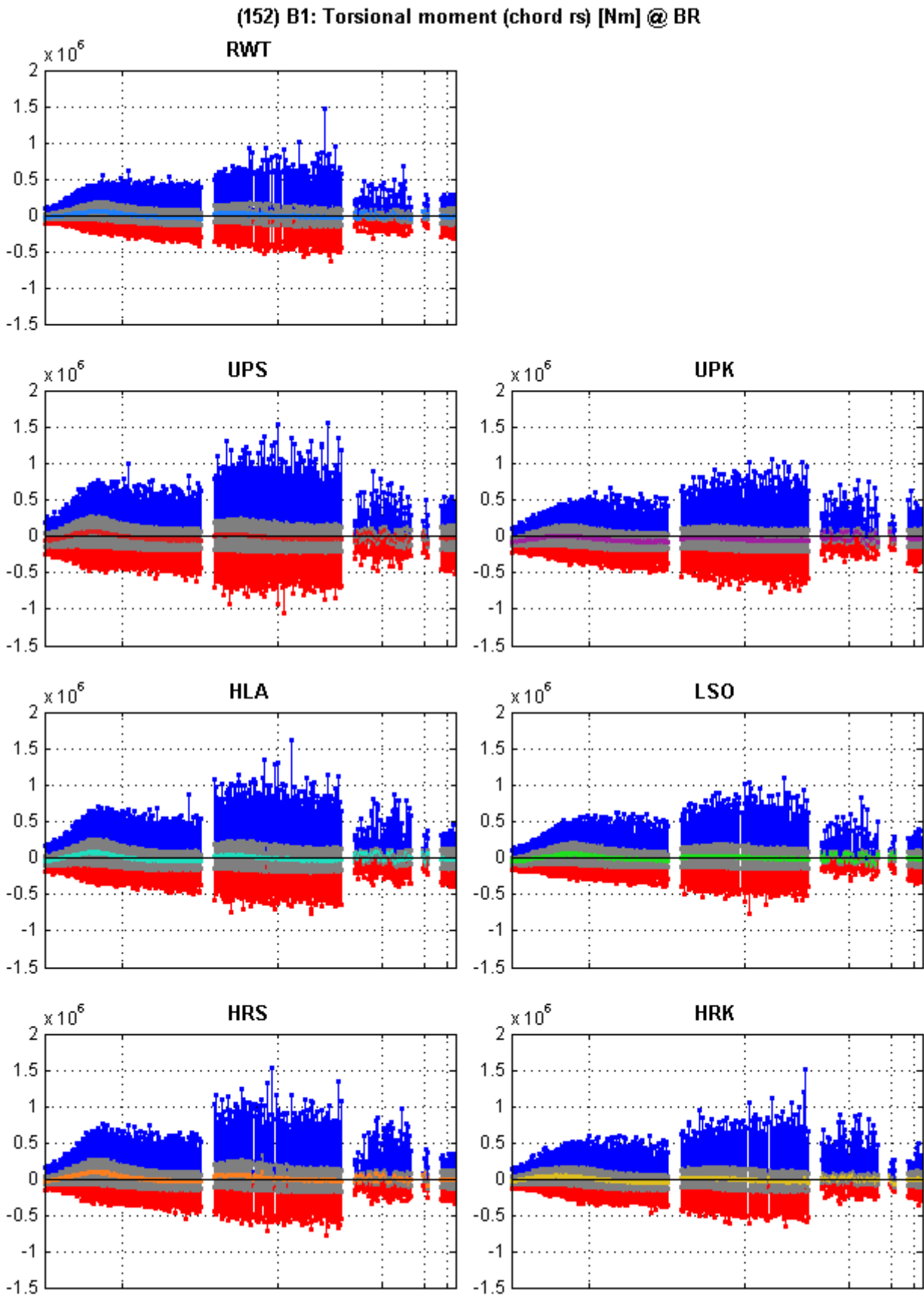


Figure 4.43: Blade 1 torsional blade root moment in the chord reference system from all DLCs for all designs

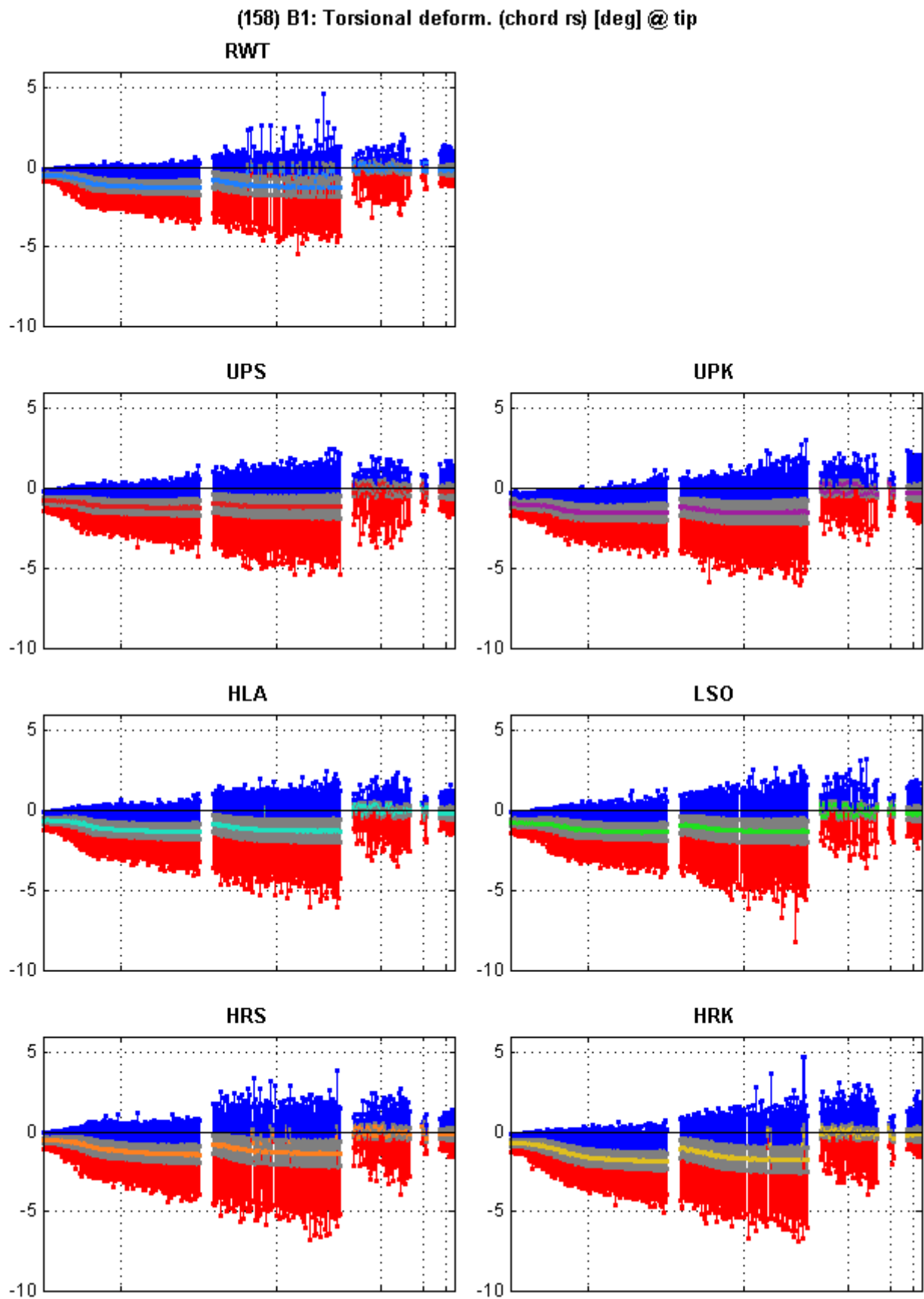


Figure 4.44: Blade 1 torsional tip displacement in the chord reference system from all DLCs for all designs

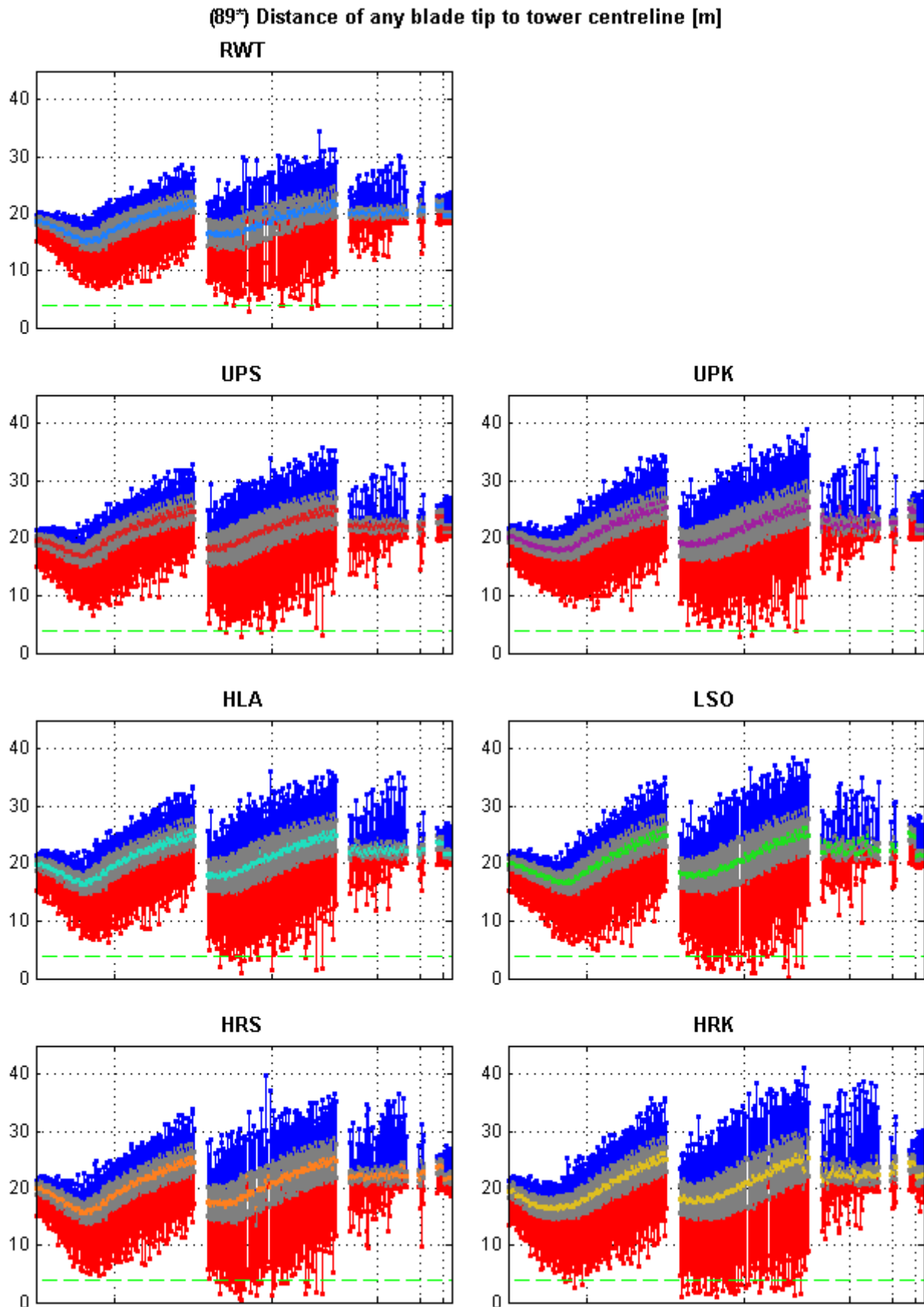


Figure 4.45: Blade tip 1, 2 or 3 clearance from centre of tower from all DLCs for all designs. (0 value in y-axis represents the tower centre and the green line/margin, the tower radius at passing point. Treated signal, $\pm 5^\circ$ window before and after passing the tower centreline)

4.5 Power Production, Damage Equivalent Loads and Fatigue Results

As described in Section 2.4, the results of power production and fatigue loads for DLC 1.2 are presented below. For the blade lifetime fatigue loads and stresses the average of moments on all three blades are used in the calculations. The graphs depicting equivalent loads versus wind speed contain the average load of the 6 seeds per wind speed. For the sake of brevity, only the flap-, edge-wise and torsional blade loads and tower fore-aft loads are presented. Additional graphs can be found in Appendix A.3 and all results of DLC 4.1 in Appendix A.4.

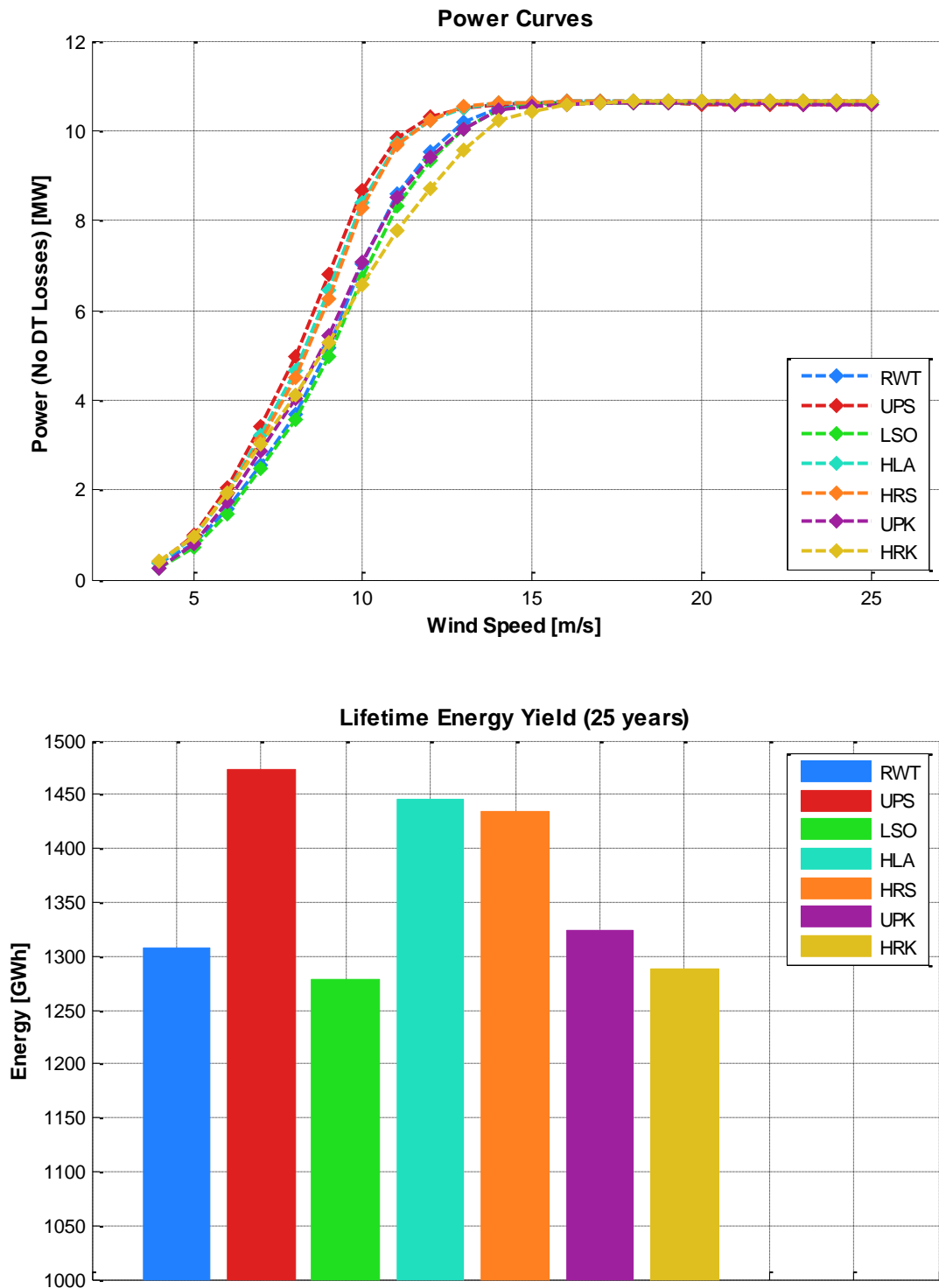


Figure 4.46: The power curves and total energy yield (per wind turbine, NOT wind farm) of all designs from all DLC 1.2 simulations

In Figure 4.46 above, it is clear that the optimal concepts (UPS, HLA and HRS) have a substantial energy production increase of about 11-12% compared to the RWT. The energy yield of sub-optimal concepts remain at a similar level close to 1300 GWh for 25 years. This happens mainly because of the reduction of the rated wind speed for the optimal concepts, providing an extra “slice” of power in the curve at the region of 6-13 m/s. The HRK concept shows a slightly higher production at the sub-rated region and slightly lower at rated region, keeping the overall production similar.

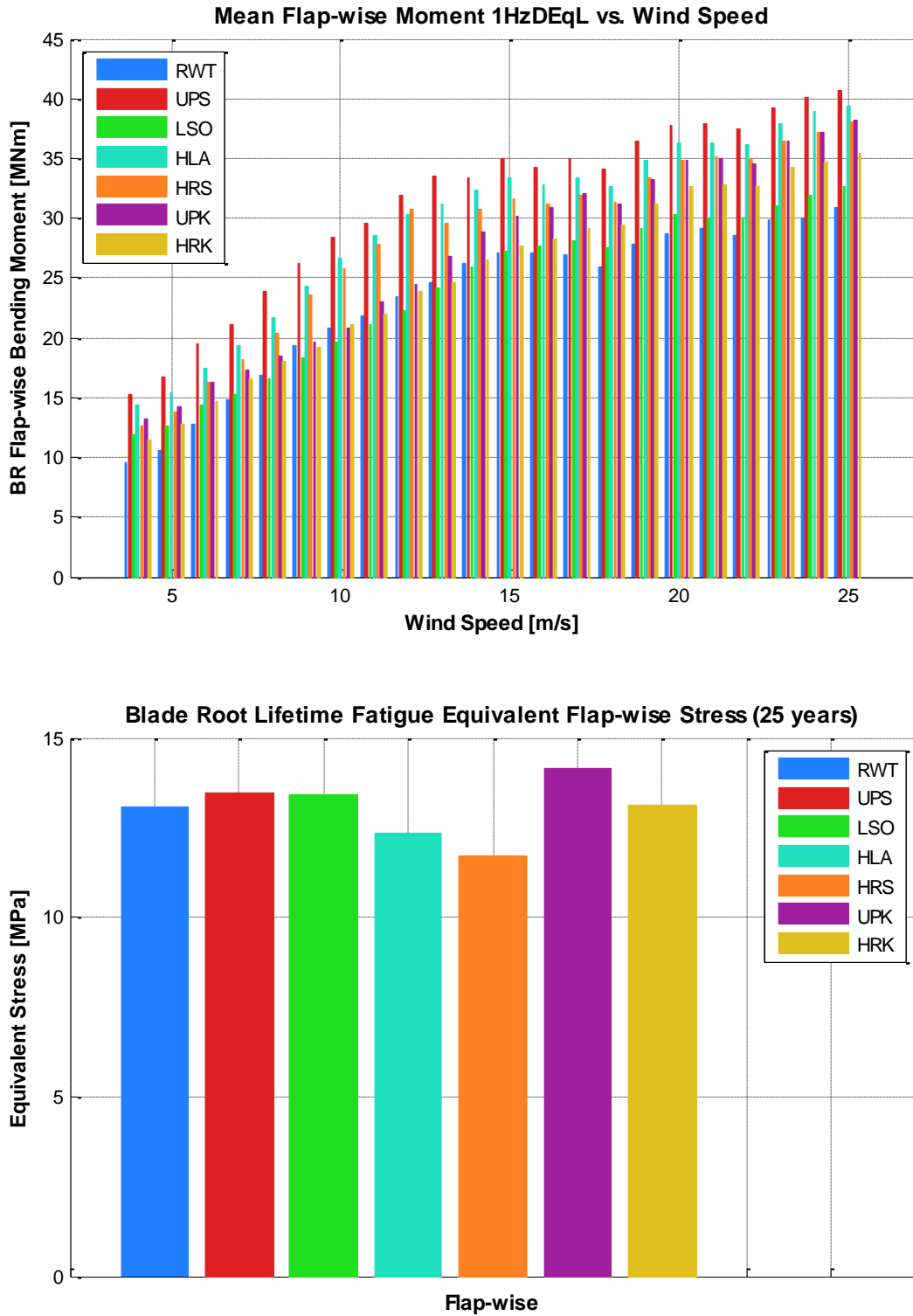


Figure 4.47: The mean flap-wise blade root bending moment versus all operating wind speeds (not Weibull-weighted) and lifetime damage equivalent stresses of all designs from all DLC 1.2 simulations

The flap-wise blade root bending moment (and the corresponding stress) is one of the most important loads in the operation of a wind turbine. There is a very interesting phenomenon appearing in Figure 4.47. The equivalent load range in the top graph shows a crude increase of 30% for the optimal designs, while the weighted lifetime stresses remain practically the same, ranging from 12 to 14 MPa ($\pm 7.7\%$). This is an extra indication that the up-scaled models were done in a realistic and useful

manner. Although the external loads increase significantly, the internal material stresses remain almost constant. The stress in the UPK is high because its design was based on a flat load at the rated region, without taking into account higher sub- and above rated region loads. The same outlook is seen in the edge-wise and torsional stresses (Figure 4.48 and Figure 4.49). This leads to a safe assumption that since the lifetime stress levels remain the same, the new damage and fatigue will not be a design driver for the new blades.

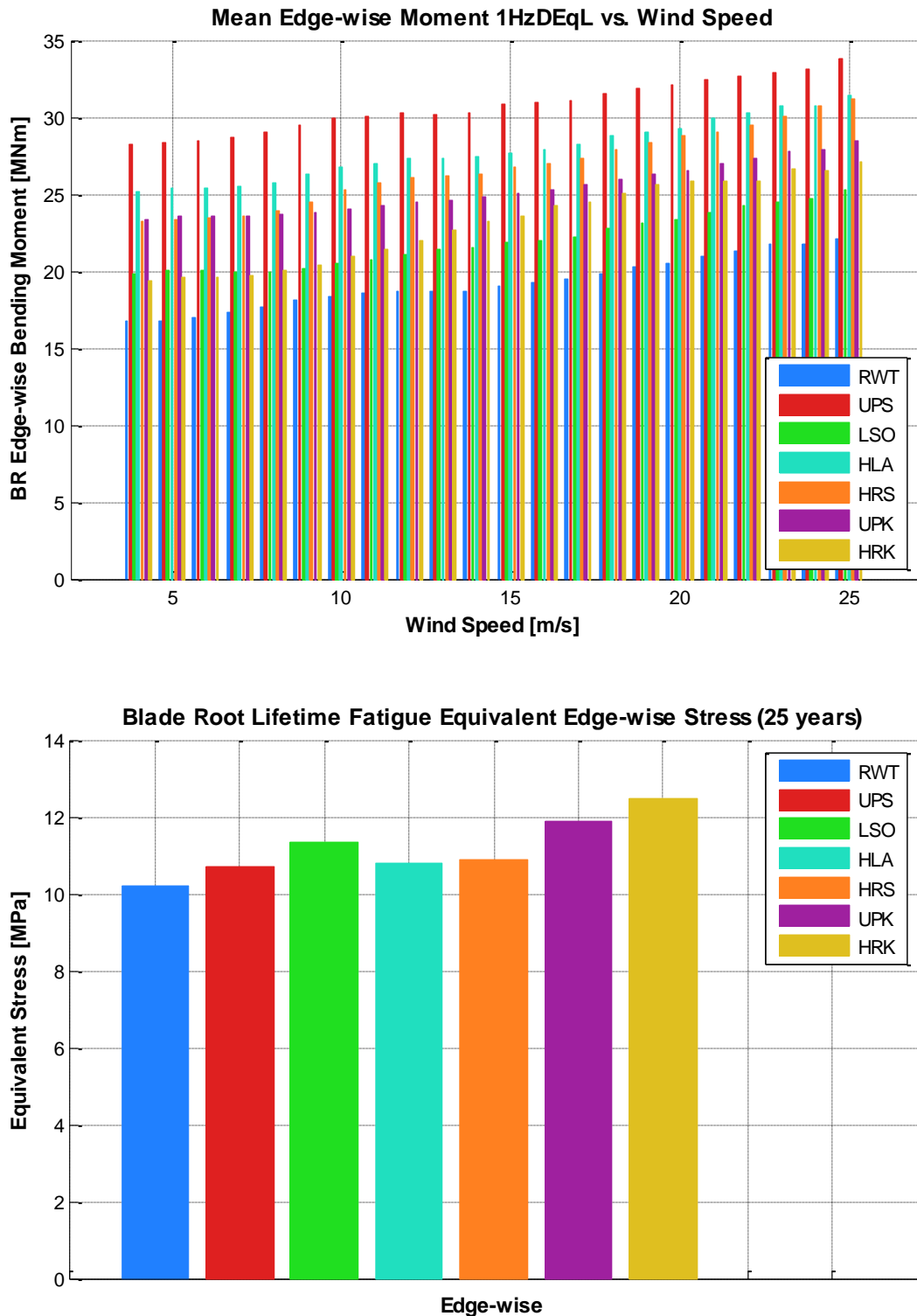


Figure 4.48: The mean edge-wise blade root bending moment versus all operating wind speeds (not Weibull-weighted) and lifetime damage equivalent stresses of all designs from all DLC 1.2 simulations

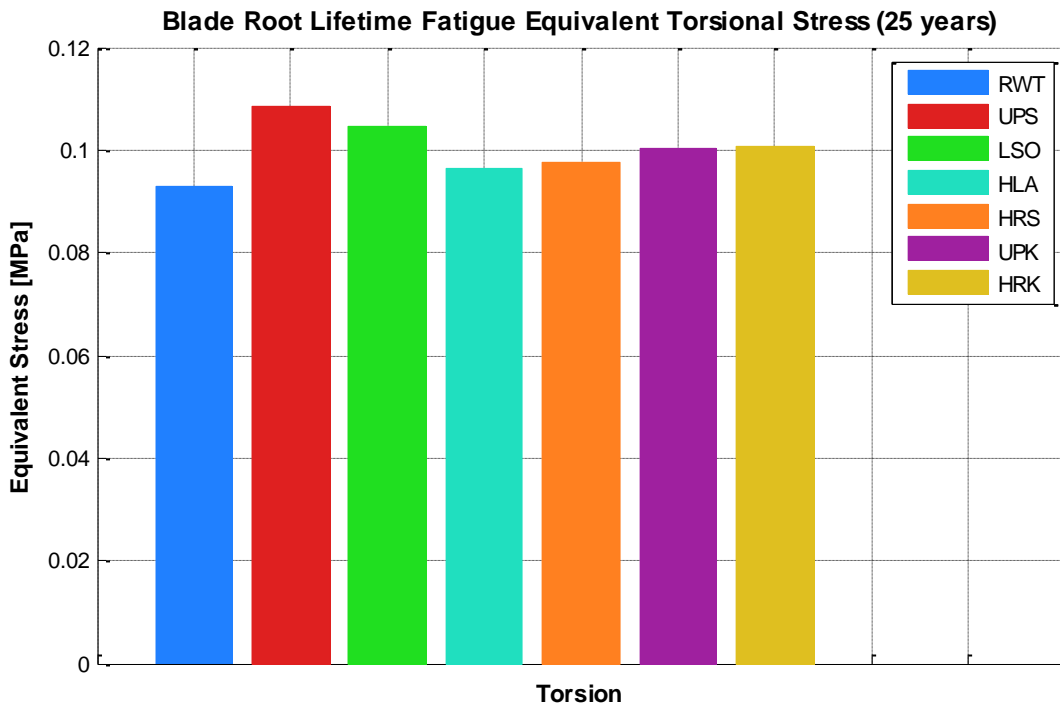
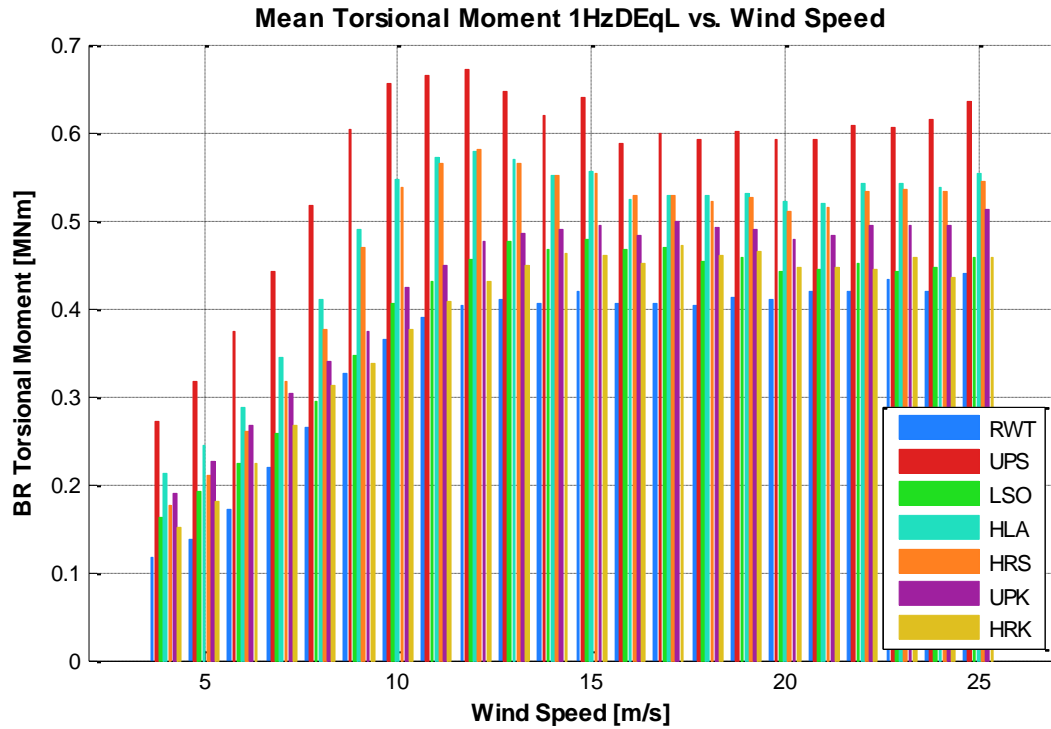


Figure 4.49: The mean torsional blade root moment versus all operating wind speeds (not Weibull-weighted) and lifetime damage equivalent stresses of all designs from all DLC 1.2 simulations

In an effort to quantify the above stresses into damage and place them in an S-N diagram to estimate the cycles to failure of the blades, quotes from experimental data were used. It must be noted, as stated before, that depending on the specifics of the composite used, these values may vary in the literature. Also different materials are used for load-carrying elements within the cross-section, so this analysis would be different. In [3], the mean UTS from static tests of six dry GFRP coupons

amounts to 457.38 MPa and a UCS of -341.64 MPa, while in [25] there is an S-N curve intersecting the shear stress axis at ca. 108 MPa. Usually, the S-N curves become practically straight and stop decreasing after 10^7 or 10^8 cycles, signifying lifetime fatigue endurance for a small enough stress range. However, for this crude estimation, in order to maintain a conservative and safe approach, the linear reduction was kept. The slope exponent used is $m = -10$.

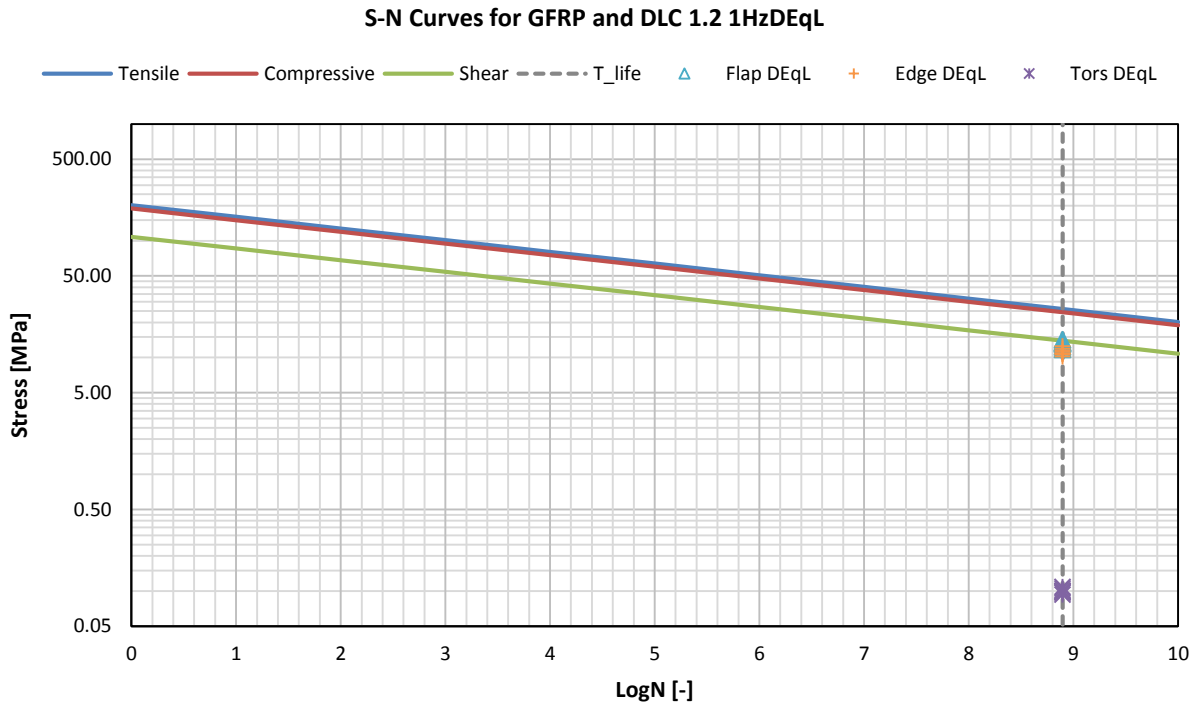


Figure 4.50: Log-log scale S-N curve for tensile, compressive and shear loadings on GFRP material, including the damage equivalent loads at the 25 year cycles

As seen in Figure 4.50 above, the shear loadings from torsion for all concepts are well below the failure line by a factor of about 100. If one considers the lower compressive curve, both the flap and edge equivalent loads are also lower by a factor of about 3. It can be concluded, that even when the most conservative safety factors (γ_m for material properties, γ_f for loads, γ_n for consequences of failure) are combined, the failure curve is still marginally above; $\gamma_{tot} = \gamma_m \cdot \gamma_f \cdot \gamma_n = 1.7 \cdot 1.35 \cdot 1.3 = 2.9835$ [20].

So the maximum increase of 30% in the moment led to an 8% increase in the stress without significantly affecting fatigue life compared to the RWT. This allows for endurance considering the wind turbine lifetime cycles. With the same rationale, the following increase of tower fore-aft moment to about +18% for the heavier UPS concept, is assumed not to transform tower fatigue damage to a design driver.

It is also very important to note that the damage equivalent loads reported below, in Figure 4.51 (and in Appendix A.3 figures for the tower) are not realistic. Unrealistic in the sense that these numbers are large and would correspond to extreme tower bottom bending moments (see Figure 4.35, Figure 4.36 and Figure 4.52) rather than lifetime equivalent moments.

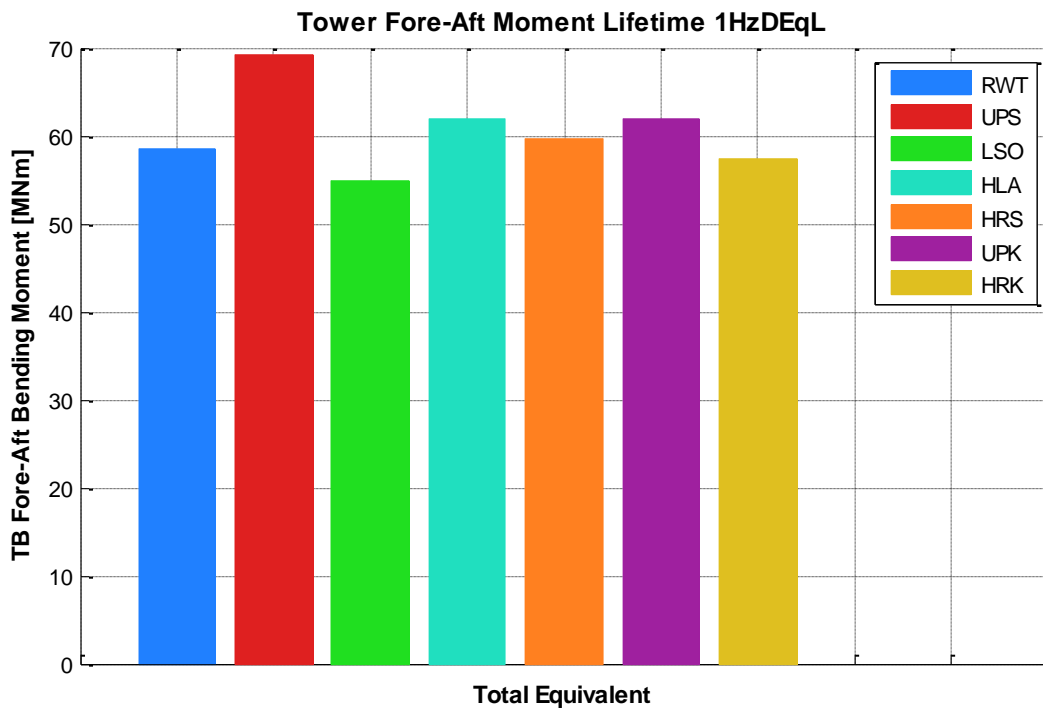
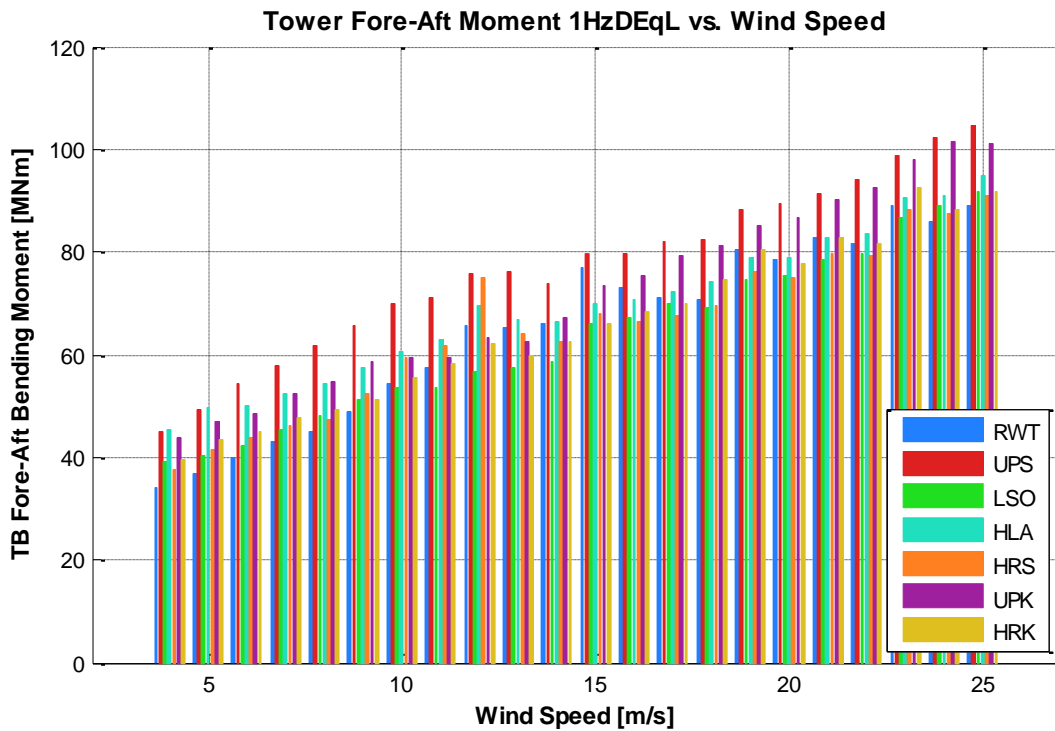


Figure 4.51: The tower bottom fore-aft moment versus all operating wind speeds (not Weibull-weighted) and lifetime damage equivalent moment of all designs from all DLC 1.2 simulations

This happens because the statistical extrapolation in the rain-flow counting and DEqL algorithms is considering the same rotor orientation for all 25 years of operation. In other words, it is suggested that the same parts of the tower cross-section is under fore-aft or side-to-side loading. However, wind direction changes throughout the year. Certain probabilities for each direction are assigned through a wind rose plot (see Figure 4.53), coming from meteorological measurements done in Horns Rev and reported in [7].

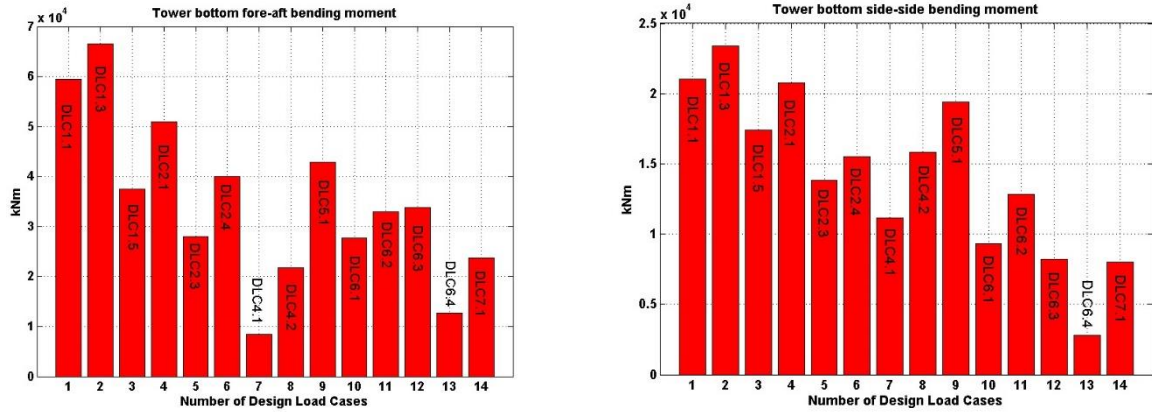


Figure 4.52: The tower bottom extreme fore-aft (left) and side-to-side (right) bending moments on the RWT tower for load cases run by DTU [5]

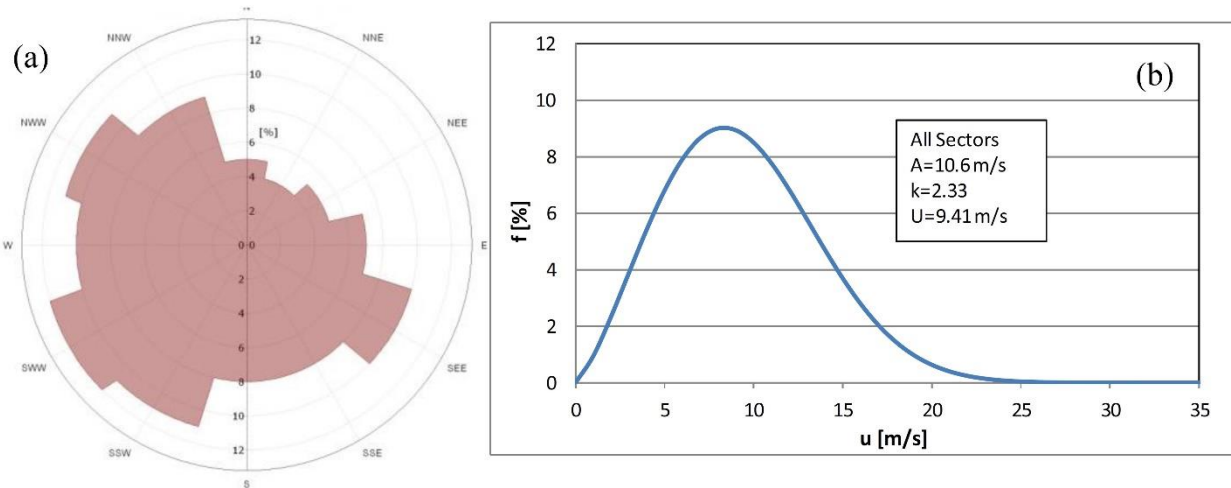


Figure 4.53: Wind rose direction probabilities (a - left) and wind speed Weibull probabilities (b - right) measured at Horns Rev, reported in [7]

So it is evident that the wind speed probabilities are not enough to describe the way the tower is under loading in the total operational lifetime. With changes in the wind direction, the tower’s axes, within the circumference of the cross-section where the loads are exerted, change as well. Taking into account the wind rose of Horns Rev farm, using $m_{steel} = 4$ as the material slope for steel and dividing the tower circumference in 360° , one should correct per-wind speed and lifetime equivalent loads by a factor of:

$$\left(\frac{[\text{max wind direction probability (SWW)}] \div [30^\circ \text{ per wind direction}]}{[12\%] \div [30]} \right)^{\frac{1}{m_{steel}}} \quad (4.1)$$

$$\left(\frac{[12\%] \div [30]}{[30]} \right)^{0.25} = 25.15\%$$

So the more realistic numbers for the loads, in Figure 4.51 above, would range from 10 MNm for 4 m/s up to 25 MNm for 25 m/s for the top graph; roughly the 25%, as per Equation (4.1). As for the lifetime moments in the bottom graph, these would range from 14 to 17.5 MNm. The material of the tower according to Bak et al. [5] is structural steel S355 (minimum yield strength 355 MPa) with a Poisson’s ratio of $\nu = 0.3$, Young’s modulus $E = 210$ GPa and density $\rho = 7855$ kg/m³ (8500 kg/m³ used to account for mass of secondary structures in the tower). In Figure 4.54, the results from the analysis

of DTU are given for comparison. DTU employs a slightly different approach in the derivation of the damage equivalent load ranges. The researchers use different reference loading cycles, lifetime cycles, and material slope exponent for steel, while there is no specific mention to the influence of wind direction.

$$DEL = \left(\frac{1}{N_{ref}} \sum_{i=1}^{n_{sim}} \left(\frac{T_{life,i}}{T_{sim,i}} \sum_{k=1}^{n_k} N_{i,k} S_{i,k}^m \right) \right)^{1/m} \quad (4.2)$$

Where: $N_{ref} = 10^7$ cycles (corresponding to 20 years, according to [5])
 $n_{sim} = 11$ wind speeds (5 to 25 m/s with steps of 2 m/s) x 3 yaw misalignment seeds
 $T_{life} =$ period that the turbine is running at a given wind speed (adds up to 18.3 years)
 $T_{sim} =$ simulation time (600 s)
 $S_{i,k} =$ the random load range
 $N_{i,k} =$ the cycles under $S_{i,k}$
 $m = 3$ for steel

In Figure 4.54 below, both blade root flap- and edge-wise equivalent loads, and fore-aft and side-to-side tower bottom equivalent loads are given, as presented by DTU. The edge-wise loads are decreasing in high wind speeds. A probable explanation is that these DEqL ranges are already weighted with their Weibull probabilities. Another one is that the coordinate system they are referring to is the global one, perpendicular to the rotational plane, and not the one of the blade chord reference system that takes pitching into account (Figure 4.48).

A similar assumption, concerning the Weibull probabilities, can also be made for the tower fore-aft loads, where they exhibit their maximum values at the rated wind speed region. The same also holds for the side-to-side loads given in Figure A.34.

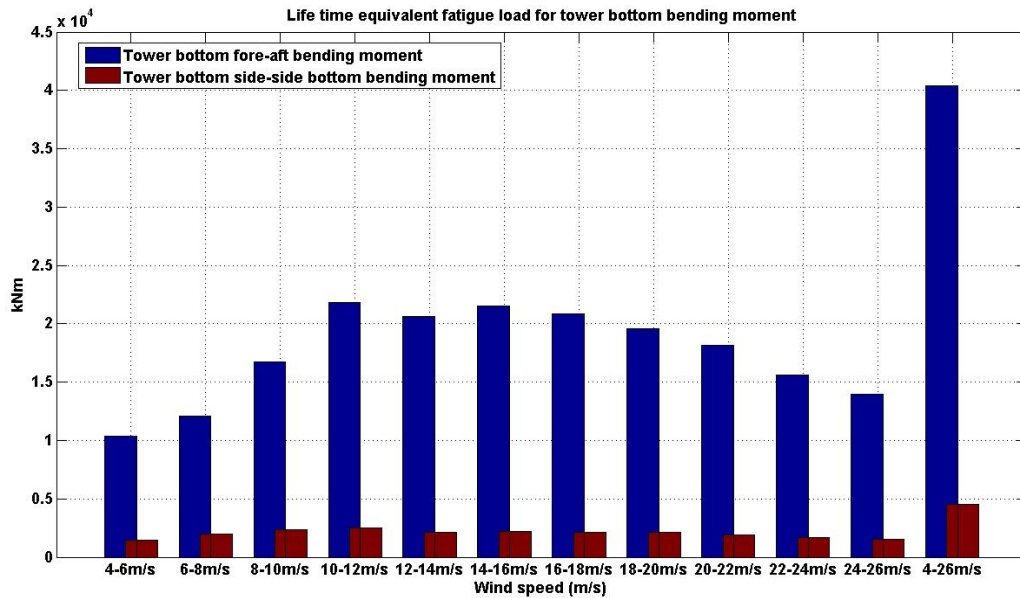
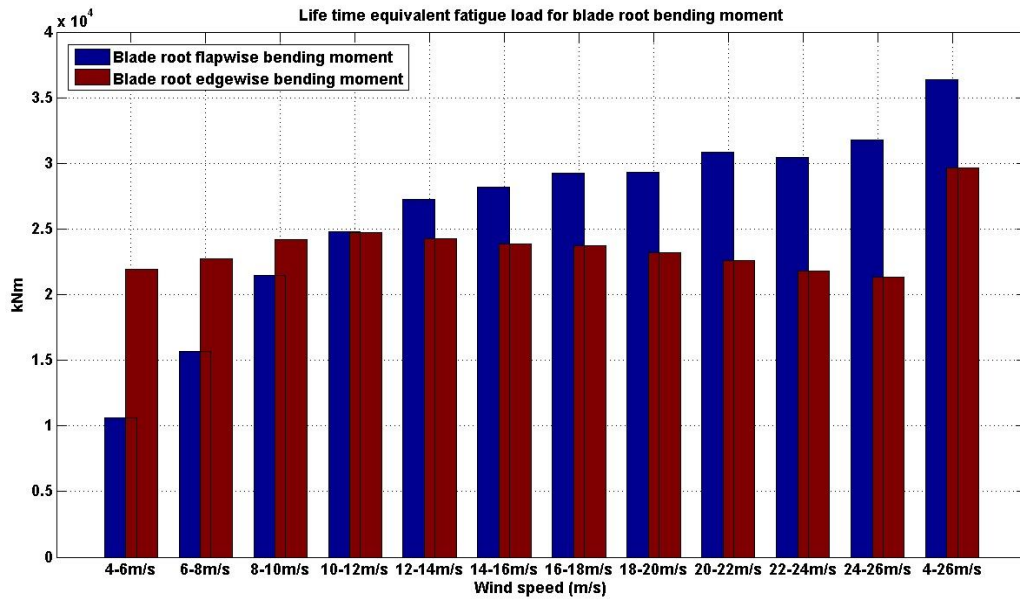


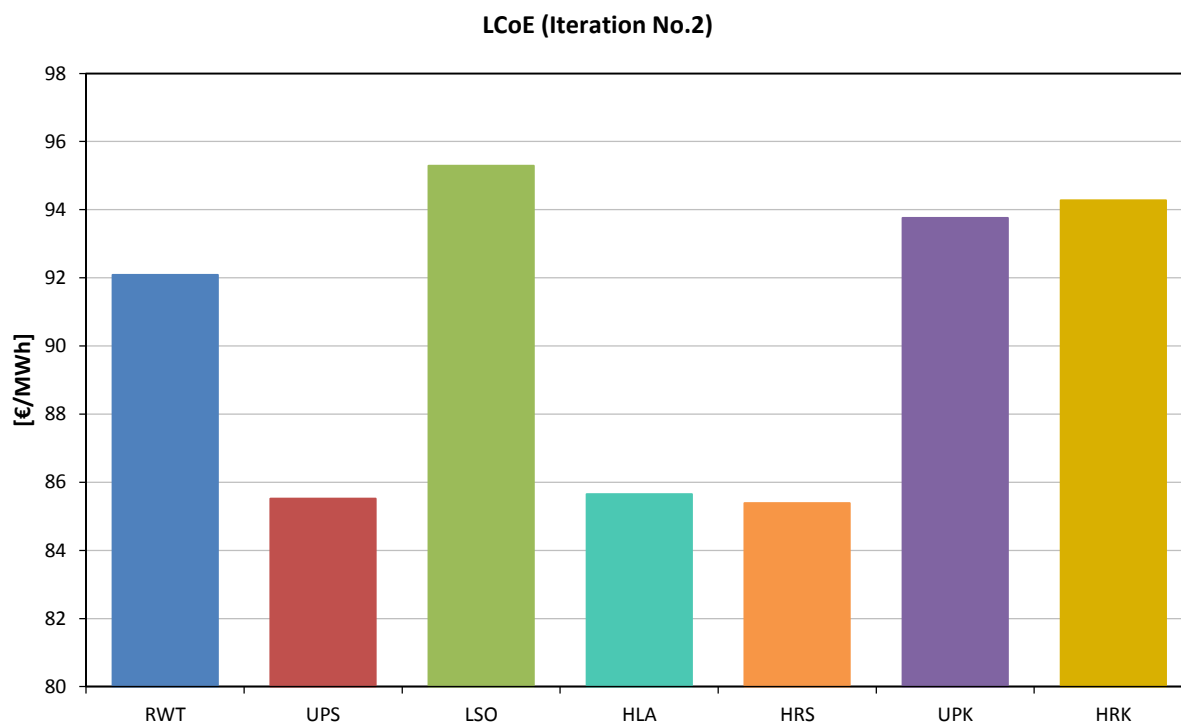
Figure 4.54: The lifetime equivalent flap- and edge-wise blade root (top) and the tower bottom fore-aft and side-to-side (bottom) bending moments versus wind speed from DTU results in [5]

4.6 LCoE (Iteration No.2) and Final Design Evaluation

As in Section 4.3, the cost model is used again to re-iterate the LCoE with the energy yield values from the extrapolation of DLC 1.2 data. The results are shown in Table 4.7 and Figure 4.55. The formulas of the cost model and losses are kept the same. The C_p values, instead of being set by the stationary analysis as before, they are manipulated so as to match the energy production, hence its values are not fully realistic. The complete cost model for each design is found in Appendix A.5.

Table 4.7: LCoE and capacity factor estimations (Iteration No.2)

	Blade Mass [kg]	C_p Equiv. [-]	Wake Losses [%]	WT capacity factor [-]	WF capacity factor [-]	Farm AEY [GWh/y]	Farm LCoE [€/MWh]
RWT	41,722	0.488	14.17	0.547	0.437	3,835	92.09
UPS	60,348	0.509	12.43	0.623	0.508	4,364	85.52
LSO	45,309	0.346	10.46	0.534	0.445	3,742	95.29
HLA	54,167	0.483	12.36	0.610	0.498	4,277	85.65
HRS	49,871	0.472	12.29	0.605	0.494	4,237	85.39
UPK	51,612	0.376	11.38	0.554	0.457	3,885	93.76
HRK	42,695	0.352	11.76	0.538	0.442	3,772	94.28

**Figure 4.55:** Graphic representation of the farm LCoE taking into account the lifetime energy yield from DLC 1.2 simulations

It can be seen from the 2nd LCoE estimation, that the optimal designs (UPS, HLA and HRS) show a considerable decrease in the cost of energy (ca. -7%), despite the heavier blades. This comes from the increase of the energy production (ca. +14% for the UPS). The LCoE of the sub-optimal designs increases slightly because of the power shedding in the effort of keeping the loads low. But this effort seems to hinder the final outcome of the design and the low mass benefits. As in the first iteration (Section 4.3), the same trends of blade mass (Figure 4.56) and wake losses (Figure 4.57) versus the LCoE are presented here. The main difference is the considerable change of the LCoE of the HRK concept due to the lower energy production than estimated at first. A dip at ca. 12.5% is seen for the wake losses again, and as for the blade mass, still having a low or high mass does not indicate a low or high LCoE.

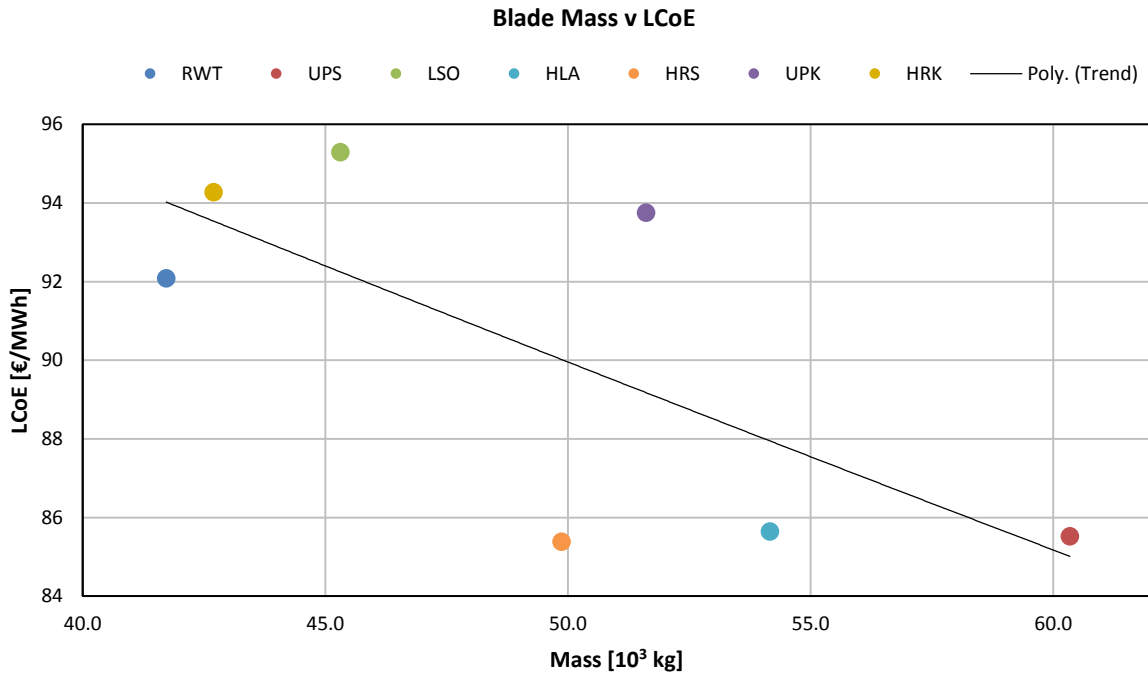


Figure 4.56: Blade mass versus LCoE (Iter. 2)

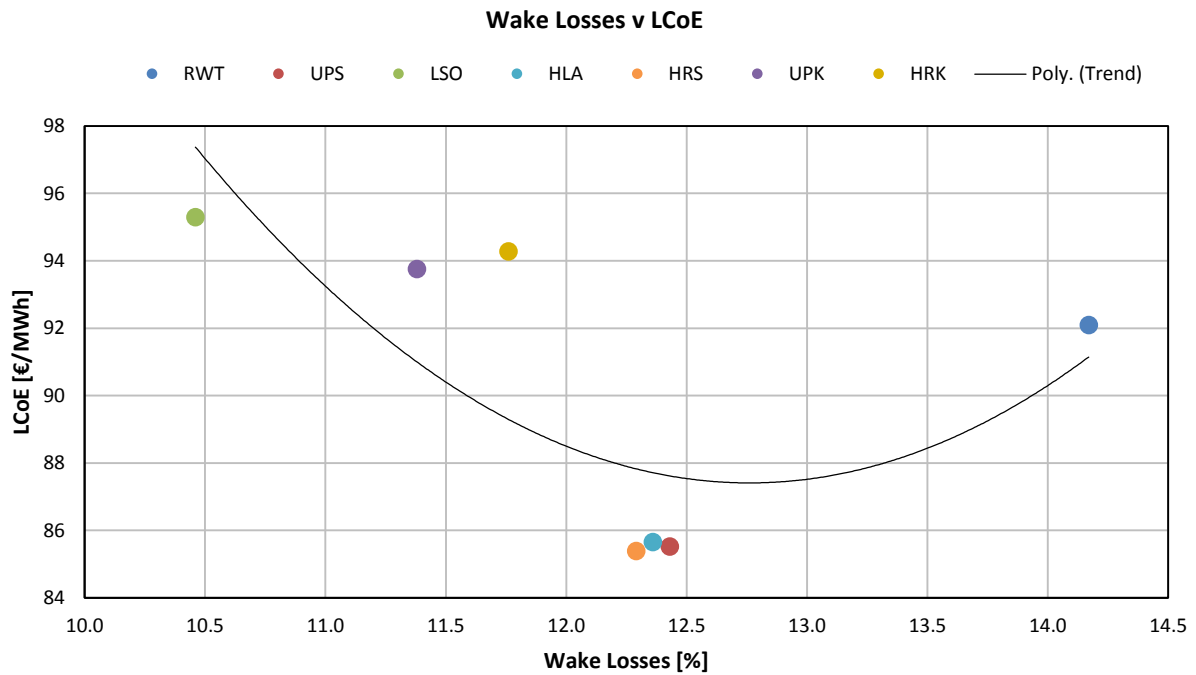


Figure 4.57: Wake losses versus LCoE (Iter. 2)

Any positive effects of the structural performance were chosen to participate in a weighted/factored final evaluation along with the LCoE with somewhat arbitrary proportions. The total ranking was done with a total of 6 parts of evaluation (Table 4.8). Three of them were reserved for the LCoE since it is the “overarching” Performance Indicator. Also because it weighs between blade mass, energy production and other farm parameters (such as secondary costs and wake losses). One part divided by four was assigned to the equivalent loads on the tower and shaft (0.25 for each of fore-

aft, side-to-side, torsion on tower bottom and shaft torque). One part was assigned to the damage equivalent stresses on the blades (0.33 for each of flap-, edge- and torsional loads). The final part was assigned to blade hits. Blade hits are defined as the number of load cases that, even for a single moment into the simulation (concerning mainly DLC 1.3), the clearance of blade tip to tower centreline became less than the tower radius (see Figure 4.45 or Figure A.24).

The ranking in each parameter was done with zero being the worst performance and unity being the best among the designs. The rankings in the tower and shaft loads group and the rankings of the blade loads group were then averaged (see Table 4.9 and Figure 4.58).

Table 4.8: The individual parameters and values participating in the evaluation

	Tower DEqL FA [MNm]	Tower DEqL SS [MNm]	Tower DEqL Tors. [MNm]	Shaft DEqL Torque [MNm]	Blade Flap- DEqL [MPa]	Blade Edge- DEqL [MPa]	Blade Tors. DEqL [MPa]	Blade Hits [-]	LCoE [€/MWh]
	(Tower and Shaft Loads Group)				(Blade Stresses Group)			-	-
RWT	58.6	17.5	10.9	1.63	13.07	10.18	0.093	2	92.09
UPS	69.2	28.8	13.6	2.45	13.48	10.70	0.109	4	85.52
LSO	54.9	25.2	10.3	2.17	13.40	11.33	0.105	27	95.29
HLA	62.0	21.1	13.0	1.82	12.37	10.81	0.097	12	85.65
HRS	59.6	17.8	12.4	1.67	11.72	10.90	0.098	32	85.39
UPK	62.0	29.7	12.3	2.18	14.14	11.89	0.100	3	93.76
HRK	57.4	17.5	11.2	1.44	13.15	12.49	0.101	48	94.28

Table 4.9: The 0 to 1 rankings of the designs by individuals and groups

	Tow. FA	Tow. SS	Tow. Tors.	Shaft Torq.	Group Mean	Bld. Flap-	Bld. Edge-	Bld. Tors.	Group Mean	Bld. Hits	LCoE#	Total
RWT	0.74	1.00	0.81	0.82	0.84	0.44	1.00	1.00	0.81	1.00	0.32	3.63
UPS	0.00	0.07	0.00	0.00	0.02	0.27	0.77	0.00	0.35	0.96	0.99	4.28
LSO	1.00	0.37	1.00	0.28	0.66	0.31	0.50	0.25	0.35	0.46	0.00	1.47
HLA	0.50	0.70	0.18	0.62	0.50	0.73	0.73	0.77	0.75	0.78	0.97	4.95
HRS	0.67	0.98	0.36	0.78	0.70	1.00	0.69	0.70	0.80	0.35	1.00	4.84
UPK	0.50	0.00	0.39	0.27	0.29	0.00	0.26	0.52	0.26	0.98	0.16	2.00
HRK	0.83	1.00	0.71	1.00	0.88	0.41	0.00	0.50	0.30	0.00	0.10	1.50

(#NOTE: The LCoE ranking in the total sum is multiplied by 3.)

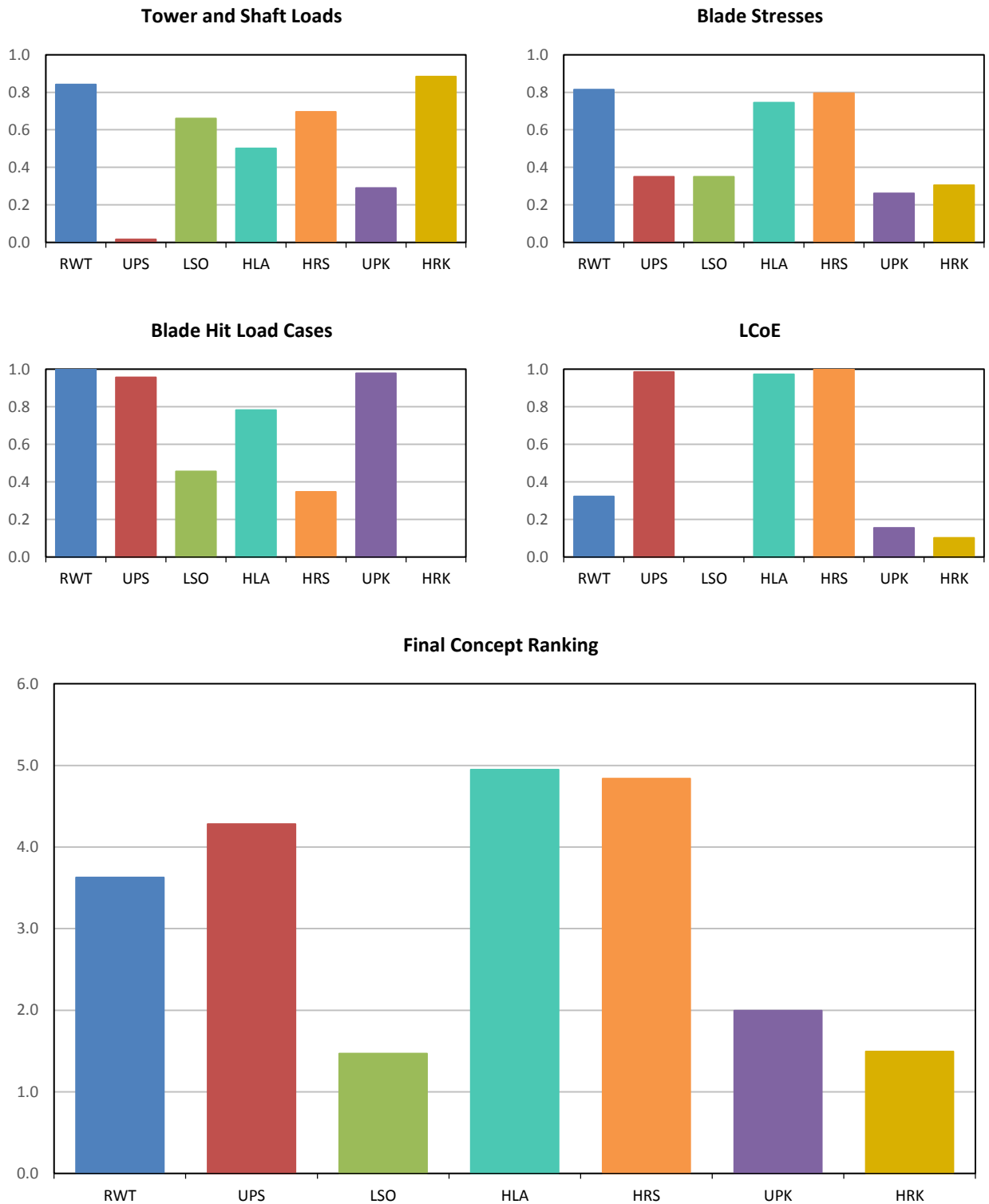


Figure 4.58: Graphic representation of the rankings by group and their final sum

In conclusion, it seems that the particular designs, the structural models generated, the simulations run and the method of evaluation used, favour the optimal concepts (UPS, HLA, and HRS) and the reference machine. The relatively faster rotating concepts (HLA and HRS) show a marginally better potential. This evaluation is done in terms of farm LCoE. Wake losses and some structural response indicators, such as fatigue loads on the blades, tower and shaft and blade hits are taken into account. It should be reminded that the blades are not pre-bent. Looking at the LCoE ranking and the final one, one can conclude that there alternative choices to be made in the designs that can provide a

better and more productive wind turbine. The so-far multi-disciplinary design provided by DTU and the INNWIND project partners, though, is indeed a very promising and balanced design. The up-scaling and larger diameter rotor is feasible and the second approach done in this thesis (aside from the initial conceptual approach in [7]) indicates that there can be a significant increase in energy production. It also comes with a decrease in the LCoE while maintaining a reasonable structural integrity.

5

CONCLUSIONS

5.1 Summary of Results and Concluding Remarks

The purpose of this thesis was to investigate six modifications on the blade structure and rotor operation of the INNWIND project 10 MW reference machine. The end-goal was the reduction of LCoE. Previous evidence showed an increase of energy production and/or decrease of loads when power density drops (increasing the rotor diameter and keeping power rating the same). The up-scaling method employed, was an effort to keep the necessary additional blade mass to a minimum. Its results were evaluated through the LCoE value of the cost model. A final ranking was produced with the combination of stresses on the blades, loads on the structure and blade hits (see Table 4.8, Figure 4.58 and Table 5.1 below).

Table 5.1: Summary of performance indicators

	RWT	UPS	LSO	HLA	HRS	UPK	HRK
Blade Mass [tn]	41.72	60.35	45.31	54.17	49.87	51.61	42.70
Farm AEP [TWh/y]	3.84	4.36	3.74	4.28	4.24	3.89	3.77
Farm LCoE [€/MWh]	92.09	85.52	95.29	85.65	85.39	93.76	94.28
Final Ranking [-/6]	3.63	4.28	1.47	4.95	4.84	2.00	1.50

An interesting phenomenon is that none of the concepts performing its best at one of the three criteria above, is deemed as the optimal one. For example, the HRK and RWT blades have the smallest masses, yet their differences in AEP, LCoE and loads set them apart in the final ranking. Similarly, the UPS has the highest AEP, but ranks only third because of loads on structure and high needed blade mass.

The top three concepts (HLA, HRS and UPS) indeed exhibit a promising potential in most aspects and should be furtherly investigated. Their main advantage over RWT is the higher AEP, which leads to a considerable cost reduction. In this particular cost model, it should be noted that the benefit of a high AEP is larger than the respective impact of a high blade mass. That is why the decrease of the power density produced favourable results for the aerodynamically optimum designs. The increased AEP comes from lowering the rated wind speed and taking advantage of that extra slice of power in the power curve. Furthermore, extra energy came from the maximum possible capture of wind in the partial load region in contrast with the sub-optimum concepts.

Another interesting thing to note is that concepts with peak-shaving included in the structural modelling (UPK and HRK) and the LSO did not produce very promising results. The resulting benefits from relative blade mass reduction were overcome by the power shedding and structural

deficiencies. So, seeking optimal C_p values is still the case for cost reduction in wind energy. Management of loads should be dealt with active components, smarter blade structuring and targeted research.

For the top three concepts, a detailed FEM analysis for buckling and stress concentration is needed. Also, after an optimal mass and stiffness allocation on the blade and its inner structure, a full IEC standard load set should be run to certify the blades. Adding pre-bend on the blades should be sufficient for eradicating blade-tower hits. This is most probably the case for the UPS, since it has similar blade hits with the “straight” RWT blade. Also, strengthening the tower should be among the considerations.

Different energy production would occur and new LCoE values would be derived. Finally, a more realistic, inclusive and detailed cost-model should be used. That would help to investigate secondary costs, such as installation, operation and maintenance costs, effects of fatigue, personnel access costs, financing and so on.

5.2 Critical Review on the Method and Proposed Corrections

Besides the actual results of the analysis of the concepts, another important part in this report is the up-scaling process devised. The structural models of the new concepts were not available and needed to be formulated. The method devised projected the steady-state operation of the RWT to the new geometries by keeping the strains on the blades the same. The bending moments changed between the designs, with ranges up to 30%. For the larger loads, more material was used and the stresses remained at a very similar level. This result confirms that up-scaling by dropping power density can still produce a sound structural response.

The short two-way study case done with the UpWind model also showed expected results and that the process can also be applied when doubling or halving the rated power as well. Additionally, if torsional forces within the aerofoils are available from the initial steady state BEM analysis, the method can probably make use of them and estimate the torsional stiffness in the same manner. BOT however did not provide this information, hence the assumption about the analogies of chords, aerofoil thickness and skin thicknesses with the relative thickness distribution.

Of course the main assumption used, is that the reference model is soundly designed and operates in good order overall. There is also need for BEM and aerodynamic forces calculations for the method to work and sufficient section-by-section detail in this analysis. At some point within the first steps of the up-scaling, it was discovered that correcting the forces (and geometry where necessary) with respect to the pitch angle (even 1 to 3°) at the maximum moment point can change the results considerably.

Another important advantage of the method is its ability to distinguish between flap-, edge- and span-wise axes for up-scaling the properties. With the use of 3 separate factors independent for each axis, modifications on the geometry and material used can be employed on-demand by the user. This was also seen with the UpWind study case where different outboard aerofoils were used. This feature also provides the ability to manually solve structural problems in a single element. However, there is no certainty whether this holds for a detailed material layup (i.e. cross-section inner structure, direction of fibres, number of layers etc.) since non-linearities may come into play. This was outside the scope of this thesis and proportional projection of the rectangular thin-walled cross-sections was assumed.

Three more issues should be noticed. The first and most important is the percentile of the chord where the aerodynamic forces are applied. Here it was assumed as 50% of the chord in the blade

root and 25% from the leading edge moving outboards, and a constant 50% of the thickness. By trial and error it was seen that when these percentages vary, but stay the same throughout the designs, the error is minimal. Considerable differences were observed when the values changed only for the up-scaled design, i.e. when using an aerofoil with a much different aerodynamic centre, e.g. at 35% of the chord from the leading edge.

Another small issue is the correction of the forces with respect to the rotor's cone and tilt angle and pre-bend when applicable. In this report, the modelling for all the designs was done by considering the rotor totally plane and perpendicular to the wind flow.

The third issue is the use of multiple criteria in the modelling process. For example, one can also investigate the static blade tip displacement. By choosing to keep the strain distribution or tip displacement constant or even by quantifying between them for inheriting the static behaviour of the reference blade. There can also be a rudimentary quest on the dynamic nature of the maximum loads and even on expected extreme loads. These values can also participate as criteria in this modelling process.

5.3 Future Work

Several steps can be taken in the future for this work to be more complete. The two most important parts and design drivers left out completely in this report is local or global buckling and flutter^(A) (over-speed) analysis. These two issues are indeed reported in literature as problematic for large blades. However, since there was a fairly large number of concepts to model, analyse and compare at a primary level, these issues were deemed secondary to investigate.

As for buckling, a short literature review shows that most of researchers or designers use a detailed FEM model with special structural codes to acquire buckling locations and modes. A basic static numerical analysis on skins, shear webs etc. was assumed not to provide high quality information on the matter, especially if cross-sectional details were to be speculated on or linearly projected.

The way flutter speed is reported is the ratio of the rotor speed where flutter occurs over the rated rotor speed. In Sandia reports [14] and [30], it is stated that flutter speeds for older wind turbines range from 2:1 until 6:1, whereas for newer, larger, more lightweight designs, the ratio may drop to 1.1:1. Practically, this means that almost no over-speed is allowed for the rotor. It must be noted that a high sampling frequency (small time increment of ca. 0.001 s) is necessary in order for the code to be able to calculate and record the high frequencies of the oscillations that indicate flutter, hence a high computational effort. A single flutter case simulation lasts almost as much as for a load set of 5 DLC groups (roughly 300 seeds). Over-speed simulations for RWT, UPS and LSO were run (not presented in the report) confirming the above statements of Sandia Labs. The RWT showed heavy oscillations at around 15 rpm, UPS at around 12 rpm and LSO at 13 rpm.

Another matter not investigated, is the influence of possible changes in the tower, whether that would concern hub height or stiffer designs for the heavier rotors. Surely, a higher tower would produce slightly more power and that is why a consistent approach was kept, so that this flat advantage would not be hindering the RWT against the new concepts. One can easily note however

^(A) Flutter is a special case of aeroelastic instability, where the rotor is left to rotate freely, without generator counter-torque, controller actions or brakes. The simulation is ran with a ramping normal profile wind speed, starting from just below rated wind speed until 25 or even 30 m/s, with the blades pitched at about 8° and the rotor is allowed to go into rotational speeds much above rated rotor speed. At a certain rotor speed, the torsional deformation of the blade increases and influences the angle of attack on the aerofoils. Lift forces change drastically and this produces recurring variations between them, also causing flap-wise oscillations. Usually, this is a coupling of the torsional and the 2nd flap-wise vibrational modes.

that with the current hub height of 119 m, the 103 m blades would come much closer to the sea level, and safety issues arise.

With all the results of this report as a starting point, one may distinguish the concepts with the best potential. Then the full IEC load set and the extra special cases can be run in order to have blades ready for certification. Also, already shown or new problems can be tackled in a step-by-step manner. Of course, such an analysis should be accompanied or followed by a proper investigation and research on the detailed structural model of the cross-sections and specifics of materials. There is also much space to be covered concerning special design alterations such as a third shear web beam, at least for the middle part of the blade, reinforcements in aerofoil edges or pressure and suction sides to tackle local buckling and fatigue.

Lastly, a small sensitivity analysis could be done on rotor configurations and their combinations. It was seen that the sum of tilt and cone angle of 7.5° was more than necessary not only for computational and numerical issues but most importantly for structural issues, such as tip-tower hits. Application of pre-bend in the blades seems to be necessary as well, because the RWT also produced a few blade hits. That would add extra 3.3 m of tip clearance. For the designs with more hits, aside from pre-bend, the values of cone and tilt angle should be increased so as to minimise and eliminate blade hits, even in conjunction with a slight increase of the stiffnesses and mass.

In conclusion, this report was an effort to approach several different designs and assess their performance as alternatives for the INNWIND reference wind turbine with the goal to increase energy production, reduce loads and the LCoE. Wind turbine design is a challenging field and only with constant research, collective knowledge and inter-institutional collaboration can there be advance and further development of wind energy. The results seem to produce interesting potentials, somewhat differentiated from the initial study of Ceyhan and Grasso; the basis of the current thesis. The structural issues that occurred from the physical formulation of the concepts did hinder some designs and favoured others. The aerodynamically optimal and heavier designs seem to be better alternatives mainly because of their higher energy production and more sound structural response.

The RWT had already a lightweight nature blade of 42 tons for 86.4 m length compared to the Sandia 114 tons blade for 100 m length. This lightweight design was up-scaled to 60 tons for the UPS concept while the structural response seemed to remain in good order signifying a huge material saving compared to the Sandia blade. Taking into account also the LCoE, energy production and fatigue issues, the other two optimal designs (HLA and HRS) also seem to be good candidates.

REFERENCES

- [1] Alberici et al., 2014. “*Subsidies and costs of EU energy, an interim report*”. ECOFYS and European Commission, October 2014.
- [2] Ashuri T, 2012. “*Beyond Classical Upscaling: Integrated Aero-servo-elastic Design and Optimization of Large Offshore Wind Turbines*”. PhD Thesis TU Delft, June 2012.
- [3] Bach PW, 1996. “*The Effect of Moisture on the Fatigue Performance of Glass Fibre Reinforced Polyester Coupons and Bolted Joints*”. Energy Research Centre of the Netherlands, February 1996.
- [4] Bak C, Bitsche R, Yde A, Kim T, Hansen MH, Zahle F, Gaunaa M, Blasques J, Døssing M, Wedel Heinen JJ, Behrens T, 2012. “*Light Rotor: The 10-MW reference wind turbine*”. DTU Wind Energy and Vestas Wind Systems A/S, EWEA (EWEC) 2012 Conference & Exhibition Proceedings, April 2012.
- [5] Bak C, Zahle F, Bitsche R, Kim T, Yde A, Henriksen LC, Natarajan A, Hansen MH, 2013. “*Description of the DTU 10 MW Reference Wind Turbine, Draft*”. DTU Wind Energy, June 2013.
- [6] Bot ETG, Ceyhan Ö, 2011. “*Blade Optimization Tool, BOT, User Manual*”. Energy Research Centre of the Netherlands, March 2011.
- [7] Ceyhan Ö, Grasso F, 2013. “*Investigation of Wind Turbine Rotor Concepts for Offshore Wind Farms*”. CAN & TORQUE Conference Proceedings, 2014.
- [8] Chaviaropoulos PK, H.J.M. Beurskens HJM, Voutsinas SG, 2013. “*Moving Towards Large(r) Rotors, Is that a good idea?*” EWEA (EWEC) 2013 Conference and Exhibition Proceedings, February 2013.
- [9] Chaviaropoulos PK, Karga C, Hendriks B, 2014. “*PI-based assessment of innovative concepts (methodology), Deliverable 1.2.3, WP1 Conceptual Design, Task 1.2 Assessment of Innovation at the Subsystem Level*”. INNWIND Project, April 2014.
- [10] Chaviaropoulos PK, Natarajan A, Mouzakis F, 2014. “*Definition of Performance Indicators (PIs) and Target Values, Deliverable 1.2.2, WP1 Conceptual Design, Task 1.2 Assessment of Innovation at the Subsystem Level*”. INNWIND Project, February 2014.
- [11] Deutsche Bundesbank, 2014. “*Exchange Rate Statistics, Euro foreign exchange reference rates of the European Central Bank, End-of-year rates and annual averages*”. June 2014.
- [12] Fingersh L, Hand M, Laxson A, 2006. “*Wind Turbine Design Cost and Scaling Model, Technical Report, NREL/TP-500-40566*”. National Renewable Energy Laboratory, December 2006
- [13] Griffin DA, 2001. “*WindPACT Turbine Design Scaling Studies Technical Area 1 - Composite Blades for 80-to 120-Meter Rotor, NREL/SR-500-29492*”. National Renewable Energy Laboratory, April 2001
- [14] Griffith DT, Ashwill TD, 2011. “*The Sandia 100-meter All-glass Baseline Wind Turbine Blade: SNL100-00*”. Sandia National Laboratories & U.S. Department of Energy, June 2011.
- [15] GWEC, 2014. “*Global Wind Report, Annual Market Update 2013*”. Global Wind Energy Council, April 2014.
- [16] Hand M et al., 2013. “*2011 Cost of Wind Energy Review, Technical Report, NREL/TP-5000-56266*”. National Renewable Energy Laboratory, March 2013.
- [17] Hendriks HB, Bulder BH, 1995. “*Fatigue Equivalent Load Cycle Method. A General Method to Compare the Fatigue Loading of Different Load Spectrums*”. Energy Research Centre of the Netherlands, October 1995.
- [18] Holierhoek JG, de Vaal JB, van Zuijlen AH, Bijl H, 2012. “*Comparing different dynamic stall models*”. Wiley Online Library, Wind Energ. 2013; 16:139-158, April 2012

- [19] INNWIND Project, <http://www.innwind.eu/> website and database.
- [20] IEC, 2005. "International Standard IEC 61400-1, Edition 3.0, Wind turbines - Part 1: Design requirements". International Electrotechnical Commission, 2005.
- [21] IEC, 2010. "International Standard IEC 61400-1, Edition 3.0, Amendment 1, Wind turbines - Part 1: Design requirements". International Electrotechnical Commission, 2010.
- [22] IEC, 2009. "International Standard IEC 61400-3, Edition 1.0, Wind turbines - Part 3: Design requirements for offshore wind turbines". International Electrotechnical Commission, 2009.
- [23] Jonkman J, Butterfield S, Musial W, Scott G, 2009. "Definition of a 5-MW Reference Wind Turbine for Offshore System Development". National Renewable Energy Laboratory, February 2009.
- [24] Johnson KE, 2004. "Adaptive Torque Control of Variable Speed Wind Turbines, NREL/TP-500-36265". National Renewable Energy Laboratory, August 2004.
- [25] Kensch CW, 2004. "Fatigue of Composites for Wind Turbines". WMC Knowledge Centre and Third International Conference on Fatigue of Composites, September 2004.
- [26] Lindenburg C, 2003. "Investigation into Rotor Blade Aerodynamics, Analysis of the stationary measurements on the UAE phase-VI rotor in the NASA-Ames wind tunnel". Energy Research Centre of the Netherlands, July 2003.
- [27] Lindenburg C, Holierhoek, JG, 2013. "Blademode v2.2 User Manual". Energy Research Centre of the Netherlands, 2013. (2.5.2 FOCUS)
- [28] Lindenburg C, 2013. "Evaluation of Phatas "JAN-2012a", with and without Supervisory control". Energy Research Centre of the Netherlands, May 2013.
- [29] Lindenburg C. "PHATAS Release "JAN-2012a" User's Manual, Program for Horizontal Axis wind Turbine Analysis and Simulation". Energy Research Centre of the Netherlands, 2013.
- [30] Lobitz DW, 2004. "Flutter Speed Predictions for MW-Sized Wind Turbine Blades". Sandia National Laboratories & U.S. Department of Energy (Wiley Online Library, Wind Energy, Vol.7, Issue 3, pp. 211-224), July 2004.
- [31] Malcolm DJ, Hansen AC, 2002. "WindPACT Turbine Rotor Design Study, NREL/SR-500-32495". Global Energy Concepts LLC, Windward Engineering, National Renewable Energy Laboratory, June 2002 (Revised April 2006).
- [32] Manwell J, McGowan J, Rogers A. "Wind energy explained: theory, design, and application - 2nd Ed.". John Wiley & Sons Ltd., 2009.
- [33] NREL, 2011. "WindPACT Turbine Design Scaling Studies Technical Area 3 - Self-Erecting Tower and Nacelle Feasibility, NREL/SR-500-29493". Global Energy Concepts LLC, National Renewable Energy Laboratory, May 2001.
- [34] Nijssen RPL, 2007. "Fatigue Life Prediction and Strength Degradation of Wind Turbine Rotor Blade Composites, SAND2006-7810P". Sandia National Laboratories, October 2007.
- [35] Ragan P and Manuel L, 2007. "Comparing Estimates of Wind Turbine Fatigue Loads using Time-Domain and Spectral Methods". Wind Engineering, Volume 31, No. 2, pp 83-99, March 2007.
- [36] Resor BR, 2013. "Definition of a 5MW/61.5m Wind Turbine Blade Reference Model". Sandia National Laboratories & U.S. Department of Energy, April 2013.
- [37] Schmidt S, Vath A, 2012. "Comparison of Existing Medium-speed Drive Train Concepts with a Differential Gearbox Approach". EWEA (EWEC) 2012 Conference & Exhibition Proceedings, April 2012.
- [38] SETIS - TPWind, 2011. "Key Performance Indicators for the European Wind Industrial Initiative, Version 3". European Commission, Directorate-General, Joint Research Centre, Strategic Energy Technologies Information System (SETIS), November 2011.

- [39] Snel H, Houwink R, Bosschers J, 1994. “*Sectional Prediction of Lift Coefficients on Rotating Wind Turbine Blades in Stall*”. Energy Research Centre of the Netherlands, December 1994.
- [40] Sieros G et al., 2011. “*Upscaling wind turbines: theoretical and practical aspects and their impact on the cost of energy*”. UpWind Project, Wiley Online Library, September 2011.
- [41] Smith K, 2001. “*WindPACT Turbine Design Scaling Studies Technical Area 2 - Turbine, Rotor, and Blade Logistics NREL/SR-500-29439*”. Global Energy Concepts LLC, National Renewable Energy Laboratory, June 2001.
- [42] Sutherland HJ, 1999. “*Fatigue Analysis of Wind Turbines. Technical Report SAND99-0089*”. Sandia National Laboratories, June 1999.
- [43] WMC Knowledge Centre & ECN. “*FOCUS6: The Integrated Wind Turbine Design Suite brochure*”. <http://www.wmc.eu/>.
- [44] Winkelaar D, 1992. “*SWIFT, Program for Three-Dimensional Wind Simulation, Part 1: Model Description and Program Verification*”. Energy Research Centre of the Netherlands, December 1992.
- [45] UpWind Project Report, 2011. “*UpWind, Design limits and solutions for very large wind turbines*”. <http://www.upwind.eu/>, March 2011.

APPENDIX

A.1 Tabular Data of Tower and Blade Properties

TOWER							
Global Height z [m]	Outer Diameter [m]	Wall Thickness [mm]	Cross Section Area [m ²]	Mass per Length [kg/m]	Second Moment of Area [m ⁴]	Torsional Stiffness Constant [m ⁴]	Radius of Gyration [m]
0.000	8.300	38.0	0.9863	8383.7	8.416	16.832	2.921
11.500	8.022	38.0	0.9531	8101.2	7.593	15.187	2.823
11.501	8.022	36.0	0.9031	7676.7	7.199	14.398	2.823
23.000	7.743	36.0	0.8716	7409.0	6.472	12.944	2.725
23.001	7.743	34.0	0.8234	6999.2	6.117	12.234	2.726
34.500	7.465	34.0	0.7937	6746.4	5.478	10.956	2.627
34.501	7.465	32.0	0.7472	6351.2	5.160	10.320	2.628
46.000	7.186	32.0	0.7192	6113.3	4.601	9.203	2.529
46.001	7.186	30.0	0.6744	5732.8	4.317	8.635	2.530
57.500	6.908	30.0	0.6482	5509.7	3.833	7.665	2.432
57.501	6.908	28.0	0.6052	5143.9	3.580	7.161	2.432
69.000	6.629	28.0	0.5807	4935.7	3.163	6.326	2.334
69.001	6.629	26.0	0.5394	4584.5	2.940	5.879	2.335
80.500	6.351	26.0	0.5166	4391.2	2.583	5.166	2.236
80.501	6.351	24.0	0.4770	4054.7	2.387	4.773	2.237
92.000	6.072	24.0	0.4560	3876.2	2.085	4.170	2.138
92.001	6.072	22.0	0.4182	3554.3	1.913	3.827	2.139
103.500	5.794	22.0	0.3989	3390.8	1.661	3.322	2.041
103.501	5.794	20.0	0.3628	3083.6	1.512	3.023	2.041
115.630	5.500	20.0	0.3443	2926.7	1.293	2.585	1.937

RWT											
Sect. No.	Span Section [m]	Chord [m]	Aero Twist [°]	Rel. Thick. [-]	Norm. Force GCS, Fn [N/m]	Norm. Force + mg LCS, Fn' [N/m]	Tang. Force GCS, Ft [N/m]	Tang. Force + mg LCS, Ft' [N/m]	Centrifugal Force (N)	Flap Bend. Moment, My LCS [N.m]	Edge Bend. Moment, Mx LCS [N.m]
1	0.000	5.380	14.500	0.999	749.0	3171.3	-72.0	11165.0	9.330E+05	2.935E+07	1.383E+07
2	1.322	5.380	14.500	0.996	797.1	3189.1	-117.9	11170.0	8.867E+05	2.861E+07	1.324E+07
3	4.011	5.381	14.499	0.953	987.9	3186.9	-143.1	10910.0	7.980E+05	2.712E+07	1.210E+07
4	6.791	5.454	14.428	0.860	1362.0	3061.6	-114.2	9986.9	7.140E+05	2.561E+07	1.100E+07
5	9.653	5.637	13.881	0.738	1811.0	2845.5	-47.7	8913.7	6.354E+05	2.407E+07	9.960E+06
6	12.587	5.867	12.537	0.610	2307.6	2639.3	89.8	8239.6	5.621E+05	2.253E+07	8.969E+06
7	15.583	6.071	10.602	0.503	4967.2	3154.1	412.0	7754.2	4.942E+05	2.097E+07	8.034E+06
8	18.630	6.185	8.890	0.430	8563.4	4049.2	820.7	7306.9	4.317E+05	1.941E+07	7.156E+06
9	21.714	6.203	7.801	0.382	11303.6	4740.9	957.8	6729.5	3.746E+05	1.787E+07	6.339E+06
10	24.824	6.143	7.024	0.349	12810.4	5082.6	978.4	6211.7	3.226E+05	1.636E+07	5.582E+06
11	27.946	6.020	6.383	0.324	13658.3	5268.8	998.9	6019.5	2.756E+05	1.489E+07	4.886E+06
12	31.065	5.849	5.778	0.305	14416.9	5424.8	1006.1	5741.4	2.334E+05	1.347E+07	4.250E+06
13	34.169	5.646	5.229	0.291	15493.9	5697.0	1006.8	5440.4	1.961E+05	1.211E+07	3.673E+06
14	37.244	5.423	4.676	0.278	16733.4	6031.7	1007.0	5172.2	1.633E+05	1.082E+07	3.155E+06
15	40.278	5.187	4.091	0.268	18006.8	6378.9	1006.9	4888.7	1.348E+05	9.598E+06	2.693E+06
16	43.257	4.944	3.491	0.260	19303.0	6737.9	1006.5	4601.9	1.104E+05	8.454E+06	2.285E+06
17	46.172	4.700	2.891	0.253	20607.5	7107.8	1005.8	4349.9	8.959E+04	7.390E+06	1.926E+06
18	49.010	4.459	2.304	0.248	21895.6	7478.9	1004.5	4100.2	7.210E+04	6.411E+06	1.613E+06
19	51.765	4.225	1.741	0.245	23139.7	7843.5	1002.6	3873.6	5.753E+04	5.517E+06	1.342E+06

20	54.427	4.001	1.212	0.243	24320.6	8194.7	1000.2	3671.0	4.550E+04	4.708E+06	1.109E+06
21	56.991	3.788	0.724	0.241	25416.3	8524.5	997.6	3475.1	3.567E+04	3.982E+06	9.097E+05
22	59.450	3.588	0.278	0.241	26411.2	8827.1	994.7	3293.9	2.772E+04	3.338E+06	7.406E+05
23	61.802	3.400	-0.125	0.241	27296.0	9098.6	991.6	3128.4	2.134E+04	2.771E+06	5.980E+05
24	64.043	3.226	-0.489	0.241	28065.4	9336.5	988.2	2963.7	1.627E+04	2.277E+06	4.787E+05
25	66.171	3.064	-0.815	0.241	28720.0	9539.9	984.1	2831.0	1.227E+04	1.851E+06	3.796E+05
26	68.188	2.915	-1.110	0.241	29264.2	9709.9	978.8	2692.3	9.158E+03	1.486E+06	2.978E+05
27	70.092	2.778	-1.379	0.241	29706.4	9847.9	972.0	2582.7	6.750E+03	1.178E+06	2.309E+05
28	71.885	2.653	-1.627	0.241	30053.4	9956.5	963.2	2467.5	4.909E+03	9.196E+05	1.766E+05
29	73.570	2.538	-1.858	0.241	30313.2	10037.8	952.0	2352.4	3.516E+03	7.062E+05	1.330E+05
30	75.150	2.433	-2.074	0.241	30485.9	10091.1	938.0	2255.3	2.475E+03	5.319E+05	9.833E+04
31	76.627	2.333	-2.277	0.241	30546.5	10107.8	920.5	2169.4	1.704E+03	3.917E+05	7.113E+04
32	78.005	2.234	-2.466	0.241	30440.5	10070.2	898.8	2080.9	1.144E+03	2.806E+05	5.010E+04
33	79.290	2.131	-2.641	0.241	30106.1	9958.0	871.6	1980.8	7.445E+02	1.945E+05	3.414E+04
34	80.484	2.021	-2.800	0.241	29497.4	9755.7	837.6	1872.8	4.661E+02	1.291E+05	2.232E+04
35	81.592	1.905	-2.942	0.241	28608.8	9461.3	795.5	1756.7	2.773E+02	8.111E+04	1.380E+04
36	82.619	1.778	-3.068	0.241	27351.1	9045.4	742.8	1627.3	1.537E+02	4.713E+04	7.898E+03
37	83.570	1.629	-3.175	0.241	25542.4	8448.0	674.9	1467.0	7.683E+01	2.439E+04	4.030E+03
38	84.448	1.444	-3.269	0.241	22939.8	7588.5	583.7	1268.2	3.249E+01	1.042E+04	1.701E+03
39	85.259	1.189	-3.356	0.241	18867.3	6242.3	446.7	1005.8	9.792E+00	3.019E+03	4.904E+02
40	86.007	0.746	-3.410	0.241	11574.3	3828.3	243.9	629.0	9.236E-01	2.462E+02	4.046E+01

RWT									
Span Section [m]	Flap Bend. Stiffness, E _{yy} LCS [N.m ²]	Edge Bend. Stiffness, E _{xx} LCS [N.m ²]	Bend. Stiffness, E _{xy} LCS [N.m ²]	Flap Strain, ε _{zx} LCS [μ]	Edge Strain, ε _{yx} LCS [μ]	EA stiffness (N)	Cross Section Area [m ²]	Mass Distr. [kg/m]	Torsional Stiffness, GJT [N.m ²]
0.000	6.187E+10	6.101E+10	0.000E+00	1328	662	1.779E+10	1.410	1189.5	2.746E+10
2.015	6.218E+10	6.112E+10	0.000E+00	1296	642	1.784E+10	1.411	1191.6	2.748E+10
3.742	6.300E+10	6.113E+10	0.000E+00	1219	610	1.808E+10	1.445	1202.8	2.732E+10
5.469	6.015E+10	5.809E+10	0.000E+00	1197	605	1.766E+10	1.433	1171.5	2.560E+10
7.196	5.456E+10	5.305E+10	0.000E+00	1206	644	1.685E+10	1.473	1113.6	2.214E+10
8.924	4.722E+10	4.774E+10	3.370E+09	1262	707	1.596E+10	1.457	1049.3	1.839E+10
10.650	3.859E+10	4.114E+10	3.869E+09	1381	830	1.483E+10	1.459	974.6	1.397E+10
12.376	3.018E+10	3.608E+10	3.707E+09	1563	965	1.385E+10	1.430	908.7	1.010E+10
14.104	2.386E+10	3.260E+10	3.399E+09	1731	1089	1.325E+10	1.419	868.9	7.448E+09
15.544	1.989E+10	3.100E+10	3.021E+09	1862	1153	1.290E+10	1.376	845.5	6.029E+09
17.698	1.525E+10	2.704E+10	2.376E+09	2061	1312	1.169E+10	1.355	775.2	4.052E+09
19.432	1.296E+10	2.508E+10	1.939E+09	2145	1373	1.101E+10	1.305	735.8	3.351E+09
21.159	1.102E+10	2.272E+10	1.594E+09	2246	1444	1.027E+10	1.263	691.1	2.638E+09
22.886	9.491E+09	2.049E+10	1.328E+09	2331	1501	9.659E+09	1.230	654.9	2.119E+09
24.613	8.258E+09	1.865E+10	1.122E+09	2409	1532	9.185E+09	1.194	625.9	1.744E+09
26.341	6.969E+09	1.867E+10	1.009E+09	2561	1418	8.712E+09	1.134	593.3	1.419E+09
28.068	6.165E+09	1.759E+10	9.109E+08	2611	1384	8.557E+09	1.104	581.0	1.243E+09
29.795	5.458E+09	1.645E+10	8.216E+08	2650	1354	8.383E+09	1.070	566.2	1.090E+09
31.523	4.850E+09	1.499E+10	7.313E+08	2687	1353	8.192E+09	1.006	548.2	9.620E+08
33.250	4.304E+09	1.349E+10	6.337E+08	2721	1362	7.953E+09	0.972	529.7	8.336E+08
34.978	3.826E+09	1.239E+10	5.489E+08	2749	1339	7.764E+09	0.895	510.3	7.447E+08
36.705	3.378E+09	1.145E+10	4.742E+08	2789	1304	7.555E+09	0.863	494.7	6.545E+08
38.433	2.977E+09	1.042E+10	4.031E+08	2825	1282	7.328E+09	0.831	477.5	5.710E+08
40.073	2.635E+09	9.451E+09	3.445E+08	2864	1268	7.108E+09	0.792	460.9	5.031E+08
41.801	2.310E+09	8.489E+09	2.862E+08	2901	1251	6.853E+09	0.749	441.8	4.434E+08
43.528	2.024E+09	7.694E+09	2.391E+08	2939	1222	6.624E+09	0.712	425.3	3.920E+08
45.255	1.764E+09	6.637E+09	1.922E+08	2979	1244	6.308E+09	0.654	401.4	3.381E+08
46.983	1.541E+09	5.967E+09	1.584E+08	3006	1211	6.058E+09	0.630	385.1	2.973E+08
48.710	1.350E+09	5.325E+09	1.289E+08	3014	1182	5.824E+09	0.567	366.0	2.642E+08
50.437	1.172E+09	4.666E+09	1.036E+08	3031	1164	5.530E+09	0.543	346.9	2.254E+08
52.251	1.017E+09	3.989E+09	8.115E+07	3024	1165	5.252E+09	0.484	326.3	1.986E+08
53.979	8.870E+08	3.538E+09	6.562E+07	3005	1122	5.007E+09	0.455	310.3	1.750E+08
55.706	7.727E+08	3.049E+09	5.124E+07	2968	1101	4.738E+09	0.414	291.7	1.526E+08

57.433	6.692E+08	2.615E+09	4.034E+07	2941	1084	4.451E+09	0.374	272.4	1.328E+08
59.161	5.787E+08	2.271E+09	3.235E+07	2893	1042	4.185E+09	0.356	257.0	1.167E+08
60.888	4.999E+08	1.921E+09	2.470E+07	2821	1015	3.902E+09	0.311	237.8	1.016E+08
62.554	4.295E+08	1.666E+09	1.991E+07	2761	965	3.635E+09	0.288	221.8	8.935E+07
64.281	3.635E+08	1.393E+09	1.555E+07	2694	934	3.337E+09	0.254	203.2	7.721E+07
66.008	3.049E+08	1.184E+09	1.201E+07	2613	875	3.050E+09	0.238	186.8	6.583E+07
67.735	2.541E+08	9.975E+08	9.617E+06	2508	814	2.776E+09	0.224	171.7	5.691E+07
69.524	2.083E+08	8.149E+08	7.116E+06	2378	758	2.489E+09	0.193	153.8	4.818E+07
71.252	1.711E+08	6.850E+08	5.822E+06	2215	676	2.243E+09	0.174	140.1	4.164E+07
72.979	1.382E+08	5.539E+08	4.347E+06	2040	608	1.981E+09	0.147	124.4	3.584E+07
74.659	1.087E+08	4.606E+08	3.526E+06	1877	519	1.720E+09	0.130	108.9	2.920E+07
76.386	8.396E+07	3.590E+08	2.588E+06	1664	447	1.467E+09	0.117	95.2	2.407E+07
78.161	6.309E+07	2.960E+08	2.326E+06	1394	333	1.250E+09	0.095	82.3	2.038E+07
79.888	4.429E+07	2.171E+08	1.650E+06	1127	252	1.006E+09	0.083	68.3	1.573E+07
81.577	2.835E+07	1.550E+08	1.311E+06	875	172	7.791E+08	0.067	54.5	1.158E+07
83.343	1.449E+07	1.004E+08	1.031E+06	592	89	5.539E+08	0.050	40.7	7.415E+06
85.071	4.504E+06	4.171E+07	5.151E+05	307	34	3.074E+08	0.035	25.2	3.167E+06
86.366	1.031E+06	1.271E+07	1.948E+05	10	1	1.722E+08	0.025	15.4	9.581E+05

UPS											
Sect. No.	Span Section [m]	Chord [m]	Aero Twist [°]	Rel. Thick. [-]	Norm. Force GCS, Fn [N/m]	Norm. Force + mg LCS, Fn' [N/m]	Tang. Force GCS, Ft [N/m]	Tang. Force + mg LCS, Ft' [N/m]	Centrifugal Force (N)	Flap Bend. Moment, My LCS [N.m]	Edge Bend. Moment, Mx LCS [N.m]
1	0.000	6.215	14.500	0.999	712.2	3958.5	-65.5	14255.0	9.592E+05	3.775E+07	2.174E+07
2	1.164	6.215	14.500	0.998	742.0	3956.6	-96.3	14208.4	9.226E+05	3.701E+07	2.100E+07
3	3.325	6.215	14.500	0.979	824.4	3991.9	-123.5	14235.0	8.573E+05	3.564E+07	1.969E+07
4	5.321	6.217	14.498	0.950	951.5	3928.7	-135.8	13826.4	8.004E+05	3.439E+07	1.853E+07
5	7.316	6.266	14.458	0.896	1155.4	3811.0	-115.9	13142.7	7.466E+05	3.316E+07	1.744E+07
6	9.145	6.340	14.325	0.836	1390.0	3673.7	-97.0	12422.6	7.000E+05	3.205E+07	1.648E+07
7	11.129	6.471	13.989	0.761	1657.7	3467.9	-58.3	11547.8	6.522E+05	3.085E+07	1.548E+07
8	13.290	6.623	13.315	0.684	1928.5	3230.8	-1.3	10774.9	6.032E+05	2.957E+07	1.446E+07
9	15.287	6.778	12.529	0.610	2207.6	3082.9	86.4	10393.6	5.605E+05	2.840E+07	1.355E+07
10	17.282	6.916	11.398	0.547	3484.2	3244.9	260.5	10125.6	5.203E+05	2.724E+07	1.269E+07
11	19.370	7.036	10.290	0.490	5229.1	3519.5	435.8	9529.8	4.805E+05	2.604E+07	1.184E+07
12	21.449	7.113	9.302	0.448	7179.9	3952.0	676.9	9216.6	4.433E+05	2.486E+07	1.103E+07
13	23.444	7.151	8.542	0.415	9136.4	4416.8	853.9	8792.1	4.096E+05	2.374E+07	1.029E+07
14	25.439	7.163	7.935	0.388	10534.7	4729.4	909.6	8380.8	3.778E+05	2.264E+07	9.585E+06
15	27.434	7.135	7.466	0.368	11546.6	4948.5	921.6	8024.8	3.478E+05	2.155E+07	8.916E+06
16	29.430	7.097	7.035	0.350	12226.5	5064.2	933.2	7644.5	3.195E+05	2.049E+07	8.279E+06
17	31.425	7.019	6.678	0.336	12700.6	5155.8	945.7	7509.1	2.928E+05	1.945E+07	7.673E+06
18	33.420	6.936	6.326	0.322	13125.3	5230.7	954.4	7350.3	2.676E+05	1.842E+07	7.098E+06
19	35.416	6.826	5.991	0.312	13540.4	5301.3	958.9	7143.4	2.440E+05	1.742E+07	6.552E+06
20	37.412	6.709	5.665	0.302	13918.3	5362.9	960.8	6931.7	2.218E+05	1.644E+07	6.035E+06
21	39.407	6.577	5.359	0.294	14528.2	5505.1	961.1	6700.2	2.010E+05	1.548E+07	5.546E+06
22	41.402	6.438	5.048	0.287	15192.5	5671.6	961.3	6514.1	1.816E+05	1.454E+07	5.084E+06
23	43.398	6.294	4.739	0.280	15857.3	5839.2	961.4	6314.2	1.635E+05	1.362E+07	4.649E+06
24	45.343	6.143	4.417	0.274	16531.1	6010.6	961.4	6115.0	1.471E+05	1.275E+07	4.249E+06
25	47.288	5.989	4.085	0.268	17227.6	6190.0	961.4	5905.4	1.319E+05	1.190E+07	3.873E+06
26	49.284	5.824	3.733	0.263	17949.5	6379.7	961.2	5718.8	1.175E+05	1.105E+07	3.510E+06
27	51.279	5.658	3.378	0.258	18685.5	6571.3	960.8	5450.1	1.041E+05	1.023E+07	3.171E+06
28	53.274	5.489	3.018	0.255	19434.4	6775.1	960.4	5276.3	9.191E+04	9.436E+06	2.854E+06
29	55.270	5.318	2.656	0.251	20191.5	6982.3	959.8	5069.0	8.070E+04	8.666E+06	2.558E+06
30	57.265	5.143	2.289	0.248	20962.8	7196.9	958.9	4872.1	7.048E+04	7.924E+06	2.283E+06
31	59.310	4.967	1.921	0.246	21740.3	7415.7	957.7	4658.2	6.096E+04	7.192E+06	2.021E+06
32	61.356	4.793	1.562	0.244	22503.7	7634.8	956.3	4493.3	5.237E+04	6.491E+06	1.780E+06
33	63.351	4.622	1.213	0.243	23248.6	7850.3	954.8	4308.9	4.483E+04	5.837E+06	1.562E+06
34	65.346	4.453	0.877	0.242	23972.2	8062.0	953.0	4111.5	3.807E+04	5.215E+06	1.363E+06
35	67.342	4.286	0.549	0.241	24674.2	8270.2	951.1	3964.6	3.205E+04	4.624E+06	1.180E+06
36	69.337	4.121	0.235	0.241	25342.2	8469.6	949.1	3776.5	2.671E+04	4.065E+06	1.013E+06

37	71.297	3.961	-0.063	0.241	25968.4	8658.4	947.0	3620.1	2.210E+04	3.549E+06	8.640E+05
38	73.257	3.802	-0.351	0.241	26560.1	8838.3	944.6	3439.8	1.806E+04	3.066E+06	7.293E+05
39	75.252	3.645	-0.631	0.241	27111.7	9007.2	941.7	3284.6	1.450E+04	2.608E+06	6.062E+05
40	77.247	3.489	-0.901	0.241	27616.6	9162.5	938.1	3142.9	1.145E+04	2.186E+06	4.964E+05
41	79.277	3.336	-1.163	0.241	28068.7	9302.7	933.3	2970.9	8.818E+03	1.794E+06	3.977E+05
42	81.309	3.187	-1.416	0.241	28456.6	9422.7	926.9	2841.4	6.627E+03	1.440E+06	3.117E+05
43	83.304	3.045	-1.661	0.241	28775.0	9522.0	918.3	2688.1	4.861E+03	1.129E+06	2.388E+05
44	85.272	2.907	-1.902	0.241	29022.7	9599.3	906.6	2531.9	3.458E+03	8.599E+05	1.777E+05
45	87.240	2.769	-2.146	0.241	29179.3	9647.0	890.2	2395.7	2.351E+03	6.276E+05	1.268E+05
46	89.262	2.624	-2.395	0.241	29155.7	9635.7	866.7	2262.9	1.483E+03	4.278E+05	8.435E+04
47	91.285	2.462	-2.640	0.241	28785.2	9511.7	832.5	2093.0	8.556E+02	2.673E+05	5.144E+04
48	93.258	2.265	-2.874	0.241	27776.4	9177.9	780.2	1892.5	4.402E+02	1.486E+05	2.793E+04
49	95.254	2.009	-3.096	0.241	25726.5	8501.4	694.2	1641.2	1.807E+02	6.545E+04	1.204E+04
50	97.271	1.614	-3.281	0.241	21305.3	7042.8	542.2	1257.7	4.587E+01	1.719E+04	3.122E+03
51	99.017	0.917	-3.394	0.241	12315.3	4068.2	299.3	759.1	3.403E+00	1.140E+03	2.127E+02

UPS									
Span Section [m]	Flap Bend. Stiffness, Elyy LCS [N.m2]	Edge Bend. Stiffness, Elxx LCS [N.m2]	Bend. Stiffness, Elxy LCS [N.m2]	Flap Strain, ϵ_{zx} LCS [μ]	Edge Strain, ϵ_{yx} LCS [μ]	EA stiffness (N)	Cross Section Area [m2]	Mass Distr. [kg/m]	Torsional Stiffness, GJT [N.m2]
0.000	9.121E+10	1.089E+11	0.000E+00	1328	662	2.265E+10	1.796	1515.1	4.434E+10
2.328	9.122E+10	1.083E+11	0.000E+00	1296	642	2.265E+10	1.792	1513.0	4.409E+10
4.323	9.179E+10	1.068E+11	0.000E+00	1219	610	2.284E+10	1.826	1519.4	4.334E+10
6.318	8.753E+10	1.013E+11	0.000E+00	1197	605	2.229E+10	1.809	1478.7	4.043E+10
8.312	7.917E+10	9.211E+10	0.000E+00	1206	644	2.123E+10	1.855	1403.1	3.466E+10
10.309	6.860E+10	8.298E+10	5.356E+09	1262	707	2.012E+10	1.837	1322.7	2.863E+10
12.302	5.611E+10	7.164E+10	6.156E+09	1381	830	1.870E+10	1.841	1229.4	2.161E+10
14.296	4.383E+10	6.253E+10	5.882E+09	1563	965	1.745E+10	1.802	1144.6	1.547E+10
16.292	3.457E+10	5.646E+10	5.384E+09	1731	1089	1.668E+10	1.787	1093.6	1.129E+10
17.956	2.887E+10	5.360E+10	4.786E+09	1862	1153	1.623E+10	1.731	1064.2	9.095E+09
20.444	2.209E+10	4.663E+10	3.756E+09	2061	1312	1.469E+10	1.703	974.5	6.058E+09
22.447	1.873E+10	4.309E+10	3.056E+09	2145	1373	1.382E+10	1.638	923.7	4.976E+09
24.442	1.591E+10	3.892E+10	2.507E+09	2246	1444	1.288E+10	1.584	866.7	3.898E+09
26.437	1.369E+10	3.503E+10	2.086E+09	2331	1501	1.210E+10	1.542	820.6	3.120E+09
28.432	1.190E+10	3.178E+10	1.757E+09	2409	1532	1.150E+10	1.494	783.4	2.559E+09
30.428	1.004E+10	3.174E+10	1.579E+09	2561	1418	1.090E+10	1.419	742.2	2.078E+09
32.423	8.867E+09	2.978E+10	1.422E+09	2611	1384	1.069E+10	1.379	725.7	1.815E+09
34.418	7.849E+09	2.780E+10	1.281E+09	2650	1354	1.047E+10	1.336	707.0	1.589E+09
36.414	6.966E+09	2.524E+10	1.137E+09	2687	1353	1.022E+10	1.254	683.7	1.400E+09
38.409	6.179E+09	2.267E+10	9.840E+08	2721	1362	9.911E+09	1.211	660.0	1.211E+09
40.405	5.487E+09	2.076E+10	8.508E+08	2749	1339	9.666E+09	1.114	635.3	1.080E+09
42.400	4.841E+09	1.912E+10	7.335E+08	2789	1304	9.396E+09	1.074	615.2	9.481E+08
44.396	4.263E+09	1.734E+10	6.223E+08	2825	1282	9.104E+09	1.032	593.3	8.257E+08
46.290	3.769E+09	1.567E+10	5.304E+08	2864	1268	8.821E+09	0.983	572.0	7.262E+08
48.286	3.308E+09	1.408E+10	4.411E+08	2901	1251	8.507E+09	0.930	548.4	6.405E+08
50.281	2.895E+09	1.270E+10	3.673E+08	2939	1222	8.209E+09	0.883	527.2	5.652E+08
52.276	2.523E+09	1.093E+10	2.949E+08	2979	1244	7.815E+09	0.810	497.2	4.872E+08
54.272	2.202E+09	9.799E+09	2.427E+08	3006	1211	7.499E+09	0.780	476.7	4.280E+08
56.267	1.928E+09	8.714E+09	1.971E+08	3014	1182	7.202E+09	0.701	452.5	3.800E+08
58.262	1.678E+09	7.644E+09	1.586E+08	3031	1164	6.843E+09	0.672	429.4	3.248E+08
60.358	1.455E+09	6.505E+09	1.239E+08	3024	1165	6.490E+09	0.598	403.3	2.859E+08
62.354	1.267E+09	5.746E+09	9.995E+07	3005	1122	6.180E+09	0.562	382.9	2.515E+08
64.349	1.106E+09	4.952E+09	7.812E+07	2968	1101	5.850E+09	0.511	360.1	2.195E+08
66.344	9.570E+08	4.227E+09	6.133E+07	2941	1084	5.488E+09	0.461	335.9	1.908E+08
68.340	8.281E+08	3.663E+09	4.915E+07	2893	1042	5.158E+09	0.439	316.7	1.678E+08
70.335	7.160E+08	3.096E+09	3.751E+07	2821	1015	4.809E+09	0.383	293.0	1.461E+08
72.259	6.157E+08	2.679E+09	3.023E+07	2761	965	4.479E+09	0.354	273.3	1.286E+08
74.254	5.222E+08	2.238E+09	2.362E+07	2694	934	4.113E+09	0.313	250.4	1.113E+08
76.249	4.391E+08	1.902E+09	1.826E+07	2613	875	3.761E+09	0.294	230.3	9.503E+07

78.244	3.678E+08	1.606E+09	1.465E+07	2508	814	3.427E+09	0.276	211.9	8.220E+07
80.311	3.030E+08	1.315E+09	1.085E+07	2378	758	3.073E+09	0.238	189.9	6.956E+07
82.307	2.498E+08	1.107E+09	8.884E+06	2215	676	2.771E+09	0.215	173.0	6.014E+07
84.302	2.028E+08	8.974E+08	6.645E+06	2040	608	2.449E+09	0.182	153.7	5.176E+07
86.242	1.610E+08	7.507E+08	5.407E+06	1877	519	2.131E+09	0.160	134.9	4.209E+07
88.237	1.263E+08	5.932E+08	3.998E+06	1664	447	1.823E+09	0.146	118.3	3.476E+07
90.288	9.678E+07	4.976E+08	3.618E+06	1394	333	1.559E+09	0.119	102.7	2.951E+07
92.283	7.018E+07	3.770E+08	2.571E+06	1127	252	1.256E+09	0.104	85.2	2.268E+07
94.234	4.680E+07	2.801E+08	2.047E+06	875	172	9.735E+08	0.084	68.1	1.668E+07
96.274	2.663E+07	2.029E+08	1.618E+06	592	89	6.937E+08	0.063	50.9	1.062E+07
98.270	9.442E+06	9.736E+07	8.147E+05	307	34	3.866E+08	0.044	31.7	4.359E+06
99.766	6.293E+06	8.884E+07	3.270E+05	10	1	2.231E+08	0.033	20.0	1.250E+06

LSO											
Sect. No.	Span Section [m]	Chord [m]	Aero Twist [°]	Rel. Thick. [-]	Norm. Force GCS, Fn [N/m]	Norm. Force + mg LCS, Fn' [N/m]	Tang. Force GCS, Ft [N/m]	Tang. Force + mg LCS, Ft' [N/m]	Centrifugal Force (N)	Flap Bend. Moment, My LCS [N.m]	Edge Bend. Moment, Mx LCS [N.m]
1	0.000	5.380	22.249	0.999	739.0	4974.8	-58.7	10527.9	8.422E+05	2.920E+07	1.430E+07
2	1.007	5.380	22.249	0.998	762.6	4954.9	-85.2	10464.1	8.133E+05	2.865E+07	1.385E+07
3	2.879	5.380	22.249	0.979	825.9	4965.1	-103.6	10435.2	7.617E+05	2.765E+07	1.305E+07
4	4.606	5.382	22.246	0.950	911.4	4911.0	-110.0	10245.9	7.164E+05	2.674E+07	1.234E+07
5	6.334	5.425	22.187	0.896	1042.6	4793.6	-93.3	9903.3	6.734E+05	2.585E+07	1.166E+07
6	7.917	5.489	21.992	0.836	1156.3	4599.5	-75.9	9462.6	6.359E+05	2.504E+07	1.107E+07
7	9.634	5.602	21.500	0.761	1271.2	4329.6	-38.1	8968.3	5.972E+05	2.418E+07	1.045E+07
8	11.505	5.734	20.513	0.684	1403.0	3980.1	29.2	8453.1	5.574E+05	2.326E+07	9.811E+06
9	13.234	5.868	19.361	0.610	1489.8	3651.6	104.1	8044.6	5.225E+05	2.242E+07	9.245E+06
10	14.961	5.987	17.703	0.547	2733.0	3769.9	381.0	7901.1	4.894E+05	2.159E+07	8.704E+06
11	16.768	6.091	16.080	0.490	4890.2	4257.7	771.5	7872.8	4.566E+05	2.073E+07	8.164E+06
12	18.568	6.157	14.632	0.448	6708.4	4568.9	998.0	7570.4	4.256E+05	1.989E+07	7.651E+06
13	20.295	6.190	13.519	0.415	7634.4	4614.9	1049.4	7198.4	3.975E+05	1.910E+07	7.182E+06
14	22.023	6.177	12.506	0.385	8615.6	4680.5	1069.9	6715.0	3.708E+05	1.833E+07	6.736E+06
15	25.876	6.091	12.055	0.372	9369.5	4711.2	1044.2	6043.1	3.159E+05	1.664E+07	5.814E+06
16	29.864	5.996	11.309	0.350	10051.4	4740.7	1032.7	5569.4	2.655E+05	1.497E+07	4.960E+06
17	31.860	5.911	10.786	0.336	10397.7	4767.7	1018.1	5432.3	2.425E+05	1.417E+07	4.567E+06
18	33.855	5.815	10.271	0.322	10736.9	4791.4	1003.9	5274.9	2.210E+05	1.338E+07	4.197E+06
19	35.850	5.708	9.779	0.312	11088.7	4819.8	991.0	5092.6	2.008E+05	1.261E+07	3.848E+06
20	37.846	5.591	9.302	0.302	11434.9	4850.7	978.5	4908.4	1.820E+05	1.186E+07	3.519E+06
21	39.842	5.467	8.853	0.294	11865.0	4915.8	971.8	4723.1	1.644E+05	1.113E+07	3.210E+06
22	41.837	5.335	8.398	0.287	12337.6	5003.2	967.9	4567.5	1.480E+05	1.042E+07	2.921E+06
23	43.832	5.199	7.945	0.280	12830.9	5098.9	965.8	4404.7	1.328E+05	9.726E+06	2.650E+06
24	45.777	5.061	7.474	0.274	13376.5	5213.8	967.0	4245.0	1.190E+05	9.072E+06	2.403E+06
25	47.723	4.917	7.085	0.268	13831.4	5305.9	963.0	4073.3	1.063E+05	8.436E+06	2.172E+06
26	49.718	4.769	6.733	0.263	14250.7	5392.2	957.1	3906.9	9.433E+04	7.805E+06	1.952E+06
27	51.713	4.619	6.378	0.258	14686.3	5479.4	952.3	3696.2	8.330E+04	7.196E+06	1.748E+06
28	53.709	4.469	6.018	0.255	15148.2	5585.9	948.9	3545.4	7.321E+04	6.608E+06	1.559E+06
29	55.704	4.319	5.656	0.251	15629.6	5698.3	946.6	3375.5	6.401E+04	6.042E+06	1.384E+06
30	57.699	4.169	5.289	0.248	16135.1	5821.4	945.2	3212.3	5.565E+04	5.499E+06	1.223E+06
31	59.744	4.018	4.921	0.246	16660.7	5952.5	944.2	3041.7	4.791E+04	4.965E+06	1.071E+06
32	61.790	3.871	4.562	0.244	17187.7	6090.5	943.6	2903.7	4.095E+04	4.457E+06	9.331E+05
33	63.786	3.728	4.213	0.243	17713.6	6229.1	943.1	2753.5	3.487E+04	3.985E+06	8.101E+05
34	65.781	3.587	3.877	0.242	18226.2	6365.4	941.9	2598.5	2.946E+04	3.537E+06	6.984E+05
35	67.776	3.450	3.549	0.241	18728.0	6503.4	940.2	2474.6	2.466E+04	3.115E+06	5.974E+05
36	69.772	3.315	3.235	0.241	19206.7	6633.6	937.7	2326.6	2.043E+04	2.718E+06	5.064E+05
37	71.731	3.183	2.937	0.241	19645.4	6754.6	933.9	2198.9	1.680E+04	2.354E+06	4.264E+05
38	73.691	3.051	2.649	0.241	20043.0	6862.6	928.4	2056.7	1.364E+04	2.016E+06	3.551E+05
39	75.686	2.918	2.369	0.241	20389.0	6956.5	921.0	1931.2	1.088E+04	1.698E+06	2.909E+05
40	77.681	2.782	2.099	0.241	20665.1	7029.2	911.1	1814.2	8.525E+03	1.408E+06	2.346E+05
41	79.712	2.642	1.837	0.241	20850.1	7071.9	897.9	1677.9	6.517E+03	1.141E+06	1.850E+05
42	81.743	2.498	1.584	0.241	20920.9	7079.6	881.2	1567.5	4.861E+03	9.031E+05	1.425E+05

43	83.739	2.350	1.339	0.241	20853.2	7041.5	860.2	1441.6	3.541E+03	6.979E+05	1.073E+05
44	85.706	2.193	1.098	0.241	20614.1	6947.6	833.8	1314.6	2.504E+03	5.231E+05	7.851E+04
45	87.674	2.021	0.854	0.241	20146.9	6779.3	799.6	1199.7	1.695E+03	3.754E+05	5.503E+04
46	89.697	1.832	0.605	0.241	19372.5	6509.6	755.0	1086.4	1.068E+03	2.512E+05	3.596E+04
47	91.719	1.625	0.360	0.241	18218.4	6113.9	698.0	958.2	6.184E+02	1.542E+05	2.157E+04
48	93.692	1.396	0.126	0.241	16561.8	5551.8	624.2	819.8	3.215E+02	8.455E+04	1.157E+04
49	95.688	1.137	-0.096	0.241	14218.3	4762.0	526.1	673.1	1.349E+02	3.715E+04	4.967E+03
50	97.705	0.862	-0.281	0.241	11186.6	3743.7	401.3	498.4	3.550E+01	1.010E+04	1.314E+03
51	99.451	0.662	-0.394	0.241	8267.0	2765.3	266.8	349.2	2.779E+00	7.747E+02	9.784E+01

LSO										
Span Section [m]	Flap Bend. Stiffness, E _{ly} LCS [N.m ²]	Edge Bend. Stiffness, E _{lx} LCS [N.m ²]	Bend. Stiffness, E _{ly} LCS [N.m ²]	Flap Strain, ε _{zx} LCS [μ]	Edge Strain, ε _{yx} LCS [μ]	EA stiffness (N)	Cross Section Area [m ²]	Mass Distr. [kg/m]	Torsional Stiffness, GJT [N.m ²]	
0.000	6.130E+10	6.253E+10	0.000E+00	1328	662	1.785E+10	1.416	1194.1	2.766E+10	
2.336	6.077E+10	6.165E+10	0.000E+00	1296	642	1.778E+10	1.406	1187.5	2.728E+10	
4.340	6.055E+10	6.063E+10	0.000E+00	1219	610	1.787E+10	1.428	1188.5	2.667E+10	
6.344	5.654E+10	5.816E+10	0.000E+00	1197	605	1.739E+10	1.411	1153.9	2.478E+10	
8.347	5.040E+10	5.364E+10	0.000E+00	1206	644	1.655E+10	1.447	1093.9	2.124E+10	
10.352	4.270E+10	4.969E+10	3.226E+09	1262	707	1.562E+10	1.426	1026.6	1.739E+10	
12.354	3.401E+10	4.338E+10	3.666E+09	1381	830	1.444E+10	1.420	948.8	1.295E+10	
14.357	2.586E+10	3.825E+10	3.473E+09	1563	965	1.341E+10	1.384	879.6	9.129E+09	
16.362	2.015E+10	3.415E+10	3.165E+09	1731	1089	1.279E+10	1.370	838.5	6.609E+09	
18.034	1.654E+10	3.195E+10	2.792E+09	1862	1153	1.240E+10	1.323	812.9	5.250E+09	
20.531	1.263E+10	2.665E+10	2.148E+09	2061	1312	1.111E+10	1.288	736.9	3.464E+09	
22.542	1.098E+10	2.416E+10	1.752E+09	2145	1373	1.047E+10	1.240	699.4	2.898E+09	
24.546	9.653E+09	2.168E+10	1.457E+09	2246	1444	9.818E+09	1.208	660.8	2.339E+09	
26.550	8.628E+09	1.919E+10	1.218E+09	2331	1501	9.250E+09	1.178	627.1	1.913E+09	
28.553	7.617E+09	1.709E+10	1.018E+09	2409	1532	8.751E+09	1.138	596.3	1.572E+09	
30.558	6.328E+09	1.642E+10	8.976E+08	2561	1418	8.218E+09	1.070	559.6	1.274E+09	
32.562	5.538E+09	1.519E+10	8.022E+08	2611	1384	8.030E+09	1.036	545.2	1.112E+09	
34.565	4.865E+09	1.402E+10	7.161E+08	2650	1354	7.826E+09	0.999	528.6	9.669E+08	
36.570	4.288E+09	1.261E+10	6.306E+08	2687	1353	7.607E+09	0.934	509.1	8.465E+08	
38.574	3.778E+09	1.121E+10	5.410E+08	2721	1362	7.349E+09	0.898	489.4	7.280E+08	
40.579	3.333E+09	1.016E+10	4.639E+08	2749	1339	7.137E+09	0.822	469.1	6.454E+08	
42.582	2.921E+09	9.261E+09	3.965E+08	2789	1304	6.909E+09	0.789	452.4	5.629E+08	
44.587	2.554E+09	8.307E+09	3.335E+08	2825	1282	6.664E+09	0.756	434.3	4.871E+08	
46.490	2.244E+09	7.427E+09	2.817E+08	2864	1268	6.429E+09	0.717	416.9	4.257E+08	
48.495	1.955E+09	6.595E+09	2.321E+08	2901	1251	6.171E+09	0.675	397.8	3.728E+08	
50.499	1.699E+09	5.881E+09	1.915E+08	2939	1222	5.928E+09	0.637	380.6	3.267E+08	
52.502	1.470E+09	5.003E+09	1.523E+08	2979	1244	5.616E+09	0.582	357.3	2.797E+08	
54.507	1.274E+09	4.431E+09	1.241E+08	3006	1211	5.363E+09	0.558	340.9	2.440E+08	
56.511	1.107E+09	3.893E+09	9.982E+07	3014	1182	5.126E+09	0.499	322.1	2.150E+08	
58.514	9.569E+08	3.374E+09	7.956E+07	3031	1164	4.847E+09	0.476	304.1	1.825E+08	
60.618	8.236E+08	2.834E+09	6.154E+07	3024	1165	4.573E+09	0.422	284.2	1.594E+08	
62.623	7.122E+08	2.472E+09	4.915E+07	3005	1122	4.334E+09	0.394	268.5	1.392E+08	
64.627	6.168E+08	2.104E+09	3.803E+07	2968	1101	4.082E+09	0.357	251.3	1.206E+08	
66.630	5.297E+08	1.773E+09	2.955E+07	2941	1084	3.809E+09	0.320	233.2	1.040E+08	
68.635	4.548E+08	1.516E+09	2.343E+07	2893	1042	3.561E+09	0.303	218.7	9.067E+07	
70.639	3.899E+08	1.264E+09	1.769E+07	2821	1015	3.302E+09	0.263	201.2	7.827E+07	
72.572	3.323E+08	1.079E+09	1.409E+07	2761	965	3.058E+09	0.242	186.6	6.826E+07	
74.576	2.789E+08	8.869E+08	1.087E+07	2694	934	2.790E+09	0.213	169.8	5.843E+07	
76.579	2.316E+08	7.411E+08	8.278E+06	2613	875	2.532E+09	0.198	155.1	4.927E+07	
78.583	1.911E+08	6.141E+08	6.545E+06	2508	814	2.290E+09	0.184	141.6	4.216E+07	
80.658	1.544E+08	4.911E+08	4.757E+06	2378	758	2.035E+09	0.158	125.7	3.514E+07	
82.663	1.244E+08	4.023E+08	3.804E+06	2215	676	1.814E+09	0.140	113.2	2.976E+07	
84.667	9.793E+07	3.155E+08	2.762E+06	2040	608	1.579E+09	0.117	99.1	2.495E+07	
86.616	7.486E+07	2.538E+08	2.171E+06	1877	519	1.350E+09	0.102	85.5	1.968E+07	
88.619	5.588E+07	1.906E+08	1.538E+06	1664	447	1.131E+09	0.091	73.4	1.569E+07	

90.679	4.016E+07	1.501E+08	1.321E+06	1394	333	9.418E+08	0.072	62.1	1.271E+07
92.682	2.704E+07	1.057E+08	8.996E+05	1127	252	7.431E+08	0.061	50.4	9.356E+06
94.642	1.665E+07	7.260E+07	6.875E+05	875	172	5.642E+08	0.048	39.4	6.598E+06
96.691	8.640E+06	4.789E+07	5.500E+05	592	89	4.045E+08	0.037	29.7	4.242E+06
98.695	3.055E+06	2.259E+07	3.122E+05	307	34	2.393E+08	0.028	19.6	1.964E+06
100.200	3.088E+06	2.957E+07	1.624E+05	10	1	1.573E+08	0.023	14.1	6.796E+05

HLA											
Sect. No.	Span Section [m]	Chord [m]	Aero Twist [°]	Rel. Thick. [-]	Norm. Force GCS, Fn [N/m]	Norm. Force + mg LCS, Fn' [N/m]	Tang. Force GCS, Ft [N/m]	Tang. Force + mg LCS, Ft' [N/m]	Centrifugal Force (N)	Flap Bend. Moment, My LCS [N.m]	Edge Bend. Moment, Mx LCS [N.m]
1	0.000	5.251	14.500	0.999	608.9	3757.2	-64.7	12788.5	1.147E+06	3.876E+07	1.893E+07
2	1.164	5.252	14.500	0.998	641.2	3755.2	-96.2	12741.2	1.103E+06	3.801E+07	1.828E+07
3	3.325	5.252	14.500	0.979	723.8	3787.7	-126.1	12755.1	1.025E+06	3.663E+07	1.712E+07
4	5.321	5.254	14.498	0.950	842.0	3722.8	-145.6	12375.6	9.566E+05	3.536E+07	1.610E+07
5	7.316	5.295	14.458	0.896	1022.5	3600.0	-143.8	11739.5	8.923E+05	3.412E+07	1.514E+07
6	9.145	5.357	14.325	0.836	1197.2	3449.6	-137.9	11078.4	8.366E+05	3.299E+07	1.430E+07
7	11.129	5.468	13.989	0.761	1390.6	3233.2	-108.6	10283.5	7.794E+05	3.178E+07	1.343E+07
8	13.290	5.597	13.315	0.684	1615.0	3005.2	-41.9	9599.5	7.208E+05	3.047E+07	1.252E+07
9	15.287	5.728	12.529	0.610	1779.6	2838.9	41.3	9262.8	6.698E+05	2.928E+07	1.173E+07
10	17.282	5.844	11.398	0.547	3278.9	3115.0	290.9	9079.7	6.217E+05	2.810E+07	1.098E+07
11	19.370	5.946	10.290	0.490	6690.8	4013.2	745.4	8710.2	5.743E+05	2.687E+07	1.023E+07
12	21.449	6.010	9.302	0.448	8263.8	4309.9	823.5	8308.4	5.298E+05	2.567E+07	9.524E+06
13	23.444	6.042	8.542	0.415	9143.3	4407.1	835.1	7832.0	4.895E+05	2.453E+07	8.879E+06
14	25.439	6.053	7.935	0.388	9992.5	4541.5	841.8	7439.9	4.515E+05	2.341E+07	8.267E+06
15	27.434	6.029	7.466	0.368	10778.2	4691.6	845.2	7117.3	4.157E+05	2.231E+07	7.686E+06
16	29.430	5.997	7.035	0.350	11450.8	4809.7	847.1	6765.0	3.818E+05	2.123E+07	7.133E+06
17	31.425	5.931	6.678	0.336	12001.5	4930.1	847.5	6626.8	3.499E+05	2.016E+07	6.608E+06
18	33.420	5.861	6.326	0.322	12547.7	5048.7	847.3	6469.3	3.199E+05	1.912E+07	6.109E+06
19	35.416	5.768	5.991	0.312	13092.1	5165.8	846.5	6272.2	2.916E+05	1.809E+07	5.637E+06
20	37.412	5.669	5.665	0.302	13630.8	5284.2	845.2	6072.6	2.651E+05	1.709E+07	5.190E+06
21	39.407	5.558	5.359	0.294	14236.4	5428.1	844.5	5862.0	2.403E+05	1.610E+07	4.767E+06
22	41.402	5.440	5.048	0.287	14868.6	5587.2	844.1	5693.3	2.171E+05	1.514E+07	4.369E+06
23	43.398	5.318	4.739	0.280	15506.4	5748.9	843.7	5512.5	1.955E+05	1.420E+07	3.993E+06
24	45.343	5.191	4.417	0.274	16165.0	5918.1	843.7	5332.4	1.759E+05	1.330E+07	3.648E+06
25	47.288	5.060	4.085	0.268	16854.1	6097.9	843.8	5143.3	1.577E+05	1.243E+07	3.324E+06
26	49.284	4.922	3.733	0.263	17584.8	6293.6	844.0	4975.0	1.404E+05	1.156E+07	3.012E+06
27	51.279	4.781	3.378	0.258	18337.7	6492.9	844.3	4733.2	1.245E+05	1.071E+07	2.720E+06
28	53.274	4.638	3.018	0.255	19115.4	6709.0	844.6	4576.8	1.099E+05	9.888E+06	2.448E+06
29	55.270	4.493	2.656	0.251	19911.6	6931.2	844.7	4390.5	9.650E+04	9.092E+06	2.194E+06
30	57.265	4.346	2.289	0.248	20733.4	7164.6	844.5	4212.1	8.428E+04	8.323E+06	1.958E+06
31	59.310	4.197	1.921	0.246	21576.4	7406.6	844.0	4020.3	7.291E+04	7.564E+06	1.733E+06
32	61.356	4.050	1.562	0.244	22414.2	7652.2	843.3	3872.9	6.263E+04	6.835E+06	1.526E+06
33	63.351	3.905	1.213	0.243	23242.1	7896.4	842.3	3706.2	5.362E+04	6.155E+06	1.340E+06
34	65.346	3.763	0.877	0.242	24057.5	8139.1	840.9	3530.2	4.554E+04	5.506E+06	1.169E+06
35	67.342	3.621	0.549	0.241	24858.8	8381.2	839.4	3398.9	3.834E+04	4.888E+06	1.013E+06
36	69.337	3.483	0.235	0.241	25633.3	8616.1	837.8	3231.3	3.196E+04	4.304E+06	8.698E+05
37	71.297	3.347	-0.063	0.241	26371.3	8842.2	836.1	3092.7	2.644E+04	3.762E+06	7.424E+05
38	73.257	3.213	-0.351	0.241	27080.6	9060.7	834.5	2932.9	2.162E+04	3.255E+06	6.272E+05
39	75.252	3.080	-0.631	0.241	27753.4	9269.4	832.6	2796.6	1.736E+04	2.773E+06	5.217E+05
40	77.247	2.948	-0.901	0.241	28386.3	9466.7	830.5	2674.6	1.371E+04	2.328E+06	4.277E+05
41	79.277	2.819	-1.163	0.241	28973.2	9650.6	827.9	2526.6	1.056E+04	1.913E+06	3.431E+05
42	81.309	2.693	-1.416	0.241	29500.8	9816.3	824.5	2417.9	7.936E+03	1.538E+06	2.693E+05
43	83.304	2.573	-1.661	0.241	29962.0	9961.6	819.6	2289.0	5.822E+03	1.208E+06	2.067E+05
44	85.272	2.456	-1.902	0.241	30355.5	10085.7	812.5	2158.6	4.142E+03	9.216E+05	1.541E+05
45	87.240	2.340	-2.146	0.241	30661.9	10181.7	801.8	2047.5	2.816E+03	6.739E+05	1.101E+05
46	89.262	2.217	-2.395	0.241	30783.2	10216.9	785.0	1940.2	1.777E+03	4.601E+05	7.345E+04
47	91.285	2.081	-2.640	0.241	30551.2	10136.3	759.4	1802.1	1.025E+03	2.881E+05	4.491E+04
48	93.258	1.914	-2.874	0.241	29648.9	9834.6	718.2	1639.1	5.276E+02	1.604E+05	2.445E+04

49	95.254	1.698	-3.096	0.241	27612.5	9157.9	645.8	1431.4	2.166E+02	7.079E+04	1.057E+04
50	97.271	1.364	-3.281	0.241	22976.8	7621.0	510.4	1104.8	5.500E+01	1.863E+04	2.752E+03
51	99.017	0.775	-3.394	0.241	13334.6	4420.6	285.3	672.8	4.082E+00	1.238E+03	1.885E+02

HLA									
Span Section [m]	Flap Bend. Stiffness, E _{lyy} LCS [N.m ²]	Edge Bend. Stiffness, E _{lxx} LCS [N.m ²]	Bend. Stiffness, E _{lxy} LCS [N.m ²]	Flap Strain, ε _{zx} LCS [μ]	Edge Strain, ε _{yx} LCS [μ]	EA stiffness (N)	Cross Section Area [m ²]	Mass Distr. [kg/m]	Torsional Stiffness, GJT [N.m ²]
0.000	8.000E+10	8.197E+10	0.000E+00	1328	662	2.042E+10	1.619	1365.7	3.618E+10
2.328	8.001E+10	8.141E+10	0.000E+00	1296	642	2.042E+10	1.615	1363.6	3.597E+10
4.323	8.055E+10	8.021E+10	0.000E+00	1219	610	2.058E+10	1.645	1369.0	3.538E+10
6.318	7.682E+10	7.597E+10	0.000E+00	1197	605	2.007E+10	1.629	1331.9	3.306E+10
8.312	6.951E+10	6.888E+10	0.000E+00	1206	644	1.911E+10	1.670	1263.0	2.845E+10
10.309	6.023E+10	6.188E+10	4.333E+09	1262	707	1.810E+10	1.652	1189.8	2.361E+10
12.302	4.925E+10	5.325E+10	4.972E+09	1381	830	1.681E+10	1.654	1105.0	1.792E+10
14.296	3.845E+10	4.634E+10	4.743E+09	1563	965	1.567E+10	1.618	1027.9	1.290E+10
16.292	3.032E+10	4.174E+10	4.335E+09	1731	1089	1.497E+10	1.603	981.3	9.483E+09
17.956	2.531E+10	3.957E+10	3.850E+09	1862	1153	1.456E+10	1.553	954.5	7.676E+09
20.444	1.937E+10	3.434E+10	3.019E+09	2061	1312	1.317E+10	1.527	873.7	5.148E+09
22.447	1.643E+10	3.170E+10	2.454E+09	2145	1373	1.239E+10	1.468	827.9	4.247E+09
24.442	1.396E+10	2.860E+10	2.013E+09	2246	1444	1.154E+10	1.420	776.7	3.339E+09
26.437	1.202E+10	2.571E+10	1.674E+09	2331	1501	1.085E+10	1.382	735.3	2.680E+09
28.432	1.045E+10	2.330E+10	1.410E+09	2409	1532	1.030E+10	1.339	701.9	2.203E+09
30.428	8.821E+09	2.327E+10	1.267E+09	2561	1418	9.765E+09	1.271	665.0	1.793E+09
32.423	7.797E+09	2.182E+10	1.141E+09	2611	1384	9.577E+09	1.235	650.2	1.568E+09
34.418	6.905E+09	2.035E+10	1.028E+09	2650	1354	9.377E+09	1.197	633.3	1.375E+09
36.414	6.132E+09	1.846E+10	9.125E+08	2687	1353	9.151E+09	1.124	612.4	1.213E+09
38.409	5.442E+09	1.656E+10	7.894E+08	2721	1362	8.877E+09	1.085	591.2	1.051E+09
40.405	4.837E+09	1.516E+10	6.825E+08	2749	1339	8.658E+09	0.998	569.1	9.387E+08
42.400	4.270E+09	1.395E+10	5.884E+08	2789	1304	8.417E+09	0.962	551.1	8.249E+08
44.396	3.763E+09	1.264E+10	4.993E+08	2825	1282	8.156E+09	0.925	531.4	7.193E+08
46.290	3.330E+09	1.142E+10	4.256E+08	2864	1268	7.902E+09	0.881	512.4	6.334E+08
48.286	2.924E+09	1.025E+10	3.539E+08	2901	1251	7.621E+09	0.833	491.3	5.594E+08
50.281	2.562E+09	9.243E+09	2.948E+08	2939	1222	7.355E+09	0.791	472.3	4.942E+08
52.276	2.235E+09	7.953E+09	2.368E+08	2979	1244	7.002E+09	0.726	445.5	4.265E+08
54.272	1.953E+09	7.127E+09	1.949E+08	3006	1211	6.720E+09	0.699	427.2	3.752E+08
56.267	1.712E+09	6.335E+09	1.583E+08	3014	1182	6.455E+09	0.628	405.6	3.335E+08
58.262	1.491E+09	5.556E+09	1.273E+08	3031	1164	6.132E+09	0.603	384.7	2.849E+08
60.358	1.295E+09	4.727E+09	9.955E+07	3024	1165	5.817E+09	0.536	361.4	2.510E+08
62.354	1.129E+09	4.175E+09	8.033E+07	3005	1122	5.540E+09	0.504	343.3	2.211E+08
64.349	9.861E+08	3.598E+09	6.274E+07	2968	1101	5.243E+09	0.458	322.7	1.927E+08
66.344	8.544E+08	3.072E+09	4.928E+07	2941	1084	4.919E+09	0.413	301.1	1.677E+08
68.340	7.403E+08	2.662E+09	3.949E+07	2893	1042	4.623E+09	0.393	283.9	1.474E+08
70.335	6.409E+08	2.250E+09	3.013E+07	2821	1015	4.310E+09	0.344	262.7	1.283E+08
72.259	5.519E+08	1.949E+09	2.428E+07	2761	965	4.014E+09	0.318	244.9	1.128E+08
74.254	4.687E+08	1.628E+09	1.896E+07	2694	934	3.685E+09	0.281	224.3	9.748E+07
76.249	3.946E+08	1.385E+09	1.465E+07	2613	875	3.369E+09	0.263	206.3	8.311E+07
78.244	3.310E+08	1.171E+09	1.176E+07	2508	814	3.070E+09	0.247	189.8	7.190E+07
80.311	2.731E+08	9.601E+08	8.719E+06	2378	758	2.755E+09	0.214	170.2	6.088E+07
82.307	2.256E+08	8.089E+08	7.144E+06	2215	676	2.485E+09	0.192	155.2	5.266E+07
84.302	1.835E+08	6.569E+08	5.349E+06	2040	608	2.198E+09	0.163	137.9	4.535E+07
86.242	1.459E+08	5.505E+08	4.357E+06	1877	519	1.913E+09	0.144	121.1	3.691E+07
88.237	1.146E+08	4.359E+08	3.226E+06	1664	447	1.638E+09	0.131	106.3	3.050E+07
90.288	8.799E+07	3.665E+08	2.919E+06	1394	333	1.400E+09	0.107	92.2	2.591E+07
92.283	6.392E+07	2.784E+08	2.075E+06	1127	252	1.129E+09	0.093	76.6	1.993E+07
94.234	4.270E+07	2.074E+08	1.652E+06	875	172	8.748E+08	0.075	61.2	1.466E+07
96.274	2.435E+07	1.507E+08	1.307E+06	592	89	6.235E+08	0.056	45.8	9.341E+06
98.270	8.648E+06	7.260E+07	6.585E+05	307	34	3.476E+08	0.040	28.5	3.837E+06
99.766	5.780E+06	6.683E+07	2.649E+05	10	1	2.008E+08	0.029	18.0	1.104E+06

HRS											
Sect. No.	Span Section [m]	Chord [m]	Aero Twist [°]	Rel. Thick. [-]	Norm. Force GCS, Fn [N/m]	Norm. Force + mg LCS, Fn' [N/m]	Tang. Force GCS, Ft [N/m]	Tang. Force + mg LCS, Ft' [N/m]	Centrifugal Force (N)	Flap Bend. Moment, My LCS [N.m]	Edge Bend. Moment, Mx LCS [N.m]
1	0.000	4.557	14.500	0.999	534.1	3410.4	-62.9	11791.6	1.298E+06	3.893E+07	1.746E+07
2	1.164	4.557	14.500	0.998	567.5	3409.3	-94.4	11745.4	1.249E+06	3.819E+07	1.686E+07
3	3.325	4.557	14.500	0.979	649.9	3440.0	-126.3	11753.6	1.160E+06	3.682E+07	1.580E+07
4	5.321	4.559	14.498	0.950	762.3	3380.3	-152.3	11395.0	1.083E+06	3.557E+07	1.486E+07
5	7.316	4.595	14.458	0.896	923.9	3265.0	-157.8	10799.2	1.011E+06	3.434E+07	1.398E+07
6	9.145	4.649	14.325	0.836	1071.3	3121.5	-159.1	10180.5	9.476E+05	3.322E+07	1.320E+07
7	11.129	4.745	13.989	0.761	1247.4	2923.6	-129.1	9445.5	8.829E+05	3.201E+07	1.240E+07
8	13.290	4.857	13.315	0.684	1396.4	2694.7	-75.8	8807.0	8.167E+05	3.072E+07	1.157E+07
9	15.287	4.970	12.529	0.610	1471.8	2517.1	-2.2	8496.0	7.590E+05	2.953E+07	1.085E+07
10	17.282	5.071	11.398	0.547	3085.5	2855.9	262.8	8343.8	7.045E+05	2.836E+07	1.015E+07
11	19.370	5.160	10.290	0.490	6654.2	3825.7	687.5	7986.1	6.508E+05	2.714E+07	9.464E+06
12	21.449	5.216	9.302	0.448	7952.3	4048.3	739.0	7609.8	6.004E+05	2.594E+07	8.814E+06
13	23.444	5.244	8.542	0.415	8822.6	4160.3	750.2	7171.7	5.549E+05	2.480E+07	8.221E+06
14	25.439	5.252	7.935	0.388	9657.2	4303.4	756.9	6811.6	5.119E+05	2.369E+07	7.658E+06
15	27.434	5.232	7.466	0.368	10451.0	4466.6	760.5	6514.7	4.713E+05	2.259E+07	7.123E+06
16	29.430	5.204	7.035	0.350	11118.3	4593.0	761.5	6191.2	4.330E+05	2.150E+07	6.614E+06
17	31.425	5.147	6.678	0.336	11651.2	4713.0	760.1	6063.6	3.968E+05	2.044E+07	6.131E+06
18	33.420	5.086	6.326	0.322	12181.8	4832.2	758.4	5918.7	3.628E+05	1.939E+07	5.672E+06
19	35.416	5.006	5.991	0.312	12713.8	4951.0	756.3	5737.3	3.308E+05	1.836E+07	5.236E+06
20	37.412	4.920	5.665	0.302	13242.3	5071.7	754.0	5553.8	3.007E+05	1.735E+07	4.824E+06
21	39.407	4.823	5.359	0.294	13846.5	5220.7	752.9	5360.8	2.726E+05	1.636E+07	4.435E+06
22	41.402	4.721	5.048	0.287	14483.0	5386.2	752.4	5206.6	2.464E+05	1.539E+07	4.067E+06
23	43.398	4.615	4.739	0.280	15129.7	5555.8	752.1	5041.4	2.219E+05	1.445E+07	3.720E+06
24	45.343	4.505	4.417	0.274	15803.7	5735.1	752.3	4877.1	1.997E+05	1.354E+07	3.402E+06
25	47.288	4.391	4.085	0.268	16513.7	5926.7	752.7	4704.2	1.790E+05	1.266E+07	3.102E+06
26	49.284	4.271	3.733	0.263	17272.3	6136.3	753.4	4551.5	1.594E+05	1.178E+07	2.814E+06
27	51.279	4.149	3.378	0.258	18057.9	6351.6	754.2	4329.5	1.414E+05	1.093E+07	2.544E+06
28	53.274	4.025	3.018	0.255	18873.5	6584.6	754.9	4187.2	1.248E+05	1.009E+07	2.291E+06
29	55.270	3.899	2.656	0.251	19711.8	6825.2	755.3	4017.7	1.096E+05	9.287E+06	2.056E+06
30	57.265	3.772	2.289	0.248	20579.8	7078.0	755.5	3855.0	9.574E+04	8.507E+06	1.837E+06
31	59.310	3.642	1.921	0.246	21472.9	7340.7	755.2	3681.5	8.283E+04	7.737E+06	1.628E+06
32	61.356	3.515	1.562	0.244	22362.4	7606.9	754.5	3549.2	7.117E+04	6.997E+06	1.436E+06
33	63.351	3.389	1.213	0.243	23243.2	7872.0	753.5	3399.2	6.093E+04	6.305E+06	1.262E+06
34	65.346	3.265	0.877	0.242	24111.6	8135.5	751.9	3240.9	5.176E+04	5.644E+06	1.103E+06
35	67.342	3.143	0.549	0.241	24967.3	8398.3	750.2	3123.9	4.357E+04	5.014E+06	9.567E+05
36	69.337	3.022	0.235	0.241	25796.6	8654.0	748.2	2973.5	3.633E+04	4.418E+06	8.231E+05
37	71.297	2.905	-0.063	0.241	26589.3	8900.5	746.3	2850.1	3.006E+04	3.865E+06	7.037E+05
38	73.257	2.788	-0.351	0.241	27354.1	9139.5	744.5	2707.2	2.457E+04	3.346E+06	5.955E+05
39	75.252	2.673	-0.631	0.241	28087.5	9370.2	742.7	2586.6	1.973E+04	2.853E+06	4.963E+05
40	77.247	2.559	-0.901	0.241	28783.5	9590.1	741.0	2479.4	1.558E+04	2.397E+06	4.077E+05
41	79.277	2.446	-1.163	0.241	29435.1	9797.0	739.1	2348.6	1.200E+04	1.972E+06	3.278E+05
42	81.309	2.337	-1.416	0.241	30027.2	9985.4	736.6	2254.3	9.015E+03	1.587E+06	2.578E+05
43	83.304	2.233	-1.661	0.241	30555.6	10154.1	733.2	2141.6	6.611E+03	1.248E+06	1.984E+05
44	85.272	2.132	-1.902	0.241	31019.9	10302.9	728.2	2027.9	4.702E+03	9.527E+05	1.483E+05
45	87.240	2.030	-2.146	0.241	31403.7	10425.4	720.4	1929.4	3.196E+03	6.974E+05	1.063E+05
46	89.262	1.924	-2.395	0.241	31613.1	10490.7	708.0	1836.5	2.017E+03	4.767E+05	7.114E+04
47	91.285	1.806	-2.640	0.241	31467.3	10439.3	688.2	1718.2	1.164E+03	2.989E+05	4.365E+04
48	93.258	1.661	-2.874	0.241	30630.6	10159.8	654.7	1575.9	5.989E+02	1.666E+05	2.386E+04
49	95.254	1.474	-3.096	0.241	28623.6	9493.2	592.9	1389.7	2.460E+02	7.364E+04	1.036E+04
50	97.271	1.183	-3.281	0.241	23911.0	7930.8	472.4	1084.9	6.247E+01	1.941E+04	2.706E+03
51	99.017	0.672	-3.394	0.241	13921.9	4615.4	266.2	662.8	4.639E+00	1.293E+03	1.857E+02

HRS									
Span Section [m]	Flap Bend. Stiffness, Elyy LCS [N.m2]	Edge Bend. Stiffness, Elxx LCS [N.m2]	Bend. Stiffness, Elxy LCS [N.m2]	Flap Strain, ϵ_{zx} LCS [μ]	Edge Strain, ϵ_{yx} LCS [μ]	EA stiffness (N)	Cross Section Area [m2]	Mass Distr. [kg/m]	Torsional Stiffness, GJT [N.m2]
0.000	7.044E+10	6.704E+10	0.000E+00	1328	662	1.881E+10	1.491	1258.0	3.070E+10
2.328	7.046E+10	6.657E+10	0.000E+00	1296	642	1.881E+10	1.488	1256.1	3.053E+10
4.323	7.097E+10	6.557E+10	0.000E+00	1219	610	1.896E+10	1.515	1261.1	3.004E+10
6.318	6.770E+10	6.207E+10	0.000E+00	1197	605	1.849E+10	1.501	1226.9	2.810E+10
8.312	6.128E+10	5.619E+10	0.000E+00	1206	644	1.760E+10	1.538	1163.1	2.422E+10
10.309	5.310E+10	5.040E+10	0.000E+00	1262	707	1.666E+10	1.521	1095.2	2.014E+10
12.302	4.341E+10	4.328E+10	0.000E+00	1381	830	1.547E+10	1.522	1016.5	1.533E+10
14.296	3.388E+10	3.760E+10	4.010E+09	1563	965	1.440E+10	1.488	945.1	1.107E+10
16.292	2.670E+10	3.382E+10	3.662E+09	1731	1089	1.376E+10	1.474	901.9	8.161E+09
17.956	2.229E+10	3.204E+10	3.251E+09	1862	1153	1.338E+10	1.427	877.1	6.622E+09
20.444	1.706E+10	2.779E+10	2.548E+09	2061	1312	1.210E+10	1.403	802.8	4.458E+09
22.447	1.448E+10	2.565E+10	2.072E+09	2145	1373	1.138E+10	1.349	760.7	3.687E+09
24.442	1.231E+10	2.314E+10	1.700E+09	2246	1444	1.060E+10	1.305	713.7	2.904E+09
26.437	1.060E+10	2.081E+10	1.414E+09	2331	1501	9.967E+09	1.270	675.8	2.336E+09
28.432	9.217E+09	1.886E+10	1.192E+09	2409	1532	9.467E+09	1.231	645.1	1.922E+09
30.428	7.782E+09	1.885E+10	1.071E+09	2561	1418	8.978E+09	1.169	611.4	1.566E+09
32.423	6.880E+09	1.768E+10	9.647E+08	2611	1384	8.806E+09	1.136	597.9	1.371E+09
34.418	6.095E+09	1.649E+10	8.694E+08	2650	1354	8.624E+09	1.101	582.5	1.204E+09
36.414	5.415E+09	1.497E+10	7.720E+08	2687	1353	8.417E+09	1.034	563.3	1.063E+09
38.409	4.808E+09	1.343E+10	6.682E+08	2721	1362	8.167E+09	0.998	543.9	9.216E+08
40.405	4.275E+09	1.230E+10	5.779E+08	2749	1339	7.967E+09	0.918	523.6	8.237E+08
42.400	3.776E+09	1.132E+10	4.985E+08	2789	1304	7.747E+09	0.885	507.2	7.243E+08
44.396	3.329E+09	1.027E+10	4.232E+08	2825	1282	7.508E+09	0.851	489.3	6.321E+08
46.290	2.947E+09	9.278E+09	3.609E+08	2864	1268	7.276E+09	0.811	471.8	5.570E+08
48.286	2.590E+09	8.337E+09	3.003E+08	2901	1251	7.019E+09	0.767	452.5	4.921E+08
50.281	2.270E+09	7.520E+09	2.503E+08	2939	1222	6.777E+09	0.729	435.1	4.350E+08
52.276	1.981E+09	6.475E+09	2.010E+08	2979	1244	6.451E+09	0.669	410.5	3.752E+08
54.272	1.732E+09	5.807E+09	1.655E+08	3006	1211	6.192E+09	0.644	393.6	3.300E+08
56.267	1.519E+09	5.167E+09	1.344E+08	3014	1182	5.948E+09	0.579	373.8	2.933E+08
58.262	1.324E+09	4.536E+09	1.081E+08	3031	1164	5.650E+09	0.555	354.5	2.503E+08
60.358	1.150E+09	3.863E+09	8.458E+07	3024	1165	5.362E+09	0.494	333.1	2.206E+08
62.354	1.004E+09	3.416E+09	6.829E+07	3005	1122	5.108E+09	0.464	316.5	1.944E+08
64.349	8.773E+08	2.947E+09	5.337E+07	2968	1101	4.836E+09	0.422	297.7	1.695E+08
66.344	7.606E+08	2.519E+09	4.195E+07	2941	1084	4.539E+09	0.381	277.8	1.475E+08
68.340	6.594E+08	2.186E+09	3.364E+07	2893	1042	4.267E+09	0.363	262.0	1.297E+08
70.335	5.713E+08	1.851E+09	2.570E+07	2821	1015	3.980E+09	0.317	242.5	1.129E+08
72.259	4.923E+08	1.605E+09	2.072E+07	2761	965	3.708E+09	0.294	226.3	9.935E+07
74.254	4.184E+08	1.344E+09	1.620E+07	2694	934	3.406E+09	0.259	207.4	8.587E+07
76.249	3.526E+08	1.145E+09	1.253E+07	2613	875	3.115E+09	0.244	190.8	7.323E+07
78.244	2.960E+08	9.700E+08	1.007E+07	2508	814	2.841E+09	0.229	175.6	6.338E+07
80.311	2.444E+08	7.969E+08	7.474E+06	2378	758	2.550E+09	0.198	157.6	5.369E+07
82.307	2.021E+08	6.729E+08	6.132E+06	2215	676	2.303E+09	0.178	143.7	4.645E+07
84.302	1.645E+08	5.478E+08	4.597E+06	2040	608	2.037E+09	0.151	127.9	4.003E+07
86.242	1.309E+08	4.603E+08	3.750E+06	1877	519	1.774E+09	0.134	112.3	3.259E+07
88.237	1.030E+08	3.654E+08	2.761E+06	1664	447	1.515E+09	0.121	98.3	2.692E+07
90.288	7.913E+07	3.083E+08	2.485E+06	1394	333	1.292E+09	0.098	85.1	2.286E+07
92.283	5.756E+07	2.350E+08	1.767E+06	1127	252	1.042E+09	0.086	70.7	1.759E+07
94.234	3.850E+07	1.757E+08	1.408E+06	875	172	8.076E+08	0.069	56.5	1.295E+07
96.274	2.198E+07	1.283E+08	1.115E+06	592	89	5.759E+08	0.052	42.3	8.253E+06
98.270	7.821E+06	6.200E+07	5.622E+05	307	34	3.212E+08	0.037	26.3	3.393E+06
99.766	5.239E+06	5.737E+07	2.267E+05	10	1	1.858E+08	0.027	16.6	9.773E+05

UPK											
Sect. No.	Span Section [m]	Chord [m]	Aero Twist [°]	Rel. Thick. [-]	Norm. Force GCS, Fn [N/m]	Norm. Force + mg LCS, Fn' [N/m]	Tang. Force GCS, Ft [N/m]	Tang. Force + mg LCS, Ft' [N/m]	Centrifugal Force (N)	Flap Bend. Moment, My LCS [N.m]	Edge Bend. Moment, Mx LCS [N.m]
1	0.000	6.215	17.928	0.999	858.8	4827.1	-75.3	12140.2	8.835E+05	3.137E+07	1.594E+07
2	1.164	6.215	17.928	0.998	891.5	4816.7	-110.1	12081.1	8.489E+05	3.070E+07	1.535E+07
3	3.325	6.215	17.928	0.979	978.8	4843.9	-137.9	12070.7	7.875E+05	2.948E+07	1.432E+07
4	5.321	6.217	17.926	0.950	1102.0	4746.1	-150.3	11691.6	7.341E+05	2.837E+07	1.341E+07
5	7.316	6.266	17.886	0.896	1290.2	4575.5	-134.8	11077.7	6.837E+05	2.728E+07	1.255E+07
6	9.145	6.340	17.753	0.836	1466.1	4375.3	-115.7	10446.3	6.401E+05	2.630E+07	1.180E+07
7	11.129	6.471	17.417	0.761	1644.3	4095.7	-73.5	9695.0	5.955E+05	2.525E+07	1.103E+07
8	13.290	6.623	16.743	0.684	1833.0	3808.7	7.2	9056.5	5.499E+05	2.413E+07	1.023E+07
9	15.287	6.778	15.957	0.610	1949.4	3605.8	102.8	8751.1	5.102E+05	2.310E+07	9.539E+06
10	17.282	6.916	14.826	0.547	3549.8	3925.4	435.2	8609.6	4.728E+05	2.210E+07	8.880E+06
11	19.370	7.036	13.718	0.490	6941.1	4817.0	999.2	8276.3	4.361E+05	2.106E+07	8.227E+06
12	21.449	7.113	12.730	0.448	8505.9	5087.4	1120.7	7892.8	4.016E+05	2.005E+07	7.613E+06
13	23.444	7.151	11.970	0.415	9310.6	5122.1	1141.3	7428.0	3.706E+05	1.909E+07	7.056E+06
14	25.439	7.163	11.363	0.388	10057.6	5190.6	1153.8	7040.4	3.413E+05	1.816E+07	6.531E+06
15	27.434	7.135	10.894	0.368	10710.1	5269.0	1158.0	6715.7	3.138E+05	1.725E+07	6.034E+06
16	29.430	7.097	10.463	0.350	11196.5	5293.9	1151.4	6360.5	2.878E+05	1.636E+07	5.564E+06
17	31.425	7.019	10.106	0.336	11509.7	5318.9	1134.3	6204.6	2.633E+05	1.549E+07	5.120E+06
18	33.420	6.936	9.754	0.322	11799.4	5334.7	1116.0	6030.9	2.404E+05	1.464E+07	4.702E+06
19	35.416	6.826	9.419	0.312	12070.0	5340.5	1096.9	5820.4	2.188E+05	1.381E+07	4.308E+06
20	37.412	6.709	9.093	0.302	12317.2	5341.7	1077.0	5607.8	1.986E+05	1.301E+07	3.937E+06
21	39.407	6.577	8.787	0.294	12628.8	5367.6	1061.5	5386.3	1.797E+05	1.222E+07	3.589E+06
22	41.402	6.438	8.476	0.287	12957.9	5409.2	1047.9	5204.6	1.621E+05	1.146E+07	3.263E+06
23	43.398	6.294	8.167	0.280	13287.1	5451.0	1035.3	5012.2	1.458E+05	1.071E+07	2.958E+06
24	45.343	6.143	7.845	0.274	13637.9	5501.2	1024.9	4821.6	1.310E+05	1.001E+07	2.680E+06
25	47.288	5.989	7.513	0.268	14011.0	5558.8	1016.0	4622.7	1.173E+05	9.329E+06	2.421E+06
26	49.284	5.824	7.161	0.263	14423.5	5633.4	1009.1	4443.0	1.043E+05	8.651E+06	2.174E+06
27	51.279	5.658	6.806	0.258	14857.9	5706.3	1003.7	4196.0	9.230E+04	7.995E+06	1.945E+06
28	53.274	5.489	6.446	0.255	15320.2	5803.6	1000.0	4027.6	8.134E+04	7.362E+06	1.733E+06
29	55.270	5.318	6.084	0.251	15804.6	5906.3	997.4	3832.0	7.132E+04	6.752E+06	1.538E+06
30	57.265	5.143	5.717	0.248	16315.5	6021.3	995.8	3644.9	6.221E+04	6.165E+06	1.358E+06
31	59.310	4.967	5.349	0.246	16848.5	6144.0	994.9	3443.9	5.373E+04	5.588E+06	1.189E+06
32	61.356	4.793	4.990	0.244	17384.5	6276.4	994.4	3283.4	4.610E+04	5.036E+06	1.035E+06
33	63.351	4.622	4.641	0.243	17919.3	6409.1	994.0	3107.7	3.942E+04	4.523E+06	8.978E+05
34	65.346	4.453	4.305	0.242	18442.7	6539.9	992.9	2922.0	3.344E+04	4.035E+06	7.738E+05
35	67.342	4.286	3.977	0.241	18955.4	6674.4	991.3	2777.4	2.812E+04	3.573E+06	6.617E+05
36	69.337	4.121	3.663	0.241	19445.8	6800.4	988.9	2600.4	2.342E+04	3.137E+06	5.609E+05
37	71.297	3.961	3.365	0.241	19900.8	6920.1	985.3	2449.6	1.936E+04	2.735E+06	4.724E+05
38	73.257	3.802	3.077	0.241	20324.0	7029.5	980.2	2280.2	1.582E+04	2.360E+06	3.936E+05
39	75.252	3.645	2.797	0.241	20712.0	7131.3	973.7	2131.7	1.270E+04	2.005E+06	3.227E+05
40	77.247	3.489	2.527	0.241	21059.1	7222.5	965.4	1996.8	1.003E+04	1.679E+06	2.605E+05
41	79.277	3.336	2.265	0.241	21361.8	7298.5	955.1	1838.5	7.727E+03	1.375E+06	2.057E+05
42	81.309	3.187	2.012	0.241	21615.7	7363.0	943.1	1715.1	5.812E+03	1.102E+06	1.588E+05
43	83.304	3.045	1.767	0.241	21820.3	7411.2	929.3	1575.7	4.270E+03	8.633E+05	1.199E+05
44	85.272	2.907	1.526	0.241	21976.2	7444.7	913.1	1437.3	3.044E+03	6.564E+05	8.787E+04
45	87.240	2.769	1.282	0.241	22067.9	7459.1	893.4	1317.9	2.076E+03	4.784E+05	6.171E+04
46	89.262	2.624	1.033	0.241	22024.7	7429.9	867.3	1203.8	1.316E+03	3.254E+05	4.039E+04
47	91.285	2.462	0.788	0.241	21717.6	7312.8	830.7	1072.6	7.641E+02	2.029E+05	2.422E+04
48	93.258	2.265	0.554	0.241	20910.9	7029.8	775.4	930.0	3.962E+02	1.124E+05	1.294E+04
49	95.254	2.009	0.332	0.241	19282.9	6473.8	688.5	775.1	1.642E+02	4.935E+04	5.488E+03
50	97.271	1.614	0.147	0.241	15828.9	5307.9	538.1	561.7	4.197E+01	1.290E+04	1.407E+03
51	99.017	0.917	0.034	0.241	9041.3	3032.1	294.6	347.3	3.112E+00	8.494E+02	9.730E+01

UPK									
Span Section [m]	Flap Bend. Stiffness, E _{lyy} LCS [N.m ²]	Edge Bend. Stiffness, E _{lxx} LCS [N.m ²]	Bend. Stiffness, E _{ly} LCS [N.m ²]	Flap Strain, ε _{zx} LCS [μ]	Edge Strain, ε _{yx} LCS [μ]	EA stiffness (N)	Cross Section Area [m ²]	Mass Distr. [kg/m]	Torsional Stiffness, GJT [N.m ²]
0.000	7.590E+10	8.009E+10	0.000E+00	1328	662	2.004E+10	1.589	1340.0	3.482E+10
2.328	7.577E+10	7.936E+10	0.000E+00	1296	642	2.001E+10	1.583	1336.5	3.455E+10
4.323	7.603E+10	7.790E+10	0.000E+00	1219	610	2.014E+10	1.609	1339.5	3.385E+10
6.318	7.230E+10	7.352E+10	0.000E+00	1197	605	1.961E+10	1.591	1301.1	3.152E+10
8.312	6.521E+10	6.644E+10	0.000E+00	1206	644	1.864E+10	1.629	1231.9	2.701E+10
10.309	5.635E+10	5.954E+10	4.111E+09	1262	707	1.763E+10	1.609	1158.9	2.234E+10
12.302	4.596E+10	5.112E+10	4.706E+09	1381	830	1.636E+10	1.609	1075.0	1.689E+10
14.296	3.579E+10	4.434E+10	4.476E+09	1563	965	1.522E+10	1.572	998.5	1.211E+10
16.292	2.815E+10	3.979E+10	4.079E+09	1731	1089	1.452E+10	1.555	951.9	8.869E+09
17.956	2.345E+10	3.759E+10	3.612E+09	1862	1153	1.410E+10	1.504	924.6	7.154E+09
20.444	1.788E+10	3.244E+10	2.819E+09	2061	1312	1.273E+10	1.476	844.3	4.773E+09
22.447	1.512E+10	2.978E+10	2.282E+09	2145	1373	1.195E+10	1.416	798.3	3.921E+09
24.442	1.281E+10	2.672E+10	1.864E+09	2246	1444	1.110E+10	1.366	747.3	3.071E+09
26.437	1.099E+10	2.389E+10	1.543E+09	2331	1501	1.041E+10	1.326	705.9	2.456E+09
28.432	9.527E+09	2.153E+10	1.294E+09	2409	1532	9.867E+09	1.283	672.3	2.012E+09
30.428	8.019E+09	2.135E+10	1.157E+09	2561	1418	9.332E+09	1.215	635.5	1.631E+09
32.423	7.067E+09	1.990E+10	1.037E+09	2611	1384	9.131E+09	1.178	619.9	1.422E+09
34.418	6.240E+09	1.843E+10	9.300E+08	2650	1354	8.919E+09	1.139	602.4	1.243E+09
36.414	5.526E+09	1.661E+10	8.217E+08	2687	1353	8.684E+09	1.066	581.1	1.093E+09
38.409	4.891E+09	1.480E+10	7.074E+08	2721	1362	8.403E+09	1.027	559.6	9.442E+08
40.405	4.334E+09	1.344E+10	6.085E+08	2749	1339	8.175E+09	0.942	537.3	8.406E+08
42.400	3.817E+09	1.228E+10	5.219E+08	2789	1304	7.927E+09	0.906	519.0	7.364E+08
44.396	3.354E+09	1.104E+10	4.405E+08	2825	1282	7.660E+09	0.868	499.2	6.402E+08
46.290	2.961E+09	9.893E+09	3.735E+08	2864	1268	7.402E+09	0.825	480.0	5.621E+08
48.286	2.594E+09	8.809E+09	3.089E+08	2901	1251	7.120E+09	0.778	459.0	4.950E+08
50.281	2.266E+09	7.870E+09	2.559E+08	2939	1222	6.852E+09	0.737	440.0	4.360E+08
52.276	1.972E+09	6.710E+09	2.043E+08	2979	1244	6.504E+09	0.674	413.9	3.752E+08
54.272	1.719E+09	5.956E+09	1.672E+08	3006	1211	6.223E+09	0.647	395.6	3.291E+08
56.267	1.503E+09	5.242E+09	1.349E+08	3014	1182	5.959E+09	0.580	374.4	2.916E+08
58.262	1.306E+09	4.550E+09	1.079E+08	3031	1164	5.646E+09	0.555	354.2	2.488E+08
60.358	1.131E+09	3.828E+09	8.381E+07	3024	1165	5.337E+09	0.492	331.6	2.186E+08
62.354	9.835E+08	3.342E+09	6.715E+07	3005	1122	5.066E+09	0.460	313.9	1.920E+08
64.349	8.570E+08	2.847E+09	5.215E+07	2968	1101	4.780E+09	0.418	294.2	1.672E+08
66.344	7.406E+08	2.402E+09	4.066E+07	2941	1084	4.469E+09	0.375	273.5	1.451E+08
68.340	6.400E+08	2.055E+09	3.237E+07	2893	1042	4.186E+09	0.356	257.0	1.273E+08
70.335	5.527E+08	1.715E+09	2.453E+07	2821	1015	3.889E+09	0.310	237.0	1.106E+08
72.259	4.747E+08	1.466E+09	1.963E+07	2761	965	3.609E+09	0.286	220.2	9.717E+07
74.254	4.020E+08	1.208E+09	1.523E+07	2694	934	3.302E+09	0.252	201.1	8.391E+07
76.249	3.376E+08	1.013E+09	1.168E+07	2613	875	3.008E+09	0.235	184.2	7.149E+07
78.244	2.824E+08	8.436E+08	9.324E+06	2508	814	2.734E+09	0.220	169.0	6.198E+07
80.311	2.323E+08	6.805E+08	6.868E+06	2378	758	2.445E+09	0.190	151.0	5.256E+07
82.307	1.913E+08	5.641E+08	5.586E+06	2215	676	2.198E+09	0.170	137.2	4.548E+07
84.302	1.551E+08	4.505E+08	4.154E+06	2040	608	1.937E+09	0.144	121.6	3.923E+07
86.242	1.229E+08	3.713E+08	3.366E+06	1877	519	1.681E+09	0.127	106.4	3.206E+07
88.237	9.630E+07	2.889E+08	2.482E+06	1664	447	1.437E+09	0.115	93.2	2.670E+07
90.288	7.363E+07	2.383E+08	2.232E+06	1394	333	1.224E+09	0.093	80.7	2.263E+07
92.283	5.327E+07	1.775E+08	1.597E+06	1127	252	9.900E+08	0.082	67.2	1.740E+07
94.234	3.542E+07	1.298E+08	1.285E+06	875	172	7.714E+08	0.066	53.9	1.281E+07
96.274	2.009E+07	9.254E+07	1.063E+06	592	89	5.623E+08	0.051	41.3	8.197E+06
98.270	7.086E+06	4.391E+07	5.650E+05	307	34	3.220E+08	0.037	26.4	3.384E+06
99.766	4.690E+06	4.071E+07	2.241E+05	10	1	1.847E+08	0.027	16.5	9.660E+05

HRK											
Sect. No.	Span Section [m]	Chord [m]	Aero Twist [°]	Rel. Thick. [-]	Norm. Force GCS, Fn [N/m]	Norm. Force + mg LCS, Fn' [N/m]	Tang. Force GCS, Ft [N/m]	Tang. Force + mg LCS, Ft' [N/m]	Centrifugal Force (N)	Flap Bend. Moment, My LCS [N.m]	Edge Bend. Moment, Mx LCS [N.m]
1	0.000	4.557	14.500	0.999	588.7	3679.4	-69.3	10111.7	1.205E+06	3.060E+07	1.307E+07
2	1.164	4.557	14.500	0.998	625.4	3673.6	-104.0	10057.2	1.158E+06	2.999E+07	1.259E+07
3	3.325	4.557	14.500	0.979	710.3	3697.1	-139.0	10038.4	1.074E+06	2.887E+07	1.174E+07
4	5.321	4.559	14.498	0.950	819.8	3620.5	-170.0	9704.2	1.002E+06	2.785E+07	1.100E+07
5	7.316	4.595	14.458	0.896	952.5	3476.8	-181.2	9170.5	9.337E+05	2.685E+07	1.029E+07
6	9.145	4.649	14.325	0.836	1070.5	3310.4	-179.6	8629.7	8.746E+05	2.594E+07	9.682E+06
7	11.129	4.745	13.989	0.761	1152.3	3069.7	-155.6	7992.5	8.140E+05	2.497E+07	9.052E+06
8	13.290	4.857	13.315	0.684	1121.0	2777.6	-117.7	7444.7	7.520E+05	2.393E+07	8.404E+06
9	15.287	4.970	12.529	0.610	960.8	2530.3	-57.2	7190.2	6.981E+05	2.297E+07	7.836E+06
10	17.282	5.071	11.398	0.547	3061.6	3080.1	329.8	7113.0	6.473E+05	2.203E+07	7.298E+06
11	19.370	5.160	10.290	0.490	5857.1	3790.6	664.2	6734.4	5.973E+05	2.106E+07	6.766E+06
12	21.449	5.216	9.302	0.448	6967.4	3957.9	723.0	6402.5	5.505E+05	2.011E+07	6.266E+06
13	23.444	5.244	8.542	0.415	7667.1	4010.9	735.1	6016.2	5.082E+05	1.921E+07	5.813E+06
14	25.439	5.252	7.935	0.388	8342.9	4097.9	743.5	5695.7	4.683E+05	1.833E+07	5.384E+06
15	27.434	5.232	7.466	0.368	8988.6	4207.6	749.1	5428.2	4.307E+05	1.746E+07	4.979E+06
16	29.430	5.204	7.035	0.350	9429.6	4251.4	743.1	5138.1	3.953E+05	1.661E+07	4.596E+06
17	31.425	5.147	6.678	0.336	9672.1	4271.8	726.8	5012.6	3.619E+05	1.577E+07	4.234E+06
18	33.420	5.086	6.326	0.322	9902.0	4287.4	710.7	4873.0	3.305E+05	1.496E+07	3.893E+06
19	35.416	5.006	5.991	0.312	10127.7	4299.3	695.0	4702.9	3.010E+05	1.416E+07	3.570E+06
20	37.412	4.920	5.665	0.302	10342.6	4310.4	679.6	4531.5	2.734E+05	1.337E+07	3.267E+06
21	39.407	4.823	5.359	0.294	10637.8	4351.1	669.1	4352.9	2.475E+05	1.261E+07	2.983E+06
22	41.402	4.721	5.048	0.287	10968.2	4410.9	661.0	4207.6	2.234E+05	1.186E+07	2.716E+06
23	43.398	4.615	4.739	0.280	11315.3	4476.5	654.5	4053.2	2.010E+05	1.113E+07	2.466E+06
24	45.343	4.505	4.417	0.274	11705.8	4557.5	650.5	3899.9	1.807E+05	1.043E+07	2.238E+06
25	47.288	4.391	4.085	0.268	12136.9	4652.1	648.3	3739.7	1.619E+05	9.753E+06	2.025E+06
26	49.284	4.271	3.733	0.263	12631.8	4770.9	648.5	3595.5	1.440E+05	9.075E+06	1.822E+06
27	51.279	4.149	3.378	0.258	13166.8	4897.0	650.2	3394.9	1.276E+05	8.416E+06	1.633E+06
28	53.274	4.025	3.018	0.255	13749.7	5049.8	653.6	3260.1	1.125E+05	7.776E+06	1.458E+06
29	55.270	3.899	2.656	0.251	14372.4	5214.6	658.1	3102.6	9.867E+04	7.156E+06	1.297E+06
30	57.265	3.772	2.289	0.248	15040.0	5397.0	663.6	2951.9	8.610E+04	6.557E+06	1.148E+06
31	59.310	3.642	1.921	0.246	15746.9	5593.1	669.6	2789.8	7.441E+04	5.964E+06	1.008E+06
32	61.356	3.515	1.562	0.244	16468.1	5800.1	675.8	2662.2	6.387E+04	5.394E+06	8.800E+05
33	63.351	3.389	1.213	0.243	17197.7	6010.6	681.9	2520.5	5.464E+04	4.861E+06	7.661E+05
34	65.346	3.265	0.877	0.242	17923.5	6221.6	687.3	2372.3	4.637E+04	4.352E+06	6.625E+05
35	67.342	3.143	0.549	0.241	18646.9	6437.0	692.3	2258.5	3.902E+04	3.867E+06	5.686E+05
36	69.337	3.022	0.235	0.241	19352.6	6646.0	696.4	2117.7	3.251E+04	3.407E+06	4.840E+05
37	71.297	2.905	-0.063	0.241	20023.8	6847.6	699.4	1999.5	2.689E+04	2.980E+06	4.094E+05
38	73.257	2.788	-0.351	0.241	20668.3	7040.8	701.4	1865.7	2.198E+04	2.580E+06	3.426E+05
39	75.252	2.673	-0.631	0.241	21282.3	7226.7	702.4	1750.2	1.765E+04	2.200E+06	2.823E+05
40	77.247	2.559	-0.901	0.241	21859.2	7402.5	702.2	1645.9	1.394E+04	1.848E+06	2.292E+05
41	79.277	2.446	-1.163	0.241	22394.6	7564.6	700.6	1522.8	1.075E+04	1.520E+06	1.821E+05
42	81.309	2.337	-1.416	0.241	22880.5	7713.3	697.7	1430.2	8.086E+03	1.222E+06	1.415E+05
43	83.304	2.233	-1.661	0.241	23315.4	7845.5	693.4	1324.0	5.942E+03	9.609E+05	1.075E+05
44	85.272	2.132	-1.902	0.241	23701.8	7962.6	687.4	1218.4	4.237E+03	7.334E+05	7.939E+04
45	87.240	2.030	-2.146	0.241	24027.5	8061.1	678.8	1129.3	2.891E+03	5.365E+05	5.620E+04
46	89.262	1.924	-2.395	0.241	24213.8	8114.1	665.2	1047.4	1.832E+03	3.664E+05	3.710E+04
47	91.285	1.806	-2.640	0.241	24110.6	8070.9	643.5	950.5	1.063E+03	2.294E+05	2.245E+04
48	93.258	1.661	-2.874	0.241	23448.0	7842.1	607.1	842.2	5.502E+02	1.277E+05	1.209E+04
49	95.254	1.474	-3.096	0.241	21857.2	7304.8	545.1	719.7	2.270E+02	5.632E+04	5.173E+03
50	97.271	1.183	-3.281	0.241	18158.6	6065.0	430.8	532.0	5.767E+01	1.480E+04	1.335E+03
51	99.017	0.672	-3.394	0.241	10484.8	3501.6	238.6	330.5	4.276E+00	9.810E+02	9.258E+01

HRK									
Span Section [m]	Flap Bend. Stiffness, Elyy LCS [N.m2]	Edge Bend. Stiffness, Elxx LCS [N.m2]	Bend. Stiffness, Elxy LCS [N.m2]	Flap Strain, ϵ_{zx} LCS [μ]	Edge Strain, ϵ_{yx} LCS [μ]	EA stiffness (N)	Cross Section Area [m2]	Mass Distr. [kg/m]	Torsional Stiffness, GJT [N.m2]
0.000	5.554E+10	5.051E+10	0.000E+00	1328	662	1.651E+10	1.309	1104.4	2.365E+10
2.328	5.550E+10	5.002E+10	0.000E+00	1296	642	1.650E+10	1.305	1101.7	2.347E+10
4.323	5.581E+10	4.904E+10	0.000E+00	1219	610	1.660E+10	1.327	1104.4	2.303E+10
6.318	5.317E+10	4.621E+10	0.000E+00	1197	605	1.617E+10	1.312	1072.8	2.149E+10
8.312	4.805E+10	4.161E+10	0.000E+00	1206	644	1.536E+10	1.343	1015.3	1.849E+10
10.309	4.158E+10	3.714E+10	0.000E+00	1262	707	1.452E+10	1.326	954.6	1.536E+10
12.302	3.394E+10	3.172E+10	0.000E+00	1381	830	1.346E+10	1.324	884.5	1.169E+10
14.296	2.645E+10	2.741E+10	3.025E+09	1563	965	1.251E+10	1.292	820.8	8.439E+09
16.292	2.082E+10	2.451E+10	2.753E+09	1731	1089	1.193E+10	1.278	782.0	6.228E+09
17.956	1.736E+10	2.312E+10	2.437E+09	1862	1153	1.158E+10	1.236	759.4	5.056E+09
20.444	1.326E+10	1.992E+10	1.902E+09	2061	1312	1.046E+10	1.212	693.6	3.406E+09
22.447	1.124E+10	1.828E+10	1.542E+09	2145	1373	9.819E+09	1.164	656.1	2.817E+09
24.442	9.544E+09	1.640E+10	1.260E+09	2246	1444	9.131E+09	1.123	614.6	2.219E+09
26.437	8.210E+09	1.466E+10	1.045E+09	2331	1501	8.568E+09	1.091	580.9	1.784E+09
28.432	7.134E+09	1.321E+10	8.775E+08	2409	1532	8.124E+09	1.056	553.6	1.468E+09
30.428	6.018E+09	1.313E+10	7.862E+08	2561	1418	7.691E+09	1.001	523.8	1.195E+09
32.423	5.317E+09	1.224E+10	7.056E+08	2611	1384	7.531E+09	0.972	511.3	1.046E+09
34.418	4.707E+09	1.134E+10	6.336E+08	2650	1354	7.362E+09	0.940	497.3	9.179E+08
36.414	4.179E+09	1.023E+10	5.606E+08	2687	1353	7.173E+09	0.881	480.0	8.099E+08
38.409	3.709E+09	9.115E+09	4.834E+08	2721	1362	6.947E+09	0.849	462.6	7.020E+08
40.405	3.297E+09	8.284E+09	4.166E+08	2749	1339	6.764E+09	0.779	444.6	6.271E+08
42.400	2.911E+09	7.574E+09	3.580E+08	2789	1304	6.565E+09	0.750	429.8	5.513E+08
44.396	2.566E+09	6.816E+09	3.027E+08	2825	1282	6.350E+09	0.720	413.8	4.810E+08
46.290	2.272E+09	6.114E+09	2.572E+08	2864	1268	6.143E+09	0.685	398.3	4.236E+08
48.286	1.996E+09	5.450E+09	2.132E+08	2901	1251	5.915E+09	0.647	381.3	3.743E+08
50.281	1.749E+09	4.876E+09	1.770E+08	2939	1222	5.698E+09	0.613	365.9	3.308E+08
52.276	1.527E+09	4.163E+09	1.416E+08	2979	1244	5.415E+09	0.561	344.5	2.856E+08
54.272	1.335E+09	3.701E+09	1.162E+08	3006	1211	5.188E+09	0.539	329.8	2.514E+08
56.267	1.171E+09	3.264E+09	9.398E+07	3014	1182	4.974E+09	0.484	312.5	2.235E+08
58.262	1.021E+09	2.839E+09	7.536E+07	3031	1164	4.717E+09	0.464	296.0	1.912E+08
60.358	8.870E+08	2.394E+09	5.865E+07	3024	1165	4.465E+09	0.412	277.4	1.684E+08
62.354	7.740E+08	2.096E+09	4.712E+07	3005	1122	4.243E+09	0.386	262.9	1.483E+08
64.349	6.766E+08	1.790E+09	3.664E+07	2968	1101	4.006E+09	0.350	246.6	1.292E+08
66.344	5.867E+08	1.515E+09	2.865E+07	2941	1084	3.751E+09	0.315	229.6	1.123E+08
68.340	5.087E+08	1.301E+09	2.285E+07	2893	1042	3.517E+09	0.299	216.0	9.867E+07
70.335	4.407E+08	1.089E+09	1.736E+07	2821	1015	3.271E+09	0.261	199.3	8.582E+07
72.259	3.797E+08	9.347E+08	1.392E+07	2761	965	3.040E+09	0.241	185.5	7.543E+07
74.254	3.227E+08	7.737E+08	1.082E+07	2694	934	2.784E+09	0.212	169.5	6.513E+07
76.249	2.719E+08	6.518E+08	8.320E+06	2613	875	2.539E+09	0.199	155.5	5.548E+07
78.244	2.282E+08	5.458E+08	6.648E+06	2508	814	2.308E+09	0.186	142.7	4.797E+07
80.311	1.884E+08	4.429E+08	4.905E+06	2378	758	2.066E+09	0.160	127.6	4.059E+07
82.307	1.557E+08	3.694E+08	3.999E+06	2215	676	1.859E+09	0.144	116.1	3.509E+07
84.302	1.267E+08	2.970E+08	2.979E+06	2040	608	1.640E+09	0.122	102.9	3.020E+07
86.242	1.008E+08	2.466E+08	2.416E+06	1877	519	1.424E+09	0.107	90.2	2.456E+07
88.237	7.924E+07	1.933E+08	1.780E+06	1664	447	1.217E+09	0.097	78.9	2.030E+07
90.288	6.083E+07	1.609E+08	1.609E+06	1394	333	1.039E+09	0.079	68.5	1.724E+07
92.283	4.419E+07	1.209E+08	1.157E+06	1127	252	8.428E+08	0.070	57.2	1.329E+07
94.234	2.951E+07	8.916E+07	9.359E+05	875	172	6.583E+08	0.056	46.0	9.805E+06
96.274	1.681E+07	6.410E+07	7.783E+05	592	89	4.812E+08	0.044	35.3	6.296E+06
98.270	5.963E+06	3.062E+07	3.954E+05	307	34	2.693E+08	0.031	22.1	2.590E+06
99.766	3.975E+06	2.867E+07	1.579E+05	10	1	1.551E+08	0.023	13.9	7.441E+05

A.2 Additional Time-domain Load Case Simulation Figures

(2) Wind speed at hub [m/s]

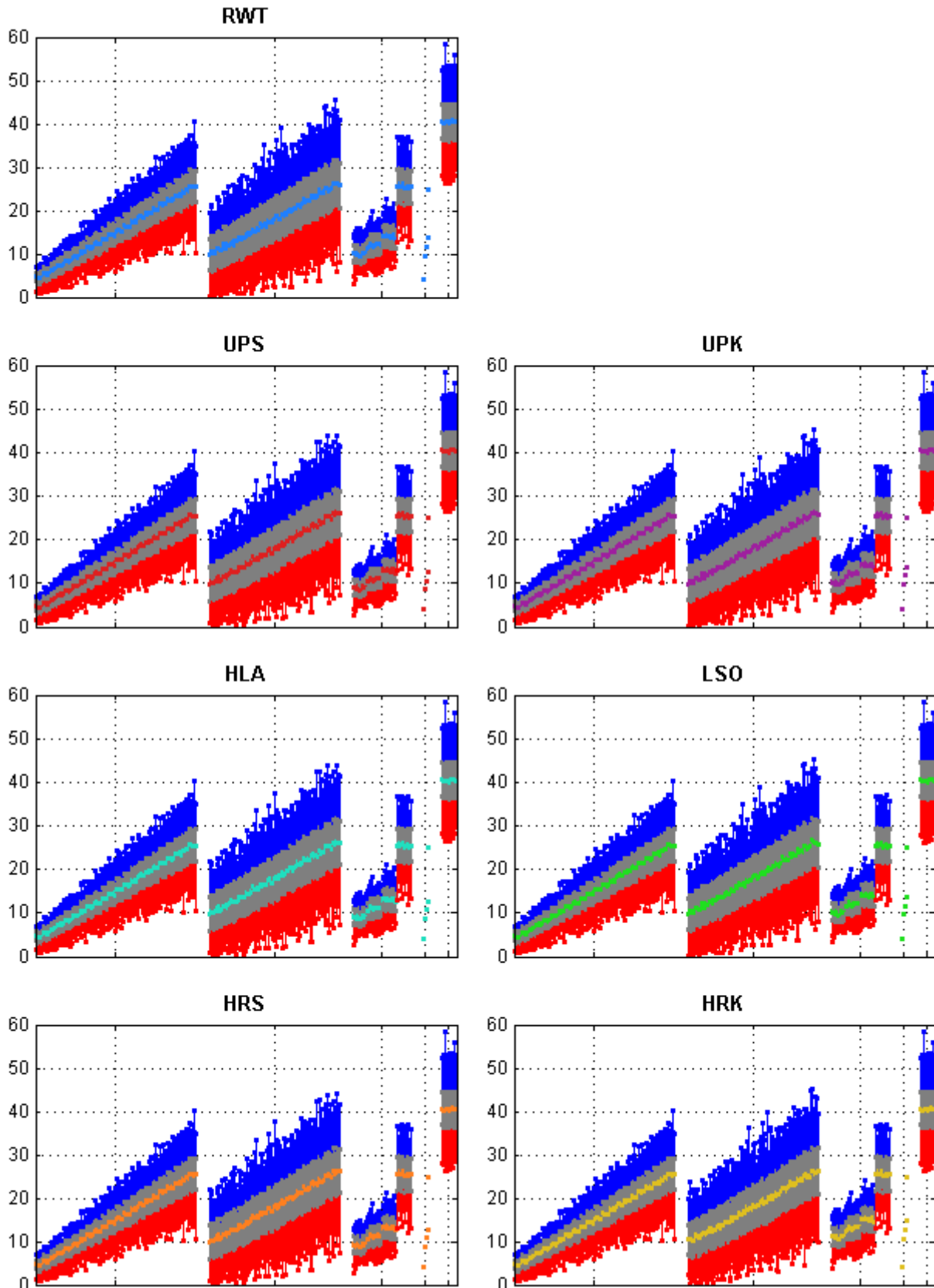


Figure A.1: Wind speed from all DLCs for all designs

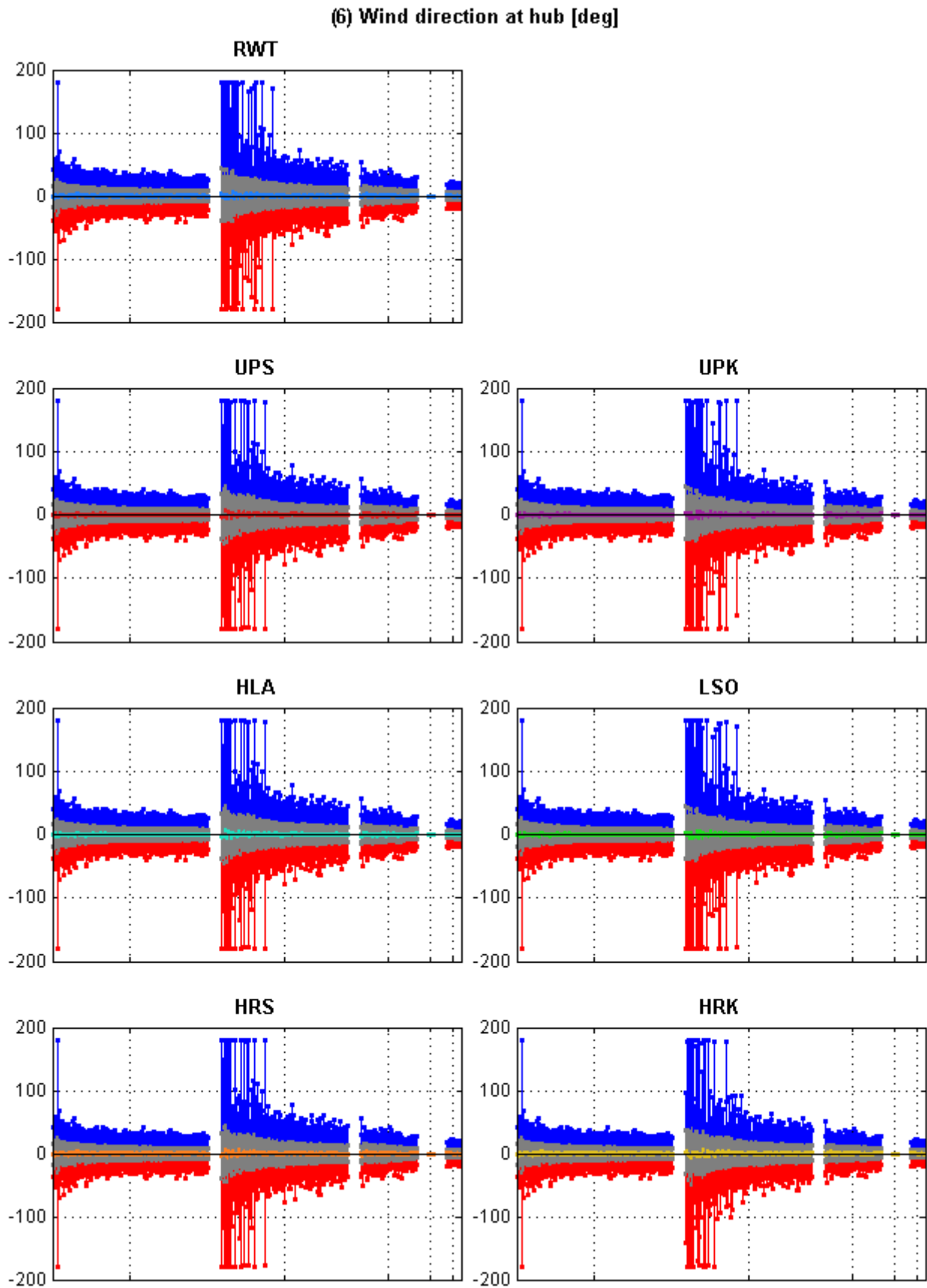


Figure A.2: Wind direction from all DLCs for all designs

(3) Aerodynamic power [W]

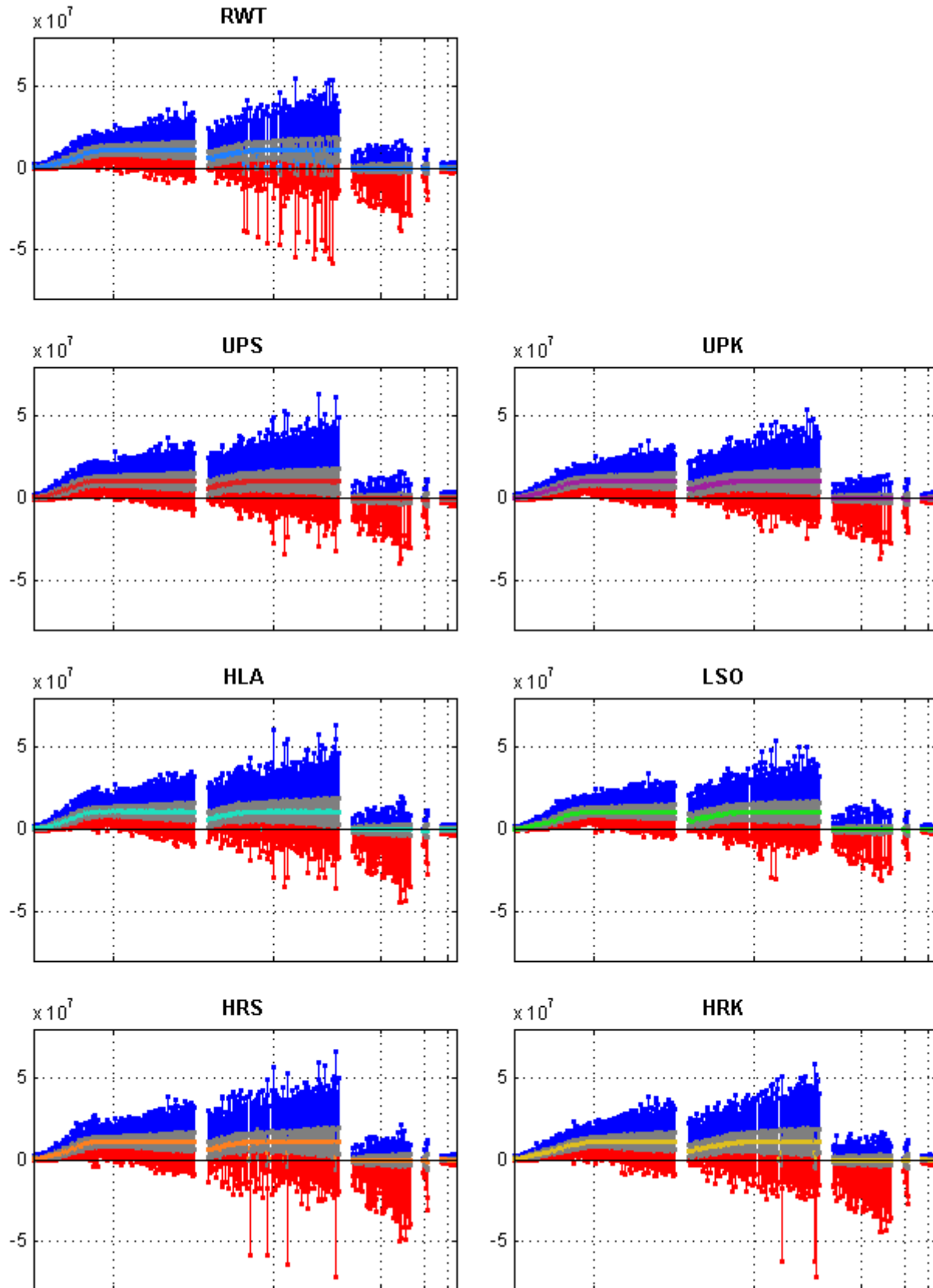


Figure A.3: Aerodynamic power from all DLCs for all designs

(91) Controller input value of rotor speed from pulse-counting [rpm]

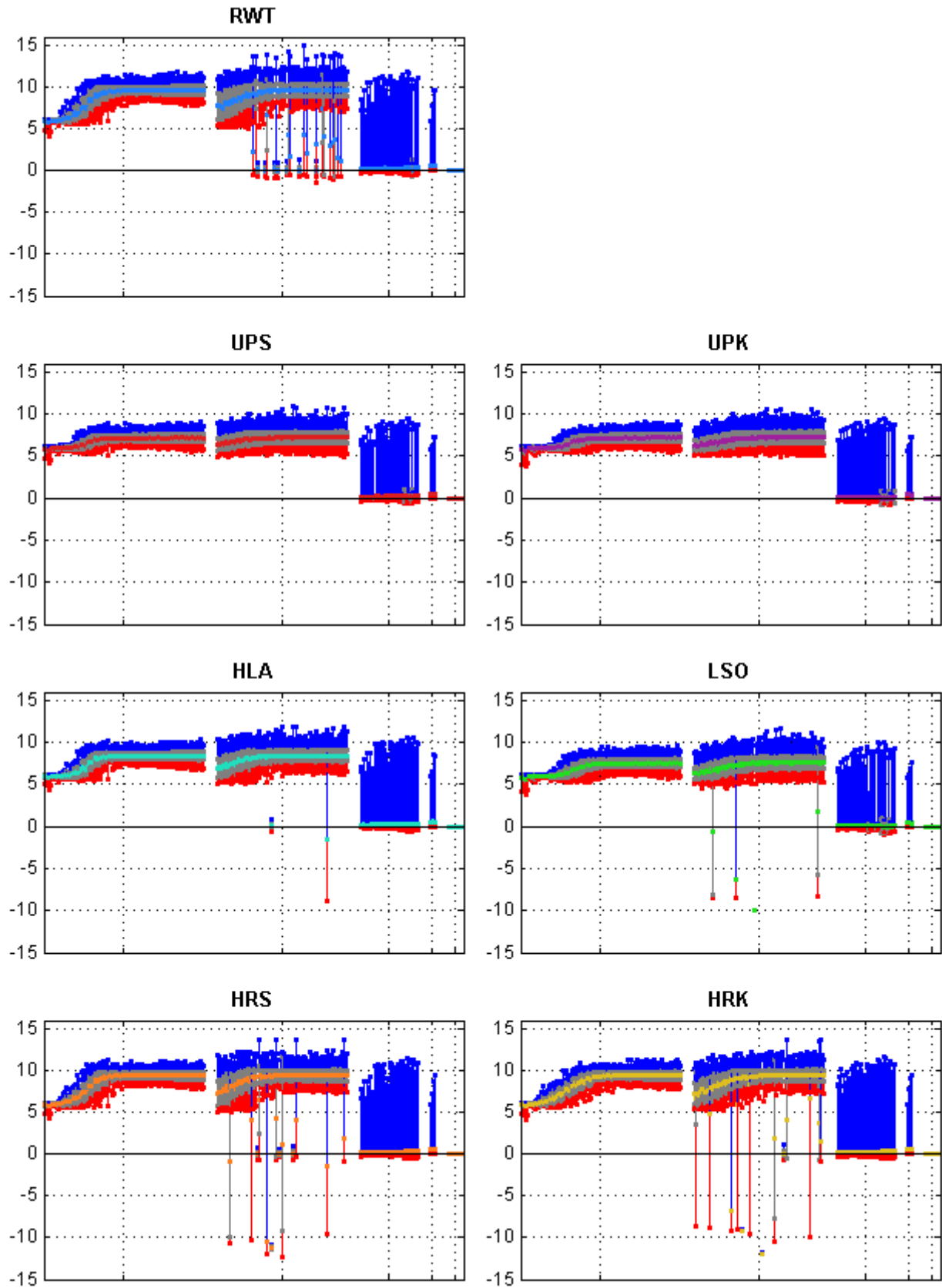


Figure A.4: Controller reference value for rotor speed from all DLCs for all designs

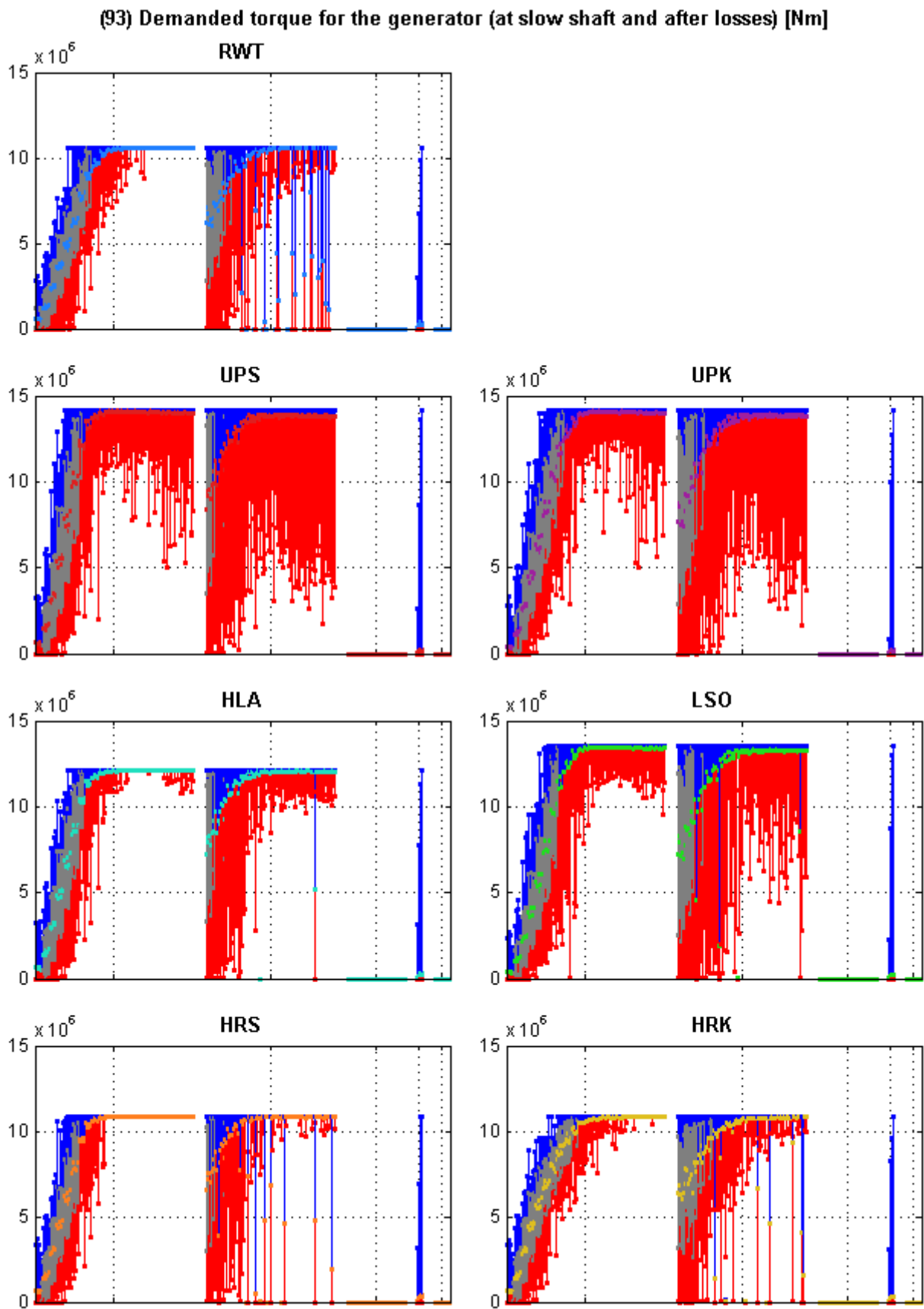


Figure A.5: Controller reference value for generator torque (transformed at slow speed shaft) from all DLCs for all designs

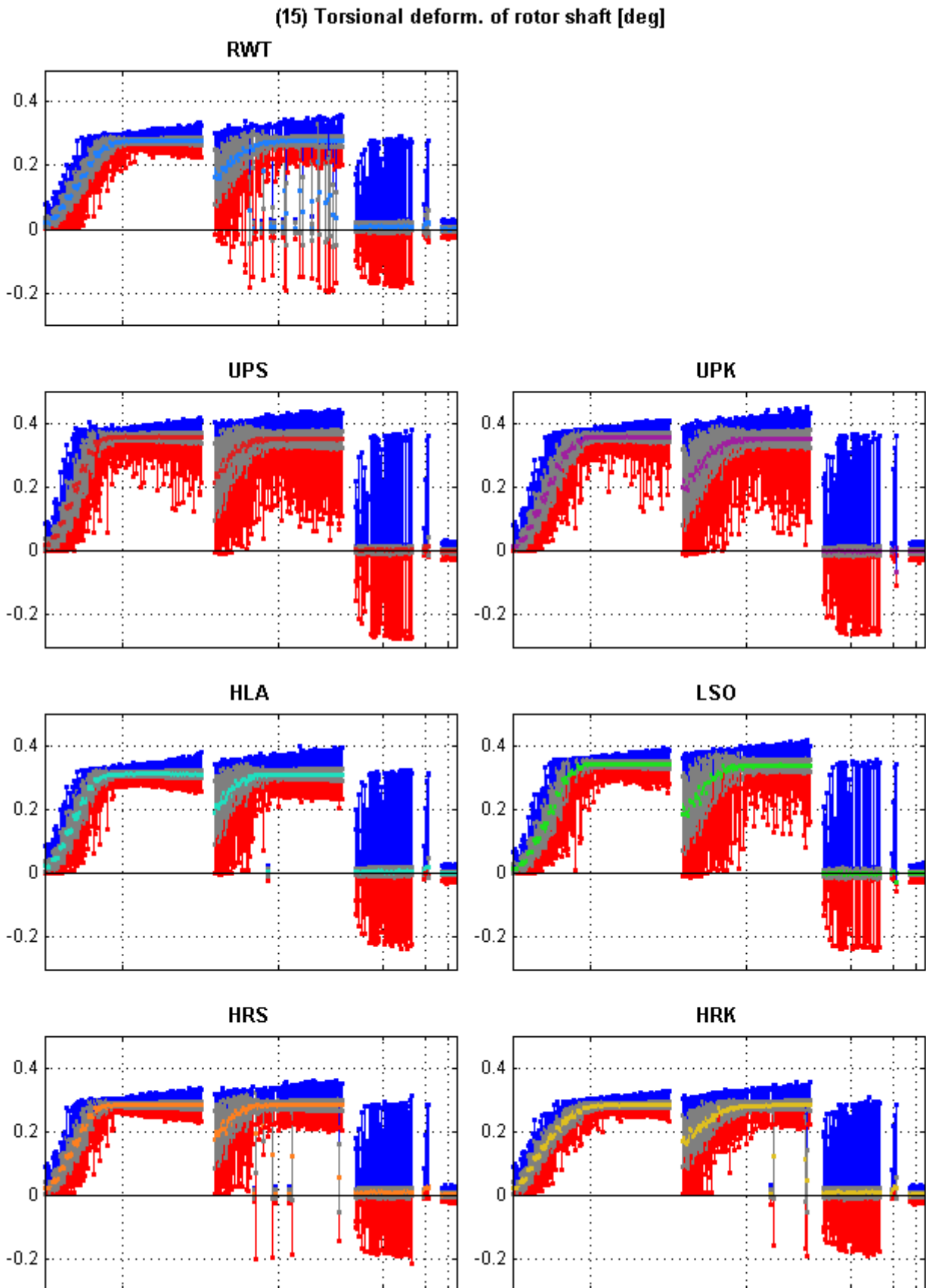


Figure A.6: Torsional deformation of rotor shaft from all DLCs for all designs

(204) B2: Pitch angle [deg]

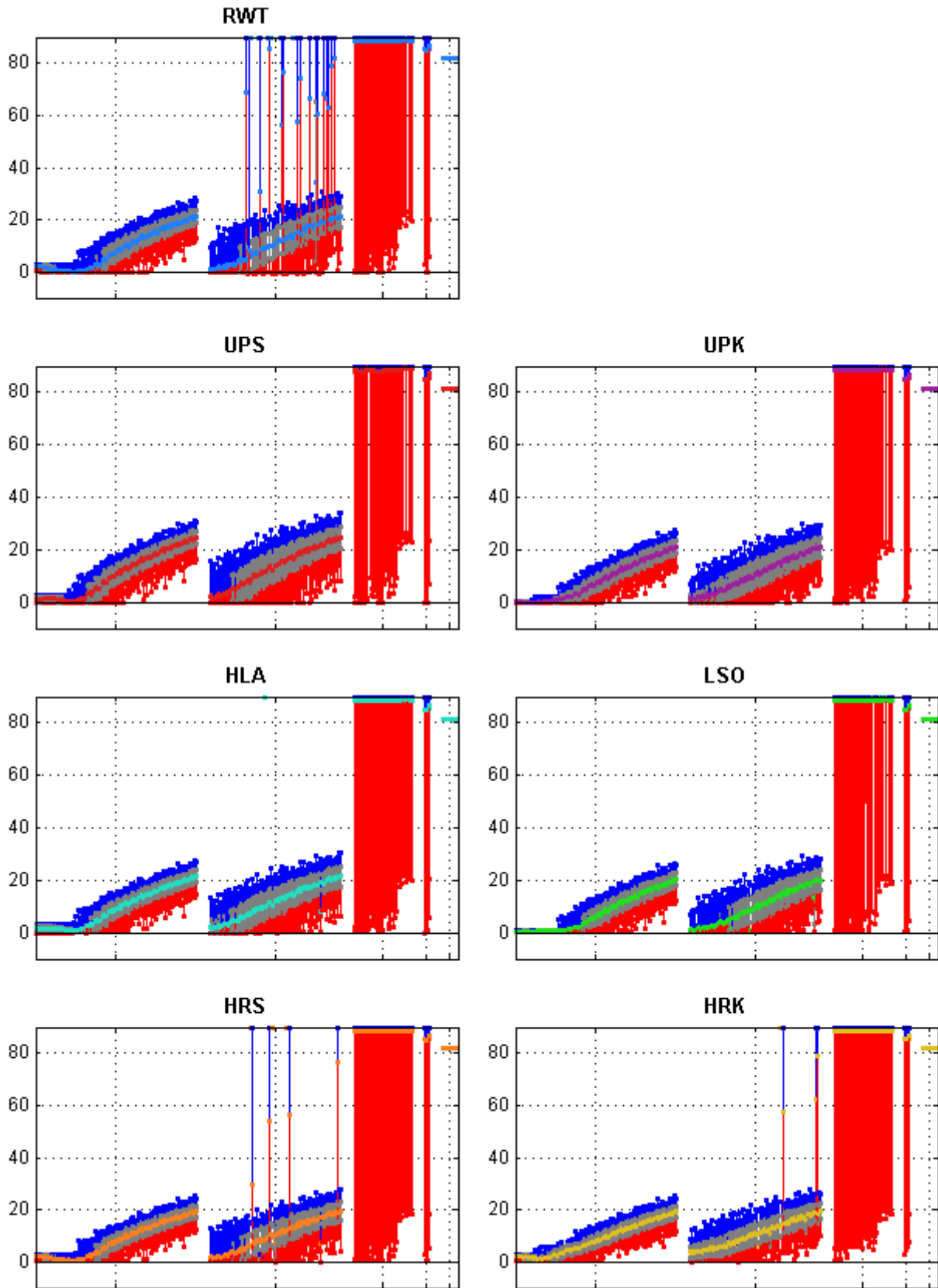


Figure A.7: Blade 2 pitch angle from all DLCs for all designs

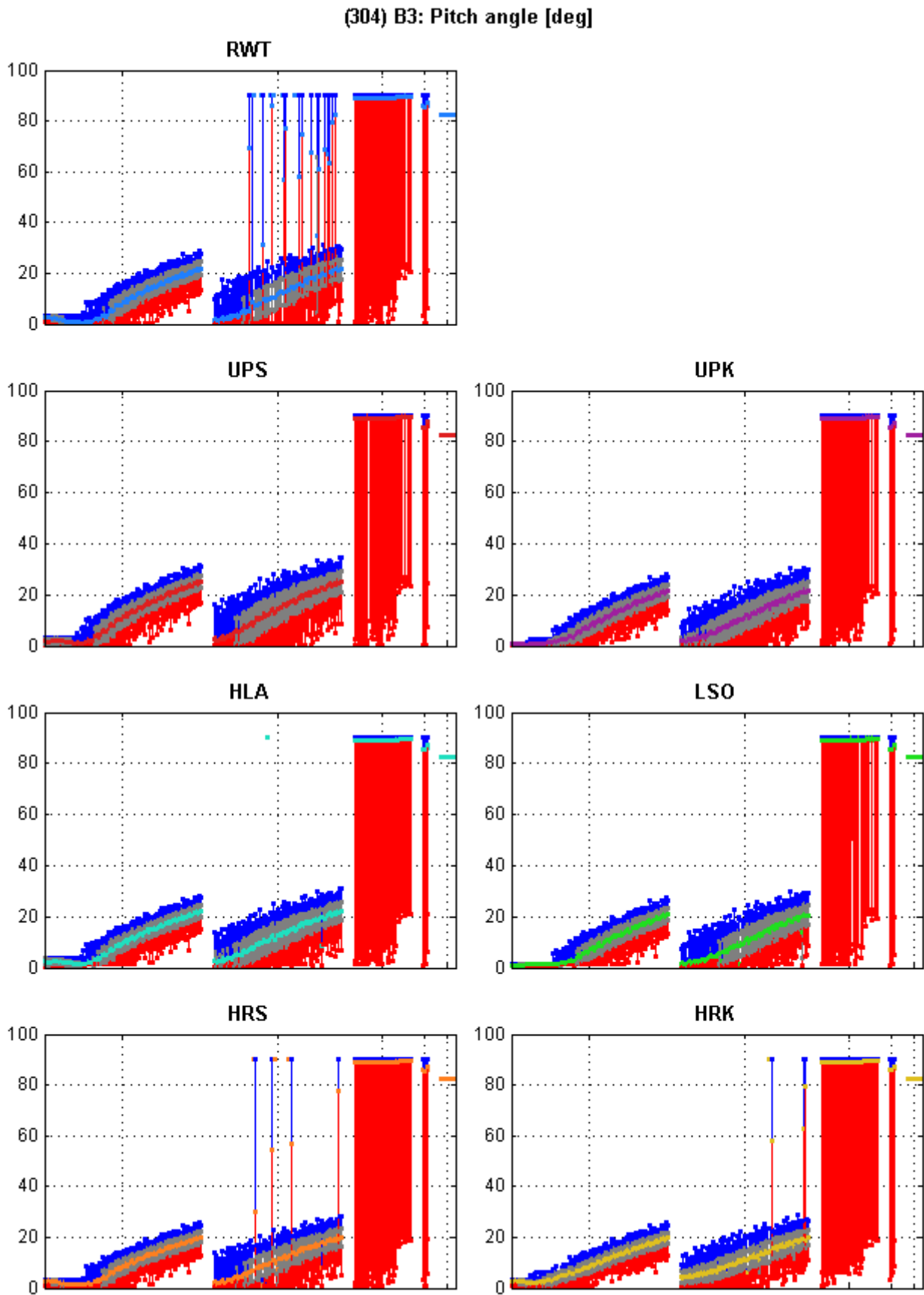


Figure A.8: Blade 3 pitch angle from all DLCs for all designs

(-153) B1: Flatwise bending moment (chord rs) [Nm] @ BR

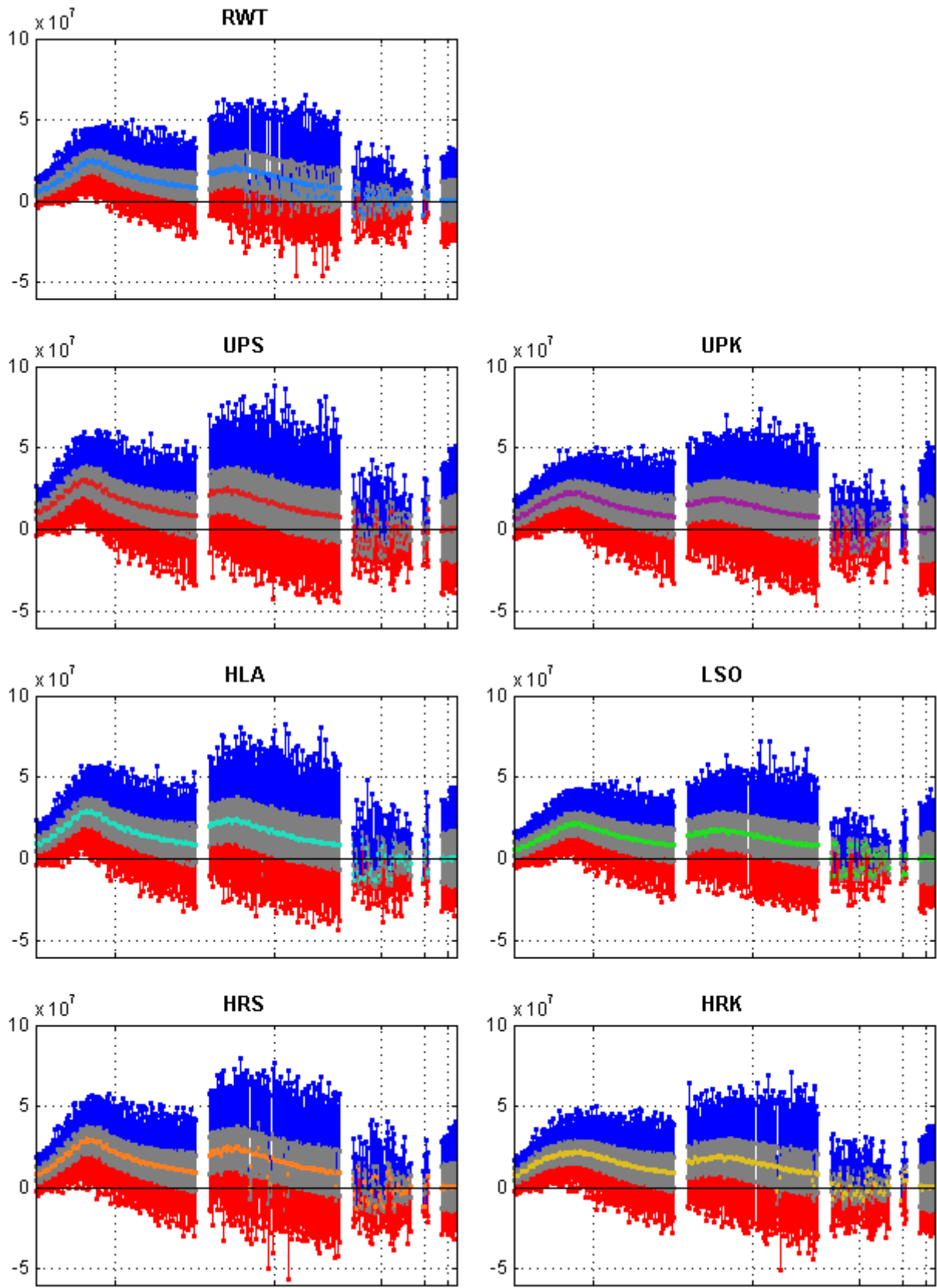


Figure A.9: Blade 1 flap-wise blade root bending moment in the chord reference system from all DLCs for all designs

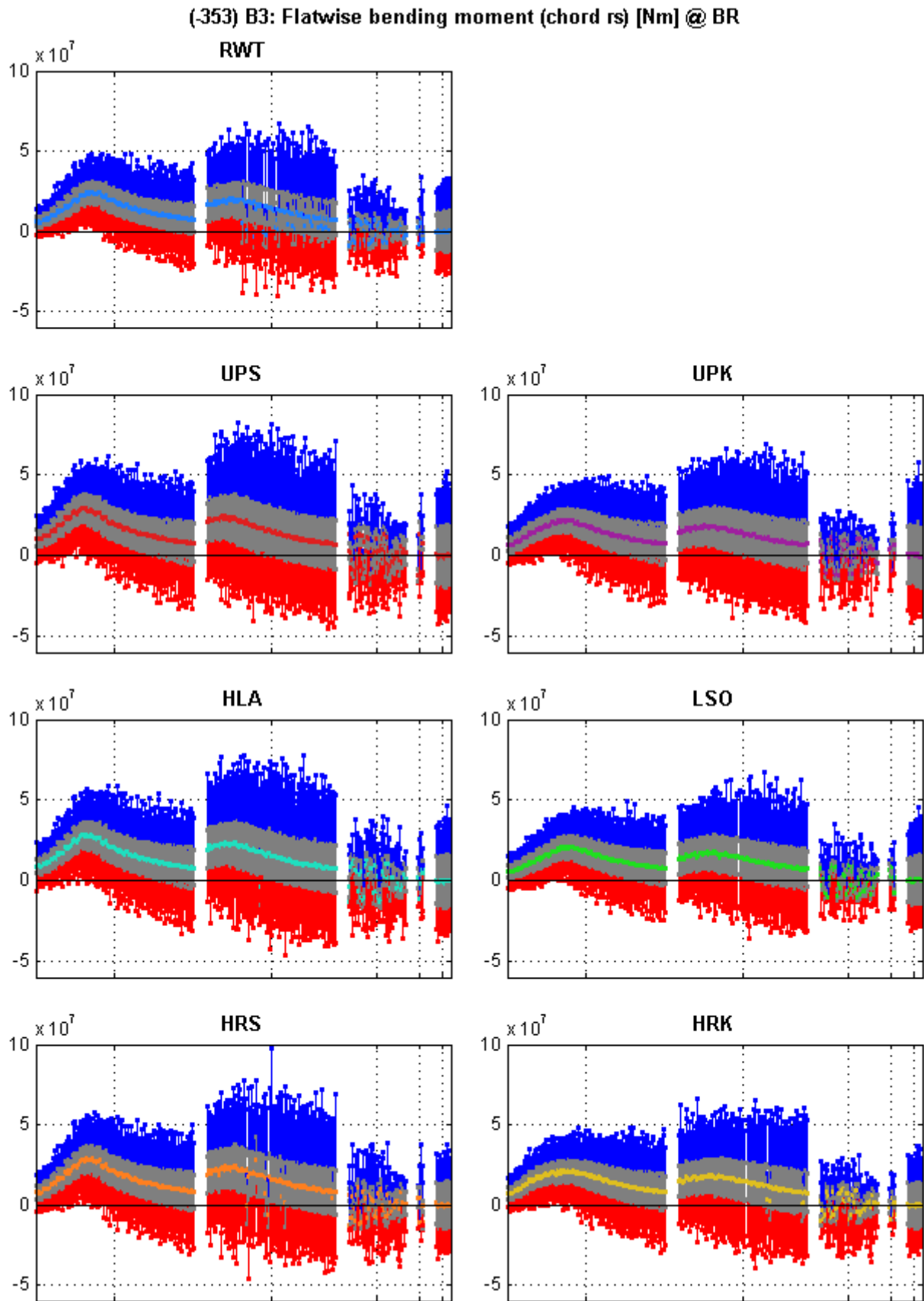


Figure A.10: Blade 3 flap-wise blade root bending moment in the chord reference system from all DLCs for all designs

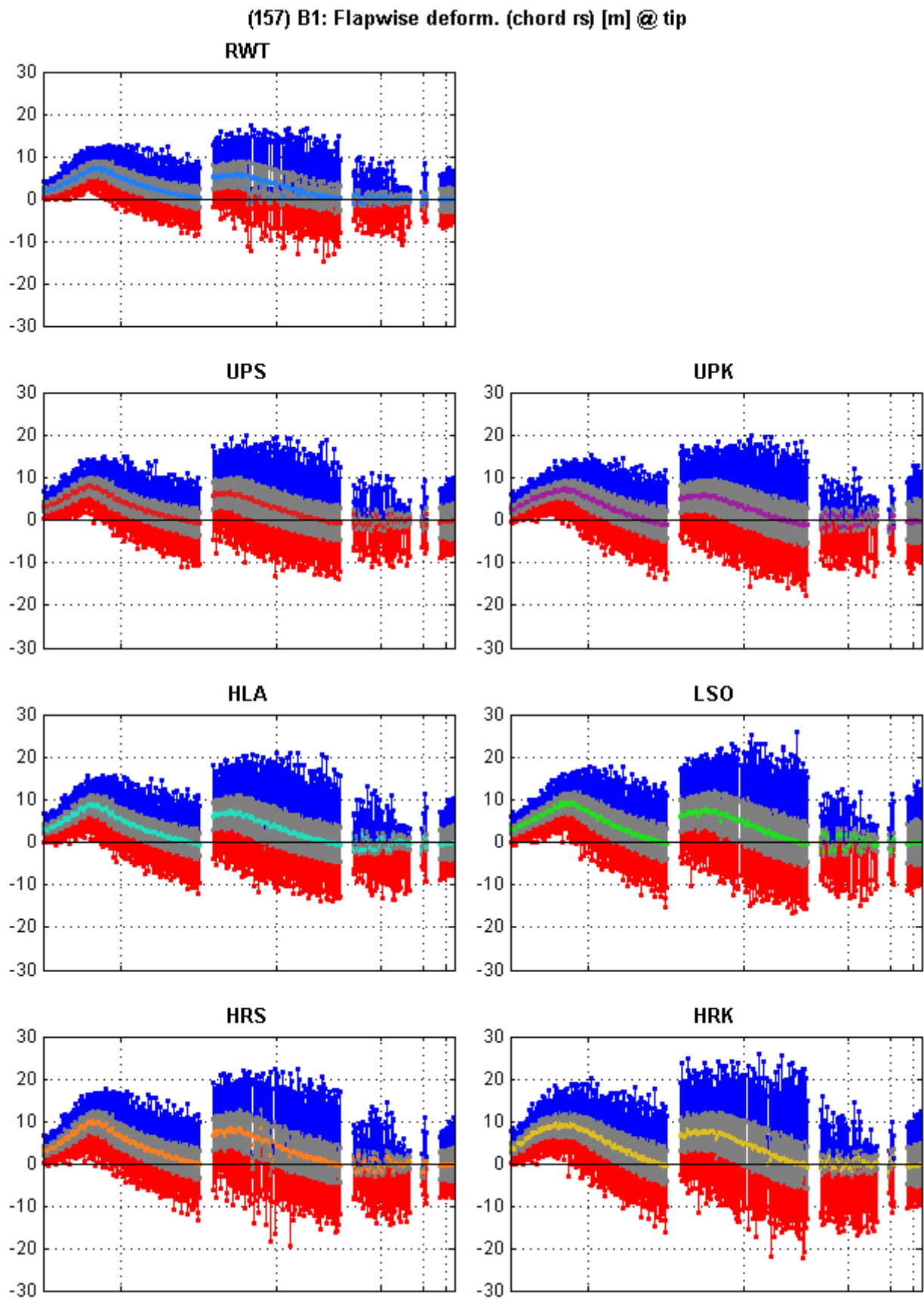


Figure A.11: Blade 1 flap-wise tip displacement in the chord reference system from all DLCs for all designs

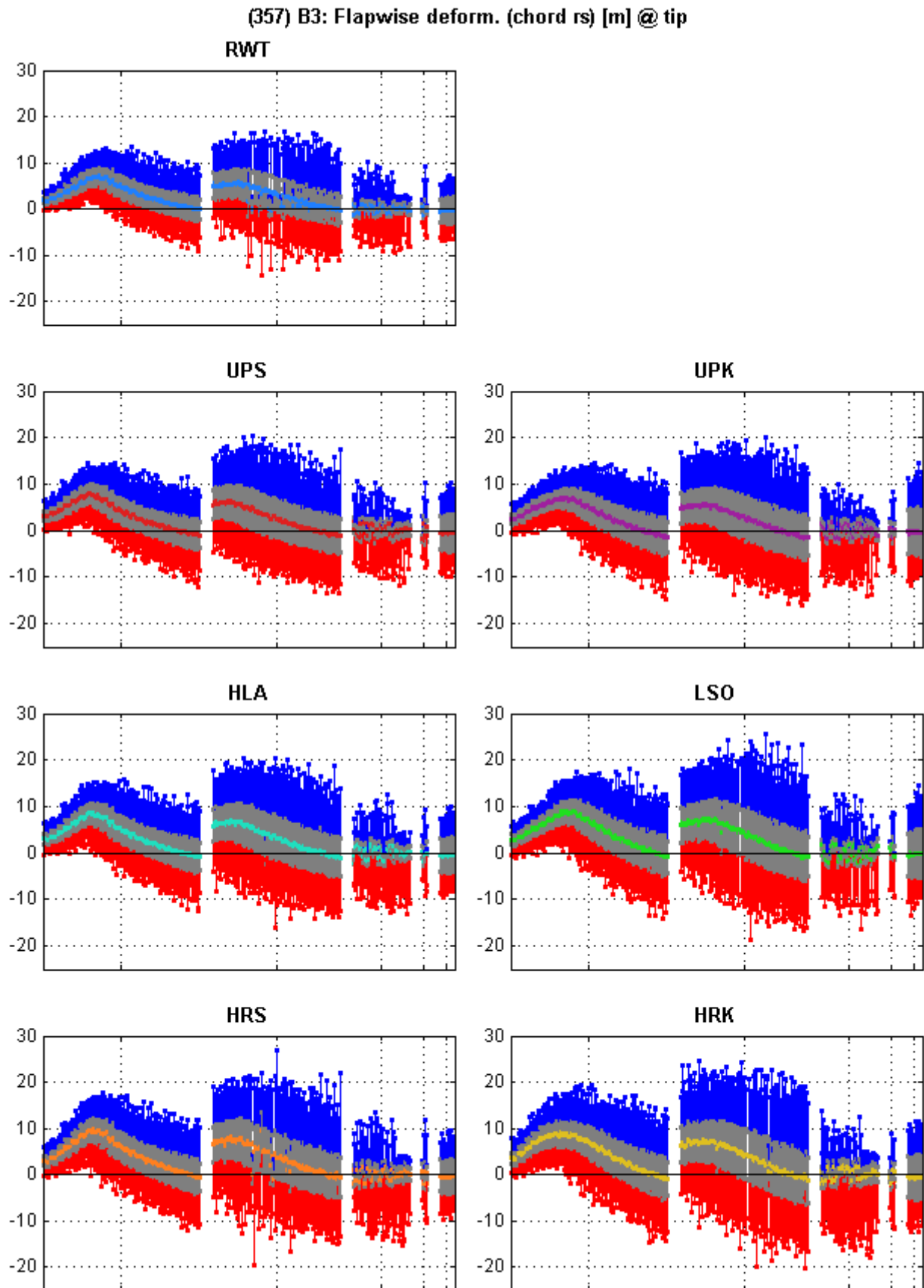


Figure A.12: Blade 3 flap-wise tip displacement in the chord reference system from all DLCs for all designs

(-251) B2: Edgewise bending moment (chord rs) [Nm] @ BR

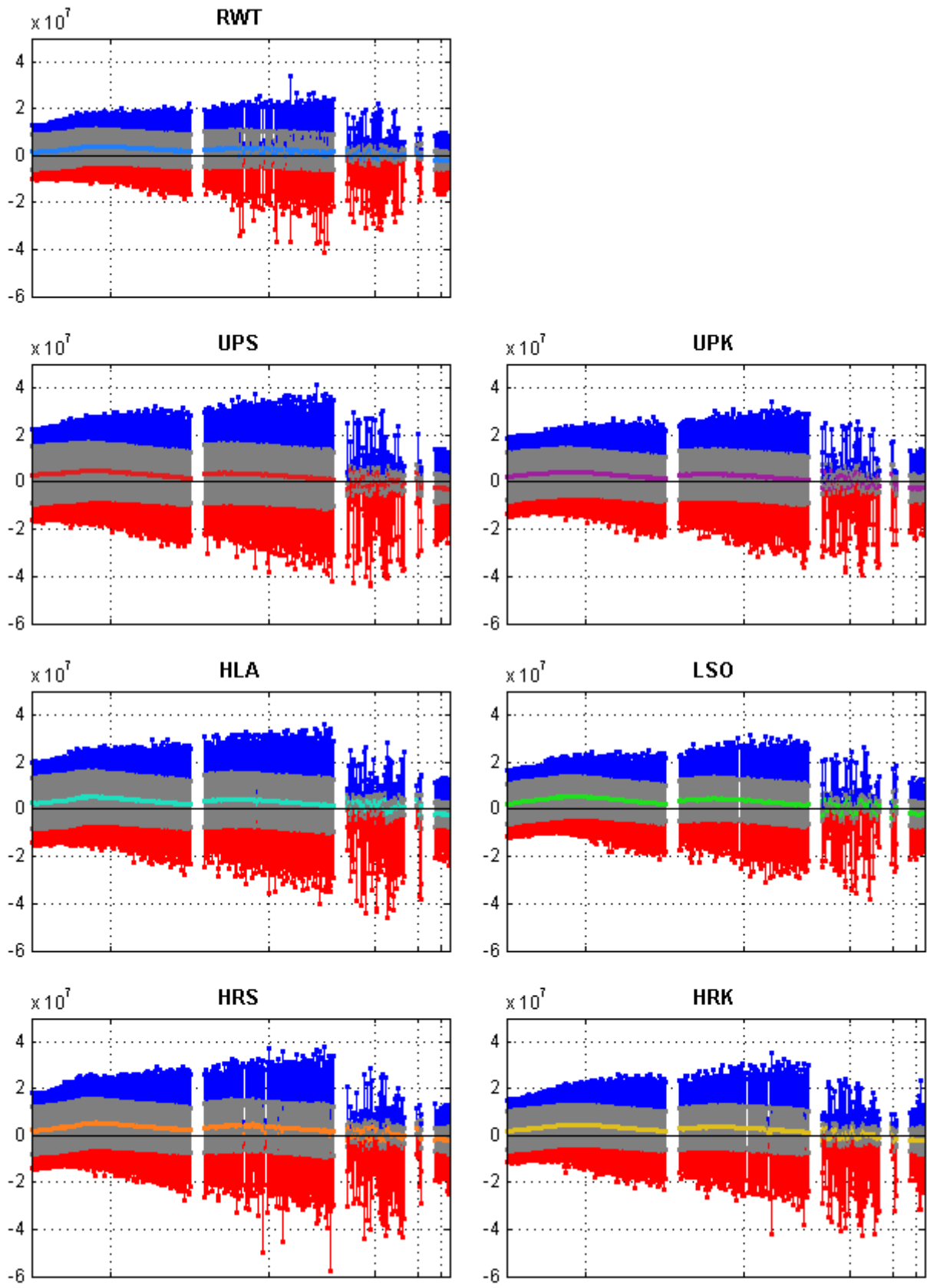


Figure A.13: Blade 2 edge-wise blade root bending moment in the chord reference system from all DLCs for all designs

(-351) B3: Edgewise bending moment (chord rs) [Nm] @ BR

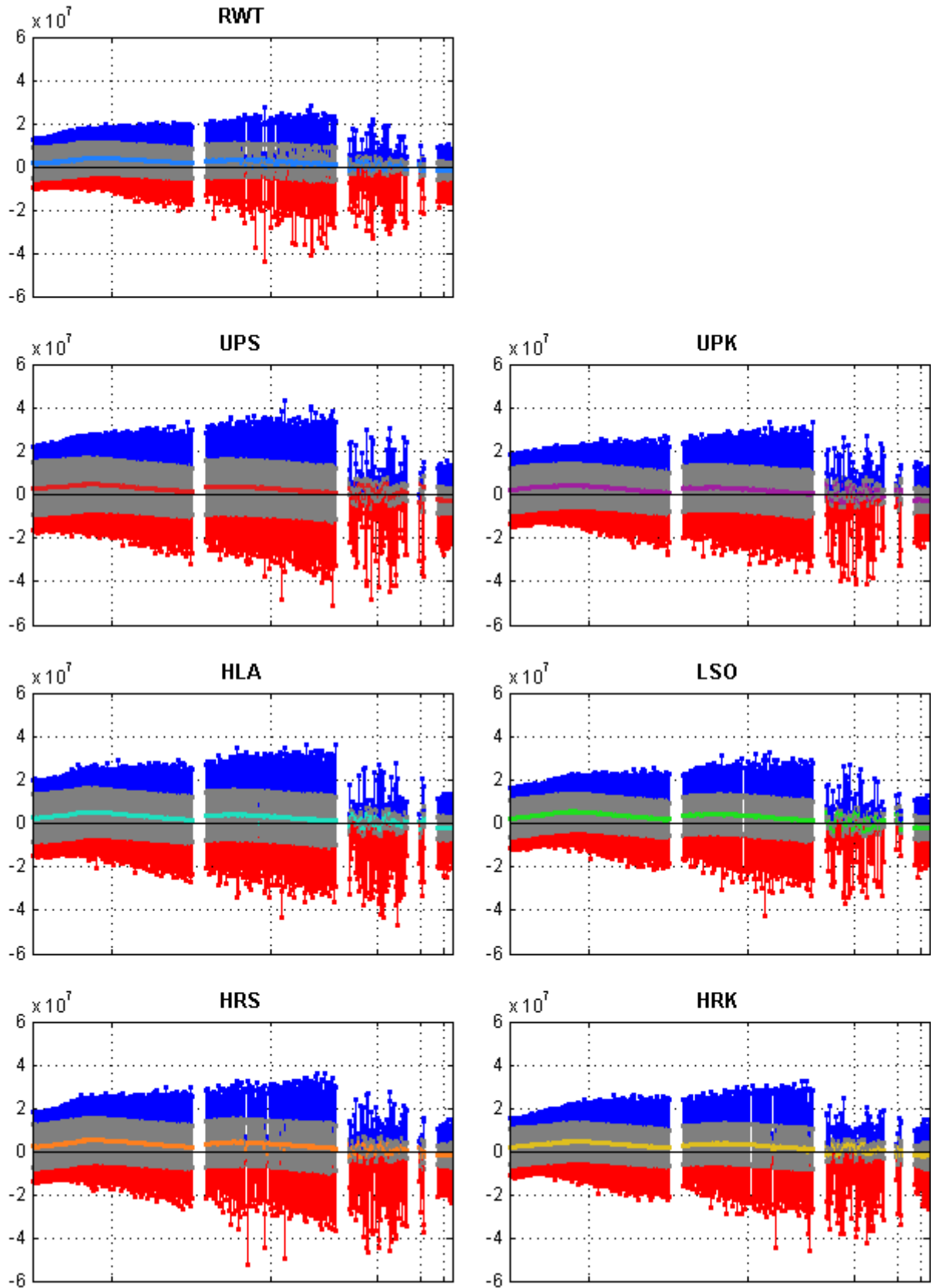


Figure A.14: Blade 3 edge-wise blade root bending moment in the chord reference system from all DLCs for all designs

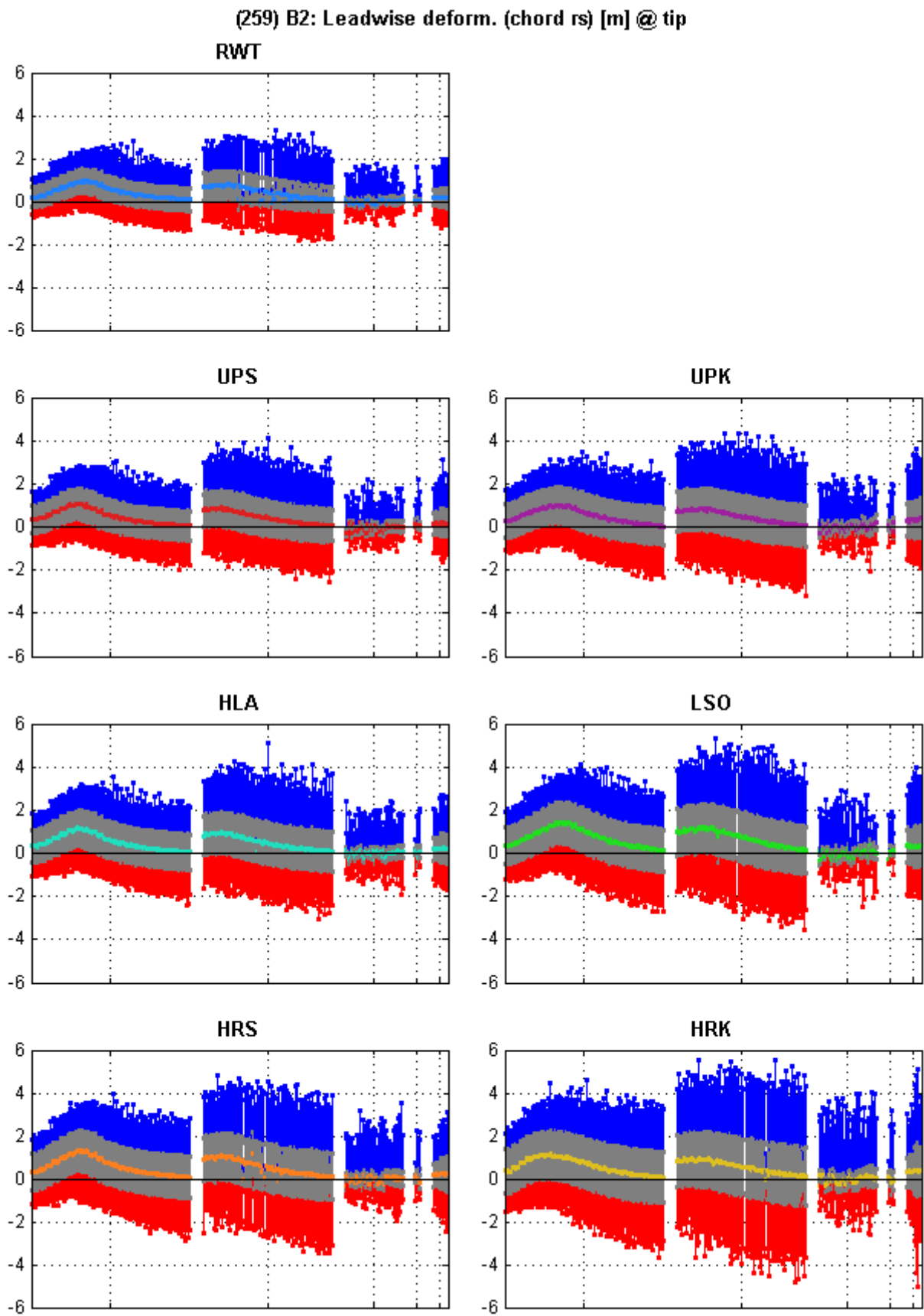


Figure A.15: Blade 2 edge-wise tip displacement in the chord reference system from all DLCs for all designs

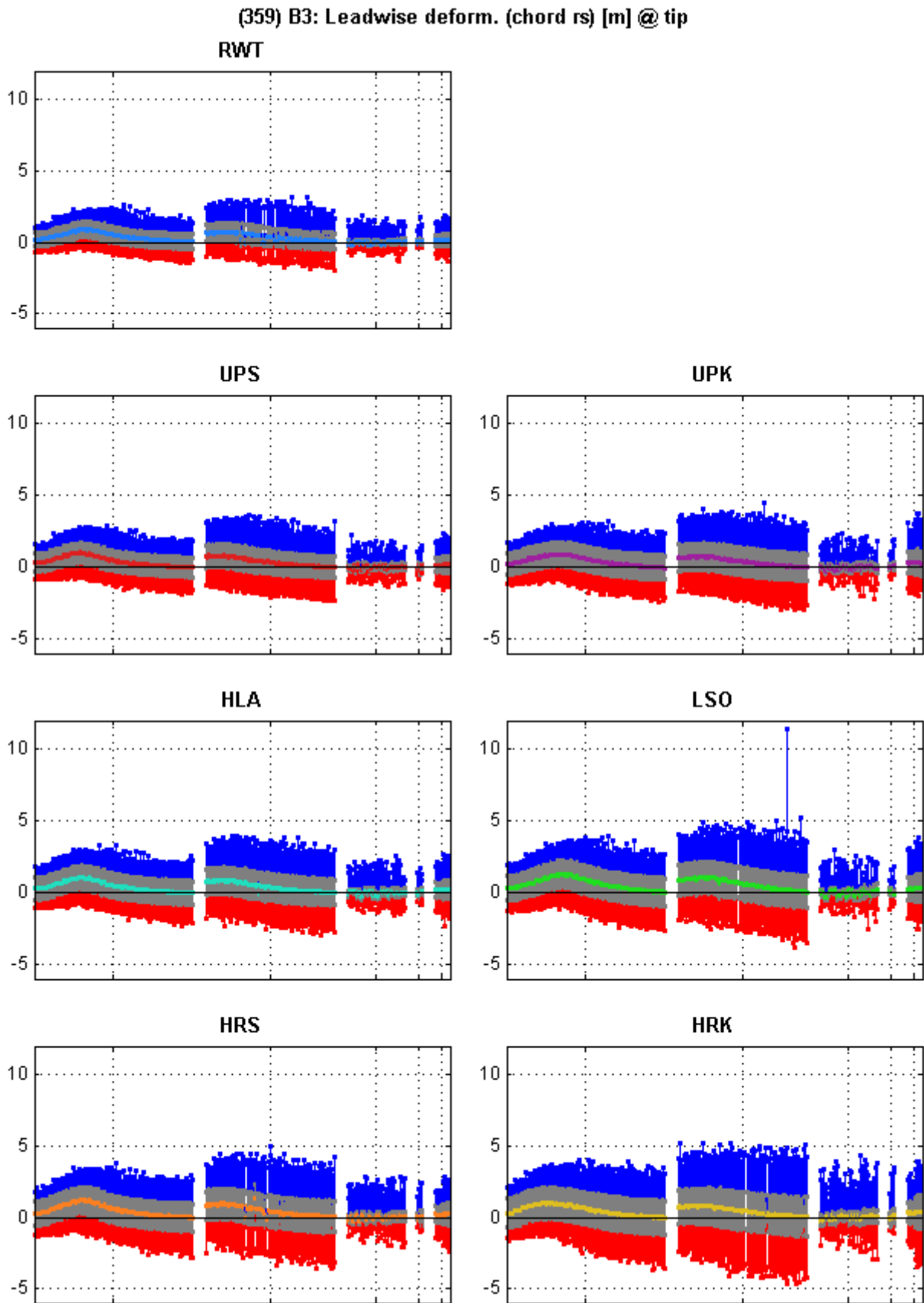


Figure A.16: Blade 3 edge-wise tip displacement in the chord reference system from all DLCs for all designs

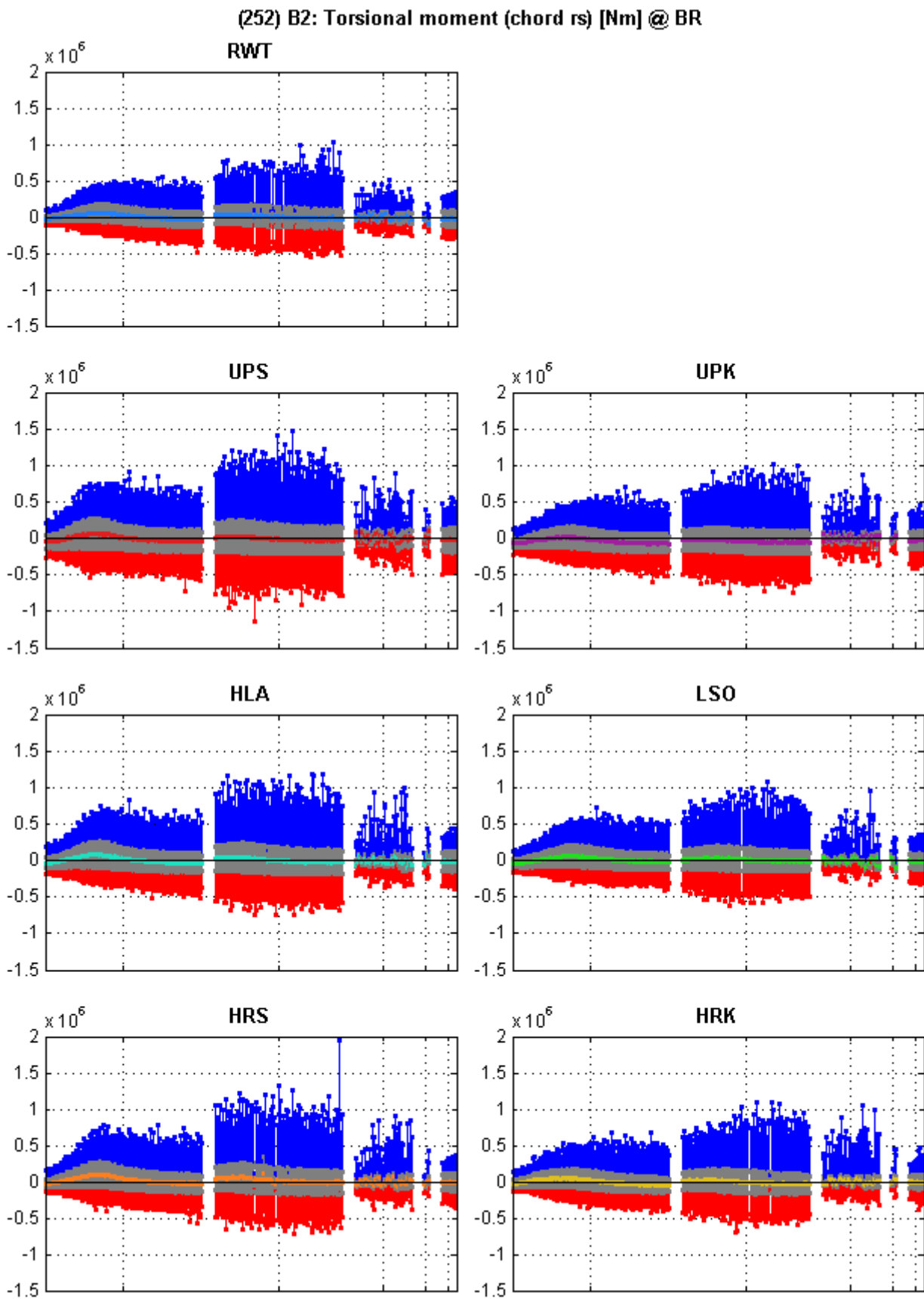


Figure A.17: Blade 2 torsional blade root moment in the chord reference system from all DLCs for all designs

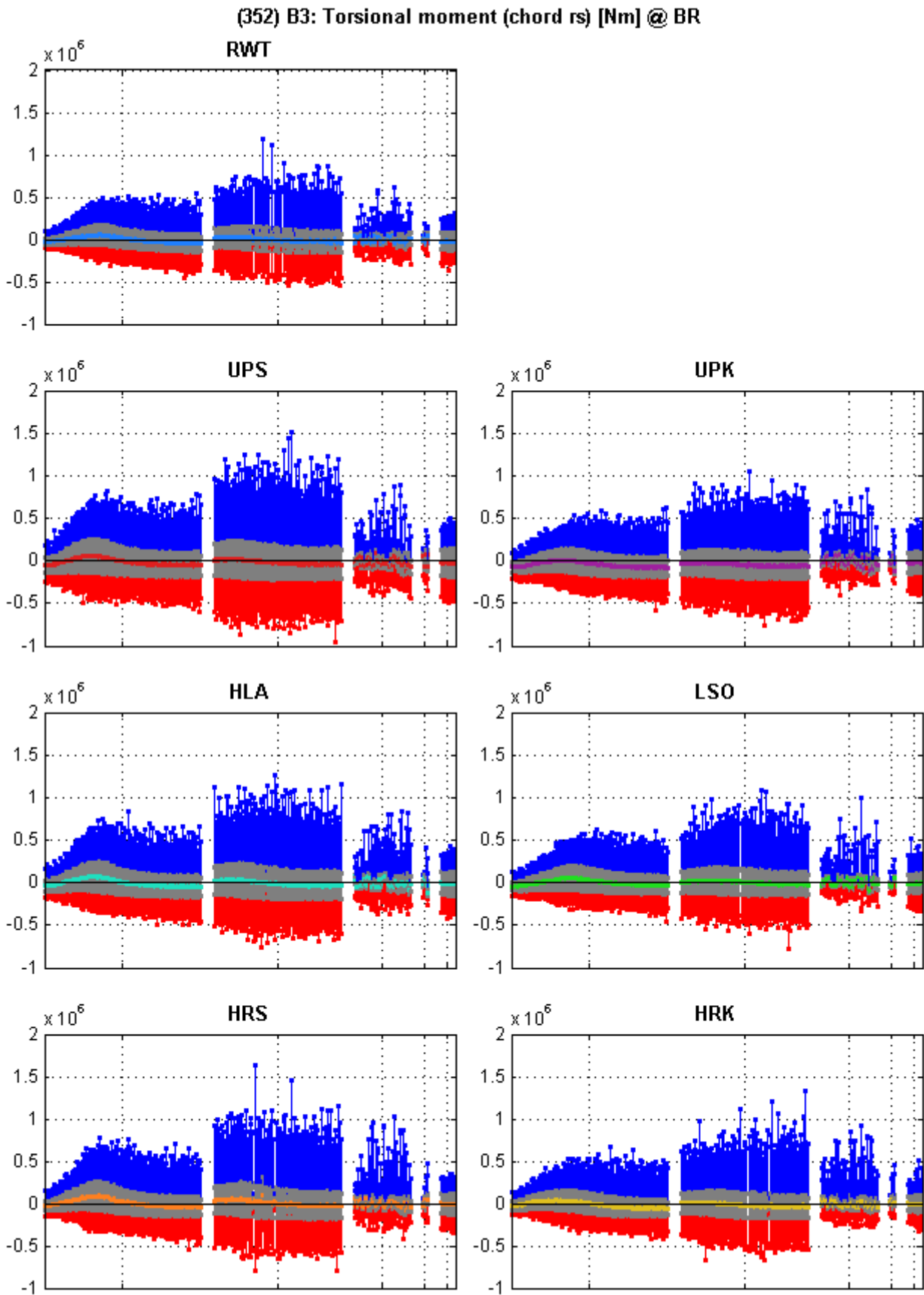


Figure A.18: Blade 3 torsional blade root moment in the chord reference system from all DLCs for all designs

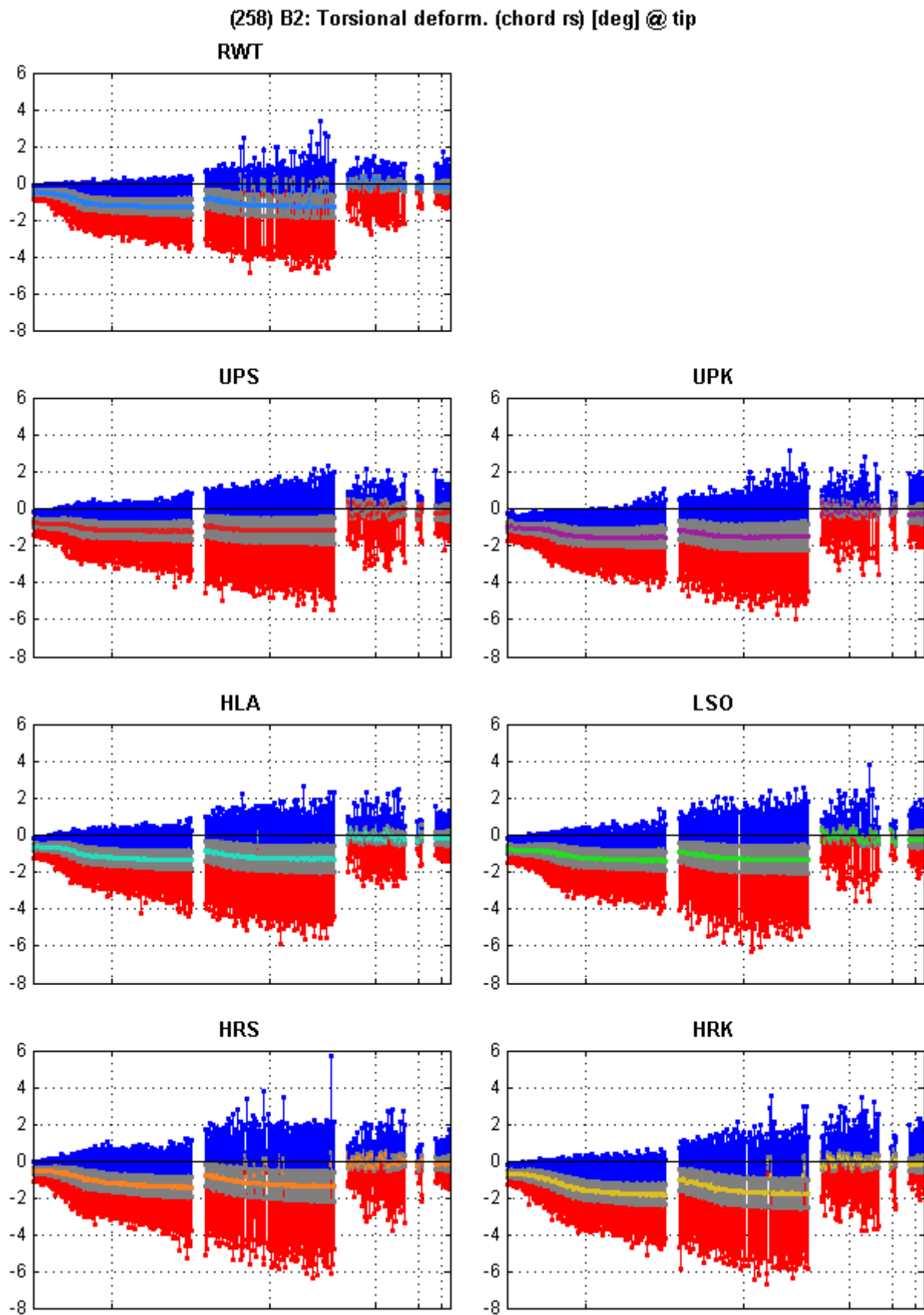


Figure A.19: Blade 2 torsional tip displacement in the chord reference system from all DLCs for all designs

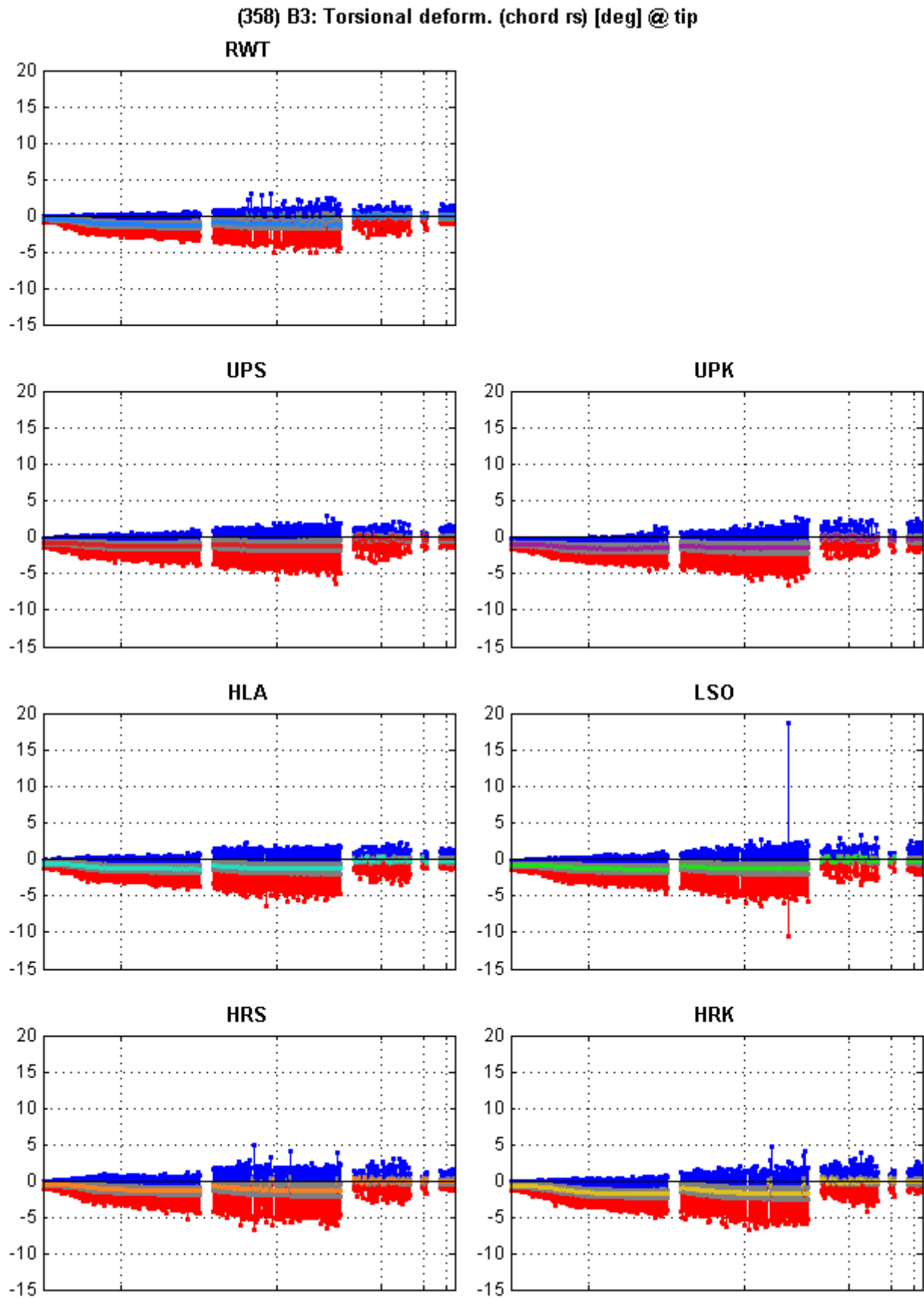


Figure A.20: Blade 3 torsional tip displacement in the chord reference system from all DLCs for all designs

(27) Nacelle displ. in X_{GL} direction (FA) [m] @ 115.63 m

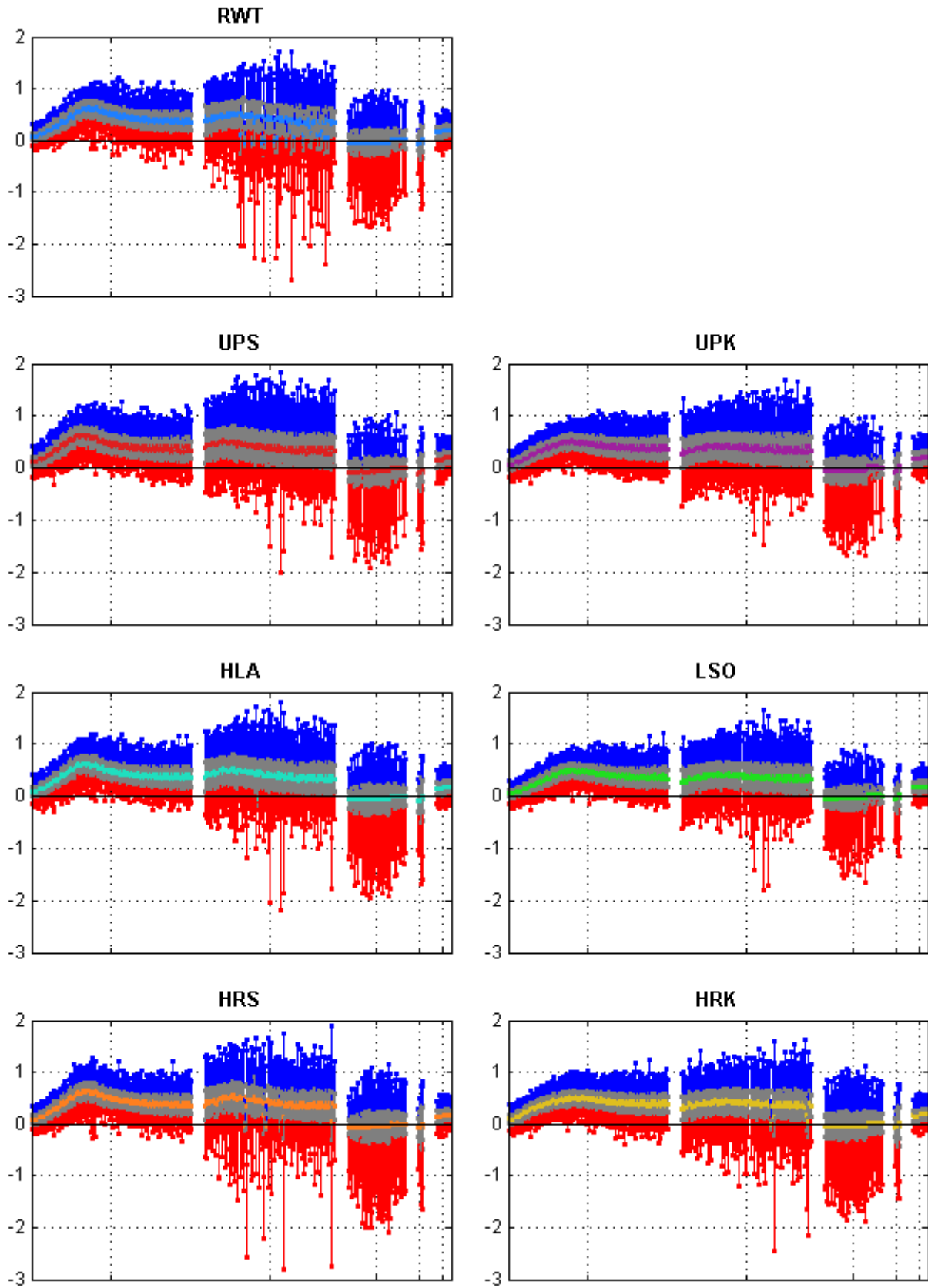


Figure A.21: Tower top/nacelle fore-aft displacement from all DLCs for all designs

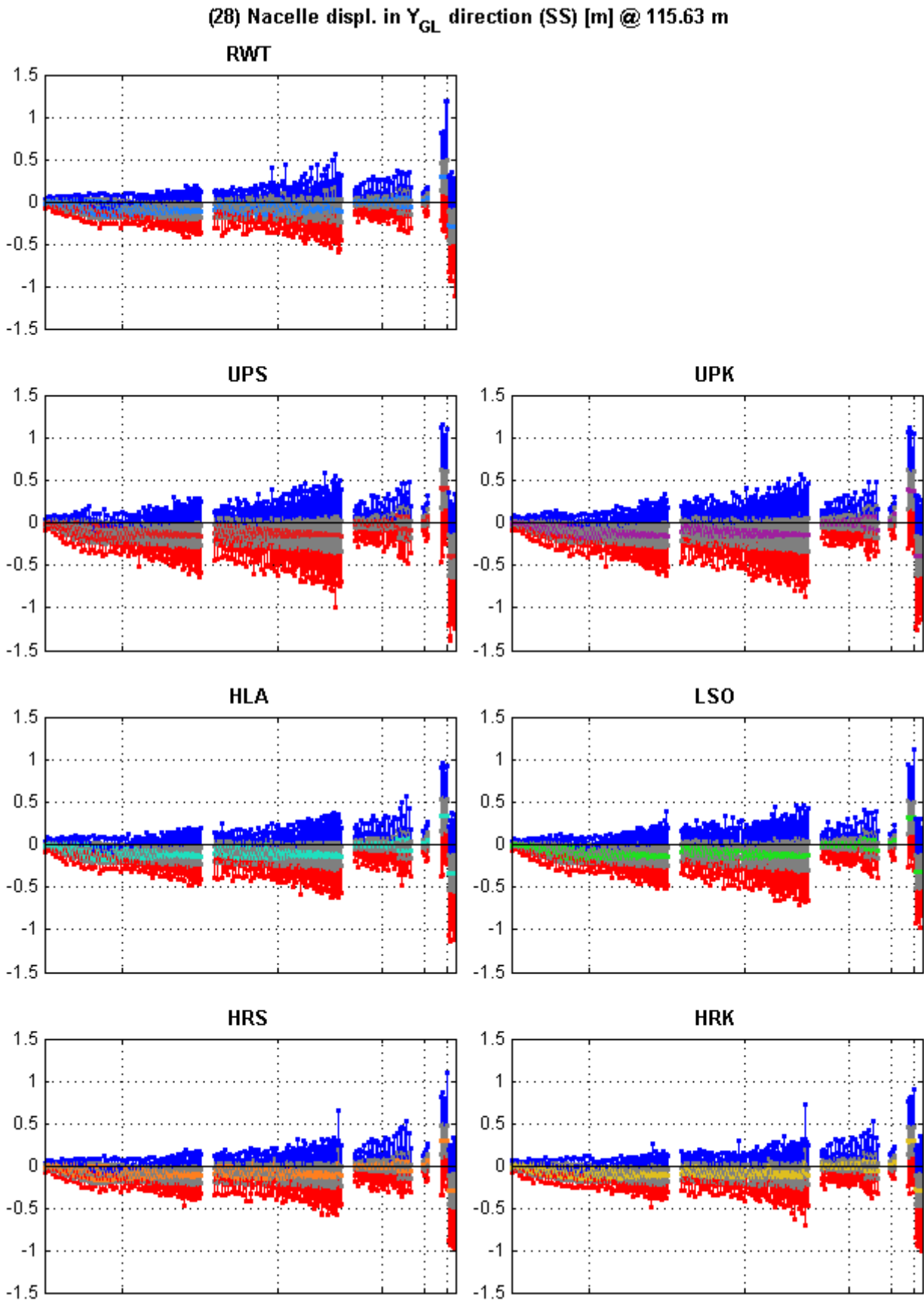


Figure A.22: Tower top/nacelle side-to-side displacement from all DLCs for all designs

(29) Torsional deform. of the tower [deg] @ 115.63 m

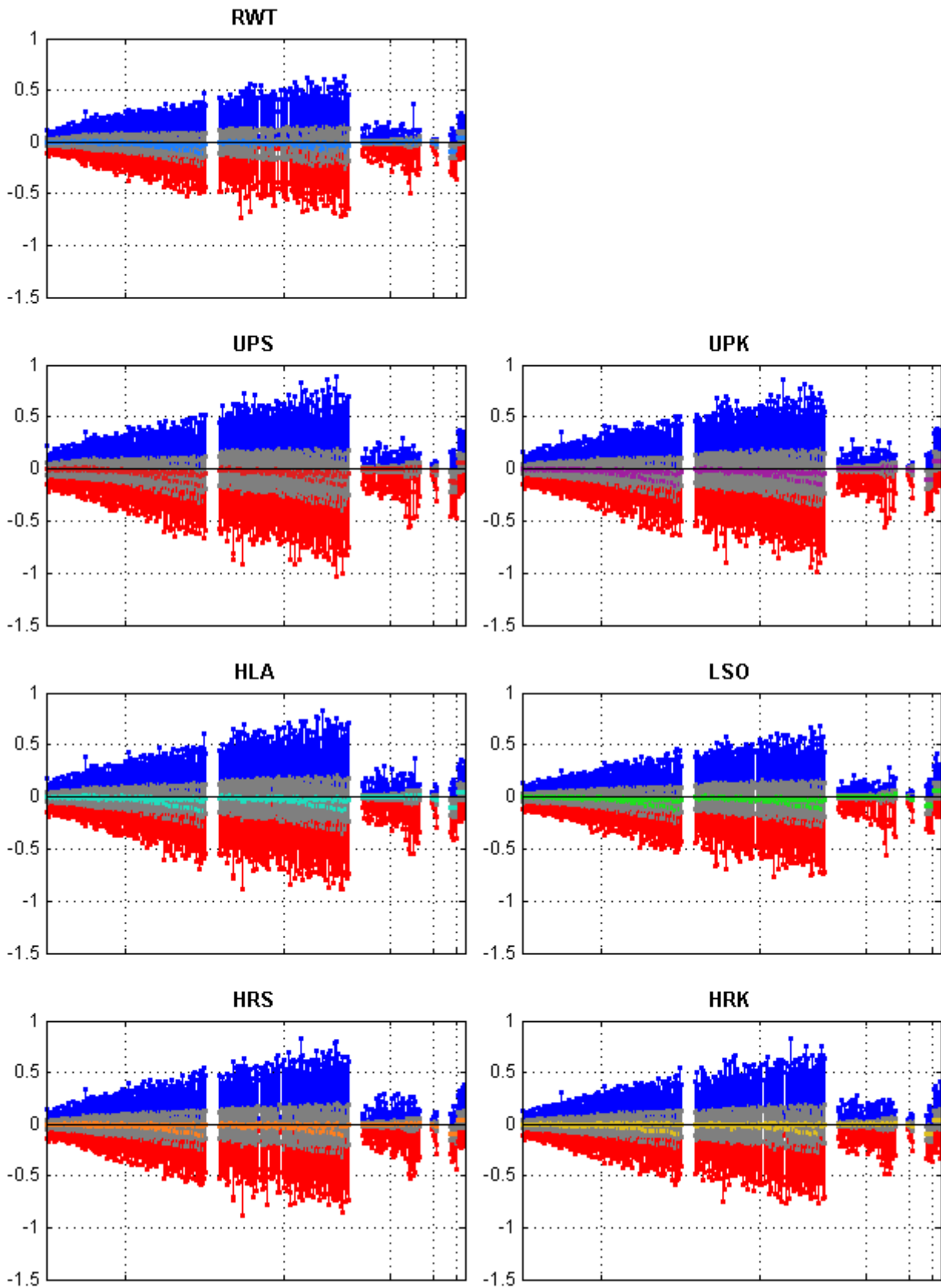


Figure A.23: Tower top/nacelle torsional displacement from all DLCs for all designs

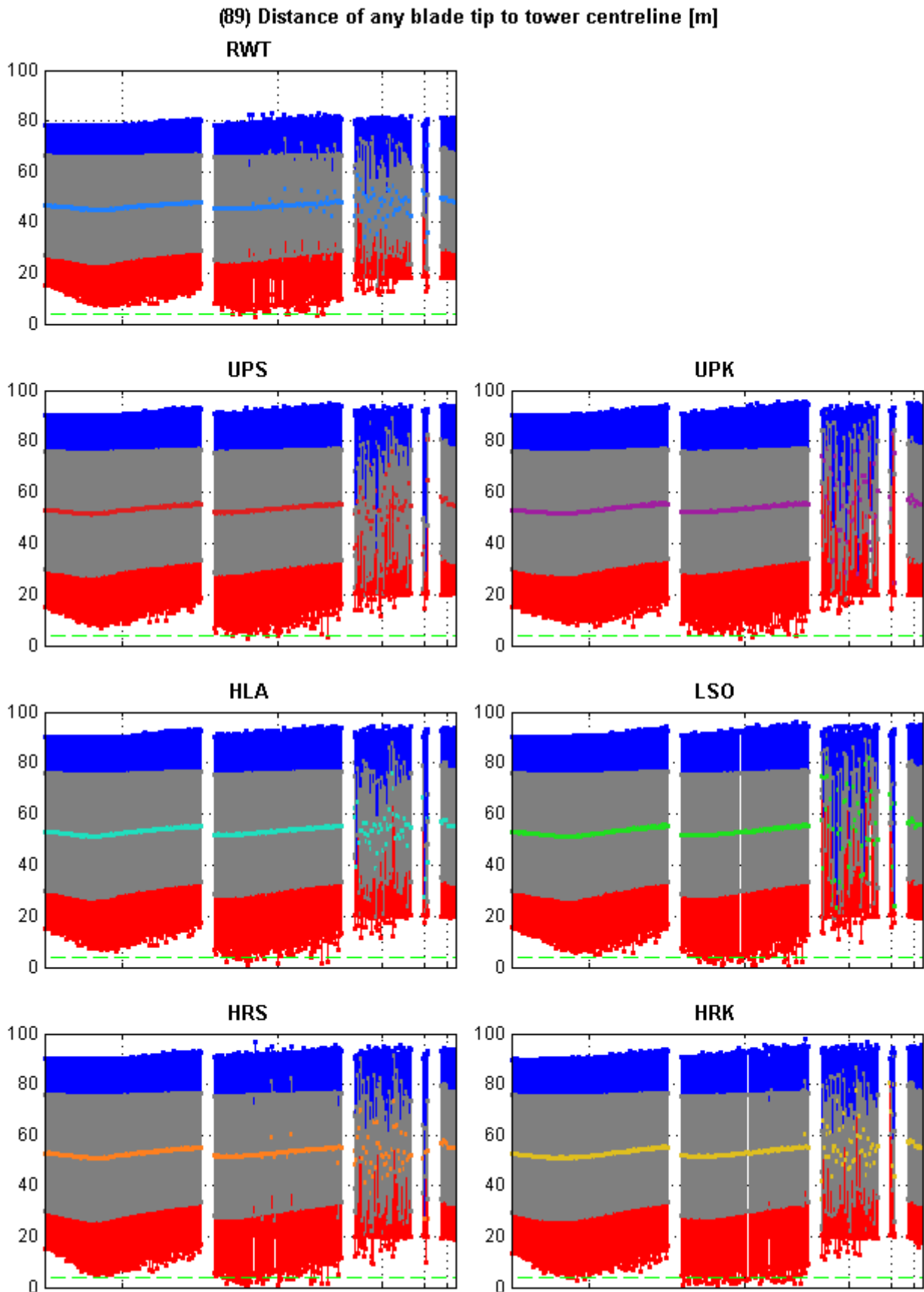


Figure A.24: Blade tip 1, 2 or 3 clearance from centre of tower from all DLCs for all designs (0 value represents tower centre and green margin tower radius at passing point. Untreated signal, $\pm 60^\circ$ window)

A.3 Additional Fatigue Loads Figures (DLC 1.2)

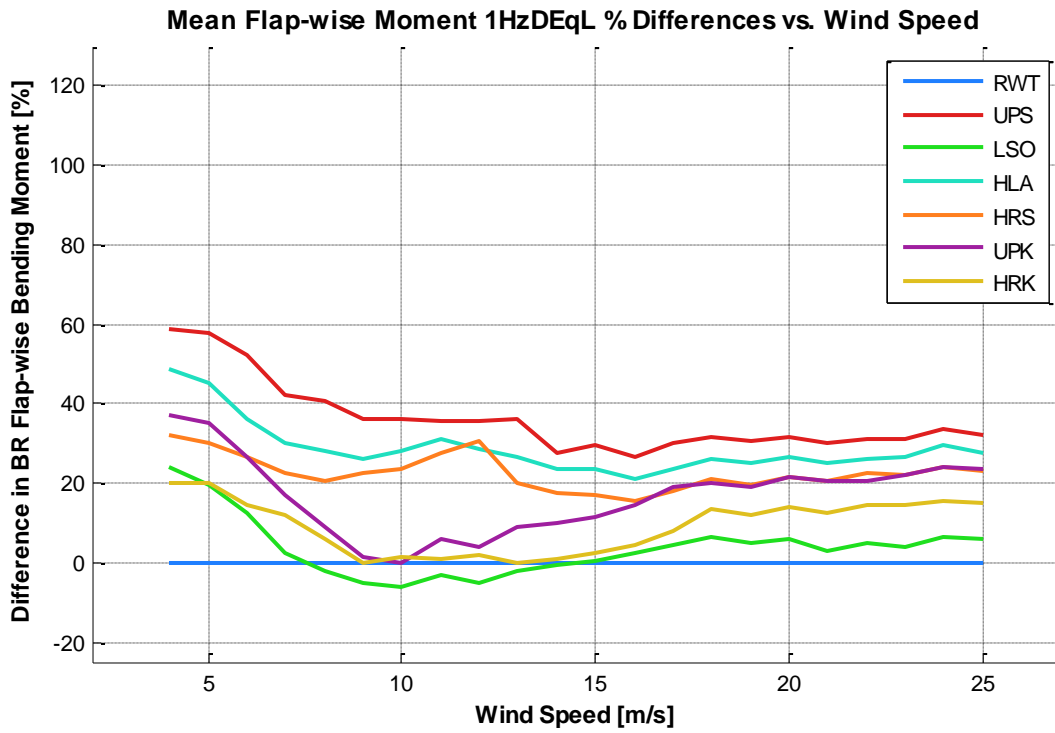


Figure A.25: The mean flap-wise blade root bending moment percent differences versus all operating wind speeds (not Weibull-weighted) for all designs from all DLC 1.2 simulations

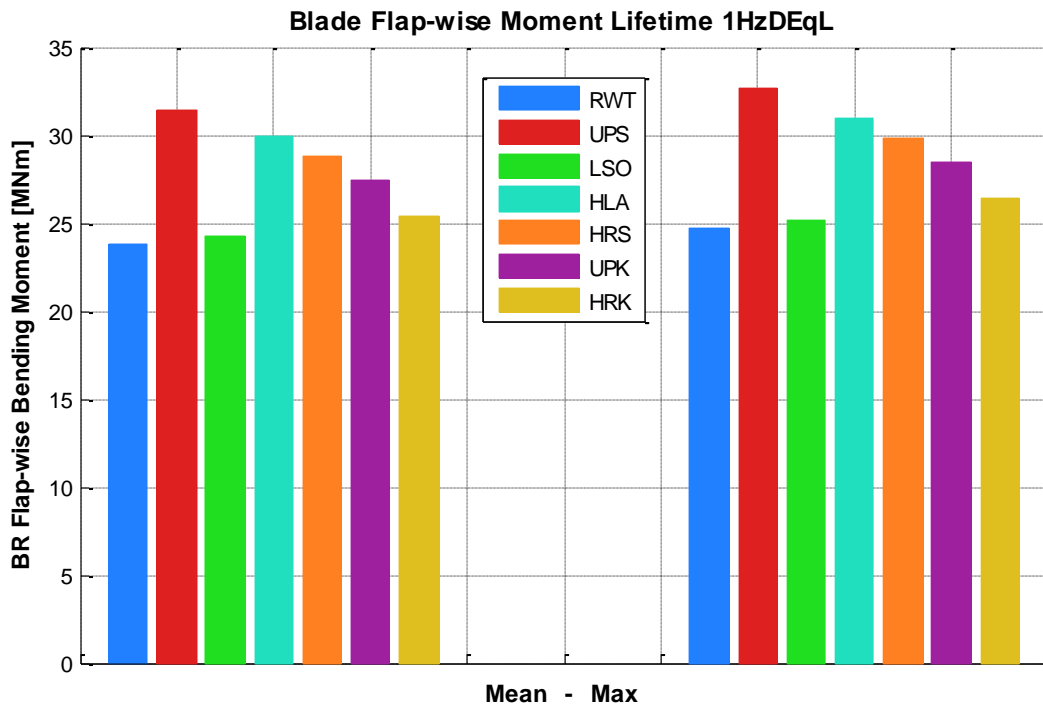


Figure A.26: Mean and maximum lifetime equivalent flap-wise blade root bending moment for all designs from all DLC 1.2 simulations

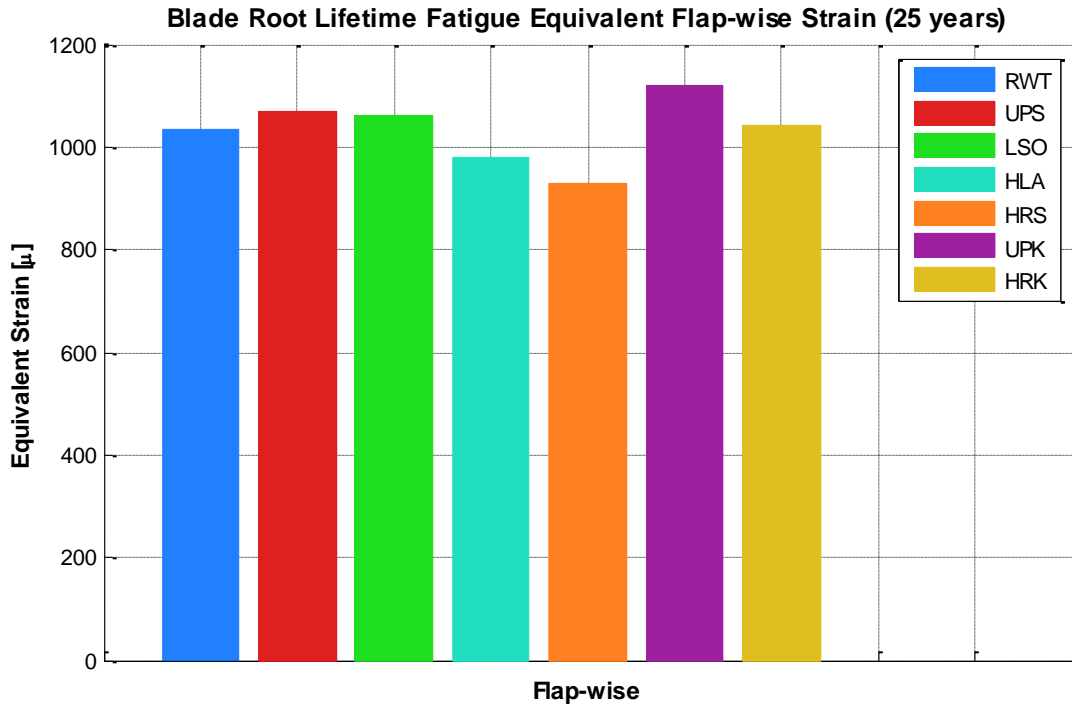


Figure A.27: Mean lifetime equivalent flap-wise blade root strain of all designs from all DLC 1.2 simulations

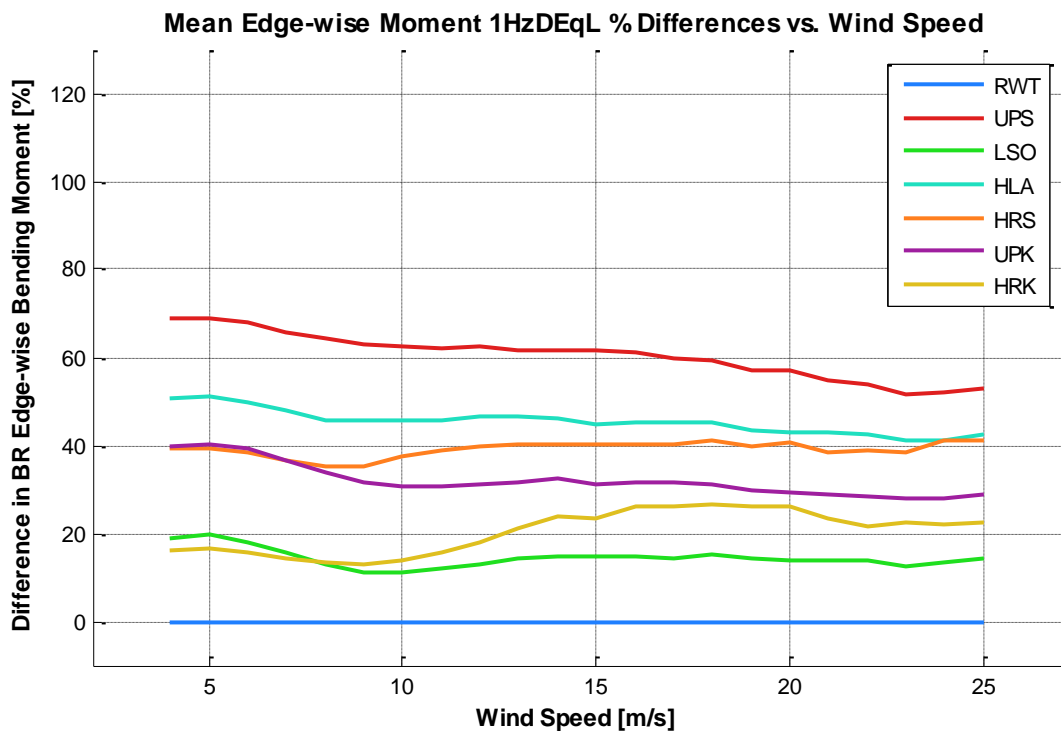


Figure A.28: The mean edge-wise blade root bending moment percent differences versus all operating wind speeds (not Weibull-weighted) for all designs from all DLC 1.2 simulations

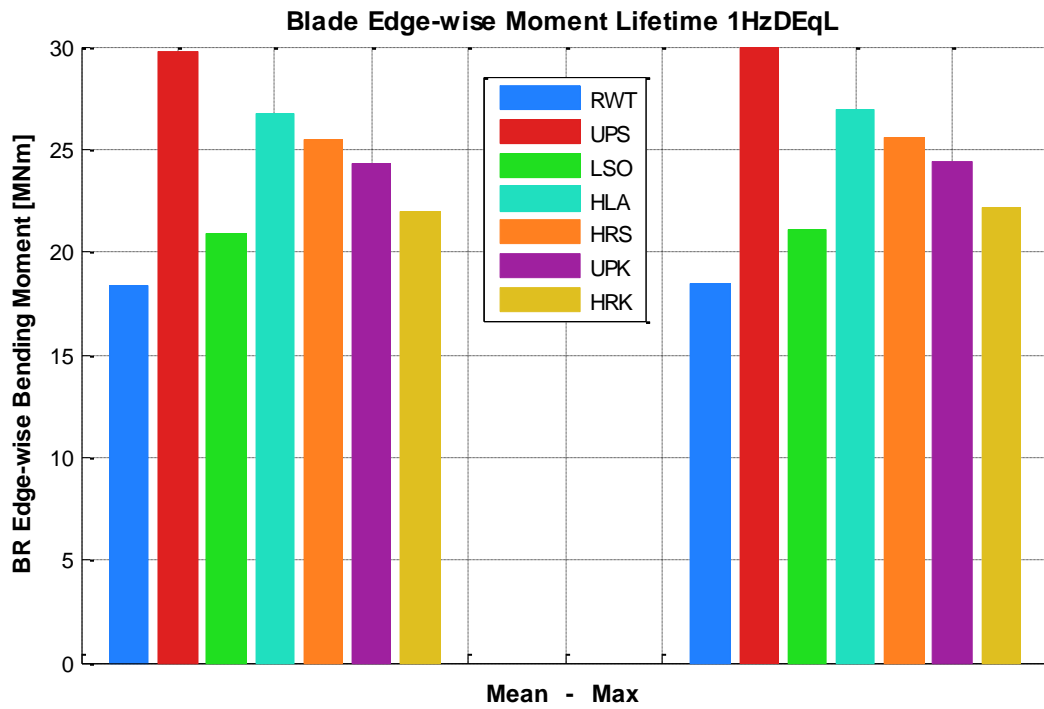


Figure A.29: Mean and maximum lifetime equivalent edge-wise blade root bending moment for all designs from all DLC 1.2 simulations

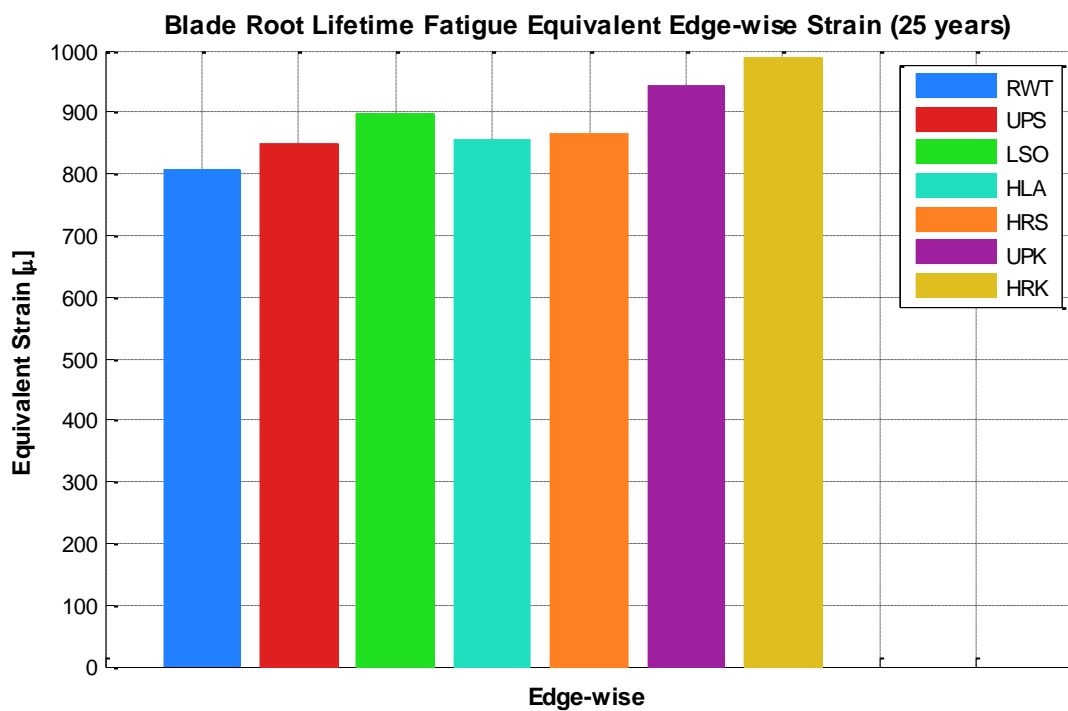


Figure A.30: Mean lifetime equivalent edge-wise blade root strain of all designs from all DLC 1.2 simulations

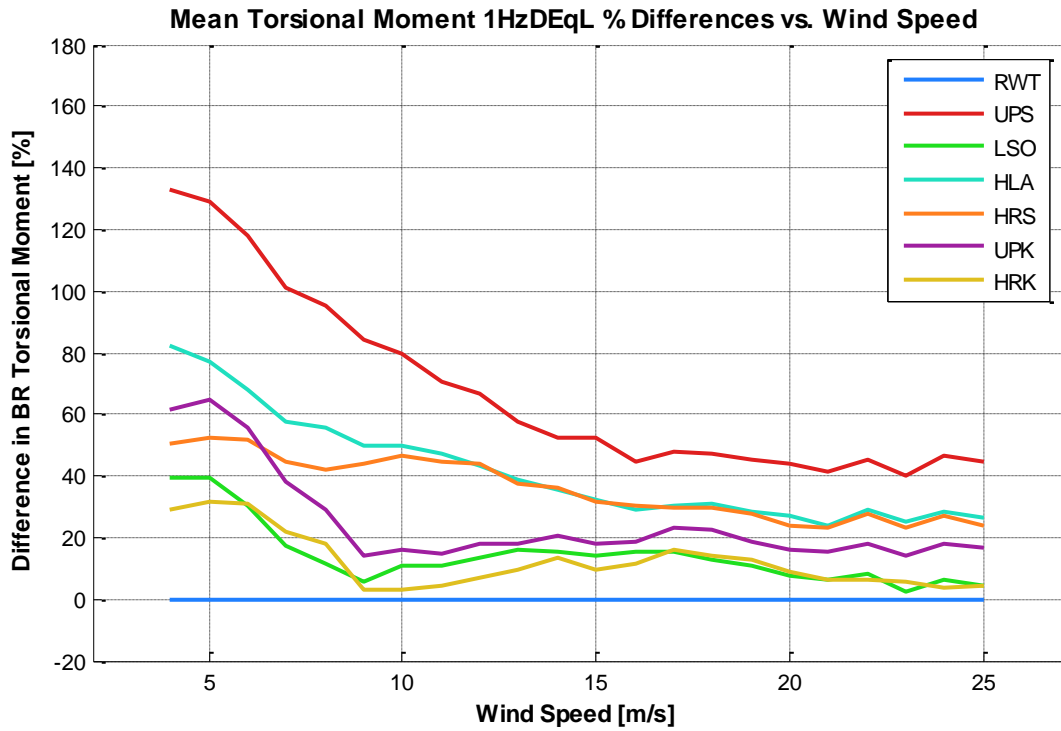


Figure A.31: The mean torsional blade root moment percent differences versus all operating wind speeds (not Weibull-weighted) for all designs from all DLC 1.2 simulations

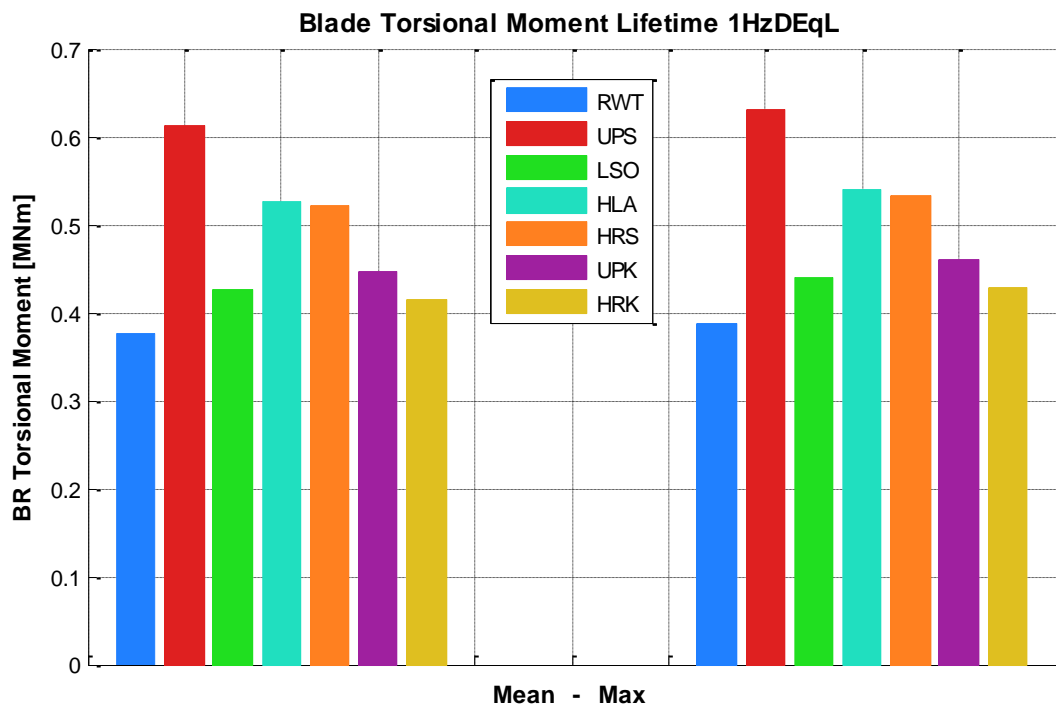


Figure A.32: Mean and maximum lifetime equivalent torsional blade root moment for all designs from all DLC 1.2 simulations

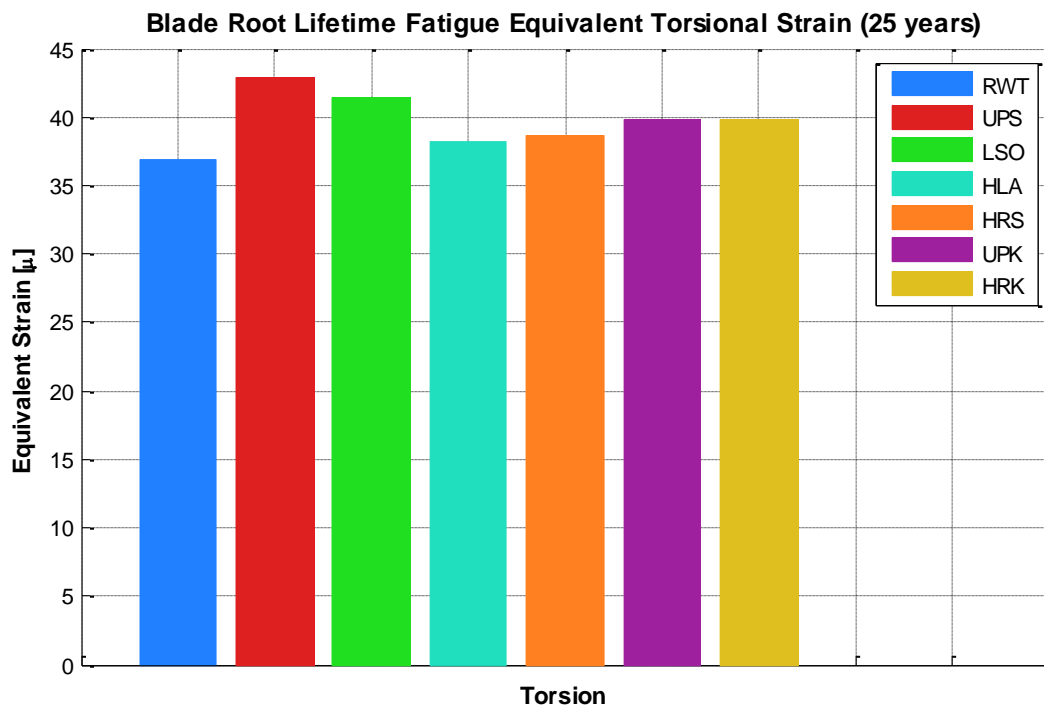


Figure A.33: Mean lifetime equivalent torsional blade root strain of all designs from all DLC 1.2 simulations

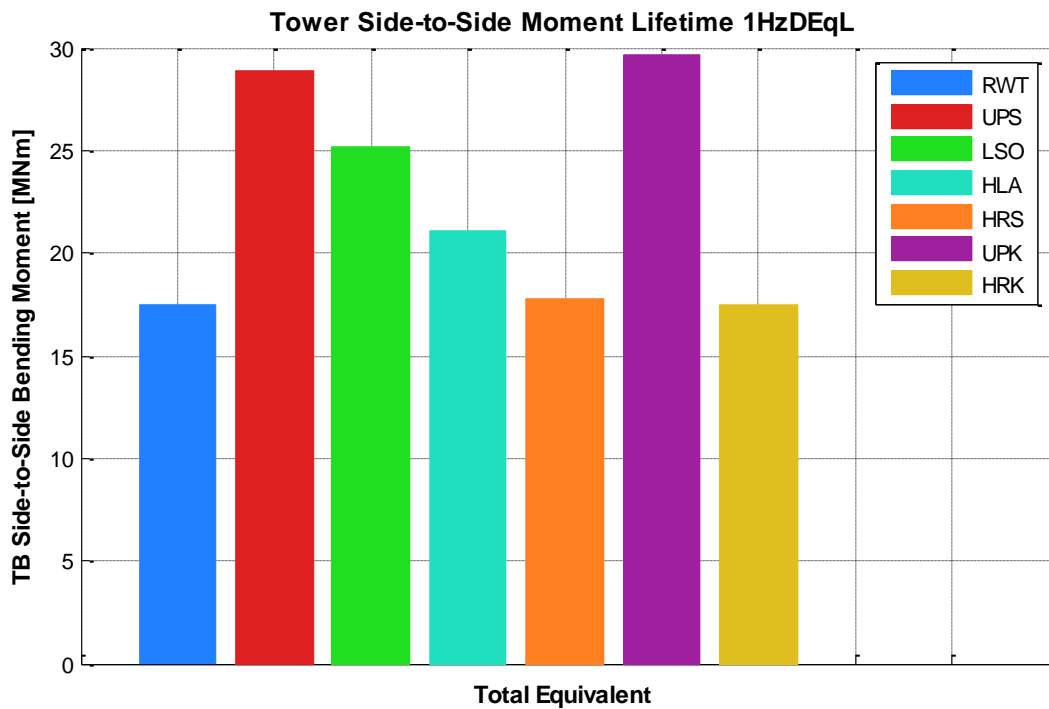
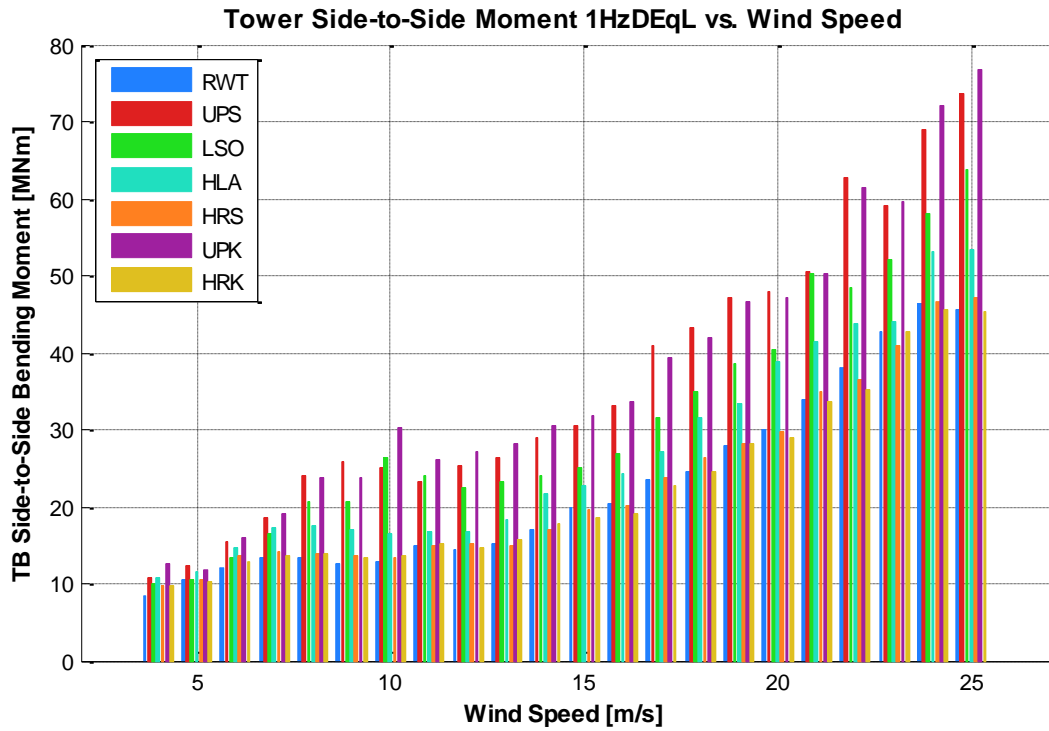


Figure A.34: The tower bottom side-to-side moment versus all operating wind speeds (not Weibull-weighted) and lifetime damage equivalent moment of all designs from all DLC 1.2 simulations

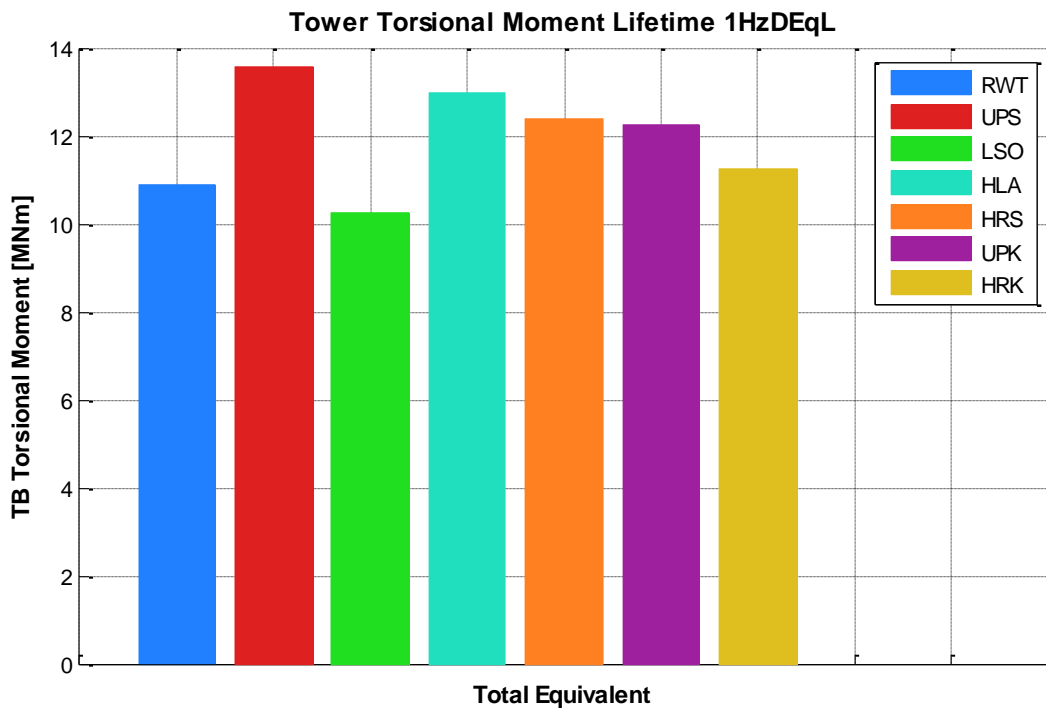
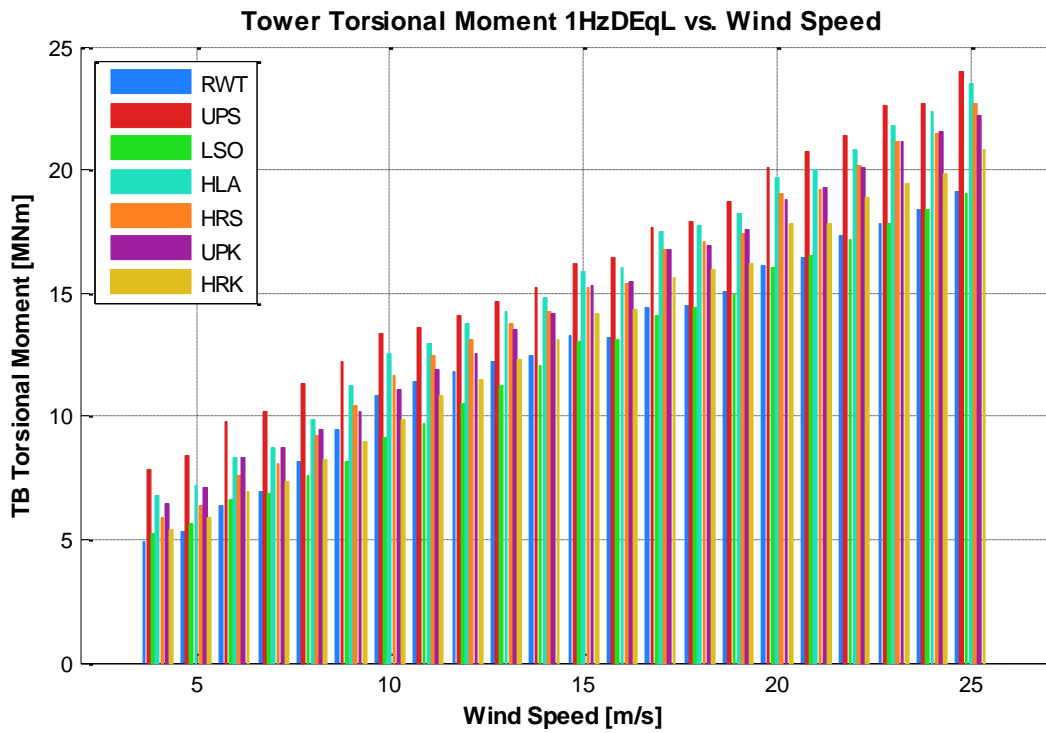


Figure A.35: The tower bottom torsional moment versus all operating wind speeds (not Weibull-weighted) and lifetime damage equivalent moment of all designs from all DLC 1.2 simulations

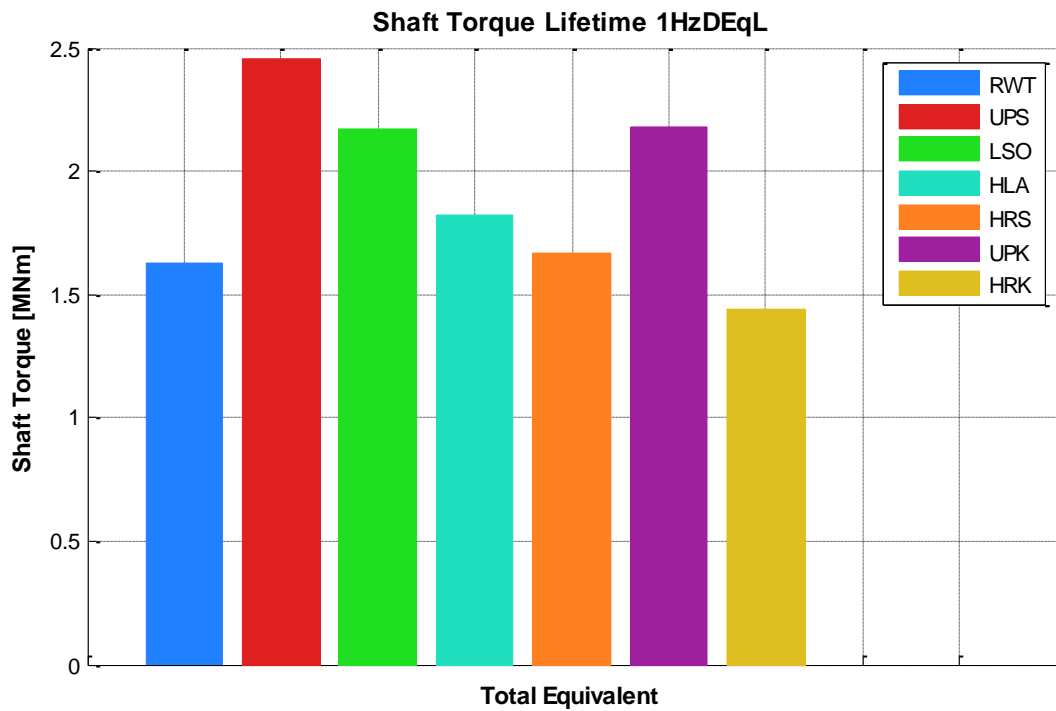
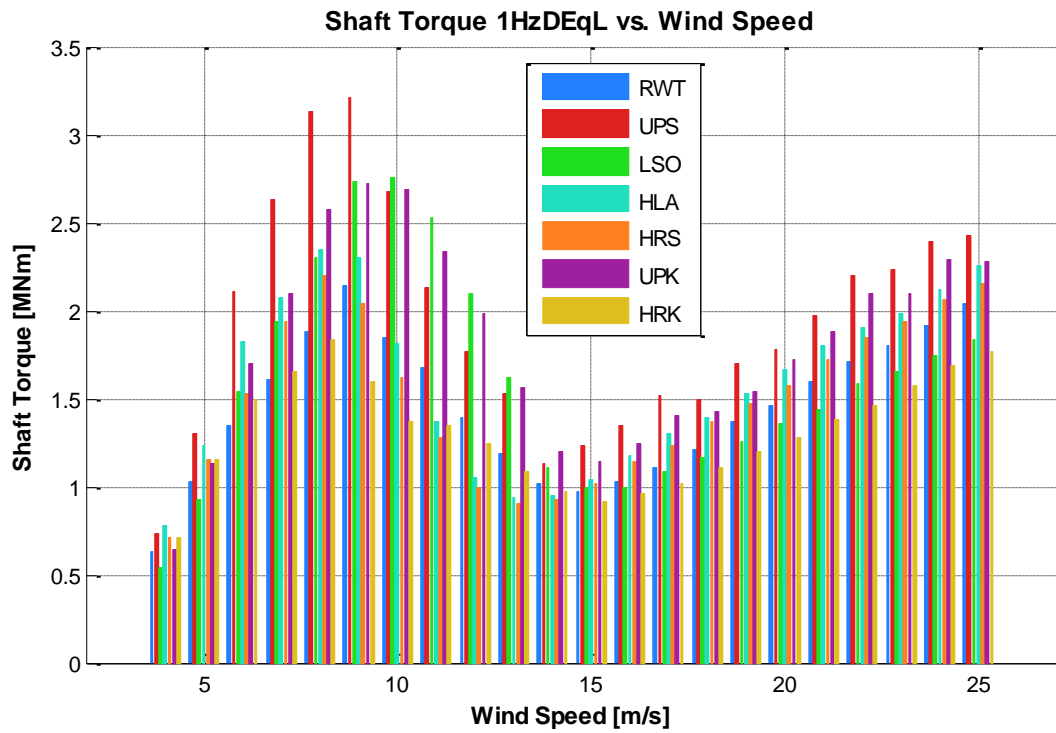


Figure A.36: The shaft torque versus all operating wind speeds (not Weibull-weighted) and lifetime damage equivalent torque of all designs from all DLC 1.2 simulations

A.4 Fatigue Loads Figures (DLC 4.1)

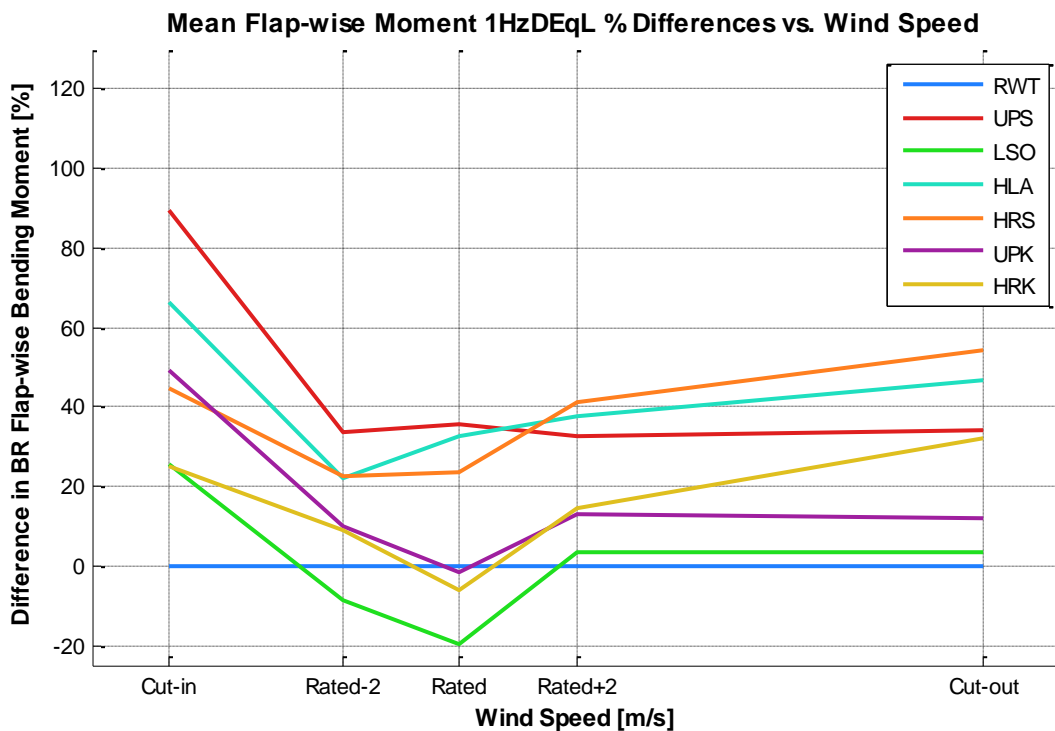
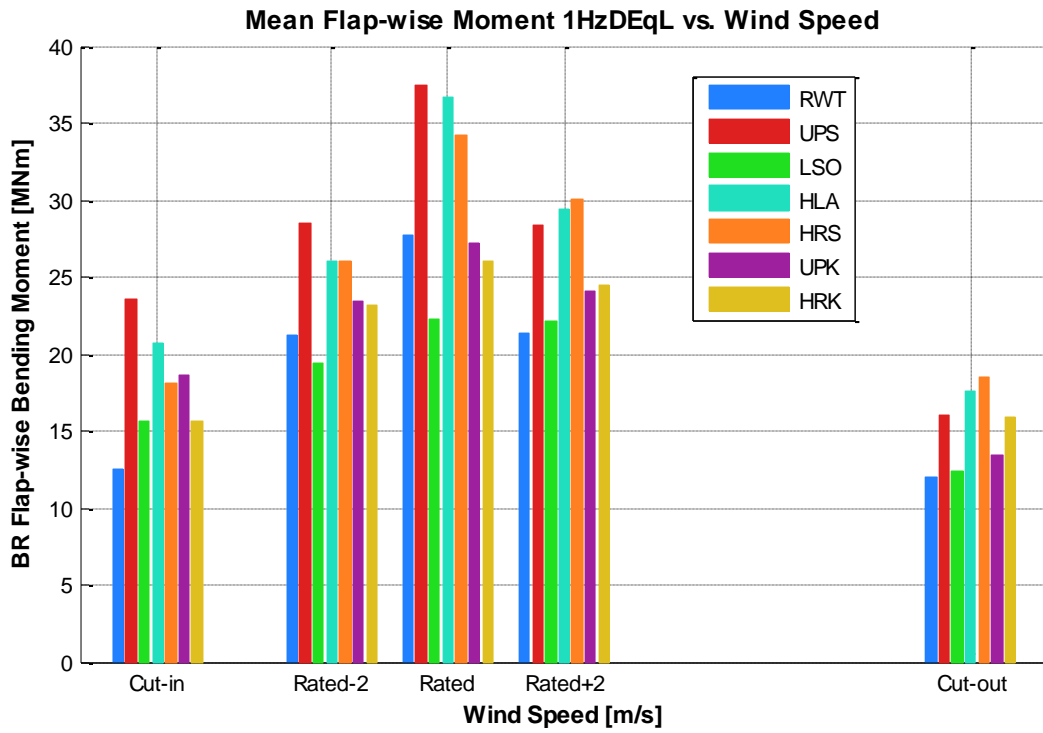


Figure A.37: The mean flap-wise blade root bending moment and percent differences versus shut-down wind speeds (not Weibull-weighted) for all designs from all DLC 4.1 simulations

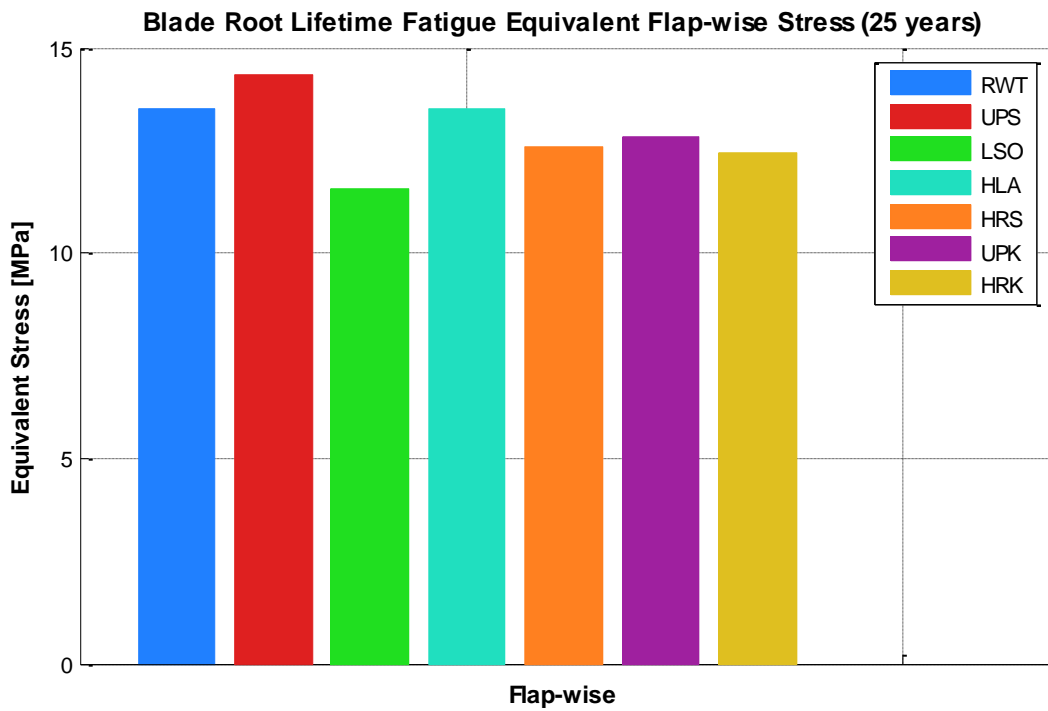
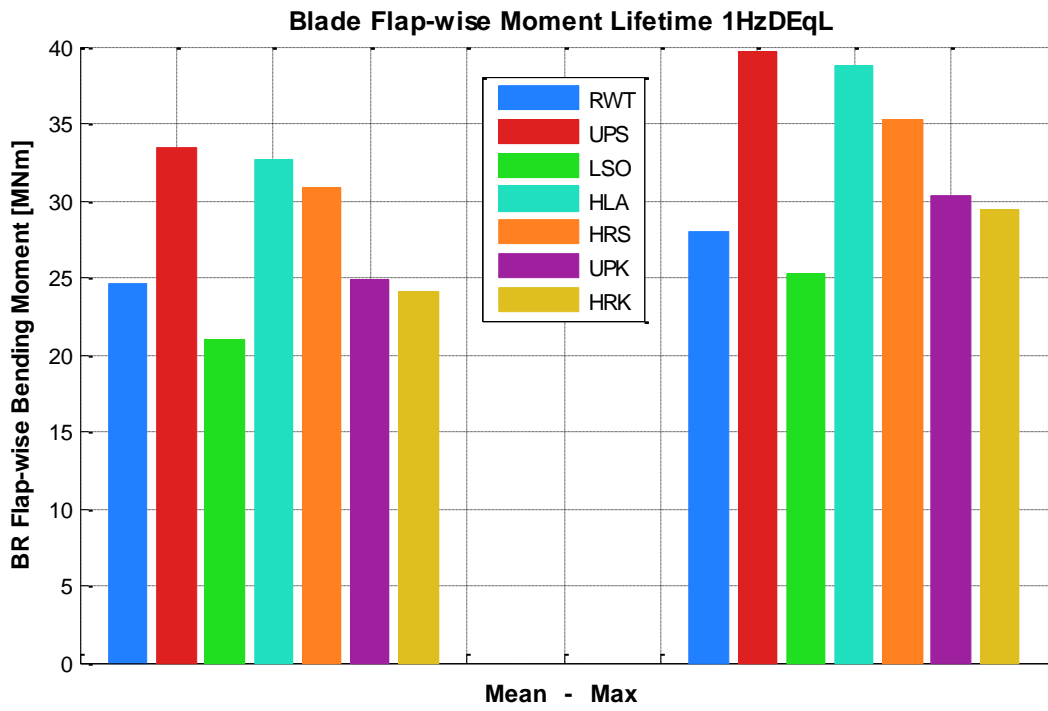


Figure A.38: Mean and maximum lifetime equivalent flap-wise blade root bending moment and stress for all designs from all DLC 4.1 simulations

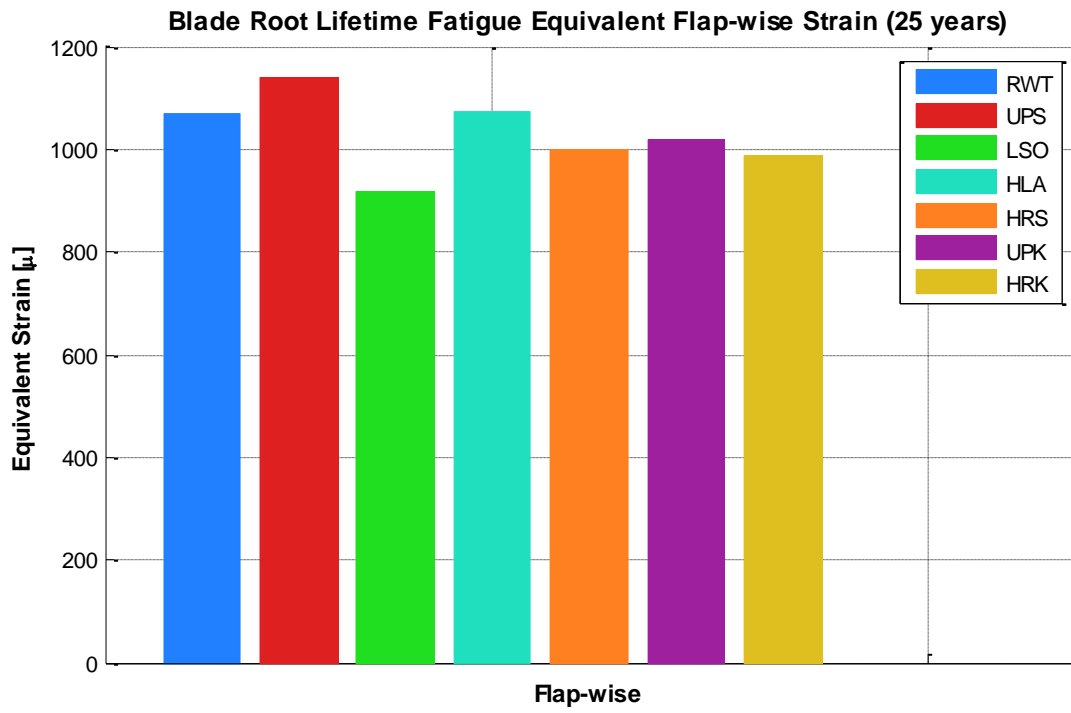


Figure A.39: Mean lifetime equivalent flap-wise blade root strain of all designs from all DLC 4.1 simulations

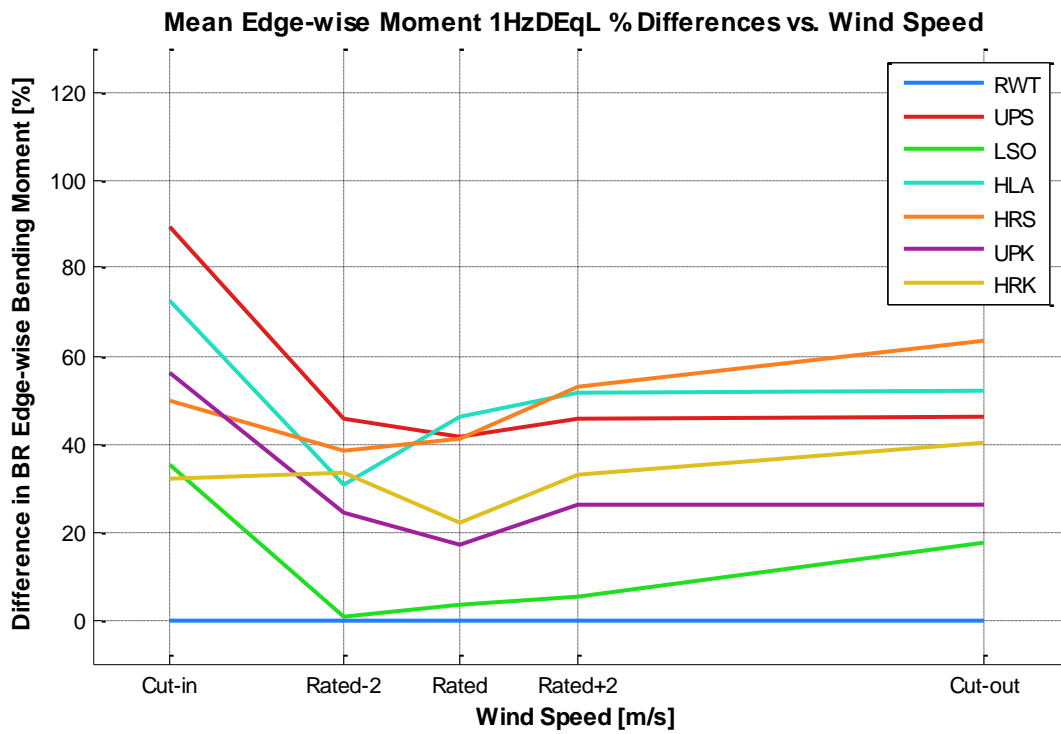
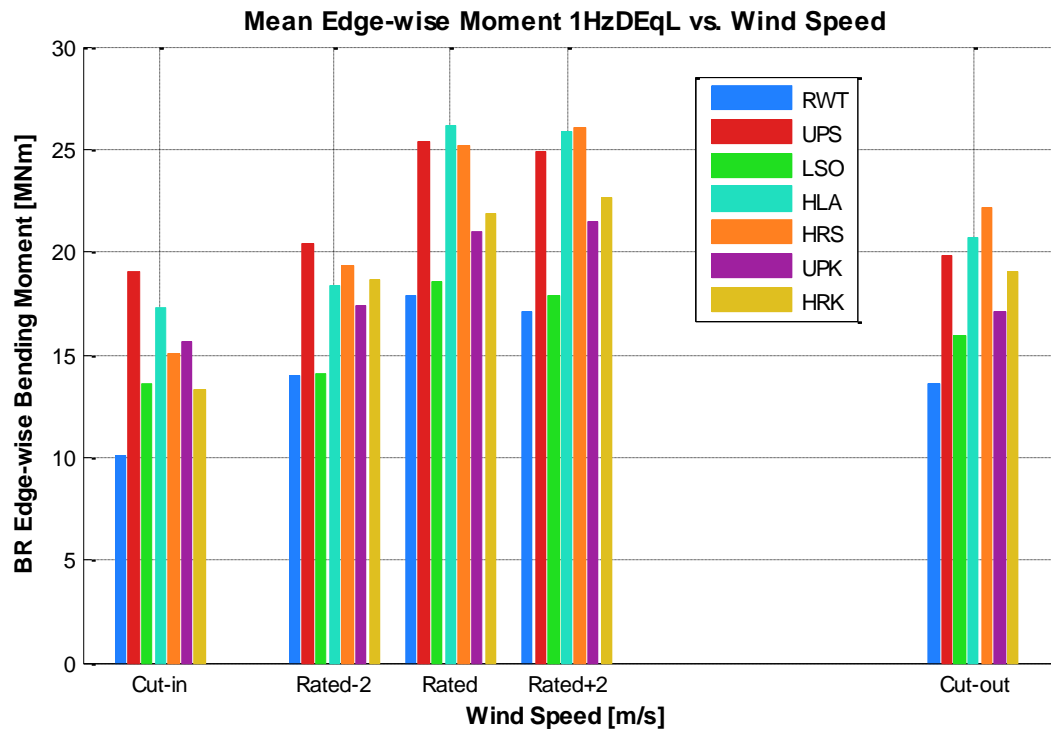


Figure A.40: The mean edge-wise blade root bending moment and percent differences versus shut-down wind speeds (not Weibull-weighted) for all designs from all DLC 4.1 simulations

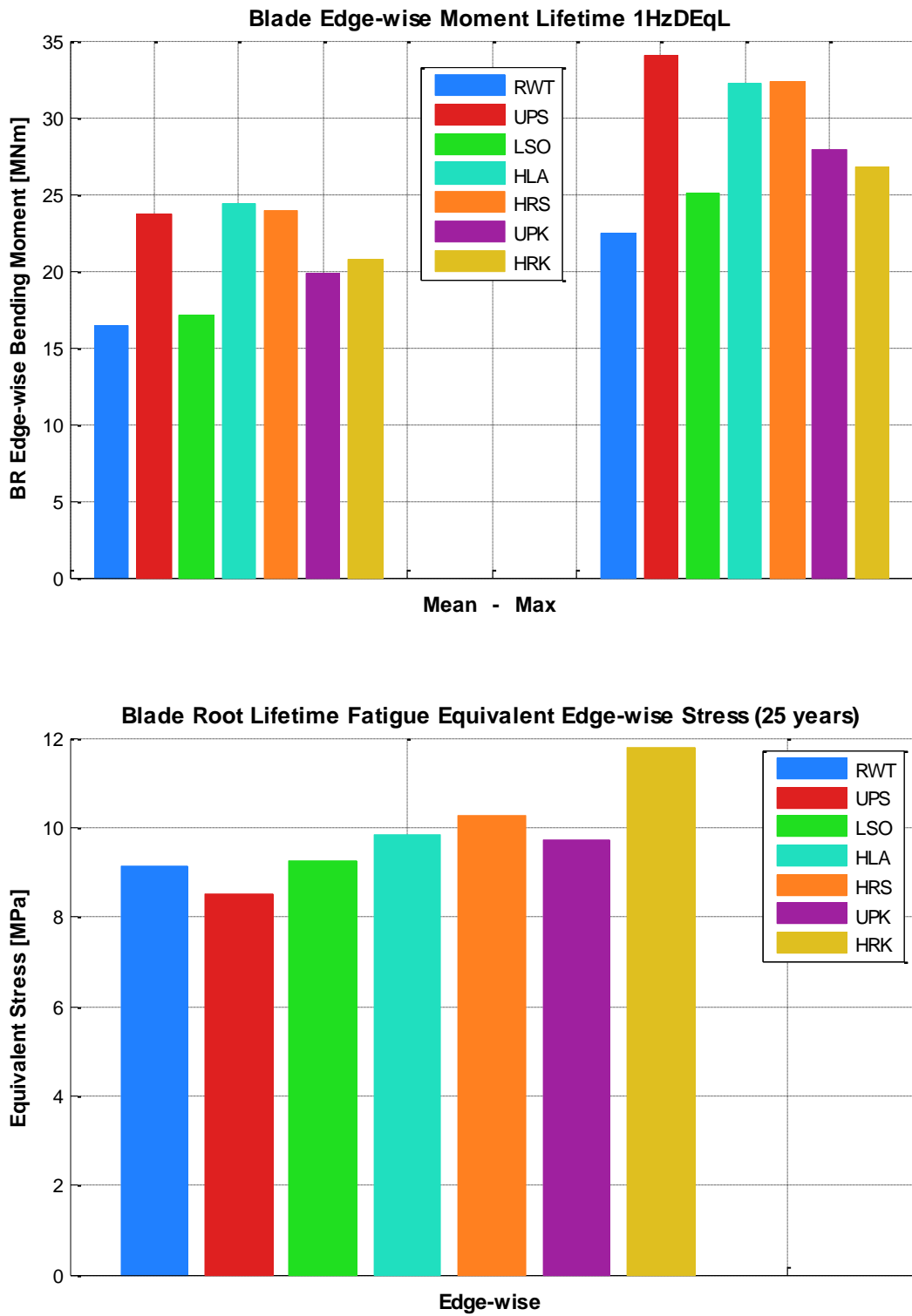


Figure A.41: Mean and maximum lifetime equivalent edge-wise blade root bending moment and stress for all designs from all DLC 4.1 simulations

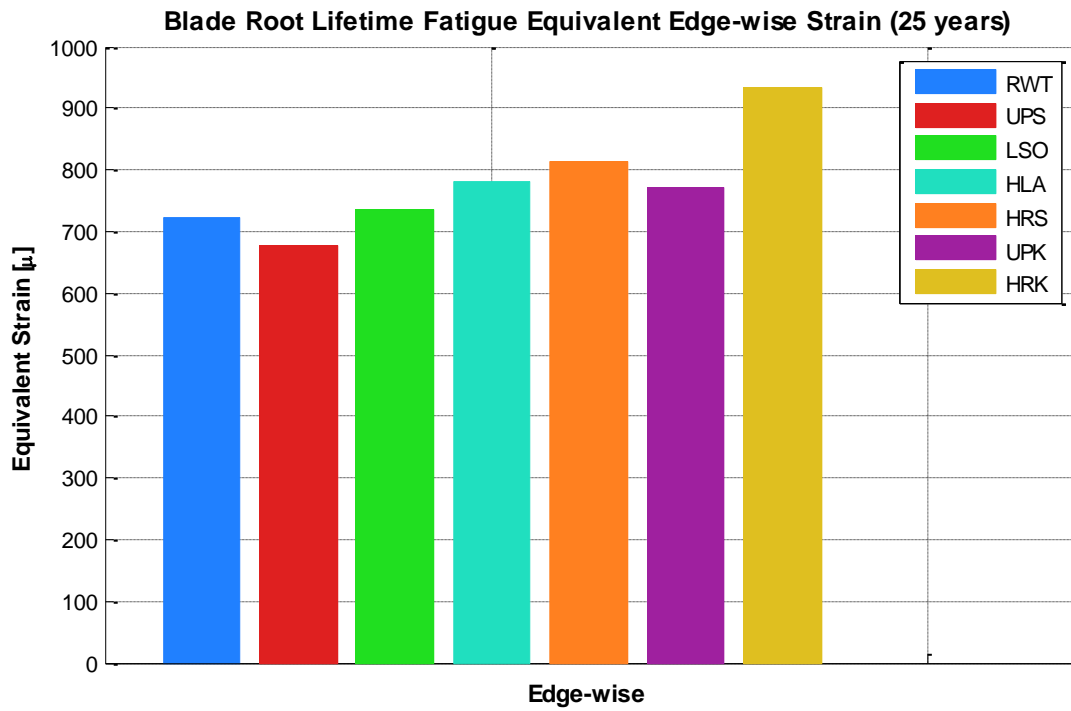


Figure A.42: Mean lifetime equivalent edge-wise blade root strain of all designs from all DLC 4.1 simulations

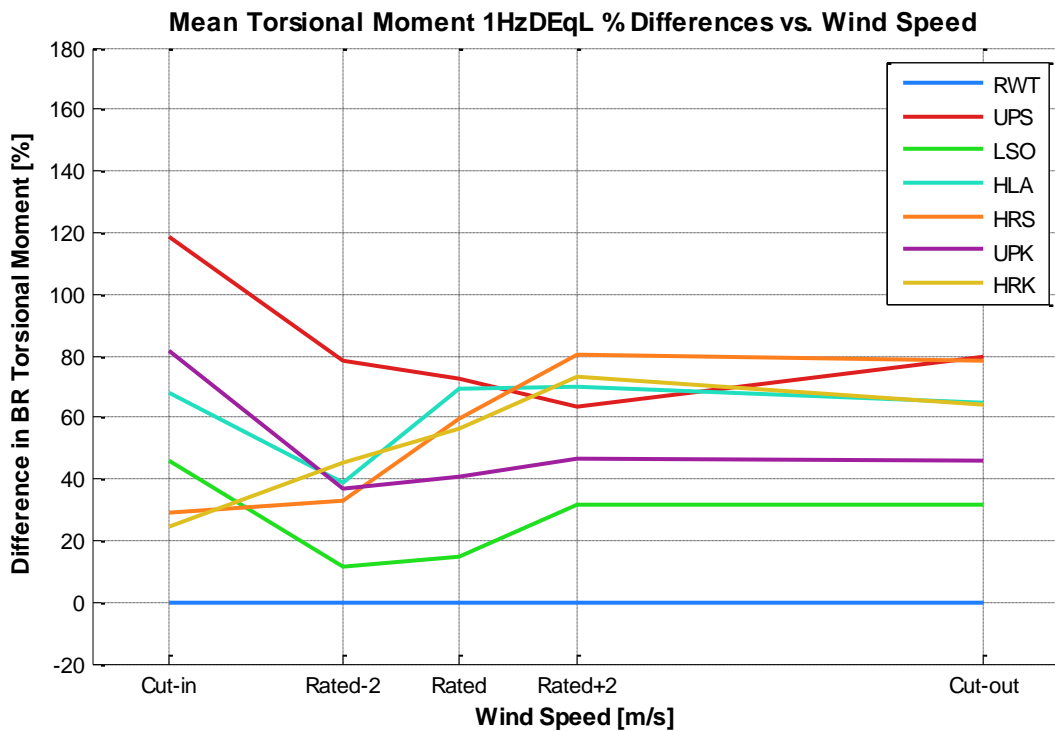
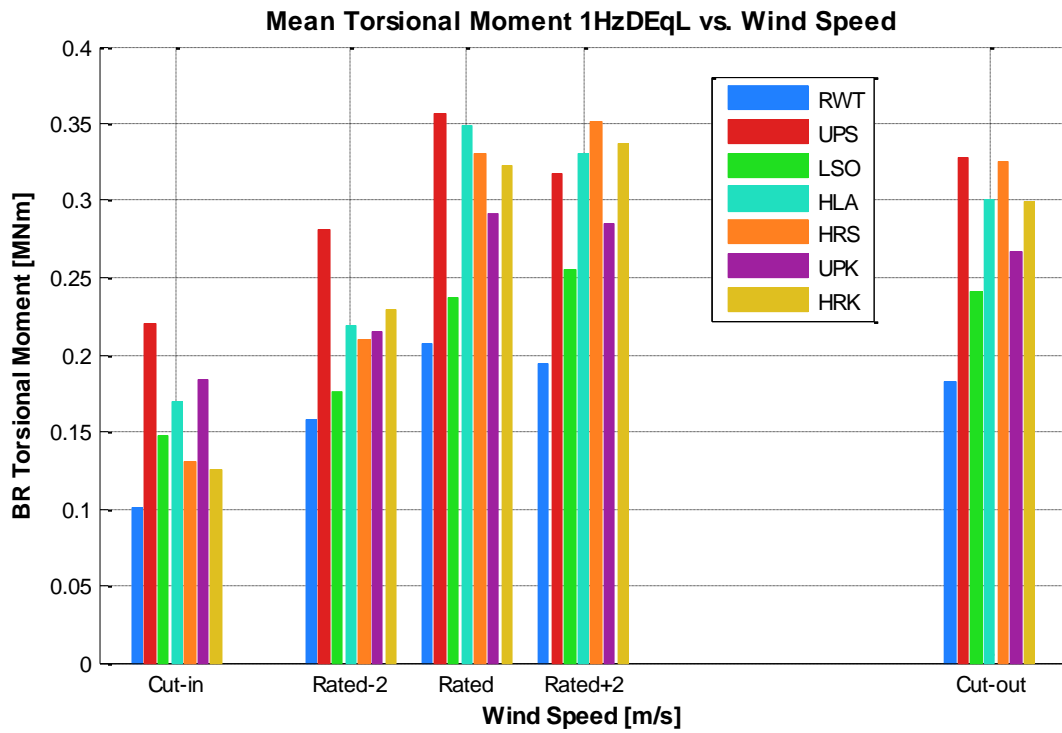


Figure A.43: The mean torsional blade root bending moment and percent differences versus shut-down wind speeds (not Weibull-weighted) for all designs from all DLC 4.1 simulations

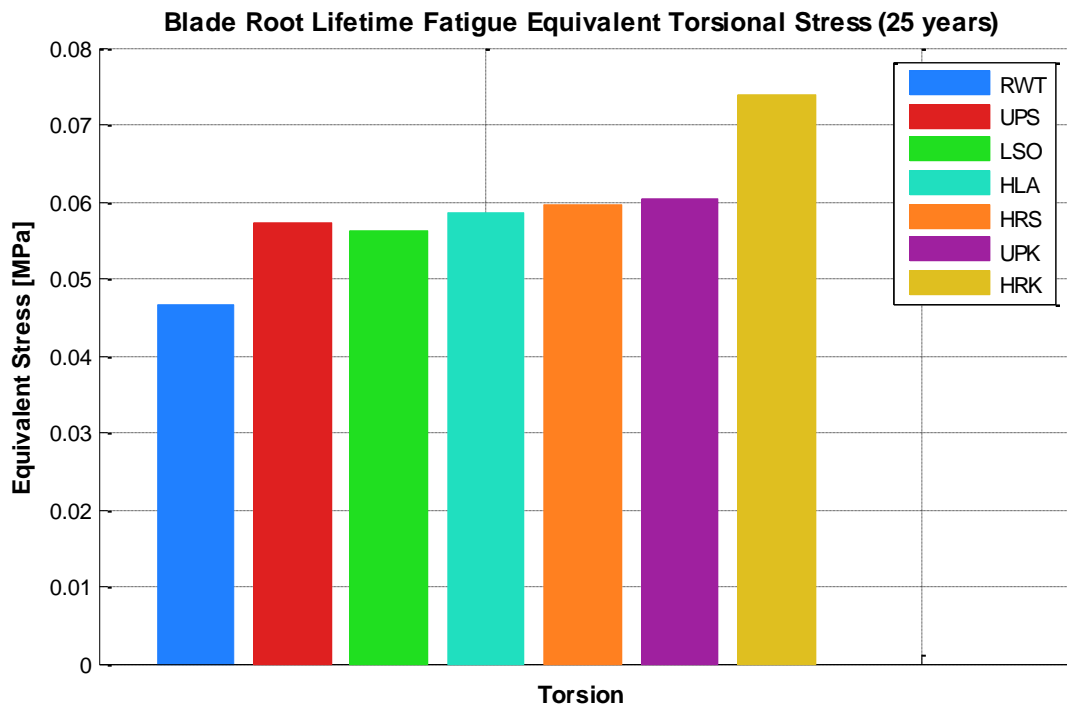
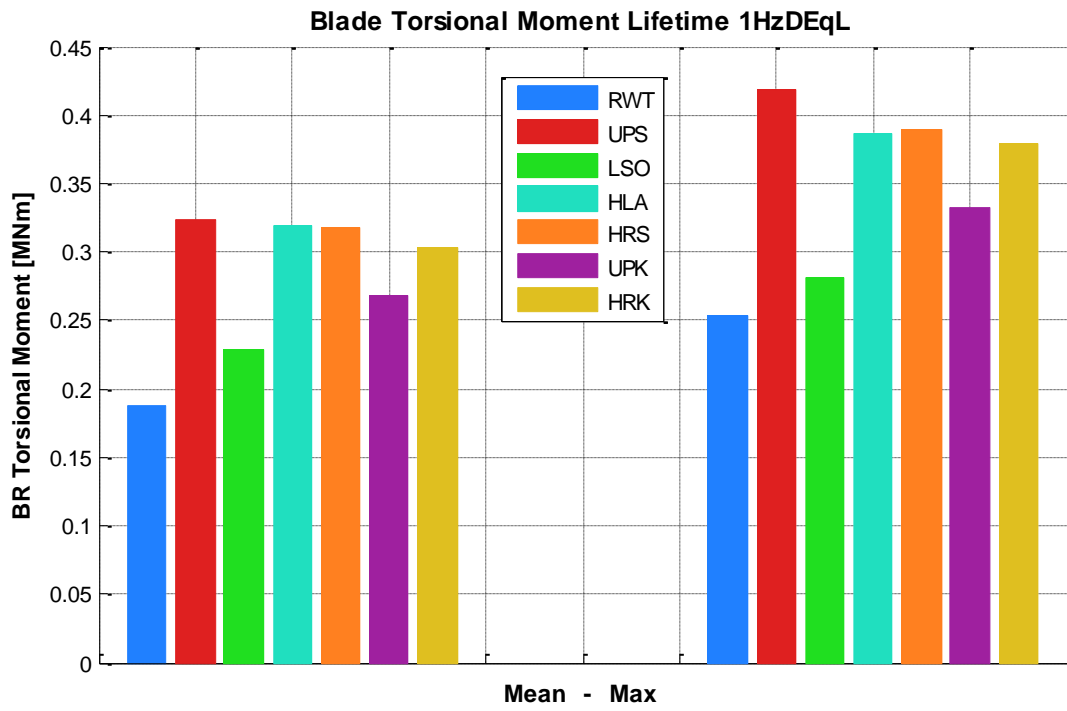


Figure A.44: Mean and maximum lifetime equivalent torsional blade root moment and stress for all designs from all DLC 4.1 simulations

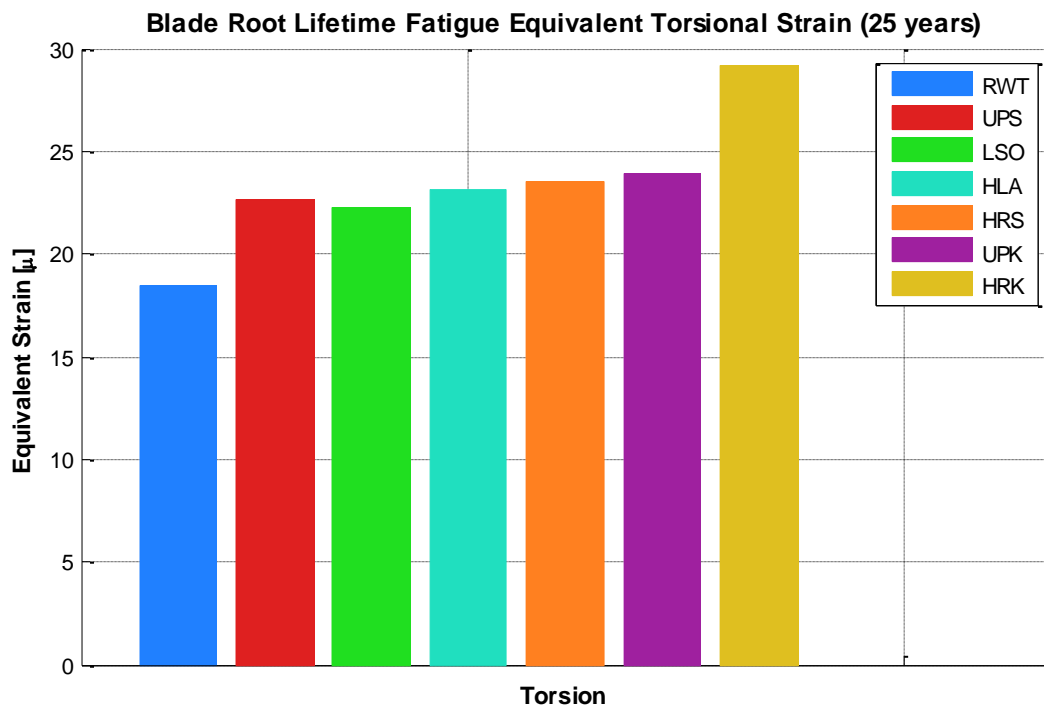


Figure A.45: Mean lifetime equivalent torsional blade root strain of all designs from all DLC 1.2 simulations

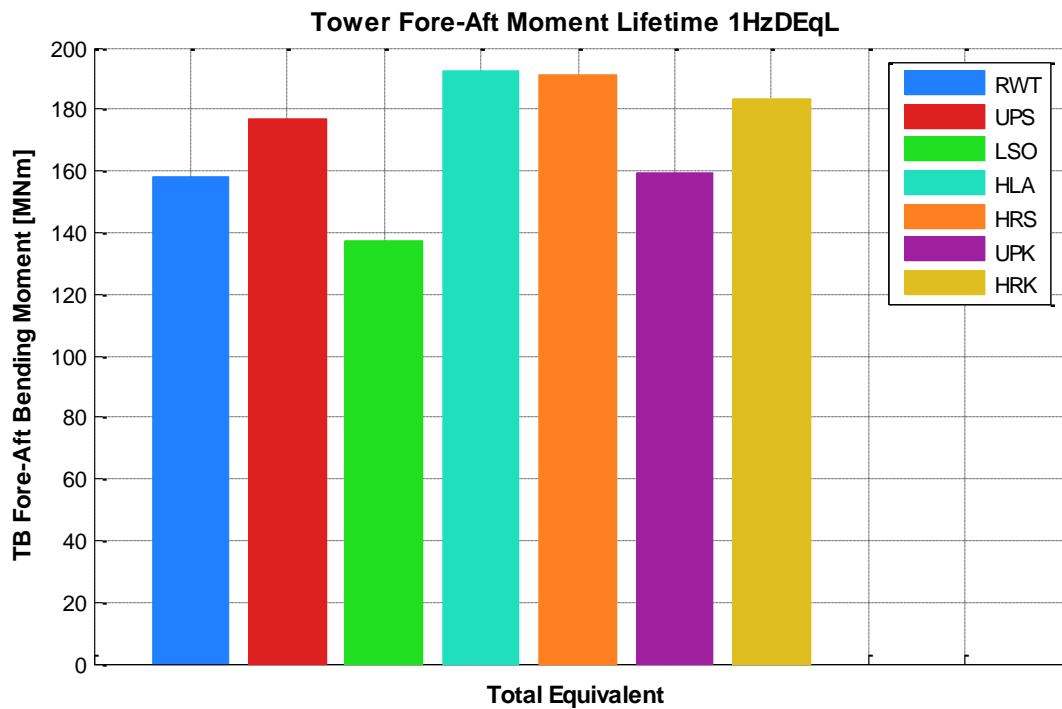
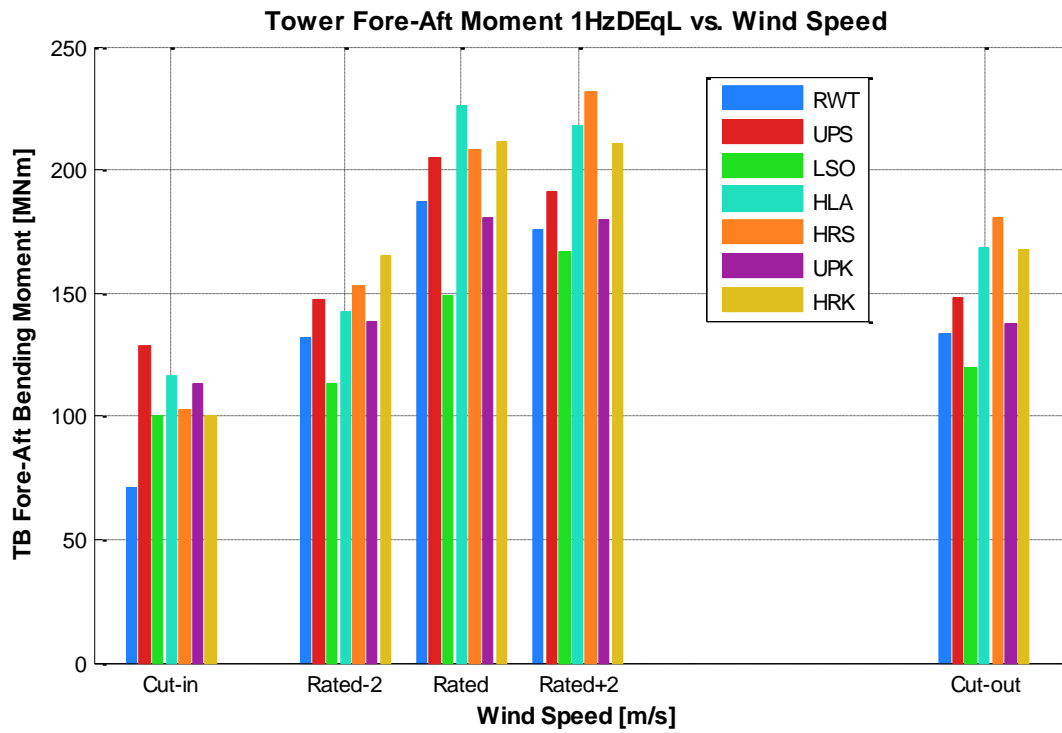


Figure A.46: The tower bottom fore-aft moment versus shut-down wind speeds (not Weibull-weighted) and lifetime damage equivalent moment of all designs from all DLC 4.1 simulations

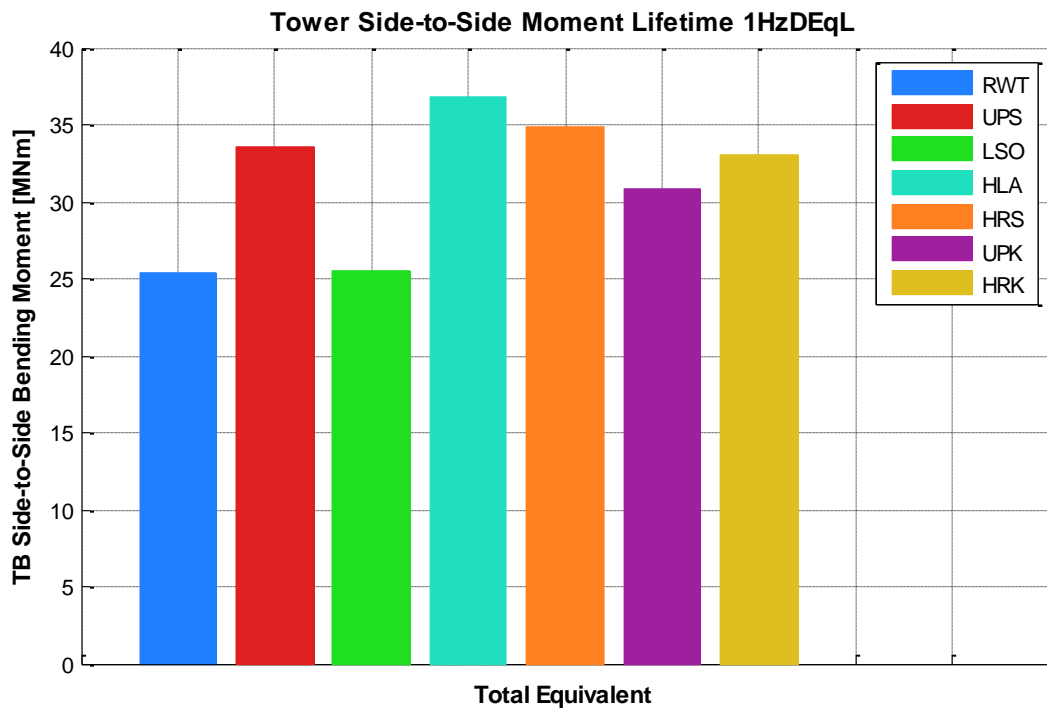
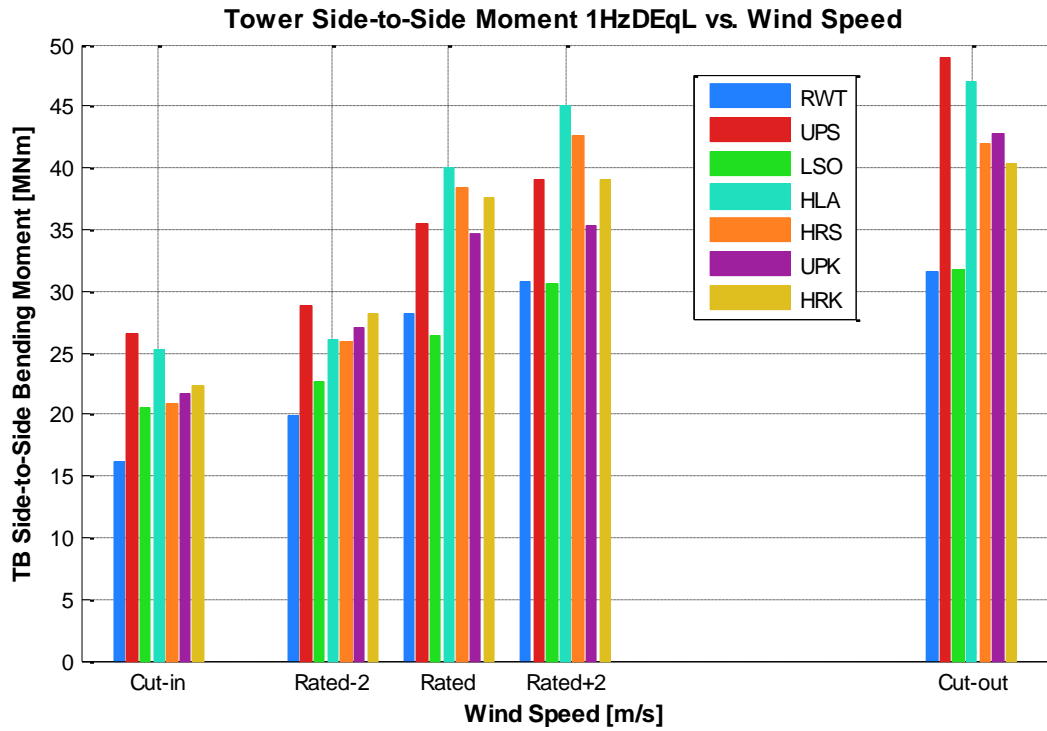


Figure A.47: The tower bottom side-to-side moment versus shut-down wind speeds (not Weibull-weighted) and lifetime damage equivalent moment of all designs from all DLC 4.1 simulations

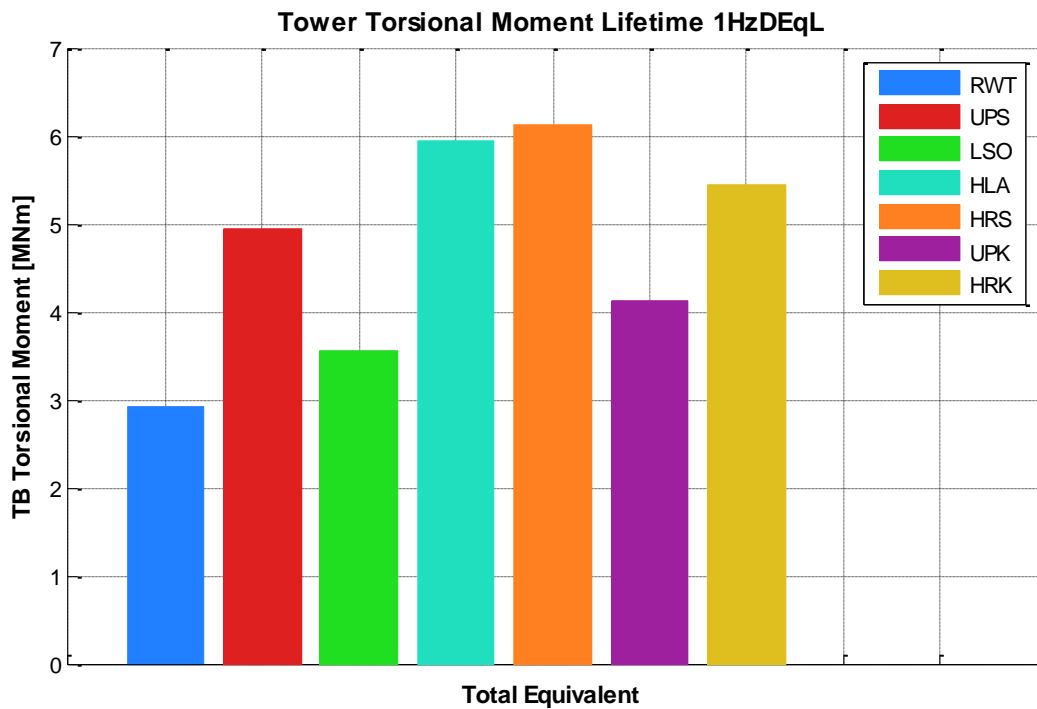
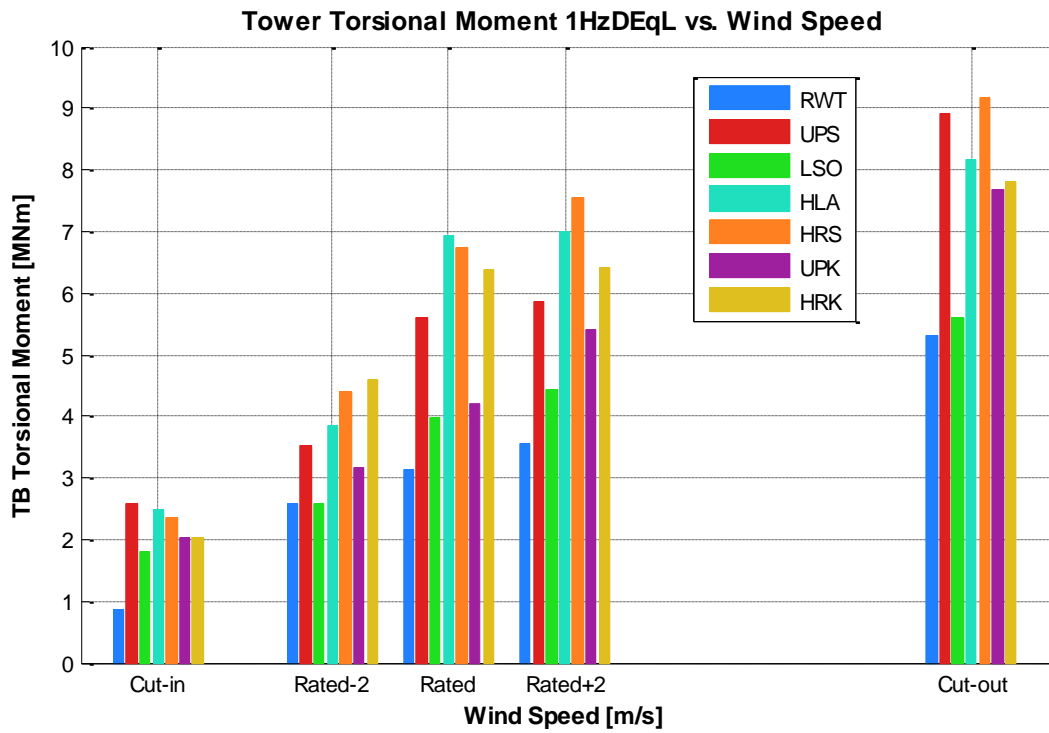


Figure A.48: The tower bottom torsional moment versus shut-down wind speeds (not Weibull-weighted) and lifetime damage equivalent moment of all designs from all DLC 4.1 simulations

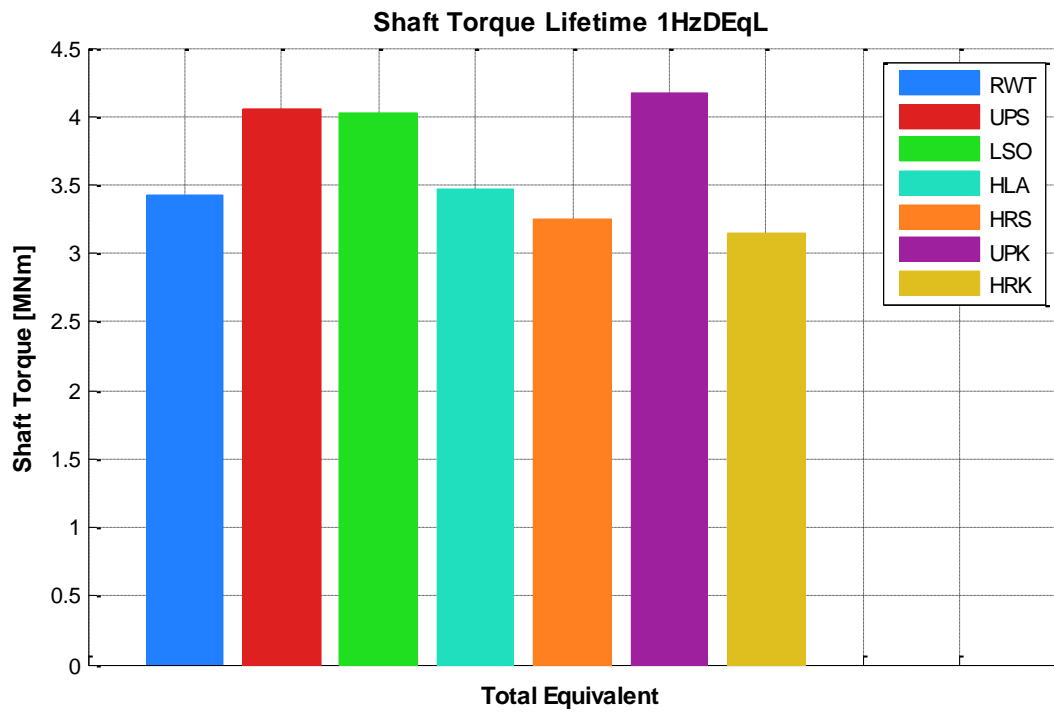
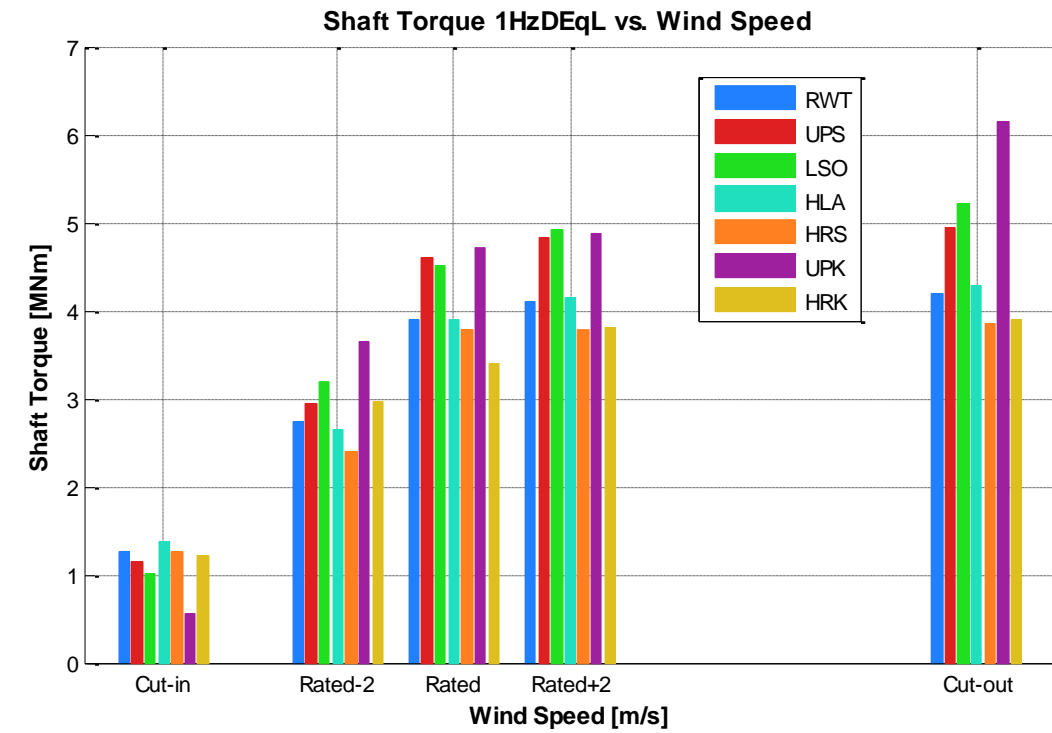


Figure A.49: The rotor shaft torque versus shut-down wind speeds (not Weibull-weighted) and lifetime damage equivalent torque of all designs from all DLC 4.1 simulations

A.5 Cost Model Tables

A.5.1 RWT

TURBINE INPUT PARAMETERS		INTERMEDIATE TURBINE RESULTS				RESULTS	
10000	Power (kW)	1.01	Omega (rad/s)			WF Capacity Factor	0.437
176.16	Diameter (m)	9.60	RPM max			Turbine Cost (M€2012/MW)	1.495
89.55	Max Tip Speed (m/s)	10582	Rated Torque (kNm)			BoP Cost (M€2012/MW)	1.695
119.0	Hub height (m)	24930	Rotor swept area (m ²)			CAPEX (M€2012/MW)	3.190
11.60	Rated speed (m/s)	0.488	Rotor Cp_max (-)			LCOE (€/MWh)	92.09
10.0	Design speed (m/s)	0.940	Drive Train Efficiency @ full load (100%)				
1	Blade Model	0.830	Drive Train Efficiency @ partial load (10%)				
2	Drive Train Model	0.547	Turbine Capacity Factor				
1	Support Structure Model						
WIND FARM DATA		SITE CONDITIONS				OTHER DATA	
800	Total Capacity (MW)	9.41	Mean Annual Wind Speed (m/s)			\$ / € (2012)	1.320
14.2%	Wake Losses (%)	2.33	Weibull shape factor k (-)			WT Price/Cost of components	1.400
2%	Electrical Losses (%)					BoP Price/Cost Multiplier	1.000
5%	Availability Losses (%)						

COMPONENT	Mass (kg)	Cost (\$2002)	Cost (€2012)	RNA	PPI	Mass (NREL)	Cost NREL (\$2009)	MADE OF NAICS code
	SF			Total				PCU
18.87% ROTOR		675,307	676,703					
12.59% Blades		1,303,779	1,305,145					
3.48% Hub 2.30	1.79	105,054	105,520					
2.64% Pitch mechanism 2.30	1.79	74,384	316,134					
0.17% Nose cone 1.00	1.00	27,894	251,047					
50.87% DRIVE TRAIN & NACELLE		2,776	15,460	18,153	55%	1.810	13,600	
2.88% Low speed shaft 3.00	3.15	445,086	4,802,348	5,430,584		125,639	2,605,600	
7.15% Main bearing 2.50	2.65	81,068	243,205	307,691	67%	16,526	166,800	
10.24% Gearbox		39,734	699,312	762,886	44%	5,400	64,400	
6.66% Generator		91,138	962,422	1,093,661	50%	39,688	877,200	
7.68% Power electronics		2,979	19,894	15,975	6%	1,053	11,000	
1.68% Bed plate (for Choice 2: 1.953 & 1.067)	2.10	49,075	661,469	711,581	42%	17,623	398,000	
1.11% Hydraulic & cooling system		790,000	819,924		37%		393,200	
0.88% Nacelle cover 2.00	2.15	69,021	152,685	179,289	55%	31,773	162,700	
5.38% ELECTRICAL CONNECTIONS		800	120,000	118,182	30%	424	77,200	
7.06% YAW SYSTEM 3.314	3.45	27,387	109,550	93,449	13%		From [2]	
0.51% CONTROL, SAFETY SYSTEM, CM		400,000	574,394		90%		308,800	
19.40% TOWER 2.00		643,811	753,552		55%	13,152	146,300	
16.36% MARINIZATION	1.71	628,471	55,000	54,167	30%		65,300	
100%	WT price	1,303,779	9,793,860	10,676,419	74%	596,520	1,491,300	
56.03% Foundation system		1,920,000	8,766,277	9,496,800	26%	866,907	6,549,400	
9.52% Offshore transportation		1,500,000	1,613,636					
1.28% Port and staging equipment		200,000	216,667					
9.59% Offshore turbine installation		1,500,000	1,625,000					
20.07% Offshore electrical I&C		2,600,000	3,401,667					
0.00% Offshore permits & engineering			0		26%		NA	
0.00% Personnel access equipment			0		26%		NA	
3.52% Scour protection		550,000	595,833		43%		403,000	
0.00% Decommissioning			0		26%		NA	
100%	Balance of Plant (BoP)	1,920,000	15,116,277	16,949,603			7,087,200	
	BoP price	15,116,277	16,949,603					
CAPEX		28,827,681	31,896,589					

LCOE CALCULATOR	
Total Plant Capacity (MW)	P 800.00
Size of Wind Turbines (MW)	Pt 10.00
Turbines Cost (€/kW)	Ct 1.495
BoP Cost (€/kW)	Cb 1.695
Capital Investment Cost (€/kW)	C 3.190
O&M Costs (€/kW/y)	O&MF 106
O&M Costs [incl. fixed annual costs, (€/MWh)]	O&M 27.67
Balancing Costs (€/MWh)	BC 3.00
Project Lifetime (y)	N 25
Capacity Factor (%)	Cf 0.44
Nominal Discount Rate (%)	dn 0.0739
Inflation Rate (%)	i 0.02112
Real Discount Rate (%)	d 0.0539
Capital Recovery Factor (%)	CRF 0.074
Summation of Discounted Future Expend	SFE 13.56
Present Value of Total O&M (€)	SO&M 1,274,242.723
Annual Energy Production (MWh/y)	E 3,064.673
Levelized Investment (€/y)	LI 188,227.161
Annual Discounted O&M (€/y)	DO&M 93,994.019
Annual O&M / Capital Investment (%)	O&M(%) 0.033
LCOE (€/MWh)	LI/E 61.42
Contribution of CAPEX (Turbines) (€/MWh)	DO&M/E 30.67
Contribution of CAPEX (BoP) (€/MWh)	
Contribution of OPEX (€/MWh)	
Contribution of CAPEX (Turbines) (%)	0.31
Contribution of CAPEX (BoP) (%)	0.35
Contribution of OPEX (%)	0.33
	1.00

COMPONENT MODELS		SF	Mass (kg)	Cost (\$2002)	Cost (€2012)	Performance	Comment on Mass	Comment on Cost	
ROTOR MODEL			41,722			CP-max 0.48769			WP2
1: Innwind.EU 10MW RWT Blade - scaled	3.00	41,722	541,442				Combination of [2] and [3]	From [1] and [5]	
2: Baseline WindPact		70,332	915,769				From [1]	From [1] and [5]	
3: Advanced WindPact		42,402	550,337				From [1]	From [1] and [5]	
4: Repower 5 MW RWT Blade - scaled	2.45	41,468	538,118				Combination of [2] and [3]	From [1] and [5]	
DRIVE TRAIN MODEL						Drive Train Efficiency at 10% load at 100% load			WP3
1: Three-stage planetary/helical									
2: Medium Speed (40:1) Innwind.EU RWT									
3: Repower 5MW RWT 3SG+HSG									
4: Direct drive									
5: SCDD NbTi									
6: SCDD MgB2									
7: SCDD AmSC - SeaTitan									
8: SCDD Jensen 2G									
9: PDD Magnomatics Gearbox									
	1	80,453	1,629,919			0.930 0.990	From [1]	From [1]	
	2	13.25	91,138	962,422	1,093,661	0.930 0.990	From [10]	From [10], €2012/kg=12	
	3	3.00	178,191	1,629,919		0.930 0.990	From [2]	From [1]	
	4		0	0		1.000 1.000			
	5		0	0		1.000 1.000			
	6		0	0		1.000 1.000			
	7		0	0		1.000 1.000			
	8		0	0		1.000 1.000			
	9		0	0		1.000 1.000			
Generator									
	1		31,630	650,000		0.896 0.968	From [1]	From [1]	
	2	13.25	49,075	661,469	711,581	0.930 0.979	From [10]	From [10], €2012/kg=14.5	
	3	2.00	34,000	650,000		0.896 0.968	From [2]	From [1]	
	4		181,659	2,193,300		0.885 0.948	From [1]	From [1]	
	5	2.35	145,000	1,528,225	1,644,000	0.800 0.950	From [9]	From [9] in €2012	
	6	2.35	165,000	2,103,634	2,263,000	0.860 0.960	From [9]	From [9] in €2012	
	7	3.15	165,000	2,212,394	2,380,000	0.860 0.960	From [9]	From [9] in €2012	
	8	3.15	70,000	8,124,507	8,740,000	0.870 0.978	From [9]	From [9] in €2012	
	9	3.15	156,000	1,078,310	1,160,000	0.880 0.989	From [9]	From [9] in €2012	
Power electronics									
	1	2.00		790,000		0.960 0.970		Rating * 79.00 \$2002/kW [1]	
	2	2.00		790,000		0.960 0.970		Rating * 79.00 \$2002/kW [1]	
	3	2.00		790,000		0.960 0.970		Rating * 79.00 \$2002/kW [1]	
	4	2.00		790,000		0.960 0.970		Rating * 79.00 \$2002/kW [1]	
	5	2.00		790,000		0.963 0.973		Rating * 79.00 \$2002/kW [1]	
	6	2.00		790,000		0.963 0.973		Rating * 79.00 \$2002/kW [1]	
	7	2.00		790,000		0.963 0.973		Rating * 79.00 \$2002/kW [1]	
	8	2.00		790,000		0.963 0.973		Rating * 79.00 \$2002/kW [1]	
	9	2.00		790,000		0.963 0.973		Rating * 79.00 \$2002/kW [1]	
Bed plate									
	1		55,556	236,082			From [1]	From [1]	
	2	2.10	69,021	152,685			From [1]	From [1]	
	3		55,556	236,082			From [1]	From [1]	
	4		30,552	51,364			From [1]	From [1]	
	5		30,552	51,364			Assuming DD equiv	Assuming DD equiv	
	6		30,552	51,364			Assuming DD equiv	Assuming DD equiv	
	7		30,552	51,364			Assuming DD equiv	Assuming DD equiv	
	8		30,552	51,364			Assuming DD equiv	Assuming DD equiv	
	9		30,552	51,364			Assuming DD equiv	Assuming DD equiv	
SUPPORT STRUCTURE MODEL									WP4
1: Jacket 10 MW RWT			1,920,000	8,766,277	9,496,800			Price = 1.2 X Fabrication cost	
2: Reference Floater for the 10 MW RWT									
3: Other									
	Transition piece for 1	2.5	330,000	1,523,077	1,650,000		From [3]	From [11], 5.0 €2012/kg	
	The jacket itself for 1	1.5	1,210,000	5,361,231	5,808,000		From [3]	From [11], 4.8 €2012/kg	
	The piles for 1	1.5	380,000	420,923	456,000		From [3]	From [11], 1.2 €2012/kg	
	Floater for 2								
	Mooring system for 2								

A.5.2 UPS

TURBINE INPUT PARAMETERS		INTERMEDIATE TURBINE RESULTS		RESULTS	
10000 305.36 77.26 119.0 10.60 10.0	Power (kW) Diameter (m) Max Tip Speed (m/s) Hub height (m) Rated speed (m/s) Design speed (m/s)	0.75 7.17 14169 33266 0.509 0.940	Omega (rad/s) RPM max Rated Torque (kNm) Rotor swept area (m2) Rotor Cp_max (-) Drive Train Efficiency @ full load (100%) Drive Train Efficiency @ partial load (10%) Turbine Capacity Factor		WF Capacity Factor Turbine Cost (M€2012/MW) BoP Cost (M€2012/MW) CAPEX (M€2012/MW) LCOE (€/MWh)
1 2 1	1: Innwind.EU 10MW RWT Blade - scal 2: Medium Speed (40-1) Innwind.EU R 1: Jacket 10 MW RWT				
WIND FARM DATA		SITE CONDITIONS		OTHER DATA	
300 12.4% 2% 5%	Total Capacity (MW) Wake Losses (%) Electrical Losses (%) Availability Losses (%)	9.41 2.33	Mean Annual Wind Speed (m/s) Weibull shape factor k (-)		\$ / € (2012) WT Price/Cost of components BoP Price/Cost Multiplier

COMPONENT	SF	Mass (kg)	Cost (\$2002)	Cost (€2012)	RNA	PPI	Mass (NREL)	Cost NREL (\$2009)	Comment on Mass	Comment on Cost	MADE OF NAICS code	PCU
		885,374	676,703	1,305,145			105,520	144,748				
19.92% ROTOR			286,608	2,940,898	2,623,115							
14.80% <i>Blades</i>			181,043	2,356,409	1,948,923	9%	53,520	1,062,300	See blade model below	See blade model below		
2.82% <i>Hub 2.30</i>	1.79	74,384	316,134	371,218	371,218	55%	60,540	130,200	Combination of [2] and [3]	Weight * 4.25 \$2002/kg [1]		
2.14% <i>Pitch mechanism 2.30</i>	1.79	27,894	251,047	281,477	281,477	48%	28,878	242,000	Combination of [2] and [3]	Weight * 9.00 \$2002/kg (Assumed)		
0.16% <i>Nose cone 1.00</i>	1.00	3,287	18,308	21,498	21,498	55%	1,810	13,600	From [1]	Weight * 5.57 \$2002/kg [1]		
53.42% DRIVE TRAIN & NACELLE			598,765	6,231,313	7,032,182			125,639	2,605,600			
2.34% <i>Low speed shaft 3.00</i>	3.15	81,068	243,205	307,691	307,691	67%	16,526	166,800	From [2]	Weight * 3.00 \$2002/kg (Assumed)		
9.83% <i>Main bearing 2.50</i>	2.65	67,392	1,188,098	1,293,925	1,293,925	44%	5,400	64,400	From [1]	Weight * 17.60 \$2002/kg [1]		
11.12% <i>Gearbox</i>		122,026	1,288,598	1,464,316	1,464,316	50%	39,688	877,200	See drive train model below	See drive train model below		
0.12% <i>Mechanical brake & couplings 3.00</i>	3.15	2,979	19,894	15,975	15,975	6%	1,053	11,000	From [2]	From [1]		
7.24% <i>Generator</i>		65,706	885,650	952,744	952,744	42%	17,623	398,000	See drive train model below	See drive train model below		
6.23% <i>Power electronics</i>			790,000	819,924	819,924	37%		393,200	NA	See drive train model below		
1.62% <i>Bed plate (for Choice 2: 1.953 & 1.067)</i>	2.10	93,438	191,535	213,166	213,166	55%	31,773	162,700	See drive train model below	See drive train model below		
0.90% <i>Hydraulic & cooling system</i>		800	120,000	118,182	118,182	30%	424	77,200	From [1]	Rating * 12.00 \$2002kW [1]		
0.71% <i>Nacelle cover 2.00</i>	2.15	27,387	100,550	93,449	93,449	13%			From [2]	Weight * 4.00 \$2002/kg		
4.36% ELECTRICAL CONNECTIONS			400,000	574,394	574,394	90%		308,800	NA	Rating * 40.00 \$2002kW [5]		
8.95% YAW SYSTEM 3.314	3.45	137,968	1,006,783	1,178,394	1,178,394	55%	13,152	146,300	From [1]	From [1]		
0.41% CONTROL, SAFETY SYSTEM, CM			55,000	54,167	54,167	30%		65,300	NA	From [5]		
15.73% TOWER 2.00	1.71	628,471	1,571,178	2,071,099	2,071,099	74%	596,520	1,491,300	Combination of [2] and [3]	Weight * (1.50 to 4.25) \$2002/kg ([1] Adj)		
10.52% MARINIZATION			1,450,358	1,384,432	1,384,432	26%		939,100	From [1]	From [1]		
100%			Cost of WT Components	12,248,746	13,164,974		866,907	6,549,400				
			WT price	17,148,245	18,430,964							
36.03% Foundation system			1,920,000	8,766,277	9,496,800	43%		2,174,700	See Foundation Model Below	See Foundation Model Below		
9.52% <i>Offshore transportation</i>				1,500,000	1,613,636	42%		1,568,300	NA	Rating * 100.00 \$2002kW ([1] Adj)		
1.28% <i>Port and staging equipment</i>				200,000	216,667	43%		144,900	NA	Rating * 20.00 \$2002kW [1]		
9.59% <i>Offshore turbine installation</i>				1,500,000	1,625,000	43%		732,800	NA	Rating * 100.00 \$2002kW [1]		
20.07% <i>Offshore electrical I&C</i>				2,600,000	3,401,667	73%		2,063,500	NA	Rating * 290.00 \$2002kW [1]		
0.00% <i>Offshore permits & engineering</i>				0	0	26%		NA				
0.00% <i>Personnel access equipment</i>				0	0	26%		NA				
3.52% <i>Scour protection</i>				550,000	595,833	43%		403,000	NA	Rating * 55.00 \$2002kW [1]		
0.00% <i>Decommissioning</i>				0	0	26%		NA				
100%			Balance of Plant (BoP)	15,116,277	16,949,603			7,087,200				
			BoP price	15,116,277	16,949,603							
CAPEX				32,264,522	35,380,567							

LCOE CALCULATOR	
Total Plant Capacity (MW)	P 800.00
Size of Wind Turbines (MW)	Pt 10.00
Turbines Cost (€/kW)	Ct 1.843
BoP Cost (€/kW)	Cb 1.695
Capital Investment Cost (€/kW)	C 3.538
O&M Costs (€/kW/y)	O&M F 106
O&M Costs (incl. fixed annual costs, €/MWh)	O&M 23.84
Balancing Costs (€/MWh)	BC 3.00
Project Lifetime (y)	N 25
Capacity Factor (%)	Cf 0.51
Nominal Discount Rate (%)	dn 0.0739
Inflation Rate (%)	i 0.02112
Real Discount Rate (%)	d 0.0539
Capital Recovery Factor (%)	CRF 0.074
Summation of Discounted Future Expend	SFE 13.56
Present Value of Total O&M (€)	SO&M 1,294,294,387
Annual Energy Production (MWh/y)	E 3,557,707
Levelized Investment (€/y)	LI 208,786,702
Annual Discounted O&M (€/y)	DO&M 95,473,122
Annual O&M / Capital Investment (%)	O&M(%) 0.030
LCOE (€/MWh)	L/E 85.52
Contribution of CAPEX (Turbines) (€/MWh)	DO&M/E 28.94
Contribution of CAPEX (BoP) (€/MWh)	
Contribution of OPEX (€/MWh)	
Contribution of CAPEX (Turbines) (%)	0.36
Contribution of CAPEX (BoP) (%)	0.33
Contribution of OPEX (%)	0.31
	-1.00

COMPONENT MODELS		SF	Mass (kg)	Cost (\$2002)	Cost (€2012)	Performance	Comment on Mass	Comment on Cost	
ROTOR MODEL			60,348			CP-max			WP2
1: Innwind.EU 10MW RWT Blade - scaled	3.00	60,348	785,136			0.50966	Combination of [2] and [3]	From [1] and [5]	
2: Baseline WindPact		107,101	1,396,851			0.480	From [1]	From [1] and [5]	
3: Advanced WindPact		61,075	794,650			0.480	From [1]	From [1] and [5]	
4: Repower 5 MW RWT Blade - scaled	2.45	41,468	538,118			0.480	Combination of [2] and [3]	From [1] and [5]	
DRIVE TRAIN MODEL						Drive Train Efficiency			WP3
						at 10% load			
						at 100% load			
1: Three-stage planetary/helical									
2: Medium Speed (40:1) Innwind.EU RWT									
3: Repower 5MW RWT 3SG+HSG									
4: Direct drive									
5: SCDD NbTi									
6: SCDD MgB2									
7: SCDD AmSC - SeaTitan									
8: SCDD Jensen 2G									
9: PDD Magnomatics Gearbox									
	1		100,403	1,629,919		0.930	0.990	From [1]	
	2	13.25	122,026	1,288,598	1,464,316	0.930	0.990	From [10]	
	3	3.00	178,191	1,629,919		0.930	0.990	From [2]	
	4		0	0		1.000	1.000	From [1]	
	5		0	0		1.000	1.000		
	6		0	0		1.000	1.000		
	7		0	0		1.000	1.000		
	8		0	0		1.000	1.000		
	9		0	0		1.000	1.000		
Generator									
	1		31,630	650,000		0.896	0.968	From [1]	
	2	13.25	65,706	885,650	952,744	0.930	0.979	From [10]	
	3	2.00	34,000	650,000		0.896	0.968	From [2]	
	4		216,804	2,193,300		0.885	0.948	From [1]	
	5	2.35	145,000	1,528,225	1,644,000	0.800	0.950	From [9]	
	6	2.35	165,000	2,103,634	2,263,000	0.860	0.960	From [9]	
	7	3.15	165,000	2,212,394	2,380,000	0.860	0.960	From [9]	
	8	3.15	70,000	8,124,507	8,740,000	0.870	0.978	From [9]	
	9	3.15	156,000	1,078,310	1,160,000	0.880	0.989	From [9]	
Power electronics									
	1	2.00		790,000		0.960	0.970	Rating * 79.00 \$2002kW [1]	
	2	2.00		790,000		0.960	0.970	Rating * 79.00 \$2002kW [1]	
	3	2.00		790,000		0.960	0.970	Rating * 79.00 \$2002kW [1]	
	4	2.00		790,000		0.960	0.970	Rating * 79.00 \$2002kW [1]	
	5	2.00		790,000		0.963	0.973	Rating * 79.00 \$2002kW [1]	
	6	2.00		790,000		0.963	0.973	Rating * 79.00 \$2002kW [1]	
	7	2.00		790,000		0.963	0.973	Rating * 79.00 \$2002kW [1]	
	8	2.00		790,000		0.963	0.973	Rating * 79.00 \$2002kW [1]	
	9	2.00		790,000		0.963	0.973	Rating * 79.00 \$2002kW [1]	
Bed plate									
	1		73,632	312,893				From [1]	
	2	2.10	93,438	181,535				From [1]	
	3		73,632	312,893				From [1]	
	4		40,492	58,063				From [1]	
	5		40,492	58,063				Assuming DD equiv	
	6		40,492	58,063				Assuming DD equiv	
	7		40,492	58,063				Assuming DD equiv	
	8		40,492	58,063				Assuming DD equiv	
	9		40,492	58,063				Assuming DD equiv	
SUPPORT STRUCTURE MODEL									WP4
1: Jacket 10 MW RWT			1,920,000	8,766,277	9,496,800			Price = 1.2 X Fabrication cost	
2: Reference Floater for the 10 MW RWT									
3: Other									
	Transition piece for 1	2.5	330,000	1,523,077	1,650,000			From [3]	
	The jacket itself for 1	1.5	1,210,000	5,361,231	5,808,000			From [3]	
	The piles for 1	1.5	380,000	420,923	456,000			From [3]	
	Floater for 2								
	Mooring system for 2								

A.5.3 LSO

TURBINE INPUT PARAMETERS		INTERMEDIATE TURBINE RESULTS		RESULTS	
10000	Power (kW)	0.79	Omega (rad/s)	WF Capacity Factor	0.445
325.36	Diameter (m)	7.53	RPM max	Turbine Cost (M€2012/MW)	1.746
91.14	Max Tip Speed (m/s)	13491	Rated Torque (kNm)	BoP Cost (M€2012/MW)	1.695
119.0	Hub height (m)	33266	Rotor swept area (m2)	CAPEX (M€2012/MW)	3.441
11.70	Rated speed (m/s)	0.346	Rotor Cp_max (-)	LCOE (€/MWh)	95.29
10.0	Design speed (m/s)	0.940	Drive Train Efficiency @ full load (100%)		
1	Blade Model	0.830	Drive Train Efficiency @ partial load (10%)		
2	Drive Train Model	0.534	Turbine Capacity Factor		
1	Support Structure Model				
WIND FARM DATA		SITE CONDITIONS		OTHER DATA	
300	Total Capacity (MW)	9.41	Mean Annual Wind Speed (m/s)	\$ / € (2012)	1.320
10.5%	Wake Losses (%)	2.33	Weibull shape factor k (-)	WT Price/Cost of components	1.400
2%	Electrical Losses (%)			BoP Price/Cost Multiplier	1.000
5%	Availability Losses (%)				

COMPONENT	Mass (kg)	Cost (\$2002)	Cost (€2012)	RNA	PPI	Mass (NREL)	Cost NREL (\$2009)	MADE OF NAICS code
	831,281	676,703						
	SF	1,459,753	1,305,145	Total				PCU
		105,565	105,520	Hub				
17.12% ROTOR		241,491	2,350,587	2,134,677		144,748	1,448,100	
11.71% Blades		135,926	1,765,098	1,460,485	9%	53,520	1,062,300	See blade model below
2.98% Hub 2.30	1.79	74,384	316,134	371,218	55%	60,540	130,200	Combination of [2] and [3]
2.26% Pitch mechanism 2.30	1.79	27,894	251,047	251,477	48%	28,878	242,000	Combination of [2] and [3]
0.17% Nose cone 1.00	1.00	3,287	18,308	21,498	55%	1,810	13,600	From [1]
55.46% DRIVE TRAIN & NACELLE		589,790	6,127,385	6,916,605		125,639	2,605,600	
2.47% Low speed shaft 3.00	3.15	81,068	243,205	307,691	67%	16,526	166,800	From [2]
10.38% Main bearing 2.50	2.65	67,392	1,186,098	1,293,925	44%	5,400	64,400	From [1]
11.18% Gearbox		116,192	1,226,992	1,394,309	50%	39,688	877,200	See drive train model below
1.13% Mechanical brake & couplings 3.00	3.15	2,979	19,894	15,975	6%	1,053	11,000	From [2]
7.27% Generator		62,565	843,308	907,195	42%	17,623	398,000	See drive train model below
6.57% Power electronics			790,000	819,924	37%		393,200	NA
1.71% Bed plate (for Choice 2: 1.953 & 1.067)	2.10	93,438	191,535	213,166	55%	31,773	162,700	See drive train model below
0.95% Hydraulic & cooling system		800	120,000	118,182	30%	424	77,200	From [1]
0.75% Nacelle cover 2.00	2.15	27,387	109,550	93,449	13%			From [2]
4.61% ELECTRICAL CONNECTIONS			400,000	574,394	90%		308,800	NA
9.45% YAW SYSTEM 3.314	3.45	137,968	1,006,783	1,178,394	55%	13,152	146,300	From [1]
0.43% CONTROL, SAFETY SYSTEM, CM			55,000	54,167	30%		65,300	NA
16.61% TOWER 2.00	1.71	628,471	1,571,178	2,071,099	74%	596,520	1,491,300	Combination of [2] and [3]
10.38% MARINIZATION			1,356,632	1,294,967	26%		939,100	From [1]
100%	Cost of WT Components	1,459,753	11,460,762	12,471,515		866,907	6,549,400	
	WT price		16,045,067	17,460,121				
56.03% Foundation system		1,920,000	8,786,277	9,496,800	43%		2,174,700	See Foundation Model Below
9.52% Offshore transportation			1,500,000	1,613,636	42%		1,568,300	NA
1.28% Port and staging equipment			200,000	216,667	43%		144,900	NA
9.59% Offshore turbine installation			1,500,000	1,625,000	43%		732,800	NA
20.07% Offshore electrical I&C			2,600,000	3,401,667	73%		2,063,500	NA
0.00% Offshore permits & engineering				0	26%		NA	
0.00% Personnel access equipment				0	26%		NA	
3.52% Scour protection			550,000	595,833	43%		403,000	NA
0.00% Decommissioning				0	26%		NA	
100%	Balance of Plant (BoP)	1,920,000	15,116,277	16,949,603			7,087,200	
	BoP price		15,116,277	16,949,603				
CAPEX		31,161,344	34,409,724					

LCOE CALCULATOR	
Total Plant Capacity (MW)	P 800.00
Size of Wind Turbines (MW)	Pt 10.00
Turbines Cost (€/kW)	Ct 1.746
BoP Cost (€/kW)	Cb 1.695
Capital Investment Cost (€/kW)	C 3.441
O&M Costs (€/kW/y)	O&M F 106
O&M Costs (incl. fixed annual costs, €/MWh)	O&M 27.19
Balancing Costs (€/MWh)	BC 3.00
Project Lifetime (y)	N 25
Capacity Factor (%)	Cf 0.45
Nominal Discount Rate (%)	dn 0.0739
Inflation Rate (%)	i 0.02112
Real Discount Rate (%)	d 0.0539
Capital Recovery Factor (%)	CRF 0.074
Summation of Discounted Future Expend	SFE 13.56
Present Value of Total O&M (€)	SO&M 1,276,452,071
Annual Energy Production (MWh/y)	E 3,118,997
Levelized Investment (€/y)	LI 203,057,592
Annual Discounted O&M (€/y)	DO&M 94,156,991
Annual O&M / Capital Investment (%)	O&M(%) 0.031
LCOE (€/MWh)	L/E 95.29
Contribution of CAPEX (Turbines) (€/MWh)	DO&M/E 30.19
Contribution of CAPEX (BoP) (€/MWh)	
Contribution of OPEX (€/MWh)	
Contribution of CAPEX (Turbines) (%)	
Contribution of CAPEX (BoP) (%)	
Contribution of OPEX (%)	

COMPONENT MODELS		SF	Mass (kg)	Cost (\$2002)	Cost (€2012)	Performance	Comment on Mass	Comment on Cost	
ROTOR MODEL			45,309			CP-max 0.34806			WP2
1: Innwind.EU 10MW RWT Blade - scaled	3.00	45,309	588,366				Combination of [2] and [3]	From [1] and [5]	
2: Baseline WindPact		107,101	1,396,851		0.480		From [1]	From [1] and [5]	
3: Advanced WindPact		61,075	794,650		0.480		From [1]	From [1] and [5]	
4: Repower 5 MW RWT Blade - scaled	2.45	41,468	538,118		0.480		Combination of [2] and [3]	From [1] and [5]	
DRIVE TRAIN MODEL						Drive Train Efficiency at 10% load at 100% load			WP3
1: Three-stage planetary/helical									
2: Medium Speed (40:1) Innwind.EU RWT									
3: Repower 5MW RWT 3SG+HSG									
4: Direct drive									
5: SCDD NbTi									
6: SCDD MgB2									
7: SCDD AmSC - SeaTitan									
8: SCDD Jensen 2G									
9: PDD Magnomatics Gearbox									
	1		96,738	1,629,919		0.930 0.990	From [1]	From [1]	
	2	13.25	116,192	1,226,992	1,394,309	0.930 0.990	From [10]	From [10], €2012/kg=12	
	3	3.00	178,191	1,629,919		0.930 0.990	From [2]	From [1]	
	4		0	0		1.000 1.000			
	5		0	0		1.000 1.000			
	6		0	0		1.000 1.000			
	7		0	0		1.000 1.000			
	8		0	0		1.000 1.000			
	9		0	0		1.000 1.000			
Generator									
	1		31,630	650,000		0.896 0.968	From [1]	From [1]	
	2	13.25	62,565	843,308	907,195	0.930 0.979	From [10]	From [10], €2012/kg=14.5	
	3	2.00	34,000	650,000		0.896 0.968	From [2]	From [1]	
	4		210,463	2,193,300		0.885 0.948	From [1]	From [1]	
	5	2.35	145,000	1,528,225	1,644,000	0.800 0.950	From [9]	From [9] in €2012	
	6	2.35	165,000	2,103,634	2,263,000	0.860 0.960	From [9]	From [9] in €2012	
	7	3.15	165,000	2,212,394	2,380,000	0.860 0.960	From [9]	From [9] in €2012	
	8	3.15	70,000	8,124,507	8,740,000	0.870 0.978	From [9]	From [9] in €2012	
	9	3.15	156,000	1,078,310	1,160,000	0.880 0.989	From [9]	From [9] in €2012	
Power electronics									
	1	2.00		790,000		0.960 0.970		Rating * 79.00 \$2002/kW [1]	
	2	2.00		790,000		0.960 0.970		Rating * 79.00 \$2002/kW [1]	
	3	2.00		790,000		0.960 0.970		Rating * 79.00 \$2002/kW [1]	
	4	2.00		790,000		0.960 0.970		Rating * 79.00 \$2002/kW [1]	
	5	2.00		790,000		0.963 0.973		Rating * 79.00 \$2002/kW [1]	
	6	2.00		790,000		0.963 0.973		Rating * 79.00 \$2002/kW [1]	
	7	2.00		790,000		0.963 0.973		Rating * 79.00 \$2002/kW [1]	
	8	2.00		790,000		0.963 0.973		Rating * 79.00 \$2002/kW [1]	
	9	2.00		790,000		0.963 0.973		Rating * 79.00 \$2002/kW [1]	
Bed plate									
	1		73,632	312,893			From [1]	From [1]	
	2	2.10	93,438	181,535			From [1]	From [1]	
	3		73,632	312,893			From [1]	From [1]	
	4		40,492	58,063			From [1]	From [1]	
	5		40,492	58,063			Assuming DD equiv	Assuming DD equiv	
	6		40,492	58,063			Assuming DD equiv	Assuming DD equiv	
	7		40,492	58,063			Assuming DD equiv	Assuming DD equiv	
	8		40,492	58,063			Assuming DD equiv	Assuming DD equiv	
	9		40,492	58,063			Assuming DD equiv	Assuming DD equiv	
SUPPORT STRUCTURE MODEL									WP4
1: Jacket 10 MW RWT			1,920,000	8,766,277	9,496,800			Price = 1.2 X Fabrication cost	
2: Reference Floater for the 10 MW RWT									
3: Other									
	Transition piece for 1	2.5	330,000	1,523,077	1,650,000		From [3]	From [11], 5.0 €2012/kg	
	The jacket itself for 1	1.5	1,210,000	5,361,231	5,808,000		From [3]	From [11], 4.8 €2012/kg	
	The piles for 1	1.5	380,000	420,923	456,000		From [3]	From [11], 1.2 €2012/kg	
	Floater for 2								
	Mooring system for 2								

A.5.4 HLA

TURBINE INPUT PARAMETERS		INTERMEDIATE TURBINE RESULTS				RESULTS	
10000	Power (kW)	0.88	Omega (rad/s)		WF Capacity Factor	0.498	
205.60	Diameter (m)	8.40	RPM max		Turbine Cost (M€2012/MW)	1.755	
90.52	Max Tip Speed (m/s)	12094	Rated Torque (kNm)		BoP Cost (M€2012/MW)	1.695	
119.0	Hub height (m)	33266	Rotor swept area (m2)		CAPEX (M€2012/MW)	3.450	
10.70	Rated speed (m/s)	0.483	Rotor Cp_max (-)		LCOE (€/MWh)	85.65	
10.0	Design speed (m/s)	0.940	Drive Train Efficiency @ full load (100%)				
1	Blade Model	0.830	Drive Train Efficiency @ partial load (10%)				
2	Drive Train Model	0.610	Turbine Capacity Factor				
1	Support Structure Model						
WIND FARM DATA		SITE CONDITIONS				OTHER DATA	
800	Total Capacity (MW)	9.41	Mean Annual Wind Speed (m/s)		\$ / € (2012)	1.320	
12.4%	Wake Losses (%)	2.33	Weibull shape factor k (-)		WT Price/Cost of components	1.400	
2%	Electrical Losses (%)				BoP Price/Cost Multiplier	1.000	
5%	Availability Losses (%)						

COMPONENT	Mass (kg)	Cost (\$2002)	Cost (€2012)	PPI	Mass (NREL)	Cost NREL (\$2009)	MADE OF NAICS code
ROTOR							
Blades	839,342	676,703	RNA				
Hub	105,565	105,520	Hub				
Blade Model	268,066	2,698,290	2,422,376		144,748	1,448,100	
Blades	162,501	2,112,801	1,748,183	9%	53,520	1,062,300	See blade model below
Hub	27,894	316,134	371,218	55%	60,540	130,200	Combination of [2] and [3]
Pitch mechanism	1,79	251,047	281,477	48%	28,878	242,000	Combination of [2] and [3]
Nose cone	1,00	3,287	21,498	55%	1,810	13,600	From [1]
DRIVE TRAIN & NACELLE							
Low speed shaft	3,15	81,068	307,691	67%	16,526	166,800	From [2]
Main bearing	2,65	67,392	1,293,925	44%	5,400	64,400	From [1]
Gearbox	3,97%	104,158	1,099,911	50%	39,688	877,200	See drive train model below
Mechanical brake & couplings	3,15	2,979	19,894	6%	1,063	11,000	From [2]
Generator	6,49%	56,085	755,965	42%	17,623	398,000	See drive train model below
Power electronics	6,54%		790,000	37%		393,200	NA
Bed plate (for Choice 2: 1.953 & 1.067)	2,10	93,438	181,535	55%	31,773	162,700	See drive train model below
Hydraulic & cooling system	0,94%	800	120,000	30%	424	77,200	From [1]
Nacelle cover	2,15	27,387	109,550	13%			From [2]
ELECTRICAL CONNECTIONS							
YAW SYSTEM	3,45	137,968	400,000	90%		308,800	NA
CONTROL, SAFETY SYSTEM, CM	8,42%		1,006,763	55%	13,152	146,300	From [1]
TOWER	1,71	628,471	55,000	30%		65,300	NA
MARINIZATION			1,374,625	26%	596,520	1,491,300	Combination of [2] and [3]
WT price		1,467,813	11,612,034		866,907	6,549,400	
Foundation system		1,920,000	8,766,277	43%	2,174,700	See Foundation Model Below	See Foundation Model Below
Offshore transportation			1,500,000	42%	1,568,300	NA	Rating * 100.00 \$2002/kW ([1] A-d)
Port and staging equipment			200,000	43%	144,900	NA	Rating * 20.00 \$2002/kW [1]
Offshore turbine installation			1,500,000	43%	732,800	NA	Rating * 100.00 \$2002/kW [1]
Offshore electrical I&C			2,600,000	73%	2,063,500	NA	Rating * 260.00 \$2002/kW [1]
Offshore permits & engineering				26%		NA	
Personnel access equipment				43%		NA	
Scour protection			550,000	43%	403,000	NA	Rating * 55.00 \$2002/kW [1]
Decommissioning				26%		NA	
Balance of Plant (BoP)		1,920,000	15,116,277			7,087,200	
BoP price			15,116,277			16,949,603	
CAPEX		31,373,125	34,502,828				

LCOE CALCULATOR		
Total Plant Capacity (MW)	P	800.00
Size of Wind Turbines (MW)	Pt	10.00
Turbines Cost (€/kW)	Ct	1.755
BoP Cost (€/kW)	Cb	1.695
Capital Investment Cost (€/kW)	C	3.450
O&M Costs (€/kW/y)	O&MF	106
O&M Costs [incl. fixed annual costs, (€/MWh)]	O&M	24.30
Balancing Costs (€/MWh)	BC	3.00
Project Lifetime (y)	N	25
Capacity Factor (%)	Cf	0.50
Nominal Discount Rate (%)	dn	0.0739
Inflation Rate (%)	i	0.02112
Real Discount Rate (%)	d	0.0539
Capital Recovery Factor (%)	CRF	0.074
Summation of Discounted Future Expend	SFE	13.56
Present Value of Total O&M (€)	SO&M	1,291,525,648
Annual Energy Production (MWh/y)	E	3,489,629
Leverized Investment (€y)	LI	203,607,019
Annual Discounted O&M (€y)	DO&M	95,268,887
Annual O&M / Capital Investment (%)	O&M(%)	0.031
	LI/E	58.35
	DO&M/E	27.30
LCOE (€/MWh)		85.65
Contribution of CAPEX (Turbines) (€/MWh)		29.68
Contribution of CAPEX (BoP) (€/MWh)		28.66
Contribution of OPEX (€/MWh)		27.30
Contribution of CAPEX (Turbines) (%)		0.35
Contribution of CAPEX (BoP) (%)		0.33
Contribution of OPEX (%)		0.32

COMPONENT MODELS		SF	Mass (kg)	Cost (\$2002)	Cost (€2012)	Performance	Comment on Mass	Comment on Cost	
ROTOR MODEL			54,167			CP-max			
1: Innwind.EU 10MW RWT Blade - scaled	3.00		704,267			0.48329	Combination of [2] and [3]	From [1] and [5]	WP2
2: Baseline WindPact			107,101	1,396,851		0.480	From [1]	From [1] and [5]	
3: Advanced WindPact			61,075	794,650		0.480	From [1]	From [1] and [5]	
4: Repower 5 MW RWT Blade - scaled	2.45		41,468	538,118		0.480	Combination of [2] and [3]	From [1] and [5]	
DRIVE TRAIN MODEL						Drive Train Efficiency			
						at 10% load			
						at 100% load			
1: Three-stage planetary/helical									
2: Medium Speed (40:1) Innwind.EU RWT									
3: Repower 5MW RWT 3SG+HSG									
4: Direct drive									
5: SCDD NbTi									
6: SCDD MgB2									
7: SCDD AmSC - SeaTitan									
8: SCDD Jensen 2G									
9: PDD Magnomatics Gearbox									
	1		89,034	1,629,919		0.930	0.990	From [1]	From [1]
	2	13.25	104,158	1,099,911	1,249,898	0.930	0.990	From [10]	From [10], €2012/kg=12
	3	3.00	178,191	1,629,919		0.930	0.990	From [2]	From [1]
	4		0	0		1.000	1.000		
	5		0	0		1.000	1.000		
	6		0	0		1.000	1.000		
	7		0	0		1.000	1.000		
	8		0	0		1.000	1.000		
	9		0	0		1.000	1.000		
Generator									
	1		31,630	650,000		0.896	0.968	From [1]	From [1]
	2	13.25	56,085	755,965	813,235	0.930	0.979	From [10]	From [10], €2012/kg=14.5
	3	2.00	34,000	650,000		0.896	0.968	From [2]	From [1]
	4		196,970	2,193,300		0.885	0.948	From [1]	From [1]
	5	2.35	145,000	1,528,225	1,644,000	0.800	0.950	From [9]	From [9] in €2012
	6	2.35	165,000	2,103,634	2,263,000	0.860	0.960	From [9]	From [9] in €2012
	7	3.15	165,000	2,212,394	2,380,000	0.860	0.960	From [9]	From [9] in €2012
	8	3.15	70,000	8,124,507	8,740,000	0.870	0.978	From [9]	From [9] in €2012
	9	3.15	156,000	1,078,310	1,160,000	0.880	0.989	From [9]	From [9] in €2012
Power electronics									
	1	2.00		790,000		0.960	0.970		Rating * 79.00 \$2002KW [1]
	2	2.00		790,000		0.960	0.970		Rating * 79.00 \$2002KW [1]
	3	2.00		790,000		0.960	0.970		Rating * 79.00 \$2002KW [1]
	4	2.00		790,000		0.960	0.970		Rating * 79.00 \$2002KW [1]
	5	2.00		790,000		0.963	0.973		Rating * 79.00 \$2002KW [1]
	6	2.00		790,000		0.963	0.973		Rating * 79.00 \$2002KW [1]
	7	2.00		790,000		0.963	0.973		Rating * 79.00 \$2002KW [1]
	8	2.00		790,000		0.963	0.973		Rating * 79.00 \$2002KW [1]
	9	2.00		790,000		0.963	0.973		Rating * 79.00 \$2002KW [1]
Bed plate									
	1		73,632	312,893				From [1]	From [1]
	2	2.10	93,438	181,535				From [1]	From [1]
	3		73,632	312,893				From [1]	From [1]
	4		40,492	58,063				From [1]	From [1]
	5		40,492	58,063				Assuming DD equiv	Assuming DD equiv
	6		40,492	58,063				Assuming DD equiv	Assuming DD equiv
	7		40,492	58,063				Assuming DD equiv	Assuming DD equiv
	8		40,492	58,063				Assuming DD equiv	Assuming DD equiv
	9		40,492	58,063				Assuming DD equiv	Assuming DD equiv
SUPPORT STRUCTURE MODEL									
1: Jacket 10 MW RWT			1,920,000	8,766,277	9,496,800				Price = 1.2 X Fabrication cost
2: Reference Floater for the 10 MW RWT									
3: Other									
	Transition piece for 1	2.5	330,000	1,523,077	1,650,000			From [3]	From [11], 5.0 €2012/kg
	The jacket itself for 1	1.5	1,210,000	5,361,231	5,808,000			From [3]	From [11], 4.8 €2012/kg
	The piles for 1	1.5	380,000	420,923	456,000			From [3]	From [11], 1.2 €2012/kg
	Floater for 2								
	Mooring system for 2								

A.5.5 HRS

TURBINE INPUT PARAMETERS		INTERMEDIATE TURBINE RESULTS		RESULTS	
10000 100.30 101.29 119.0 10.80 10.0	Power (kW) Diameter (m) Max Tip Speed (m/s) Hub height (m) Rated speed (m/s) Design speed (m/s)	0.98 9.40 10807 33266 0.472 0.940	Omega (rad/s) RPM max Rated Torque (kNm) Rotor swept area (m2) Rotor Cp_max (-) Drive Train Efficiency @ full load (100%) Drive Train Efficiency @ partial load (10%) Turbine Capacity Factor		WF Capacity Factor Turbine Cost (M€2012/MW) BoP Cost (M€2012/MW) CAPEX (M€2012/MW) LCOE (€/MWh)
1 2 1	Blade Model Drive Train Model Support Structure Model		0.830 0.605		
WIND FARM DATA		SITE CONDITIONS		OTHER DATA	
300 12.3% 2% 5%	Total Capacity (MW) Wake Losses (%) Electrical Losses (%) Availability Losses (%)	9.41 2.33	Mean Annual Wind Speed (m/s) Weibull shape factor k (-)	\$ / € (2012) WT Price/Cost of components BoP Price/Cost Multiplier	1.320 1.400 1.000

COMPONENT	SF	Mass (kg)	Cost (\$2002)	Cost (€2012)	RNA	PPI	Mass (NREL)	Cost NREL (\$2009)	Comment on Mass	Comment on Cost	MADE OF NAICS code	PCU
		899,407	1,437,879	1,305,145			Total	144,748				
18.82% ROTOR			255,179	2,529,674	2,282,858							
13.26% Blades			105,565	105,520	105,520							
3.06% Hub 2.30	1.79		74,384	316,134	371,218	55%	60,540	130,200	Combination of [2] and [3]	Weight * 4.25 \$2002/kg [1]		
2.32% Pitch mechanism 2.30	1.79		27,894	251,047	281,477	48%	28,878	242,000	Combination of [2] and [3]	Weight * 9.00 \$2002/kg (Assumed)		
0.18% Nose cone 1.00	1.00		3,287	18,308	21,498	55%	1,910	13,600	From [1]	Weight * 5.57 \$2002/kg [1]		
53.24% DRIVE TRAIN & NACELLE			554,229	5,716,507	6,458,793			125,639	2,605,600			
2.54% Low speed shaft 3.00	3.15		81,068	243,205	307,691	67%	16,526	166,800	From [2]	Weight * 3.00 \$2002/kg (Assumed)		
10.67% Main bearing 2.50	2.65		67,392	1,186,098	1,293,925	44%	5,400	64,400	From [1]	Weight * 17.60 \$2002/kg [1]		
9.21% Gearbox			93,078	982,899	1,116,931	50%	39,688	877,200	See drive train model below	See drive train model below		
1.13% Mechanical brake & couplings 3.00	3.15		2,979	19,894	15,975	6%	1,053	11,000	From [2]	From [1]		
5.99% Generator			50,119	675,543	726,721	42%	17,623	398,000	See drive train model below	See drive train model below		
6.76% Power electronics				790,000	819,924	37%		393,200	NA	See drive train model below		
1.76% Bed plate (for Choice 2: 1.953 & 1.067)	2.10		93,438	191,535	213,166	55%	31,773	162,700	See drive train model below	See drive train model below		
0.97% Hydraulic & cooling system			800	120,000	118,182	30%	424	77,200	From [1]	Rating * 12.00 \$2002/kW [1]		
0.77% Nacelle cover 2.00	2.15		27,387	109,550	93,449	13%			From [2]	Weight * 4.00 \$2002/kg		
4.73% ELECTRICAL CONNECTIONS				400,000	574,394	90%		308,800	NA	Rating * 40.00 \$2002/kW [5]		
9.71% YAW SYSTEM 3.314	3.45		137,968	1,006,783	1,178,394	55%	13,152	146,300	From [1]	From [1]		
0.45% CONTROL, SAFETY SYSTEM, CM				55,000	54,167	30%		65,300	NA	From [5]		
17.07% TOWER 2.00	1.71		628,471	1,571,178	2,071,099	74%	596,520	1,491,300	Combination of [2] and [3]	Weight * (1.50 to 4.25) \$2002/kg ([1] Ad)		
10.43% MARINIZATION				1,325,208	1,264,972	26%		939,100		From [1]		
100%			Cost of WT Components	1,437,879	11,196,568	12,131,848		866,907	6,549,400			
			WT price	15,675,195	16,984,587							
56.03% Foundation system			1,920,000	8,766,277	9,496,800	43%		2,174,700	See Foundation Model Below	See Foundation Model Below		
9.52% Offshore transportation				1,500,000	1,613,636	42%		1,568,300	NA	Rating * 100.00 \$2002/kW ([1] Ad)		
1.28% Port and staging equipment				200,000	216,667	43%		144,900	NA	Rating * 20.00 \$2002/kW [1]		
9.59% Offshore turbine installation				1,500,000	1,625,000	43%		732,800	NA	Rating * 100.00 \$2002/kW [1]		
20.07% Offshore electrical I&C				2,600,000	3,401,667	73%		2,063,500	NA	Rating * 290.00 \$2002/kW [1]		
0.00% Offshore permits & engineering					0	26%		NA				
0.00% Personnel access equipment					0	26%		NA				
3.52% Scour protection				550,000	595,833	43%		403,000	NA	Rating * 55.00 \$2002/kW [1]		
0.00% Decommissioning					0	26%		NA				
100%			Balance of Plant (BoP)	1,920,000	15,116,277	16,949,603			7,087,200			
			BoP price	15,116,277	16,949,603							
CAPEX				30,791,472	33,934,190							

LCOE CALCULATOR		P	800.00
Total Plant Capacity (MW)	Pt		10.00
Size of Wind Turbines (MW)	Ct		1.698
Turbines Cost (€/kW)	Cb		1.695
BoP Cost (€/kW)	C		3.393
Capital Investment Cost (€/kW)	O&M		106
O&M Costs (€/kW/y)	O&M		24.51
O&M Costs (incl. fixed annual costs, €/MWh)			
Balancing Costs (€/MWh)	BC		3.00
Project Lifetime (y)	N		25
Capacity Factor (%)	Cf		0.49
Nominal Discount Rate (%)	dn		0.0739
Inflation Rate (%)	i		0.02112
Real Discount Rate (%)	d		0.0539
Capital Recovery Factor (%)	CRF		0.074
Summation of Discounted Future Expend	SFE		13.56
Present Value of Total O&M (€)	SO&M		1,290,320,204
Annual Energy Production (MWh/y)	E		3,459,989
Levelized Investment (€/y)	LI		200,251,388
Annual Discounted O&M (€/y)	DO&M		95,179,968
Annual O&M / Capital Investment (%)	O&M(%)		0.031
LCOE (€/MWh)	LJ/E		57.88
Contribution of CAPEX (Turbines) (€/MWh)	DO&M/E		27.51
Contribution of CAPEX (BoP) (€/MWh)			28.97
Contribution of OPEX (€/MWh)			28.91
Contribution of CAPEX (Turbines) (%)			0.34
Contribution of CAPEX (BoP) (%)			0.34
Contribution of OPEX (%)			0.32
			1.00

COMPONENT MODELS		SF	Mass (kg)	Cost (\$2002)	Cost (€2012)	Performance	Comment on Mass	Comment on Cost	
ROTOR MODEL			49,871			CP-max			
1: Innwind.EU 10MW RWT Blade - scaled	3.00	49,871	648,062			0.471771	Combination of [2] and [3]	From [1] and [5]	WP2
2: Baseline WindPact		107,101	1,396,851			0.480	From [1]	From [1] and [5]	
3: Advanced WindPact		61,075	794,650			0.480	From [1]	From [1] and [5]	
4: Repower 5 MW RWT Blade - scaled	2.45	41,468	538,118			0.480	Combination of [2] and [3]	From [1] and [5]	
DRIVE TRAIN MODEL						Drive Train Efficiency			
						at 10% load			
						at 100% load			
1: Three-stage planetary/helical									
2: Medium Speed (40:1) Innwind.EU RWT									
3: Repower 5MW RWT 3SG+HSG									
4: Direct drive									
5: SCDD NbTi									
6: SCDD MgB2									
7: SCDD AmSC - SeaTitan									
8: SCDD Jensen 2G									
9: PDD Magnomatics Gearbox									
	1	81,748	1,629,919			0.930 0.990	From [1]	From [1]	
	2	13.25	93,078	982,899	1,116,931	0.930 0.990	From [10]	From [10]	
	3	3.00	178,191	1,629,919		0.930 0.990	From [2]	From [10], €2012/kg=12	
	4		0	0		1.000 1.000		From [1]	
	5		0	0		1.000 1.000			
	6		0	0		1.000 1.000			
	7		0	0		1.000 1.000			
	8		0	0		1.000 1.000			
	9		0	0		1.000 1.000			
Generator									
	1		31,630	650,000		0.896 0.968	From [1]	From [1]	
	2	13.25	50,119	675,543	726,721	0.930 0.979	From [10]	From [10], €2012/kg=14.5	
	3	2.00	34,000	650,000		0.896 0.968	From [2]		
	4		183,991	2,193,300		0.885 0.948	From [1]		
	5	2.35	145,000	1,528,225	1,644,000	0.800 0.950	From [9]	From [9] in €2012	
	6	2.35	165,000	2,103,634	2,263,000	0.860 0.960	From [9]	From [9] in €2012	
	7	3.15	165,000	2,212,394	2,380,000	0.860 0.960	From [9]	From [9] in €2012	
	8	3.15	70,000	8,124,507	8,740,000	0.870 0.978	From [9]	From [9] in €2012	
	9	3.15	156,000	1,078,310	1,160,000	0.880 0.989	From [9]	From [9] in €2012	
Power electronics									
	1	2.00		790,000		0.960 0.970		Rating * 79.00 \$2002KW [1]	
	2	2.00		790,000		0.960 0.970		Rating * 79.00 \$2002KW [1]	
	3	2.00		790,000		0.960 0.970		Rating * 79.00 \$2002KW [1]	
	4	2.00		790,000		0.960 0.970		Rating * 79.00 \$2002KW [1]	
	5	2.00		790,000		0.963 0.973		Rating * 79.00 \$2002KW [1]	
	6	2.00		790,000		0.963 0.973		Rating * 79.00 \$2002KW [1]	
	7	2.00		790,000		0.963 0.973		Rating * 79.00 \$2002KW [1]	
	8	2.00		790,000		0.963 0.973		Rating * 79.00 \$2002KW [1]	
	9	2.00		790,000		0.963 0.973		Rating * 79.00 \$2002KW [1]	
Bed plate									
	1		73,632	312,893			From [1]	From [1]	
	2	2.10	93,438	181,535			From [1]	From [1]	
	3		73,632	312,893			From [1]	From [1]	
	4		40,492	58,063			From [1]	From [1]	
	5		40,492	58,063			Assuming DD equiv	Assuming DD equiv	
	6		40,492	58,063			Assuming DD equiv	Assuming DD equiv	
	7		40,492	58,063			Assuming DD equiv	Assuming DD equiv	
	8		40,492	58,063			Assuming DD equiv	Assuming DD equiv	
	9		40,492	58,063			Assuming DD equiv	Assuming DD equiv	
SUPPORT STRUCTURE MODEL									
1: Jacket 10 MW RWT			1,920,000	8,766,277	9,496,800			Price = 1.2 X Fabrication cost	
2: Reference Floater for the 10 MW RWT									
3: Other									
	Transition piece for 1	2.5	330,000	1,523,077	1,650,000		From [3]	From [11], 5.0 €2012/kg	
	The jacket itself for 1	1.5	1,210,000	5,361,231	5,808,000		From [3]	From [11], 4.8 €2012/kg	
	The piles for 1	1.5	380,000	420,923	456,000		From [3]	From [11], 1.2 €2012/kg	
	Floater for 2								
	Mooring system for 2								

A.5.6 UPK

TURBINE INPUT PARAMETERS		INTERMEDIATE TURBINE RESULTS				RESULTS	
10000	Power (kW)	0.75	Omega (rad/s)			WF Capacity Factor	0.457
205.80	Diameter (m)	7.16	RPM max			Turbine Cost (M€2012/MW)	1.798
77.16	Max Tip Speed (m/s)	14188	Rated Torque (kNm)			BoP Cost (M€2012/MW)	1.695
119.0	Hub height (m)	33266	Rotor swept area (m2)			CAPEX (M€2012/MW)	3.493
11.80	Rated speed (m/s)	0.376	Rotor Cp_max (-)			LCOE (€/MWh)	93.76
10.0	Design speed (m/s)	0.940	Drive Train Efficiency @ full load (100%)				
1	1: Innwind.EU 10MW RWT Blade - scal	0.830	Drive Train Efficiency @ partial load (10%)				
2	2: Medium Speed (40-11) Innwind.EU R1	0.554	Turbine Capacity Factor				
1	1: Jacket 10 MW RWT						
	Support Structure Model						
WIND FARM DATA		SITE CONDITIONS				OTHER DATA	
800	Total Capacity (MW)	9.41	Mean Annual Wind Speed (m/s)			\$ / € (2012)	1.320
11.4%	Wake Losses (%)	2.33	Weibull shape factor k (-)			WT Price/Cost of components	1.400
2%	Electrical Losses (%)					BoP Price/Cost Multiplier	1.000
5%	Availability Losses (%)						

COMPONENT	SF	Mass (kg)	Cost (\$2002)	Cost (€2012)	RNA	PPI	Mass (NREL)	Cost NREL (\$2009)	Comment on Mass	Comment on Cost	MADE OF NAICS code	PCU
		859,428	676,703									
18.22% ROTOR		260,400	2,597,991	2,339,396			144,748	1,448,100				
12.97% <i>Blades</i>		154,835	2,012,502	1,665,193		9%	53,520	1,062,300	See blade model below	See blade model below		
2.89% <i>Hub 2.30</i>	1.79	74,384	316,134	371,218		55%	60,540	130,200	Combination of [2] and [3]	Weight * 4.25 \$2002/kg [1]		
2.19% <i>Pitch mechanism 2.30</i>	1.79	27,894	251,047	281,477		48%	28,878	242,000	Combination of [2] and [3]	Weight * 9.00 \$2002/kg (Assumed)		
0.17% <i>Nose cone 1.00</i>	1.00	3,287	18,308	21,498		55%	1,810	13,600	From [1]	Weight * 5.57 \$2002/kg [1]		
54.79% DRIVE TRAIN & NACELLE		599,028	6,234,349	7,035,537			125,639	2,605,600				
2.40% <i>Low speed shaft 3.00</i>	3.15	81,068	243,205	307,691		67%	16,526	166,800	From [2]	Weight * 3.00 \$2002/kg (Assumed)		
10.08% <i>Main bearing 2.50</i>	2.65	67,392	1,186,098	1,293,925		44%	5,400	64,400	From [1]	Weight * 17.60 \$2002/kg [1]		
11.42% <i>Gearbox</i>		122,197	1,290,398	1,466,361		50%	39,688	877,200	See drive train model below	See drive train model below		
0.12% <i>Mechanical brake & couplings 3.00</i>	3.15	2,979	19,894	15,975		6%	1,053	11,000	From [2]	From [1]		
7.43% <i>Generator</i>		65,798	886,896	954,075		42%	17,623	398,000	See drive train model below	See drive train model below		
6.39% <i>Power electronics</i>		790,000		819,924		37%		383,200	NA	See drive train model below		
1.66% <i>Bed plate (for Choice 2: 1.953 & 1.067)</i>	2.10	93,438	181,535	213,166		55%	31,773	162,700	See drive train model below	See drive train model below		
0.92% <i>Hydraulic & cooling system</i>		800	120,000	118,182		30%	424	77,200	From [1]	Rating * 12.00 \$2002/kg [1]		
0.73% <i>Nacelle cover 2.00</i>	2.15	27,387	109,550	93,449		13%			From [2]	Rating * 4.00 \$2002/kg [5]		
4.47% ELECTRICAL CONNECTIONS			400,000	574,394		90%		308,800	NA	From [1]		
9.18% YAW SYSTEM 3.314	3.45	137,968	1,006,783	1,178,394		55%	13,152	146,300	From [1]	From [1]		
8.42% CONTROL, SAFETY SYSTEM, CM			55,000	54,167		30%		65,300	NA	From [5]		
16.13% TOWER 2.00	1.71	628,471	1,571,178	2,075,009		74%	596,520	1,491,300	Combination of [2] and [3]	Weight * (1.15 to 4.25) \$2002/kg ([1] A-d)		
16.44% MARINIZATION			1,404,475	1,340,635		26%		939,100		From [1]		
100%	Cost of WT Components	1,487,899	11,862,994	12,840,824			866,907	6,549,400				
	WT price		16,608,192	17,977,154								
56.03% Foundation system		1,920,000	8,766,277	9,496,800		43%		2,174,700	See Foundation Model Below	See Foundation Model Below		
9.52% Offshore transportation			1,500,000	1,613,636		42%		1,568,300	NA	Rating * 100.00 \$2002/kg ([1] A-d)		
1.28% Port and staging equipment			200,000	216,667		43%		144,900	NA	Rating * 20.00 \$2002/kg [1]		
9.59% Offshore turbine installation			1,500,000	1,625,000		43%		732,800	NA	Rating * 100.00 \$2002/kg [1]		
20.07% Offshore electrical I&C			2,600,000	3,401,667		73%		2,063,500	NA	Rating * 260.00 \$2002/kg [1]		
0.00% Offshore permits & engineering				0		26%		NA				
0.00% Personnel access equipment				0		26%		NA				
3.32% Scour protection			550,000	595,833		43%		403,000	NA	Rating * 55.00 \$2002/kg [1]		
0.00% Decommissioning				0		26%		NA				
100%	Balance of Plant (BoP)	1,920,000	15,116,277	16,949,603				7,087,200				
	BoP price		15,116,277	16,949,603								
CAPEX			31,724,469	34,926,757								

LCOE CALCULATOR	
Total Plant Capacity (MW)	P 800.00
Size of Wind Turbines (MW)	Pt 10.00
Turbines Cost (€/kW)	Ct 1.798
BoP Cost (€/kW)	Cb 1.695
Capital Investment Cost (€/kW)	C 3.493
O&M Costs (€/MWh)	O&Mf 106
O&M Costs [incl. fixed annual costs, (€/MWh)]	O&M 26.46
Balancing Costs (€/MWh)	BC 3.00
Project Lifetime (y)	N 25
Capacity Factor (%)	Cf 0.46
Nominal Discount Rate (%)	dn 0.0739
Inflation Rate (%)	i 0.02112
Real Discount Rate (%)	d 0.0539
Capital Recovery Factor (%)	CRF 0.074
Summation of Discounted Future Expend	SFE 13.56
Present Value of Total O&M (€)	SO&M 1,279,967,154
Annual Energy Production (MWh/y)	E 3,205,426
Levelized Investment (€y)	LI 206,108,690
Annual Discounted O&M (€y)	DO&M 94,416,279
Annual O&M / Capital Investment (%)	O&M(%) 0.030
	LI/E 64.30
	DO&M/E 29.46
LCOE (€/MWh)	93.76
Contribution of CAPEX (Turbines) (€/MWh)	33.10
Contribution of CAPEX (BoP) (€/MWh)	31.20
Contribution of OPEX (€/MWh)	29.46
Contribution of CAPEX (Turbines) (%)	0.35
Contribution of CAPEX (BoP) (%)	0.33
Contribution of OPEX (%)	0.31
	1.00

COMPONENT MODELS		SF	Mass (kg)	Cost (\$2002)	Cost (€2012)	Performance	Comment on Mass	Comment on Cost	
ROTOR MODEL			51,612			CP-max			WP2
1: Innwind.EU 10MW RWT Blade - scaled	3.00	51,612	670,834			0.37582	Combination of [2] and [3]	From [1] and [5]	
2: Baseline WindPact		107,101	1,396,851			0.480	From [1]	From [1] and [5]	
3: Advanced WindPact		61,075	794,650			0.480	From [1]	From [1] and [5]	
4: Repower 5 MW RWT Blade - scaled	2.45	41,468	538,118			0.480	Combination of [2] and [3]	From [1] and [5]	
DRIVE TRAIN MODEL						Drive Train Efficiency			WP3
						at 10% load			
1: Three-stage planetary/helical									
2: Medium Speed (40:1) Innwind.EU RWT									
3: Repower 5MW RWT 3SG+HSG									
4: Direct drive									
5: SCDD NbTi									
6: SCDD MgB2									
7: SCDD AmSC - SeaTitan									
8: SCDD Jensen 2G									
9: PDD Magnomatics Gearbox									
1		100,505	1,629,919			0.930 0.990	From [1]	From [1]	
2	13.25	122,197	1,290,398	1,466,361		0.930 0.990	From [10]	From [10], €2012/kg=12	
3	3.00	178,191	1,629,919			0.930 0.990	From [2]	From [1]	
4		0	0			1.000 1.000			
5		0	0			1.000 1.000			
6		0	0			1.000 1.000			
7		0	0			1.000 1.000			
8		0	0			1.000 1.000			
9		0	0			1.000 1.000			
Generator									
1		31,630	650,000			0.896 0.968	From [1]	From [1]	
2	13.25	65,798	886,886	954,075		0.930 0.979	From [10]	From [10], €2012/kg=14.5	
3	2.00	34,000	650,000			0.896 0.968	From [2]	From [1]	
4		216,988	2,193,300			0.885 0.948	From [1]	From [1]	
5	2.35	145,000	1,528,225	1,644,000		0.800 0.950	From [9]	From [9] in €2012	
6	2.35	165,000	2,103,634	2,263,000		0.860 0.960	From [9]	From [9] in €2012	
7	3.15	165,000	2,212,394	2,380,000		0.860 0.960	From [9]	From [9] in €2012	
8	3.15	70,000	8,124,507	8,740,000		0.870 0.978	From [9]	From [9] in €2012	
9	3.15	156,000	1,078,310	1,160,000		0.880 0.989	From [9]	From [9] in €2012	
Power electronics									
1	2.00		790,000			0.960 0.970		Rating * 79.00 \$2002KW [1]	
2	2.00		790,000			0.960 0.970		Rating * 79.00 \$2002KW [1]	
3	2.00		790,000			0.960 0.970		Rating * 79.00 \$2002KW [1]	
4	2.00		790,000			0.960 0.970		Rating * 79.00 \$2002KW [1]	
5	2.00		790,000			0.963 0.973		Rating * 79.00 \$2002KW [1]	
6	2.00		790,000			0.963 0.973		Rating * 79.00 \$2002KW [1]	
7	2.00		790,000			0.963 0.973		Rating * 79.00 \$2002KW [1]	
8	2.00		790,000			0.963 0.973		Rating * 79.00 \$2002KW [1]	
9	2.00		790,000			0.963 0.973		Rating * 79.00 \$2002KW [1]	
Bed plate									
1		73,632	312,893				From [1]	From [1]	
2	2.10	93,438	181,535				From [1]	From [1]	
3		73,632	312,893				From [1]	From [1]	
4		40,492	58,063				From [1]	From [1]	
5		40,492	58,063				Assuming DD equiv	Assuming DD equiv	
6		40,492	58,063				Assuming DD equiv	Assuming DD equiv	
7		40,492	58,063				Assuming DD equiv	Assuming DD equiv	
8		40,492	58,063				Assuming DD equiv	Assuming DD equiv	
9		40,492	58,063				Assuming DD equiv	Assuming DD equiv	
SUPPORT STRUCTURE MODEL									WP4
1: Jacket 10 MW RWT			1,920,000	8,766,277	9,496,800			Price = 1.2 X Fabrication cost	
2: Reference Floater for the 10 MW RWT									
3: Other									
Transition piece for 1	2.5	330,000	1,523,077	1,650,000			From [3]	From [11], 5.0 €2012/kg	
The jacket itself for 1	1.5	1,210,000	5,361,231	5,808,000			From [3]	From [11], 4.8 €2012/kg	
The piles for 1	1.5	380,000	420,923	456,000			From [3]	From [11], 1.2 €2012/kg	
Floater for 2									
Mooring system for 2									

A.5.7 HRK

TURBINE INPUT PARAMETERS		INTERMEDIATE TURBINE RESULTS			RESULTS	
10000 100.38 101.29 119.0 12.70 10.0	Power (kW) Diameter (m) Max Tip Speed (m/s) Hub height (m) Rated speed (m/s) Design speed (m/s)	0.98 9.40 10807 33266 0.352 0.940	Omega (rad/s) RPM max Rated Torque (kNm) Rotor swept area (m2) Rotor Cp_max (-)		WF Capacity Factor Turbine Cost (M€2012/MW) BoP Cost (M€2012/MW) CAPEX (M€2012/MW) LCOE (€/MWh)	0.441 1.661 1.695 3.356 94.42
1 2 1	1: Innwind.EU 10MW RWT Blade - scal 2: Medium Speed (40-1) Innwind.EU R 1: Jacket 10 MW RWT	0.830 0.537	Drive Train Efficiency @ full load (100%) Drive Train Efficiency @ partial load (10%) Turbine Capacity Factor			
WIND FARM DATA		SITE CONDITIONS			OTHER DATA	
300 11.8% 2% 5%	Total Capacity (MW) Wake Losses (%) Electrical Losses (%) Availability Losses (%)	9.41 2.33	Mean Annual Wind Speed (m/s) Weibull shape factor k (-)		\$ / € (2012) WT Price/Cost of components BoP Price/Cost Multiplier	1.320 1.400 1.000

COMPONENT	SF	Mass (kg)	Cost (\$2002)	Cost (€2012)	RNA	PPI	Mass (NREL)	Cost NREL (\$2009)	Comment on Mass	Comment on Cost	MADE OF NAICS code	PCU
		787,877	676,703	1,305,145			Total	144,748				
17.28% ROTOR												
11.60% Blades		1,416,349	1,305,145	2,049,774								
3.13% Hub 2.30	1.79	105,565	105,520	307,691								
2.37% Pitch mechanism 2.30	1.79	74,384	316,134	371,218								
0.18% Nose cone 1.00	1.00	27,894	251,047	281,477								
54.45% DRIVE TRAIN & NACELLE		554,229	5,716,507	6,458,793								
2.59% Low speed shaft 3.00	3.15	81,068	243,205	307,691								
10.91% Main bearing 2.50	2.65	67,392	1,188,098	1,293,925								
9.42% Gearbox		93,078	982,899	1,116,931								
1.13% Mechanical brake & couplings 3.00	3.15	2,979	19,894	19,975								
6.13% Generator		50,119	675,543	726,721								
6.91% Power electronics			790,000	819,924								
1.80% Bed plate (for Choice 2: 1.953 & 1.067)	2.10	93,438	191,535	213,166								
1.00% Hydraulic & cooling system		800	120,000	118,182								
0.79% Nacelle cover 2.00	2.15	27,387	109,550	93,449								
4.84% ELECTRICAL CONNECTIONS			400,000	574,394								
9.93% YAW SYSTEM 3.314	3.45	137,968	1,006,783	1,178,394								
0.46% CONTROL, SAFETY SYSTEM, CM			55,000	54,167								
17.46% TOWER 2.00	1.71	628,471	1,571,178	2,071,099								
10.36% MARINIZATION			1,287,179	1,228,671								
100%		Cost of WT Components	1,416,349	10,876,839	11,862,463		866,907	6,549,400				
		WT price	15,227,575	16,607,448								
56.03% Foundation system		1,920,000	8,766,277	9,496,800		43%	2,174,700	See Foundation Model Below	See Foundation Model Below			
9.52% Offshore transportation		1,500,000	1,500,000	1,613,636		42%	1,568,300	NA	Rating * 100.00 \$2002kW [(1) Adj]			
1.28% Port and staging equipment		200,000	200,000	216,667		43%	144,900	NA	Rating * 20.00 \$2002kW [(1)]			
9.59% Offshore turbine installation		1,500,000	1,625,000			43%	732,800	NA	Rating * 100.00 \$2002kW [(1)]			
20.07% Offshore electrical I&C		2,600,000	3,401,667			73%	2,063,500	NA	Rating * 260.00 \$2002kW [(1)]			
0.00% Offshore permits & engineering			0	0		26%	NA					
0.00% Personnel access equipment			0	0		26%	NA					
3.52% Scour protection			550,000	595,833		43%	403,000	NA	Rating * 55.00 \$2002kW [(1)]			
0.00% Decommissioning			0	0		26%	NA					
100%		Balance of Plant (BoP)	1,920,000	15,116,277	16,949,603			7,087,200				
		BoP price	15,116,277	16,949,603								
CAPEX			30,343,852	33,557,051								

LCOE CALCULATOR	
Total Plant Capacity (MW)	P 800.00
Size of Wind Turbines (MW)	Pt 10.00
Turbines Cost (€/kW)	Ct 1.661
BoP Cost (€/kW)	Cb 1.695
Capital Investment Cost (€/kW)	C 3.356
O&M Costs (€/kW/y)	O&MF 106
O&M Costs (incl. fixed annual costs, €/MWh)	O&M 27.41
Balancing Costs (€/MWh)	BC 3.00
Project Lifetime (y)	N 25
Capacity Factor (%)	Cf 0.44
Nominal Discount Rate (%)	dn 0.0739
Inflation Rate (%)	i 0.02112
Real Discount Rate (%)	d 0.0539
Capital Recovery Factor (%)	CRF 0.074
Summation of Discounted Future Expend	SFE 13.56
Present Value of Total O&M (€)	SO&M 1,275,423,181
Annual Energy Production (MWh/y)	E 3,093,698
Levelized Investment (€/y)	LI 198,025,826
Annual Discounted O&M (€/y)	DO&M 94,081,095
Annual O&M / Capital Investment (%)	O&M(%) 0.032
LCOE (€/MWh)	LI/E 64.01
Contribution of CAPEX (Turbines) (€/MWh)	DO&M/E 30.41
Contribution of CAPEX (BoP) (€/MWh)	
Contribution of OPEX (€/MWh)	
Contribution of CAPEX (Turbines) (%)	0.34
Contribution of CAPEX (BoP) (%)	0.34
Contribution of OPEX (%)	0.32
	1.00

COMPONENT MODELS		SF	Mass (kg)	Cost (\$2002)	Cost (€2012)	Performance	Comment on Mass	Comment on Cost	
ROTOR MODEL			42,694			CP-max			
1: Innwind.EU 10MW RWT Blade - scaled	3.00		554,162			0.35233	Combination of [2] and [3]	From [1] and [5]	WP2
2: Baseline WindPact			107,101	1,396,851		0.480	From [1]	From [1] and [5]	
3: Advanced WindPact			61,075	794,650		0.480	From [1]	From [1] and [5]	
4: Repower 5 MW RWT Blade - scaled	2.45		41,468	538,118		0.480	Combination of [2] and [3]	From [1] and [5]	
DRIVE TRAIN MODEL						Drive Train Efficiency			
						at 10% load			
						at 100% load			
1: Three-stage planetary/helical									
2: Medium Speed (40:1) Innwind.EU RWT									
3: Repower 5MW RWT 3SG+HSG									
4: Direct drive									
5: SCDD NbTi									
6: SCDD MgB2									
7: SCDD AmSC - SeaTitan									
8: SCDD Jensen 2G									
9: PDD Magnomatics Gearbox									
	1		81,748	1,629,919		0.930	0.990	From [1]	From [1]
	2	13.25	93,078	982,899	1,116,931	0.930	0.990	From [10]	From [10], €2012/kg=12
	3	3.00	178,191	1,629,919		0.930	0.990	From [2]	From [1]
	4		0	0		1.000	1.000		
	5		0	0		1.000	1.000		
	6		0	0		1.000	1.000		
	7		0	0		1.000	1.000		
	8		0	0		1.000	1.000		
	9		0	0		1.000	1.000		
Generator									
	1		31,630	650,000		0.896	0.968	From [1]	From [1]
	2	13.25	50,119	675,543	726,721	0.930	0.979	From [10]	From [10], €2012/kg=14.5
	3	2.00	34,000	650,000		0.896	0.968	From [2]	From [1]
	4		183,991	2,193,300		0.885	0.948	From [1]	From [1]
	5	2.35	145,000	1,528,225	1,644,000	0.800	0.950	From [9]	From [9] in €2012
	6	2.35	165,000	2,103,634	2,263,000	0.860	0.960	From [9]	From [9] in €2012
	7	3.15	165,000	2,212,394	2,380,000	0.860	0.960	From [9]	From [9] in €2012
	8	3.15	70,000	8,124,507	8,740,000	0.870	0.978	From [9]	From [9] in €2012
	9	3.15	156,000	1,078,310	1,160,000	0.880	0.989	From [9]	From [9] in €2012
Power electronics									
	1	2.00		790,000		0.960	0.970		Rating * 79.00 \$2002KW [1]
	2	2.00		790,000		0.960	0.970		Rating * 79.00 \$2002KW [1]
	3	2.00		790,000		0.960	0.970		Rating * 79.00 \$2002KW [1]
	4	2.00		790,000		0.960	0.970		Rating * 79.00 \$2002KW [1]
	5	2.00		790,000		0.963	0.973		Rating * 79.00 \$2002KW [1]
	6	2.00		790,000		0.963	0.973		Rating * 79.00 \$2002KW [1]
	7	2.00		790,000		0.963	0.973		Rating * 79.00 \$2002KW [1]
	8	2.00		790,000		0.963	0.973		Rating * 79.00 \$2002KW [1]
	9	2.00		790,000		0.963	0.973		Rating * 79.00 \$2002KW [1]
Bed plate									
	1		73,632	312,893				From [1]	From [1]
	2	2.10	93,438	181,535				From [1]	From [1]
	3		73,632	312,893				From [1]	From [1]
	4		40,492	58,063				From [1]	From [1]
	5		40,492	58,063				Assuming DD equiv	Assuming DD equiv
	6		40,492	58,063				Assuming DD equiv	Assuming DD equiv
	7		40,492	58,063				Assuming DD equiv	Assuming DD equiv
	8		40,492	58,063				Assuming DD equiv	Assuming DD equiv
	9		40,492	58,063				Assuming DD equiv	Assuming DD equiv
SUPPORT STRUCTURE MODEL									
1: Jacket 10 MW RWT			1,920,000	8,766,277	9,496,800				Price = 1.2 X Fabrication cost
2: Reference Floater for the 10 MW RWT									
3: Other									
	Transition piece for 1	2.5	330,000	1,523,077	1,650,000			From [3]	From [11], 5.0 €2012/kg
	The jacket itself for 1	1.5	1,210,000	5,361,231	5,808,000			From [3]	From [11], 4.8 €2012/kg
	The piles for 1	1.5	380,000	420,923	456,000			From [3]	From [11], 1.2 €2012/kg
	Floater for 2								
	Mooring system for 2								

